

CHEMOURS DELISLE PLANT
2017 HWDIR EXEMPTION PETITION REISSUANCE APPLICATION
SECTION 2.0 GEOLOGY

TABLE of CONTENTS

2.0 GEOLOGY	1
2.1 INTRODUCTION	1
2.2 Regional Geology	3
2.2.1 Historical Regional Geology.....	3
2.2.2 Regional Surface Geology	4
2.2.3 Structure.....	5
2.2.3.1 Faulting	5
2.2.4 Data Documenting Lack of Faulting.....	6
2.2.5 Seismicity.....	7
2.2.5.1 Natural Seismicity.....	7
2.2.5.2 Induced Seismicity.....	8
2.2.6 Stratigraphy.....	11
2.2.6.1 Washita-Fredericksburg Group.....	11
2.2.6.2 Tuscaloosa Formation.....	11
2.2.6.3 Eutaw Formation.....	13
2.2.6.4 Selma Formation.....	13
2.2.6.5 Midway Group	13
2.2.6.6 Wilcox Group.....	14
2.2.6.7 Claiborne/Jackson Group.....	15
2.2.6.8 Vicksburg Group.....	16
2.2.6.8.1 Chickasawhay Formation.....	16
2.2.6.9 Undifferentiated Sand and Shales	16
2.2.6.9.1 Fleming Group	16
2.2.6.9.2 Graham Ferry Formation	17
2.2.6.9.3 Citronelle Formation	17
2.2.6.10 Pleistocene and Holocene Deposits	18
2.2.7 Mineral Resources	19

2.3	LOCAL GEOLOGY	20
2.3.1	Injection Interval, Injection Zone, and Confining Zone Defined	20
2.3.2	Structure	21
2.3.3	Stratigraphy of the Injection Zone	21
2.3.3.1	Washita-Fredericksburg	21
2.3.3.1.1	Fracture Pressure Estimate for the Washita-Fredericksburg Injection Interval	22
2.3.3.2	Tuscaloosa Formation	22
2.3.3.2.1	Fracture Pressure Estimate for Tuscaloosa Massive Sand Injection Interval	23
2.3.3.3	Eutaw Formation	24
2.3.3.4	Basal Selma Shale/Chalk	24
2.3.4	Stratigraphy of the Confining Zone	24
2.3.4.1	Selma Shale/Chalk	24
2.3.4.2	Midway Shale	25
2.4	GROUNDWATER HYDROLOGY	25
2.4.1	Regional Geology and Hydrology	25
2.4.2	Local Hydrology	27
2.4.3	Chemours Monitoring Program	29

FIGURES

- Figure 2-1 Chemours DeLisle Plant, Lithologic Column
- Figure 2-2 Electric Log Stratigraphic Column – Well No. 5
- Figure 2-3 Composite Electric Log Stratigraphic Column
- Figure 2-4 Regional Mississippi Stratigraphic Column
- Figure 2-5 Distribution of Cretaceous and Cenozoic Continental Margins in the Northwestern Gulf of Mexico
- Figure 2-6 Surface Geologic Map of Mississippi
- Figure 2-7 Tectonic Map of the Northern Gulf Coast Region
- Figure 2-8 Tectonic and Subsurface Structural Features of Mississippi (from Miss. Bureau of Geology)
- Figure 2-9 Earthquake Events within a 250km Radius of the Chemours DeLisle Plant through March 2017
- Figure 2-10 Detailed Tectonic Setting Southern Mississippi Salt Basin
- Figure 2-11 Mississippi Index Map of oil and gas fields with County Key
- Figure 2-12 Washita-Fredericksburg Injection Interval Electric Log Correlation
- Figure 2-13 Miocene Aquifer System (State of Mississippi)
- Figure 2-14 Excerpts from Ground Water Atlas of the United States
- Figure 2-15 Location of Monitor Wells (Google Maps)

TABLES

Table 2-1	Index of Geologic Maps within the DeLisle Petition Reissuance Geology Section
Table 2-2	Estimated Dip of Formations Below the Top of the Confining Zone at the DeLisle Plant
Table 2-3	Thicknesses of Formations Below the Top of the Confining Zone at the DeLisle Plant
Table 2-4	Modified Mercalli Intensity Scale of 1931
Table 2-5	Calculated Injection Interval Pressure Increase at the DeLisle Plant
Table 2-6	Upper Washita-Fredericksburg Injection Intervals
Table 2-7	Geological Data Used for Establishing Porosity and Permeability of the Washita-Fredericksburg Injection Sand
Table 2-8	Injection Well No. 2 - Washita-Fredericksburg X-Ray Diffraction Analysis
Table 2-9	Injection Well No. 5 - Washita-Fredericksburg X-Ray Diffraction Analysis
Table 2-10	Injection Well No. 5 - Average Reservoir Properties of Sampled Zones
Table 2-11	Geologic Column and Hydrologic Characteristics of Aquifers in Mississippi
Table 2-12	Freshwater Sand Depths in Harrison County, Mississippi
Table 2-13	Chemical Quality of Water from Miocene Aquifers
Table 2-14	Freshwater Aquifer Characteristics
Table 2-15	Analytical Results of DeLisle Monitoring Well Water Samples
Table 2-16	Chemical Analysis of Water Well No. 4
Table 2-17	Formation Fluid Analysis Well No. 5 - Tuscaloosa Massive Sand
Table 2-18	Sidetrack Injection Wells Reservoir Fluid Sampling Results

APPENDICES

Appendix 2-1	Well Location Map
Appendix 2-2	Cross-Section Index Map (A-A' and B-B')
Appendix 2-3	North-South Structural Cross-Section A-A'
Appendix 2-4	West-East Structural Cross-Section B-B'
Appendix 2-5	Top of Midway Shale (Top of Confining Zone) Structure Map
Appendix 2-6	Top of Selma Chalk Structure Map
Appendix 2-7	Top of Eutaw Structure Map
Appendix 2-8	Top of Upper and Middle Tuscaloosa Formation Structure Map
Appendix 2-9	Top of Lower Tuscaloosa Formation Structure Map
Appendix 2-10	Top of Tuscaloosa Massive Sand Structure Map
Appendix 2-11	Top of Washita-Fredericksburg Sand (Injection Interval) Structure Map
Appendix 2-12	Midway Shale Isopach Map
Appendix 2-13	Selma Chalk Isopach Map
Appendix 2-14	Eutaw Isopach Map
Appendix 2-15	Upper and Middle Tuscaloosa Formation Isopach Map
Appendix 2-16	Lower Tuscaloosa Formation Isopach Map
Appendix 2-17	Tuscaloosa Massive Sand (Net Sand) Isopach Map
Appendix 2-18	Washita-Fredericksburg Sand (Injection Interval) Isopach Map
Appendix 2-19	Interpreted Seismic Line Union Oil Line 2 – (BUSINESS CONFIDENTIAL)
Appendix 2-20	Synthetic Seismogram (Injection Well No. 4) – (BUSINESS CONFIDENTIAL)
Appendix 2-21	David Leeds and Associates Seismic Study 1989 and 1998
Appendix 2-22	MDEQ Earthquake Epicenter Map
Appendix 2-23	Gulf Coast Seismicity Map

- Appendix 2-24 Seismic Hazard Map of Mississippi
- Appendix 2-25 1990 – 2001 Seismicity of Mississippi
- Appendix 2-26 Seismic Hazard Map for Continuous United States
- Appendix 2-27 NEIC: Earthquake Search Results USGS Earthquake Database for the State of Mississippi
- Appendix 2-28 Location Sample Service, Inc. Petrographic Core Analysis Monitor Well No. 1
- Appendix 2-29 Location Sample Service, Inc. Petrographic Core Analysis Plant Well No. 2 Original Borehole (1979)
- Appendix 2-30 Omni Laboratories, Inc. Petrographic Study Final Report Plant Well No. 2 Sidetrack No. 1 (1996)
- Appendix 2-31 Omni Laboratories, Inc. Petrographic Study Final Report Plant Well No. 3 Sidetrack No. 1 (1999)
- Appendix 2-32 O'Malley Laboratories Inc. Core Analysis Plant Well No. 4 Original Borehole (1982)
- Appendix 2-33 Omni Laboratories, Inc. Petrographic Study Final Report Plant Well No. 4 Sidetrack No. 1 (1994)
- Appendix 2-34 Envirocorp Services and Technology, Inc. Core Analysis Report Plant Well No. 5 (1993)

2.0 GEOLOGY

This section contains an evaluation and review of the subsurface regional geology and local geology present at the Chemours DeLisle Mississippi Plant site and directly focuses on the suitability of the injection and containment formations.

2.1 INTRODUCTION

The siting of the injection wells at the Chemours DeLisle Plant meets all the requirements of 40 CFR 146.62. The injection formation is located approximately 7,000 feet beneath the lowermost aquifer that meets the criteria for being an underground source of drinking water (USDW) as defined in 40 CFR 144.3 (Figure 2-1). There are no withdrawals of drinking water from the lowermost USDW.

The wells are sited in an area that is geologically suitable. Suitability has been determined based upon:

- 1) an analysis of the region's structural and stratigraphic geology, hydrogeology, and seismicity;
- 2) an analysis of the geology and hydrogeology of the well site, including detailed information on the stratigraphy, structure and rock properties, aquifer hydrodynamics, and mineral resources; and,
- 3) an analysis of the ability to accurately describe the geology of the area based upon the availability of subsurface data, multiple core samples of the principal strata, and the availability of accurate models to predict waste fate and transport.

The massive sandstones of the Washita-Fredericksburg provide an effective injection unit in terms of lateral extent, mineralogical composition, and petrophysical characteristics. The Washita-Fredericksburg Injection Interval has adequate permeability, porosity, thickness, and area extent to allow injection of the waste volume generated by the facility. This conclusion is based on 37 years of experience injecting into this interval.

The Containment Interval includes the overlying shales of the uppermost Washita-Fredericksburg, Tuscaloosa, Eutaw, and the chinks and shales of the Selma Chalk (Figure 2-1). The Containment Interval is laterally extensive and possess attributes required for the effective and direct confinement of injected waste fluids. The Containment Interval overlies the Washita-Fredericksburg Injection Interval and is contained with the Injection Zone. The shales of the Selma/Midway Confining Zone are laterally continuous and free of transecting, transmissive faults or fractures over an area sufficient to prevent the movement of fluids into a USDW. The Confining Zone overlies the Injection Zone and contains more than one formation of sufficient thickness with lithologic and stress characteristics capable of preventing vertical propagation of fractures. Figure 2-2 presents a “type log” containing subsurface formation depths and thicknesses. This type log is a well log that was selected as being representative of the of the subsurface at the Chemours DeLisle Plant site.

In addition, the Confining Zone (top of the Midway Shale at approximately 6,100 feet below ground level (referenced as “BGL” in the remainder of the document)) is separated from the base of the lowermost USDW (at approximately 2,750 feet BGL) by many sequences of permeable and less permeable strata. These strata will provide added layers of protection for the USDW in the event of fluid movement up an unlocated borehole or transmissive fault. A simplified version of Figure 2-2, the “type log”, is presented as Figure 2-3. The net effect of interbedded layers is the retardation of any potential upward fluid movement to such an extent that it would never reach the USDW, but rather exit laterally into one of the numerous buffer saline aquifers.

The geologic structure, stratigraphy, hydrogeology, and seismicity of the region support the Chemours DeLisle Plant site as an acceptable location for injection operations. There are no known usable subsurface mineral resources in the Washita-Fredericksburg within the immediate area. The geology of the area is described within this section. Geological data was used to establish accurate inputs for a Sandia Waste Isolation Flow and Transport (SWIFT) numerical model to predict injection interval pressurization, lateral waste transport, and waste containment within the Injection Zone.

2.2 Regional Geology

2.2.1 Historical Regional Geology

The earliest record of sedimentation in the Gulf of Mexico Basin occurred during the Late Triassic to Early Jurassic when initial phases of tensional rifting resulted in the deposition of non-marine red beds and deltaic sandstones, conglomerates, siltstones, and shales of the Eagle Mills Formation (Figure 2-4). During the Middle Jurassic, these sediments were overlain by a thick succession of anhydrite and salt beds (Werner Anhydrite and Louann Salt). As much as 13,000 feet of Louann Salt accumulated in the major sub-basins of the Gulf Coast. In the eastern Gulf, regressive sandstones of the Norphlet Formation subsequently covered the thick evaporate section. Area well logs show that the Norphlet Sand in the state of Mississippi can exceed 1,000 feet in thickness. The early Late Jurassic was a period of shallow warm seas, resulting in the deposition of the Smackover carbonates. It was also at this time that the ancestral Mississippi River drainage system first established itself as a dominant factor in the basin.

The Late Jurassic period concluded with the deposition of a succession of shallow-water clastics and interbedded carbonates; also by this time, the Gulf had completed its spreading and achieved full connection to the Atlantic (Salvador, 1987). Jurassic non-skeletal carbonate sands and mud accumulated on a ramp-type shelf, while reefal buildups developed on subtle topographic highs (Baria et al., 1982). A highly terrigenous clastic influx in eastern Louisiana, Mississippi, and the Florida panhandle deposited the Haynesville Formation, which diminishes and grades westward into the Gilmer Limestone in East Texas. The Haynesville Formation is overlain by the Cotton Valley Group of Late Jurassic - Early Cretaceous age. The Cotton Valley Group is prevalent throughout the Gulf Coast and contains the Knowles Limestone, which is a widely recognized regional marker bed. During the balance of the Early Cretaceous, a period of shelf stability and decreased terrigenous sediment influx allowed for the development of extensive sandy carbonates and carbonates. Early Cretaceous geologic units include the Sligo, Pine Island, Rodessa, and Mooringsport formations of the Trinity Group. Terrigenous influx increased again toward the end of the Early Cretaceous, resulting in the deposition of the Paluxy Formation and the Fredericksburg and Washita groups.

Following a prominent hiatus in deposition, known as the Middle Cretaceous Unconformity, increasing tectonism in the western United States and northern Mexico accelerated the influx of clastic sediments to the Gulf of Mexico basin. The resulting Tuscaloosa Massive Sand of the

Eastern Gulf (time-equivalent to the Woodbine sands of east Texas) effectively shut off the production of carbonates except in the distal regions of the Florida platform. As the rate of terrigenous influx exceeded the rate of basin subsidence, significant progradation of sediments occurred on the continental shelf (Figure 2-5).

The geometry of Cenozoic deposition in the Gulf Coast Basin was primarily controlled by the interaction of the following factors:

- 1) Changes in the rate of sediment input and the shifting location(s) of maximum sedimentation,
- 2) Changes in the relative position of sea level, resulting in the development of a series of widespread depositional cycles throughout Cenozoic time,
- 3) Diapiric intrusion of salt and shale in response to sediment loading, and
- 4) Flexures and growth faults due to sediment loading and gravitational instability.

Early Tertiary sediments are thickest in the Rio Grande Embayment of south Texas, reflecting the role of the ancestral Rio Grande River and Nueces River as sediment sources to the Gulf of Mexico. By Oligocene time, deposition rates increased to the northeast, suggesting the ancestral Colorado, Brazos, Sabine, and Mississippi rivers were gaining in importance. The Miocene was marked by an abrupt decrease in the amount of sediment entering the Rio Grande Embayment, with a coincident increase in the rate of sediment supply in southeast Texas, Louisiana, and Mississippi. Throughout the Pliocene and Pleistocene, maximum depocenters of sedimentation were controlled by the Mississippi River and were located offshore of Louisiana and Texas.

2.2.2 Regional Surface Geology

The regional surface geology of Mississippi is depicted in Figure 2-6. Regional structure and isopach maps, prepared for this permit renewal, are listed below, with their corresponding appendix number. The mapped area extends approximately 26 miles in an east-west direction and 30 miles in a north-south direction. These maps are presented herein on a Tobin digital oil and gas base map (Appendix 2-1). Geostock Sandia, LLC, prepared current updates and revisions to the maps. Electric log data and correlation data from offset petroleum exploration wells that penetrate the injection/confining zones and the site injection wells are annotated on the base, isopach and structure maps. Table 2-1 presents an Index of Geologic Maps that are referenced within this section.

An index base map showing the location of two regional cross-sections is included in Appendix 2-2. The two regional cross-sections oriented approximately north-south and west-east are included as Appendices 2-3 and 2-4. The north-south cross-section A-A' (Appendix 2-3) illustrates the southerly regional dip, while the west-east cross-section B-B' (Appendix 2-4) illustrates the strike of the strata and the structuring onto Waveland Field west of the plant. The Confining Zone, Injection Zone, and Injection Interval are labeled on both geologic cross-sections (Appendices 2-3 and 2-4).

2.2.3 Structure

The Chemours DeLisle Plant is located within the Mississippi Embayment of the Central Gulf Coast Basin, approximately midway between the Mississippi Salt Dome Basin and the South Louisiana Salt Dome Basin (Figure 2-7). The area is structurally stable and unfaulted. Regional dip is to the south-southwest (Figure 2-8). Here, the Late Cretaceous clastic section and major Tertiary progradational wedges were less affected by growth faulting than the equivalent downdip expanded sedimentary sections located offshore beyond the Cretaceous shelf edge.

Structure maps of all of the formations illustrate regional southerly dip (Appendices 2-5 through 2-11). Formation dip rates for the region and the plant site are summarized in Table 2-2.

Isopach maps of the deeper formations indicate the following thicknesses for the regional area, with the following values for Washita-Fredericksburg Sand net sand thickness (Appendices 2-12–2-18). Table 2-3 summarizes the thicknesses of formations below the top of the Confining Zone at the Chemours DeLisle Plant site.

2.2.3.1 Faulting

There are no known or suspected faults near the DeLisle Plant. The closest identified fault is located in Ansley Field, approximately 16 miles southwest of the plant site (DuPont, 1974). Subsurface well control indicates that this fault has limited lateral extent and a throw of less than 100 feet. The Baton Rouge fault system is a major regional tectonic feature that marks the Cretaceous shelf margin. At its closest point, the Baton Rouge fault system is located 25 miles south of the plant site (DuPont, 1974). This fault system strikes east-west and trends along the north edge of Lake Pontchartrain, Louisiana, eastward through the Chandeleur Sound into the Gulf of Mexico (Figure 2-7).

Evaluation of geophysical well logs, geologic structure maps, and cross-sections from the surrounding area provides substantial evidence that no faulting exists near the plant site. Furthermore, gravity data indicate that no salt diapirs occur in the area between the Mississippi Salt Dome Basin (Figure 2-8) and the South Louisiana Salt Dome Basin (DuPont, 1974).

2.2.4 Data Documenting Lack of Faulting

Additional evidence for the absence of faulting is offered by evaluation of a north-south seismic line shot by Union Oil. Union Oil Line 627-2 is a north-south line that passes through the DeLisle Plant and is located immediately west of the injection field (Appendix 2-19). This data must be considered **BUSINESS CONFIDENTIAL**, and is to be stored under **LOCK AND KEY**. This seismic line should be viewed only by individuals on a need-to-know basis as cleared through Chemours. The license agreement also prohibits unauthorized reproduction of the seismic line as per terms of the license.

The interpreted/annotated version of Union Oil seismic line 672-2 shows the location of Plant Well No. 4, along with the approximate tops of the Confining Zone, Injection Zone, and Injection Interval. The inset location map orients Seismic Line 672-2 as a north-south transect near the western boundary of the Chemours DeLisle Plant and Well No. 4. Included with this display are a Time-Depth Curve and a Synthetic Seismogram Section (Appendix 2-20: this appendix is also **BUSINESS CONFIDENTIAL**) that are constructed from the sonic/acoustic log of Well No. 4. These data were used to identify the time-depths of both formation tops and regulatory units on Seismic Line 672-2.

Along the entire seven-mile length of Seismic Line 627-2 lateral continuity is clearly indicated for all strata from the top of the Confining Zone through the Injection Zone, indicating no evidence of faulting in the area.

In summary, the subsurface geologic data gives no indication that transmissive faults or fractures are present within the defined Injection Zone; and that lateral continuity of the Injection and Confining Zones exists. As there is a thick confining interval isolating the Injection Zone from the base of the lowermost USDW and no known breached formations exist.

2.2.5 Seismicity

Evaluations have been performed to determine the possible effects of natural and induced seismic events on (1) the integrity of well construction materials; and, (2) the integrity of both the Injection and Confining Zones beneath the DeLisle Plant. A review of “The National Earthquake Information Center” (<http://earthquake.usgs.gov/contactus/golden/neic.php>) indicates that the DeLisle area has a low potential for seismic activity (see Figure 2-9, and Appendices 2-21 through 2-27). David J. Leeds, a certified geophysicist and engineering geologist, conducted a regional evaluation for the site (Appendix 2-21). Leeds (1989) identified seismogenic sources, modeled a “design earthquake,” and discussed the effects of the “design” earthquake on the Injection and Confining Zones.

In an additional study performed by DuPont, the probability of induced seismicity was evaluated using the very conservative “zero-cohesion Mohr-Coulomb failure criterion” recommended by the U.S. Geological Survey (Wesson and Nicholson, 1987). This study is discussed below (Section 2.2.3.2, Induced Seismicity).

The natural seismicity by the Leads’ study and the DuPont “zero-cohesion Mohr-Coulomb failure criterion” study of the potential to cause induced seismicity, both indicate that seismicity is not a significant issue at the DeLisle site.

2.2.5.1 Natural Seismicity

Seismically, the Gulf Coastal Plain is one of the least active regions of North America (Figure 2-9). This area of Mississippi and adjacent states has either a zero rating or the very lowest rating for seismicity. The regional epicenter map (Appendix 2-22) shows all regional seismic events (events plotted) in the National Geophysical Data Center files as of 2017. A more detailed version shows historically recorded earthquakes in the Gulf Coast region from 1790 to present (Appendix 2-23). The oldest earthquake plotted was an event in western Florida during 1780, which exhibited an Intensity VI (Table 2-4, Modified Mercalli Intensity Scale) and was located approximately 125 miles east of the DeLisle Plant. Destructive earthquake ground motion has not been experienced in the DeLisle area in 200+ years of recorded earthquakes (Leeds, 1989).

Natural seismicity in the Gulf Coastal Plain is attributed primarily to flexure of sediments along hinge-lines that parallel the coast. This flexure is due to compression and down warping of the immature Gulf of Mexico basin sediments in response to extreme sediment loading. Structural

features such as salt domes and growth faults, although capable of storing and releasing some seismic energy, are weak and ineffective in generating even modest ground motion.

Salt domes are the result of plastic flowage of salt that pierces or ruptures adjacent sedimentary layers, or causes doming in the overlying sedimentary layers. These sediments have low density, poor cementation, and low shear strength which results in a low shear moduli. It is doubtful that a salt dome could develop earthquakes with a magnitude greater than 3.0 on the Richter Scale. Small earthquakes may be felt locally but are unlikely to propagate damaging ground motions. As indicated in Section 2.2.1.1, the DeLisle Plant is not located near any salt diapirs as the plant is situated between the Mississippi Salt Dome Basin (Figure 2-10) and the South Louisiana Salt Dome Basin (DuPont, 1974).

Growth faults may be responsible for some seismic activity, *i.e.*, several low magnitude events within about 50 miles of the coast. A 1983 event at Lake Charles was from a depth of 14+ km and had a Mercalli magnitude of approximately IV (dishes rattling). This depth is located well below injection depths beneath the DeLisle Plant. Even more distant seismic regions (*e.g.*, New Madrid Zone in southeastern Missouri) have not developed events great enough to cause damage at the DeLisle Plant (Leeds, 1989).

By using data from the largest historic event of the province and modeling a “design earthquake”, the hypothetical modeling results show an event with little damage to engineered structures or facilities. Ground motion due to seismic activity is attenuated with depth. Thus, no damage to the well systems would be anticipated. The few historical seismic events in the Gulf Coast area indicate that there is little chance of an event occurring in the vicinity of DeLisle Plant (Leeds, 1989).

2.2.5.2 Induced Seismicity

Documented fluid-injection induced earthquakes are quite rare, and are probably caused by increased pore pressure from injection operations that reduce frictional resistance to failure. This mechanism has been successful in explaining the best known case of injection-induced seismicity which occurred at Rocky Mountain Arsenal near Denver, Colorado (Wesson and Nicholson, 1987). Injection at Rocky Mountain Arsenal was directly emplaced into relatively impermeable crystalline basement rocks with hydrologic properties that were unfavorable to injection operations.

Gulf Coast reservoirs that are characterized by high transmissibility and storativity are capable of receiving fluid at low injection pressures and are not likely to be the site of an induced earthquake (Wesson and Nicholson, 1987). Injection at DeLisle Plant meets these conditions, because injection occurs into deep, incompetent (relatively soft, high porosity, moderate to high permeability) formations over a broad area not subject to natural earthquakes. In addition, each injection well is operated at comparatively low injection pressures.

The probability of the waste injection process inducing an earthquake is extremely remote in the Gulf Coast area. Geology and regional tectonic conditions do not provide the high stress accumulation required for earthquake generation; therefore, there is no apparent risk of inducing seismic events from subsurface waste disposal at the DeLisle Plant.

The potential for induced seismicity at the Chemours DeLisle Plant can be evaluated using the very conservative "zero-cohesion Mohr-Coulomb failure criterion," recommended by the U.S. Geological Survey (Wesson and Nicholson, 1987). This method is based on the following equation:

$$P_{crit} = \frac{S_v (3\alpha - 1)}{2} \quad (1)$$

where,

P_{crit} = the critical injection zone fluid pressure required to initiate slippage along faults and fractures;

S_v = the total overburden stress gradient that represents the maximum principal stress in the Gulf Coast region; and

α = the ratio of the minimum principal stress (horizontal in the Gulf Coast region) to the maximum principal stress (overburden stress).

Equation 1 contains a number of conservative assumptions that produce a "worst-case" lower value for the critical fluid pressure that would induce seismicity by:

- Neglecting the cohesive strength of the sediments;
- Assuming that a fault or fracture is oriented at the worst possible angle; and
- Assuming a worst-case value of 0.6 for the coefficient of friction of the rock (Wesson and Nicholson, 1987).

For this evaluation, Equation 1 can be expressed in a more convenient form by introducing the matrix stress ratio K_i (Matthews and Kelly, 1967; Eaton, 1969), defined as the ratio of the minimum to the maximum "effective" principal stresses. Effective principal stress is equal to actual principal stress minus fluid pore pressure p_o . Thus,

$$K_i = \left(\frac{\alpha S_v - p_o}{S_v - p_o} \right) \quad (2)$$

Substituting Equation 2 into Equation 1 and performing algebraic manipulations results in Equation 3, which is used to evaluate induced seismicity at the Chemours DeLisle Plant:

$$\Delta P_{crit} = \left(\frac{3K_i - 1}{2} \right) (S_v - p_o) \quad (3)$$

Where,

ΔP_{crit} is the critical injection zone pressure buildup required to induce seismicity, with:

$$P_{crit} = p_o + \Delta P_{crit} \quad (4)$$

Section 3.0 - Reservoir Modeling indicates that, at all injection depths, the initial pore pressure (p_o) is less than 0.47 psi per foot of depth. Eaton (1969) provides a plot of the effective overburden stress (S_v) as a function of depth for locations along the Gulf Coast. According to this plot, at depths greater than 3,000 feet, (S_v) exceeds 0.88 psi per foot of depth. Matthews and Kelly (1967) provides a plot of the matrix stress ratio (K_i) for tectonically relaxed sediments along the Texas Gulf Coast. This plot indicates that, at all depths greater than 3,000 feet, K_i exceeds a value of

0.54. Substituting these values for p_o , S_v , and K_i into Equation 3, it is found that, at DeLisle, P_{crit} is greater than .125 psi per foot of depth, or, 125 psi per 1,000 feet of depth.

The calculated injection interval pressure increases at the DeLisle Plant as derived from historical modeling performed in the reservoir mechanics section of the permit application are presented in Table 2-5 and indicates that induced seismicity is unlikely to be a problem at the Chemours DeLisle site.

2.2.6 Stratigraphy

The following sections describe those formations penetrated by the DeLisle Plant injection wells and Monitor Well No. 1. Formations below the maximum depth of the injection wells are not described because they have no bearing on injection operations. The formations penetrated by the injection wells are described in ascending order beginning with the Washita-Fredericksburg Group, which contains the sandstone unit presently receiving injected waste (Figures 2-1 and 2-4).

A more detailed description of the Injection Zone beneath the plant can be found in Section 2.3.3 of this permit application.

2.2.6.1 Washita-Fredericksburg Group

Contemporaneous with uplift and erosion in southern Arkansas and northern Louisiana, Washita-Fredericksburg sands and shale were deposited basinward. Sub-regionally, the basin was enhanced as a result of salt withdrawal and a tectonic adjustment to the uplift. The basin became stranded behind the residual high formed by the stacking of Jurassic and Early Cretaceous shelf edges. As mixed fluvial-deltaic sands and shales entered the basin along the strandline, some sediment was redistributed farther offshore on the shallow marine platform. Following a significant unconformity of Middle Cretaceous age, clastic deposition resumed during the early Late Cretaceous with the deposition of the Tuscaloosa Massive Sand (Chasteen, 1983).

2.2.6.2 Tuscaloosa Formation

In southern Mississippi, the basal Late Cretaceous Tuscaloosa Formation overlies the Washita-Fredericksburg group. In southwest Mississippi and southeast Louisiana, the lower Tuscaloosa

Formation is divided into a non-marine facies and an overlying marine facies (Berg and Cook, 1968; Chasteen, 1983; Hearne and Lock, 1985; and, Stancliffe and Adams, 1986; Shirley, 1987). The non-marine facies is the Tuscaloosa Massive Sand, which is composed of a basal braided stream deposit and a meander belt point-bar complex.

The Tuscaloosa Massive Sand is composed of stacked massive sandstones with few well-defined shale breaks. Chert-conglomerate is commonly present at the base of the stacked channel sand (Chasteen, 1983). The Tuscaloosa Massive Sand sediments are structureless, well-sorted, micaceous, locally fossiliferous (marine bivalves), calcareous, glauconitic, fine-grained, and quartz rich. All of these characteristics are indicative of a more marginal marine (more downdip equivalent) environment of deposition than the lower Tuscaloosa section in southwestern Mississippi and eastern Louisiana (Mancini et al., 1987). The stacking of channel sandstones with basal conglomerates is typical of a braided-stream environment. Regional isopach maps of the braided-stream unit show a sheet-like geometry with thick sand areas corresponding to persistent drainage patterns where major streams existed (Chasteen, 1983). Overlying the braided-stream deposits are meander belt point bar and associated facies deposits.

The overlying marine unit is composed of sandstones interbedded with siltstones and shales that exhibit intense bioturbation. This intense bioturbation suggests deposition in shallow water, brackish to marine environment. In addition, cores and sample logs commonly record the presence of oysters as solitary and bedded forms in the shales, which would support a shallow-water marine origin for the unit (Chasteen, 1983). Sandstones in the marine interval of the Lower Tuscaloosa Formation are generally thin, exhibit a lenticular nature, and are commonly intensely bioturbated (Chasteen, 1983).

Continued transgression caused by a major global rise in sea level during the early Late Cretaceous inundated the marginal marine Tuscaloosa sequence, leading to the deposition of middle marine shales of the Middle and Upper Tuscaloosa (Vail et al., 1977; Stancliffe and Adams, 1986). Microfauna analysis of samples from Liberty Field in Amite County, Mississippi, show a vertical change from a fauna dominated by the agglutinated species *Ammobaculites* and *Trochammina* to one characterized by the calcareous species *Heterohelix* and *Lenticulina* (Stancliffe and Adams, 1986). This faunal succession suggests a transition from restricted marine to open marine neritic conditions for Middle and Upper Tuscaloosa shales (Stancliffe and Adams, 1986). The marine Tuscaloosa shales along the basin contain a diverse assemblage of macrofossils, including ammonites, gastropods, inoceramids, other bivalves, and a rich assemblage of planktonic

foraminifera and calcareous nannofossils typical of Cretaceous open-shelf environments (Mancini et al., 1987). Fluvial deposition was confined to extreme updip positions in the northern Gulf of Mexico Basin (Chasteen, 1983).

2.2.6.3 Eutaw Formation

The Eutaw Formation conformably overlies the Upper Tuscaloosa Shale Formation. The Eutaw Formation and overlying Selma Chalk deposits represent marine shelf deposition and a continuation of the Late Cretaceous global sea-level rise. The Eutaw Formation consists mainly of fossiliferous, calcareous claystone grading to micaceous, calcareous, glauconitic, fine-grained sandstone near the updip marine margin (Mancini et al., 1987).

2.2.6.4 Selma Formation

The Late Cretaceous global rise in sea level reached its maximum extent soon after the end of Eutaw deposition. Much of the Gulf Coast (including most of Mississippi) was inundated and remained below sea level through the end of Cretaceous time. The Selma Formation was deposited in a relatively shallow epicontinental sea and consists of chalk, marl, shale, and minor beds of sandstones. In west-central Mississippi, reefal limestone was deposited on uplifted shallow platforms that formed in response to igneous intrusions. The Late Cretaceous sea remained relatively shallow throughout deposition of the Selma Formation, with sedimentation and subsidence in near equilibrium.

2.2.6.5 Midway Group

The Paleocene Midway Group sediments were deposited during the first major Tertiary regressive cycle. Conformably overlying marine Cretaceous sediments is the Clayton Formation. The faunal succession across the Upper Cretaceous/Tertiary boundary shows a sharp break in both macro-fauna and micro-fauna types, making it possible to accurately determine the base of the Tertiary in the Gulf Coast Basin (Rainwater, 1964a). At the beginning of the Tertiary, an epicontinental sea still covered most of the Mississippi Embayment, with the Clayton Formation being deposited in an open marine environment. The unit is generally less than 50 feet thick and is composed of thin marls, marly chalk, or calcareous clays (Rainwater, 1964a).

As the epicontinental sea became partially restricted in the Mississippi Embayment, the Porters Creek clay was deposited on the Clayton marl. Fossil evidence, although scarce, indicates a lagoonal to restricted marine environment for the Porters Creek Formation (Rainwater, 1964b). The Porters Creek Formation is composed mainly of massively bedded montmorillonitic clay. In southeastern Mississippi, both the Clayton and Porters Creek Formations are absent.

Open marine circulation was re-established in the Mississippi Embayment during the deposition of the shallow marine Matthews Landing Formation. The Matthews Landing Formation was deposited above the Porters Creek clay in a shallow marine environment, and is composed primarily of fossiliferous, glauconitic shales with minor sandstone beds (Rainwater, 1964a).

A major regression marks the deposition of the late Paleocene Naheola Formation that overlies the Matthews Landing Formation. Uplift in the sediment source areas of the Rocky Mountains, Plains, and Appalachian regions supplied an abundance of coarse-grained fluvial sediments for the first time in the Tertiary. Sedimentation rates along the Gulf Coast exceeded subsidence rates and produced the first major regressive cycle in the Tertiary. Alluvial environments dominated throughout most of Naheola time. The Naheola Formation consists of alternating sand, silt, and shale, with lignite interbeds near the top of the unit (Rainwater, 1964a).

2.2.6.6 Wilcox Group

The lower Eocene Wilcox Group is a thick clastic succession that flanks the margin of the Gulf Coast Basin. The Wilcox Group is divided into the Nanafalia, Tusahoma, Bashi, and Hatchetigbee Formations in Mississippi. The Wilcox Group is characterized by the deposition of regressive lobate and bird-foot delta complexes along the Gulf Coast, with major fluvial axes closely corresponding to present-day river patterns (Fisher and McGowen, 1967; Galloway, 1968). Beach barrier and strand plain facies were deposited between delta lobes (Self et al., 1986). The Holly Springs Delta System of the Nanafalia Formation comprises most of the lower part of the Wilcox Group in the north-central Gulf Coast Basin. The broad apex of the Holly Springs delta system was centered along the axis of the Mississippi River trough. Deposits of prodelta facies of the restricted shelf system occur basinward of the prograding delta lobes and consist of thick sequences of lignitic, micaceous, and gray mud. The top of the Lower Wilcox is marked by regionally transgressive shale, historically called the “Big Shale” in Louisiana and Mississippi (Rainwater, 1964a; Galloway, 1968).

The Tuscahoma Formation (middle Wilcox) is composed of non-marine sands and shales similar to those of the Paleocene Naheola and the early Hatchetigbee formations. The Tuscahoma Formation is regressive, thereby indicating sedimentation rates greater than either subsidence or eustatic sea level rise.

Although less well studied, the upper Wilcox Group is generally considered to be transgressive with locally regressive delta lobes deposited during a global rise in sea level. An increase in the carbonate content and glauconite content in upper Wilcox sediments suggests an increase in marine conditions compared to lower Wilcox. An examination of Wilcox hydrocarbon producing trends in Louisiana and Mississippi led Paulson (1972) to conclude that the Wilcox is a transgressive sequence. During deposition of Bashi sediments, the transgressive sea extended as far north as central Alabama and Mississippi (Rainwater, 1964a). Deposition of the Wilcox ended with the regressive Hatchetigbee Formation, which is lithologically similar to other non-marine sections of the early Tertiary. The sediments of the Hatchetigbee Formation were deposited primarily in coastal plain environments with deltaic deposition occurring along the marine margin (Rainwater, 1964a).

2.2.6.7 Claiborne/Jackson Group

The Claiborne Group in Mississippi is composed of two transgressive marine sequences (Tallahatta-Winona formations and the Cook Mountain Formation) and two regressive sequences (Zilpha-Sparta and Cockfield formations). Along the coastal area, a thin limestone was also deposited on the shelf under shallow open sea conditions. Small restricted basins were present when the siliceous Tallahatta claystone was deposited. The overlying Winona and Cook Mountain limestone and marls were deposited primarily in shallow neritic environments. The overlying regressive sequences of the Claiborne Group were deposited in alluvial and marginal marine environments. The slow subsidence rate in southern Mississippi during the regressive cycle limited the amount of sediment carried by local streams. Consequently, deltas which were built at the time are generally small.

Immediately overlying the Claiborne Group are transgressive marine deposits of the Jackson Group (Yazoo Clay). At the beginning of the early Eocene, the marine shoreline transgressed rapidly over the low-lying coastal plain and covered southern and western Mississippi. In the Mississippi Salt Dome Basin, where over 500 feet of shale was deposited, subsidence was much greater than on the carbonate shelf to the south where less than 100 feet of limestone was deposited.

By the end of middle Eocene time, the shoreline had transgressed to a position similar to present day.

2.2.6.8 Vicksburg Group

The early Oligocene Vicksburg Group of the Central Gulf Coast Basin is represented by clastic deposits in western Mississippi, carbonate deposits in northern Florida, and interfingering of both units across eastern Mississippi and Alabama (Waters and Mancini, 1982). The complexity of the lithofacies changes in this region has caused problems in establishing geologic ages and correlating formations (Hazel et al., 1980; Bybell, 1982; Waters and Mancini, 1982). The Vicksburg Group is divided into the Red Bluff Formation, Marianna Formation, Glendon Formation, Byram Formation, and Bucatunna Formation. Sediments of the Vicksburg Group were deposited in marginal marine environments, with clastic sediments grading into carbonate sediments across the basin. The terrigenous clastic deposits were sourced from older coastal plain sediments and Appalachian terrains.

2.2.6.8.1 Chickasawhay Formation

The late Oligocene of the Gulf Coast Basin was characterized by a broad regional transgressive event that deposited the Chickasawhay Limestone in Mississippi and Alabama. During the late Oligocene, the carbonate province expanded farther to the west than at any other time during the Tertiary (Rainwater, 1968). To the west, the Chickasawhay Limestone grades into its clastic equivalent, the Anahuac shale of Louisiana and Texas. The Chickasawhay Limestone was deposited in shallow to neritic environments and consists of bluish-gray glauconitic marl and beds of white limestone (Copeland, 1968).

2.2.6.9 Undifferentiated Sand and Shales

2.2.6.9.1 Fleming Group

The Miocene-aged Fleming Group of the Central Gulf Coast was deposited mainly under regressive conditions following the final Oligocene Chickasawhay transgression. The Fleming Group in Mississippi is divided in ascending order into the Catahoula Formation, the Hattiesburg Formation, and the Pascagoula Formation. Terrigenous clastics of the Miocene section were

derived from the Eocene and Cretaceous terrane of the Mississippi Embayment as well as from the Appalachian terrane (Rainwater, 1964b).

The Catahoula Formation is characterized by gray and greenish-gray silty clays, and unconsolidated to indurated, fine- to coarse-grained alluvial sands. Farther basinward, a few limestone and marl beds are present (Rainwater, 1964b). The exposed Catahoula section is approximately 300 feet thick, and thickens into the subsurface to 1,000 feet thick near the Louisiana border. Most of the Miocene sediments of southern Mississippi are referred to as the Hattiesburg and Pascagoula formations. The marine shoreline was located south of the present-day Mississippi shoreline during most of the Miocene, although at least two major marine transgressions are recorded in the late Miocene section (Rainwater, 1964b).

2.2.6.9.2 Graham Ferry Formation

The Pliocene Graham Ferry Formation occurs above the Miocene Pascagoula Formation (Newcombe, 1975). Sediments of the Graham Ferry Formation are heterogeneous sands and shales common to deltaic facies deposits. Terrigenous and brackish water deposits predominate, although in its type locality the Graham Ferry contains numerous marine fossils (Brown et al., 1944).

2.2.6.9.3 Citronelle Formation

Disconformably overlying the Pliocene Graham Ferry Formation are terrace deposits of the Pliocene Citronelle Formation. The Citronelle Formation was deposited on broad coalescing flood plains that occupied a wide belt between the Mississippi River and the Atlantic coast. Heavy mineral spectra of the unit indicate an Appalachian metamorphic belt source area.

The Citronelle Formation ranges in thickness from a thin veneer to a maximum of 160 feet (Brown et al., 1944). The most common feature of the Citronelle Formation is the strongly oxidized brick-red sands that form ridge crests at the surface (Brown et al., 1944). Road cuts through the Citronelle Formation exhibit large-scale fluvial cross-beds in the coarse sands and gravels. Citronelle sediments are interpreted to be erosional remnants of distributary channel deposits (Brown et al., 1944).

2.2.6.10 Pleistocene and Holocene Deposits

Terrace and coastal deposits, loess, and Mississippi River Valley alluvium comprise the most recent sediments in the area.

2.2.7 Mineral Resources

Three oil and gas fields (Kiln, Ansley, and Waveland) are located in Hancock County, approximately 10 to 16 miles west-southwest of the plant site. Kiln Field (now abandoned) and Ansley Field have produced oil and gas from the Cuevas sand. The Cuevas sand is approximately 700 feet stratigraphically lower than the Washita-Fredericksburg sand that is used for injection at the DeLisle Plant site. Several hundred feet of non-permeable shale and limestone separate the Cuevas sand from the injection interval.

Waveland Field, located 16 miles southwest of the plant site, produces gas from the Mooringsport Formation at a depth of 13,500 feet, which is approximately 3,800 feet stratigraphically below the injection interval at the DeLisle Plant site. There is no evidence for any possibility of interconnection between these two sands.

The nearest oil and/or gas production from the Washita-Fredericksburg interval used for injection at the DeLisle Plant site is found at the Pistol Ridge Field, located 40 miles north of the DeLisle Plant. Because of the great distance involved, there is no possibility that waste disposal could have any effect on the Pistol Ridge or any other field (DuPont, 1974).

The E. I. du Pont de Nemours & Co., 1-Lester Earnest well (later designated as Monitor Well No. 1) was drilled in 1974 as a stratigraphic test well for purposes of identifying waste disposal and containment intervals. The well encountered no oil or gas deposits to a depth of 10,030 feet beneath the DeLisle Plant site. All porous rocks penetrated by the well contained either fresh or salt water. Analyses of electrical logs, cores, and drill stem test recoveries also proved that no oil or gas was encountered (DuPont, 1974). The absence of hydrocarbon deposits was again verified by the drilling of Injection Well No. 5 to the north of the other injection wells.

In addition, there are no other known mineral resources in the vicinity of the DeLisle Plant site (Figure 2-11). Quaternary coastal sand and silt deposits are exposed at the surface and contain no known or suspected commercial mineral deposits (DuPont, 1974).

2.3 LOCAL GEOLOGY

2.3.1 Injection Interval, Injection Zone, and Confining Zone Defined

The injection and confinement system present at the DeLisle Plant is composed of sediments that range in age from late Early Cretaceous to Paleocene. The Upper Washita-Fredericksburg Injection Interval sands are presented on Table 2-6.

Although Well Nos. 2, 3, 4, and 5 are not currently permitted to inject wastes into the Tuscaloosa Massive Sand, the interval is recognized as a back-up disposal interval. Authorization for any future use of the Tuscaloosa Massive Sand would require approval and a revised permit for Wells Nos. 2, 3, 4, and 5. (see Section 1.0 for the current permits).

The injection zone is defined as the sedimentary column within which all waste must be contained. The plant injection wells are permitted to inject waste at a depth below 8,800 feet BGL; therefore, the top of the Injection Zone beneath the DeLisle Plant is located at a depth of approximately 8,000 feet BGL to include the Containment Interval of the overlying shales of the uppermost Washita-Fredericksburg, Tuscaloosa, Eutaw, and the chinks and shales of the Selma Chalk. This depth falls within the Selma Chalk and is located approximately 185 feet above the base of the Selma Chalk and the top of the Eutaw Formation. The base of the Selma Chalk is located at 8,180 feet BGL. The base of the Injection Zone is assigned to the base of a sandstone interval of the upper Washita-Fredericksburg Group, at a depth of 10,100 feet BGL.

The Confining Zone beneath the plant consists of the Midway Group and Selma Formation and is approximately 1,865 feet thick in the plant site area (Figures 2-1 and 2-3). The top of the Midway occurs at a depth of approximately 6,140 feet BGL. Additional low permeability shale and limestone intervals and high permeability saline aquifer sands occur between the top of the Confining Zone and the base of the lowermost USDW, which is located at a depth of approximately 2,750 feet BGL (Figure 2-3). These saline aquifers effectively satisfy the regulatory requirements for a “buffer aquifer,” which provides an additional margin of safety for containment.

2.3.2 Structure

Structurally, the DeLisle Plant is located within the Mississippi Embayment, approximately midway between the Wiggins Anticline to the north and the south Louisiana Salt Dome Basin to the south (Figures 2-5, 2-7, 2-8 and 2-10). The Washita-Fredericksburg Injection Interval dips south from the Hancock County High across the plant site, then basinward toward the Gulf.

2.3.3 Stratigraphy of the Injection Zone

The petrography of the formations penetrated by Monitor Well No. 1 and the DeLisle Plant Wells is summarized in Table 2-7. Detailed petrographic analyses are contained in Appendices 2-28 through 2-34.

2.3.3.1 Washita-Fredericksburg

Injection of waste water at the DeLisle Plant occurs directly into sands of the Upper Washita-Fredericksburg Group (Figures 2-2 and 2-12). A net sand isopach map of the injection interval shows that the plant site is located along the north-south axis of a thick section of stacked fluvial-deltaic sands (Appendix 2-18). The net sand thickness of the injection interval sand ranges from 160 feet to 210 feet in the plant wells. Regional cross-sections show the broad lateral continuity of both the injection interval sands and the overlying containing shale units (Appendices 2-3 and 2-4). Whole core and sidewall core analyses (see Appendices 2-28 through 2-34 for copies of all core analyses) show an average porosity of 24 percent and a permeability of 554 millidarcies (md) (Johnson, 1974a) for the injection interval sand, indicating excellent reservoir properties.

The Washita-Fredericksburg section was conventionally cored for Monitor Well No. 1 (DuPont Lester Earnest No. 1) in 1974, Well No. 5 in 1993, Well No. 4 in 1995, Well No. 2 in 1996, and Well No. 4 in 1999. Petrographic examination and X-ray diffraction analyses were performed on selected samples from the cored section.

The mineralogy of the Washita-Fredericksburg sand was determined by X-ray diffraction tests on cores from Well Nos. 2 and 5. Results are summarized in Table 2-8 and 2-9, respectively.

2.3.3.1.1 Fracture Pressure Estimate for the Washita-Fredericksburg Injection Interval

The fracture gradient for the Washita-Fredericksburg injection interval sands can be estimated by the Eaton method, as described by Moore, 1974:

$$FG = \frac{P_{ob}-P_r}{1-e} + P_r \quad (5)$$

where:

FG = Fracture Gradient, psi/ft

P_{ob} = Overburden Gradient, 0.9412 psi/ft (Moore, 1974)

P_r = Original Reservoir Pressure Gradient, 0.4624 psi/foot

e = Poisson's Ratio, 0.4486 (Moore, 1974)

Following Eaton's Method, the calculated fracture gradient for the Washita-Fredericksburg is 0.852 psi/foot. At the reference pressure depth for the Washita-Fredericksburg Injection Interval (see Section 3.0), located at a below ground level depth of 9,850 feet, the estimated fracture pressure is calculated as:

$$9,850 \text{ feet} \times 0.852 \text{ psi/foot} = 8,391 \text{ psig}$$

2.3.3.2 Tuscaloosa Formation

Sands and shales of the Tuscaloosa Formation overlie the Washita-Fredericksburg section. The Tuscaloosa Massive Sand represent possible future backup waste injection intervals for the DeLisle Plant. Additionally, the thick Tuscaloosa shales serve as additional containment layers for the Washita-Fredericksburg injection sands. Tuscaloosa Massive Sand were conventionally cored during drilling of Monitor Well No. 1. The Lower Tuscaloosa section is composed of a basal non-marine section and an overlying marine section (Hearne and Lock, 1985). The marine

sands display horizontal, low-angle, inclined, and ripple-drift laminations, and contain up to 10 percent glauconite. The sand is moderately to well-sorted, fine- to very fine-grained, subrounded to rounded, and subarkosic (Hearne and Lock, 1985). The marine sandstones are interbedded with intensely burrowed, dark gray siltstones and black laminated shales. The majority of the sands in the non-marine section appear to be homogeneous and structureless, although traces of faint, low-angle and high-angle laminations, and ripple-drift laminations are visible (Hearne and Lock, 1985). These sands are moderately to well-sorted, rounded, medium to fine-grained, subarkosic, and interbedded with black laminated shales (rare), bioturbated shales, and dark burrowed siltstones (Hearne and Lock, 1985). The Lower Tuscaloosa Massive Sand section in Appendix 2-16 shows that the plant site is probably located on the margin of a fluvial-deltaic lobe. Net sand thickness of the Lower Tuscaloosa ranges from 270 feet to 335 feet at the plant.

Net sand thickness of the Tuscaloosa Massive Sand ranges from 240 feet to 285 feet at the plant (Appendix 2-17). Petrographic examination and partial X-ray diffraction clay studies were performed on the Tuscaloosa Massive Sand samples from Cores 9, 10 and 13 in Monitor Well No. 1.

2.3.3.2.1 Fracture Pressure Estimate for Tuscaloosa Massive Sand Injection Interval

The fracture gradient for the Tuscaloosa Massive Sand injection interval sands can be estimated by the Eaton method, as described by Moore, 1974:

$$FG = \frac{P_{ob}-P_r}{1-e} + P_r \quad (6)$$

where:

FG = Fracture Gradient, psi/ft

P_{ob} = Overburden Gradient, 0.9389 psi/ft (Moore, 1974)

P_r = Original Reservoir Pressure Gradient, 0.4624 psi/foot

e = Poisson's Ratio, 0.4460 (Moore, 1974)

Following Eaton's Method, the calculated fracture gradient for the Tuscaloosa Massive Sand is 0.846 psi/foot. At the reference pressure depth for the Tuscaloosa Massive Sand Injection Interval (see Section 3.0), located at a below ground level depth of 9,473 feet, the estimated fracture pressure is calculated as:

$$9,473 \text{ feet} \times 0.846 \text{ psi/foot} = 8,014 \text{ psig}$$

2.3.3.3 Eutaw Formation

The Eutaw Formation comprises the uppermost portion of the Injection Zone and provides additional containment to the injection interval. At the plant, the thickness of the Eutaw ranges from 200 feet to 240 feet (see Appendix 2-10).

2.3.3.4 Basal Selma Shale/Chalk

The basal section of the Selma Shale/Chalk forms the uppermost portion of the Injection Zone. Near the plant, this basal portion of the Selma Shale/Chalk within the Injection Zone is approximately 170 feet thick. Geophysical well log data show the chalk to be a tight, low porosity interval.

2.3.4 Stratigraphy of the Confining Zone

The Confining Zone consists of the upper portion of the Selma Chalk and the Midway Shale, forming a 1,870-foot thick secondary containment interval to the underlying Injection Zone.

2.3.4.1 Selma Shale/Chalk

The upper portion of the Selma Shale/Chalk forms the lower portion of the Confining Zone. In the vicinity of the plant site, the Selma Shale/Chalk is approximately 800 feet to 850 feet thick. Geophysical well log data show the chalk to be a tight, low porosity interval. A whole core from the middle of the chalk was taken in Well No. 5, within the Confining Zone. The test results described an average porosity of 8 percent and air permeability of 8.4×10^{-5} darcies, which demonstrates the lack of porosity and permeability development and shows the excellent confining capabilities of the Selma Shale/Chalk.

2.3.4.2 Midway Shale

The Midway Shale forms the upper portion of the confining zone. In the vicinity of the plant site, the Midway Shale is approximately 1,150 feet thick. Geophysical logs show the Midway is predominantly shale, with thin interbeds of sandstone. A whole core from the lower portion of the midway shale was taken in Well No. 5. The results described an average porosity of 16 percent, and air permeability is 2.45×10^{-3} darcys. Average brine permeability from four measurements from vertical plugs is 3.273×10^{-8} darcys. These test results of extremely low permeability demonstrate the excellent confining capabilities of the Midway Shale.

Table 2-9 contains a summary of the mineralogic data derived from the 10 whole cores sampled from Well No. 5. Properties such as porosity and permeability are listed in Table 2-10.

Collectively, the plant data show the excellent secondary confining capability of the confining zone strata. The extremely low permeability, thickness, and broad extent of the confining zone are more than adequate to provide containment, should the Injection Zone be breached.

2.4 GROUNDWATER HYDROLOGY

2.4.1 Regional Geology and Hydrology

The DeLisle Plant is located in the Gulf Coast geosyncline which has been slowly subsiding for millions of years due to the deposition of large quantities of sediments carried by streams and rivers to the Gulf of Mexico. The major axis of the Gulf Coast Geosyncline is approximately parallel to the coastline, resulting in an east-southeast strike of the strata. Dip of the beds is generally south and increases toward the Gulf due to basinward subsidence (Newcombe et al., 1968). Sedimentary units dip from 30 to 100 feet per mile, with the rate of dip being least near the surface (Newcombe, 1975).

Except for regional strike and dip, correlation of the near-surface strata over long distances is extremely difficult. The strata consist of irregular and locally lenticular sediments (Trmal, 1982). There are no thick, consistently traceable clay beds, and the thickness and extent of the sand beds are irregular. However, sub-regional “zones” in which sand is dominant can be identified and traced laterally (Newcombe et al., 1968).

The strata that contain aquifers are composed of estuarine and deltaic sediments which range in age from Miocene to Holocene. Formations of importance from the Fleming Group (Miocene) are the Catahoula, Hattiesburg, and Pascagoula Formations (Rainwater, 1964b); and the Graham Ferry Formation of Pliocene age (Newcombe, 1975). These formations represent a stratigraphic thickness of up to 5,000 feet (Brahana and Dalsin, 1977). The boundaries between the Miocene formations cannot be reliably identified or traced in the subsurface, and the Pliocene Graham Ferry Formation cannot be easily distinguished from the underlying Miocene units. As a result, all sediments between the Citronelle Formation (late Pliocene) and the Vicksburg Group (Oligocene) are commonly considered to comprise the “Miocene aquifer system” (Newcombe, 1975; Brahana and Dalsin, 1977). Figure 2-4 is a stratigraphic column of Mississippi, and Table 2-11 is a chart of shallow Mississippi aquifers and their hydrologic characteristics.

The sediments that contain freshwater are composed of clean quartz sand, ranging in grain size from very fine to very coarse (Newcombe et al., 1968). At any particular location, the amount of sand in the freshwater section may range from 10 to 70 percent (Newcombe, 1975). Bed thickness and grain size vary considerably within short distances. Clay beds occur irregularly throughout the freshwater section (Newcombe et al., 1968).

In Harrison County near the coast, freshwater aquifers occur as deep as 2,500 feet (Newcombe et al., 1968). The average thickness of the freshwater section in Mississippi is 1,500 feet. Freshwater sand intervals range in thickness from less than 10 feet to as much as 450 feet. In some locations there are up to 12 distinct aquifers, and in all areas there are at least three aquifers (Newcombe, 1975). Table 2-12 lists the depths of 8 freshwater aquifer sands present in the subsurface of Harrison County, Mississippi.

The Miocene aquifers occur under confined conditions except in areas where the strata crop out. The confining beds consist of clay or sandy clay. In southern Mississippi, water moves gulf ward from unconfined aquifers down gradient into confined aquifers. Little is known about the hydraulic interaction between the various sand layers (Brahana and Dalsin, 1977). Recharge to the Miocene aquifer system includes (1) precipitation directly on outcrops located of Harrison County, (2) inter-aquifer movement through the clay and silt beds that separate the sand units, and (3) infiltration from overlying surficial deposits (Citronelle and younger sediments). The deepest layers of the Miocene aquifer system contain some salty water, especially in southern Mississippi. Figures 2-13 and 2-14 show the configuration of the base and thickness of the Miocene aquifer

system, respectively. Figure 2-13 shows the configuration of the base of freshwater in the Miocene aquifer system.

Minor aquifers include the Citronelle Formation, which is composed of quartz sand, chert gravel, and lenses of clay. The aquifer is only partially saturated and is thus a water table aquifer (Gandl, 1982). Much of the Citronelle sediments have been removed by erosion (Brahana and Dalsin, 1977); as a result, water levels vary from place to place. The shallowest aquifers in southern Mississippi consist of sand and gravel terrace deposits. These are Pleistocene to Holocene in age and vary in lateral extent and in saturation thickness (Brahana and Dalsin, 1977). Figure 2-13 shows the outcrop of the Citronelle aquifers and overlying coastal deposits.

The quality of groundwater in southern Mississippi is good, and the water usually requires little or no treatment (Brahana and Dalsin, 1977). Because of the thickness, areal extent, and permeability of the Miocene aquifer system, it is the largest potential source of groundwater in Mississippi. Vast reservoirs of freshwater remain untapped in the deeper aquifers of the system, as only the upper few hundred feet have been developed (Newcombe, 1975). Miocene aquifers have a large water-transmitting capacity (hydraulic conductivity) (Brahana and Dalsin, 1977). The water is generally a soft, sodium bicarbonate type, and is generally uniform throughout the area (Newcombe, 1975). Table 2-13 provides chemical analyses of water from the important Miocene aquifers throughout the region, and Table 2-11 lists the hydrologic characteristics of the aquifers. Water from the Miocene system supplies small domestic wells, large municipal wells, and industrial wells (Gandl, 1982). Over the years, artesian pressure has been reduced in the Miocene aquifers as a result of withdrawals (Newcombe et al., 1968). Water levels are declining regionally at a rate of one to two feet per year, and at greater rates near centers of heavy pumping (Newcombe et al., 1968).

The Citronelle Formation is drained naturally by streams and springs, and therefore cannot be used for large industry or municipal demands. However, the Citronelle Formation does supply local small municipal and industrial users. The overlying alluvial and terrace deposits are used for domestic and stock supplies (Brahana and Dalsin, 1977).

2.4.2 Local Hydrology

Sediments in St. Louis Bay consist of sandy silts, sandy muds, and sand. Holocene sediments are 10 to 20 feet thick in the plant vicinity (Otvos, 1982). Water from the near-surface is not utilized

at the DeLisle Plant due to the abundance of freshwater in the deeper aquifers discussed above. Freshwater (equal to or less than 1,000 parts per million total dissolved solids) occurs to a depth of approximately 2,300 feet in the immediate plant area (Trmal, 1982). Table 2-14 summarizes the representative depth, thickness, and total dissolved solids (TDS) of the six main Miocene aquifer layers at the plant site. The depth to strata that contains water with 10,000 mg/L TDS or less is approximately 2,750 feet below land surface at the plant site (Clark, 1986).

The base of the lowermost USDW (<10,000 mg/l TDS), determined by detailed log analysis of the Gulf Coast injection sites, has a formation resistivity (R_f) of 2.0 ohm-m on the long-spaced resistivity tool. The three most productive freshwater sand layers beneath the plant site are Miocene in age and occur at depths of 640 to 980 feet, 1,640 to 1,790 feet, and 1,870 to 1,990 feet (Table 2-14). Water production wells for both domestic and municipal supplies in the local area are developed in the uppermost sand layer (640 to 980 feet). A list of water wells has been compiled for an area within 2.0 miles of DeLisle Plant and a map showing their locations are presented in Figure 2-15.

Four water production wells used at the DeLisle Plant are developed in the aquifer that occurs at a depth of 1,640 to 1,790 feet. This zone was chosen because (1) it is virtually undeveloped, (2) the water supply is of high quality and has a high specific capacity, and (3) because use of the water does not affect the shallower zone used for domestic and municipal supplies (Barlow, 1974; Trmal, 1982). Tables 2-15 and 2-16 contain the results of analyses performed on recovery of samples taken from the completed aquifer from the site and surrounding area water production water wells.

The site's water production wells have high capacities which range from 1,400 to 2,400 gpm/well, and are the deepest freshwater supply wells in the area. The site's production wells also serve as groundwater monitoring wells, allowing for continuous ambient monitoring of the USDW water intervals, Injection Interval, and Confining Zone.

Table 2-17 contains the results of a laboratory analysis of formation fluid from the Tuscaloosa Massive Sand as performed on a sample of fluid obtained from the Plant Well No. 5 during drilling and completion of the well.

Table 2-7 provides a summary of core sample results used to establish porosity, permeability and thickness of the Washita-Fredericksburg injection sand.

Table 2-18 shows additional sample results to characterize reservoir formation fluids in the Tuscaloosa Massive Sand Massive and Washita-Fredericksburg injection sands.

2.4.3 Chemours Monitoring Program

The current groundwater monitoring plan was developed in 1986, as required by the Mississippi Underground Injection Control Permit, to monitor the freshwater aquifers above the injection well disposal zone. The monitoring plan requires taking samples from two on-site monitoring wells once per calendar quarter, and taking samples from six off-site community water supply wells once per calendar year. Samples of water from all monitoring wells are analyzed for the following parameters: pH, total iron, total dissolved solids, temperature, chlorides, conductivity, total iron, total chromium, total vanadium, total mercury, total cadmium and total lead. Table 2-15 shows the analytical results of the samples for calendar 2013, 2014, and 2015. There is no evidence of contamination by the “signature” parameters that Part I Section B Paragraph 1.a of the permit rightly describes as the “signature” contaminants characteristic of iron chloride waste from the DeLisle site: iron, chromium, lead, manganese and vanadium.

The draft of permit MS11001 provided by MDEQ on October 4, 2016 is shown in Appendix 1-1. This permit reduces the number of off-site wells from six to two wells located hydrologically “downstream” –to the Southeast—of the injection wells. The permit also makes changes in the analytes for the monitor well samples. It requires analyzing for the “signature” contaminants that would signal contamination with iron chloride waste from the DeLisle site: pH, total iron, total chromium, total vanadium, and total manganese.

REFERENCES

- Baria, L. R., D. L. Stoudt, P. M. Harris, and P. D. Crevello, 1982, Upper Jurassic reefs of Smackover Formation, United States Gulf Coast: American Association of Petroleum Geologists Bulletin, v. 66, 1449-1482.
- Barlow, A. C., 1974, Review of electric log indicates ten freshwater sands [0109247].
- Berg, R. B. and B. C. Cook, 1968, Petrography and origin of Lower Tuscaloosa sandstones, Mallalieu Field, Lincoln County, Mississippi: Gulf Coast Association of Geological Societies Transactions, v. 18, 242-255 [0111358].
- Brahana, J. V. and G. J. Dalsin, 1977, Water for industrial development in George, Hancock, Pearl River, and Stone Counties, Mississippi: USGS and Mississippi Research and Development Center, 70 [0109261].
- Brown, G. F., V. M. Foster, R. W. Adams, E. W. Reed, and H. D. Padgett, 1944, Geology and groundwater resources of the coastal area in Mississippi: Mississippi State Geological Survey, Bulletin 60, 232 [0110092].
- Bybell, L. M., 1982, Late Eocene to early Oligocene calcareous nannofossils in Alabama and Mississippi: Gulf Coast Assoc. Geol. Socs. Trans., v. 32, 295-302.
- Chasteen, H. R., 1983, Reevaluation of the lower Tuscaloosa and Dantzer Formations (Mid-Cretaceous) with emphasis on depositional environments and time-stratigraphic relationships: Gulf Coast Association of Geological Societies Transactions, v. 33, 31-40 [0111360].
- Clark, J. E., 1986, Groundwater monitoring plan for Mississippi UIC Permit [0110147].
- Copeland, C. W., 1968, Geology of the Alabama Coastal Plain: A guidebook: Geological Survey of Alabama, Circular 47.
- DuPont, 1974, Technical Data Summary-Waste Well 1 [0107399].
- Fisher, W. L. and J. H. McGowen, 1967, Depositional systems in the Wilcox Group of Texas and their relationship to the occurrence of oil and gas: Gulf Coast Association of Geological Societies Transactions, v. 17, 105-125.

- Galloway, W. E., 1968, Depositional systems of the lower Wilcox Group, North-central Gulf Coast Basin: Gulf Coast Association of Geological Societies Transactions, v. 18, 275-289 [0111139].
- Gandl, L. A., 1982, Characterization of aquifers designated as potential drinking water sources in Mississippi: USGS Water-Resources Investigations Open-File Report 81-550, 90, [0111354].
- Harry, D.L. and J. Londono, 2004, Structure and evolution of the central Gulf of Mexico continental margin and coastal plain, southeast United States: Geological Society of America, v.116, i. 1-2, p. 188-199.
- Hazel, J. E.; M. D. Mumma; and W. J. Huff, 1980, Ostracode biostratigraphy of the lower Oligocene (Vicksburgian) of Mississippi and Alabama: Gulf Coast Association of Geological Societies Transactions, v. 30, 361-380.
- Hearne, J. H. and B. E. Lock, 1985, Diagenesis of the Lower Tuscaloosa as seen in the du Pont de Nemours No. 1 Lester Earnest, Harrison County, Mississippi: Gulf Coast Association of Geological Societies Transactions, v 35, 387-393 [0108889].
- Johnson, W. B., 1974a, Petrographic study of massive sand: 6 [0107570].
- Johnson, W. B., 1974b, Petrographic study of massive sand: 4 [0107575].
- Leeds, D. J., 1989, Seismicity--natural and induced, DeLisle Plant, Mississippi [0113346].
- Mancini, E. A., R. M. Mink, J. W. Payton, and B. L. Bearden, 1987, Environments of deposition and petroleum geology of Tuscaloosa Group (Upper Cretaceous), South Carlton and Pollard Fields, Southwestern Alabama: American Association of Petroleum Geologists Bulletin, v. 71, 1128-1142.
- Moore, P. L., 1974. Drilling Practices Manual: PennWell Books, Tulsa, Oklahoma.
- Newcombe, R., Jr., 1975, The Miocene aquifer system in Mississippi: Jackson, Mississippi, USGS Water Resources Investigations Map, 46-75 [0107349].
- Newcombe, R., Jr., D. E. Shattles, and C. P. Humphreys, Jr., 1968, Water for the growing needs of Harrison County, Mississippi: USGS Water-Supply Paper 1856, 106 [0110094].

- Otvos, E. G., 1982, Coastal geology of Mississippi, Alabama and adjacent Louisiana areas: New Orleans Geological Society, Field Trip, June 1982, 47 [0111363].
- Paulson, O. L., 1972, Various factors influence Wilcox deposits in the “Golden Triangle”: Oil and Gas Journal, 86-87 [0111141].
- Rainwater, E. H., 1964a, Regional stratigraphy of the Midway and Wilcox in Mississippi: Mississippi Geological Survey Bulletin 102, 29 [0111362].
- Rainwater, E. H., 1964b, Stratigraphy Gulf Coast Miocene: Gulf Coast Association of Geological Societies Transactions, v. 14,. 76-77 [0111138].
- Salvador, A., 1987, Late Triassic-Jurassic Paleogeography and Origin of the Gulf of Mexico Basin: AAPG Bulletin, v. 71, No. 4, 419-451.
- Self, G. A., S. Q. Breard, H. P. Rael, J. A. Stein, P. A. Thayer, M. O. Traugott, and W. D. Easom, 1986, Lockhart Crossing Field: new Wilcox trend in southeastern Louisiana: American Association of Petroleum Geologists Bulletin, v. 70, 501-515.
- Shirley, K., 1987, Trend spins seismic success story: American Association of Petroleum Geologists Explorer, v. 8, No. 10, 14.
- Stancliffe, R. J. and E. R. Adams, 1986, lower Tuscaloosa fluvial channel styles at Liberty Field, Amite County, Mississippi: Gulf Coast Association of Geological Societies Transactions., v. 36, 305-313 [0111357].
- Trmal, C., 1982, DeLisle Groundwater study [0109281].
- Vail, P. R., R. M. Mitchum, and S. Thompson, 1977, Seismic stratigraphy and global changes in sea-level, Part 4: global cycles of relative changes in sea-level, in Payton, C. E., ed., Seismic stratigraphy-applications to hydrocarbon exploration: American Association of Petroleum Geologists Memoir 26, 82-97.
- Vesic, A. S., 1974, Results of high-pressure permeability tests on core samples of shale: Duke University, 5 [0107158].
- Waters, L. A. and E. A. Mancini, 1982, Lithostratigraphy and biostratigraphy of upper Eocene and lower Oligocene strata in southwest Alabama and southeast Mississippi: Gulf Coast Association of Geological Societies Transactions, v. 32, 302-307.

Wesson, R. L. and C. Nicholson, 1987, Earthquake hazard associated with deep well injection: U. S. Geological Survey Open-File Report 87-331, 72 [0109424]

Glossary

Aquifer

A geological formation, group of formations, or part of a formation that is capable of yielding a significant amount of water to a well or spring.

Borehole

A shaft bored or drilled into the ground either vertically or horizontally.

Confining Zone

A geological formation that is capable of limiting fluid movement above an injection zone. It is composed of rock layers that are impermeable or distinctly less permeable (shales for example) than the injection zone beneath it.

Containment Interval

Geological formation(s) capable of limiting fluid movement above the injection interval(s). It overlies the injection intervals and is contained within the injection zone.

Fault

A surface or zone of rock fracture along which there has been displacement.

Formation

Body of rock forming a separate and identifiable geological unit base on the rock characteristics.

Geophysical Well Log

Recording of a variety of subsurface properties made by lowering detectors into the well.

Groundwater

Subsurface fresh water, potable water, or water that is or can be potentially used as a drinking water supply.

Injection Interval

The geological formation targeted to receive the injected fluids. The injection interval is contained within the injection zone.

Injection Zone

A geological formation or group of formations (sandstones for example) receiving fluids through an injection well. The injection zone extends from the bottom of the lowermost injection interval to the top of the containment interval.

Lithology

The physical character of a rock.

Permeability

A measure of the resistance to the flow of a fluid through a rock. If it takes a lot of pressure to squeeze fluid through a rock, that rock has low permeability. Permeability is expressed in units called millidarcies.

Porosity

A measure of the ability of a rock to hold fluid. It is the open space in a rock divided by the total rock volume (solid + space or holes). Porosity is expressed as a percentage of the total rock taken up by pore space. A sandstone may have 10% porosity, meaning that 90% of the rock is solid and 10% is open.

Sandstone

A sedimentary rock composed of sand-sized grainer of mineral, rock, or organic material. In the subsurface, sandstone often serves as an aquifer for groundwater or as a reservoir for oil and natural gas.

Seismicity

The occurrence or frequency of earthquakes in a region.

Shale

A fine-grained sedimentary rock that forms from the compaction of silt and clay mineral particles that we commonly call “mud.” In the subsurface, black shales contain organic material that sometimes breaks down to form natural gas or oil. Other shales can be crushed and mixed with water to produce clays.

Strata

A bed or layer of sedimentary rock this is visually distinguishable from adjacent beds or layers.

Stratigraphy

The order and relative position of strata and their relationship to the geological time scale.

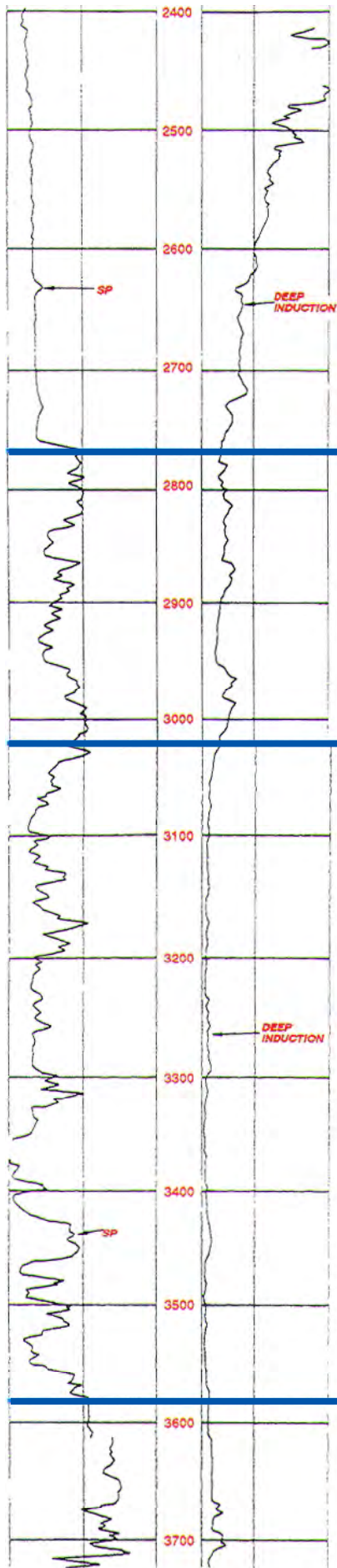
Structure

The description and interpretation of deformation in the earth’s crust.

Wellbore

See Borehole

FIGURES



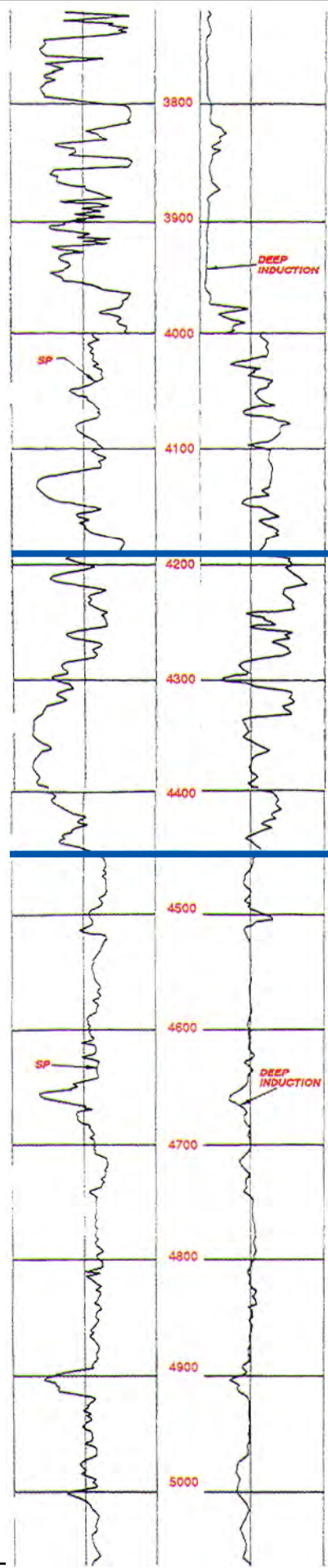
**Approximate
Base of Lowermost USDW**

**Undifferentiated
Shale
(270 ft.)**

**Undifferentiated
Sands
and
Shales
(550 ft.)**

**Catahoula
Shales and Sands
(630 ft.)**

Figure 2-3 Composite Electric Log Stratigraphic Column



**Catahoula
Shales
and
Sands
(630 ft.)**

**Het Limestone
(300 ft.)**

**Jackson
Shale
(750 ft.)**

Figure 2-3 Composite Electric Log Stratigraphic Column

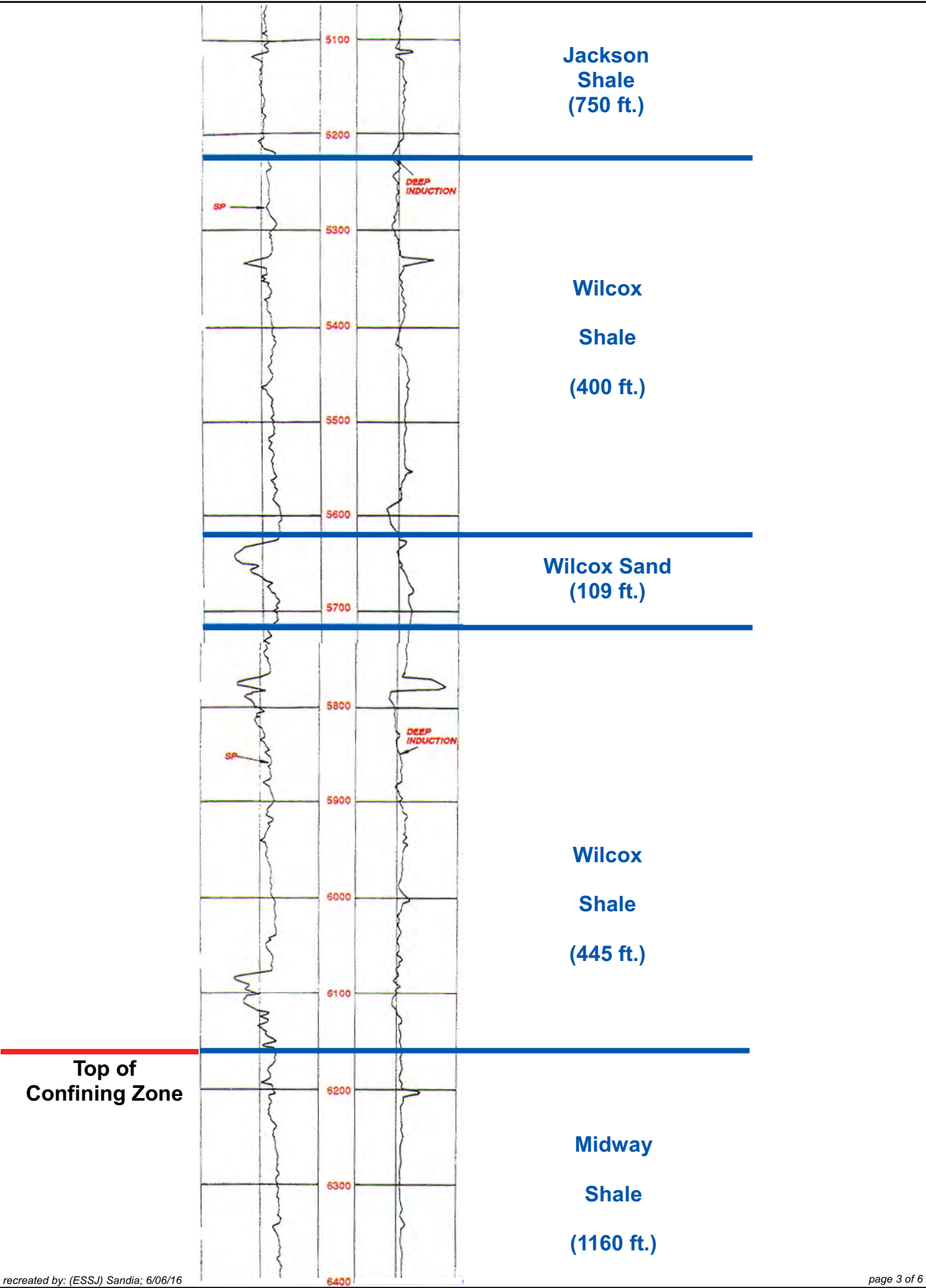
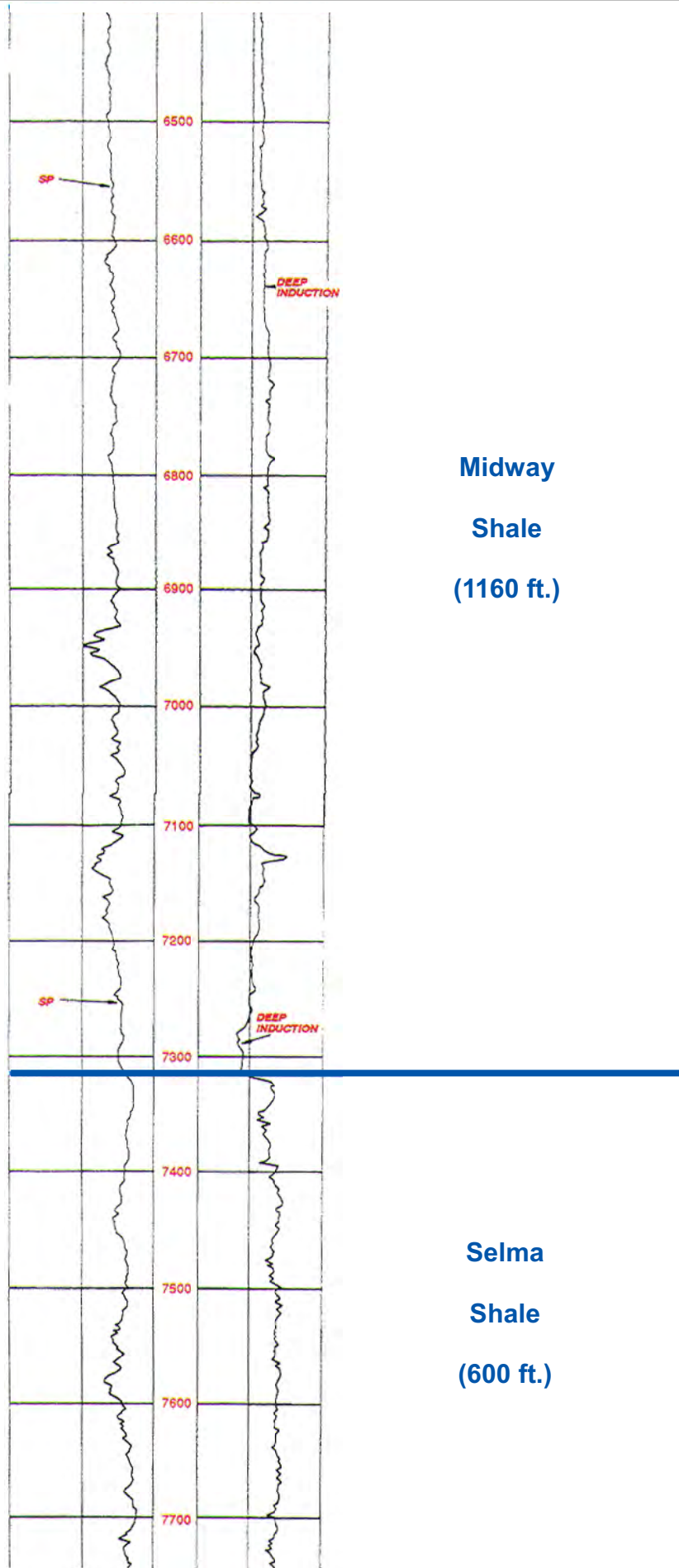


Figure 2-3 Composite Electric Log Stratigraphic Column



**Midway
Shale
(1160 ft.)**

**Selma
Shale
(600 ft.)**

Figure 2-3 Composite Electric Log Stratigraphic Column

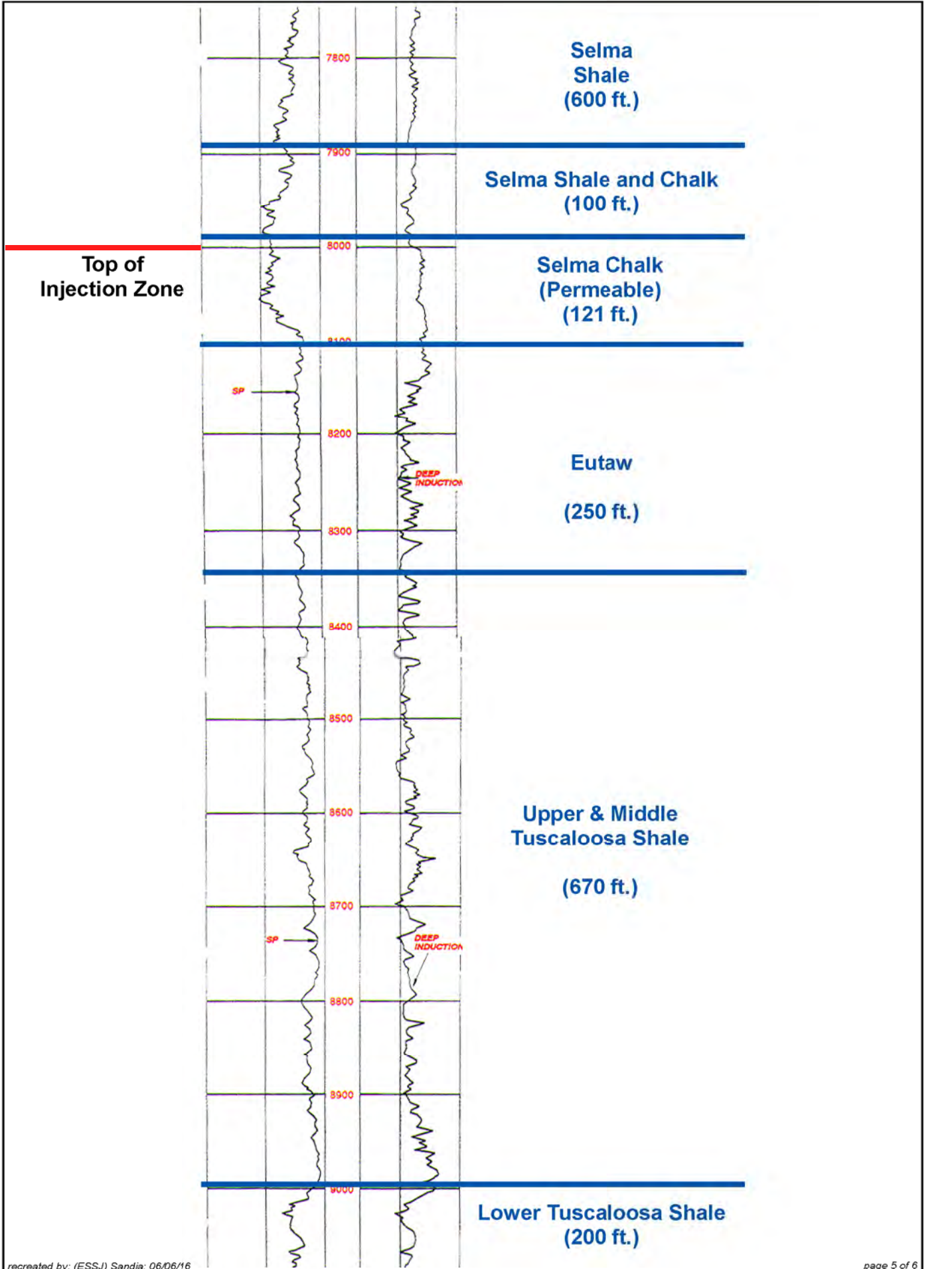


Figure 2-3 Composite Electric Log Stratigraphic Column

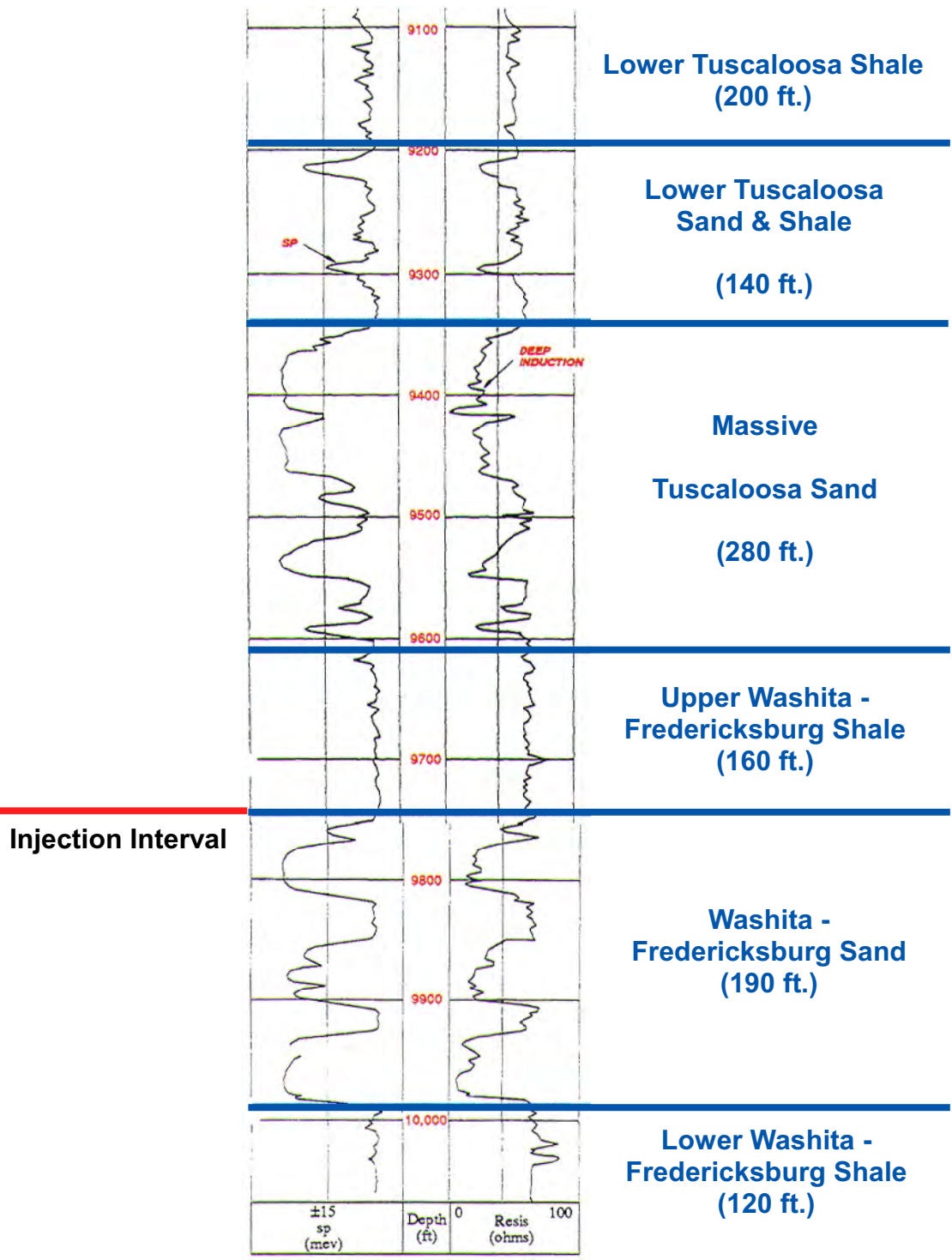


Figure 2-3 Composite Electric Log Stratigraphic Column

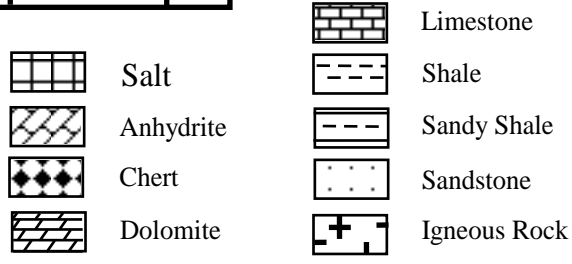
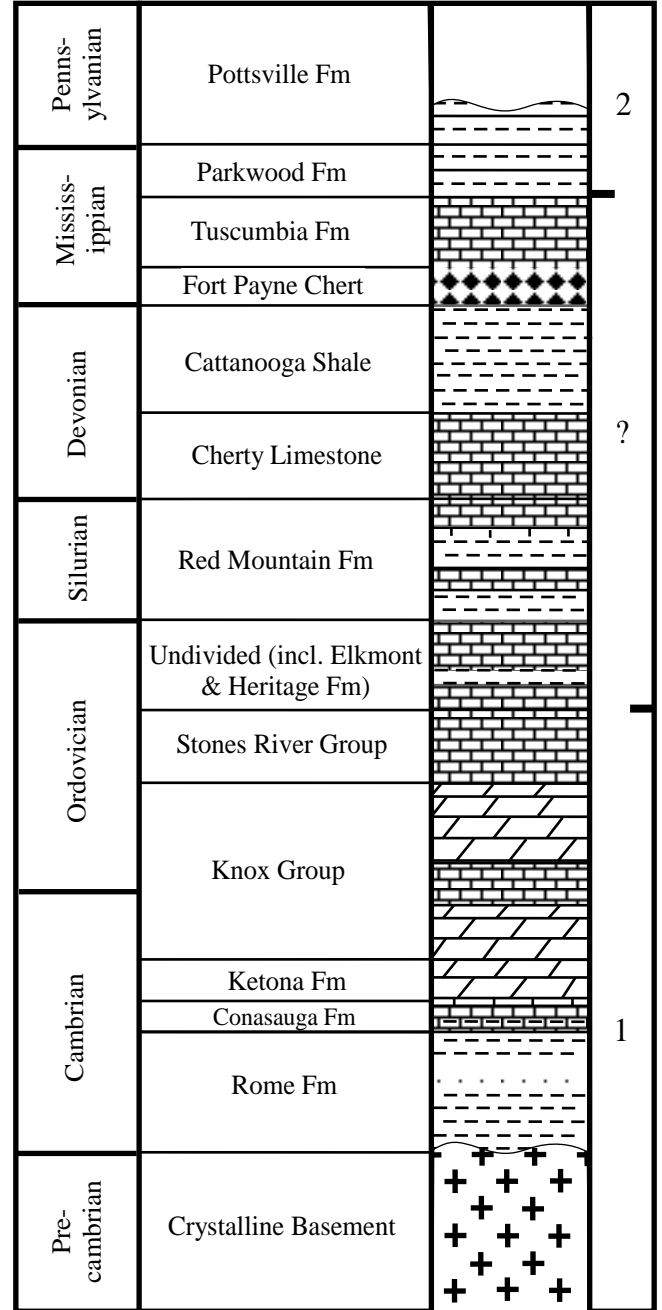
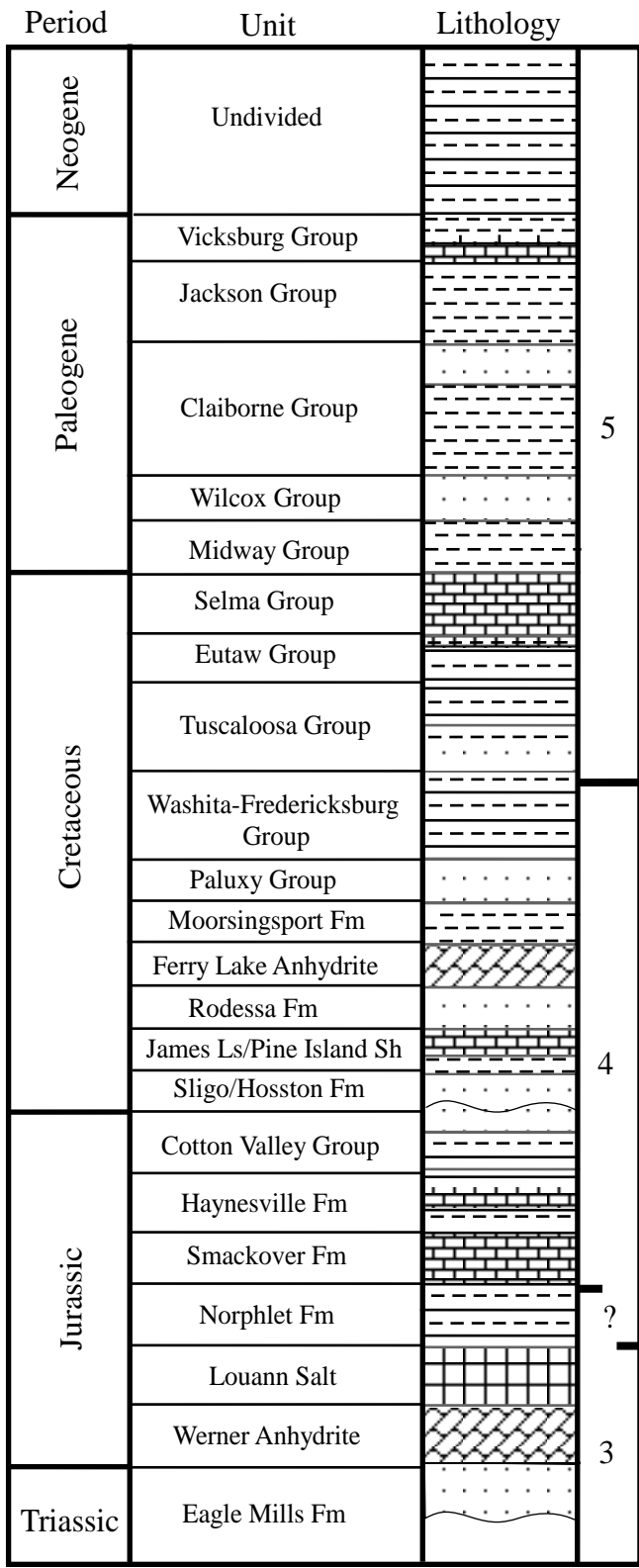


Figure 2-4 Regional Mississippi Stratigraphic Column
(from Geologic Society of America Bulletin 116)

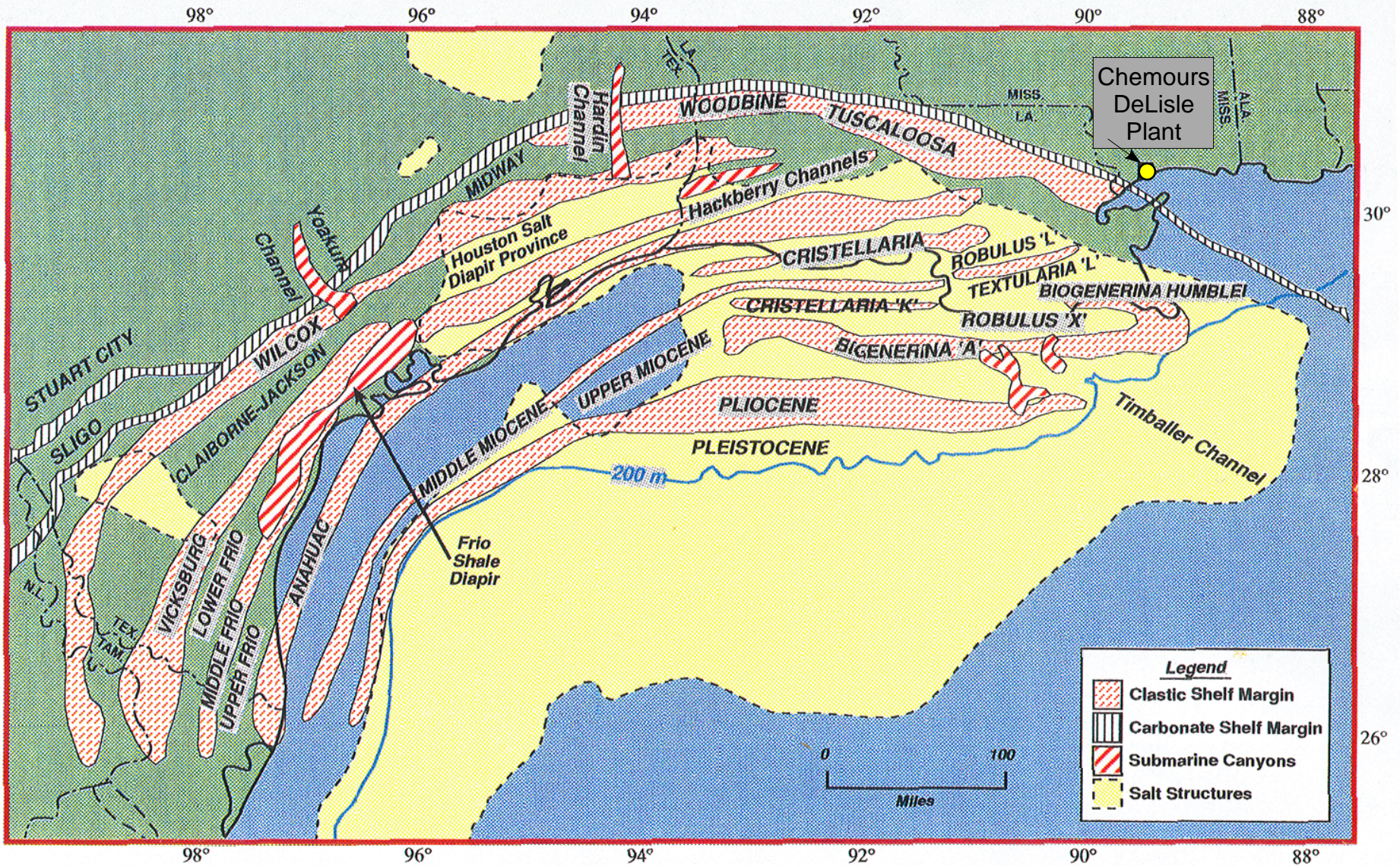
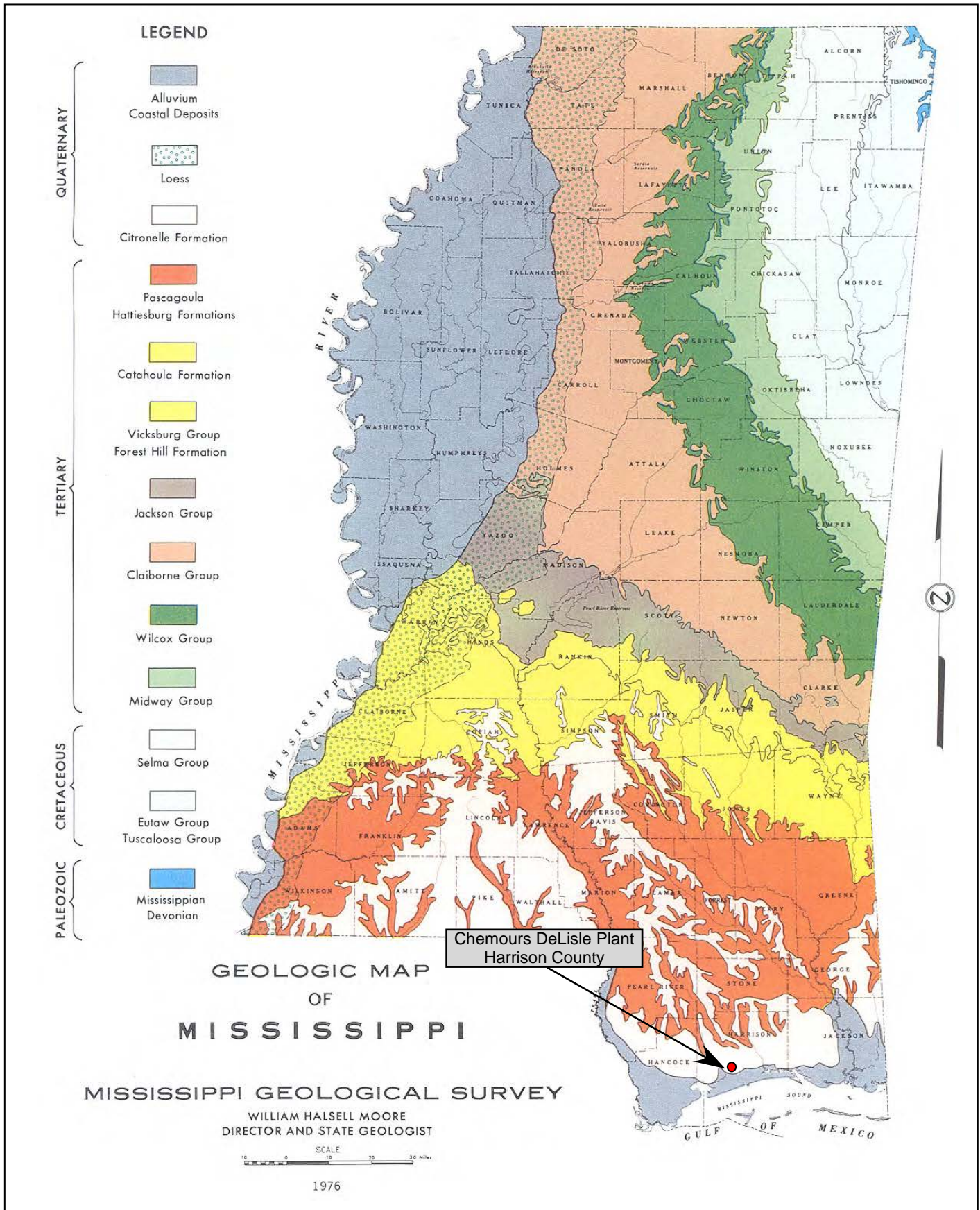
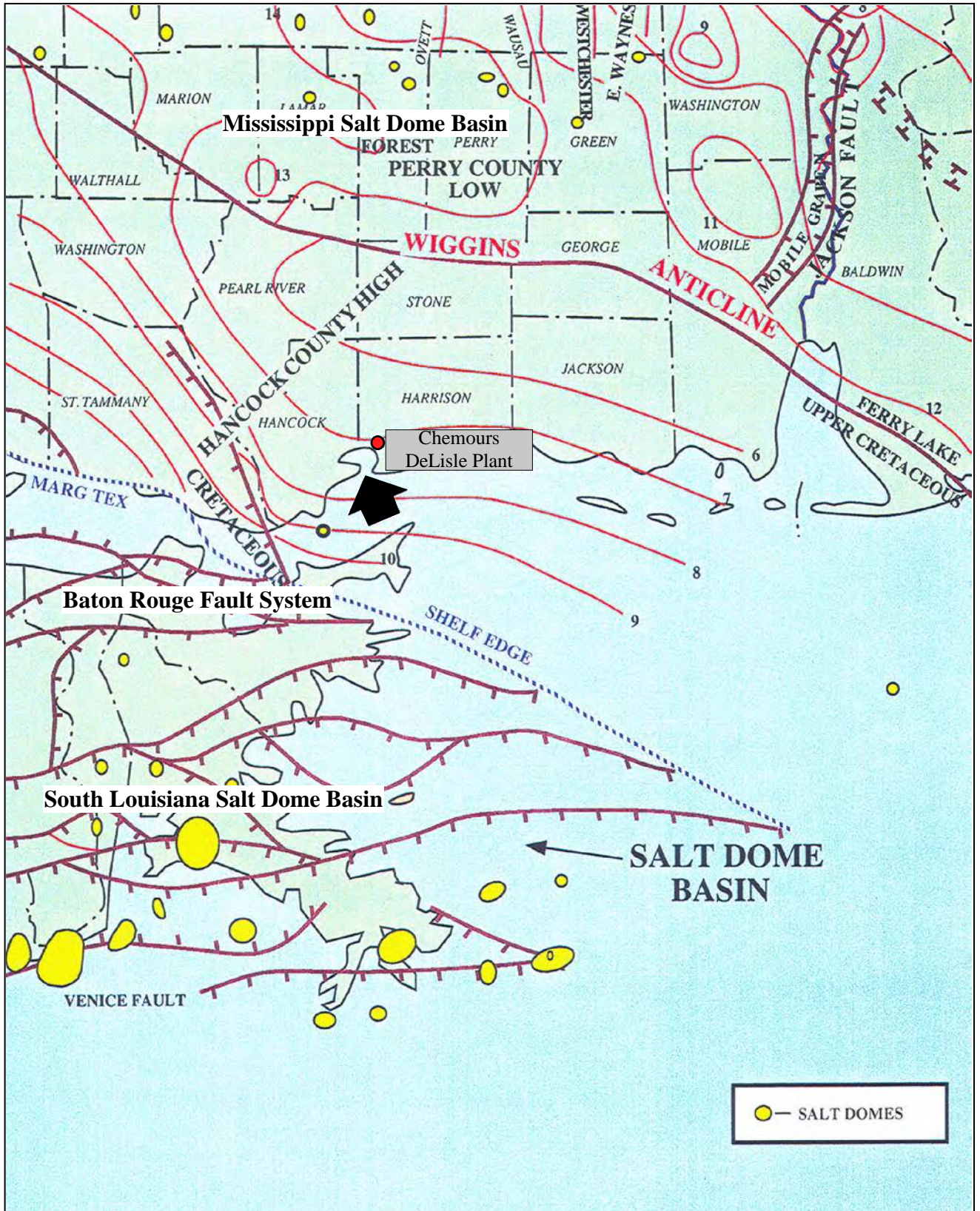


Figure 2-5 Distribution of Cretaceous and Cenozoic continental Margins in the Northeastern Gulf of Mexico. (from Jackson and Galloway, 1984)



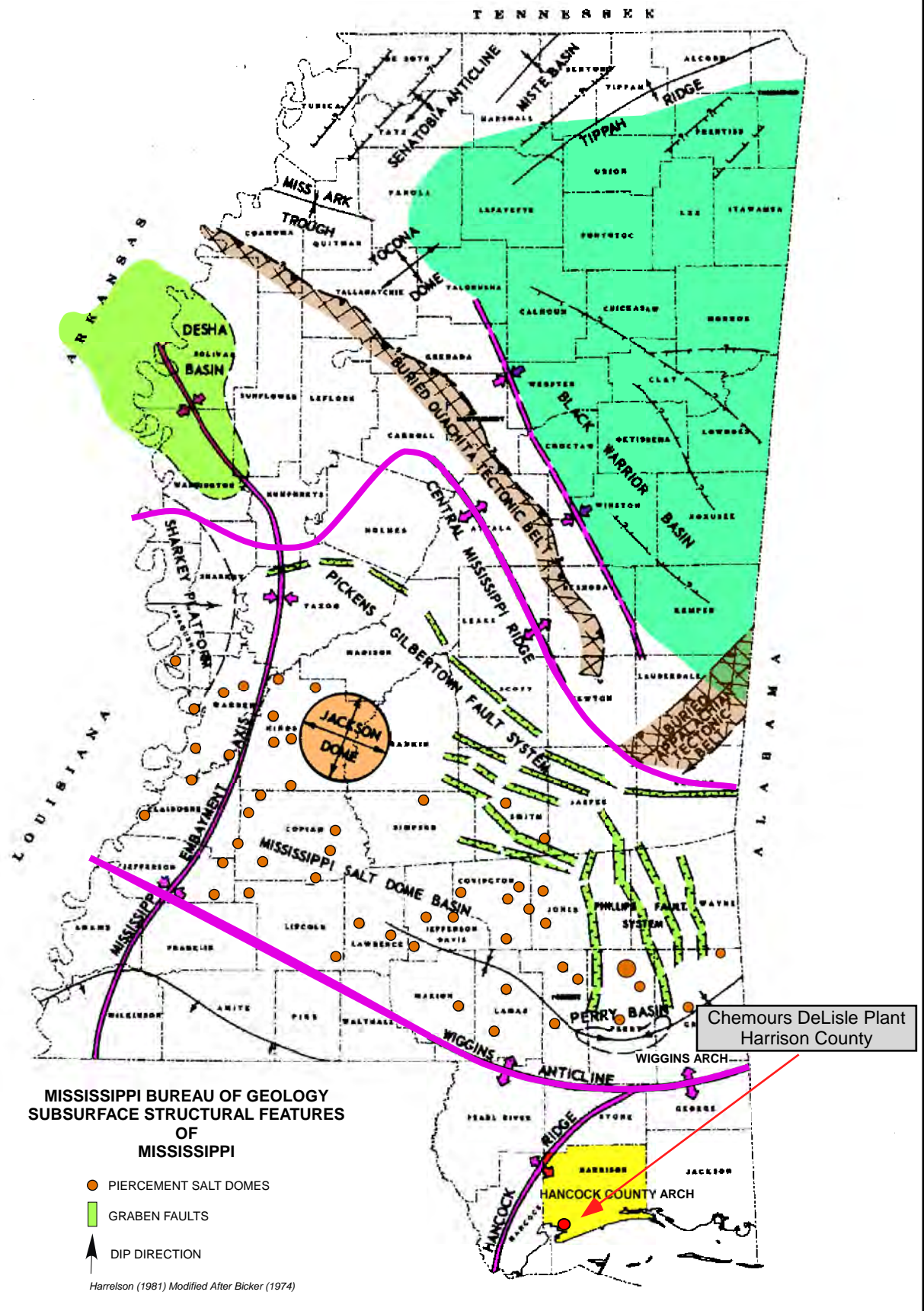
Adapted from: Mississippi Geological Survey 1976
 9/5/06 ESSJ-Sandia

Figure 2-6 Surface Geologic Map of Mississippi



adapted by: ESSJ Sandia 9/12/06

Figure 2-7 Tectonic Map of Northern Gulf Coast Region
 (Modified from Decker & Associates, Inc., June 1984)



Adapted from: "Subsurface Cretaceous Strata of Mississippi", Dora M. Devery 1982
9/13/06 ESSJ-Sandia

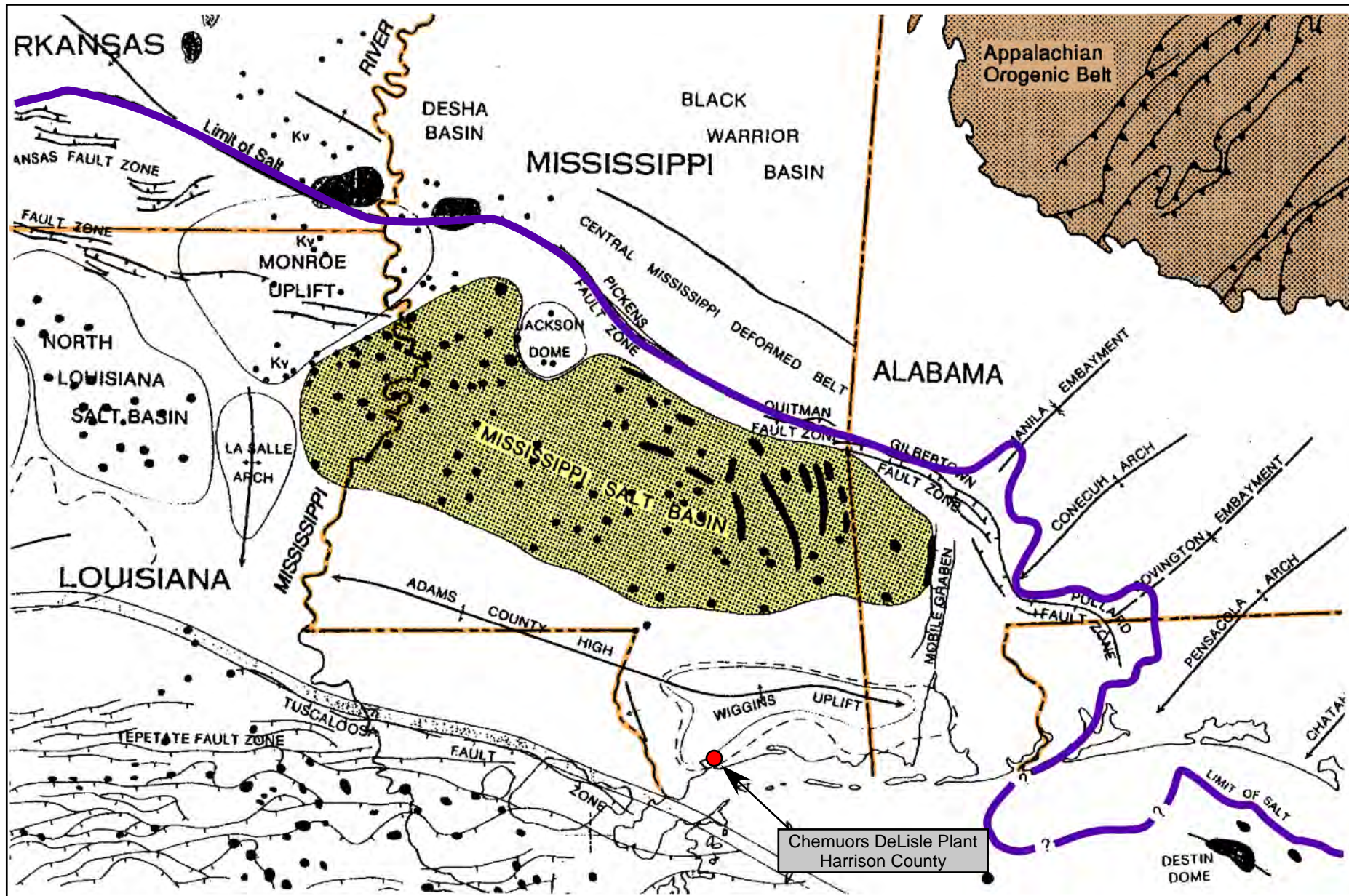
Figure 2-8 Tectonic and Subsurface Structural Features of Mississippi
(from Mississippi Bureau of Geology)



US Geological Survey - National Earthquake Information Center

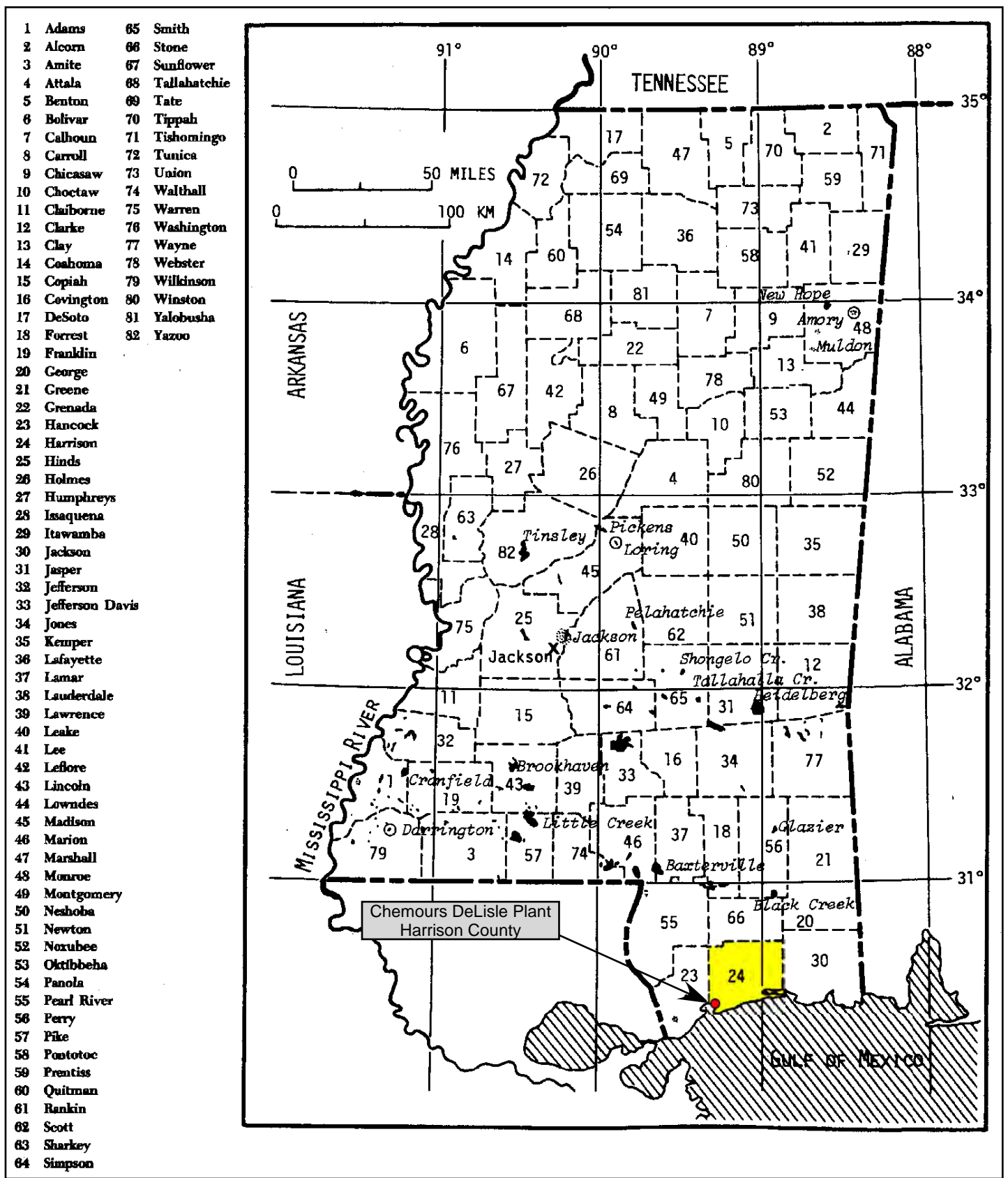
- ★ Location of The Chemours DeLisle Plant
- Earthquake in closest proximity to Chemours
Location: 30.662°N 89.248°W(5km depth)
Date & Time: 1975-09-09 ; 11:52:44
- Earthquakes

Figure 2-9 Earthquake Events Within a 250 km Radius of the Chemours DeLisle Plant through June 2017



Adapted from: "Petroleum Frontiers - Mississippi Salt Dome Basin" Vol. 13 No. 2 1996
 9/13/06 ESSJ-Sandia

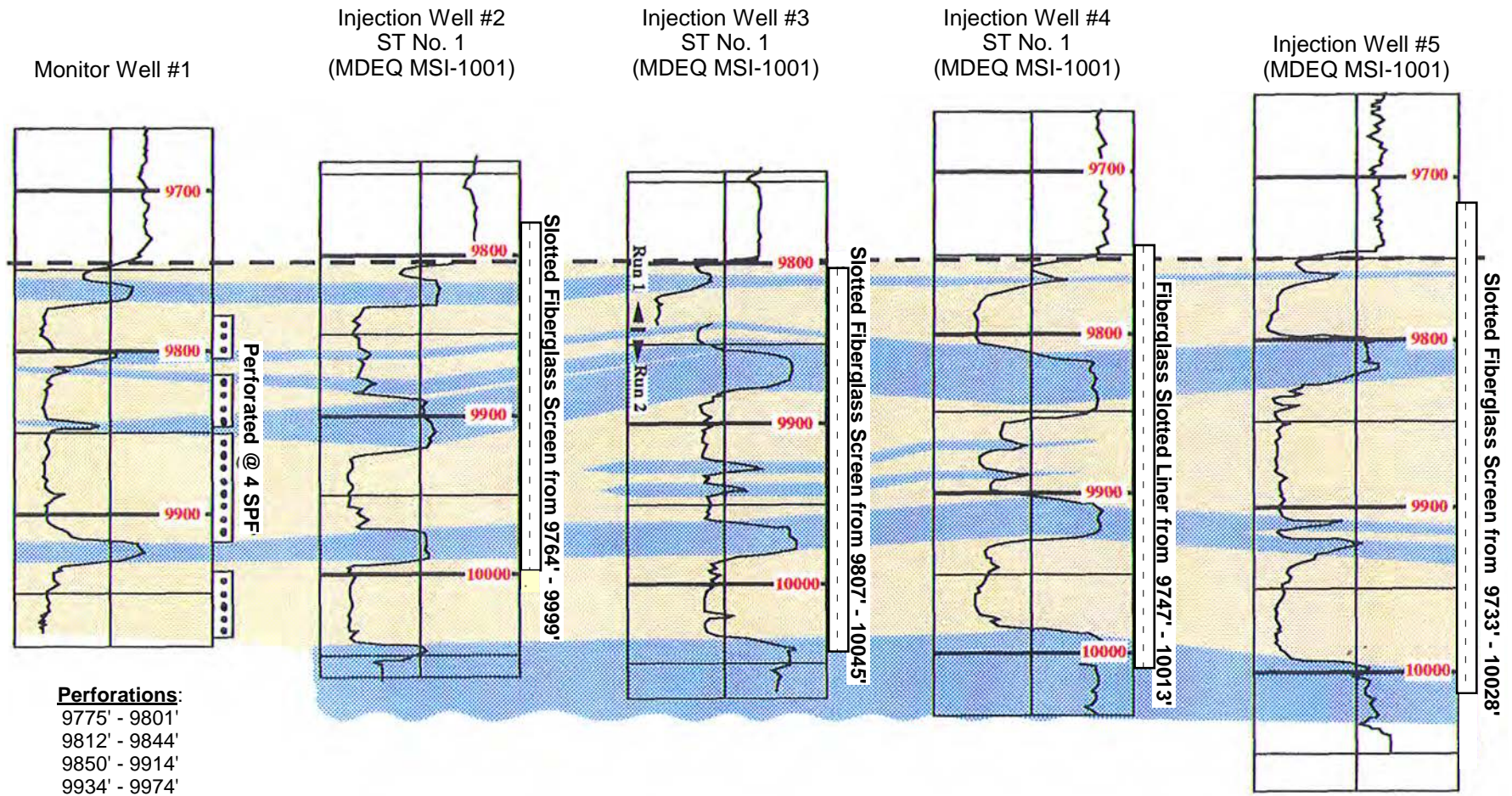
Figure 2-10 Detailed Tectonic Setting, Southern Mississippi Salt Basin.



Adapted from: "Petroleum Geology of the United States"
9/5/06 ESSJ-Sandia

Figure 2-11 Mississippi Index Map of Oil and Gas Fields with County Key.

Chemours DeLisle Plant - Washita Fredericksburg Sand



Perforations:
 9775' - 9801'
 9812' - 9844'
 9850' - 9914'
 9934' - 9974'

(Log curves are Spontaneous Potential)

adapted by: ESSJ Sandia 1/04/07

Figure 2-12 Washita-Fredericksburg Injection Interval Electric Log Correlation

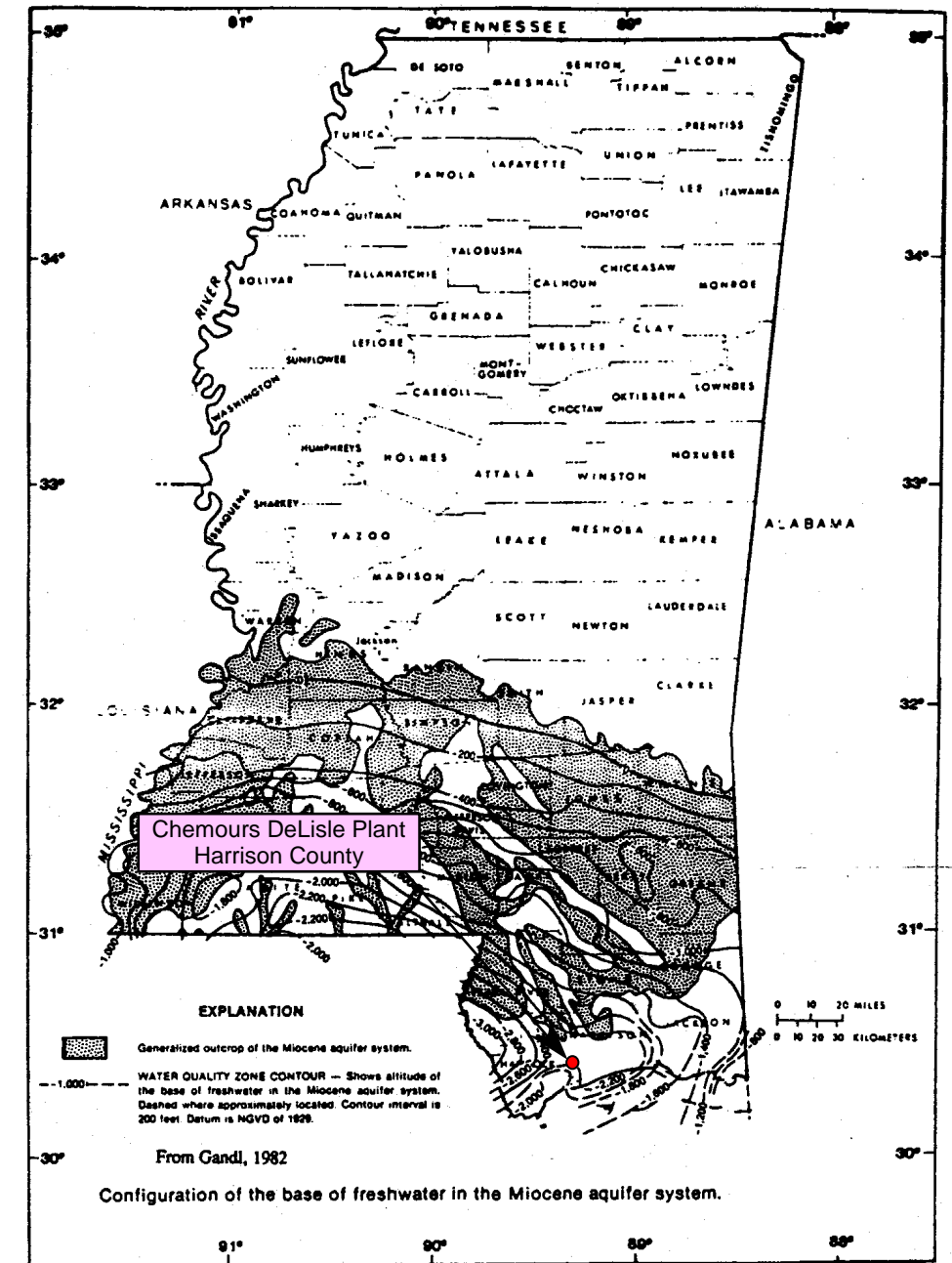
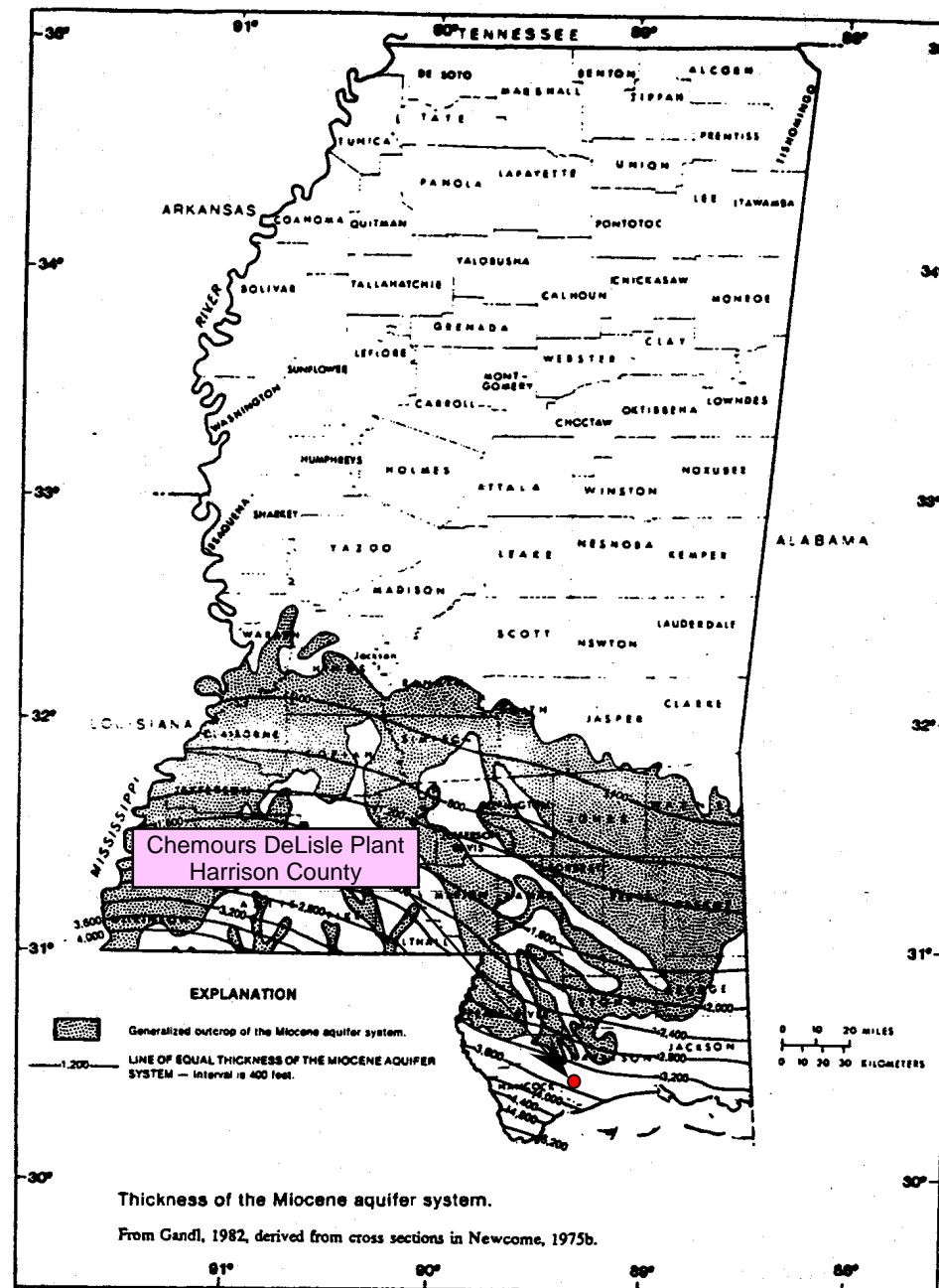
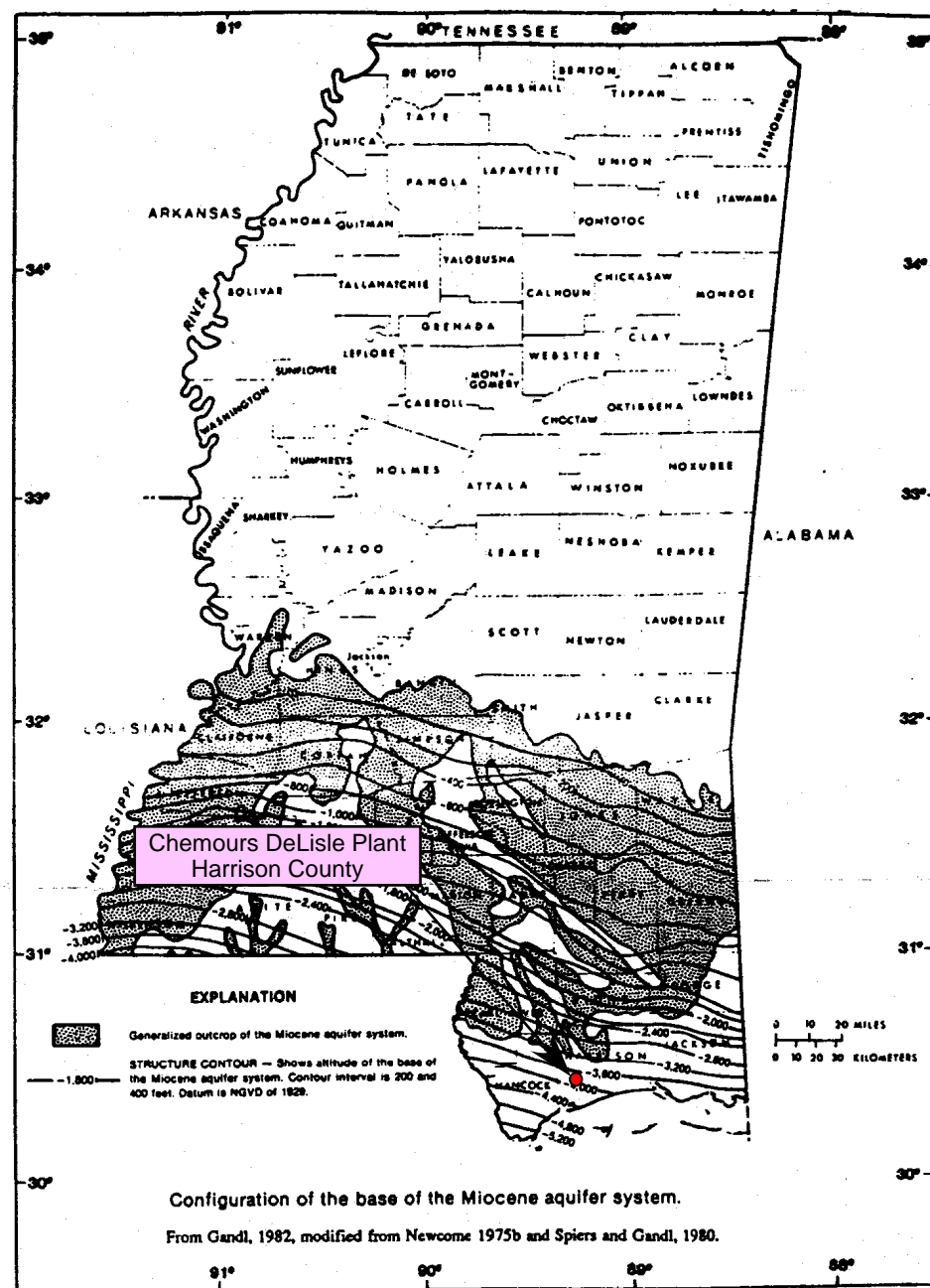


Figure 2-13 Miocene Aquifer System (State of Mississippi)

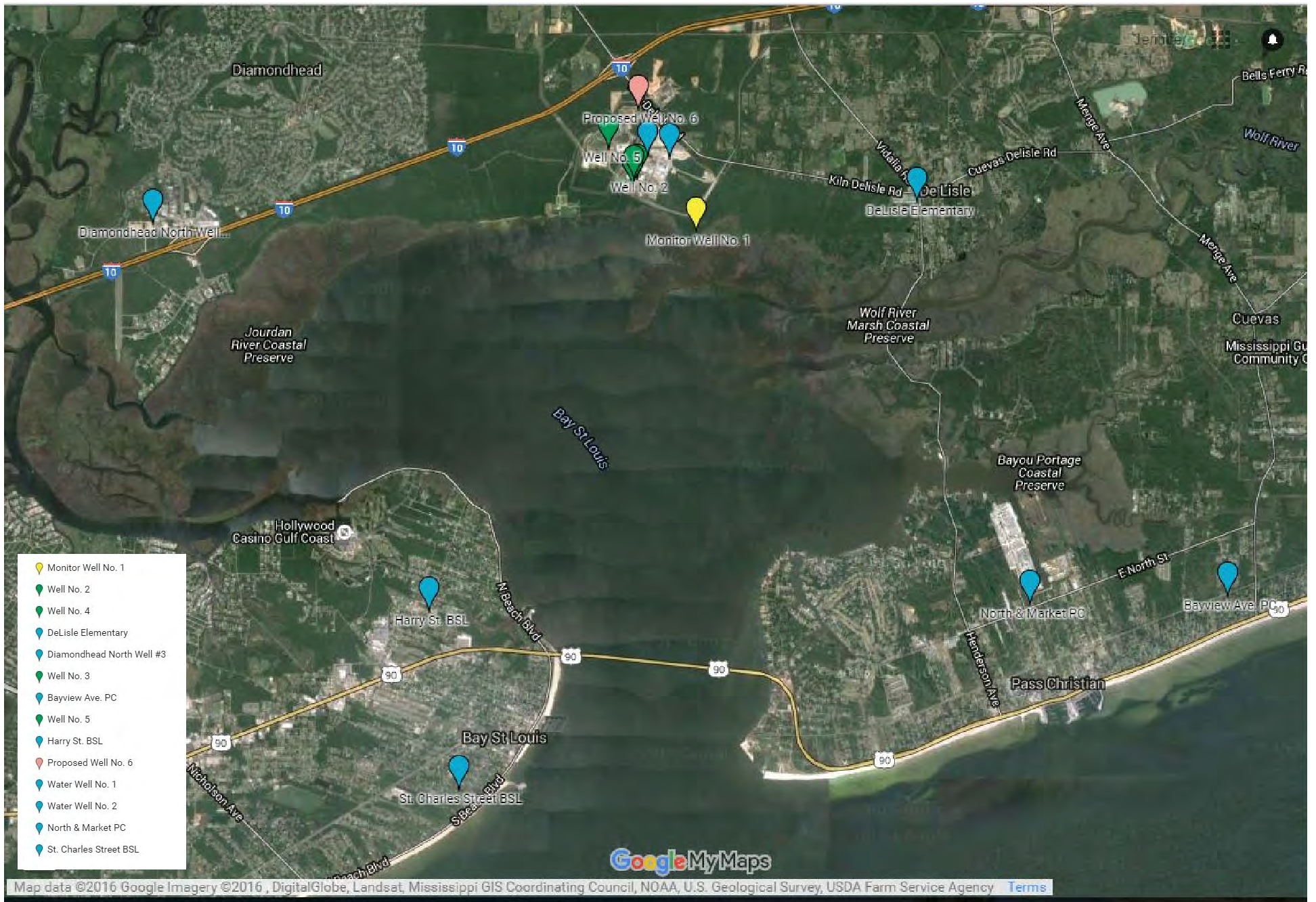


Figure 2-15 Monitor Well Locations

TABLES

Table 2-1**Index of Geologic Maps within the DeLisle Petition Reissuance Geology Section**

Regulatory Unit	Geologic Formation	Appendix Numbers	
		Structure Maps	Isopach Maps
Confining Zone	Midway Shale	2 - 5	2 - 12
	Selma Chalk	2 - 6	2 - 13
Injection Zone	Eutaw Shale	2 - 7	2 - 14
	Upper & Middle Tuscaloosa Massive Sand	2 - 8	2 - 15
	Lower Tuscaloosa Massive Sand	2 - 9	2 - 16
	Tuscaloosa Massive Sand	2 - 10	2 - 17
Injection Interval	Washita-Fredericksburg Sand	2 - 11	2 - 18

Table 2-2**Estimated Dip of Formations Below the Top of the Confining Zone at the DeLisle Plant**

Formation	Regional Area (ft/mile)	Near Plant Site (ft/mile)
Midway Shale	33 to 210	110
Selma Chalk	45 to 180	83
Eutaw Shale	42 to 132	73
Upper and Middle Tuscaloosa Massive Sand	45 to 120	72
Lower Tuscaloosa Massive Sand	42 to 210	60
Tuscaloosa Massive Sand	33 to 110	72
Washita-Fredericksburg (injection sand interval) Sand	37 to 132	60

Table 2-3**Thicknesses of Formations Below the Top of the Confining Zone at the DeLisle Plant**

Formation	Lithology	Regional Area (ft)	At Site Fig 2-2 (ft)
Midway	Shale	935 to 1,475	1180
Selma	Chalk/Shale	300 to 1,125	840
Eutaw	Shale/Lime	110 to 265	290
Upper & Middle Tuscaloosa Shale	Shale	550 to 800	560
Lower Tuscaloosa Massive Sand/Shale	Sand/Shale	95 to 480	270
Tuscaloosa Massive Sand	Sand	135-360	317
Upper Washita-Fredericksburg Shale	Shale	20 to 190	160
Washita-Fredericksburg Sand (Injection Interval)	Sand/Shale	100 to 240	246
Lower Washita-Fredericksburg Shale	Shale	120 to 240	120

Table 2-4
Modified Mercalli Intensity Scale of 1931

(Abridged)

- I. Not felt except by a very few under especially favorable circumstances. (I Rossi-Forel Scale.)
- II. Felt only by a few persons at rest, especially on upper floors of buildings. Delicately suspended objects may swing. (I to II Rossi-Forel Scale.)
- III. Felt quite noticeably indoors, especially on upper floors of buildings, but many people do not recognize it as an earthquake. Standing motorcars may rock slightly. Vibration like passing of truck. Duration estimated. (III Rossi-Forel Scale.)
- IV. During the day felt indoors by many, outdoors by few. At night some awakened. Dishes, windows, doors disturbed; walls make creaking sound. Sensation like heavy truck striking building. Standing motorcars rocked noticeably. (IV to V Rossi-Forel Scale.)
- V. Felt by nearly everyone, many awakened. Some dishes, windows, etc., broken; a few instances of cracked plaster; unstable objects over turned. Disturbances of trees, poles, and other tall objects sometimes noticed. Pendulum clocks may stop. (V to VI Rossi-Forel Scale.)
- VI. Felt by all, many frightened and run outdoors. Some heavy furniture moved; a few instances of fallen plaster or damaged chimneys. Damage slight. (VI to VII Rossi-Forel Scale.)
- VII. Everybody runs outdoors. Damage negligible in buildings of good design and construction; slight to moderate in well-built ordinary structures; considerable in poorly built or badly designed structures; some chimneys broken. Noticed by persons driving motorcars. (VIII Rossi-Forel Scale.)
- VIII. Damage slight in specially designed structures; considerable in ordinary substantial buildings with partial collapse; great in poorly build structures. Panel walls thrown out of frame structures. Fall of chimneys, factory stacks, columns, monuments, walls. Heavy furniture overturned. Sand and mud ejected in small amounts. Changes in well water. Persons driving motorcars disturbed. (VIII+ to IX- Rossi-Forel Scale.)
- IX. Damage considerable in specially designed structures; well-designed frame structures thrown out of plumb; great in substantial buildings, with partial collapse. Buildings shifted off foundations. Ground cracked conspicuously. Underground pipes broken. (IX+ Rossi-Forel Scale.)
- X. Some well-built wooden structures destroyed; most masonry and frame structures destroyed with foundations; ground badly cracked. Rails bent. Landslides considerable from river banks and steep slopes. Shifted sand and mud. Water splashed (slopped) over banks. (X Rossi-Forel Scale.)
- XI. Few, if any, (masonry) structures remain standing. Bridges destroyed. Broad fissures in ground. Underground pipelines completely out of service. Earth slumps and land slips in soft ground. Rails bent greatly.
- XII. Damage total. Waves seen on ground surface. Lines of sight and level distorted. Objects thrown upward into the air.

Table 2-5**Calculated Injection Interval Pressure Increases at the DeLisle Plant**

Formation	Formation Depth (ft)	Conservative Model Calculated Pressure Buildup ¹ (psi)	Seismicity Calculated Pressure Buildup (psi)	Margin of Safety (psi)
Washita- Fredericksburg	9,850	967	1,231	264
Tuscaloosa Massive Sand	9,455	344	1,182	838

Note¹: These values are retrieved from Section 3.0 of this petition, as seen in Tables 3-13 and 3-1

Table 2-6**Upper Washita-Fredericksburg Injection Intervals**

Well No.	Log (ft)	Depth
Well No. 2	9,779 - 10,018	
Well No. 3	9,797 - 10,043	
Well No. 4	9,754 - 10,023	
Well No. 5	9,744 - 10,043	
Proposed Well No. 6	9,700 - 10,100*	
Proposed Well No. 7	9,700 - 10,100*	

*Estimated, to be established by final well log and report

Table 2-7**Geological Data Used for Establishing Porosity, Permeability and Thickness of the Washita Fredericksburg Injection Sand**

Well No.	Core No.	Formation Sampled	Dominant Lithology	Depth (ft)	Core Plug Samples	Average Air Permeability (md)	Average Porosity (%)
5	7	Washita-Fredericksburg	Shale/Silt/Sand	9,606 - 9,637	15	0.631	8
1	17	Washita-Fredericksburg	Shale	9652-9660	7	0	4.3
1	18	Washita-Fredericksburg	Shale	9660-9676	16	0.00	4.53
5	8	Washita-Fredericksburg	Shale	9,667 - 9,697	7	0.209	6
4		Washita-Fredericksburg	Sand	9757		1691.0	20.7
1	19	Washita-Fredericksburg	Sand	9767-9798	29	191.13	14.52
4		Washita-Fredericksburg	Calc/Sand	9778		61.0	23.4
4		Washita-Fredericksburg	Sand/Ankerite	9779		16.0	12.3
4		Washita-Fredericksburg	Sand	9782		41.0	20.4
4		Washita-Fredericksburg	Sand	9786		810.0	28.7
4		Washita-Fredericksburg	Shale	9789		0.10	5.9
4		Washita-Fredericksburg	WALLCAKE	9790			
4		Washita-Fredericksburg	Sand	9794		672.0	27.2

Table 2-7 (continued)

Well No.	Core No.	Formation Sampled	Dominant Lithology	Depth (ft)	Core Plug Samples	Average Air Permeability (md)	Average Porosity (%)
2		Washita-Fredericksburg Shale	Sand with calcite cementation	9796		<0.01	3.9
4		Washita-Fredericksburg	Calc/Sand	9798		118.0	23.8
1	20	Washita-Fredericksburg	Sand	9798- 9826	28	418.43	19.38
2		Washita-Fredericksburg	Sand	9800		462	23.4
4		Washita-Fredericksburg	Calc/Sand	9800		84.0	22.9
2		Washita-Fredericksburg	Sand	9802		682	24.1
4		Washita-Fredericksburg	Calc/Sand	9802		312.0	24.2
4		Washita-Fredericksburg	Calc/Sand	9804		525.0	26
4		Washita-Fredericksburg	Calc/Sand	9806		492.0	25.8
4		Washita-Fredericksburg	Calc/Sand	9808		364.0	23.5
2		Washita-Fredericksburg	Sand	9810		460	12.9
4		Washita-Fredericksburg	Sh/Calc/Sand	9810		28.0	20.7
4		Washita-Fredericksburg	Calc/Sand	9812		31.0	22.3
4		Washita-Fredericksburg	Calc/Sand	9814		236.0	24.1

Table 2-7 (continued)

Well No.	Core No.	Formation Sampled	Dominant Lithology	Depth (ft)	Core Plug Samples	Average Air Permeability (md)	Average Porosity (%)
5	9	Washita-Fredericksburg	Sand	9,817 - 9,849	31	1024.00	23
4		Washita-Fredericksburg	Shaly/Sand	9820		0.0	13.7
2		Washita-Fredericksburg	Sand	9820		1133	21.8
3	4	Washita-Fredericksburg	Sand/Shale	9822		0.09	9.2
3	5	Washita-Fredericksburg	Sand/Graded Bedding	9826		12	13
1	21	Washita-Fredericksburg	Sand	9829-9851	22	332.77	21.95
3	6	Washita-Fredericksburg	Sand	9838		1087.00	20.3
4		Washita-Fredericksburg	Sand	9842		200.0	21.2
2		Washita-Fredericksburg	Sand	9843		230	18.1
3	7	Washita-Fredericksburg	Sand	9844		2042	22.6
3	8	Washita-Fredericksburg	Sand	9848		2502	22.6
5	10	Washita-Fredericksburg	Sand	9,849 - 9,907	58	799	21
2		Washita-Fredericksburg	sand	9850		264	24.1
2		Washita-Fredericksburg	mudstone (shale)	9852		*	*

Table 2-7 (continued)

Well No.	Core No.	Formation Sampled	Dominant Lithology	Depth (ft)	Core Plug Samples	Average Air Permeability (md)	Average Porosity (%)
4		Washita-Fredericksburg	Calc/Sand	9854		36.0	22.6
3	9	Washita-Fredericksburg	Sand	9856		1247.00	22.1
1	22	Washita-Fredericksburg	Sand	9857-9917	43	370.81	24.31
3	10	Washita-Fredericksburg	Sand	9861		824	22.6
3		Washita-Fredericksburg	Sand/Shale	9866		0.52	7.7
3		Washita-Fredericksburg	Shale	9871		0.01	5.1
4		Washita-Fredericksburg	Shale	9876		0.15	3.8
4		Washita-Fredericksburg	Calc/Sand	9880		18.0	20.3
4		Washita-Fredericksburg	Calc/Sand	9882		15.0	20.1
4		Washita-Fredericksburg	Calc/Sand	9884		34.0	22.6
3		Washita-Fredericksburg	Sand/carbonate cement	9887		90	17
4		Washita-Fredericksburg	Calc/Sand	9892		17.0	21
4		Washita-Fredericksburg	Calc/Sand	9896		31.0	21.7
2		Washita-Fredericksburg	Shale/Sand/Silt	9896		0.02	4.1

Table 2-7 (continued)

Well No.	Core No.	Formation Sampled	Dominant Lithology	Depth (ft)	Core Plug Samples	Average Air Permeability (md)	Average Porosity (%)
4		Washita-Fredericksburg	Calc/Sand	9898		194.0	23.9
3		Washita-Fredericksburg	Sand	9899		509	19.5
2	4	Washita-Fredericksburg	Shale/Sand	9900-9955	47	241.01	19.93
4		Washita-Fredericksburg	Lig/Sand	9900		12.0	18.4
2		Washita-Fredericksburg	Sand	9902		222	21.3
3		Washita-Fredericksburg	Sand	9904		618	20.3
4		Washita-Fredericksburg	Dense Calc/Sand	9906		0.0	9.1
4		Washita-Fredericksburg	Sand	9907		510.0	25.5
3		Washita-Fredericksburg	Sand	9916		391	20.3
4		Washita-Fredericksburg	Sand	9917		200.0	23.3
2		Washita-Fredericksburg	Sand/Shale	9921		1.9	12.7
2		Washita-Fredericksburg	Sand	9928		274	24
4		Washita-Fredericksburg	Sand	9928		571.0	23.8

Table 2-7 (continued)

Well No.	Core No.	Formation Sampled	Dominant Lithology	Depth (ft)	Core Plug Samples	Average Air Permeability (md)	Average Porosity (%)
3		Washita-Fredericksburg	Sand	9929		419	19.7
4		Washita-Fredericksburg	Calc/Sand	9930		84.0	18.6
4		Washita-Fredericksburg	Calc/Sand	9932		72.0	21.6
1		Washita-Fredericksburg	Sand	9932-9950	10	196.17	27.72
2		Washita-Fredericksburg	Sand	9934		*	21.9
3		Washita-Fredericksburg	Sand	9938		400	20.9
4		Washita-Fredericksburg	Sand	9938		558.0	22.1
4		Washita-Fredericksburg	Sand	9940		614.0	22.5
4		Washita-Fredericksburg	Calc/Sand	9942		238.0	21.4
4		Washita-Fredericksburg	Calc/Sand	9948		78.0	20.8
4		Washita-Fredericksburg	Shale	9952		0.0	2.7
3		Washita-Fredericksburg	Sand/Silt/calcite cement	9952		0.01	4.3
4		Washita-Fredericksburg	Calc/Sand	9956		32.0	18.9

Table 2-7 (continued)

Well No.	Core No.	Formation Sampled	Dominant Lithology	Depth (ft)	Core Plug Samples	Average Air Permeability (md)	Average Porosity (%)
4		Washita-Fredericksburg	Calc/Sand	9958		46.0	19.4
2		Washita-Fredericksburg	Sand	9962		449	23
3		Washita-Fredericksburg	Sand/Siderite cement	9962		39	17.7
4		Washita-Fredericksburg	Calc/Sand	9962		71.0	20.2
4		Washita-Fredericksburg	Calc/Sand	9964		63.0	19.7
4		Washita-Fredericksburg	Sand	9968		578.0	23.6
4		Washita-Fredericksburg	Sand	9970		620.0	24.2
2		Washita-Fredericksburg	Sand	9970		324	23.5
3		Washita-Fredericksburg	Sand/Quartz and Siderite cement	9970		35	14.7
4		Washita-Fredericksburg	Calc/Sand	9982		142.0	21.3
4		Washita-Fredericksburg	Sand	9984		117.0	21
2	5	Washita-Fredericksburg	Shale/Sand	9985-10045	48	427.28	23.52
3		Washita-Fredericksburg	Sand/quartz and carbonate cement	9992		18	14.1

Table 2-7 (continued)

Well No.	Core	Formation Sampled	Dominant Lithology	Depth (ft)	Core Plug	Average Air	Average Porosity (%)
3		Washita-Fredericksburg	Sand/Laminated	9996		47	17.8
3		Washita-Fredericksburg	Sand/Laminated	10008		0.14	10.4
3		Washita-Fredericksburg	Sand	10016		259	20.2
3		Washita-Fredericksburg	Sand	10023		508	20.4

Table 2-8
Chemours DeLisle Plant
Injection Well No. 2
X-Ray Diffraction Analysis Results (in Wt. %)

Depth	9908A	9908B	9910	9915	9920	9939	10000A	10000B	10025A	10025B
Quartz	71	71	65	68	62	74	69	70	64	67
Feldspar	6	6	8	8	7	6	8	8	10	9
Dolomite	2	2	2	2	5	2	3	3	1	1
Kaolinite	10	10	12	10	13	10	10	8	10	12
Illite	4	4	6	4	5	4	4	2	8	6
Smectite and Mixed Layer Clay	5	5	5	6	6	2	4	7	5	3
Chlorite	2	2	2	2	2	2	2	2	2	2

Reference: Halliburton, 1979, Mineral content of cores from DeLisle Injection Well 2 [0109692].

Table 2-9
Chemours DeLisle Plant
Injection Well No. 5 Washita-Fredericksburg
X-Ray Diffraction Analysis Results (in Wt. %)

Sample No.	129 - 140	141 - 150	151 - 160	161 - 170	171 - 180	181 - 190	191 - 200	201 - 210	211 - 218
Depths	9,817-29	9,829-39	9,839-49	9,849-59	9,859-69	9,869-79	9,879-89	9,889-99	9,899-9,907
Quartz	90	95	93	92	92	91	86	91	82
Feldspar									
Plagioclase	7.0	3.5	5.3	6.3	5.4	5.7	9.7	6.8	5.6
K-spar	1.9	0.6	0.8	1.1	1	0.3	1.6	2.1	1.3
Calcite	0.1	0	0	0	0	0.1	0	0	7.9
Dolomite	0 - 1	0	0 - 1	0 - 1	0 - 7	0 - 2	0 - 3	0 - 1	0 - 5
Siderite	0	0	0	0	0	0.5	0.5	0	0
Kaolinite	1	1	1	1	1 - 2	1 - 2	1 - 2	1	1
Illite	1	1	1	1	1	1 - 3	1	1	1 - 3
Chlorite	0	0	0.1	0.4	0.2	0.1	0.1	0.1	0.3
Smectite	0	0	0	0	0.1	0.2	0.2	0	0.3

Reference: Envirocorp, 1983, Mineral content of cores from DeLisle Injection Well 5--Draft report.

Table 2-10
Chemours DeLisle Injection Well No. 5
Average Reservoir Properties of Sampled Zones

Core No.	Formation Sampled	Dominant Lithology	Depth (ft)	Core Samples	Plug	Average Air Permeability (md)	Average Porosity (%)
1	Midway	Shale	6,912 - 6,942	18		2.45	16
2	Selma	Chalk	7,679 - 7,711	31		0.084	8
3	Eutaw	Shale	8,311 - 8,340	10		0.766	7
4	Tuscaloosa (Upper/Middle)	Shale	8,785 - 8,815	--		--	--
5	Tuscaloosa (Lower)		9,100 - 9,132	14		65.5	17
6	Tuscaloosa (Massive)	Sand	9,386 - 9,418	32		2,100.0	24
7	Washita-Fredericksburg	Shale/Silt/Sand	9,606 - 9,637	15		0.631	8
8	Washita-Fredericksburg	Shale	9,667 - 9,697	7		0.209	6
9	Washita-Fredericksburg	Sand	9,817 - 9,849	31		1,024.0	23
10	Washita-Fredericksburg	Sand	9,849 - 9,907	58		799.0	21

Note: Data obtained from Envirocorp Analysis Report, May 1983.

Table 2-11

Geologic Column and Hydrologic Characteristics of Aquifers in Mississippi (after Gandl, 1982)

Era	System	Series	Group	Formation	Lithology	Thickness (ft)	Water Bearing Characteristics	Transmissivity (ft ² /d)	Specific Conductance (gal/min/ft)	Hydraulic Conductivity (ft/d)	Mineral Potential Type	Mineral Potential Location		
Cenozoic	Quaternary	Holocene		Mississippi River Valley Alluvium	Silty clay, sand, gravel	50 – 200	Mississippi River Valley alluvial aquifer	13,000 – 79,000	10 - 168	170 – 190	Sand and gravel	Throughout outcrop area		
		Pleistocene		Loess	Silt	--	Not an aquifer	--	--	--	--	--	--	
				Terrace Deposits (includes coastal deposits)	Sand, gravel silt and clay	--	Minor aquifers	--	--	--	--	--	--	--
	Tertiary	Pliocene		Citronelle Fm	Clay, sand and gravel	0 – 100	Citronelle aquifers	4,000 – 13,000	6.2 - 66	82 - 200	gravel	Throughout outcrop area		
				Graham Ferry Fm	Clay and sand	0 – 100	Local aquifer							
		Miocene		Pascagoula Fm	Sand and clay	0 – 5000	Miocene aquifer system	13,000	Up to 30	95	Minor amounts of lignite	Scattered throughout		
				Hattiesburg FM	Sand and clay									
				Catahoula SS	Sand and clay									
				Paynes Hammock Sand	Sandy marl, clay and silty limestone	20	Not an aquifer	--	--	--	--	--	--	
				Chickasawhay Ls	Impure limestone, marl and clay	30	Not an aquifer	--	--	--	--	--	--	--
		Oligocene	Vicksburg		Bucatanna Fm	clay	--	Confining unit	--	--	--	--	--	--
					Byram Fm	Clay, marl, limestone and sand	100 - 250	Oligocene aquifer system	120 - 3300	1.5 - 12	3 - 60	Glauconite and bentonite	Outcrop area	
				Glendon Fm										
	Marinna Fm		Silty limestone											
	Mint Spring Fm		Sandy marl											
	Forest Hill Fm		Clay and marl in extreme east											
	Red Bluff Fm		Sand and clay elsewhere											

Table 2-12
Chemours DeLisle Plant
Freshwater Sand Depths in Harrison County, Mississippi
(Data from Water Well 1 & Monitor Well No. 1 Electric Log)

Major Sand Unit	Monitor Well 1 Log Depths (feet)
Aquifer 1 ¹	640 – 980
Aquifer 2 ¹	1,530 – 1,580
Aquifer 3 ¹	1,640 – 1,790
Aquifer 4 ¹	1,885 – 1,990
Aquifer 5 ¹	2,010 – 2,060
Aquifer 6 ¹	2,300 – 2,345
Aquifer 7	2,370 – 2,480
Brackish Transition Aquifer 8	2,500 – 2,750
Base of Lowermost USDW – 2,750	

1. A.C. Barlow 1/28/74 Memo

Table 2-13
Chemours DeLisle Plant
Chemical Quality of Water from Miocene Aquifers

Parameter	Maximum	Minimum	Median
Bicarbonate	37.0	155.0	480.0
Dissolved solids	67.0	195.0	1,030.0
Hardness (as CaCO ₃)	0.0	5.0	80.0
pH (standard units)	6.4	7.7	9.0
Calcium	0.0	1.1	21.0
Chloride	2.0	4.6	432.0
Fluoride	0.0	0.2	1.1
Iron	0.0	0.08	2.9
Magnesium	0.0	0.3	6.7
Nitrate	0.0	0.1	2.7
Potassium	0.2	0.9	14.0
Silica	12.0	31.0	61.0
Sodium	5.2	66.0	391.0
Sulfate	0.0	8.6	13.0

Constituents and hardness in milligrams per liter.
 Values calculated from 99 analyses.
 From: Newcombe, 1975.

Table 2-14
Chemours DeLisle Plant
Freshwater Aquifer Characteristics

Age	Depth (feet)	Thickness (feet)	TDS (mg/L)
Miocene	640 - 980	340	187
Miocene	1,530 - 1,580	50	N/A
Miocene	1,640 - 1,790	150	214
Miocene	1,885 - 1,990	105	N/A
Miocene	2,010 - 2,060	50	N/A
Miocene	2,300 - 2,345	45	N/A

N/A = Not Analyzed

From: Clark, 1986

Table 2-15**Analytical Results of DeLisle Monitoring Well Water Samples**Analytical Results of **DeLisle Plant Water Well #1** (USGS ID N104) Samples 2013-2016

Latitude 30.3834; Longitude -89.3088; Township 8S, Range 13W, Section 5; Screen Base Depth 1,755 ft

Quarterly Report	Chlorides, mg/l	Total Dissolved Solids, mg/l	Total Mercury, mg/l	Total Cadmium, mg/l	Total Chromium, mg/l	Total Iron, mg/l	Total Lead, mg/l	Total Vanadium, mg/l	pH, s.u.	Specific Conductance, micro-seimen
1Q2016	42.2	275	<0.0020	<0.005	<0.010	<0.050	<0.001	<0.050	8.78	492
4Q2015	44.0	271	<0.0020	<0.005	<0.010	<0.050	<0.001	<0.050	8.66	1240
3Q2015	45.2	245	<0.0020	<0.005	<0.010	0.072	<0.001	<0.050	8.73	463
1Q2015	50.9	285	<0.0020	<0.005	<0.010	<0.050	<0.001	<0.050	8.20	482
4Q2014	48.7	248	<0.0020	<0.005	<0.010	<0.050	<0.001	<0.050	8.83	483
3Q2014	45.8	260	<0.0020	<0.005	<0.010	<0.050	<0.050	<0.050	8.89	474
2Q2014	49.1	391	<0.0020	<0.005	<0.010	<0.050	<0.050	<0.050	8.73	474
1Q2014	45.5	274	<0.0020	<0.005	<0.010	0.053	<0.001	<0.050	8.23	472
4Q2013	50.0	271	<0.0020	<0.005	<0.010	<0.050	<0.050	<0.050	8.71	478
3Q2013	47.4	265	<0.0020	<0.005	<0.010	<0.050	<0.050	<0.050	8.34	479
2Q2013	50.8	261	<0.0020	<0.003	<0.005	<0.025	<0.025	<0.025	8.27	483
1Q2013	48.8	320	<0.0020	<0.005	<0.010	<0.050	<0.050	<0.050	8.33	480

Table 2-15 (Continued)Analytical Results of **DeLisle Plant Water Well #2** (USGS ID N291) Samples 2013-2016

Latitude 30.3831; Longitude -89.3055; Township 8S, Range 13W, Section 4; Screen Base Depth 1,760 ft

Quarterly Report	Chlorides, mg/l	Total Dissolved Solids, mg/l	Total Mercury, mg/l	Total Cadmium, mg/l	Total Chromium, mg/l	Total Iron, mg/l	Total Lead, mg/l	Total Vanadium, mg/l	pH, s.u.	Specific Conductance, micro-seimen
1Q2016	54.2	286	<0.0020	<0.005	<0.010	<0.050	<0.001	<0.050	8.60	514
4Q2015	53.8	292	<0.0020	<0.005	<0.010	<0.050	<0.001	<0.050	8.53	983
3Q2015	60.7	285	<0.0020	<0.005	<0.010	0.072	<0.001	<0.050	8.67	505
1Q2015	57.7	288	<0.0020	<0.005	<0.010	<0.050	<0.001	<0.050	8.20	506
4Q2014	109	270	<0.0020	<0.005	<0.010	<0.050	<0.001	<0.050	8.81	512
3Q2014	58.0	319	<0.0020	<0.005	<0.010	0.098	<0.050	<0.050	8.67	505
2Q2014	60.4	286	<0.0020	<0.005	<0.010	0.143	<0.050	<0.050	8.63	518
1Q2014	58.2	275	<0.0020	<0.005	<0.010	0.120	<0.001	<0.050	8.15	508
4Q2013	61.3	287	<0.0020	<0.005	<0.010	<0.050	<0.050	<0.050	8.64	508
3Q2013	59.6	289	<0.0020	<0.005	<0.010	<0.050	<0.050	<0.050	8.18	510
2Q2013	62.1	276	<0.0020	<0.003	<0.005	0.027	<0.025	<0.025	8.23	513
1Q2013	60.2	296	<0.0020	<0.005	<0.010	<0.050	<0.050	<0.050	8.09	518

Table 2-15 (Continued)Analytical Results of **DeLisle Elementary Well** (USGS ID N286) Samples 2013-2015

Latitude 30.3775; Longitude -89.2685; Township 8S, Range 13W, Section 8; Screen Base Depth 557 ft

Quarterly Report	Chlorides, mg/l	Total Dissolved Solids, mg/l	Total Mercury, mg/l	Total Cadmium, mg/l	Total Chromium, mg/l	Total Iron, mg/l	Total Lead, mg/l	Total Vanadium, mg/l	pH, s.u.	Specific Conductance, micro-seimen
2Q2015	19.0	311	<0.0020	<0.001	<0.001	<0.025	<0.001	<0.001	8.85	536
2Q2014	21.6	318	<0.0020	<0.005	<0.001	<0.050	<0.001	<0.005	8.79	521
2Q2013	20.7	304	<0.0020	<0.005	<0.010	<0.050	<0.001	<0.050	8.75	530

Analytical Results **City of Pass Christian Well at North and Market Streets** (USGS ID N327) Samples 2013-2015

Longitude 30.3256; Longitude -89.2517; Township 8S, Range 13W Section 25; Screen Base Depth 852 ft

Quarterly Report	Chlorides, mg/l	Total Dissolved Solids, mg/l	Total Mercury, mg/l	Total Cadmium, mg/l	Total Chromium, mg/l	Total Iron, mg/l	Total Lead, mg/l	Total Vanadium, mg/l	pH, s.u.	Specific Conductance, micro-seimen
2Q2015	42.6	362	<0.0020	<0.001	<0.001	<0.025	<0.001	<0.001	9.01	663
2Q2014	47.4	368	<0.0020	<0.005	<0.001	<0.050	<0.001	<0.050	8.89	641
2Q2013	47.0	361	<0.0020	<0.005	<0.001	0.263	0.010	<0.050	8.97	651

Table 2-15 (Continued)**Analytical Results of City of Pass Christian Bayview Avenue (Fire Department) Well (USGS ID O006) Samples 2013-2015**

Latitude 30.3267; Longitude -89.2222; Township 8S, Range 13W, Section 19; Screen Base Depth 891 ft

Quarterly Report	Chlorides, mg/l	Total Dissolved Solids, mg/l	Total Mercury, mg/l	Total Cadmium, mg/l	Total Chromium, mg/l	Total Iron, mg/l	Total Lead, mg/l	Total Vanadium, mg/l	pH, s.u.	Specific Conductance, micro-seimen
2Q2015	32.6	360	<0.0020	<0.001	<0.001	0.030	<0.001	<0.001	8.97	641
2Q2014	34.6	352	<0.0020	<0.005	<0.001	<0.050	<0.001	<0.050	8.94	622
2Q2013	34.3	349	<0.0020	<0.005	<0.001	<0.050	0.002	<0.050	8.99	632

Analytical Results City of Diamondhead North Well #3 (USGS ID N470) Samples 2013-2015

Latitude 30.3794; Longitude -89.3202; Township 8S, Range 14W, Section 35; Screen Base Depth 720 ft

Quarterly Report	Chlorides, mg/l	Total Dissolved Solids, mg/l	Total Mercury, mg/l	Total Cadmium, mg/l	Total Chromium, mg/l	Total Iron, mg/l	Total Lead, mg/l	Total Vanadium, mg/l	pH, s.u.	Specific Conductance, micro-seimen
2Q2015	70.8	294	<0.0020	<0.001	<0.001	0.251	0.003	<0.001	8.14	555
2Q2014	4.96	186	<0.0020	<0.005	<0.001	<0.050	<0.001	<0.050	8.50	298
2Q2013	5.32	191	<0.0020	<0.005	<0.001	<0.050	0.003	<0.050	8.66	306

Table 2-15 (Continued)Analytical Results of **City of Bay St. Louis Harry Street Well** (USGS ID K377) Samples 2013-2015

Latitude 30.3248; Longitude -89.3414, Township 8S, Range 14W, Section 41; Screen Base Depth 1,062 ft

Quarterly Report	Chlorides, mg/l	Total Dissolved Solids, mg/l	Total Mercury, mg/l	Total Cadmium, mg/l	Total Chromium, mg/l	Total Iron, mg/l	Total Lead, mg/l	Total Vanadium, mg/l	pH, s.u.	Specific Conductance, micro-seimen
2Q2015	59.5	401	<0.0020	<0.001	<0.001	<0.025	<0.001	<0.001	8.93	734
2Q2014	58.2	396	<0.0020	<0.005	<0.001	<0.050	<0.001	<0.050	8.54	711
2Q2013	51.2	384	<0.0020	<0.005	<0.001	<0.050	<0.001	<0.050	8.91	724

Analytical Results **City of Bay St. Louis St. Charles Street Well** (USGS ID K004) Samples 2013-2015

Latitude 30.3017; Longitude -89.3369, Township 8S, Range 13W, Section 30; Screen Base Depth 1,210 ft

Quarterly Report	Chlorides, mg/l	Total Dissolved Solids, mg/l	Total Mercury, mg/l	Total Cadmium, mg/l	Total Chromium, mg/l	Total Iron, mg/l	Total Lead, mg/l	Total Vanadium, mg/l	pH, s.u.	Specific Conductance, micro-seimen
2Q2015	34.3	393	<0.0020	<0.001	<0.001	<0.025	<0.001	<0.001	8.93	734
2Q2014	36.7	413	<0.0020	<0.005	<0.001	<0.050	<0.001	<0.050	8.85	708
2Q2013	46.8	346	<0.0020	<0.005	<0.001	<0.050	0.003	<0.050	8.23	702

Table 2-16
Chemours DeLisle Plant
Chemical Analysis of Water, Production Well No. 4

Constituent	Value	Units
Arsenic	< 0.001	mg/L
Calcium	6.1	mg/L
Chloride	138.0	mg/L
Copper	< 0.05	mg/L
Cyanide	0.53	mg/L
Fluoride	0.23	mg/L
Iron	0.1	mg/L
Magnesium	1.0	mg/L
Manganese	< 0.05	mg/L
N-Nitrate-aqueous	0.846	mg/L
Phenols (color. aq.)	< 0.10	mg/L
Potassium	1.9	mg/L
Silica	8.9	mg/L
Sodium	204.0	mg/L
Sulfate (aqueous)	0.017	mg/L
Zinc	< 0.02	mg/L
Alkalinity (bicarbonate)	150.0	mg/L
Alkalinity (carbonate)	40.0	mg/L
Hardness	18.0	mg/L
Specific conductance	702.0	µmhos/cm
Total dissolved solids	436.0	mg/L
Total suspended solids	1.0	mg/L
pH	8.6	units
Specific gravity	1.0	mg/L

Date Sampled: January 10, 1990

Table 2-17
Chemours DeLisle Plant
Formation Fluid Analysis Waste Disposal Well No. 5
Tuscaloosa Massive Sand

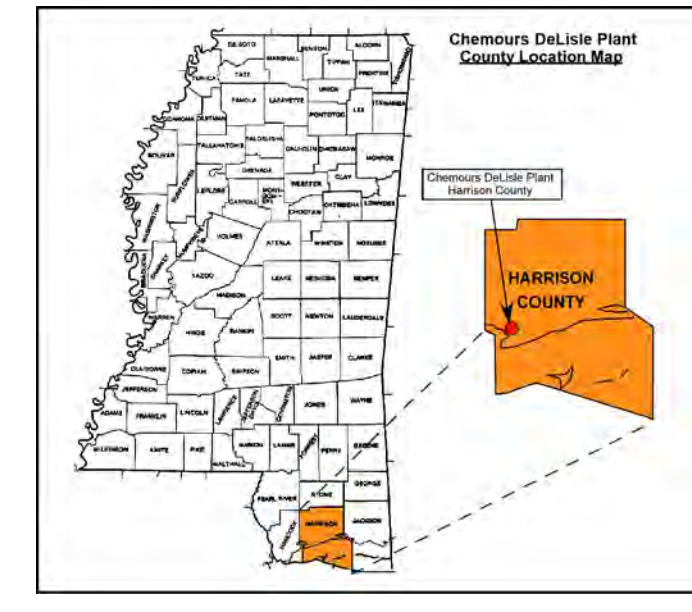
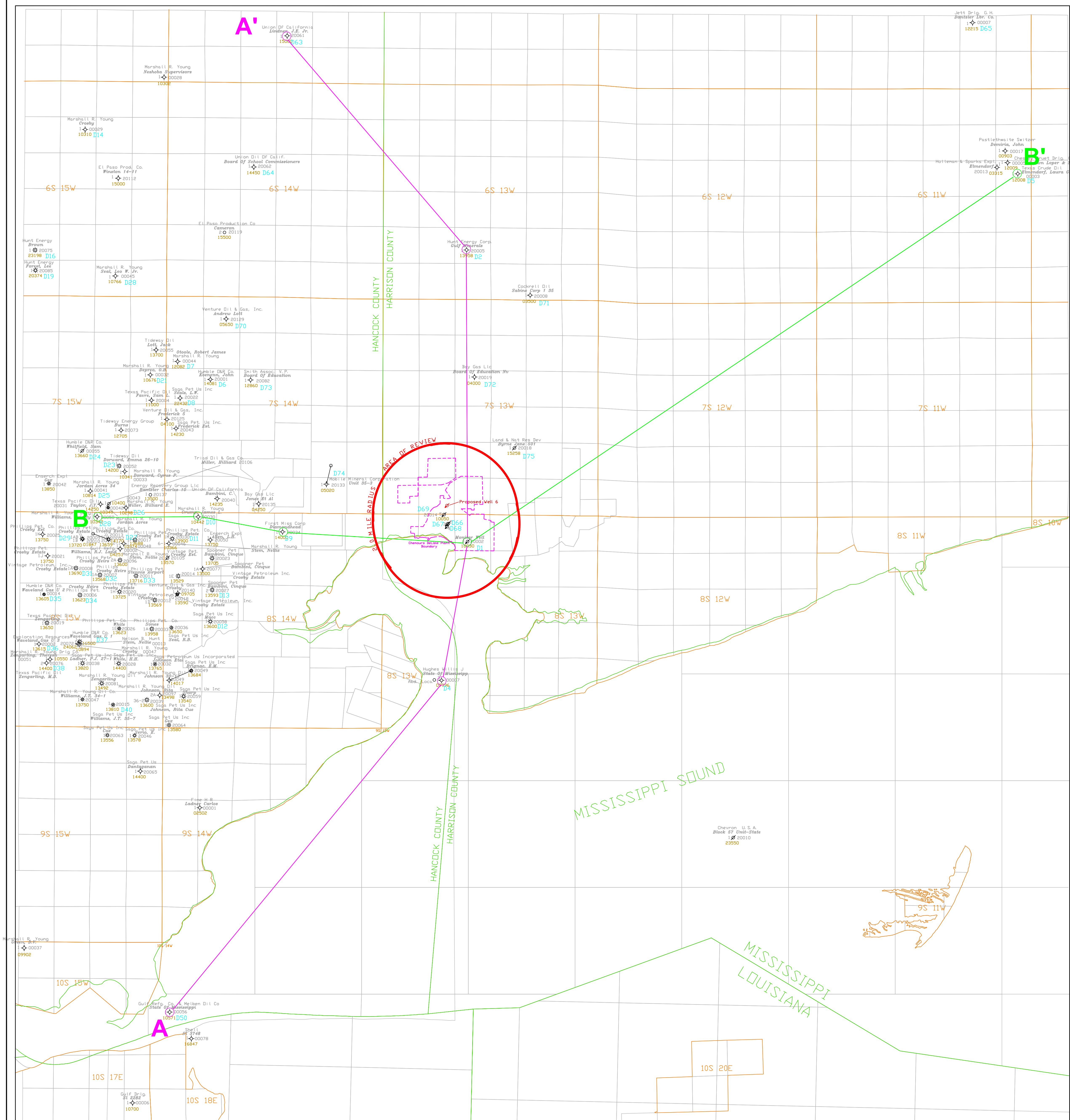
Constituent	Concentration	Units
Barium	4.3	ppm
Bromide	546.0	mg/L
Cadmium	0.007	ppm
Carbonate	199.0	mg/L
Chloride	71,750.0	mg/L
Cyanide	< 0.1	mg/L
Fluoride	0.42	mg/L
Nitrate	< 0.1	mg/L
Phosphate (total)	< 0.05	mg/L
Strontium	4.5	ppm
Sulfate	131.0	mg/L
Sulfite	< 10.0	mg/L
Specific gravity	1.085	g/cc
Total dissolved solids	105,000.0	mg/L
Total suspended solids	1,608.0	mg/L

Table 2-18

Chemours DeLisle Plant Sidetrack Injection Wells Reservoir Fluid Sampling Results

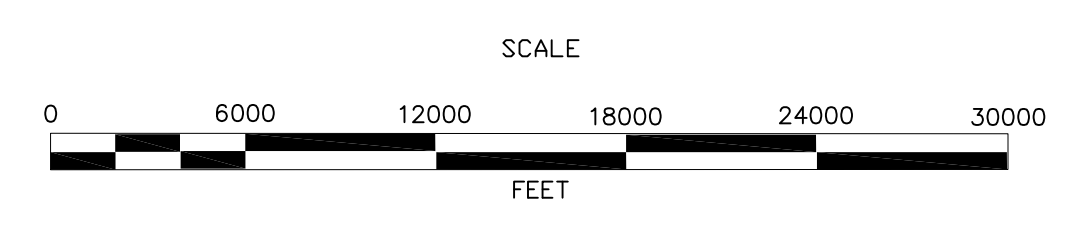
Constituents	units	Injection Well No. 2 Sidetrack No. 1				Tusc. Massive 01-15-99	Injection Well No. 3 Sidetrack No. 1				Injection Well No. 4 Sidetrack No. 1			
		WF-1 11-23-95	WF-2 11-23-95	WF-3 11-23-95	WF-4 11-23-95		WF-1 01-15-99	WF-2 01-15-99	WF-3 01-15-99	WF-1 06-28-95	WF-2 06-28-95	WF-3 06-28-95	WF-4 06-28-95	
Depth		9560'	9902'	9966'	9806'	9496'	9848'	9916'	9996'	9792'	9879'	9946'	9807'	
Total Organic Carbon	(mg/l)	400.0	<10	40.0	<10	157.00	104.00	59.00	194.00	128.0	48.4	99.9	123.0	
Aluminum	(mg/l)	19.0	7,170.0	45.9	3,770.0	2.31	804.00	133.00	5.95	6,036.0	4,988.0	4,462.0	2,890.0	
Antimony	(mg/l)	--	--	--	--	--	--	--	--	<0.25	<0.25	<0.25	<0.25	
Arsenic	(mg/l)	<0.01	<0.01	<0.1	<0.01	<0.007	0.086	0.184	<0.07	0.625	<0.125	0.69	<0.125	
Barium	(mg/l)	8.18	4.08	45.00	55.10	23.2	8.4	22.3	15.0	11.60	51.30	16.20	20.30	
Beryllium	(mg/l)	<0.02	<0.02	<0.02	<0.02	<0.001	0.085	0.078	<0.001	1.90	3.04	1.26	0.89	
Boron	(mg/l)	23.5	<0.5	316	<0.5	19.6	95.9	50.1	27.8	--	--	--	--	
Cadmium	(mg/l)	<0.01	<0.01	<0.01	<0.01	<0.01	0.030	<0.01	<0.01	<0.25	0.27	<0.25	<0.25	
Chromium	(mg/l)	0.10	344.0	1.10	419.0	<0.02	21.200	3.320	<0.02	160.0	90.4	102.0	20.8	
Cobalt	(mg/l)	0.34	6.6	1.28	50.5	1.81	1.7	11.9	3.05	8.98	18.2	14.0	12.01	
Copper	(mg/l)	5.89	13.5	5.04	97.8	0.019	<0.04	1.490	0.310	<1.50	2.21	4.75	<1.50	
Iron	(mg/l)	134	53,500	696	62,100	96.6	27,200	13,800	151	42,550	56,400	38,420	47,680	
Lead	(mg/l)	0.14	72.6	0.50	54.1	0.18	80.6	60.9	1.06	59.4	54.2	86.3	75.4	
Manganese	(mg/l)	5.3	2,860	24.1	2,800	8.897	1,902	1,066	8.09	1,858	2,029	1,758	2,251	
Mercury	(mg/l)	<0.005	0.009	<0.005	0.11	<0.0002	<0.0002	<0.0002	<0.0002	0.095	0.02	<0.0002	<0.0002	
Nickel	(mg/l)	1.86	58.4	6.31	261	1.25	13	0.95	1.11	24.2	41.6	32.7	13.9	
Selenium	(mg/l)	<0.05	<0.05	<0.05	<0.05	<0.09	<0.09	<0.09	<0.09	<0.125	<0.125	<0.125	<0.125	
Silver	(mg/l)	0.13	<0.02	<0.02	<0.02	0.24	0.35	0.34	0.26	<0.02	<0.02	<0.02	<0.02	
Strontium	(mg/l)	495	8.99	520	9.19	346	24.5	18.2	378	18.6	19.8	17.7	16.9	
Thallium	(mg/l)	<0.02	<0.02	<0.02	<0.02	<0.16	0.046	<0.4	<0.02	<0.25	<0.25	<0.25	<0.25	
Titanium	(mg/l)	0.26	0.06	0.08	55.9	<0.02	<0.02	<0.02	<0.4	2.64	3.26	3.13	3.22	
Vanadium	(mg/l)	0.12	377	1.06	504	<0.05	7.31	<0.05	<0.05	318	502	142	111	
Zinc	(mg/l)	4.26	85.6	5.32	82.3	5.64	95	53.3	7	57	89.6	71.6	65.9	
Chloride	(mg/l)	--	--	--	--	--	--	--	--	107,000	123,000	120,000	118,000	
Potassium	(mg/l)	800	1,420	1,547	547	721	880	1286	702	740	1,230	970	730	
Sodium	(mg/l)	50,500	16,900	50,000	15,100	30,740	6,120	6,860	32,620	10,600	7,300	11,700	11,100	
Acidity as CaCO3	(mg/l)	790	153,000	2,200	184,000	282	21,470	11,400	92	*see note	*see note	*see note	*see note	
Hardness (CaCO3)	(mg/l)	--	--	--	--	--	--	--	--	--	--	--	--	
Calcium	(mg/l)	129,000	1,320	13,500	467	16,630	11,690	7,520	16,900	1,820	4,697	7,486	6,920	
Magnesium	(mg/l)	1,140	1,450	1,210	1,380	831	2022	2432	1400	2,764	2,375	1,474	2,462	
Hardness as CaCO3	(mg/l)	--	--	--	--	--	--	--	--	15,927	21,508	24,763	27,418	
Resistivity	(ohm-cm)	9.60	11.00	9.50	6.70	6.44	9.65	6.31	6.55	2.31E-03	2.14E-03	1.97E-03	2.15E-03	
Specific Gravity (60/60)		1.110	1.180	1.120	1.190	1.090	1.190	1.190	1.100	1.1667	1.1876	1.1906	1.1806	
Total Dissolved Solids	(mg/l)	165,986	246,948	187,898	261,036	130,000	187,000	207,000	140,000	195,000	221,000	202,000	219,000	
Total Suspended Solids	(mg/l)	798	871	3045	176	172	90	290	244	427	876	376	374	
Viscosity	(cst)	1.00	1.00	1.00	1.00	0.88	1.19	1.26	0.90	1.19	1.29	1.30	1.25	
pH	(units)	5.13	2.32	4.32	<0.80	6.130	2.880	5.770	4.060	2.37	2.44	2.18	2.00	

APPENDICES



Legend

- Deviated Well Spot
- ◇ P&A Oil and Gas Well
- ◆ Injection Well
- ⚡ Proposed Injection Well
- ⊛ Gas Well
- Oil Well
- ⊘ Dry & Abandoned Well
- 4658 Post Numbers
- D40 Map ID Wells
- 11600 Total Depth
- 31290 API Number
- NDE Log Not Deep Enough
- NL No Log



Chemours The Chemours Company FC, LLC
Titanium Technologies
Harrison County, MS

Appendix 2-2: Cross Section Index Map
(A-A' and B-B')
Contour Interval = N/A

Base Map Prepared & compiled from Tobin International, Ltd. digital Map Data
Compiled & Drafted by: (ESSJ, WGR) Sandia Scale: 1" = 6000' Date: July 2016

GEOSTOCK SANDIA
ENTREPOSE

A

South

A'

North

D50
Gulf Ref. Co. & Melbren Oil Co.
#1 State of Mississippi
TD: 10,555'

D4
J. Willis Hughes
#3 State of Mississippi
TD: 10,015'

D1
Chemours
#1 Lester Earnest
(Monitor Well 1)
TD: 10,020'

D2
Hunt Energy
#1 Gulf Mineral
TD: 13,971'

D63
Union Oil of California
#1 J.E. Lindert, Jr. 27-11
TD: 15,240'

12.0 Miles

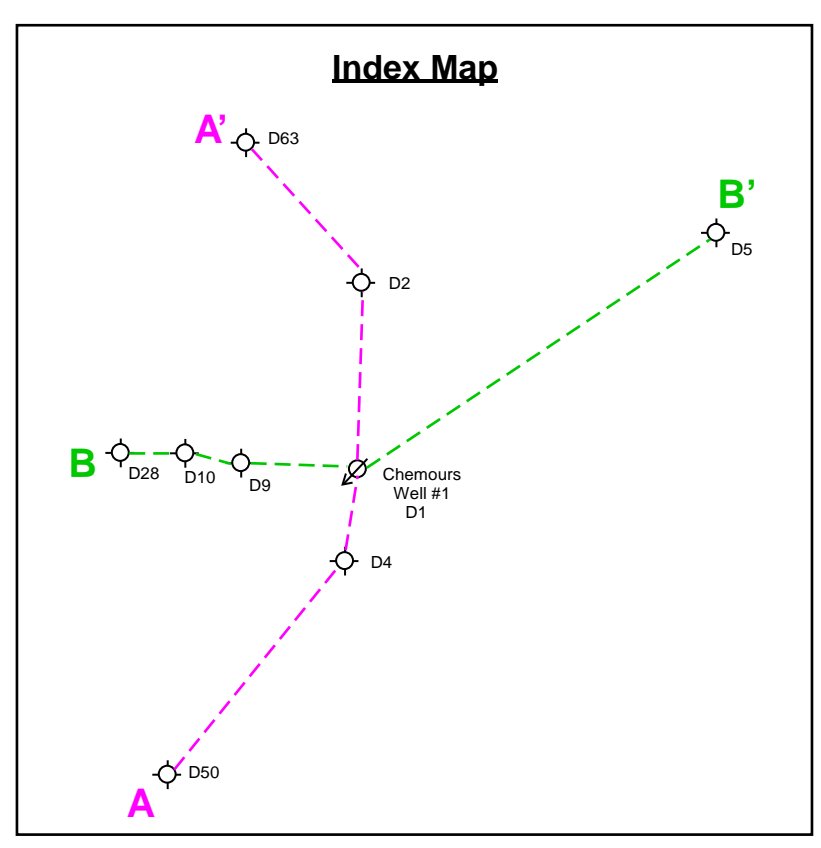
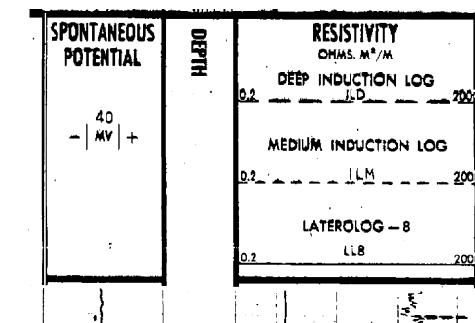
4.0 Miles

8.2 Miles

7.8 Miles

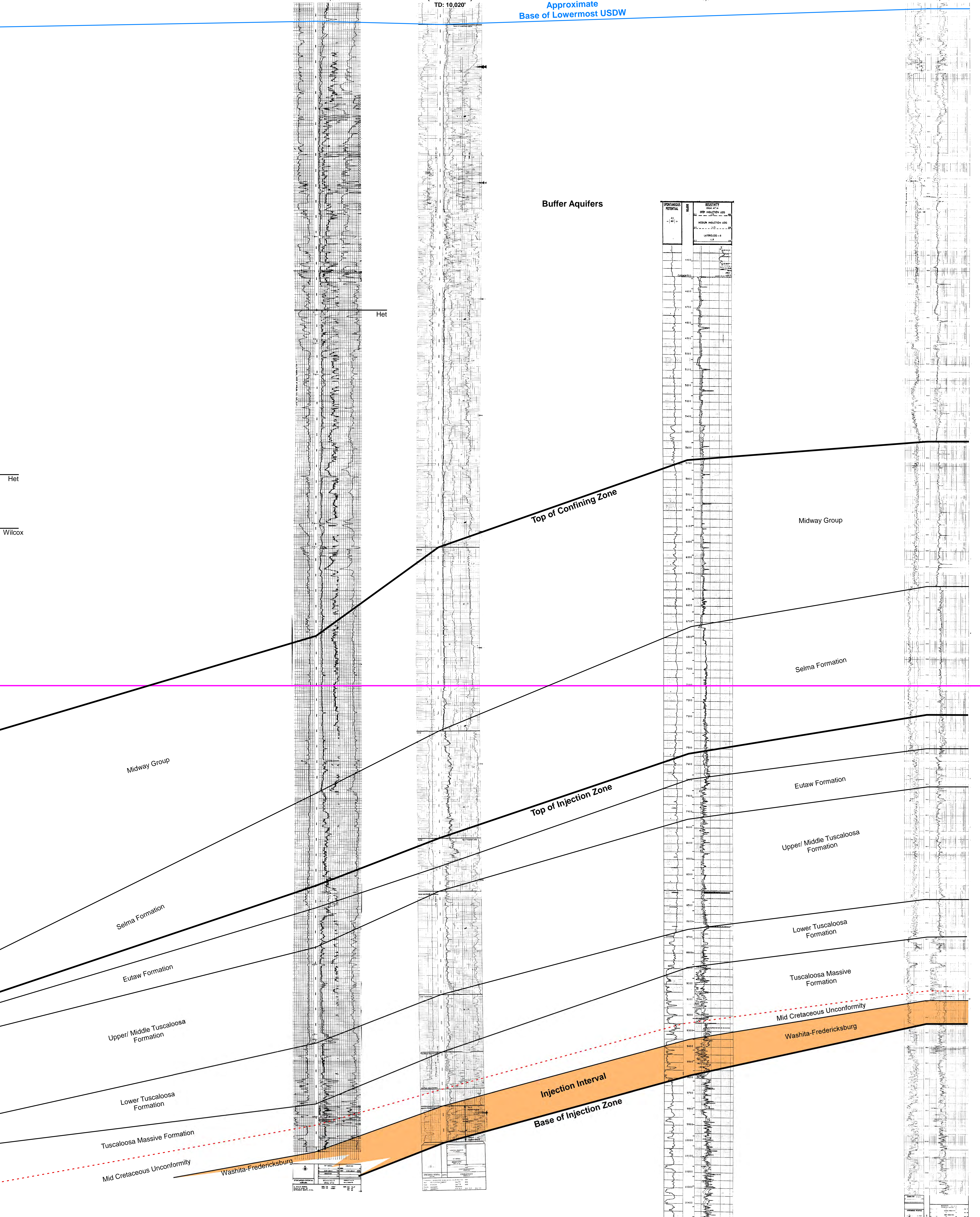
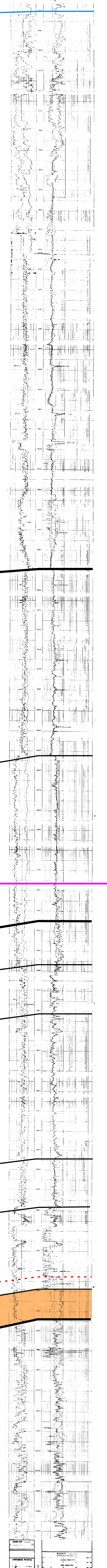
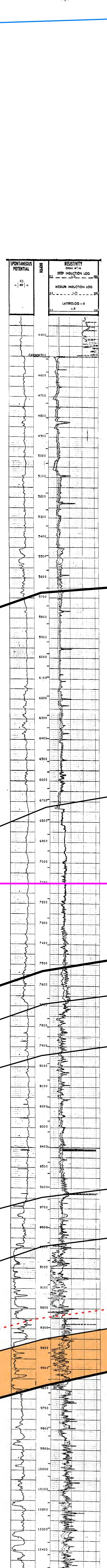
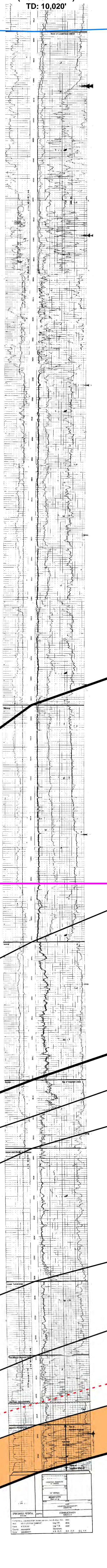
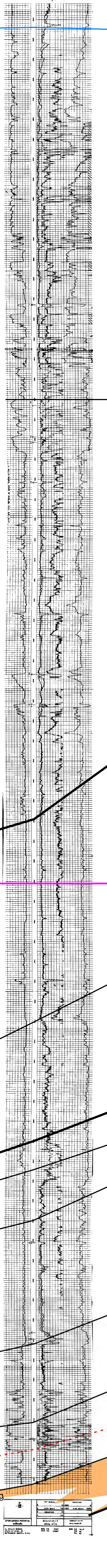
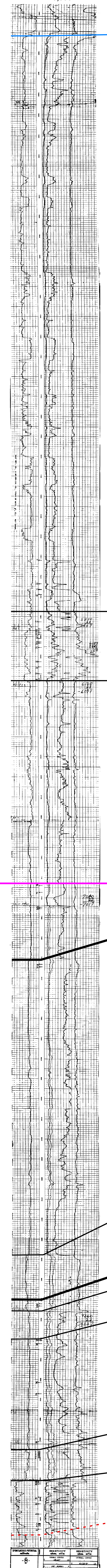
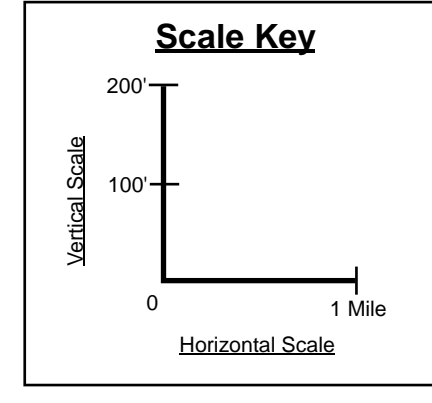
Approximate
Base of Lowermost USDW

Buffer Aquifers



-7000
Subsurface Datum

7000
Subsurface Datum



Chemours The Chemours Company FC, LLC
Titanium Technologies
Harrison County, Mississippi

Appendix 2-3
South - North
Structural Cross Section A-A'

Created by: ESSJ
Designed by: WDX, PWS, JUC
Scale: on Scale Key
Date: 7/2016

ENTREPOSE
GEOSTOCK SANDIA

ENTREPOSE: 2880 Enterspace Drive, Princeton, NJ 08542-3209, Tel: 609-334-4547, Fax: 609-334-3122

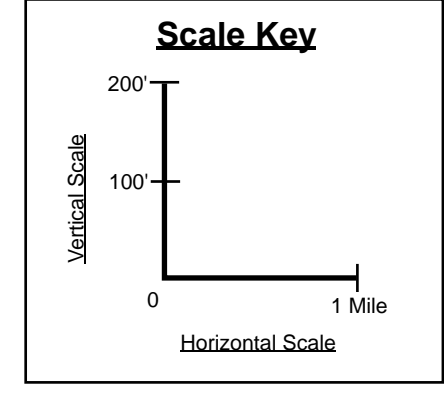
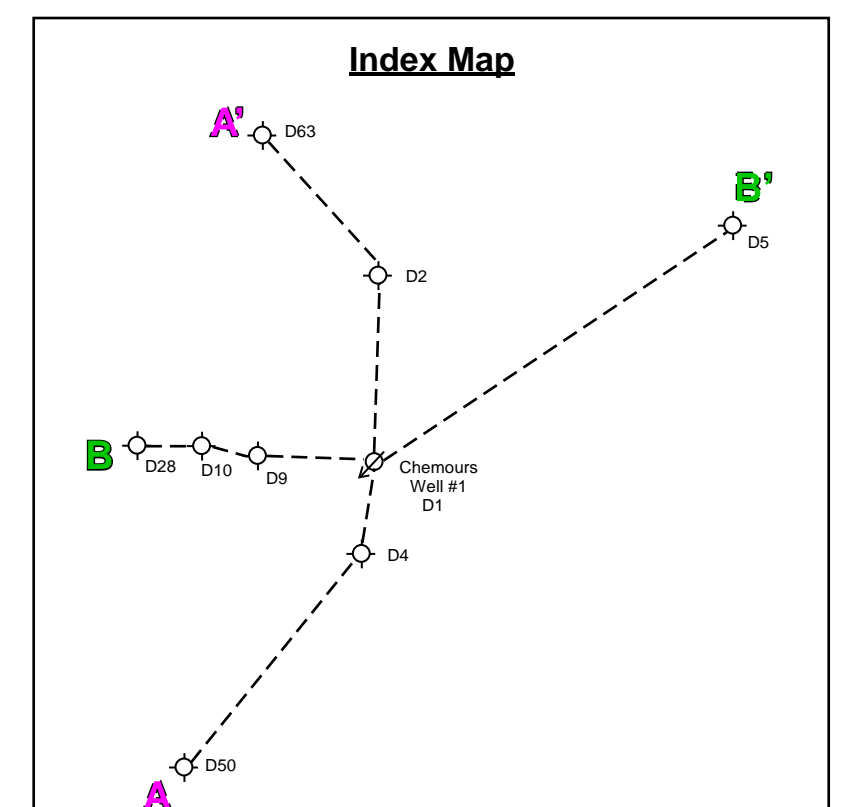
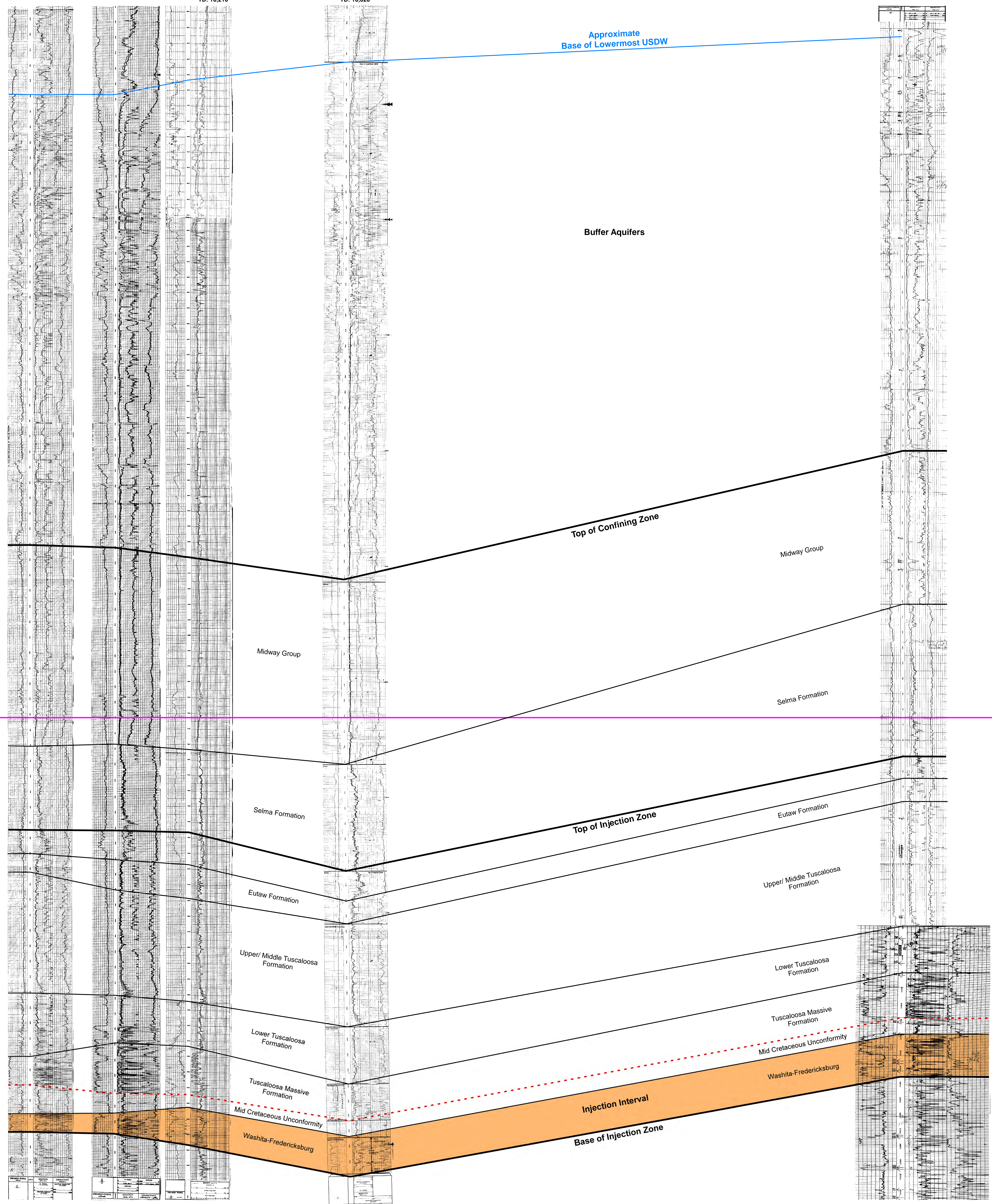
B

West

B'

East

D28 Marshall R. Young Drilling Co. #1 Trinity Williams TD: 10,342' 2.8 Miles D10 Marshall R. Young Drilling Co. #1 Crump TD: 10,442' 2.4 Miles D9 First Mississippi Corp. & Diamondhead Explor. #1 Diamondhead TD: 10,210' 5.1 Miles D1 Chemours #1 Lester Earnest (Monitor Well 1) TD: 10,020' 18.3 Miles D5 Texas Crude Oil Corp. #1 Laura C. Elmendorf TD: 12,038'

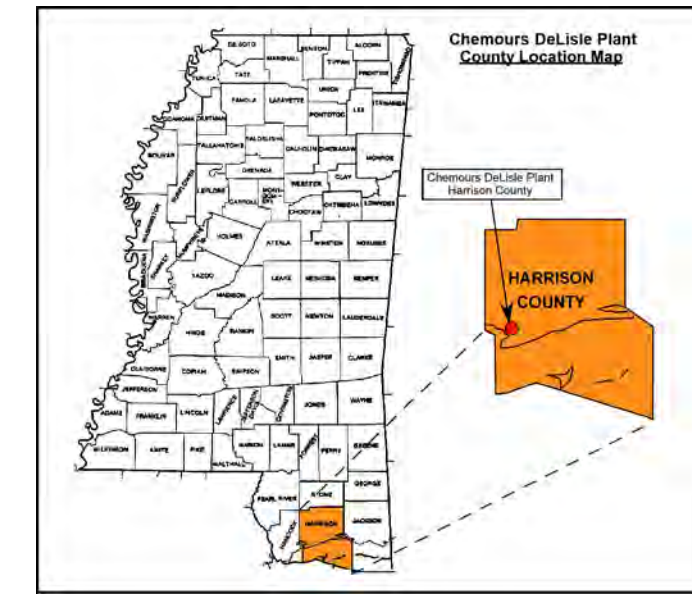
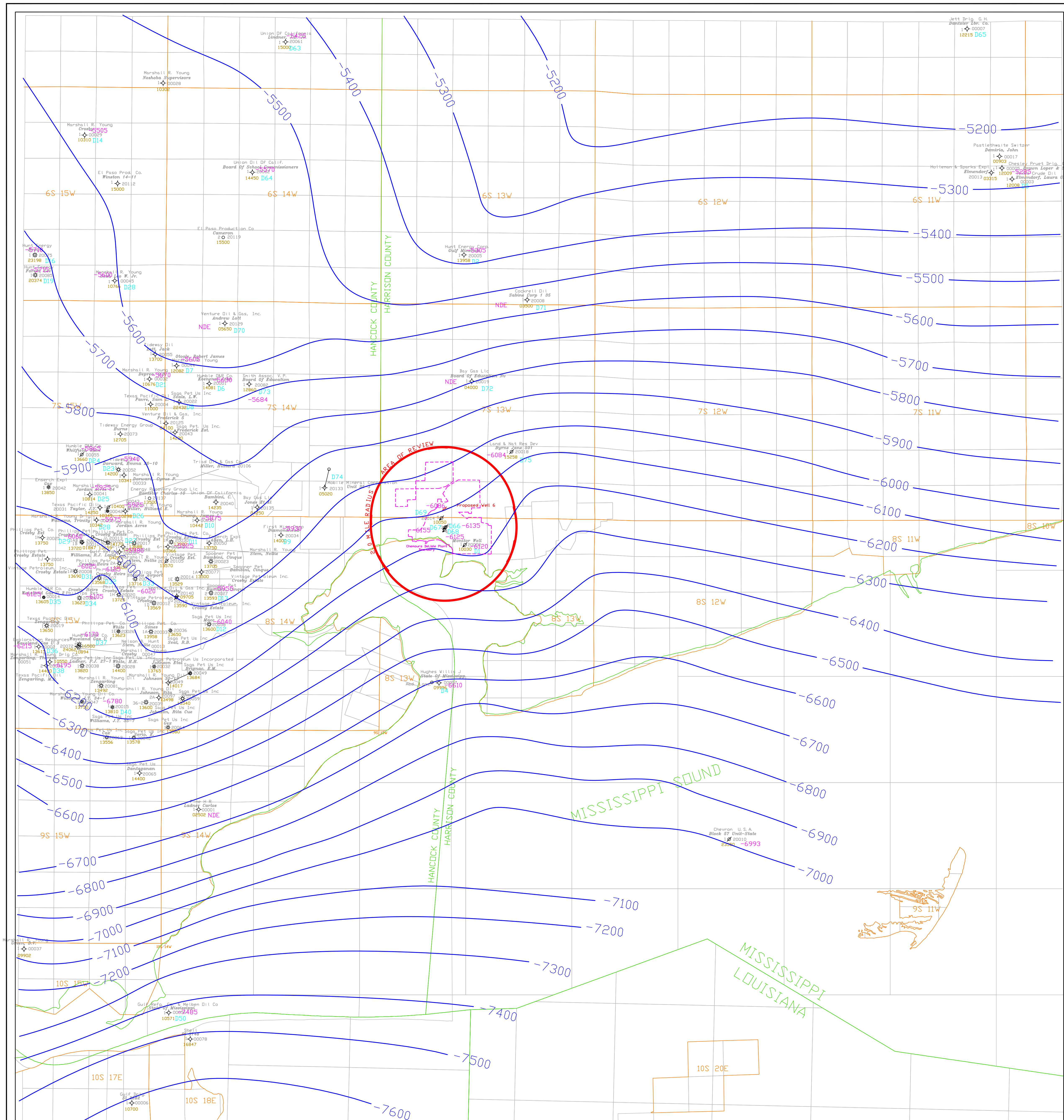


Chemours The Chemours Company FC, LLC
 Titanium Technologies
 Harrison County, Mississippi

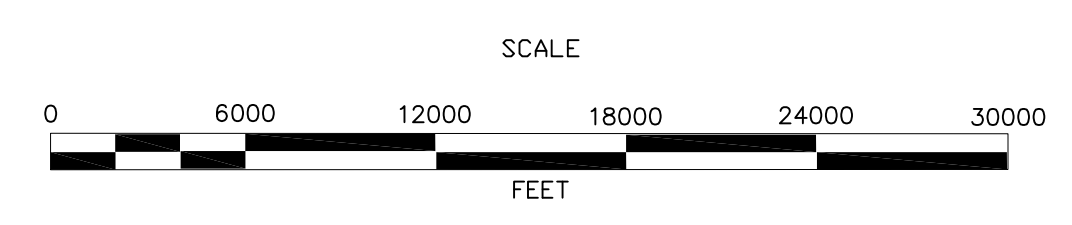
Appendix 2-4
 West - East
 Structural Cross Section B-B'

Created by: ESEJ
 Checked by: MFC, PRC, DUC Scale: on Scale Key Date: 7/2016

GEOSTOCK SANDIA
 ENTREPOSE
8000 Lakeside Drive, Suite 100, San Diego, CA 92123 USA, Tel: (619) 594-0461 Fax: (619) 491-9172



- Legend**
- Deviated Well Spot
 - ◇ P&A Oil and Gas Well
 - ◆ Injection Well
 - ⚡ Proposed Injection Well
 - ⊛ Gas Well
 - Oil Well
 - ⊘ Dry & Abandoned Well
 - 4658 Post Numbers
 - D40 Map ID Wells
 - 11600 Total Depth
 - 31290 API Number
 - NDE Log Not Deep Enough
 - NL No Log

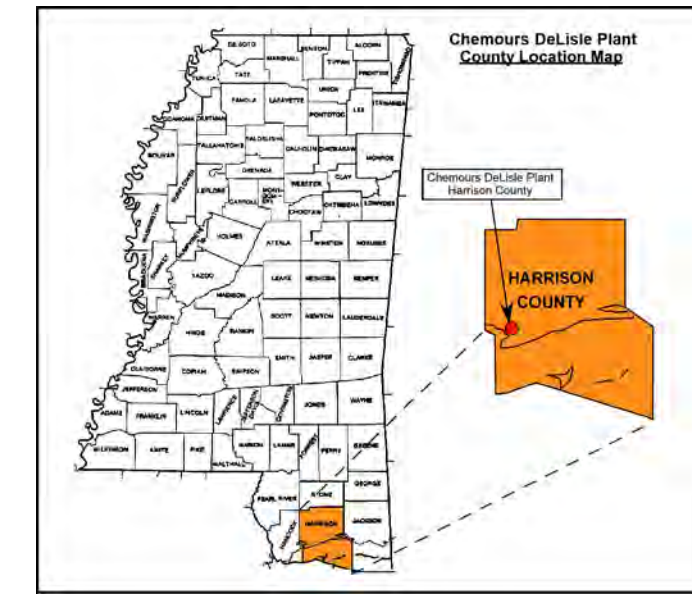
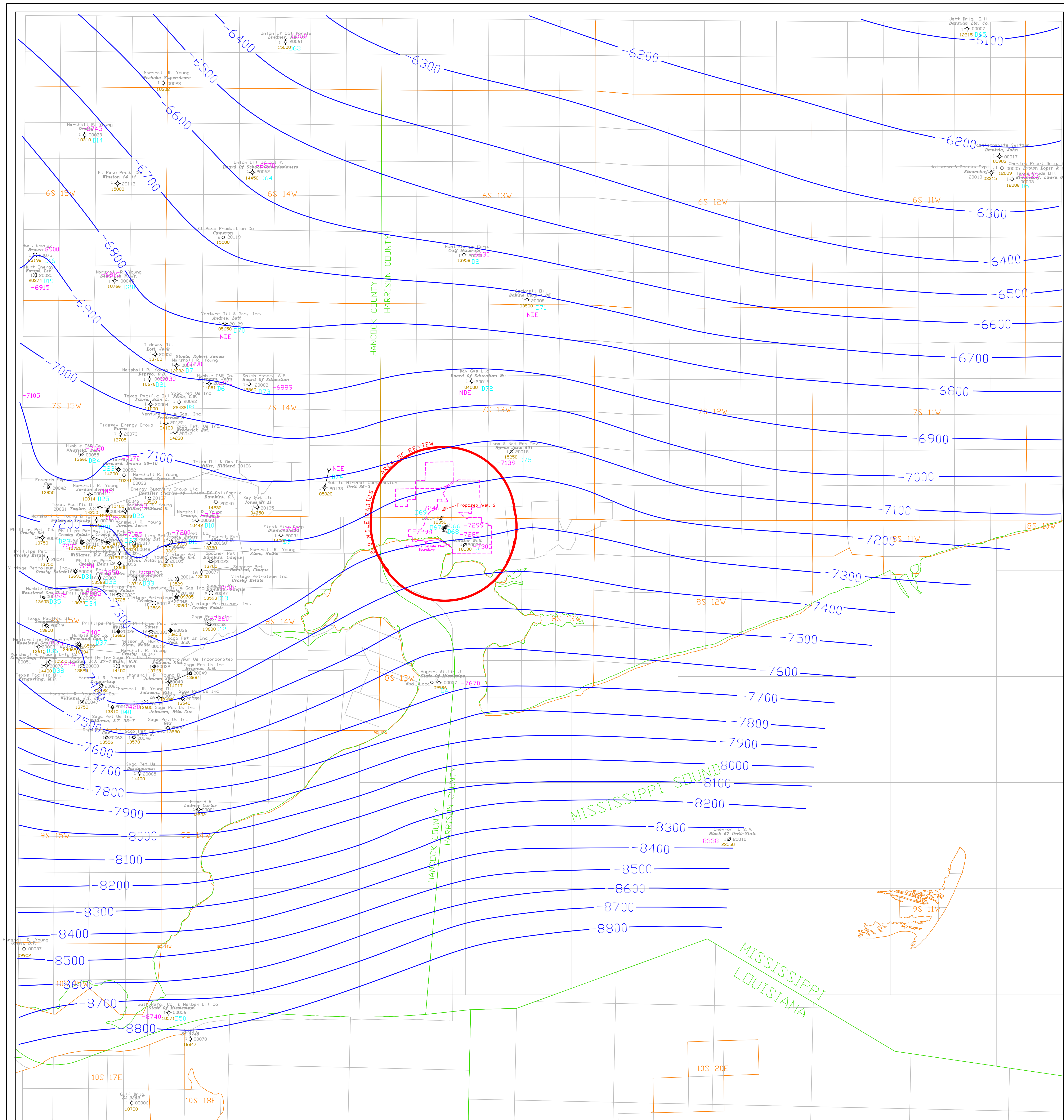


Chemours The Chemours Company FC, LLC
Titanium Technologies
Harrison County, MS

Appendix 2-5: Top of Midway Shale (Top of Confining Zone)
Structure Map
Contour Interval = 100'

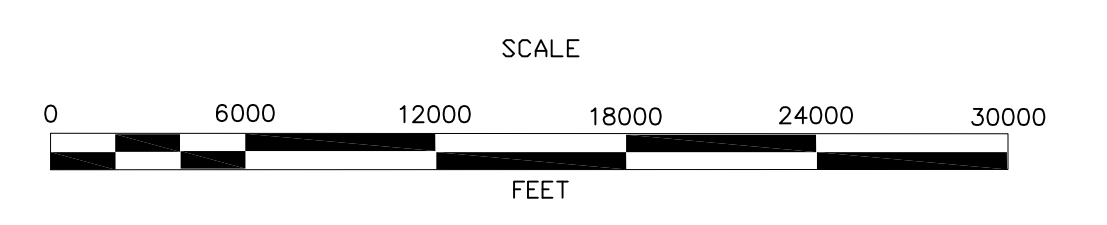
Base Map Prepared & compiled from Tobin International, Ltd. digital Map Data
Compiled & Drafted by: (ESSJ, WGR) Sandia Scale: 1" = 6000' Date: July 2016

GEOSTOCK SANDIA
ENTREPOSE



Legend

- Deviated Well Spot
- ◇ P&A Oil and Gas Well
- ⊕ Injection Well
- ⊕ Proposed Injection Well
- ⊕ Gas Well
- Oil Well
- ⊕ Dry & Abandoned Well
- 11600 Total Depth
- 31290 API Number
- NDE Log Not Deep Enough
- NL No Log

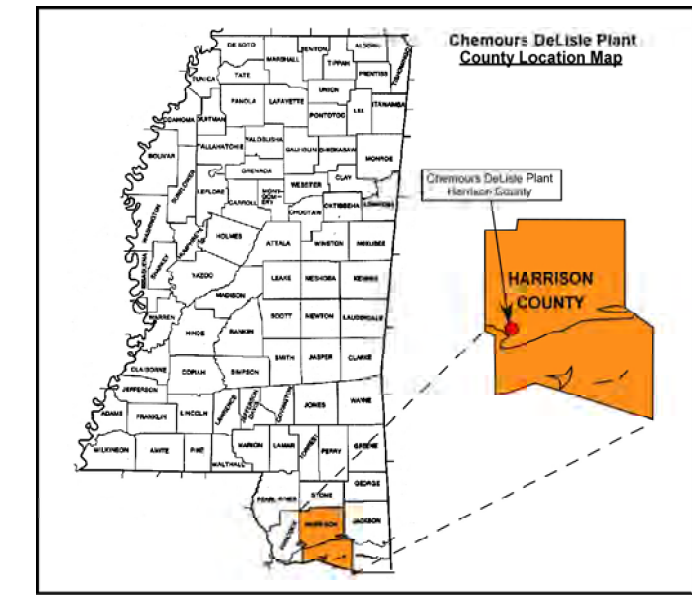
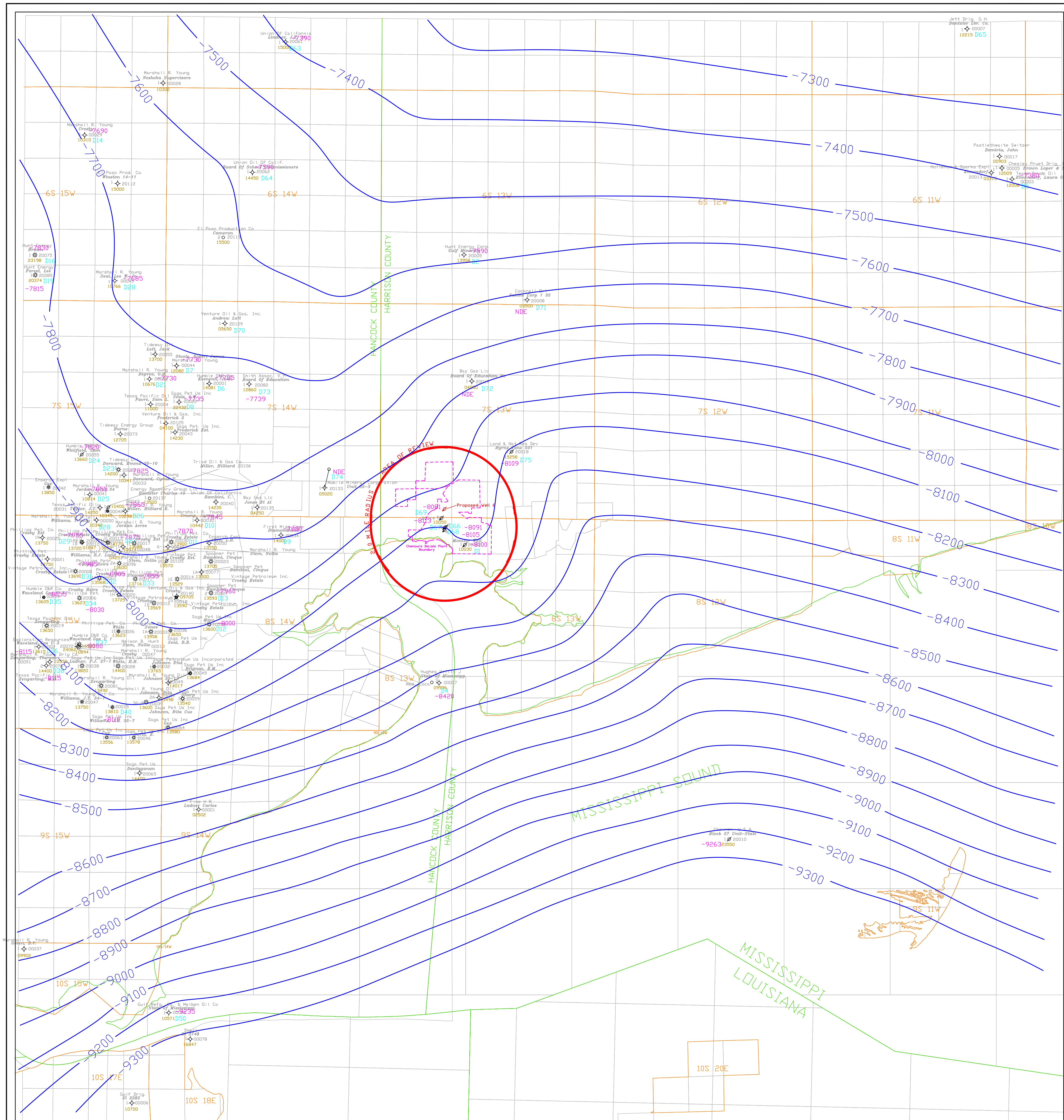


Chemours The Chemours Company FC, LLC
Titanium Technologies
Harrison County, MS

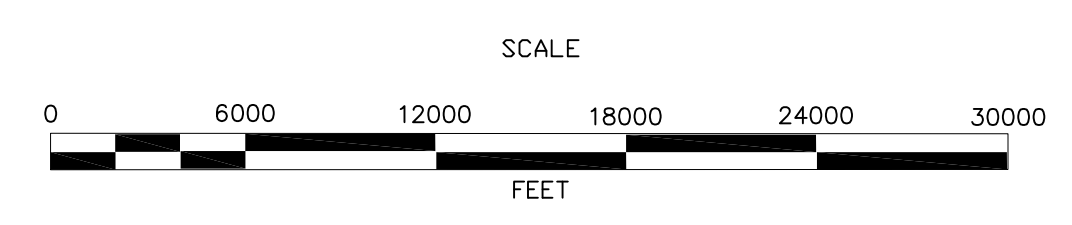
Appendix 2-6: Top of Selma Chalk
Structure Map
Contour Interval = 100'

Base Map Prepared & compiled from Tobin International, Ltd. digital Map Data
Compiled & Drafted by: (ESSJ, WGW) Sandia Scale: 1" = 6000' Date: July 2016

GEOSTOCK SANDIA
ENTREPOSE



- Legend**
- Deviated Well Spot
 - ◇ P&A Oil and Gas Well
 - ⊕ Injection Well
 - ⊕ Proposed Injection Well
 - ⊕ Gas Well
 - Oil Well
 - ⊕ Dry & Abandoned Well
 - 4658 Total Depth
 - D40 Map ID Wells
 - 11600 Total Depth
 - 31290 API Number
 - NDE Log Not Deep Enough
 - NL No Log

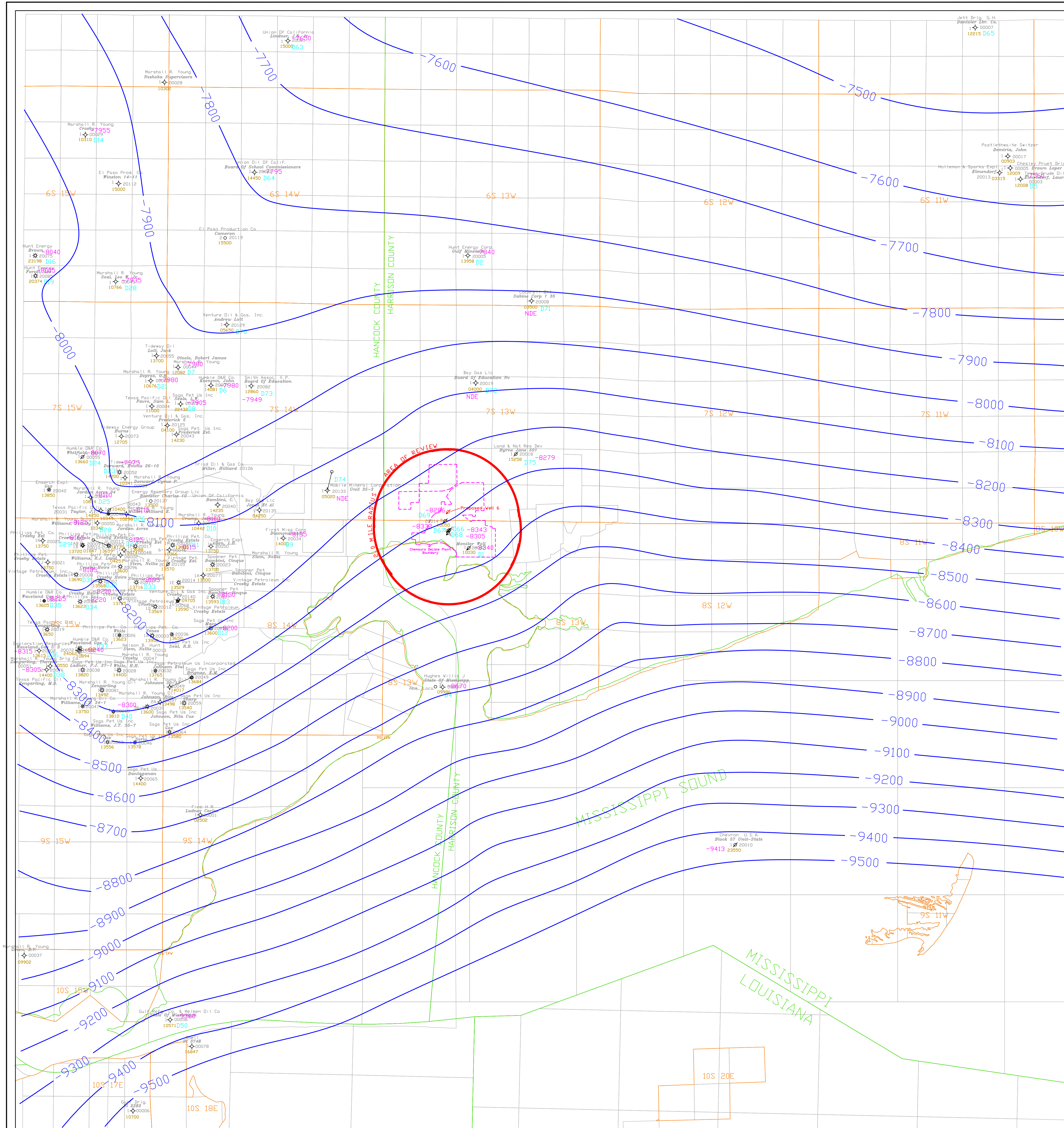


Chemours The Chemours Company FC, LLC
Titanium Technologies
Harrison County, MS

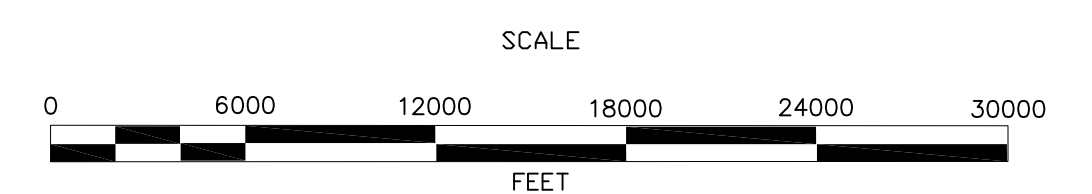
Appendix 2-7: Top of Etaw
Structure Map
Contour Interval = 100'

Base Map Prepared & compiled from Tobin International, Ltd. digital Map Data
Compiled & Drafted by: (ESS), WGM/Sandia Scale: 1" = 6000' Date: 7/2016

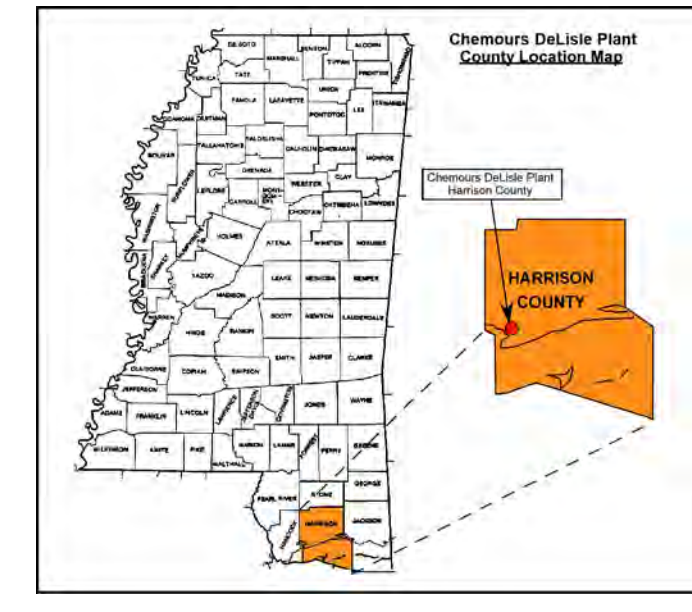
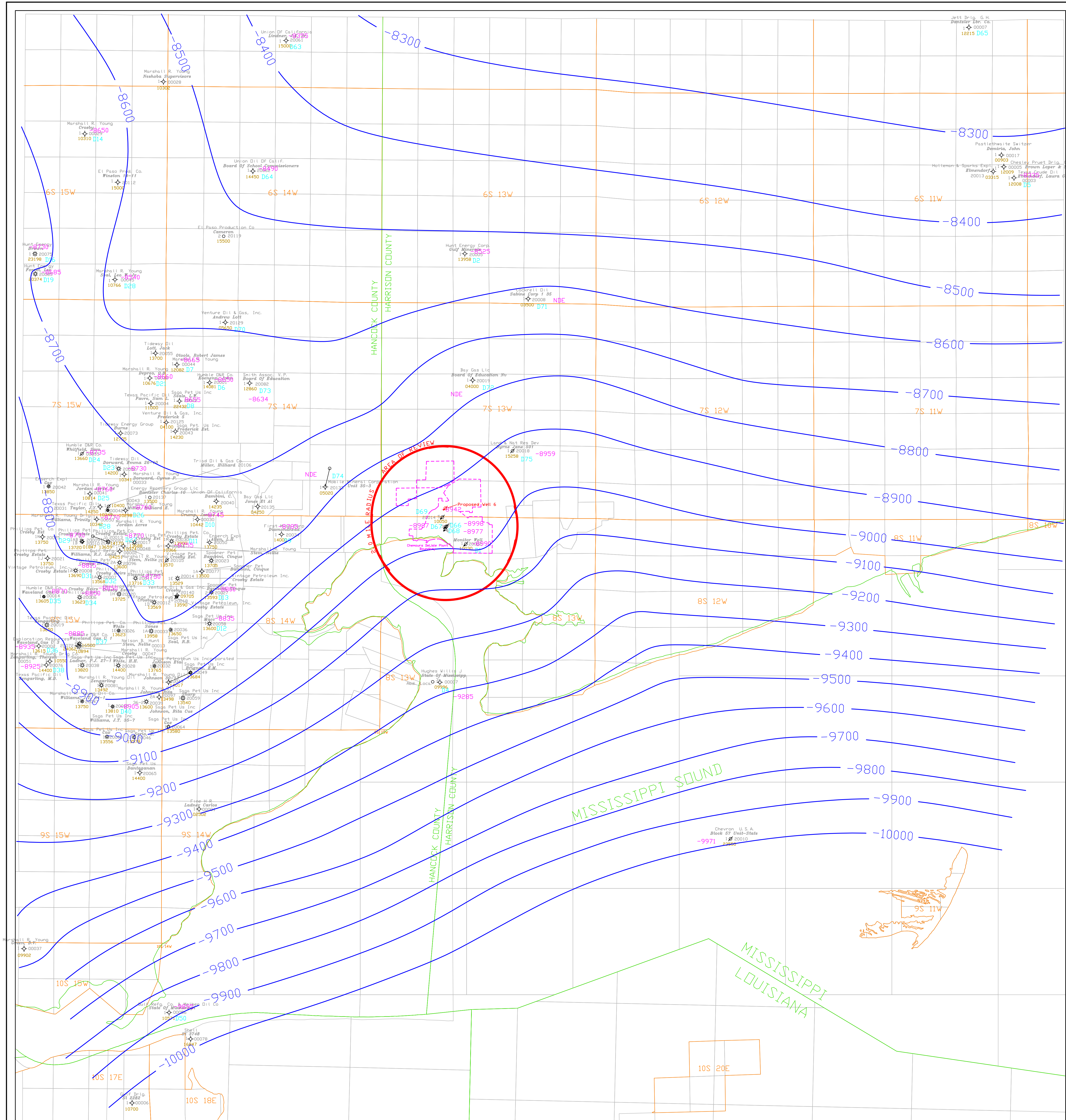
GEOSTOCK SANDIA
ENTREPOSE



Legend	
○	Deviated Well Spot
◇	P&A Oil and Gas Well
◆	Injection Well
♣	Proposed Injection Well
✱	Gas Well
○	Oil Well
⊕	Dry & Abandoned Well
-4658	Post Numbers
D40	Map ID Wells
11600	Total Depth
31290	API Number
NDE	Log Not Deep Enough
NL	No Log

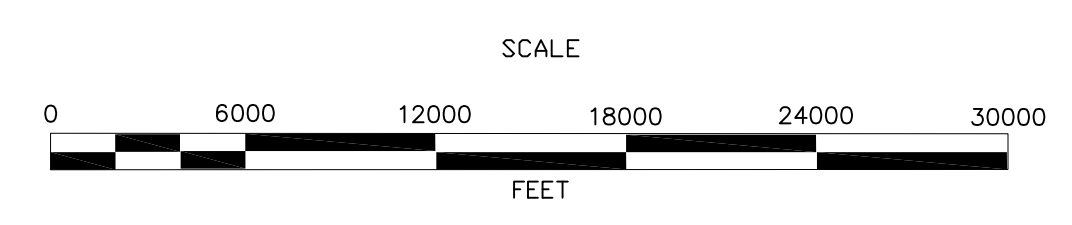


	The Chemours Company FC, LLC Titanium Technologies Harrison County, MS	
	Appendix 2-8: Top of Upper & Middle Tuscaloosa Formation Structure Map Contour Interval = 100'	
<small>Base Map Prepared & compiled from Tobin International, Ltd. digital Map Data</small>		
<small>Compiled & Drafted by: (ESSJ, WGW) Sandia</small>	<small>Scale: 1"= 6000'</small>	<small>Date: July 2016</small>



Legend

- Deviated Well Spot
- ◆ P&A Oil and Gas Well
- ⊕ Injection Well
- ⊕ Proposed Injection Well
- ⊕ Gas Well
- Oil Well
- ⊕ Dry & Abandoned Well
- 4658 Post Numbers
- D40 Map ID Wells
- 11600 Total Depth
- 31290 API Number
- NDE Log Not Deep Enough
- NL No Log

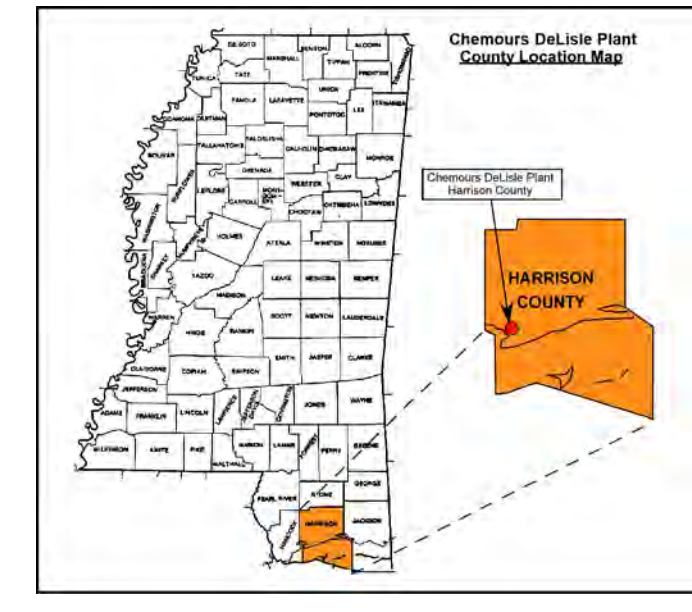
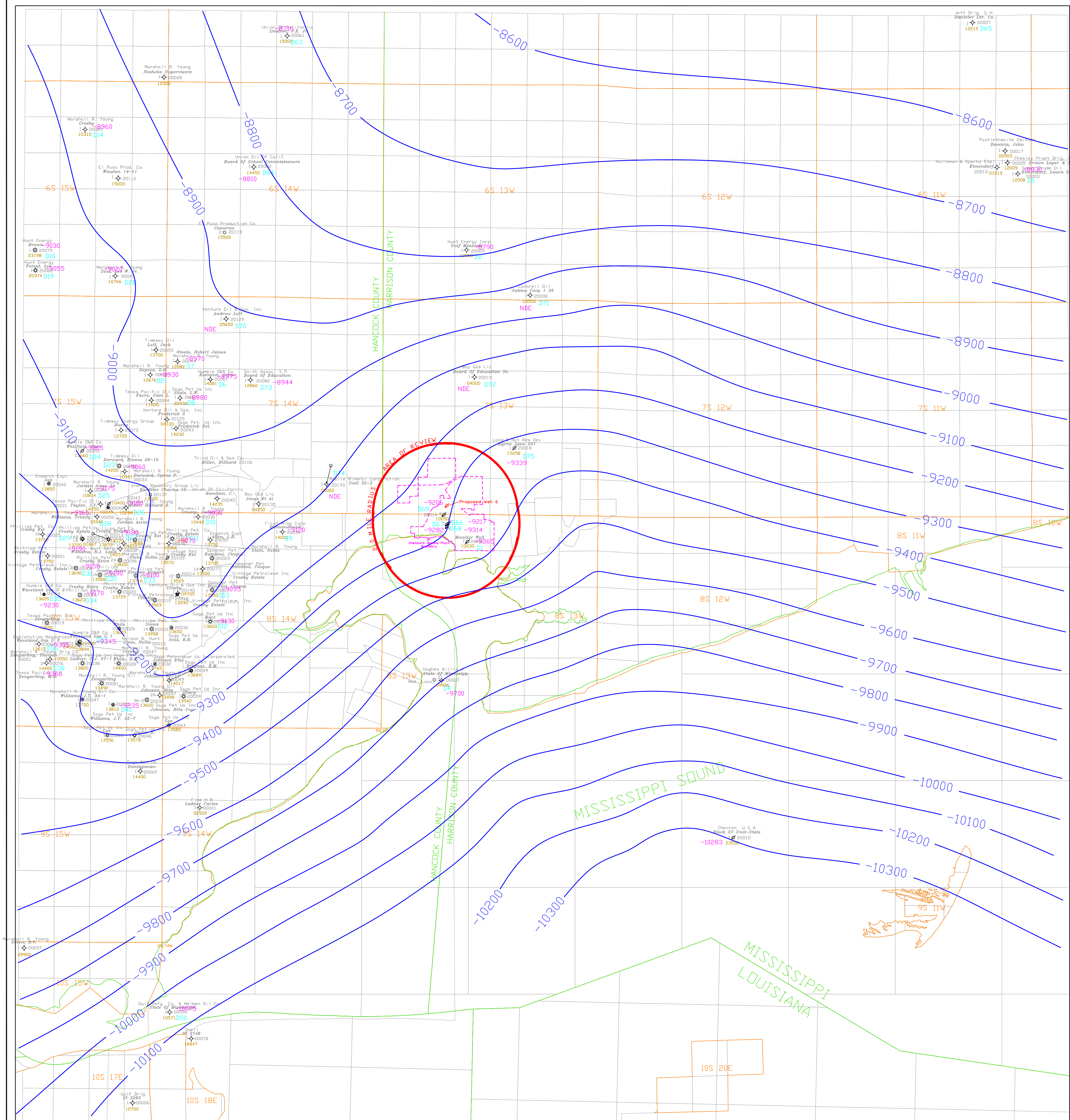


Chemours The Chemours Company FC, LLC
Titanium Technologies
Harrison County, MS

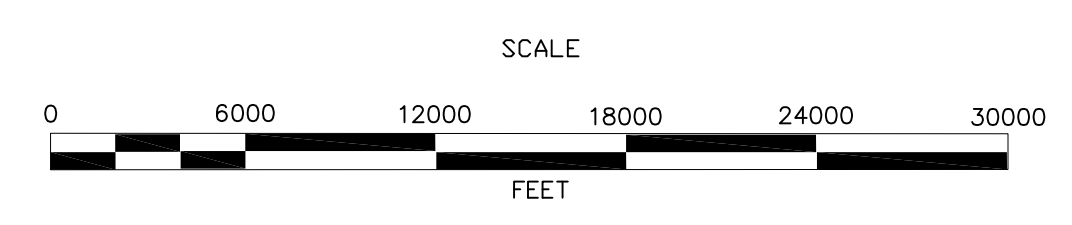
Appendix 2-9: Top of Lower Tuscaloosa Formation
Structure Map
Contour Interval = 10'

Base Map Prepared & compiled from Tobin International, Ltd. digital Map Data
Compiled & Drafted by: (ESSJ, WGR) Sandia Scale: 1" = 6000' Date: July 2016

GEOSTOCK SANDIA
ENTREPOSE



- Legend**
- Deviated Well Spot
 - ◆ P&A Oil and Gas Well
 - ◇ Injection Well
 - ⚡ Proposed Injection Well
 - ⊛ Gas Well
 - Oil Well
 - ⊘ Dry & Abandoned Well
 - 4658 Post Numbers
 - D40 Map ID Wells
 - 11600 Total Depth
 - 31290 API Number
 - NDE Log Not Deep Enough
 - NL No Log



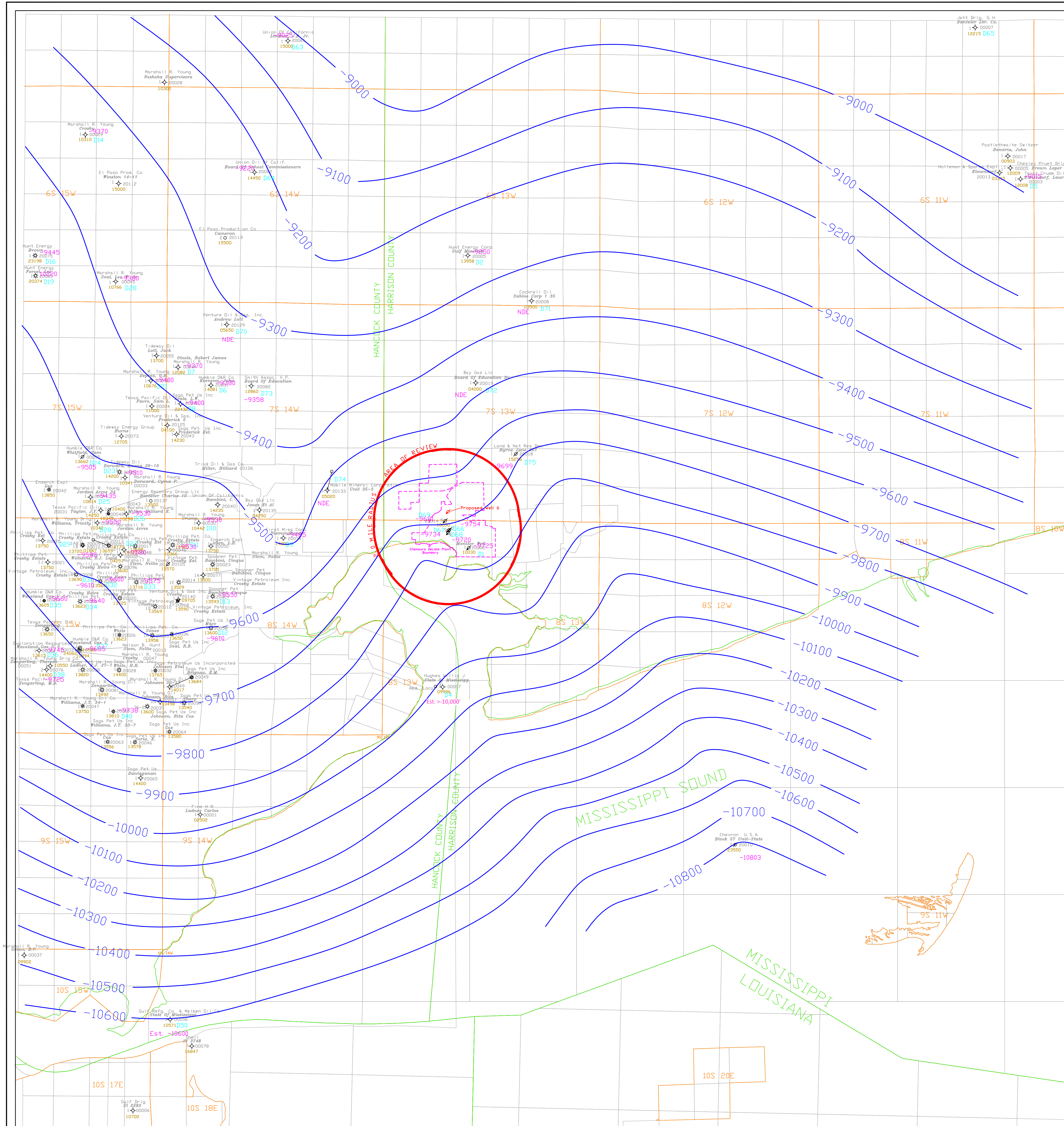
Chemours The Chemours Company FC, LLC
Titanium Technologies
Harrison County, MS

Appendix 2-10: Top of Tuscaloosa Massive Sand
Structure Map
Contour Interval = 100'

Base Map Prepared & compiled from Tobin International, Ltd. digital Map Data

Compiled & Drafted by: (ESSJ, WGR) Sandia	Scale: 1" = 6000'	Date: July 2016
---	-------------------	-----------------

GEOSTOCK SANDIA
ENTREPOSE



- Legend**
- Deviated Well Spot
 - ◆ P&A Oil and Gas Well
 - ⊕ Injection Well
 - ⊕ Proposed Injection Well
 - ⊕ Gas Well
 - Oil Well
 - ⊕ Dry & Abandoned Well
 - 4658 Post Numbers
 - D40 Map ID Wells
 - 11600 Total Depth
 - 31290 API Number
 - NDE Log Not Deep Enough
 - NL No Log

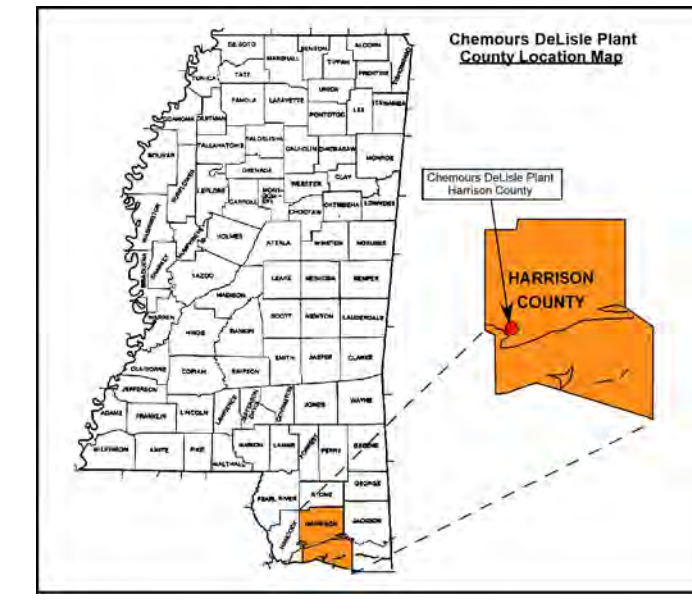
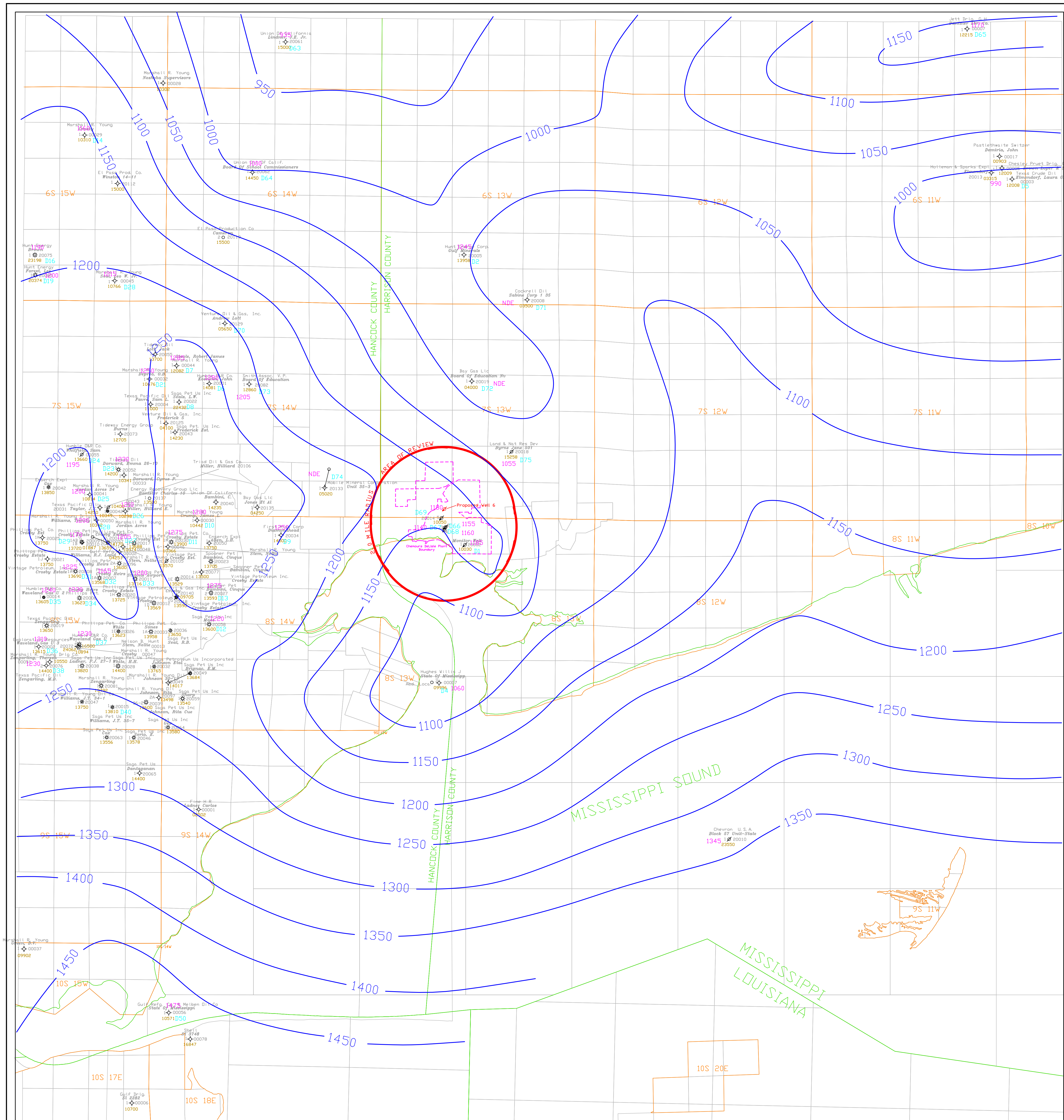


Chemours The Chemours Company FC, LLC
Titanium Technologies
Harrison County, MS

Appendix 2-11: Top of Washita-Fredericksburg Sand
(Injection Interval) Structure Map
Contour Interval = 100'

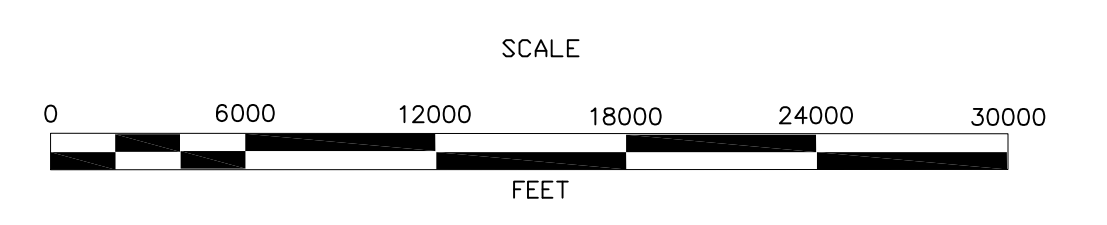
Base Map Prepared & compiled from Tobin International, Ltd. digital Map Data
Compiled & Drafted by: (ESSJ, WGR) Sandia Scale: 1" = 6000' Date: July 2016

GEOSTOCK SANDIA
ENTREPOSE



Legend

- Deviated Well Spot
- ◇ P&A Oil and Gas Well
- ⊕ Injection Well
- ⊕ Proposed Injection Well
- ⊕ Gas Well
- Oil Well
- ⊕ Dry & Abandoned Well
- 4658 Post Numbers
- D40 Map ID Wells
- 11600 Total Depth
- 31290 API Number
- NDE Log Not Deep Enough
- NL No Log

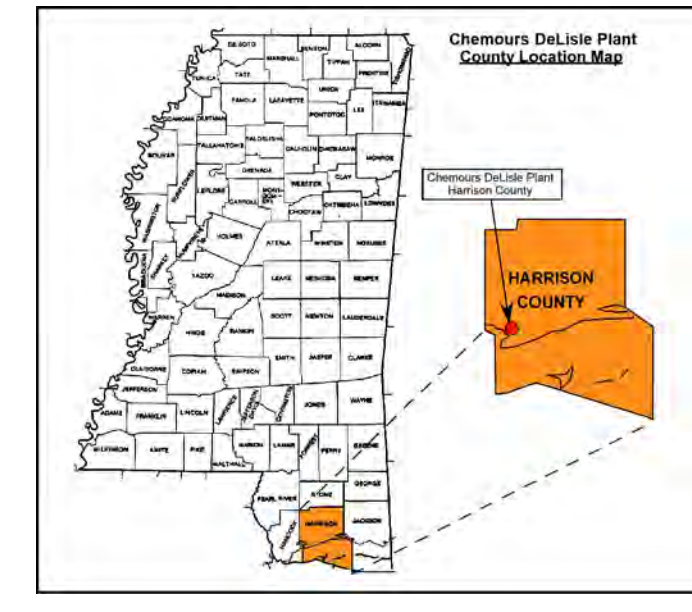
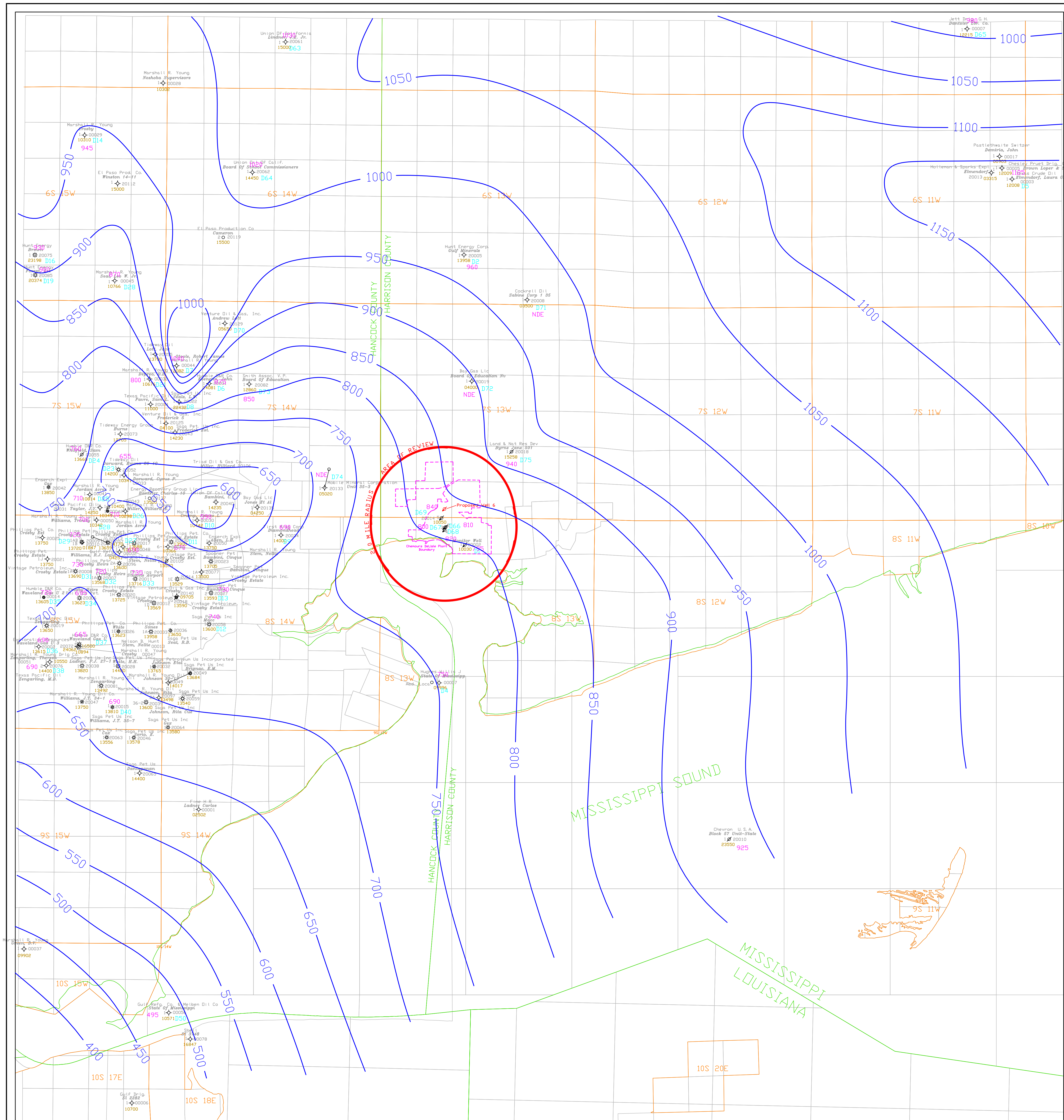


Chemours The Chemours Company FC, LLC
Titanium Technologies
Harrison County, MS

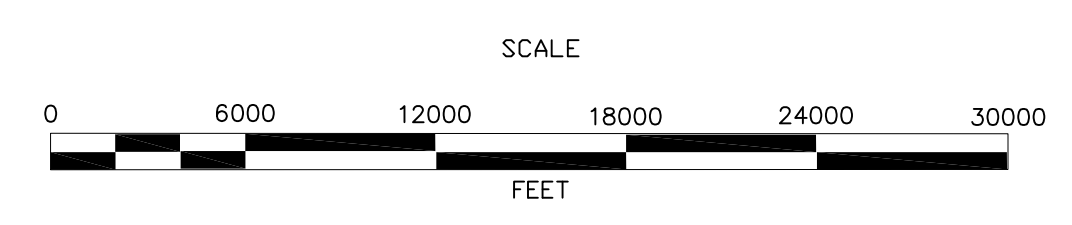
Appendix 2-12: Midway Shale
Isopach Map
Contour Interval = 50'

Base Map Prepared & compiled from Tobin International, Ltd. digital Map Data
Compiled & Drafted by: (ESSJ, WGR) Sandia Scale: 1" = 6000' Date: July 2016

GEOSTOCK SANDIA
ENTREPOSE



- Legend**
- Deviated Well Spot
 - ◇ P&A Oil and Gas Well
 - ♣ Injection Well
 - ♣ Proposed Injection Well
 - ♣ Gas Well
 - Oil Well
 - ♣ Dry & Abandoned Well
 - 11600 Total Depth
 - 31290 Map ID Wells
 - 11600 Total Depth
 - 31290 Map ID Wells
 - NDE Log Not Deep Enough
 - NL No Log

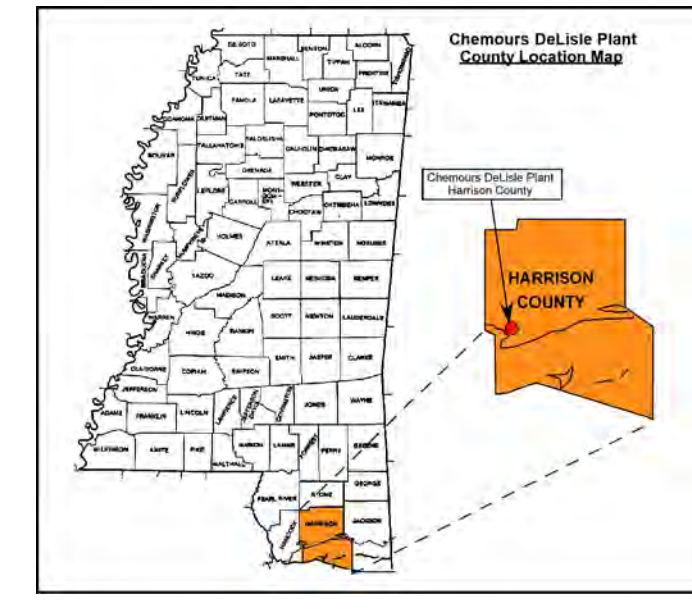
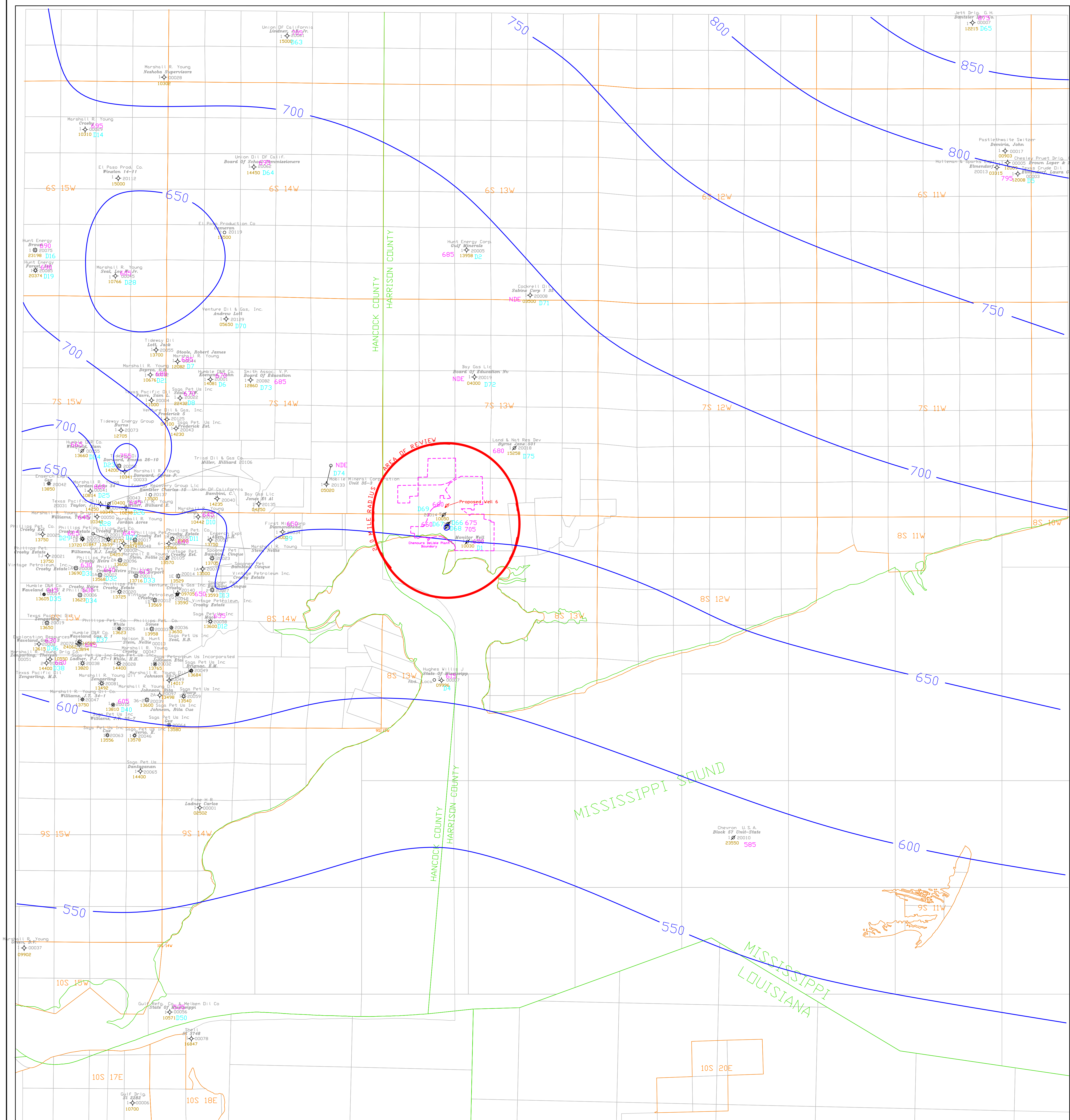


Chemours The Chemours Company FC, LLC
Titanium Technologies
Harrison County, MS

Appendix 2-13: Selma Chalk
Isopach Map
Contour Interval = 50'

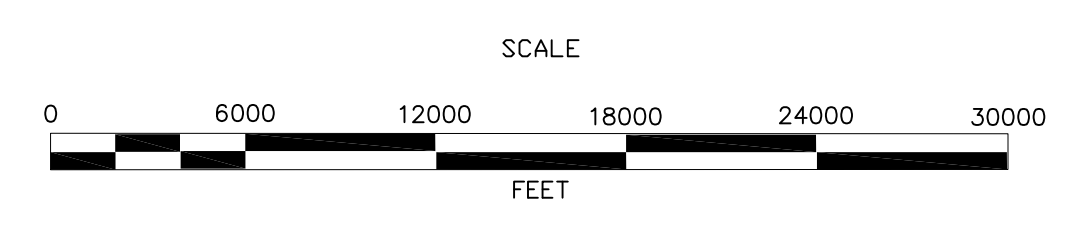
Base Map Prepared & compiled from Tobin International, Ltd. digital Map Data
Compiled & Drafted by: (ESSJ, WGR) Sandia Scale: 1" = 6000' Date: July 2016

GEOSTOCK SANDIA
ENTREPOSE



Legend

- Deviated Well Spot
- ◆ P&A Oil and Gas Well
- ⊕ Injection Well
- ⊕ Proposed Injection Well
- ⊕ Gas Well
- Oil Well
- ⊕ Dry & Abandoned Well
- 4658 Post Numbers
- D40 Map ID Wells
- 11600 Total Depth
- 31290 API Number
- NDE Log Not Deep Enough
- NL No Log

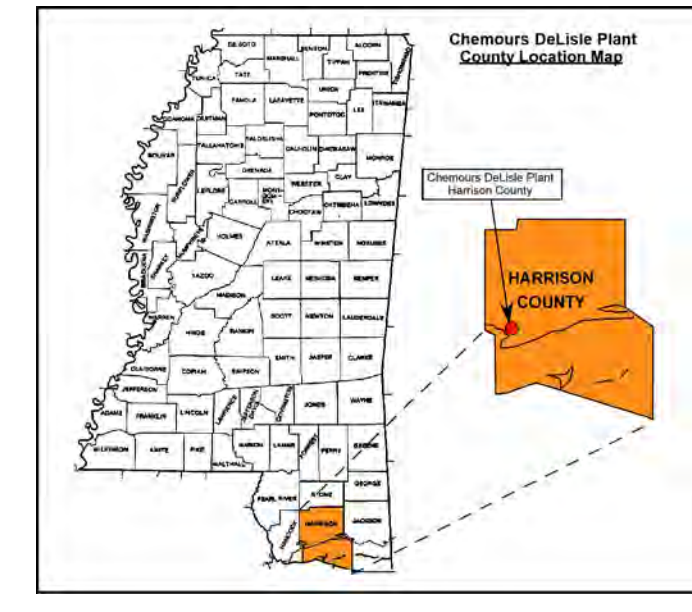
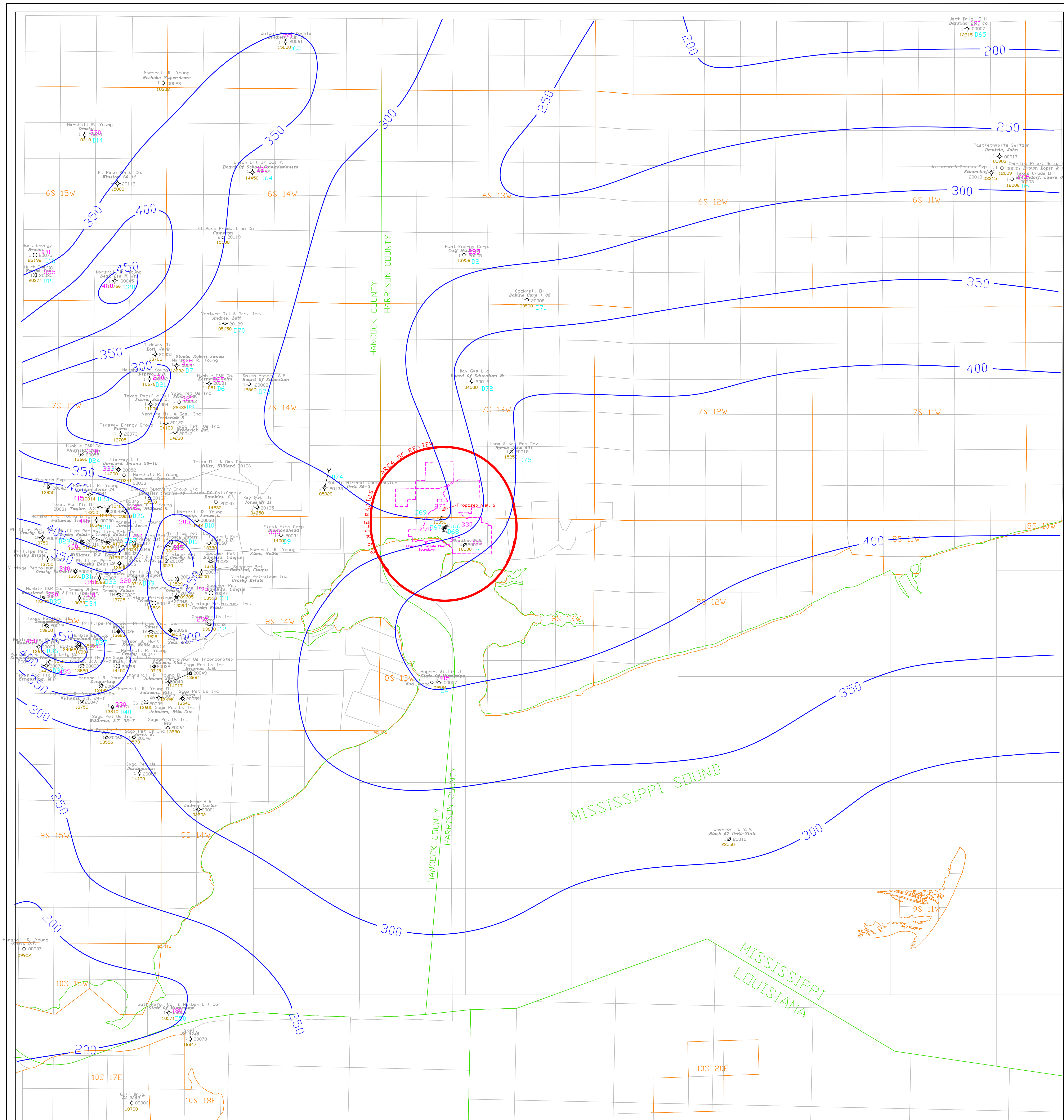


Chemours The Chemours Company FC, LLC
Titanium Technologies
Harrison County, MS

Appendix 2-15: Upper & Middle Tuscaloosa Formation
Isopach Map
Contour Interval = 50'

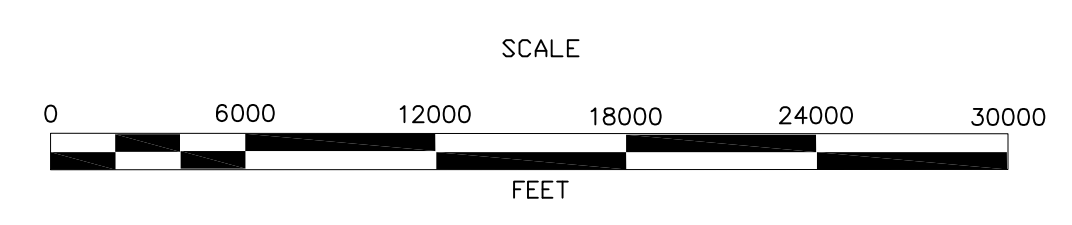
Base Map Prepared & compiled from Tobin International, Ltd. digital Map Data
Compiled & Drafted by: (ESSJ, WGR) Sandia Scale: 1" = 6000' Date: July 2016

GEOSTOCK SANDIA
ENTREPOSE

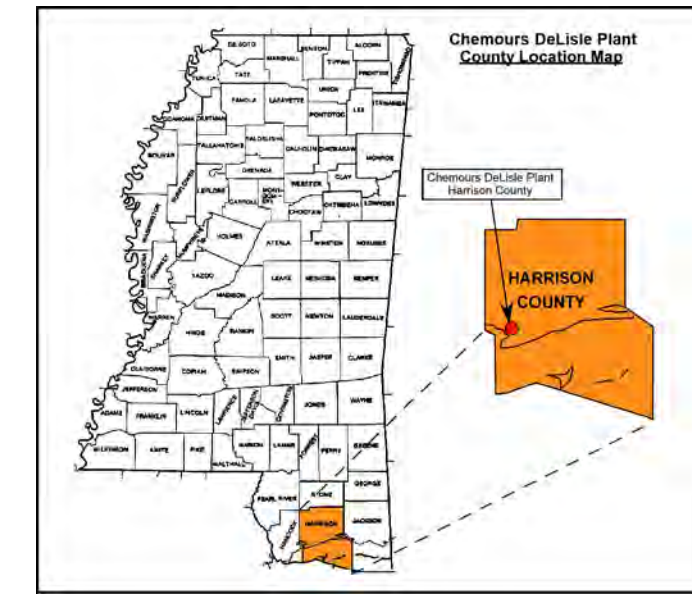
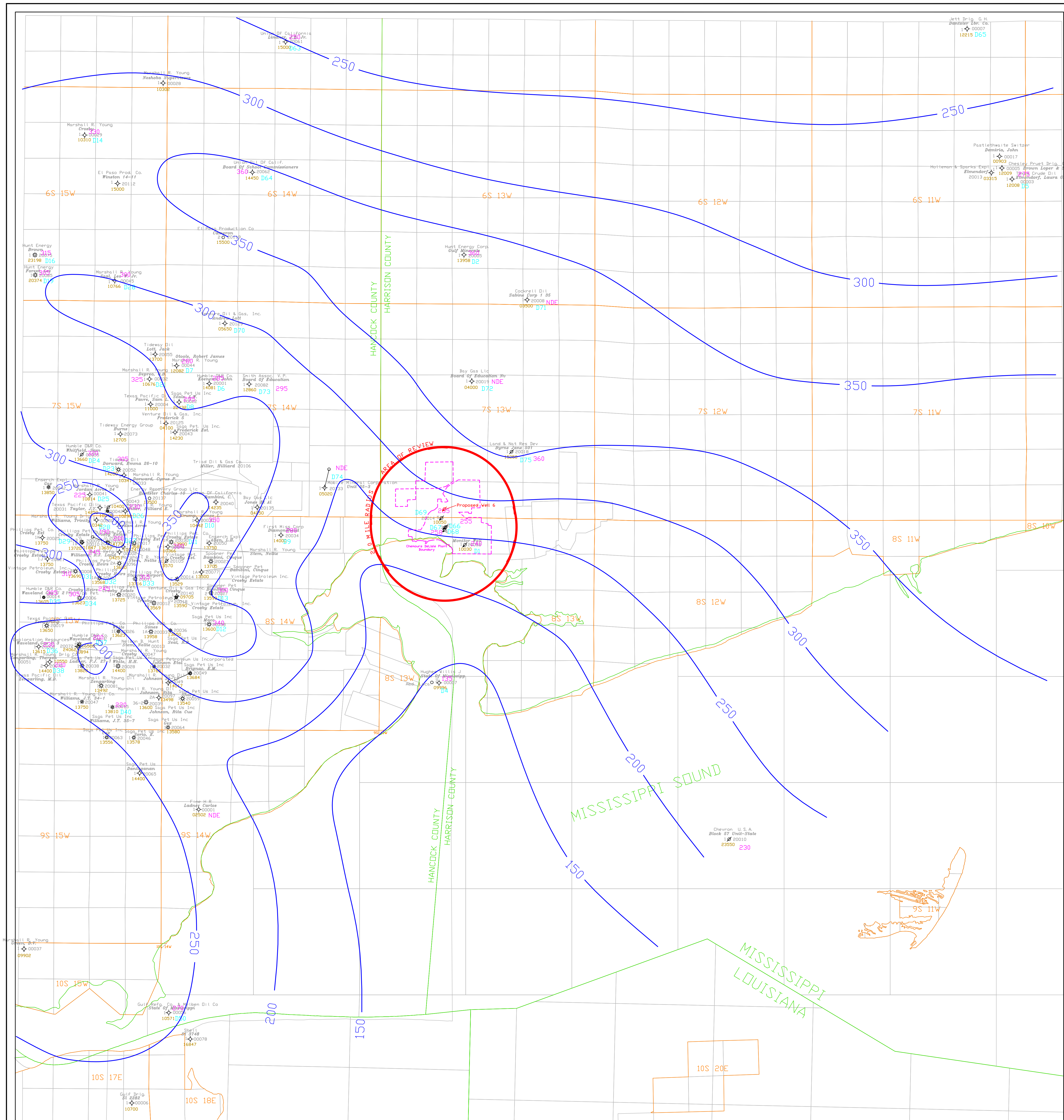


Legend

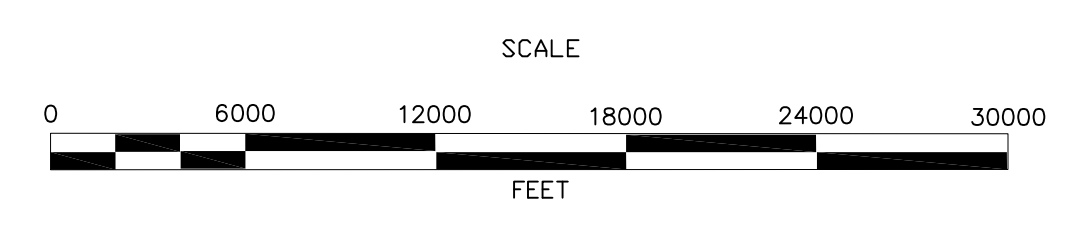
- Deviated Well Spot
- ◇ P&A Oil and Gas Well
- ⊕ Injection Well
- ⊕ Proposed Injection Well
- * Gas Well
- Oil Well
- ⊕ Dry & Abandoned Well
- 4658 Post Numbers
- D40 Map ID Wells
- 11600 Total Depth
- 31290 API Number
- NDE Log Not Deep Enough
- NL No Log



	The Chemours Company FC, LLC Titanium Technologies Harrison County, MS	
	Appendix 2-16: Lower Tuscaloosa Formation Isopach Map Contour Interval = 50'	
<small>Base Map Prepared & compiled from Tobin International, Ltd. digital Map Data</small>		
<small>Compiled & Drafted by: (ESSJ, WGR) Sandia</small>	<small>Scale: 1" = 6000'</small>	<small>Date: July 2016</small>



- Legend**
- Deviated Well Spot
 - ◇ P&A Oil and Gas Well
 - ⊕ Injection Well
 - ⊕ Proposed Injection Well
 - ⊕ Gas Well
 - Oil Well
 - ⊕ Dry & Abandoned Well
 - 4659 Post Numbers
 - D40 Map ID Wells
 - 11600 Total Depth
 - 31290 API Number
 - NDE Log Not Deep Enough
 - NL No Log

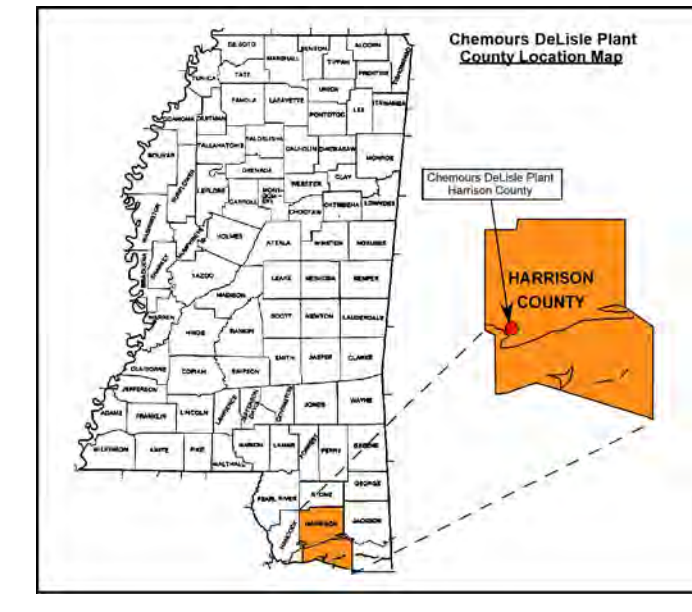
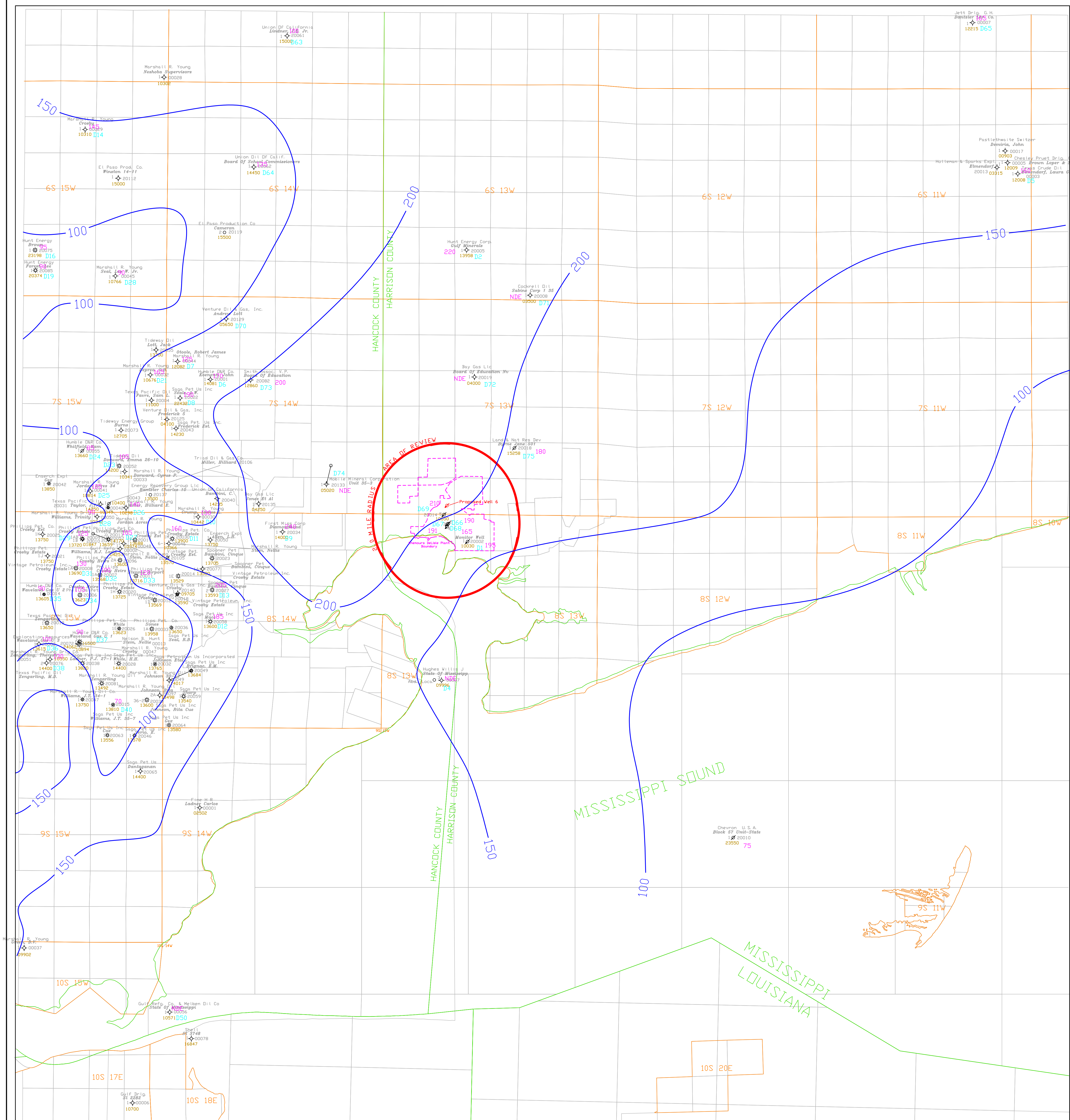


Chemours The Chemours Company FC, LLC
Titanium Technologies
Harrison County, MS

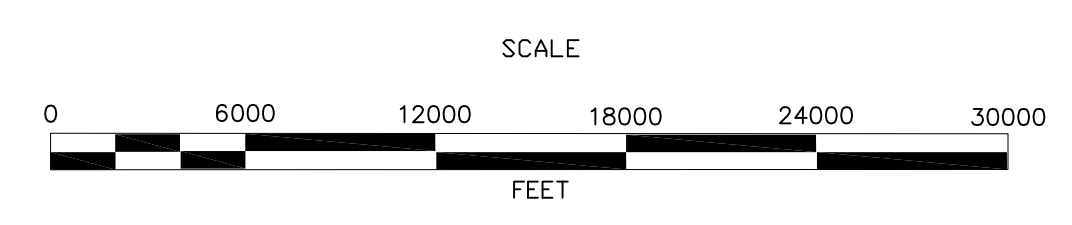
Appendix 2-17: Tuscaloosa Massive Sand
(Net Sand) Isopach Map
Contour Interval = 5'

Base Map Prepared & compiled from Tobin International, Ltd. digital Map Data
Compiled & Drafted by: (ESSJ, WGR) Sandia Scale: 1" = 6000' Date: July 2016

GEOSTOCK SANDIA
ENTREPOSE



- Legend**
- Deviated Well Spot
 - ◇ P&A Oil and Gas Well
 - ◆ Injection Well
 - ♣ Proposed Injection Well
 - ✱ Gas Well
 - Oil Well
 - ♠ Dry & Abandoned Well
 - 4658 Post Numbers
 - D40 Map ID Wells
 - 11600 Total Depth
 - 31290 API Number
 - NDE Log Not Deep Enough
 - NL No Log

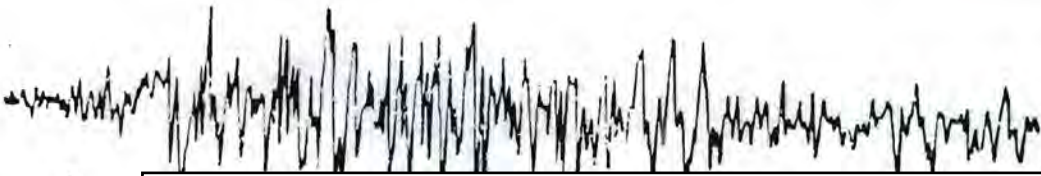


Chemours The Chemours Company FC, LLC
Titanium Technologies
Harrison County, MS

Appendix 2-18: Washita-Fredericksburg Sand
(Injection Interval) Isopach Map
Contour Interval = 50'

Base Map Prepared & compiled from Tobin International, Ltd. digital Map Data
Compiled & Drafted by: (ESS), WGR/Sandia Scale: 1" = 6000' Date: July 2016

GEOSTOCK SANDIA
ENTREPOSE



Appendix 2-21 David Leeds and Associates Seismic Study 1989 and 1998

DAVID J. LEEDS AND ASSOCIATES

11972 Chalon Road
Los Angeles, CA 90049
(213) 472-0282

Consultants in Engineering Seismology/Geology/Geophysics

E.I. du Pont de Nemours & Co.
Engineering Service Division
Gulf Coast Regional Consulting
PO Box 3269
Beaumont, TX 77704

DJLA 89-154-03
21 July 1989

Attention: Ms Diane K Sparks:

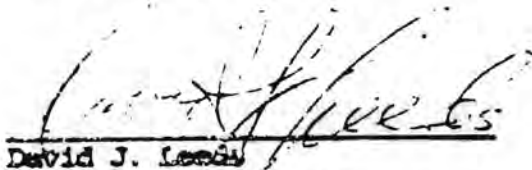
Re: Seismicity—
Natural & Induced
Beaumont Works
Texas

We take pleasure in submitting our report on the seismicity of the region near your Beaumont Works, the possibility of earthquake damage to the injection process, and the potential for induced seismicity with damage to the confining and injection zones. The report contains the detail which supports our conclusions.

In our opinion there is no hazard of natural earthquake damage to the facility (presuming the installations conform to usual engineering practice) or of induced seismicity generated by the injection process. We do not believe that there has ever been destructive earthquake ground motion at your site.

We hope that this report meets your requirements. Please feel free to contact us if we can be of further assistance.

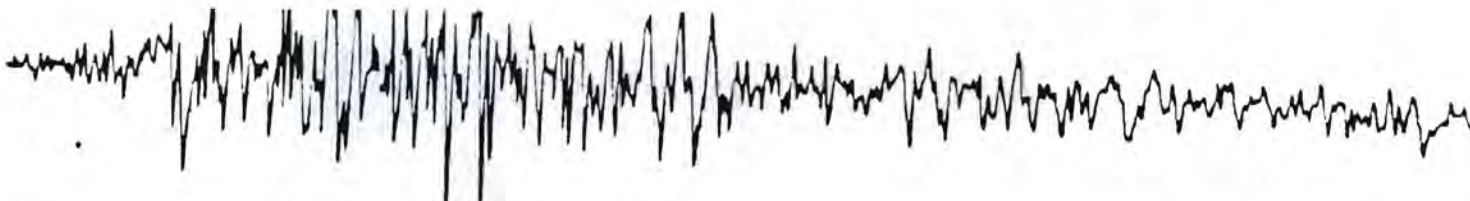
Very truly yours,


David J. Leeds

DAVID J. LEEDS AND ASSOCIATES
CA Registered Geologist #940
CA Registered Geophysicist #GP 17
CA Certified Engineering Geologist #EG 373
MPE Certified Professional Geologist #674

DJL:z

MS\DJLA\8915403.ltr



DAVID J. LEEDS AND ASSOCIATES

Consultants in Engineering Seismology/Geology/Geophysics

11972 Chalon Road
Los Angeles, CA 90049
(213) 472-0282

DJLA 89-154-03
July 15, 1989

SEISMIC EFFECTS/DU PONT BEAUMONT WORKS

General

This report addresses potential natural and induced seismic effects on and of fluid waste disposal injection wells at the Du Pont Beaumont Works located approximately 5 miles southeast of Beaumont, Texas. The principal elements of the report address the following concerns:

- A. The natural seismicity of the region.
- B. Possible damage by earthquakes to the injection and confining zones of the facility.
- C. The possibility of the injection process triggering earthquakes.

The report will:

- 1. Describe the seismic environment in terms of the seismic history of the region.
- 2. Postulate a "design earthquake" for the subsurface and discuss its effects on the injection and confining zones.
- 3. Present case histories of induced seismicity.
- 4. Compare the geologic/seismic environment at other sites where induced seismicity has been observed with conditions at the Du Pont Beaumont Works.
- 5. Present conclusions with respect to the above.
- 6. Provide three sets of references, on induced seismicity, Louisiana seismology, and on Texas seismology.

Location

The Du Pont Beaumont Works is situated on the Texas Coastal Plain approximately 28 miles inland (northwest) of the Gulf of Mexico and about 5 miles southeast of Beaumont.

General Geology

The Texas Coastal Plain at Jefferson County presents an enormous thickness of Tertiary sands and shales with overall persistent and continuous subsurface geology. This wedge of sediments is punctuated with intrusions of Jurassic salt. These domal and anticlinal areas are fragmented by faulting; however, there is no indication of current activity. The geology of the area is described in detail in other reports so will not be repeated here.

Texas Seismicity

Seismic activity of the Texas Coastal Plain is among the lowest in the nation. The major part of the state, except for the Rio Grande rift area of Texas, the Panhandle, and the eastern Texas-Oklahoma border, has had either zero coefficients assigned or the very lowest elements of seismicity. See Figure 1. These coefficients are developed through historical seismicity (the record of felt earthquakes), instrumental seismicity (seismograph records), and the structural geologic framework. In a highly seismically active area, the historic record can be extended backward using paleoseismicity. This is not usually an option in Texas.

Earthquakes are measured in terms of:

Intensity - effect of the ground motion on man, his work, and on natural features. The measure currently in use (since 1931) is known as the Modified Mercalli Intensity Scale (MMI). Before 1931 the quite similar Rossi-Forel Intensity Scale was used. However, observations before 1931 have been converted to the MMI scale, so there should be no confusion. The MMI shown in Table I has been updated to adjust to current construction practice. Intensity observations are employed to construct isoseismal maps wherein the areas of equal shaking are contoured.

Magnitude - instrumental measure of an earthquake. It is the response of a specified instrument (seismograph) with narrowly defined dynamic response. With the magnitude scale (see Figure 2), earthquakes can be measured at a distance. Seismic stations should all achieve similar determinations from the same event since adjustments are made for distance and instrumental constants. The magnitude scale was devised by Dr. Charles F. Richter and frequently carries his name.

However, there are now several iterations of the magnitude scale, depending on the type of seismic wave observed, the epicentral distance, and several other factors.

Instrumental seismology is equally as important as the historic record, for instrumentation permits the measurement and location of seismic events much smaller than those which may be felt. Thus, a catalog of seismic events may contain events that are instrumentally recorded but not felt by man. Also, since seismic ground motion attenuates with distance and the entire country is not adequately covered by seismographs, many small events are felt but not recorded or escape all detection.

The epicenter map (Figure 3) shows all seismic events in the National Geophysical Data Center (NGDC) files as of June 9, 1989 for the area of interest. The accompanying list (Table II) includes several small events (near Houston Hobby Airport) that have not received adequate documentation so are not plotted. Table II has been developed from the NGDC printout, supplemented by data in the files of David J. Leeds and Associates. The epicenters for events plotted in Figure 3 are identified in Figure 4, which is an enlargement from Figure 3 of the coastal plain region of South Texas. Some caution must be exercised in the use of the plotting of Figures 3 and 4 since NGDC frequently prints more than one location for the same event (from the solutions of different investigators) as well as overprinting several events at the same location. Neither the instrumental nor the historical record can be considered complete or accurate.

The oldest earthquake included in the larger plot of epicenters (Figure 3) is an 1843 New Orleans Intensity III earthquake. The oldest Texas earthquake on the map is an Intensity IV in 1873. An earlier unconfirmed 1847 event is listed near Seguin. A total of 281 seismic events are plotted, some a repetition at the same site and some duplicated by conflicting reports. A smaller area, within a 100-mile radius of the Beaumont Works, has only a handful of events except for the maximum $M=4.2$ swarm approximately 90 miles north.

The largest ground motion experienced in this portion of the Gulf Coast was in the Lake Charles, Louisiana earthquake of October 16 1983, approximately 55 miles east of the Du Pont Beaumont Works. While the NGDC tabulation indicates $MMI=III$, field investigation turned up several reports of $MMI=V$. (See Stevenson & Agnew, 1985, in the "References" section). Closest epicenters to the Beaumont Works are the 1966 instrumental location near Beaumont and the 1952 event 25 miles east near Orange. Their magnitudes were 3.0 and 3.8, respectively. The 1966 Beaumont event was recorded instrumentally but not reported felt. The 1952 Orange event was felt: "Linesman atop a pole felt it quiver. Buildings swayed and windows rattled". (*United States Earthquakes, 1952*). Note that in all cases shown within about 200 miles of the Beaumont Works in the 140+ years of record earthquake ground motion has been limited to the rattling of dishes, doors, and windows. The $MMI=VII$, $M_b=3.8$, 1891 Rusk Event 140 miles northwest is not an exception. The Rusk event has been documented as a severe thunderstorm (Kilbourne and Lutschak, 1974).

Even in other parts of Texas, in quite different geologic/seismic regimes, earthquake damage has not exceeded the fall of a chimney or two. The Beaumont area is only very slightly active, with an intensity of IV being the norm. It is certain that destructive earthquake ground motion has never been experienced in the Beaumont area.

Seismogenic Sources

A source mechanism is required for the development of a model earthquake. It is usual to have a known active fault system with a known, measurable strain or stress field. The more active regions of the earth have faults with strain (movement across the fault without a rupture) developing at a rate up to 5 centimeters per year or greater. As a meter or more of strain develops, stress accumulates; eventually the system releases this stored strain energy in the form of elastic waves (i.e., an earthquake).

The Texas Gulf Coast has several structural geological features capable of storing and releasing some energy although all are weak or ineffective in terms of generating even modest ground motion.

The salt structures have developed gravimetrically by the flow of the lower density salt through weaker zones of the thick sediments. The salt is so plastic that it tends to flow rather than develop large fractures. The surrounding sediments are badly faulted by the intrusion and are almost as physically incompetent as the salt, also having low densities, poor cementation, and low shear strength with resulting low shear moduli. It is doubtful that the salt dome as a seismogenic source could develop earthquakes with magnitudes greater than 3.0 and intensity MMI=IV. These events may be locally felt but are unlikely to propagate damaging ground motions. Reference to the historical catalog presented in Table II shows a relationship between magnitude and maximum intensity. The events might be perceptible, but the level of shaking could not be called damaging.

Growth faults have also developed along the Texas Gulf Coast which may be responsible for some seismic activity. Considering the Gulf Coast as a whole, a level of $M_b=4.2$ is considered an upper level for this source in this area. The several low magnitude events within about 50 miles of the coastline are probably attributable to this mechanism.

The possibility that growth faults may be triggered by faults in the basement is suggested by Stevenson and Agnew (1985) in their discussion of the Lake Charles Earthquake. Details of the event were developed from recordings of Department of Energy supported microearthquake networks monitoring geothermal experiments in southwestern Louisiana. The depths of 14+ km for these events are deeper than have previously been reported and well below injection depths. Stevenson (Pers. comm. 1989) stated that no events were attributable to the geothermal operations (extraction and reinjection of brine).

Design Earthquake

A body-wave magnitude, M_b , of 4.2 ± 0.2 appears to be a conservative working postulate for a design earthquake at this site. The source area would have to be along one of the growth faults, parallel to the Coast, and probably near the site. The event generated by salt dome activity would be somewhat less.

Design Seismic Ground Motion

The maximum ground motion generated by the design earthquake on the surface would be close to an intensity of $MMI=V$. We suggest that this intensity would equate with horizontal surface acceleration of $0.05g$, generally at foundation levels of a structure. This is the same value used as an Operating Basis Earthquake (OBE) for certain Gulf Coast nuclear power plant electric generating stations. The empirical record equating intensity to acceleration has a wide spread of data, with recordings varying from horizontal acceleration of 0.025 to $0.15g$ for an Intensity V surface observation.

OBE is a term used by the Nuclear Regulatory Commission to define the design level of a nuclear power reactor at which the facility is required to remain functional. It is a level of ground motion that the reactor has a reasonable chance of experiencing at least once per 100 years. Nuclear criteria are based primarily on life safety, with economic risk secondary, so are usually considered conservative. These considerations are minimal for an injection facility.

A second, higher level, criterion known as the Safe Shutdown Earthquake (SSE), is used as an ultraconservative maximum level based on the largest potential of the geologic/seismic system. This is the level at which point the reactor is required to go through a safe and orderly shutdown. It should be noted that the OBE is usually 50% of the SSE.

Since vertical motions are usually considered to be from one-half to two-thirds of horizontal motion, we can omit their discussion here.

Our premise for a design earthquake is based on the empirical data of normal shallow focus (≤ 20 km) earthquakes on soft sites. It is assumed that the Gulf coastal seismic environment, with its release of energy from less competent materials than usual, would have longer rise times. Therefore, the spectra of ground motion would be biased to longer periods (lower frequencies) than usual, with resulting low accelerations, large displacements, and long durations.

Subsurface Ground Motion

Studies over the years of the effect of depth on seismic ground motion have all noted the attenuation that is realized with depth. Observations in deep mines

and boreholes have confirmed this phenomenon. In a 1972 paper¹ the work to that date was summarized and strongly indicated a diminution of amplitude with depth. As a reasonable average, it can be assumed that the ground motions at depth are approximately one-half the surface motion or less. Some researchers give multipliers of as much as five. For small motions, wherein the materials remain completely elastic, the amplification may be as much as ten.

Effect of Ground Motion

The effect of ground motion on saturated granular soils is buildup in pore water pressure. If the water table is near the surface (within about 15 to 20 feet), if the sands are reasonably well sorted and clean (free of clay), and if accelerations exceed about 0.25g, a type of soil failure known as liquefaction can occur. This causes a loss of shear strength of the soil, ejection of sand and water to the surface (sand boils), and collapse of the foundation of structures supported by the soils. In extreme cases, multistory buildings have rolled over (Niigata, Japan Earthquake 1964) and buried tanks have floated to the surface. There is settlement and an ensuing densification of the soil. Without the above conditions liquefaction does not occur.

These conditions (i.e., shallow saturated sands and high ground motion) have been duplicated in the laboratory and procedures developed so that the prediction of soil behavior can be made.² The Beaumont Works site does not meet the conditions required for seismic-triggered liquefaction since the predicted acceleration levels are only about one-fifth of that required.

At depth, conditions are even better (i.e., there is less ground motion). While pore pressure could increase, the soils are not used as support. Furthermore, in the short interval of shaking there is just no time or place for the fluid to go. Thus, it remains incompressible.

Another question that might be asked concerns possible interaction between horizons due to casing penetration and cementation. Since there is only minor differential movement as the seismic wave passes through the medium, there should be no effect. Quantitatively, there might be several centimeters of displacement over the wavelength of the seismic wave. The normal elasticity of the casing and tubing should accommodate the strain.

In an extreme case (Kern County, California 1952) where surface motion reached 0.50g and there were many miles of surface rupture, approximately 2% of the wells in the area had some surface damage due to settlement of surficial soils. This

¹ Leeds, D.J., "The Underground Seismic Environment," Proceedings, 1st North American Rapid Excavation and Tunneling Conference, SME, AIME (1972).

² Dobry, R., et al., Prediction of Pore Water Pressure Buildup and Liquefaction of Sands During Earthquakes by the Cyclic Strain Method, NBS Building Science Series 138 (July 1982).

caused some subsurface damage such as collapsing the tubing near the surface. A sharp rise in casing pressure accompanied the shock. However, all wells returned to normal within 2 or 3 weeks.

Induced Seismicity

Earthquakes may be triggered by the impounding of large bodies of surface water (dams and reservoirs) and by the withdrawal or injection of fluids. The withdrawal of fluids (water, oil) may result in a decrease of fluid pressure and compaction of subsurface deposits which could lead to land surface subsidence. As a result of this subsidence small shallow earthquakes may occur. Rarely does fluid extraction result in seismic activity; the Wilmington Oil Field south of Los Angeles is an extreme exception.

Water flooding and hydrofracturing to increase oil recovery, and mining activity are also infrequent causes of microearthquake activity. The injection of fluid into the subsurface may also produce earthquakes by increasing fluid pressure at depth. These rarely result in seismic activity; however, a few classic examples follow. The Rocky Mountain Arsenal waste disposal well north of Denver, and the Rangely Oil Field in western Colorado are two well documented cases. These two injection sites are described below and their characteristics compared with those of the Beaumont Works in Table III. See Figures 5 through 11.

Wilmington Oil Field, California. The Wilmington field is a gently arched anticlinal fold plunging northwest with five main faults trending approximately north (Figure 5). The area is underlain by sediments of Holocene to Miocene age about 6000 feet thick that overlie pre-Tertiary basement schist. The major producing oil zones range from a depth of about 2500 to 6000 feet.

During subsidence, the rocks are subjected to stresses caused by the subsidence. These stresses can be relieved by minor faulting. Such movement occurred in claystone and soft shale beds between 1500 and 2000 feet below the surface (Mayuga, 1968)³. Six such earthquakes were recorded between December 1947 and April 1961; these events are shown in Figure 6. A movement of 9 inches was observed along one horizon at about 1550 feet after one of the earthquakes (Kovach, 1974)⁴. The movement damaged the casings of several hundred oil wells. A slow continuing, or "creeping", horizontal movement was evident between the periods of the earthquakes because many oil wells were continually being damaged along suspected planes of movement. These earthquakes were not due to tectonic factors.

³ Mayuga, M. N., *Geology and Development of California's Giant--The Wilmington Oil Field*, Preprint of a paper presented to American Association of Petroleum Geologists, 83rd Annual Meeting, Oklahoma City (1968).

⁴ Kovach, R. L., *Source Mechanisms for Wilmington Oil Field, California, Subsidence Earthquakes*, Bulletin of the Seismological Society of America, Vol. 64, No. 3, p. 866-717 (1974).

Microearthquake monitoring of the area has been accomplished by Teng, et al. (1973 through 1985)⁶. Their findings in 1973 suggest a correlation of microearthquake occurrence with water flooding and oil pumping "despite the fact that the locations of hypocenters are predominantly inside the basement complex (below 10,000 feet) and water flooding is primarily carried out at a depth between 3000 and 5000 feet". They also note (1975) that "most of the earthquakes in the Los Angeles basin originate from a depth far deeper than the region where water injection is in operation".

Rocky Mountain Arsenal, Colorado. The Rocky Mountain Arsenal disposal well is located northeast of Denver on the gently dipping east flank of the Denver-Julesburg basin (Figure 7). The disposal well penetrated 11,970 feet of sedimentary rock and 75 feet of Precambrian gneiss (Evans⁶). The very competent basement gneiss contains vertical fractures. Pressure injection tests were conducted on the well in January 1962, and contaminated waste was injected during March 1962.

Evans showed a correlation between the fluid injection and the number of earthquakes (Figure 8). Healy et al. (1968)⁷ presented evidence to indicate that the seismic activity has a tectonic origin wherein the fluid injected into the basement rock released stored tectonic strain. The earthquakes appear to be related to right-slip faulting in the basement gneiss.

Rangely Oil Field, Colorado. The Rangely Oil Field is a closed anticlinal fold in westernmost Colorado (Figure 9; Raleigh, 1972)⁸. A northeast trending normal fault with about 50 feet of displacement cuts across the anticline (Figure 10). Production is from the Paleozoic Weber sandstone; the wells have an average depth of 6700 feet (Munson, 1970)⁹. The field was discovered in 1933, but expansion of operations began during World War II. In December 1957, water flooding by fluid injection was started to recover the maximum amount of oil from the reservoir.

⁶ Teng, T. L., et al. "Microearthquakes and Water Flooding in Los Angeles." *Bulletin of the Seismological Society of America*, Vol. 43, No. 3, Berkeley, p. 888-873, (1973). A series of annual reports, *Microearthquake Monitoring in the City of Long Beach Area*, were published by Prof. Teng and his group at the University of Southern California through 1986 until support from the Department of Oil Properties of the City of Long Beach was withdrawn.

⁸ Evans, D.M., "The Denver Area Earthquakes and the Rocky Mountain Arsenal Disposal Well." *Engineering Geology Case Histories*, No. 8, Geological Society of America, Boulder, p.28-32 (1970).

⁷ Healy, J. H., W. M. Rubey, D. T. Griggs, and C. B. Raleigh, "The Denver Earthquakes", *Science*, Vol. 161, No. 3846, p.1301-1310 (1968). (See also Healy et al. "The Denver Earthquakes", *Man's Impact on Environment*, T. R. Detweiler, Editor, McGraw-Hill Book Co., p.428-441 (1970).)

⁸ Raleigh, C. B., "Earthquakes and Fluid Injection", *Underground Waste Management and Environmental Implications*, Memoir 18, American Association of Petroleum Geologists, Tulsa, p.273-276 (1972).

⁹ Munson, R. C., "Relationship and Effect of Waterflooding of the Rangely Oil Field on Seismicity", *Engineering Geology Case Histories*, No. 8, Geological Society of America, p. 38-40 (1970).

Munson compared the net fluid injected and the number of earthquakes (Figure 11). Raleigh (*loc. cit.* 1972) noted that the earthquakes originated at depths between 6000 and 12000 feet (i.e., within or below the injection zone) and that most of the events had a three-dimensional spatial relationship between earthquakes, a pre-existing fault, and fluid pressure (Figure 11). Control of the earthquakes has been shown to be feasible by controlling the injection of fluids (Bredenhoeft et al, 1974).¹⁰

Other Injection-Induced Seismicity

The Geysers Geothermal Field, California, has recorded microearthquakes in the magnitude range from 0.5 to 2.7. Their location is within the San Andreas Fault System, an active right-lateral shear zone associated with a plate boundary. The mechanism is not well understood, but there has been an injection of condensate along with the production of steam.

Sleepy Hollow Oil Field, Southwestern Nebraska, has recorded a number of earthquakes in the magnitude range from 0.6 to 2.9 during a period of fluid injection although there is a possibility of tectonic origin. Fluid injection has increased pore pressure to probably greater than 50% of the overburden pressure, but ambient stress is nearly capable of generating earthquakes and there is an historic record of seismicity.

Fenton Hill, New Mexico, was the location of hydraulic geothermal fracturing experiment in crystalline rock. Microearthquakes were generated in low permeability granitic rocks.

Northeastern Ohio Earthquake of 31 January 1986, has provoked discussion of the possibility of the $M_b=5.0$ earthquake having been induced. The most recent publication (February 1988) highlights the historical seismicity of the area but points out the coincidence of injection wells near the epicenter. The actual pressure elevation at the wells was no more than 40 bars, and probably much less. The data are not conclusive.

Gobles Oil Field, Southwestern Ontario, has generated small tremors with magnitudes from 1.0 to 2.0 in a 4-year period starting in 1980, associated with secondary oil recovery methods.

Snipe Lake Oil Field, North-central Alberta, the March 8, 1970 earthquake, $M_b=5.1$, coincided with water injection operations.

Induced Seismicity at the Du Pont Beaumont Works

¹⁰ Bredenhoeft, J. D., C. B. Raleigh, and J. H. Healy. "Control of Earthquakes at Rangely, Colorado". *ABA Bulletin of the American Association of Petroleum Geologists*, Vol. 66, No. 7, p. 1433. (1974)

Site geologic/seismologic conditions at the several sites where seismicity has been triggered by fluid withdrawal or injection are compared with conditions at the Beaumont Works site in Table III. As shown, conditions are sufficiently different that these effects need not be a consideration at the site. For example, Wilmington had 24 feet of subsidence from fluid withdrawal before subsurface adjustments began to take place. And the Rocky Mountain Arsenal injection was at extremely high pressures into fractured, hard rocks. Furthermore, Rangely is a closed anticlinal fold severely fractured by a near-surface fault.

In several cases cited the natural stress field (the potential for natural earthquakes) is almost unstable, requiring only a moderate artificially induced increase in pressure to trigger a seismic event. On the other hand, injection at Beaumont is at comparatively low pressures (above formation pressure) into deep, incompetent (soft, high porosity, granular) formations over a broad area in an area very infrequently subject to very small natural earthquakes. Obviously, there is little parallel between the quoted case histories and the Beaumont site; stress buildup would be insignificant.

Conclusions

On the basis of our analysis, we have reached the following conclusions:

1. The seismic environment of Gulf Coastal Texas near the Beaumont site is such that damaging earthquakes are unknown. The site has experienced only quite small earthquakes within historic time. The largest historic earthquake of the province is MMI=V. We conclude that a design earthquake should be MMI=V, with acceleration at the surface of 0.05g. Such an event would not be damaging to engineered structures or facilities. Subsurface motion would be much less, with no damage anticipated.

2. The probability of the injection process triggering an earthquake (induced seismicity) is extremely remote. The geology and regional tectonic conditions do not support the high stress accumulation required for earthquake generation.

Three tables, eleven figures, and three lists of references complete this report.

Should there be any questions about the report, do not hesitate to contact me.



David J. Leeds

DAVID J. LEEDS AND ASSOCIATES
CA Registered Geologist #940
CA Registered Geophysicist #GP 17
CA Certified Engineering Geologist #EG 373
AIPG Certified Professional Geologist #674



DJL:z

TABLE I

MODIFIED MERCALLI INTENSITY (DAMAGE) SCALE OF 1931
(Abridged)

- I. Not felt except by a very few under especially favorable circumstances. (I Rossi-Forel Scale.)
- II. Felt only by a few persons at rest, especially on upper floors of buildings. Delicately suspended objects may swing. (I to II Rossi-Forel Scale.)
- III. Felt quite noticeably indoors, especially on upper floors of buildings, but many people do not recognize it as an earthquake. Standing motorcars may rock slightly. Vibration like passing of truck. Duration estimated. (III Rossi-Forel Scale.)
- IV. During the day felt indoors by many, outdoors by few. At night some awakened. Dishes, windows, doors disturbed; walls make creaking sound. Sensation like heavy truck striking building. Standing motorcars rocked noticeably. (IV to V Rossi-Forel Scale.)
- V. Felt by nearly everyone, many awakened. Some dishes, windows, etc., broken; a few instances of cracked plaster; unstable objects overturned. Disturbances of trees, poles, and other tall objects sometimes noticed. Pendulum clocks may stop. (V to VI Rossi-Forel Scale.)
- VI. Felt by all, many frightened and run outdoors. Some heavy furniture moved; a few instances of fallen plaster or damaged chimneys. Damage slight. (VI to VII Rossi-Forel Scale.)
- VII. Everybody runs outdoors. Damage negligible in buildings of good design and construction; slight to moderate in well-built ordinary structures; considerable in poorly built or badly designed structures; some chimneys broken. Noticed by persons driving motorcars. (VIII Rossi-Forel Scale.)
- VIII. Damage slight in specially designed structures; considerable in ordinary substantial buildings with partial collapse; great in poorly built structures. Panel walls thrown out of frame structures. Fall of chimneys, factory stacks, columns, monuments, walls. Heavy furniture overturned. Sand and mud ejected in small amounts. Changes in well water. Persons driving motorcars disturbed. (VIII+ to IX-Rossi-Forel Scale.)
- IX. Damage considerable in specially designed structures; well-designed frame structures thrown out of plumb; great in substantial buildings, with partial collapse. Buildings shifted off foundations. Ground cracked conspicuously. Underground pipes broken. (IX+ Rossi-Forel Scale.)
- X. Some well-built wooden structures destroyed; most masonry and frame structures destroyed with foundations; ground badly cracked. Rails bent. Landslides considerable from river banks and steep slopes. Shifted sand and mud. Water splashed (slopped) over banks. (X Rossi-Forel Scale.)
- XI. Few, if any, (masonry) structures remain standing. Bridges destroyed. Broad fissures in ground. Underground pipelines completely out of service. Earth slumps and land slips in soft ground. Rails bent greatly.
- XII. Damage total. Waves seen on ground surface. Lines of sight and level discorded. Objects thrown upward into the air.

REVISIONS
BY _____ DATE _____

DILA

FILE

BY _____ DATE _____
CHECKED BY _____

DAVID J. LEEDS AND ASSOCIATES

GULF COASTAL EARTHQUAKES 1843-1989
 LAT 27°-34°N; LONG 88°-99°W

Date	SMT Time	Lat N°	Long W°	MMI	Mb	Localc
1843 02 14	---	29.9	90.1	III	3.0	
1843 02 15	---	30.0	90.0	III	---	
1847 02 14	02:--	29.6	99.0	V	3.3	Seguin
1872 05 01	04:30	30.2	97.7	IV	3.6	Manor
1882 04 12	05:--	29.9	90.1	III	3.4	
1882 10 22	22:15	33.6	95.6	VIII	5.5	
1886 01 22	16:38	30.4	92.0	II	3.0	
1886 02 05	01:--	32.8	88.0	V	---	
1886 02 13	---	32.8	88.0	-	---	
1887 01 05	17:57	30.15	97.06	VI	3.8	Paige
1887 01 31	22:14	30.52	96.2	IV	3.0	Wellborn
1891 01 08	08:--	31.7	95.2	VII	3.8	Rusk
1902 10 09	18:00	30.10	97.6	V	3.8	Creedmoor
1905 02 03	---	30.5	91.1	V	3.0	Baton Rouge, LA
1910 05 08	17:30	30.1	96.0	IV	3.8	Hempstead, Waller
1910 05 11	---	30.1	96.0	IV	3.6	Waller & Wash. Co
1910 05 12	---	30.1	96.0	IV	3.8	
1911 03 31	16:57	33.8	92.2	VI	4.7	
1911 03 31	18:10	33.8	92.2	V	4.0	
1914 12 30	01:--	30.5	95.9	V	3.5	Anderson Co
1925		29.5	94.8			Goose Creek
1927 11 13	16:21	32.3	90.2	IV	4.2	
1927 12 15	04:30	28.9	89.4	IV	4.2	
1929 06 13	14:44	30.7	88.0	III	---	
1929 07 28	17:--	28.9	89.4	IV	3.8	
1930 10 19	12:17	30.1	91.0	VI	4.7	Donaldsonville, LA
1931 12 17	03:36	33.8	90.1	VI	4.7	
1932 04 09	10:15	31.6	96.2	VI	4.0	Mexia-Wortham
1934 04 11	17:40	33.8	95.5	V	4.2	Trout Switch
1936 03 14	17:20	34.0	95.1	V	4.2	SE Oklahoma
1939 06 19	21:43	33.3	92.5	-	---	
1940 12 02	16:16	33.0	94.0	IV	3.8	
1941 08 28	18:30	32.3	90.8	IV	3.6	
1947 09 20	21:30	31.9	92.6	V	4.0	
1950 03 20	13:24	33.4	97.4	IV	3.8	Chico
1952 10 17	15:48	30.1	93.7	IV	3.8	Orange
1955 02 01	14:45	30.4	89.1	V	4.2	
1956 01 08	00:35	29.3	94.8	IV	3.8	
1956 09 27	14:15	31.9	88.5	IV	---	
1957 03 19	16:37	32.6	94.7	V	4.3	Gladewater
1957 03 19	17:41	32.6	94.7	III	3.0	Gladewater
1957 03 19	22:36	32.6	94.7	III	3.0	Gladewater
1957 03 19	22:45	32.6	94.7	III	3.0	Gladewater
1958 11 06	23:08	29.9	90.1	IV	3.8	New Orleans, LA
1958 11 19	18:15	30.5	91.2	V	4.2	Baton Rouge, LA
1959 10 15	15:45	29.8	93.1	IV	3.9	
1963 11 05	22:45	27.8	92.4	-	4.8	
1964 04 24	01:21	31.5	93.8	V	3.8	Hemphill
1964 04 28	21:18	31.2	93.9	VI	4.2	Hemphill
[Approx. 20 aftershocks through 1964 08 19 max MMI VI, Mb 4.2]						
1964 08 03	09:37	31.0	94.0	IV	3.6	
1964 10 22	16:00	31.18	89.59	VI	4.6	
1966 02 24	23:45	30.0	94.0	-	2.0	
1967 06 04	16:14	33.6	90.9	VI	4.5	

Date	GMT Time	Lat N°	Long W°	MMI	Mb	Locality
1967 06 29	13:57	33.6	90.9	V	3.4	
1967 10 24	14:34	32.7	89.3	-	2.6	
1968 10 11	02:25	34.0	96.4	III	2.3	
1968 10 11	08:55	34.0	96.4	III	2.8	
1968 10 14	14:42	34.0	96.4	VI	3.5	
1968 10 18	21:14	34.0	96.4	-	2.8	
1969 02 02	12:49	33.3	95.8	-	2.8	
1969 06 12	15:34	29.38	98.16	II	1.5	Houston Hobby Apt*
1969 06 18	15:20	29.38	98.16	II	1.5	Houston Hobby Apt*
1970 02 03	---	31.0	97.0	IV	3.8	Travis Peak
1971 03 14	18:43	23.0	88.1	-	2.9	
1971 03 15	14:53	32.8	88.3	-	3.5	
1971 03 16	02:37	32.8	88.3	-	3.7	
1971 03 17	05:04	33.1	88.1	-	3.0	
1973 01 08	09:11	33.8	90.6	III	3.5	
1973 04 25	14:32	33.9	90.8	-	3.2	
1973 05 25	14:40	33.9	90.6	IV	2.9	
1973 12 25	02:48	29.0	98.0	IV	3.0	Fashing
1974 02 15	22:32	33.95	93.09	III	3.8	
1974 02 15	22:49	34.0	93.0	V	4.0	
1974 04 20	23:48	29.0	98.0	-	3.0	South Texas
1974 06 24	18:03	29.0	98.0	-	3.4	South Texas
1974 08 01	13:33	29.0	98.0	-	3.0	South Texas
1975 03 01	11:50	33.5	88.0	IV	3.2	
1975 09 09	11:52	30.7	89.3	IV	2.9	
1976 10 23	00:40	32.2	88.9	-	3.1	
1977 05 04	02:00	31.96	88.44	V	3.5	
1977 09 12	02:36	32.95	95.24	-	2.5	
1977 11 04	11:21	33.93	89.17	IV	3.4	
1978 01 08	11:34	32.78	88.25	-	3.1	
1978 06 09	23:15	32.04	88.6	-	3.3	
1978 09 23	07:34	33.97	91.92	V	3.1	
1978 12 11	02:08	31.91	88.47	V	3.5	
1979 07 25	03:15	33.97	97.55	V	2.7	
1979 12 09	23:12	33.99	97.35	III	2.5	
1980 07 08	01:34	34.0	97.35	-	2.5	
1980 12 05	00:07	33.91	97.28	-	2.4	
1981 02 13	02:15	30.0	91.8	IV	---	
1981 02 18	08:33	29.56	91.46	-	3.0	
1981 06 09	01:48	32.142	94.399	IV	3.0	Center
1981 11 06	12:36	32.021	95.262	IV	3.2	Jacksonville
1982 03 28	23:24	29.849	98.465	-	3.0	South Texas
1983 07 23	15:24	28.743	98.131	IV	3.4	Fashing
1983 10 16	19:40	30.243	93.393	III	3.4	
1983 12 09	20:52	33.183	92.704	IV	3.0	
1983 12 10	09:24	33.183	92.704	-	2.4	
1984 03 03	01:03	28.852	98.461	IV	3.8	Pleasanton
1984 03 02	01:58	28.852	98.461	IV	3.2	Pleasanton
1984 08 08	01:31	29.133	98.362	IV	3.0	Pleasanton
1985 09 18	15:54	33.548	97.051	V	3.3	
1986 05 12	04:18	27.700	88.727	-	3.6	

MMI = Modified Mercalli Intensity

Mb = Magnitude

* Press report--not on map printout

E.I. DUPONT DE NEMOURS & COMPANY, INC.
 BEAUMONT PLANT WORKS, TEXAS

Updated Seismicity Table : 1987-1997

Lat 27° - 34° N; Long 88° - 99°W

(Data obtained from National Geophysical Data Center, US Geological Survey)

Date	Time	Lat N°	Long W°	MMI	Mb	Locale
1987	8 11	20 : 31	33.105	92.889	-	-
1988	12 12	13 : 10	33.109	92.978	-	-
1989	2 5	8 : 37	32.727	92.884	-	-
1989	2 5	8 : 37	33.201	92.778	-	-
1991	7 20	23 : 38	28.908	98.042	IV	-
1992	4 7	12 : 10	30.100	96.500	-	-
1992	8 10	1 : 57	29.000	98.500	-	-
1993	4 9	12 : 29	28.811	98.124	V	4.1
1993	5 16	15 : 30	28.810	98.170	IV	-
1994	6 10	23 : 34	33.013	92.671	III	-
1995	1 4	1 : 46	29.450	96.950	IV	-
1996	2 18	11 : 6	33.970	95.450	-	2.0
1996	2 18	11 : 6	33.970	95.459	-	2.1
1996	3 25	14 : 15	32.131	88.671	-	-
1996	3 25	14 : 15	32.131	88.671	-	-
1996	8 11	18 : 17	33.577	90.874	-	-
1996	8 11	18 : 17	33.577	90.874	-	-
1996	8 11	18 : 17	33.580	90.870	-	-
1996	8 11	18 : 17	33.580	90.870	-	-
1997	1 3	16 : 55	33.940	97.940	-	-
1997	1 9	3 : 7	33.200	92.600	-	-
1997	3 24	22 : 31	27.717	98.054	V	-
1997	3 24	22 : 31	27.580	98.030	-	3.9
1997	5 31	3 : 26	33.182	95.966	-	-
1997	12 24	18 : 32	33.200	92.750	-	-

TABLE III
INDUCED SEISMICITY COMPARISON

Wilmington Oil Field, California		
Producing rock	Sandstone	
Withdrawal/injection depth	-2500 to -6000 feet	
Structure	Anticline; 5 major faults cut producing zone	
Area	Elliptical ~3 x 11 mi.	
Induced seismicity	Horizontal movement along claystone and soft shale above producing zone, at -1550 feet. Shocks barely felt at surface	
Rocky Mountain Arsenal, Colorado		
Injection rock	Crystalline	
Injection depth	-12,000 feet	
Structure	Crystalline basement, highly fractured	
Area	N/A	
Induced seismicity	~-12,000 feet and below	
Rangely Oil Field, Colorado		
Producing rock	Sandstone	
Withdrawal/injection depth	-6700± feet	
Structure	Anticline; one major fault cuts producing zones	
Area	Elliptical, ~6 x 12 mi.	
Induced seismicity	In producing zone to depth of ~-12,000 feet	
DuPont Beaumont Works, Texas		
Injection zones	Mio.Oakville Fm	Olig.Frio Fm
Rock	Sands	Sands
Injection depth, ft	~4100	~7400
Rate, gpm	470	135
Porosity, %	31	27
Permeability, Darcys	1.5	1.14
Structure	Structural saddle between two salt domes	
Area	500 acres	
Induced seismicity	None reported or anticipated	

BY _____ DATE 6-15-89
CHECKED BY _____

FILE _____
DJLA 89-154-02

REVISIONS
BY _____ DATE _____

DAVID J. LEEDS AND ASSOCIATES

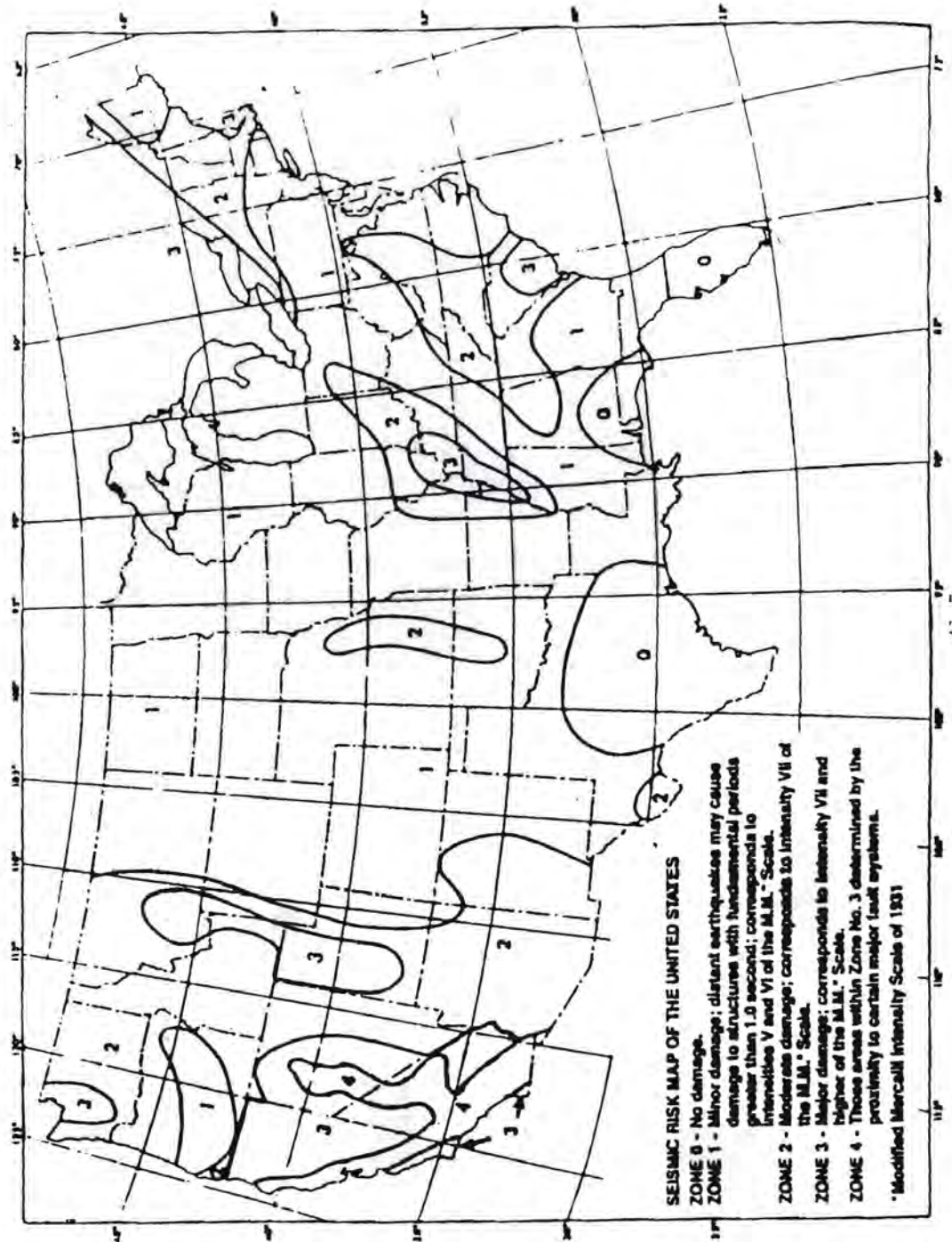


FIGURE NO. 1 - SEISMIC ZONE MAP OF THE UNITED STATES

BY _____ DATE _____
CHECKED BY _____
FILE _____
REVISIONS BY _____ DATE _____

DAVID J. LEEDS AND ASSOCIATES

The Magnitude Scale is a means of indicating the size of an earthquake on the basis of instrumental records.

Dr. C. F. Richter, Seismological Laboratory, California Institute of Technology, developed a magnitude scale which is based on the maximum recorded amplitude of a standard seismograph located at a distance of 100 km from the source of a shallow earthquake. The magnitude is defined by the relationship :

$$M = \log A - \log A_0$$

In this relationship, A is the recorded trace amplitude for a given earthquake at a given distance written by a standard instrument, and A_0 is the trace amplitude for a particular earthquake selected as a standard. The zero of the scale is arbitrarily fixed to fit the smallest recorded earthquakes. The largest known earthquake magnitudes are on the order of $8 \frac{3}{4}$. This magnitude is the result of observations and not an arbitrary scaling. The upper magnitude limit is not known, but is estimated to be about 9.

Empirical relationships between earthquake magnitude and energy release have been developed by several investigators. There is no exact relationship between earthquake magnitude and energy for large earthquakes, and these empirical relationships should be considered no more than approximations.

RICHTER MAGNITUDE DEFINITION
(sheet 1 of 2)

C. F. Richter, 1958
Elementary Seismology

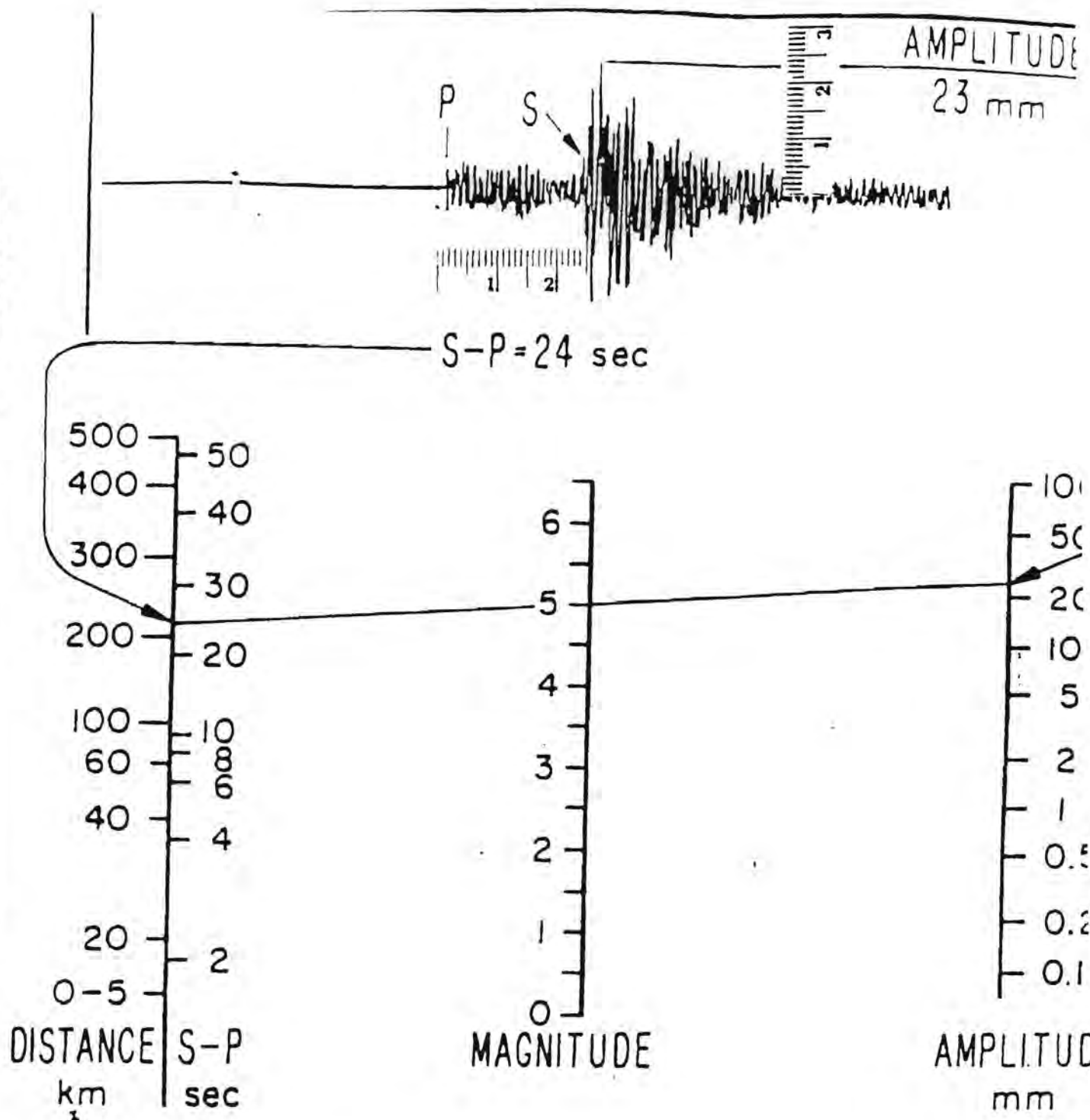
Figure 2a

REVISIONS BY _____ DATE _____

FILE _____

BY _____ DATE _____

CHECKED BY _____



TO DETERMINE THE MAGNITUDE OF AN EARTHQUAKE WE CONNECT ON THE CHART

A. THE MAXIMUM AMPLITUDE RECORDED BY A STANDARD SEISMOMETER, AND

B. THE DISTANCE OF THAT SEISMOMETER FROM THE EPICENTER OF THE EARTHQUAKE (OR THE DIFFERENCE IN TIMES OF ARRIVAL OF THE P AND S WAVES)

BY A STRAIGHT LINE, WHICH CROSSES THE CENTER SCALE AT THE MAGNITUDE

RICHTER MAGNITUDE DEFINITION
(sheet 2 of 2)

BY _____ DATE 6-30-89
CHECKED BY _____

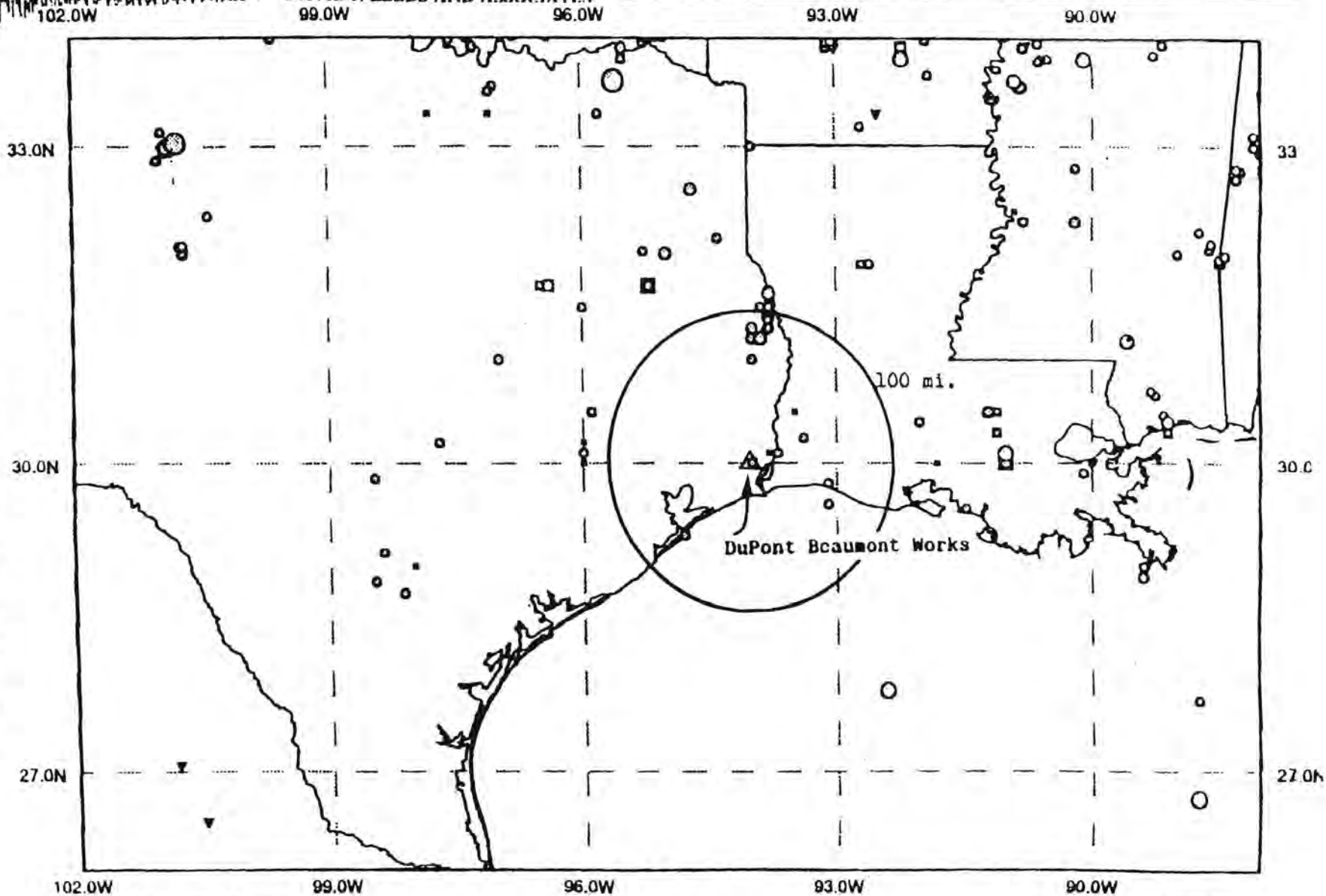
FILE DJLA 89-154-03

REVISIONS
BY _____ DATE _____

DAVID J. LEEDS AND ASSOCIATES

NCDC June 1989

GULF COAST SEISMICITY



MAGNITUDES

<4.0 ○
5.0 ○
6.0 ○

281 EARTHQUAKES PLOTTED

1843 - 1989

INTENSITIES

I-IV .
V -

NO INTENSITY OR MAGNITUDE

FILE 5119

BY _____ DATE May 12, 1989

CHECKED BY _____

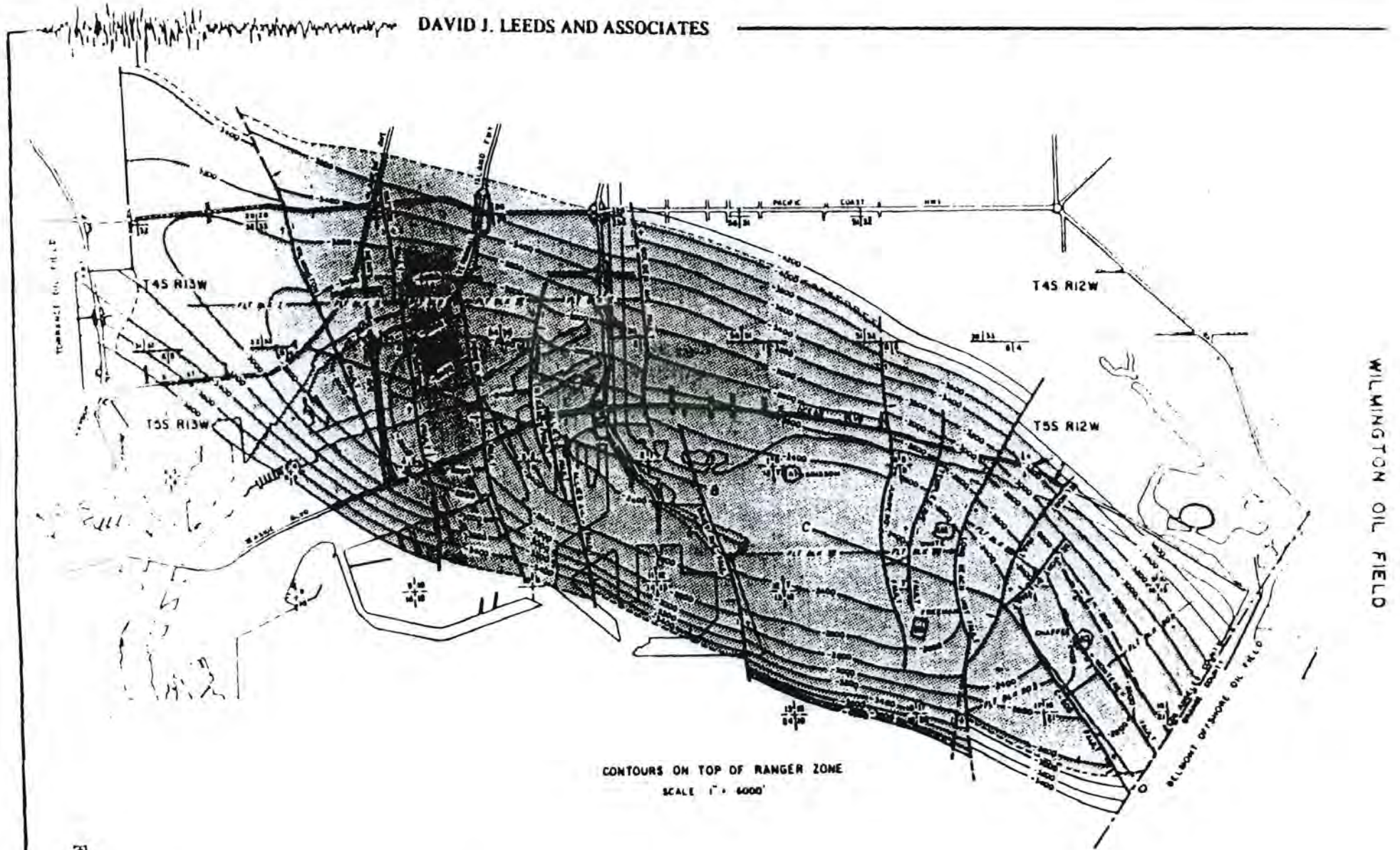
FILE DJLA 89 4-01/-02

REVISIONS

BY _____ DATE 6-15-07

"Calif. Oil & Gas Fields", Vol. II, Calif Div.011 & Gas, 1974

DAVID J. LEEDS AND ASSOCIATES



CONTOURS ON TOP OF RANGER ZONE
SCALE 1" = 6000'

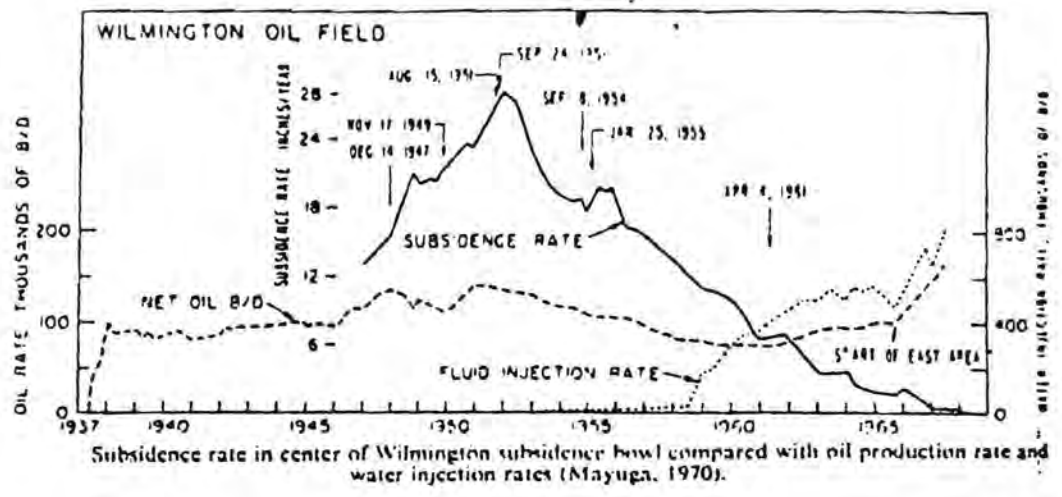
Figure 5a

BY _____ DATE 12 May 1989
CHECKED BY _____

FILE _____ DJLA 89-154-01 / -02

REVISIONS
BY _____ DATE 6-1-89

[Handwritten signature]
DAVID J. LEEDS AND ASSOCIATES



Wilmington Oil Field
Subsidence Rate
and Earthquakes

BY _____ DATE 12 May 1989

CHECKED BY _____ FILE _____

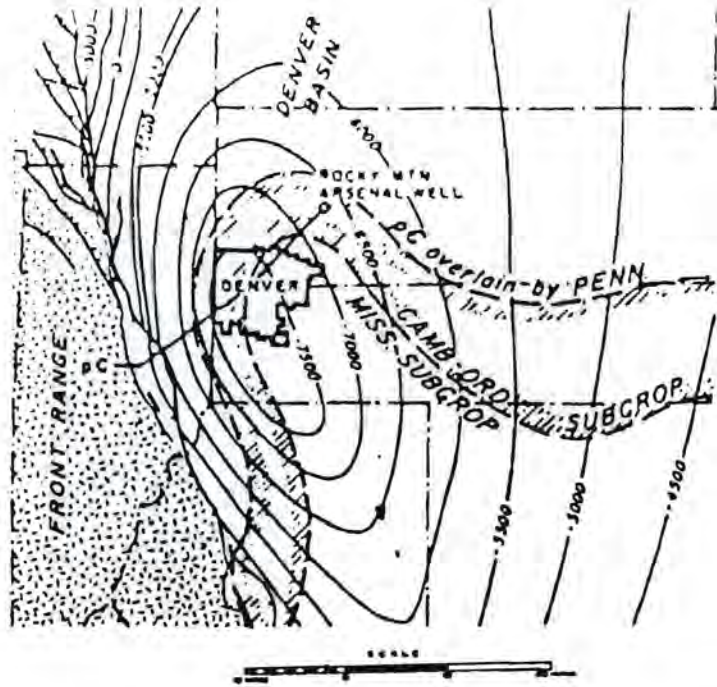
DJLA 89-154-01 / -02

REVISIONS

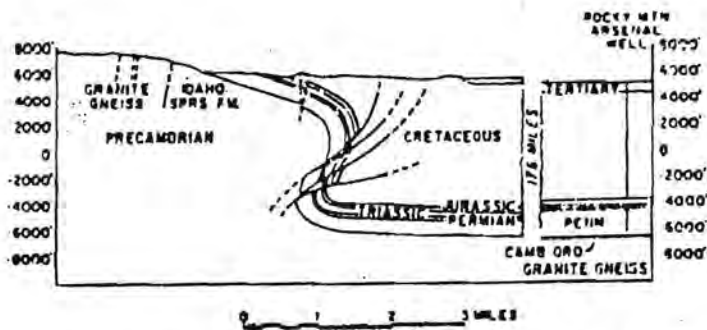
BY _____ DATE _____

6-1

DAVID J. LEEDS AND ASSOCIATES



(a) Structural map of a portion of the Denver-Julesburg Basin (after Anderman and Ackman, 1963), showing the location of the Rocky Mountain Arsenal well.

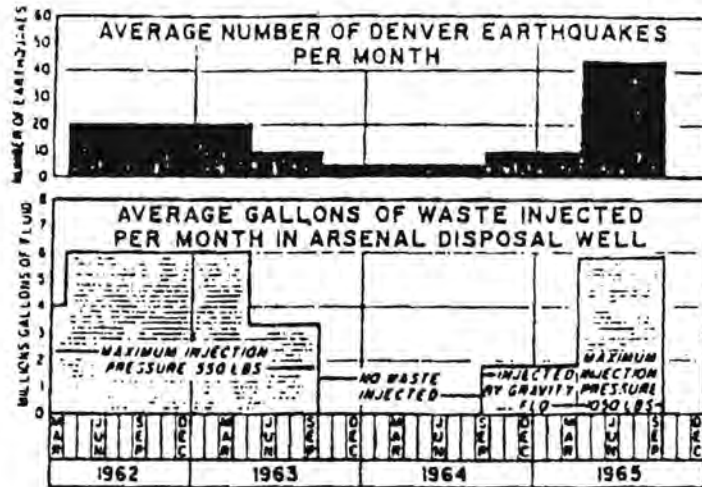


(b) Cross-section showing the subsurface geology from the Arsenal well to the outcrop of Precambrian granite gneiss west of Denver (after H. F. and C. F. Boos, and H. H. Odiorne). The line of cross-section is shown in Figure 1.

Denver-Julesburg Basin

BY _____ DATE 12 May 1989 FILE _____ DATA 89-154-01 / -02 REVISIONS 6-11
 CHECKED BY _____ BY _____ DATE _____

DAVID J. LEEDS AND ASSOCIATES



Earthquake frequency - waste injection relationships during five characteristic periods.

Rocky Mountain Arsenal
 Induced Seismicity

BY _____ DATE 12 May 1989

CHECKED BY _____

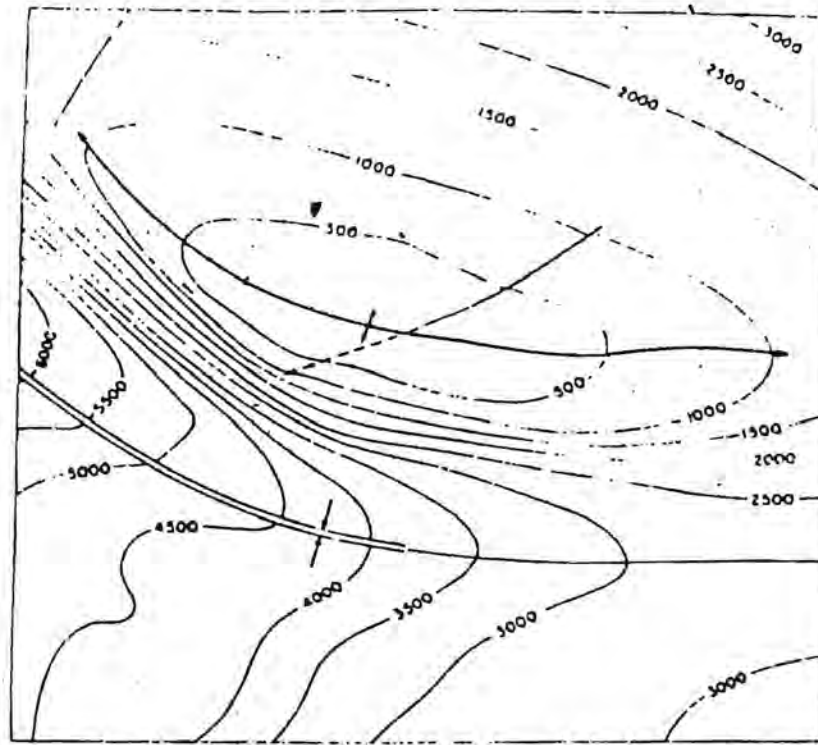
FILE _____

DJLA 89-174-01 /02

REVISIONS

BY _____ DATE 6-15-

DAVID J. LEEDS AND ASSOCIATES



Structure contours of top of Weber Sandstone near Rangely, Colorado. Rangely field is located in closed anticline. Faults shown are mapped from displacements in elevation of upper contact of Weber Sandstone (courtesy Chevron Oil Company).

Rangely Oil Field
Structural Contour Map

BY _____ DATE 12 May 1989

CHECKED BY _____

FILE _____

DATA 89-154-01/-02

REVISIONS

BY _____ DATE _____

6-15

DAVID J. LEEDS AND ASSOCIATES



Epicenters of earthquakes in Rangely field (outlined by dashed line) between October 1969 and November 1970. Contours give bottomhole pressure (psi) measured in September 1969 (courtesy Chevron Oil Company). Triangles represent seismograph stations; circles, experimental wells; square, well in which stresses were measured by hydraulic fracturing.

Rangely Oil Field
Induced Seismicity

BY _____ DATE 12 May 1989

CHECKED BY _____

FILE _____

DJLA 89-154-01 / -02

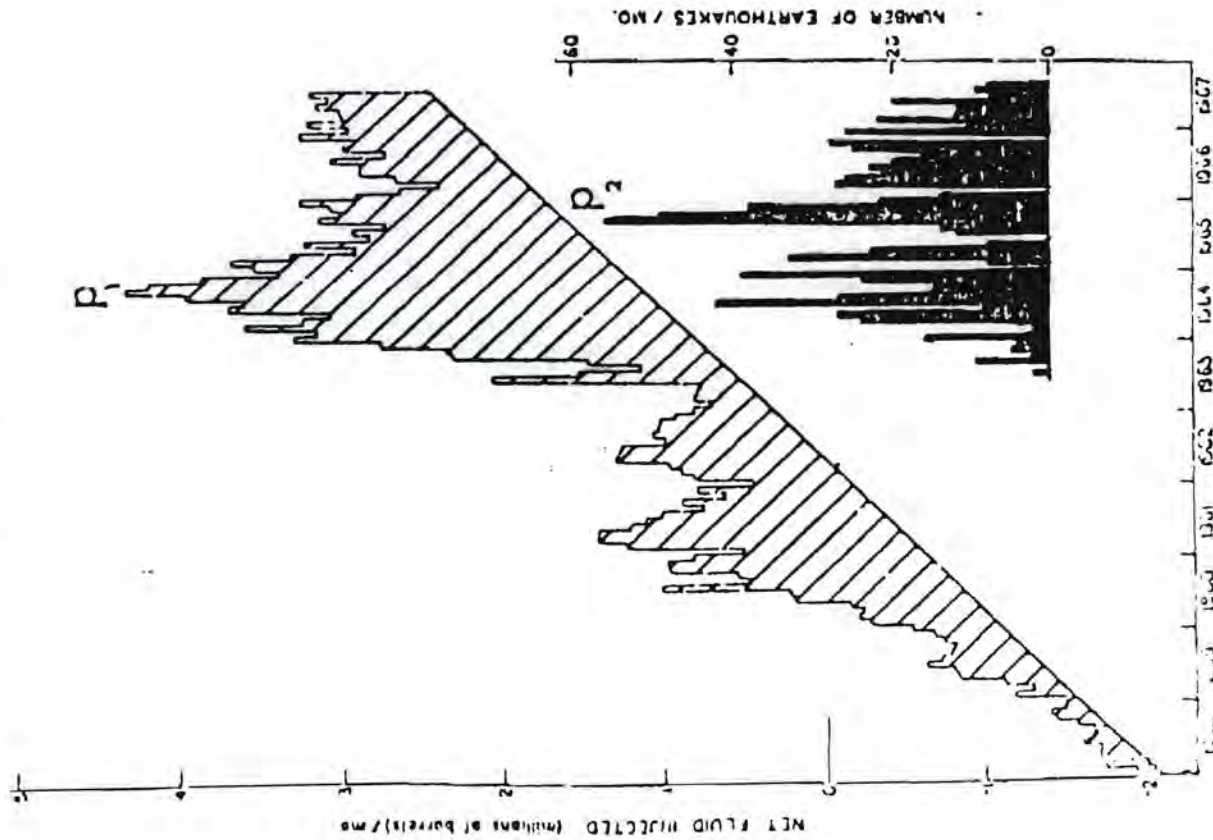
REVISIONS

BY _____ DATE _____

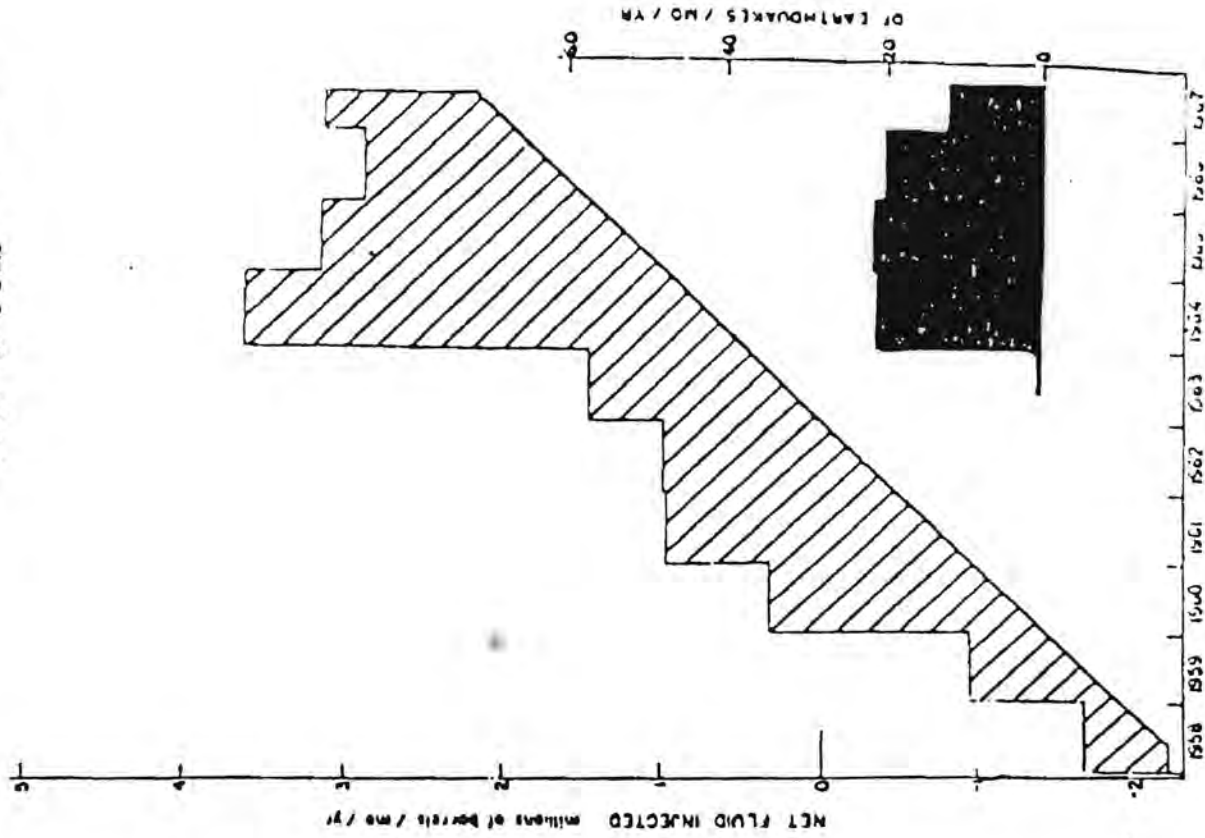
6-15

DAVID J. LEEDS AND ASSOCIATES

Monthly Values



Monthly Values Averaged
Over a Year



REFERENCES: INDUCED SEISMICITY

- Ahmad, MU and JA Smith, Earthquakes, Injection Wells, and the Perry Nuclear Power Plant, Cleveland, Ohio, *USA Geology*, Vol 16, No. 8, pp 739-742 (1988).
- Allis, RG, Mechanisms of Induced Seismicity at The Geysers Geothermal Reservoir, California, *Geophys. Res. Lett.*, Vol 9, pp 629-632 (1982).
- Armbruster, JG and L Seeber, Spatial Correlation Between the Aftershocks of the 1886 Charleston, S.C. Earthquake and Recent Induced Seismicity in the Southeastern U.S., *Seis. Soc. Am. 1985 Annual Mtg, Austin, TX, Earthquake Notes*, Vol 55, No. 1, pp 25-26 (1985).
- Bardwell, GE, Some Statistical Features of the Relationship Between Rocky Mountain Arsenal Waste Disposal and Frequency of Earthquakes, *Mountain Geologist*, Vol 3, pp 37-42 (1966).
- Borcherdt, RD, ed., Preliminary Report on Aftershock Sequence for Earthquake of January 31, 1986 near Painesville, Ohio (Time Period: 2/1/86-2/10/86), *U.S. Geol. Surv. Open-file Report 86-181*, 109 pp (1986).
- Bredhoeft, JD et al., Control of Earthquakes at Rangely, Colorado (abstract), *Bull. Am. Assn. Petrol. Geol.*, Vol 58, No. 7, p 1432 (1974).
- Davis, SD, Investigations of Natural and Induced Seismicity in the Texas Panhandle, MS thesis, 230 pp, University of Texas, Austin, TX (1985).
- Davis, SD and FJ Mauk, Seismicity Induced by Geopressured/Geothermal Well Development in the Texas and Louisiana Gulf Coast (abstract), *EOS*, Vol 63: No. 45, p 1044 (1982).
- Davis, SD and WD Pennington, A Barrier-Asperity Model for Injection Induced Deformation in the Cogdell Oil Field, Kent and Scurry Counties, Texas, *Seismol. Soc. Am. 1985 Annl Mtg, Austin, TX, Earthquake Notes*, Vol 55, No. 1, p 18 (1985).
- Davis, SD and WD Pennington, Induced Seismic Deformation in the Cogdell Oilfield of West Texas, *Bull. Seismol. Soc. Am.*, preprint (1987).

- Denlinger, RP and CG Bufe, Reservoir Conditions Related to Induced Seismicity at the Geysers Steam Reservoir, Northern California, *Bull. Seismol. Soc. Am.*, Vol 72, pp 1317-1327 (1982).
- Diao, S-Z, Zhou H-P, and Guo, A-X, Induced Earthquakes by Injecting and Leaking Water in Jiao 7 Oil Well, Shandong Province: Characteristics of the Focal Parameters and Earthquake Sequences, *Seismol. Bur. Shandong Prov., China, Seismology and Geology*, Vol 9, No. 3, pp 84-89 (1987). (in Chinese; summaries in English)
- Dieterich, JH, CB Raleigh, and JD Bredehoeft, Earthquake Triggering by Fluid Injection at Rangely, Colorado, *Proc. Int. Soc. Rock Mech. and Int. Assoc. Eng. Symp. Paper T2-B* (1972).
- Eberhart-Phillips, D and DH Oppenheimer, Induced Seismicity in the Geysers Geothermal Area, California, *J. Geophys. Res.*, Vol 89, No. 2, pp 1191-1207 (1984).
- Evans, DG and DW Steeples, Microearthquakes near the Sleepy Hollow Oilfield, Southwestern Nebraska, *Bull. Seismol. Soc. Am.*, Vol 77, No. 1, pp 132-140 (1987).
- Evans, DM, The Denver Area Earthquakes and the Rocky Mountain Arsenal Disposal Well, *Mountain Geologist*, Vol 3, pp 23-36 (1966).
- Fehler, M, Spectral Studies of Very Small Earthquakes Induced by Hydraulic Fracturing, *Seismol. Soc. Am. 1985 Annu Mtg, Austin, TX, Earthquake Notes*, Vol 55, No. 1, p 12 (1985).
- Fletcher, JB and LR Sykes, Earthquakes Related to Hydraulic Mining and Natural Seismic Activity in Western New York State, *J. Geophys. Res.*, Vol 82, pp 3767-3780 (1977).
- Gibbs, JF et al., Seismicity in the Rangely, Colorado, Area: 1962-1970, *Bull. Seismol. Soc. Am.*, Vol 63, pp 1557-1570 (1973).
- Glassmoyer, GR et al., Source and Propagation Characteristics for Aftershock Sequence near Painesville, Ohio (abstract), *EOS Trans. AGU*, Vol 67, p 314 (1986).

Induced Seismicity;
OJLA 89-154-03
July 15, 1989
Page 3

- Cough, DI, *Induced Seismicity, The Assessment and Mitigation of Earthquake Risk*, pp 91-117, UNESCO, Paris (1978).
- Haimson, BC, *Earthquake Stresses at Rangely, Colorado, New Horizons in Rock Mechanics: Earthquakes and Other Dynamic Phenomena*, HR Hardy and R Stefanko, eds., *Proc. U.S. Symp. Rock Mechanics*, Vol 14, pp 680-708 (1972).
- Harding, ST, *Induced Seismicity in the Cogdell Canyon Reef Oil Field, U.S. Geol. Surv. Open-file Report 81-333*, p 547 (1981).
- Harding, ST et al., *The Scurry County, Texas, Earthquake Series of 1977-1978: Induced Seismicity?* (abstract), *Earthquake Notes*, Vol 49, No. 3, pp 14-15 (1978).
- Healy, JH et al., *The Denver Earthquakes, Science*, Vol 161, pp 1301-1310 (1968).
- Herrmann, RD, S-K Park, and CY Wang, *The Denver Earthquakes of 1967-1968, Bull. Seismol. Soc. Am.*, Vol 71; pp 731-745 (1981).
- Holmes and Narver, *Geothermal Induced Seismicity Program Plan, Report HN-00020-1094*, 21 pp (1981).
- House, L, *Locating Microearthquakes Induced by Hydraulic Fracturing in Crystalline Rock, Geophys. Res. Ltr*, Vol 14, No. 9, pp 919-921 (1987).
- House, LS and N McFarland, *Locations of Microearthquakes Induced by Hydraulic Fracturing at Fenton Hill, New Mexico, in May 1984* (abstract), *Earthquake Notes*, Vol 55, No. 1, p 12 (1985).
- Hsieh, PA and JS Bredehoeft, *A Reservoir Analysis of the Denver Earthquakes: A Case of Induced Seismicity, J. Geophys. Res.*, Vol 86, pp 903-920 (1981).
- Johnson, SJ and EL Krinitzsky, *Reservoirs and Induced Seismicity at Corps of Engineers Projects, Final Report, Waterways Experiment Station, Misc. Paper S-77-3*, 14 pp (1977).

- Knappe, BK (compiler), *Underground Injection Operations in Texas: A Classification and Assessment of Underground Injection Activities*, Texas Dept. of Water Resources Rep. 291 (1984).
- Li, X and R Yang, An Induced Event by Water Injection and Its Seismological Implication, Seismol. Bur. Jilin Prov., China, *Earthquake Research in China*, Vol 2, No. 4, pp 95-99 (1986).
- Lu, S-A et al., Induced Earthquakes by Injecting and Leaking Water in Jiao 7 Oil Well, Shandong Province: Macroscopic Phenomena on Ground Surface and Characteristics of Earthquake Swarm Activity, Seismol. Bur. Shandong Prov., China, *Seismology and Geology*, Vol 9, No. 3, pp 79-83 (1987). (in Chinese; summaries in English)
- Mereu, RF et al., A Study of the Microearthquakes of the Gobles Oilfield Area of Southwestern Ontario, *Bull. Seismol. Soc. Am.*, Vol 76, pp 1215-1223 (1986).
- Milne, WG, The Snipe Lake, Alberta Earthquake of March 6, 1970, *Can. J. Earth Sci.*, Vol 7, pp 1564-1567 (1970).
- Milne, WG and MJ Berry, Induced Seismicity in Canada, *Eng. Geol.*, Vol 10, pp 219-226 (1976).
- Munson, RC, Relationship of Effect of Water Flooding of the Rangely Oil Field on Seismicity, in *Engineering Geology*, WM Adams, ed., *Geol. Soc. Am. Eng. Case Hist. 8*, pp 39-49 (1970).
- Nicholson, C, E Roeloffs, and RL Wesson, The Northeastern Ohio Earthquake of January 31, 1986: Was It Induced? *EOS Trans. AGU*, Vol 68, pp 354-355 (1987). Also *Bull. Seismol. Soc. Am.*, Vol 78, No. 1, pp 188-217 (1988).
- Nottis, GN, A Chronology of Events and Review of the Association of Seismicity with Well #11 and #12 at the Dale Brine Field, Dale, New York, 19 pp, Geoscience Services, Summit, NJ (1986).
- Ohtake, M, Seismic Activity Induced by Water Injeciton at Matsushiro, Japan, *J. Phys. Earth*, Vol 22, pp 163-174 (1974).

- Orr, CD and GR Keller, Keyston Field, Winkler County, Texas: An Examination of Seismic Activity, In-Situ Stresses, Effective Stresses, and Secondary Recovery (abstract), *Earthquake Notes*, Vol 52, pp 29-30 (1981).
- Patrick, DM, Microearthquake Monitoring at Corps of Engineers Facilities, Interim Report, Waterways Experiment Station, *Technical Report 77-2*, 88 pp (1977).
- Pearson, C, The Relationship Between Microseismicity and High Pore Pressures During Hydraulic Stimulation Experiments in Low Permeability Granitic Rocks, *J. Geophys. Res.*, Vol 86, pp 7855-7864 (1981).
- Pennington, WD, Comments on the Usefulness of Studies of Oil- and Gas-Field Seismicity (abstract), *Earthquake Notes*, Vol 55, No. 3, p 13 (1984).
- Pennington, WD and SD Davis, Changing Pore-fluid Pressures and the Evolution of Seismic Barriers and Asperities in Texas Oil and Gas Fields (abstract), *Seismol. Soc. Am. 1985 Annl Mtg, Austin, TX*, *Earthquake Notes*, Vol 55, No. 1, pp 17-18 (1985).
- Pennington, WD and SD Davis, Fluid Flow, Shear Fractures, and Earthquakes in Texas Oil and Gas Fields, *Soc. Expl. Geophys. 38th Annl Midwest Regional Mtg, San Antonio, Geophysics*, Vol 50: No. 7, p 1205 (1985).
- Pennington, WD et al., The Evolution of Seismic Barriers and Asperities Caused by the Depressuring of Fault Planes in Oil and Gas Fields of South Texas, *Bull. Seismol. Soc. Am.*, Vol 76, pp 939-948 (1986).
- Raleigh, CB, Earthquakes and Fluid Injection, *Underground Waste Management and Environmental Implications*, *Am. Assn Petrol. Geol. Memoir 18*, pp 273-279 (1972).
- Raleigh, CB, JH Healy, and JD Bredenhoeft, An Experiment in Earthquake Control at Rangely, -Colorado, *Science*, Vol 191, pp 1230-1237 (1976).
- Roeloffs, EA, Shear Faulting in Porous Media Accompanied by Fluid Injection: A Solution in Terms of Biot's Three Waves, *AGU 1982 Spring Mtg: abstracts; also EOS, Trans. AGU*, Vol 63, No. 18, 372 pp (1982).

Induced Seismicity
DOLA 89-154-03
July 15, 1989
Page 6

- Rothe, GH and C-Y-Lui, Possibility of Induced Seismicity in the Vicinity of the Sleepy Hollow Oil Field, Southwestern Nebraska, *Bull. Seismol. Soc. Am.*, Vol 73, pp 1357-1367 (1983).
- Sanford, AD and TR Topozada, Seismicity of Proposed Radioactive Waste Disposal Site in Southeastern New Mexico, *New Mexico Bur. Mines & Min. Res. Circ. 143*, 15 pp (1974).
- Sanford, AD et al., Seismicity in the Area of the Waste Isolation Pilot Plant (WIPP), *Sandia Laboratories Rep. SAND 80-7096* (1980).
- Scopel, LJ, Pressure Injection Disposal Well, Rocky Mountain Arsenal, Denver, Colorado, *GSA Engr. Geol. Case Histories*, No. 8, pp 19-24 (1979). Also *The Mountain Geologist*, Vol 1, No. 1, pp 35-42.
- Seeber, L et al., A Concentrated Source of Seismicity Associated with Flooding of the Deep Witherbee/Mineville Iron Mine, *Seismol. Soc. Am. 1985 Annual Mtg*, Austin, TX, *Earthquake Notes*, Vol 55, No. 1, pp 18-19 (1985).
- Seeber, L, JG Armbruster, and K Evans, Recent Historic Seismicity in Northeastern Ohio; Reactivation of Precambrian Faults and the Role of Deep Fluid Injection, *Geol. Soc. Am. 22nd Annual Mtg*, North-Central Section, *Abstracts with Programs* 20:5, 387 pp (1988).
- Segall, P, Stress and Subsidence Resulting from Subsurface Fluid Withdrawal in the Epicentral Region of the 1983 Coalinga Earthquake, *J. Geophys. Res.*, Vol 90, No. 8, pp 6801-6816 (1985).
- Segall, P and JW Rudnicki, Stress and Pore-pressure Changes Resulting from Fluid Extraction and Injection: Application to the 1983 Coalinga, California, Earthquake, *Seismol. Soc. Am. 1985 Annl Mtg*, Austin, TX, *Earthquake Notes*, Vol 55, No. 1, p 17 (1985).
- Segall, P and RF Yerkes, Stress and Fluid Pressure Changes Associated with Oil Field Operations: A Critical Assessment of Effects in the Focal Region of the 1983 Coalinga Earthquake, *U.S. Geol. Surv. Open-file Report 85-44*, pp 313-343 (1985).
- Simpson, DW, Seismicity Changes Associated with Reservoir Impounding, *Eng. Geol.*, Vol 10, pp 371-375 (1976).

Induced Seismicity
DJLA 89-154-03
July 15, 1989
Page 7

- Simpson, DW, Triggered Earthquakes, *Ann. Rev. Earth Sci.*, Vol 14, pp 21-42 (1986).
- Simpson, D, Reservoir-induced Earthquakes and the Hydraulic Properties of the Shallow Crust (abstract), *EOS Trans. AGU*, Vol 67, p 242 (1986).
- Simpson, DW and SK Negmatullaev, Induced Seismicity at the Murek Reservoir, Tadjikistan, U.S.S.R., *Bull. Seismol. Soc. Am.*, Vol 71, pp 1561-1586 (1981).
- Snow, DT, Hydrogeology of Induced Seismicity and Tectonism: Case Histories of Kariba and Koyna, *Geol. Soc. Am. Spec. Paper 189*, pp 3117-3360 (1982).
- Steeple, DW, Induced Seismicity in the Sleepy Hollow Oil Field, Red Willow County, Nebraska, *U.S. Geol. Surv. Open-file Report 85-464*, pp 429-432 (1985).
- Talebi, S and F Cornet, Analysis of the Microseismicity Induced by a Fluid Injection in a Granitic Rock Mass, *Geophys. Res. Lett.*, Vol 14, No. 3 (pp 227-230 (1987).
- Talwani, P, Induced Seismicity: A Review, *Int'l Assoc. Seismol. & Physics of Earth's Interior Regional Assembly: Abstracts*, Hyderabad, India Oct 31-Nov 7, 1984, Natl Geophys. Res. Inst. India, 88 pp (1984).
- Talwani, P and S Acree, Deep Well Injection at the Calhio Wells and the Leroy, Ohio Earthquake of January 31, 1986, *A Report to the Cleveland Electric Illuminating Co.*, North Perry, OH, 92 pp (1986).
- Talwani, P and SD Acree, Did Deep Well Injection Induce the Leroy, Ohio Earthquake of January 31, 1986? *Geol. Soc. Am. 22nd Annual Mtg, North-Central Section: Abstracts with Programs* 20:5, 391 pp (1988).
- Teng, TL, CR Real, and TL Henyey, Microearthquakes and Water Flooding in Los Angeles, *Bull. Seismol. Soc. Am.*, Vol 63, pp 859-875 (1973).
- Terashima, T, Survey on Induced Seismicity at Mishraq Area in Iraq, *J. Phys. Earth*, Vol 29, pp 371-375 (1981). Also in *Jishin*, Vol 33, No. 4, pp 443-463 (1980) (in Japanese; summaries in English).

Induced Seismicity
DJLA 89-154-C3
July 15, 1989
Page 8

Turbitt, T et al., Monitoring the Background and Induced seismicity for the Hot Dry Rock Programme in Cornwall, *European Geothermal Update: Third International Seminar on the Results of EC Geothermal Energy Research, Nov 29-Dec 1, 1983, Munich, D Reidel Publ. Co., pp 712-716 (1985).*

van Poolen, HK and DB Hoover, Waste Disposal and Earthquakes at the Rocky Mountain Arsenal, Derby, Colorado, *J. Petrol. Tech., Vol 22, pp 983-993 (1970).*

Voss, JA and RB Herrmann, A Surface Wave Study of the June 16, 1978 Texas Earthquake, *Earthquake Notes, Vol 51, pp 3-14 (1980).*

Wesson, RL, and Nicholson, C, Earthquake Hazard Associated with Deep Well Injection: A Report to the U.S. Environmental Protection Agency, *U.S. Geol. Surv. Open-file Report 87-331, 107 pp (1987).*

Wesson, RL et al., Possible Role of Fluid Injection, *Studies of the January 31, 1986 Northeastern Ohio Earthquake, U.S. Geol. Surv. Open-file Report 86-331, pp 12-24 (1986).*

REFERENCES: TEXAS SEISMOLOGY

- Bell, DE and VA Brill, Active Faulting in Lavaca County, Texas, *Bull. Am. Assn Petrol. Geol.*, Vol 22, No. 1, pp 104-106 (1938).
- Bornhauser, M, Gulf Coast Tectonics, *World Oil*, pp 113-124 (1956).
- Brazee, RJ and WK Cloud, Earthquake of March 19, 1957, *United States Earthquakes 1957*, pp 16-18 (1959).
- Bryan, F, Evidence of Recent Movements Along Faults of the Balcones System in Central Texas, *Bull. Am. Assn Petrol. Geol.* Vol 20, No. 10, pp 1357-1371 (1936).
- Bryan, F, Recent Movements on a Fault of the Balcones System, McLennon County, Texas, *Bull. Am. Assn Petrol. Geol.* Vol 17, No. 4, pp 439-442 (1933).
- Burr, JG, The Probable Earthquake Origin of Caddo Lake (Texas-Louisiana) (abstract), *Texas Acad. Sci. Proc.* 1942, p 132 (1943). Full text in *Shreveport Times*, March 1943.
- Byerly, P, The Texas Earthquake of August 16, 1931, *Bull. Seismol. Soc. Am.*, Vol 24, No. 2, pp 81-99 and Vol 24, No. 3, pp 303-325 (1934).
- Carlson, SM, S Davis, and W Pennington, Recent Earthquakes in the Gulf Coast of Texas, *EOS*, Vol 64, No. 45, p 750 (1983).
- Carlson, SM and WD Pennington, The Seismicity of East Texas, *Geol. Soc. Am. Abstracts with Programs*, Vol 15, No. 1, p 39 (1983).
- Carlson, SM, WD Pennington, and SD Davis, Seismicity of East Texas (abstract), *Earthquake Notes*, Vol 55, No. 3, p ii (1984).
- Carlson, S, Investigations of Recent and Historical Seismicity in East Texas, MS thesis, 197 pp, University of Texas, Austin, TX (1984).

Texas Seismology;
DOLA 89-154-04
July 15, 1989
Page 2

- Castle, RO and TL Youd, Discussion: The Houston Fault Problem, *Bull. Assn Engr. Geol.*, Vol 9, No. 1, pp 57-77 (1972).
- Clanton, US, Active Faults in Southwest Harris County, Texas, *Envir. Geol.*, Vol 1, No. 3 (1975).
- Crosby, GW, Gravity and Mechanical Study of the Great Bend in the Mexia-Talco Fault Zone, Texas, *J. Geophys. Res.*, Vol 76, No. 11, pp 2690-2705 (1971).
- Davis, SD, Historical Seismicity of Texas - A Summary, *Bull. Am. Assn Petrol. Geol.*, Vol 69, No. 9, p 149 (1985).
- Davis, SD, Investigations of Natural and Induced Seismicity in the Texas Panhandle, MS thesis, 230 pp, University of Texas, Austin, TX (1985).
- Davis, SD and WD Pennington, A Barrier-Asperity Model for Injection Induced Deformation in the Cogdell Oil Field, Kent and Scurry Counties, Texas, *Earthquake Notes, Seismol. Soc. Am. Annl Mtg, Austin, TX*, p 18 (1985).
- Davis, SD and WD Pennington, Induced Seismic Deformation in the Cogdell Oilfield of West Texas, *Bull. Seismol. Soc. Am.*, preprint (1987).
- Davis, SD and WD Pennington, Seismicity of the Texas Panhandle, *Earthquake Notes*, Vol 55, No. 3, pp 11-12 (1984).
- Davis, SD, WD Pennington, and SM Carlson, Historical Seismicity of the State of Texas - A Summary, *Trans. Gulf Coast Assn Geol. Soc.*, Vol XXXV, pp 39-43 (1985).
- Dawson, RF, A Review of the Land Subsidence Problems in the Texas Gulf Coast Area, preprint, Surveying & Mapping Div., Am. Soc. Civ. Engr. Mtg, Houston, TX (1962).
- Doser, DI, The 16 August 1931 Valentine, Texas, Earthquake: Evidence for Normal Faulting in West Texas, *Bull. Seismol. Soc. Am.*, Vol 77, No. 6, pp 2005-2017 (1987).

Texas Seismology;
DJLA 89-154-C4
July 15, 1989
Page 3

- Dumas, DB, Active Seismic Focus near Snyder, Texas, *Bull. Seismol. Soc. Am.*, Vol 69, No. 4, pp 1295-1299 (1979).
- Dumas, DB, HJ Dorman, and GV Latham, A Reevaluation of the August 16, 1931 Texas Earthquake, *Bull. Seismol. Soc. Am.*, Vol 70, No. 4, pp 1171-1180 (1980).
- Dumas, DB, HJ Dorman, and GV Latham, The August 16, 1931 Texas Earthquake, *EOS*, Vol 60, No. 46, p 894 (1979).
- Dumas, DB, Erratum to Active Seismic Focus near Snyder, Texas, *Bull. Seismol. Soc. Am.*, Vol 70, No. 4, p 1427 (1980).
- Eppley, RA and WK Cloud, Earthquake of June 17, 1959, *United States Earthquakes 1959*, pp 11-12 (1961).
- Foley, LL, Mechanics of the Balcones and Mexia Faulting, *Bull. Am. Assn Petrol. Geol.*, Vol 10, pp 1261-1269 (1926).
- Frolich, C and DB Dumas, The Seismicity of the Gulf of Mexico (abstract), *EOS Trans. AGU*, Vol 61, pp 288 (1980).
- Frolich, C, Seismicity of the Central Gulf of Mexico, *Geology*, Vol 10, pp 103-106 (1982).
- Gabrysch, RK, Land-surface Subsidence in the Houston-Galveston Region, Texas, *Land Subsidence, Proc. Tokyo Symposium IASH/AISH-UNESCO*, pp 43-55 (1969).
- Gray, E, The Geology, Ground-water, and Surface Subsidence of the Baytown-La Porte Area, Harris County, Texas (unpub. thesis), Texas A&M Univ., 10 pp (1958).
- Harding, ST, Induced Seismicity in the Cogdell Canyon Reef Oil Field, *U.S. Geol. Surv. Open-file Report 81-333*, p 547 (1981).
- Harding, ST et al., The Scurry County, Texas, Earthquake Series of 1977-1978: Induced Seismicity? (abstract), *Earthquake Notes*, Vol 49, No. 3, pp 14-15 (1978).

- Henley, AD, Seismic Activity near the Texas Gulf Coast, *Engr. Geol.*, Vol 3, No. 1-2, pp 33-39 (1966).
- Hull, LV, New Dallas Seismological Observatory at SMU, *Bull. Seismol. Soc. Am.*, Vol 46, No. 4, pp 321-330 (1956).
- Humphreys, WJ, Seismological Reports for October, November and December, 1914, *Monthly Weather Review*, U.S. Weather Bur., Vol 42, p 689 (1914).
- Jenneman, VF, Microseisms at Corpus Christi (abstract), *Union Geod. et Geophys. Int. Assn Seismol. Comptes Rendus*, No. 9, p 24 (1949); also *Geophysical Abstracts* 139, p 278 (1949).
- Jurkowski, G, J Ni, and L Brown, Modern Uparching of the Gulf Coastal Plain, Paper 4B0463, *J. Geophys. Res.*, Vol 89, No. B7, pp 6247-6255 (1984).
- Keller, GR and SE Cebull, Plate Tectonics and the Ouachita System in Texas, Oklahoma, and Arkansas (abstract), *Bull. Geol. Soc. Am.* (1973).
- Keller, GR et al., A Seismicity and Seismotectonic Study of the Kermit Seismic Zone, Texas, *U.S. Geol. Surv. Open-file Report 81-37* (1981).
- Kilbourne, RT and W Lutschak, The Rusk, Texas "Earthquake" of January 8, 1891, *Geol. Soc. Am. Abstracts with Programs*, Vol 6, No. 7 (1974).
- King, PB, Tectonics of Quaternary Time in Middle North America, *The Quaternary of the United States*, HE Wright, Jr and DG Frey, eds., pp 831-870 (1965).
- Knappe, BK (compiler), Underground Injection Operations in Texas: A Classification and Assessment of Underground Injection Activities, *Texas Dept. of Water Resources Report 291* (1984).
- Li, TMC et al., High-Frequency Seismic Noise at Lajitas, Texas, *Bull. Seismol. Soc. Am.*, Vol 74, No. 5, pp 2015-2033 (1984).
- Lynch, SA and P Weaver, Pavement Disruption by Recent Earth Movement, *11th Annu Symp. Hwy. Engr. Geol.*, Tallahassee, FL (1960).

Texas Seismology;
DJLA 89-154-04
July 15, 1989
Page 5

- Mickey, WV, Reservoir Seismic Effects, *Proc. COWAR Int. Symp. Manmade Lakes*, Knoxville, TN (1971).
- Miller, WD and DL Reddell, Alaskan Earthquake Damages Texas High Plains Water Wells, *Trans. Am. Geophys. Un.*, Vol 45, No. 4, pp 659-663 (1964).
- Monthly Weather Review*, Earthquakes [Earthquake of October 22, 1882], pp 22-23 (1882).
- Muehlberger, WR, Late Paleozoic Movement along the Texas Lineament, *Trans. NY Acad. Sci.*, Ser. II, Vol 17, No. 4, pp 385-392 (1965).
- Muehlberger, WR, and AE Kurie, Fracture Study of Central Travis County, Texas, *Gulf Coast Assn Geol. Soc.*, *Trans.* 6, pp 43-49 (1956).
- Muehlberger, WR, RC Belcher, and LK Goetz, Quaternary Faulting in Trans-Pecos Texas, *Geology*, Vol 4, pp 67-93 (1978).
- Murphy, LM and WK Cloud, *United States Earthquakes 1951* [Earthquake of June 20, 1951], U.S. Coast & Geod. Surv. Serial 762, p 8 (1953).
- Murphy, LM and WK Cloud, *United States Earthquakes 1952* [Earthquakes of April 9 and October 17, 1952], U.S. Coast & Geod. Surv. Serial 773, pp 6-9 (1954).
- Murphy, LM and WK Cloud, *United States Earthquakes 1955* [Earthquake of January 26, 1955], U.S. Coast & Geod. Surv., p 9 (1957).
- Murphy, LM and FP Ulrich, *United States Earthquakes 1951* [Earthquake of March 11, 1948], U.S. Coast & Geod. Surv. Serial 746 (1951).
- Murphy, LM and FP Ulrich, *United States Earthquakes 1951* [Earthquake of March 20, 1950], U.S. Coast & Geod. Surv. Serial 755, p 6 (1952).
- Neumann, F, *Seismological Report, 1924-1927*, U.S. Coast & Geod. Surv. Serial Nos. 328//503 (1926-1932).

Neumann, F, The Texas Earthquake of July 30, 1925 (abstract), *Bull. Seismol. Soc. Am.*, Vol 16, No. 2, p 158 (1926).

Neumann, F, *United States Earthquakes 1931* [Earthquake of August 16, 1931], U.S. Coast & Geod. Surv. Serial 553, pp 10-13 (1932).

Neumann, F, *United States Earthquakes 1934* [Earthquake of April 11, 1934], U.S. Coast & Geod. Surv. Serial 593, pp 9-10 (1936).

Neumann, F, *United States Earthquakes 1936*, U.S. Coast & Geod. Surv. Serial 610, pp 8-10 (1938).

Ni, JF, RE Reilinger, and LD Brown, Vertical Crustal Movements in the Vicinity of the 1931 Valentine, Texas, Earthquake, *Bull. Seismol. Soc. Am.*, Vol 71, No. 3, pp 857-863 (1981).

Orr, CD and GR Keller, Keyston Field, Winkler County, Texas: An Examination of Seismic Activity, In-Situ Stresses, Effective Stresses, and Secondary Recovery (abstract), *Earthquake Notes*, Vol 52, pp 29-30 (1981).

Orr, CD and GR Keller, A Seismicity Study of a Delaware Basin Gas Field, West Texas (abstract), *Seismol. Soc. Am. Annl Mtg*, Seattle, WA, pp 7-8 (1980).

Orr, CD and GR Keller, A Study of Seismicity and Regional Stresses in the Delaware Basin-Central Basin Platform Region of West Texas and Southern New Mexico (abstract), *Earthquake Notes*, p 18 (1985).

Pennington, WD, Comments on the Usefulness of Studies of Oil- and Gas-Field Seismicity (abstract), *Earthquake Notes*, Vol 55, No. 3, p 13 (1984).

Pennington, WD and Carlson, SM, The Seismicity of East Texas (abstract), *Earthquake Notes*, Vol 54, No. 1, p 86 (1983).

Pennington, WD and SD Davis, Changing Pore-fluid Pressures and the Evolution of Seismic Barriers and Asperities in Texas Oil and Gas Fields (abstract), *Earthquake Notes*, Vol 56, pp 17-18 (1985).

Texas Seismology;
DOLA 89-154-04
July 15, 1989
Page 7

Pennington, WD and SD Davis, Fluid Flow, Shear Fractures, and Earthquakes in Texas Oil and Gas Fields (abstract), *Geophysics*, Vol 50, No. 7, p 1205 (1985).

Pennington, WD, S Davis, and S Carlson, Earthquakes Induced by Fluid Withdrawal and Fault Strengthening, Fashing Gas Field, South Texas, *Earthquake Notes*, Vol 55, No. 1, p 21 (1984).

Pennington, WD et al., The Evolution of Seismic Barriers and Asperities Caused by the Depressuring of Fault Planes in Oil and Gas Fields of South Texas, *Bull. Seismol. Soc. Am.*, Vol 76, pp 939-948 (1986).

Person, WJ, Earthquakes, May-June 1981, *Earthquake Info. Bull.*, Vol 13, No. 6, pp 225-227 (1981).

Pratt, WE, An Earthquake in the Panhandle of Texas, *Bull. Seismol. Soc. Am.*, Vol 16, No. 2, pp 146-149 (1926).

Pratt, WE and DW Johnson, Local Subsidence of the Goose Creek Oil Field [Texas], *J. Geol.*, Vol 34, No. 7, pp 577-590 (1926).

Reagor, BG, CW Stover, and ST Algermissen, Seismicity Map of the State of Texas, U.S. Geol. Surv. Misc. Field Studies Map MF-1388, 2 sheets (1982).

Reasor, DD, Balcones Fault System - Its Northeast Extent, *Bull. Am. Assn Petrol. Geol.*, Vol 45, No. 10, pp 1759-1762 (1961).

Reid, WM, Active Faults in Houston, Texas (doctoral dissertation), Univ. Texas, Austin, 122 pp (1973).

Reid, WM, Displacement of Active Surface Faults in Houston, Texas (abstract), *Am. Geophys. Un. Fall Mtg, San Francisco, EOS*, 1971.

Roberts, EB and FP Ulrich, Seismological Activities of the U.S. Coast and Geodetic Survey in 1948 [Earthquake of March 11, 1948], *Bull. Seismol. Soc. Am.*, Vol 40, No. 3, pp 201-203 (1950).

Texas Seismology
DJLA 89-154-04
July 15, 1989
Page 3

- Rockwood, CG, Notes on American Earthquakes, No. 12 [Earthquake of October 22, 1882], *Am. J. Sci.*, Vol 125, p 359 (1883).
- Rogers, AM and A Malkiel, A Study of Earthquakes in the Permian Basin of Texas-New Mexico, *Bull. Seismol. Soc. Am.*, Vol 69, pp 843-865 (1979).
- Sansom, JW Jr and DH Shurbet, Microearthquake Studies in Texas, *Bull. Assn Engr. Geol.*, Vol XX, No. 3, pp 267-269 (1983).
- Sellards, EH, The Borger, Texas, Earthquake of June 19, 1936, *Univ. Texas Pub.* 3945, pp 699-704 (1940).
- Sellards, EH, The Texas-Oklahoma Earthquake of April 11, 1934, *Univ. Texas Bull.* 3501, pp 259-266 (1936).
- Sellards, EH, The Valentine Texas Earthquake, *Univ. Texas Bull.* 3201, pp 113-138 (1932).
- Sellards, EH, The Wortham-Mexia, Texas, Earthquake, *Univ. Texas Bull.* 3201, pp 105-112 (1932).
- Sheets, MM, Active Surface Faulting in the Houston Area, Texas, *Houston Geol. Soc. Bull.*, Vol 13, No. 7, reprint, 10 pp (1971).
- Sheets, MM, Diastrophism During Historic Time in Gulf Coast Plain, *Bull. Am. Assn. Petrol. Geol.*, Vol 31, No. 2, pp 201-226 (1947).
- Shurbet, DH, Development of the Gulf Coast Geosyncline, *Texas J. Sci.*, Vol 20, No. 3, pp 243-247 (1969).
- Shurbet, DH, Increased Seismicity in Texas, *Texas J. Sci.*, Vol 21, pp 37-41 (1969).
- Stenzel, HB, Faulting in Northwest Houston County, Texas, *Texas Mineral Resources*, Univ. Texas Publication 4301, 390 pp (1946).

Texas Seismology;
DJLA 89-154-04
July 15, 1989
Page 9

Udden, JA, The Southwest Earthquake of July 30, 1925, *Univ. Texas Bull.* 2609, 32 pp (1926).

UED Earth Sciences Div., Teledyne Systems Co., *Texas-Louisiana Earthquake 24 April 1964*, Long Range Seismic Measurements Project 8.4, Seismic Data Lab. Rpt 114, 17 pp (1965);

U.S. Coast & Geodetic Survey, Preliminary Report on the Southwest Texas Earthquake of August 16, 1931, *Earthquake Notes*, Vol 3, No. 3, pp 1-3 (1931).

von Hake, CA, Earthquake History of Texas, *Earthquake Information Bull.*, U.S. Geol. Surv., Vol 9, No. 3, pp 30-32 (1977).

von Hake, CA and WK Cloud, United States Earthquakes 1969 [Earthquake of May 12, 1969], NOAA (1971).

Voss, JA and RB Herrmann, A Surface Wave Study of the June 16, 1978 Texas Earthquake, *Earthquake Notes*, Vol 51, pp 3-14 (1980).

REFERENCES: LOUISIANA SEISMOLOGY

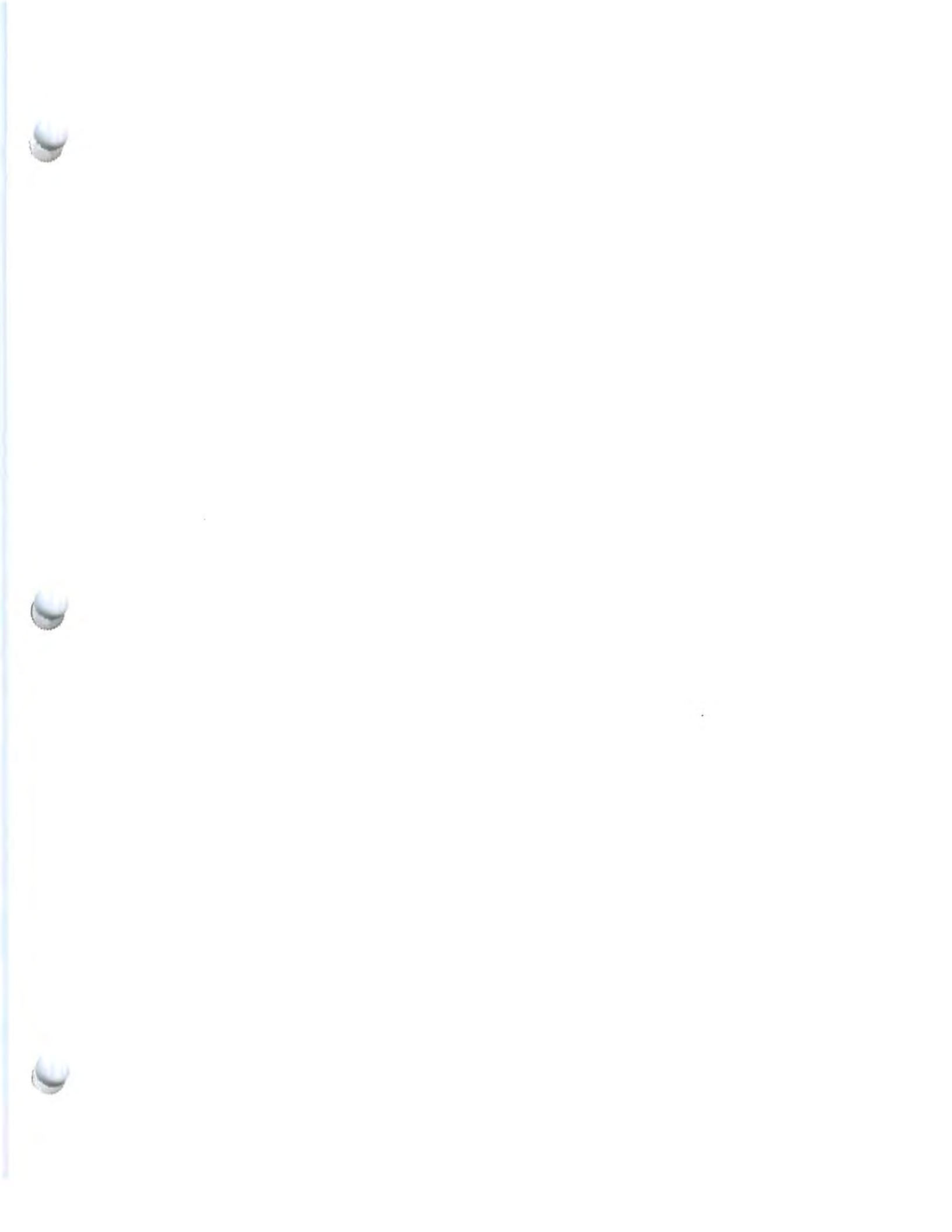
- Agnew, J et al., Observations of Microseismic and Tilt Activity Induced by Fluid Injection and Withdrawal from Deep Reservoirs in Western Coastal Louisiana (abstract), *Earthquake Notes*, Vol 54, No. 1, p 86 (1983).
- Brazee, RJ and WK Cloud, *United States Earthquakes 1958* [New Orleans Earthquake of November 6, 1958] p 9; [Baton Rouge Earthquake of November 19, 1958] p 12 (1960).
- Eppley, RA and WK Cloud, *United States Earthquakes 1959* [Southwestern Louisiana Earthquake of October 15, 1959] p 11 (1961).
- Fuller, ML, The New Madrid Earthquake, *U.S. Geological Survey Bulletin 494*, Washington (1912).
- Louisiana Power & Light, *Final Safety Analysis Report, Waterford Steam Electric Station Unit No. 3*, pp 2.5-42, Fig 2.5-43 (undated).
- Mississippi Power & Light Co., *Preliminary Safety Analysis Report, Grand Gulf Nuclear Station, Units 1 and 2* (1972).
- McKeown, FA and LC Pakiser (eds.), Investigation of the New Madrid, Missouri, Earthquake Region, *U.S. Geological Survey Professional Paper 1236*, Washington (1982).
- Neumann, F and RR Bodle, Donaldsonville, Louisiana Earthquake of October 19, 1930, *United States Earthquakes 1930*, U.S. Coast & Geodetic Survey Serial 539, Washington (1932).
- Stevenson, DA, Geopressured-Geothermal Well Development and Seismic Activity in Gulf Coast Louisiana (abstract), *Earthquake Notes*, Seismol. Soc. Am. Annl Mtg, Austin, TX, p 18 (1985).
- Stevenson, DA and JD Agnew, Lake Charles, Louisiana, Earthquake of 16 October 1983, *Bull. Seismol. Soc. Am.*, Vol 78, No. 4, pp 1463-1474 (1988).

Louisiana Seismology
DJLA 89-154-03
July 20, 1989
Page 2

Stover, CW, BG Reagor, and ST Algermissen, Seismicity Map of the State of Louisiana, U.S. Geolog. Surv. Misc. Field Studies Map MF-1081 (1979).

Stover, CW (ed.), *United States Earthquakes, 1983*, U.S. Geolog. Surv. Bull. 1698 [Southwestern Louisiana Earthquake of 16 October 1983] p 69 (1983).

DJLA\8915403.LA





DAVID J. LEEDS AND ASSOCIATES

Consultants in Engineering Seismology/Geology/Geophysics

11972 Chalon Road
Los Angeles, CA 90049
(213) 472-0282

DJLA 87-1154-03
May 29, 1998

E.I. du Pont de Nemours & Co.
Engineering Service Division
Gulf Coast Regional Consulting
PO Box 3269
Beaumont, TX 77704

Attention: Mr. James Clark

Re: Seismicity--
Natural & Induced
Beaumont Works
Texas

We take pleasure in submitting an update of our report on the seismicity of the region near your Beaumont Works, the possibility of earthquake damage to the injection process, and the potential for induced seismicity with damage to the confining and injection zones. The report contains the detail which supports our conclusions.

In our opinion there is no hazard of natural earthquake damage to the facility (presuming the installations conform to usual engineering practice) or of induced seismicity generated by the injection process. We do not believe that there has ever been destructive earthquake ground motion at your site.

We hope that this report meets your requirements. Please feel free to contact us if we can be of further assistance.

Very truly yours,

David J. Leeds

Registered Geologist CA#940; Registered Geophysicist CA#GP17
Certified Engr. Geol. CA#EG 373;
Amer. Inst. Prof. Geologists, Cert. Prof. Geologist #674

E.I. DUPONT DE NEMOURS & COMPANY, INC
BEAUMONT PLANT WORKS, TEXAS

Updated Seismicity Table, 1987-1997
Latitude 27° - 34° North; Longitude 88° - 99° West
Basic data from National Geophysical Data Center, US Geological Survey
Edited (from additional sources) by David J. Leeds, 1998

Date	Time	Lat N°	Lng W°	MMI	Mb	Locale
1987	8 11	20:31	33.105	92.889	—	—
1988	12 12	13:10	33.109	92.978	—	—
1989	2 5	8:37	32.727	92.884	—	—
1989	2 5	8:37	33.201	92.778	—	??
1991	7 20	23:38	28.908	98.042	IV	3.6 Falls City, Kames Co.
1992	4 7	12:10	30.100	96.500	—	—
1992	8 10	1:57	29.000	98.500	—	*
1993	4 9	12:29	28.811	98.124	VI	4.3 Fashing, Atacosa Co.
1993	5 16	15:30	28.810	98.170	IV	—
1994	6 10	23:34	33.013	92.671	III	—
1995	1 4	1:46	29.450	96.950	IV	—
1996	1 18	11:6	33.970	95.459	—	2.1
1996	3 25	14:15	32.131	88.671	—	—
1996	8 11	18:17	33.577	90.874	—	—
1997	1 3	16:55	33.940	97.940	—	—
1997	1 9	3:7	33.200	92.600	—	—
1997	3 24	22:31	27.717	98.054	V+	3.8
1997	5 31	3:26	33.182	95.968	—	—
1997	12 24	18:32	33.200	92.750	—	—

* Events are instrumentally located, not reported felt, and are tentative.

Addenda to Bibliography 1989-1998:

- "A compendium of earthquake activity in Texas"
S. D. Davis, W. D. Pennington, and S. M. Carlson
Univ. Texas Bureau of Economic Geology Circular. 89-3, 1989.
27 printed pages, 219 microfiche. [SDD: USGS Memphis;
Pennington: Marathon Oil, Littleton CO; SMC: Union Oil, Houston]
- "Felt Reports from the 20 July 1991 Falls City earthquake, Karnes
Co., Texas", D. R. Olson, and C. Frohlich, *Seismological
Research Letters*. 63:4, Oct-Dec 1992, pp 603-604. [All UTex.]
- "The 9 April 1993 earthquake in south-central Texas: Was it
induced by fluid withdrawal?", S. D. Davis, P. A.
Nyffenegger, and C. Frohlich", *Bulletin of the Seismological
Society of America*, 85:6, Dec. 1995. pp 1888-1895. [Davis:
USGS, Memphis; Others UTex.]
- "Calibration Studies at TXAR", Ileana Tibuleac and Eugene Herrin
Seismological Research Letters. 68:2, Mar-Apr 1997 pp 353-362,
(Earthquake of April 14, 1995 [SMU])
- "Felt Reports from the Alice, Texas, Earthquake of 24 March 1997"
Andria Bilich, Stephen Clark, Brian Creighton, Cliff Frohlich
Seismological Research Letters, March/April 1998 pp 117-122
[All UTex.]

David J. Leeds
11972 Chalon Road
Los Angeles CA 90049

wp51\djla\9815403

REFERENCES: LOUISIANA SEISMOLOGY

- Agnew, J et al., Observations of Microseismic and Tilt Activity Induced by Fluid Injection and Withdrawal from Deep Reservoirs in Western Coastal Louisiana (abstract), *Earthquake Notes*, Vol 54, No. 1, p 86 (1983).
- American Press, Data Sought on Southwestern Louisiana Earthquake October 20, 1959, Lake Charles, LA (1959).
- American Press, Earth Tremor Reported in This Area October 15, 1959, Lake Charles, LA (1959).
- Anonymous, Earthquake History of Louisiana, *EQe Info Bull.*, pp 26-29 (Mar 1973).
- Braze, RJ and WK Cloud, *United States Earthquakes 1958* [New Orleans Earthquake of November 6, 1958] p 9; [Baton Rouge Earthquake of November 19, 1958] p 12 (1960).
- Bruce, CH, Pressured Shale and Related Sediment Deformation: Mechanism for Development of Regional Contemporaneous Faults, *Am. Assn Pet. Geol. Bull.* Vol 57, pp 878-886 (1973).
- Burr, JG, The Probable Earthquake Origin of Caddo Lake (Texas-Louisiana), (abstract), *Texas Acad. Sci. Proc.* 1942, Vol 26, p 132 (1943). Full text in *Shreveport Times* (Mar 1943).
- Coffman, JL and CA Von Hake, *Earthquake History of the United States*, NOAA, No. 41-1 (1973).
- Docekal, J, *Earthquakes of the Stable Interior, with Emphasis on the Mid-continent*, Vol 2 (PhD thesis), Univ. of Nebraska, 332 pp (1970).
- Eppley, RA and WK Cloud, *United States Earthquakes 1959* [Southwestern Louisiana Earthquake of October 15, 1959] p 11 (1961).
- Fuller, ML, The New Madrid Earthquake, *U.S. Geol. Surv. Bull.* 494, Washington DC (1912).
- Hales, AL, Crustal Structure Study of Gulf Coast of Texas, *Am. Assn Pet. Geol. Bull.* Vol 54, pp 2040-2057 (1970).
- Louisiana Geological Survey, *Technical Support for Geopressured Geothermal Well Activities in Louisiana*, Final Report for 1 Nov 1983 - 31 Oct 1984, submitted to U.S. Dept of Energy.
- Louisiana Power & Light, *Final Safety Analysis Report, Waterford Steam Electric Station Unit No. 3*, pp 2.5-42, Fig 2.5-43 (undated).
- Mississippi Power & Light Co., *Preliminary Safety Analysis Report, Grand Gulf Nuclear Station, Units 1 and 2* (1972).
- McKeown, FA and LC Pakiser (eds.), Investigation of the New Madrid, Missouri, Earthquake Region, *U.S. Geol. Surv. Prof. Paper* 1236, Washington, DC (1982).
- Murphy, BF, Particle Motions Near Explosions in Halite, *Project COWBOY, Final Report, December 1959-March 1960*, Winnfield, Louisiana, Sandia Corp. SC-4440 (RR). Prepared for U.S. Atomic Energy Commission (1960).

Texas Seismology
David J. Leeds
May 26, 1998

REFERENCES: TEXAS SEISMOLOGY

- Acharya, H, *Palo Duro Seismographic Network Operation for July to December 1987*, App. C, Report 8, ONWI/SUB/87/E512-0500-T61, Stone & Webster Engineering Corp. Prepared for Office of Nuclear Waste Isolation, Battelle Memorial Institute, Columbus, OH (1988).
- Acharya, HR et al., *Microearthquake Monitoring of Texas Panhandle*, *Bull. Seismol. Soc. Am.*, Vol 79, No. 5, pp 1645-1650 (1989).
- Acharya, HR and LM Tyralla, *Palo Duro Microearthquake Network Operation Report for January to June 1986*, Report 3, ONWI/SUB/86/E512-0500-T46. Prepared by Stone & Webster Engineering Corp. for Office of Nuclear Waste Isolation, Battelle Memorial Institute, Columbus, OH (1985).
- *Algermissen, ST, *Seismicity Map of the State of Texas*, *Misc. Field Studies (U.S. Geological Survey, Map MF-1388*, (1982).
- Anonymous, *Earthquake History of Texas*, U.S. Geol. Surv., *Earthquake Info. Bull.* (May-Jun 1977).
- Baker, MR, DB Mason, and DI Doser, *Seismicity (1978-1979) Associated with the War-Wink Gas Field, Ward County, Texas (abstract)*, *Seismol. Res. Ltrs*, Vol 61, No. 1, p 31 (1989).
- Bechtel, Inc., *Report on Event at Rusk, Texas, January 7-8, 1891, Gulf States Utilities Blue Hills Station Units 1 and 2, Preliminary Safety Analysis Report, Appendix 2H, Docket 50-510, 50-511* (1974).
- Bell, DE and VA Brill, *Active Faulting in Lavaca County, Texas*, *Bull. Am. Assn Petrol. Geol.*, Vol 22, No. 1, pp 104-106 (1938).
- *Bilich, Andrea, Stephen Clark, Brian Creighton, Cliff Frohlich, *Felt Reports from the Alice, Texas, Earthquake of 24 March 1997*, *Seis. Res. Ltrs*, (March/April 1998) pp 117-122. [Authors all UTex.]
- Bornhauser, M, *Gulf Coast Tectonics, World Oil*, pp 113-124 (1956).
- Brazeel, RJ and WK Cloud, *Earthquake of March 19, 1957, United States Earthquakes 1957*, pp 16-18 (1959).
- Bryan, F, *Evidence of Recent Movements Along Faults of the Balcones System in Central Texas*, *Bull. Am. Assn Petrol. Geol.* Vol 20, No. 10, pp 1357-1371 (1936).
- Bryan, F, *Recent Movements on a Fault of the Balcones System, McLennon County, Texas*, *Bull. Am. Assn Petrol. Geol.* Vol 17, No. 4, pp 439-442 (1933).
- Burr, JG, *The Probable Earthquake Origin of Caddo Lake (Texas-Louisiana) (abstract)*, *Texas Acad. Sci. Proc.* 1942, p 132 (1943). Full text in *Shreveport Times*, March 1943.
- Byerly, P, *The Texas Earthquake of August 16, 1931*, *Bull. Seismol. Soc. Am.*, Vol 24, No. 2, pp 81-99 and Vol 24, No. 3, pp 303-325 (1934).

Louisiana Seismology
DJLA 89-154-06
December 12, 1989
Page 2

- Neumann, F. *United States Earthquakes 1940*, U.S. Coast & Geodetic Survey, [Earthquake of December 2, 1940], Serial 647, Washington, DC (1942).
- Neumann, F and RR Bodle, Donaldsonville, Louisiana Earthquake of October 19, 1930, *United States Earthquakes 1930*, U.S. Coast & Geodetic Survey Serial 539, Washington, DC (1932).
- Nunn, JA, State of Stress on the Northern Gulf Coast, *Geology*, Vol 13, pp 429-432 (1985).
- Ocamb, RD, Growth Faults of South Louisiana, *Trans. Gulf Coast Assoc. Geol. Soc. Vol II*, pp 139-175 (1961).
- Shelton, JW, Role of Contemporaneous Faulting During Basin Subsidence, *Am. Assn Pet. Geol. Bull.* Vol 52, pp 399-413 (1968).
- Stevenson, DA, Geopressured-Geothermal Well Development and Seismic Activity in Gulf Coast Louisiana (abstract), *Earthquake Notes*, Seismol. Soc. Am. Annl Mtg, Austin, TX, p 18 (1985).
- Stevenson, DA, *Technical Support for Geopressured-Geothermal Well Activities in Louisiana*, Final Report for the Period 1 Nov 1983-31 Oct 1984, LSU, DOE/NV/10174-5, pp 73-128 (1985).
- Stevenson, DA, *Technical Support for Geopressured-Geothermal Well Activities in Louisiana*, Final Report for the Period 1 Nov 1984-31 Dec 1985, LSU, DOE/NV/10425-1, pp 89-128 (1987).
- Stevenson, DA and JD Agnew, Lake Charles, Louisiana, Earthquake of 16 October 1983, *Bull. Seismol. Soc. Am.*, Vol 78, No. 4, pp 1463-1474 (1988).
- Stover, CW (ed.), *United States Earthquakes 1983*, U.S. Geolog. Surv. Bull. 1698 [Lake Charles Earthquake of 16 October 1983] p 69 (1987).
- Stover, CW, BG Reagor, and ST Algermissen, Seismicity Map of the State of Louisiana, U.S. Geolog. Surv. Misc. Field Studies Map MF-1081 (1979).
- Thornbrough, AD, ES Ames, and HL Hawk, Instrumentation Systems, *Project COWBOY, Winnfield, Louisiana* December 1959-March 1960, Sandia Corp. SC-4470 (RR). Prepared for U.S. Atomic Energy Commission (1960).
- Thorsen, CZ, Age of Growth Faulting in Southeastern Louisiana, *Trans. Gulf Coast Assoc. Geol. Soc.*, Vol 13, pp 103-110 (1963).
- Veutsch, AC, *Geological Survey of Louisiana Report for 1899* [...Shreveport Area...] pp 152, 159, 185.
- Von Hake, CA and WK Cloud, *United States Earthquakes 1964*, U.S. Coast & Geodetic Survey [Louisiana Earthquakes of April 1964] (1966).

WP5\DJLA\8915406.LA

Reviewed May 29 1998
No additional entries.

Texas Seismology
David J. Leeds
May 26, 1998

- Carlson, SM, S Davis, and W Pennington, Recent Earthquakes in the Gulf Coast of Texas, *EOS*, Vol 64, No. 45, p 750 (1983).
- Carlson, SM and WD Pennington, The Seismicity of East Texas, *Geol. Soc. Am. Abstracts with Programs*, Vol 15, No. 1, p 39 (1983).
- Carlson, SM, WD Pennington, and SD Davis, Seismicity of East Texas (abstract), *Earthquake Notes*, Vol 55, No. 3, p 11 (1984).
- Carlson, S, *Investigations of Recent and Historical Seismicity in East Texas* (MS thesis), 197 pp, University of Texas, Austin, TX (1984).
- Castle, RO and TL Youd, Discussion: The Houston Fault Problem, *Bull. Assn Engr. Geol.*, Vol 9, No. 1, pp 57-77 (1972).
- Clanton, US, Active Faults in Southwest Harris County, Texas, *Envir. Geol.*, Vol 1, No. 3 (1975).
- Crosby, GW, Gravity and Mechanical Study of the Great Bend in the Mexia-Talco Fault Zone, Texas, *J. Geophys. Res.*, Vol 76, No. 11, pp 2690-2705 (1971).
- Dale, D, Reevaluation of Critical Historical Earthquakes [Rusk, Texas January 8, 1891], *Earthquake Engr. Res. Inst. Newsletter*, Vol 10, No. 4, pp 19-20 (1976).
- Davis, SD, Historical Seismicity of Texas - A Summary, *Bull. Am. Assn Petrol. Geol.*, Vol 69, No. 9, p 149 (1985).
- Davis, SD, *Investigations of Natural and Induced Seismicity in the Texas Panhandle* (MS thesis), 230 pp, University of Texas, Austin, TX (1985).
- *Davis, SD, PA Nyffenegger, and C Frohlich, The 9 April 1993 earthquake in south-central Texas: Was it induced by fluid withdrawal?, *Bull. Seis. Soc. Amer.*, 85:6, Dec. 1995. pp 1888-1895. (Authors: Davis: USGS, Memphis; Others UTex.)
- Davis, SD and WD Pennington, A Barrier-Asperity Model for Injection Induced Deformation in the Cogdell Oil Field, Kent and Scurry Counties, Texas, *Earthquake Notes*, *Seismol. Soc. Am. Annl Mtg*, Austin, TX, p 18 (1985).
- Davis, SD and WD Pennington, Induced Seismic Deformation in the Cogdell Oilfield of West Texas, *Bull. Seismol. Soc. Am.*, Vol 79, No. 5, pp 1477-1495 (1989).
- Davis, SD and WD Pennington, Seismicity of the Texas Panhandle, *Earthquake Notes*, Vol 55, No. 3, pp 11-12 (1984).
- *Davis, SD, WD Pennington, and SM Carlson, A Compendium of Earthquake Activity in Texas, *Univ. Texas Bur. Econ. Geol. Circ. 89-3*, 1989. 27 printed pages, 219 microfiche. (Authors: Davis: USGS Memphis; Others unknown)
- Davis, SD, WD Pennington, and SM Carlson, Historical Seismicity of the State of Texas - A Summary, *Trans. Gulf Coast Assn Geol. Soc.*, Vol XXXV, pp 39-43 (1985).
- Dawson, RF, A Review of the Land Subsidence Problems in the Texas Gulf Coast Area, preprint, *Surveying & Mapping Div., Am. Soc. Civ. Engr. Mtg*, Houston, TX (1962).

Texas Seismology
David J. Leeds
May 26, 1998

- Doser, DI, The 16 August 1931 Valentine, Texas, Earthquake: Evidence for Normal Faulting in West Texas, *Bull. Seismol. Soc. Am.*, Vol 77, No. 6, pp 2005-2017 (1987).
- Doser, DI, MB Baker, and DB Mason, Seismicity in the War-Wink Gas Field, Delaware Basin, West Texas, and its Relationship to Petroleum, *Bull. Seismol. Soc. Am.*, Vol 81, No. 3, pp 971-986 (1991).
- Dumas, DB, Active Seismic Focus near Snyder, Texas, *Bull. Seismol. Soc. Am.*, Vol 69, No. 4, pp 1295-1299 (1979).
- Dumas, DB, HJ Dorman, and GV Latham, A Reevaluation of the August 16, 1931 Texas Earthquake, *Bull. Seismol. Soc. Am.*, Vol 70, No. 4, pp 1171-1180 (1980).
- Dumas, DB, HJ Dorman, and GV Latham, The August 16, 1931 Texas Earthquake, *EOS*, Vol 60, No. 46, p 894 (1979).
- Dumas, DB, Erratum to Active Seismic Focus near Snyder, Texas, *Bull. Seismol. Soc. Am.*, Vol 70, No. 4, p 1427 (1980).
- Eppley, RA and WK Cloud, Earthquake of June 17, 1959, *United States Earthquakes 1959*, pp 11-12 (1961).
- Erdlac, RJ, Jr, A Mathematical Model of Push-up Block Formation: An Example from the Big Bend Region, Texas, USA (abstract), *AGU GAP (Apr 1992)*.
- Foley, LL, Mechanics of the Balcones and Mexia Faulting, *Bull. Am. Assn Petrol. Geol.*, Vol 10, pp 1261-1269 (1926).
- Frolich, C and DB Dumas, The Seismicity of the Gulf of Mexico (abstract), *EOS Trans. AGU*, Vol 61, pp 288 (1980).
- Frolich, C, Seismicity of the Central Gulf of Mexico, *Geology*, Vol 10, pp 103-106 (1982).
- Gabrysch, RK, Land-surface Subsidence in the Houston-Galveston Region, Texas, *Land Subsidence, Proc. Tokyo Symposium IASH/AISH-UNESCO*, pp 43-55 (1969).
- Gray, E, The Geology, Ground-water, and Surface Subsidence of the Baytown-La Porte Area, Harris County, Texas (unpub. thesis), Texas A&M Univ., 10 pp (1958).
- Harding, ST, *Induced Seismic Cogdell Canyon Reef Oil Field*, U.S. Geol. Surv. Open-file Report 81-167 (1981).
- Harding, ST, *Induced Seismicity in the Cogdell Canyon Reef Oil Field*, U.S. Geol. Surv. Open-file Report 81-333, p 547 (1981).
- Harding, ST et al., The Scurry County, Texas, Earthquake Series of 1977-1978: Induced Seismicity? (abstract), *Earthquake Notes*, Vol 49, No. 3, pp 14-15 (1978).
- Henley, AD, Seismic Activity near the Texas Gulf Coast, *Engr. Geol*, Vol 3, No. 1-2, pp 33-39 (1966).
- Hull, LV, New Dallas Seismological Observatory at SMU, *Bull. Seismol. Soc. Am.*, Vol 46, No. 4, pp 321-330 (1956).

Texas Seismology
David J. Leeds
May 26, 1998

- Humphreys, WJ, Seismological Reports for October, November and December, 1914, *Monthly Weather Review*, U.S. Weather Bur., Vol 42, p 689 (1914).
- Jenneman, VF, Microseisms at Corpus Christi (abstract), *Union Geod. et Geophys. Int. Assn Seismol. Comptes Rendus*, No. 9, p 24 (1949); also *Geophysical Abstracts* 139, p 278 (1949).
- Jurkowski, G, J Ni, and L Brown, Modern Uparching of the Gulf Coastal Plain, Paper 4B0463, *J. Geophys. Res.*, Vol 89, No. B7, pp 6247-6255 (1984).
- Keller, GR and SE Cebull, Plate Tectonics and the Ouachita System in Texas, Oklahoma, and Arkansas (abstract), *Bull. Geol. Soc. Am.* (1973).
- Keller, GR et al., A Seismicity and Seismotectonic Study of the Kermit Seismic Zone, Texas, *U.S. Geol. Surv. Open-file Report* 81-37 (1981).
- *Keller, GR, AM Rogers, and CD Orr, Seismic activity in the Permian Basin area of West Texas and southeastern New Mexico, 1975-1979, *Seis. Res. Ltrs.*, Vol 58, No 2, pp 63-70, 1987.
- Kilbourne, RT and W Lutschak, The Rusk, Texas "Earthquake" of January 8, 1891, *Geol. Soc. Am. Abstracts with Programs*, Vol 6, No. 7 (1974).
- King, PB, Tectonics of Quaternary Time in Middle North America, *The Quaternary of the United States*, HE Wright, Jr and DG Frey, eds., pp 831-870 (1965).
- Knape, BK (compiler), Underground Injection Operations in Texas: A Classification and Assessment of Underground Injection Activities, *Texas Dept. of Water Resources Report* 291 (1984).
- Li, TMC et al., High-Frequency Seismic Noise at Lajitas, Texas, *Bull. Seismol. Soc. Am.*, Vol 74, No. 5, pp 2015-2033 (1984).
- Lynch, SA and P Weaver, Pavement Disruption by Recent Earth Movement, *11th Annl Symp. Hwy. Engr. Geol.*, Tallahassee, FL (1960).
- Mickey, WV, Reservoir Seismic Effects, *Proc. COWAR Int. Symp. Manmade Lakes*, Knoxville, TN (1971).
- Miller, WD and DL Reddell, Alaskan Earthquake Damages Texas High Plains Water Wells, *Trans. Am. Geophys. Un.*, Vol 45, No. 4, pp 659-663 (1964).
- Monthly Weather Review* [Earthquake of October 22, 1882], pp 22-23 (1882).
- Muehlberger, WR, Late Paleozoic Movement along the Texas Lineament, *Trans. NY Acad. Sci.*, Ser. II, Vol 17, No. 4, pp 385-392 (1965).
- Muehlberger, WR, and AE Kurie, Fracture Study of Central Travis County, Texas, *Gulf Coast Assn Geol. Soc.*, *Trans.* 6, pp 43-49 (1956).
- Muehlberger, WR, RC Belcher, and LK Goetz, Quaternary Faulting in Trans-Pecos Texas, *Geology*, Vol 4, pp 67-93 (1978).
- Murphy, LM and WK Cloud, *United States Earthquakes 1951* [Earthquake of June 20, 1951], *U.S. Coast & Geod. Surv. Serial* 762, p 8 (1953).
- Murphy, LM and WK Cloud, *United States Earthquakes 1952* [Earthquakes of April 9 and Oct 17, 1952], *U.S. Coast & Geod. Surv. Serial* 773, pp 6-9 (1954).

Texas Seismology
David J. Leeds
May 26, 1998

- Murphy, LM and WK Cloud, *United States Earthquakes 1955* [Earthquake of January 26, 1955], U.S. Coast & Geod. Surv., p 9 (1957).
- Murphy, LM and FP Ulrich, *United States Earthquakes 1951* [Earthquake of March 11, 1948], U.S. Coast & Geod. Surv. Serial 746 (1951).
- Murphy, LM and FP Ulrich, *United States Earthquakes 1951* [Earthquake of March 20, 1950], U.S. Coast & Geod. Surv. Serial 755, p 6 (1952).
- Neumann, F, *Seismological Report, 1924-1927*, U.S. Coast & Geod. Surv. Serial Nos. 328//503 (1926-1932).
- Neumann, F, The Texas Earthquake of July 30, 1925 (abstract), *Bull. Seismol. Soc. Am.*, Vol 16, No. 2, p 158 (1926).
- Neumann, F, *United States Earthquakes 1931* [Earthquake of August 16, 1931], U.S. Coast & Geod. Surv. Serial 553, pp 10-13 (1932).
- Neumann, F, *United States Earthquakes 1934* [Earthquake of April 11, 1934], U.S. Coast & Geod. Surv. Serial 593, pp 9-10 (1936).
- Neumann, F, *United States Earthquakes 1936*, U.S. Coast & Geod. Surv. Serial 610, pp 8-10 (1938).
- Ni, JF, RE Reilinger, and LD Brown, Vertical Crustal Movements in the Vicinity of the 1931 Valentine, Texas, Earthquake, *Bull. Seismol. Soc. Am.*, Vol 71, No. 3, pp 857-863 (1981).
- *Olson, DR., and C Frohlich, Felt Reports from the 20 July 1991 Falls City Earthquake, Karnes Co., Texas", *Seis. Res. Ltrs.* 63:4, Oct-Dec 1992, pp 603-604. (Authors U.Tex.)
- Orr, CD and GR Keller, Keyston Field, Winkler County, Texas: An Examination of Seismic Activity, In-Situ Stresses, Effective Stresses, and Secondary Recovery (abstract), *Earthquake Notes*, Vol 52, pp 29-30 (1981).
- Orr, CD and GR Keller, A Seismicity Study of a Delaware Basin Gas Field, West Texas (abstract), *Seismol. Soc. Am. Annl Mtg*, Seattle, WA, pp 7-8 (1980).
- Orr, CD and GR Keller, A Study of Seismicity and Regional Stresses in the Delaware Basin-Central Basin Platform Region of West Texas and Southern New Mexico (abstract), *Earthquake Notes*, p 18 (1985).
- Pennington, WD, Comments on the Usefulness of Studies of Oil- and Gas-Field Seismicity (abstract), *Earthquake Notes*, Vol 55, No. 3, p 13 (1984).
- *Pennington, WD, The evolution of seismic barriers and asperities caused by the depressuring of fault planes in oil and gas fields of south Texas, *Bull. Seismo. Soc. Amer.*, Vol 78, No 4, pp 939-948, (1986).
- Pennington, WD and Carlson, SM, The Seismicity of East Texas (abstract), *Earthquake Notes*, Vol 54, No. 1, p 86 (1983).
- Pennington, WD and SD Davis, Changing Pore-fluid Pressures and the Evolution of Seismic Barriers and Asperities in Texas Oil and Gas Fields (abstract), *Earthquake Notes*. Vol 56, pp 17-18 (1985).
- Pennington, WD and SD Davis, Fluid Flow, Shear Fractures, and Earthquakes in

Texas Seismology
David J. Leeds
May 26, 1998

- Texas Oil and Gas Fields (abstract), *Geophysics*, Vol 50, No. 7, p 1205 (1985).
- Pennington, WD, S Davis, and S Carlson, Earthquakes Induced by Fluid Withdrawal and Fault Strengthening, Fashing Gas Field, South Texas, *Earthquake Notes*, Vol 55, No. 1, p 21 (1984).
- Pennington, WD et al., The Evolution of Seismic Barriers and Asperities Caused by the Depressuring of Fault Planes in Oil and Gas Fields of South Texas, *Bull. Seismol. Soc. Am.*, Vol 76, pp 939-948 (1986).
- Person, WJ, Earthquakes, May-June 1981, *Earthquake Info. Bull.*, Vol 13, No. 6, pp 225-227 (1981).
- Pratt, WE, An Earthquake in the Panhandle of Texas, *Bull. Seismol. Soc. Am.*, Vol 16, No. 2, pp 146-149 (1926).
- Pratt, WE and DW Johnson, Local Subsidence of the Goose Creek Oil Field [Texas], *J. Geol.*, Vol 34, No. 7, pp 577-590 (1926).
- Railroad Commission of Texas, *A Survey of Enhanced Recovery Operations to 1974*, Austin, TX, 481 pp (1975).
- Railroad Commission of Texas, *A Survey of Secondary and Enhanced Recovery Operations to 1976* (also to 1978, 1980, and 1982), Austin, TX (1977 through 1983).
- Railroad Commission of Texas, *A Survey of Secondary Recovery and Pressure Maintenance Operations in Texas to 1960* (also to 1962, 1964, 1966, 1968, 1970, and 1972), Austin, TX (1961 through 1973).
- Reagor, BG, CW Stover, and ST Algermissen, Seismicity Map of the State of Texas, U.S. Geol. Surv. Misc. Field Studies Map MF-1388, 2 sheets (1982).
- Reasor, DD, Balcones Fault System - Its Northeast Extent, *Bull. Am. Assn Petrol. Geol.*, Vol 45, No. 10, pp 1759-1762 (1961).
- Regan, TR and PJ Murphy, *Faulting in the Northern Palo Duro Basin, Texas*, Rev. 1, ONWI/SUB/86/E512-0500-T30. Prepared by Stone & Webster Engineering Corp. for Office of Nuclear Waste Isolation, Battelle Memorial Institute, Columbus, OH (1985).
- Reid, WM, Active Faults in Houston, Texas (doctoral dissertation), Univ. Texas, Austin, 122 pp (1973).
- Reid, WM, Displacement of Active Surface Faults in Houston, Texas (abstract), Am. Geophys. Un. Fall Mtg, San Francisco, EOS, 1971.
- Roberts, EB and FP Ulrich, Seismological Activities of the U.S. Coast and Geodetic Survey in 1948 [Earthquake of March 11, 1948], *Bull. Seismol. Soc. Am.*, Vol 40, No. 3, pp 201-203 (1950).
- Rockwood, CG, Notes on American Earthquakes, No. 12 [Earthquake of October 22, 1882], *Am. J. Sci.*, Vol 125, p 359 (1883).
- Rogers, AM and A Malkiel, A Study of Earthquakes in the Permian Basin of Texas-New Mexico, *Bull. Seismol. Soc. Am.*, Vol 69, pp 843-865 (1979).

Texas Seismology
David J. Leeds
May 26, 1998

- *Sanford, A, Seismicity in the area of the Waste Isolation Pilot Plant (WIPP), *Sandia National Laboratories, Sand80-7096*, (1980).
- Sansom, JW Jr and DH Shurbet, Microearthquake Studies in Texas, *Bull. Assn Engr. Geol*, Vol XX, No. 3, pp 267-269 (1983).
- Sellards, EH, The Borger, Texas, Earthquake of June 19, 1936, *Univ. Texas Pub.* 3945, pp 699-704 (1940).
- Sellards, EH, The Texas-Oklahoma Earthquake of April 11, 1934, *Univ. Texas Bull.* 3501, pp 259-266 (1936).
- Sellards, EH, The Valentine Texas Earthquake, *Univ. Texas Bull.* 3201, pp 113-138 (1932).
- Sellards, EH, The Wortham-Mexia, Texas, Earthquake, *Univ. Texas Bull.* 3201, pp 105-112 (1932).
- Sheets, MM, Active Surface Faulting in the Houston Area, Texas, *Houston Geol. Soc. Bull.*, Vol 13, No. 7, reprint, 10 pp (1971).
- Sheets, MM, Diastrophism During Historic Time in Gulf Coast Plain, *Bull. Am. Assn Petrol. Geol*, Vol 31, No. 2, pp 201-226 (1947).
- Shurbet, DH, Development of the Gulf Coast Geosyncline, *Texas J. Sci.*, Vol 20, No. 3, pp 243-247 (1969).
- Shurbet, DH, Increased Seismicity in Texas, *Texas J. Sci*, Vol 21, pp 37-41 (1969).
- Stenzel, HB, Faulting in Northwest Houston County, Texas, *Texas Mineral Resources*, Univ. Texas Publication 4301, 390 pp (1946).
- Teledyne Geotech, *Pleasant Bayou Test Well - Brazoria County, Texas*, Seismic Array Quarterly Progress Report, 42 p (January-March 1983).
- ibid.*, 45 p (April-June 1983).
- Texaco, Certification by Texaco Inc. for Self-Certification of a Tertiary Recovery Project for the Cogdell Canyon Reef Unit, Cogdell Field, Kent and Scurry Counties, Texas; Tertiary Method Being Certified: Polymer Augmented Waterflood. Document of hearing before Texas Railroad Commission, Sep 29, 1983 (1983).
- *Tibuleac, Ileana and Eugene Herrin, Calibration Studies at TXAR, *Seis. Res. Ltrs.* 68:2, (Mar-Apr 1997) pp 353-362. [Earthquake of April 14, 1995; Authors: SMU.]
- Udden, JA, The Southwest Earthquake of July 30, 1925, *Univ. Texas Bull.* 2609, 32 pp (1926).
- UED Earth Sciences Div., Teledyne Systems Co., *Texas-Louisiana Earthquake 24 April 1964*, Long Range Seismic Measurements Project 8.4, Seismic Data Lab. Rpt 114, 17 pp (1965);
- U.S. Coast & Geodetic Survey, Preliminary Report on the Southwest Texas Earthquake of Aug 16, 1931, *Earthquake Notes*, Vol 3, No. 3, pp 1-3 (1931).

Texas Seismology
David J. Leeds
May 26, 1998

von Hake, CA, Earthquake History of Texas, *Earthquake Information Bull.*, U.S. Geol. Surv., Vol 9, No. 3, pp 30-32 (1977).

von Hake, CA and WK Cloud, *United States Earthquakes 1969* [Earthquake of May 12, 1969], NOAA (1971).

Voss, JA and RB Herrmann, A Surface Wave Study of the June 16, 1978 Texas Earthquake, *Earthquake Notes*, Vol 51, pp 3-14 (1980).

* 1998 additions to list.

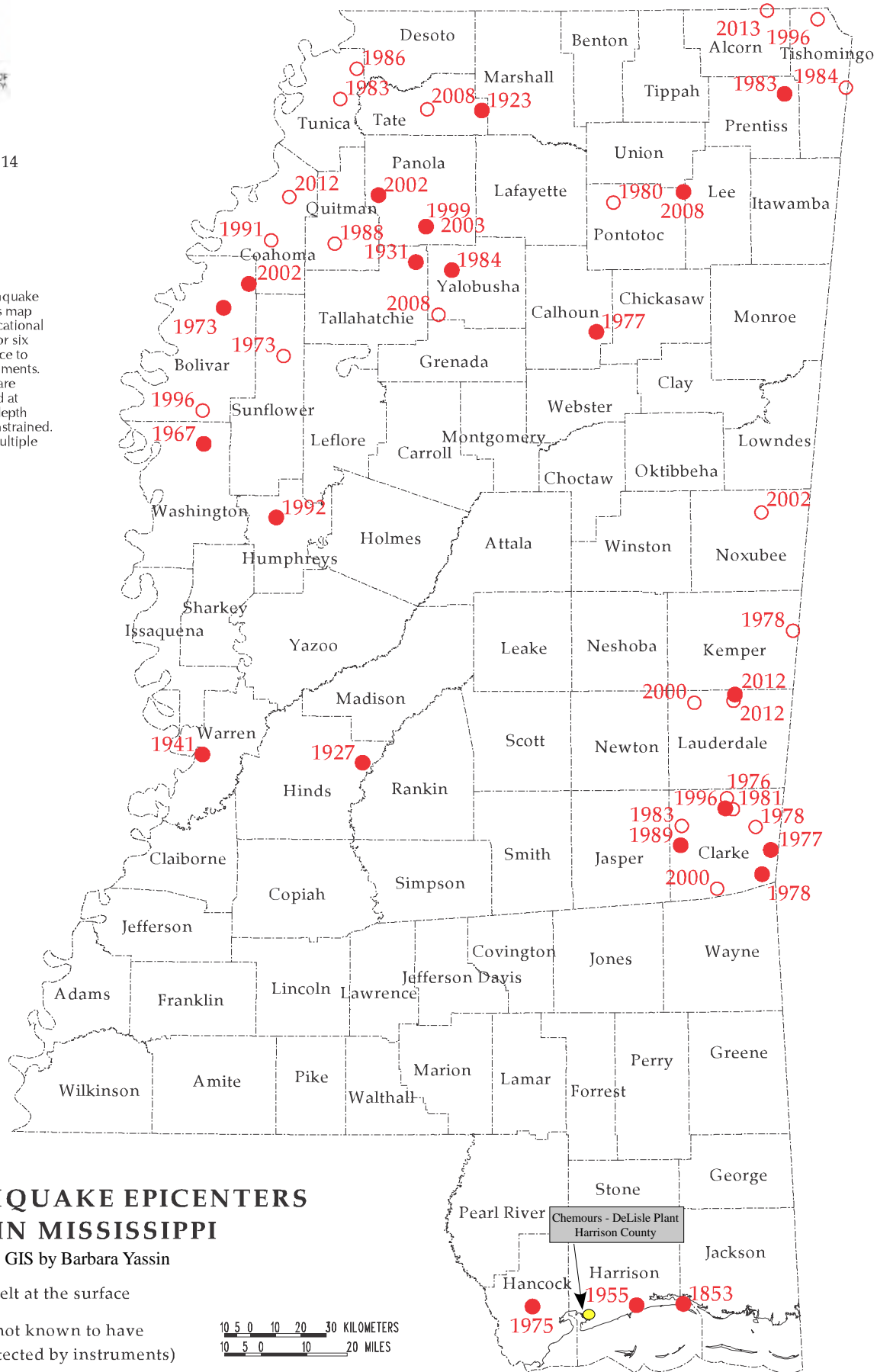
WP51\DJLA\eqbiblio.TX
Updated May 6, 1992.
Updated May 26, 1998



Fact Sheet 1
revised April 2014

DISCLAIMERS

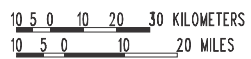
The locations of the earthquake epicenters plotted on this map are approximate. The locational uncertainty of up to five or six miles is due to the distance to the nearest seismic instruments. All of these earthquakes are believed to have occurred at shallow depths, but the depth information is poorly constrained. Some points represent multiple events.



EARTHQUAKE EPICENTERS IN MISSISSIPPI

GIS by Barbara Yassin

- Earthquake felt at the surface
- Earthquake not known to have been felt (detected by instruments)





EARTHQUAKES IN MISSISSIPPI

Michael B. E. Bograd



This is a list of earthquakes originating, or with epicenters, within the State of Mississippi. Given are the date, location, whether or not it was felt, maximum intensity (in the Modified Mercalli Intensity scale of I-XII), and magnitude (a relative measure of the energy released).

- September 11, 1853 - Biloxi, felt
March 27, 1923 - Wyattte, Tate Co., intensity IV
November 13, 1927 - Jackson, intensity IV
December 16, 1931 - Batesville-Charleston area, intensity VI-VII, mag. 4.7, damage in northern Miss., felt over 65,000 square miles in Miss., Ala., Ark., Tenn., and Mo.
June 28, 1941 - Vicksburg, intensity III-IV
February 1, 1955 - Gulfport, intensity V, felt along the Coast
June 4, 1967 - Greenville, intensity VI, mag. 3.8, felt over 25,000 square miles in Mississippi, Arkansas, Louisiana, and Tennessee
June 29, 1967 - Greenville, intensity V, mag. 3.4, felt in 3 counties
January 8, 1973 - Sunflower County, not felt, mag. 3.5
May 25, 1973 - Bolivar County, felt
September 9, 1975 - Hancock Co., intensity IV, mag. 2.9
October 23, 1976 - northern Clarke County, not felt, magnitude 3.0
May 3, 1977 - southeastern Clarke County, intensity V, magnitude 3.6
November 4, 1977 - Vardaman, Calhoun Co., intensity V, magnitude 3.4
January 8, 1978 - Kemper County-Alabama border, not felt, magnitude 3.0
June 9, 1978 - eastern Clarke County, not felt, mag. 3.3
December 10, 1978 - southeastern Clarke County, intensity V, magnitude 3.5
October 12, 1980 - northwestern Pontotoc County, not felt, magnitude 2.1
February 15, 1981 - Clarke County, not felt, magnitude 2.4
January 29, 1983 - northeastern Prentiss County, not felt, magnitude 2.4
February 5, 1983 - northeastern Prentiss County, intensity V, magnitude 2.9
April 25, 1983 - Tunica County, not felt, magnitude 1.6
May 30, 1983 - western Clarke County, not felt, mag. 2.4
March 23, 1984 - Tishomingo County-Alabama border, not felt, magnitude 2.0
September 24, 1984 - northwestern Yalobusha County, felt, magnitude 2.5
May 11, 1986 - northeastern Tunica Co., not felt, mag. 1.6
August 1, 1988 - Quitman County, not felt, magnitude 2.1
August 23, 1989 (2 events) - Pachuta, Clarke County, felt
August 25, 1989 - Pachuta, Clarke County, felt
November 26, 1989 (2 events) - Pachuta, Clarke Co., felt
February 11, 1991 - Clarksdale, Coahoma Co., not felt, magnitude 2.7

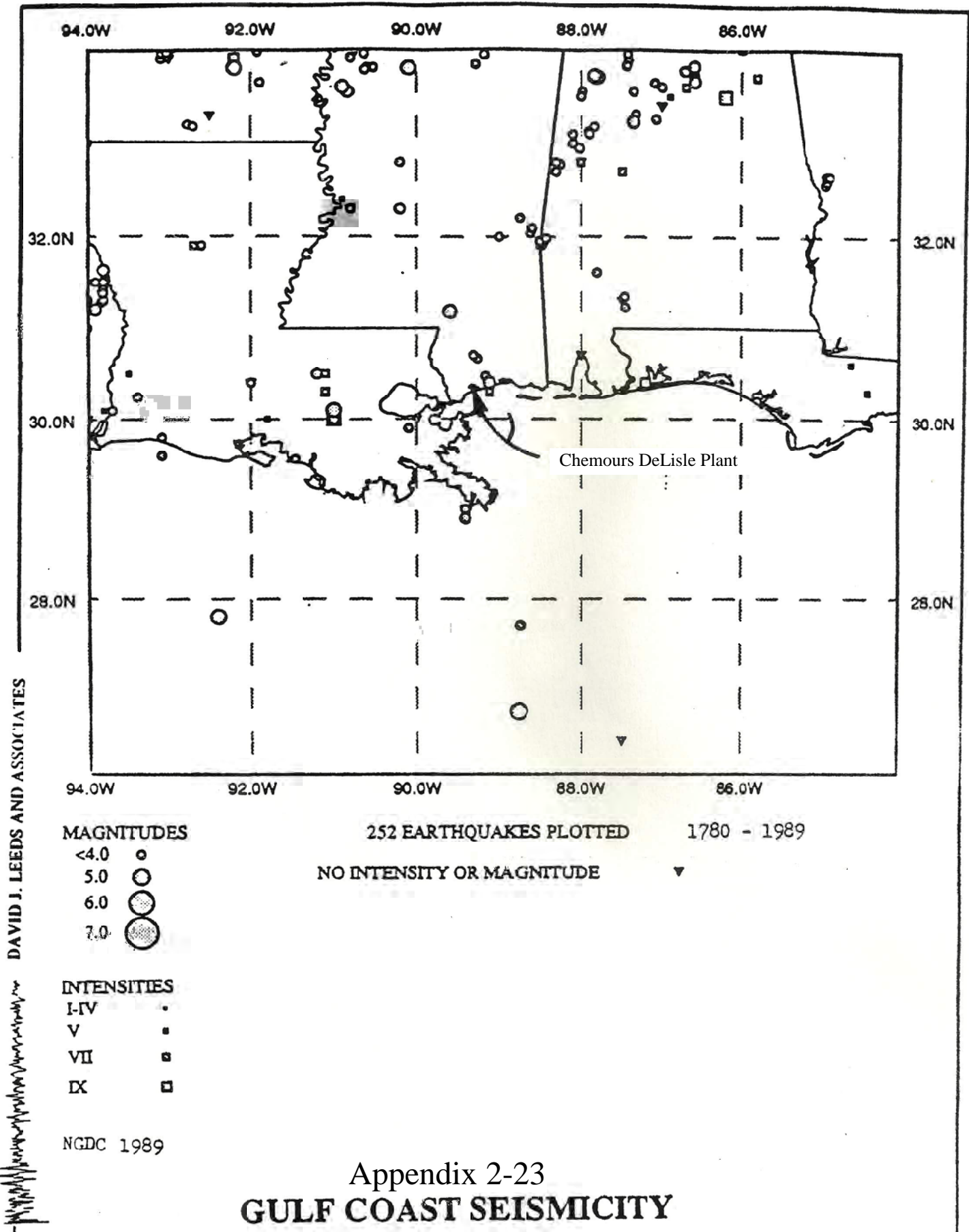
- December 11, 1992 (2 events) - Belzoni, Humphreys County, both felt, first quake was magnitude 2.4
March 25, 1996 (2 events) - Clarke County, felt in Quitman and much of Clarke County, mag. 3.5; an after-shock of mag. 2.5 was felt about 30 minutes later
May 13, 1996 - northern Tishomingo Co., not felt, mag. 2.7
August 11, 1996 - southern Bolivar Co., not felt, mag. 3.1
Feb. 24, 1999 - southern Panola County, int. IV, mag. 2.8
January 28, 2000 - Shubuta, Clarke Co., not felt, mag. 2.7
October 10, 2000 - northwestern Lauderdale County, not felt, magnitude 2.3
January 6, 2002 - near Brooksville, Noxubee County, not felt, magnitude 2.2
August 11, 2002 - western Panola County, felt, mag. 2.8
October 26, 2002 - northern Bolivar County, felt, mag. 3.1
February 26, 2003 - Courtland, Panola Co., felt
January 20, 2008 - southwestern Yalobusha County, not felt, magnitude 1.7
May 10, 2008 - Belden, Lee Co., int. IV, magnitude 3.1
June 2, 2008 - near Senatobia, Tate Co., not felt, mag. 2.2
July 27, 2012 - Meridian Station, Lauderdale Co., felt, magnitude 2.1
July 29, 2012 - Meridian Station, Lauderdale Co., not felt, magnitude 1.6
October 9, 2012 - Jonestown, Coahoma Co., not felt, magnitude 2
August 30, 2013 - near Corinth, Alcorn Co., not felt, magnitude 2.0

EARTHQUAKE RISK

The map indicates that earthquakes have occurred throughout Mississippi. It is expected that earthquakes of low magnitude will continue to occur. Many earthquakes in neighboring (and distant) states have been felt in parts of Mississippi. However, the greatest risk to Mississippi from earthquakes is from a strong earthquake in the New Madrid Seismic Zone, the southern end of which is about 40 miles from the northwest corner of Mississippi. The great New Madrid earthquake series of 1811-1812 included at least four shocks strong enough to shake northern Mississippi at damaging intensities and be felt throughout the state. The 1843 earthquake at the southern end of the zone shook the northern third of Mississippi strongly enough to cause damage. People in Mississippi should take precautions for another strong earthquake on the New Madrid Seismic Zone.

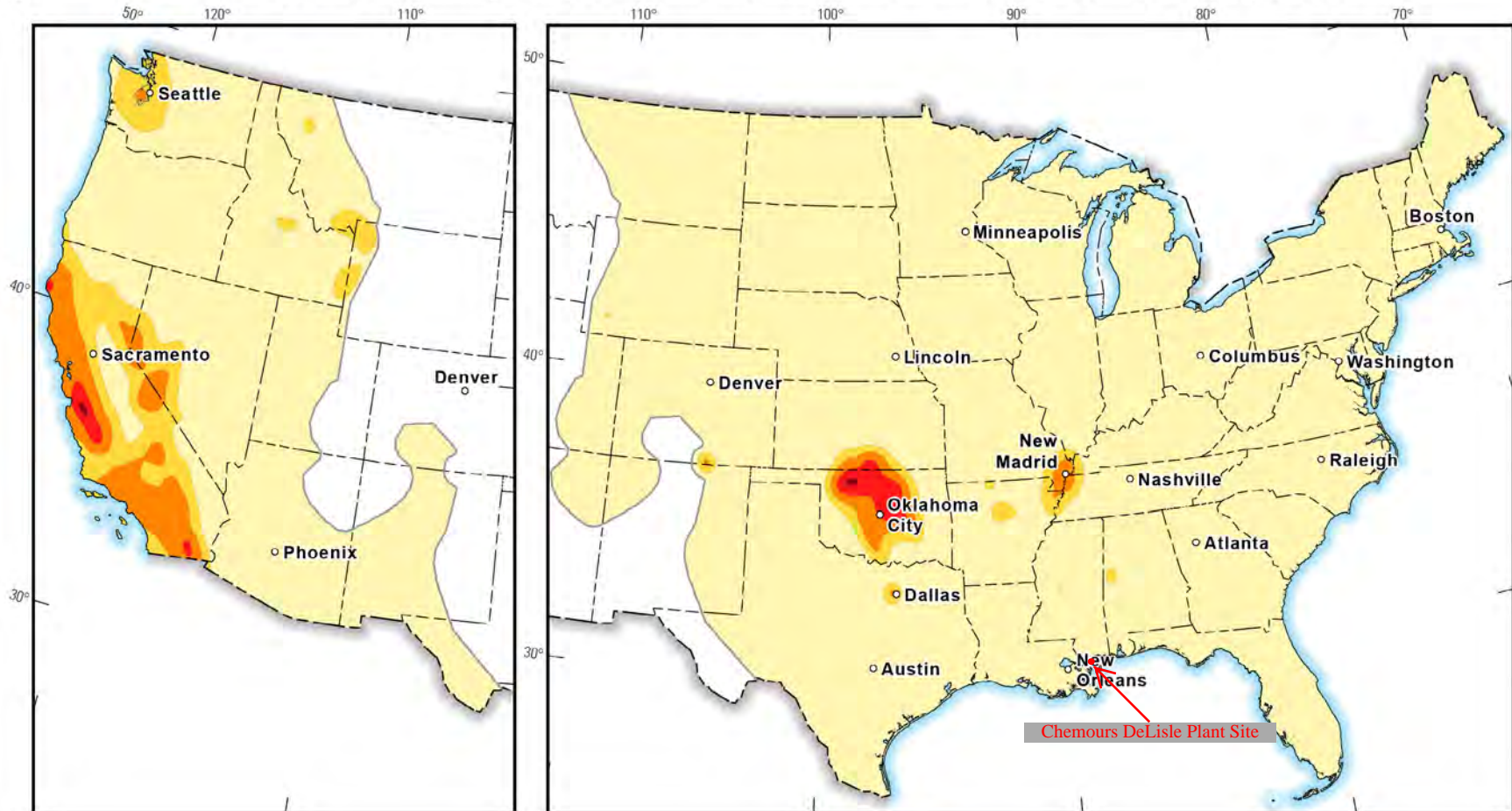
SOURCES

The listings were compiled from published catalogs of earthquakes. The more recent, instrumentally recorded locations were taken from publications of the U.S. Geological Survey, National Earthquake Information Center, and the Center for Earthquake Research and Information at the University of Memphis.



Appendix 2-23
GULF COAST SEISMICITY

Chance of damage based on the average of horizontal spectral response acceleration for 1.0-second period and peak ground acceleration



Based on results from the 2014
National Seismic Hazard Model

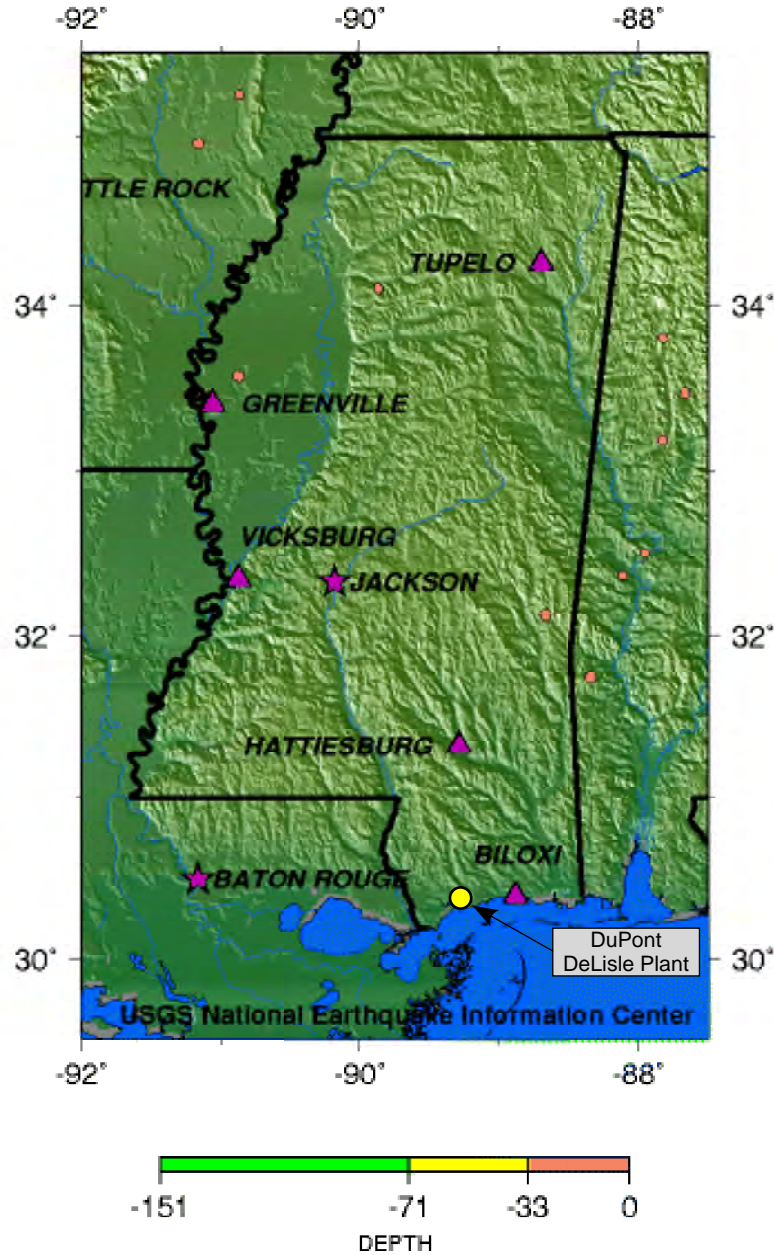
Based on results from this study

Chance of damage from an earthquake in 2016



Appendix 2-24 Seismic Hazard Map for the Continuous United States

1990 - 2001 Seismicity of Mississippi



- Purple Triangles: Cities
- Purple Star: Capital City
- Circles: Earthquakes (color represents depth range)

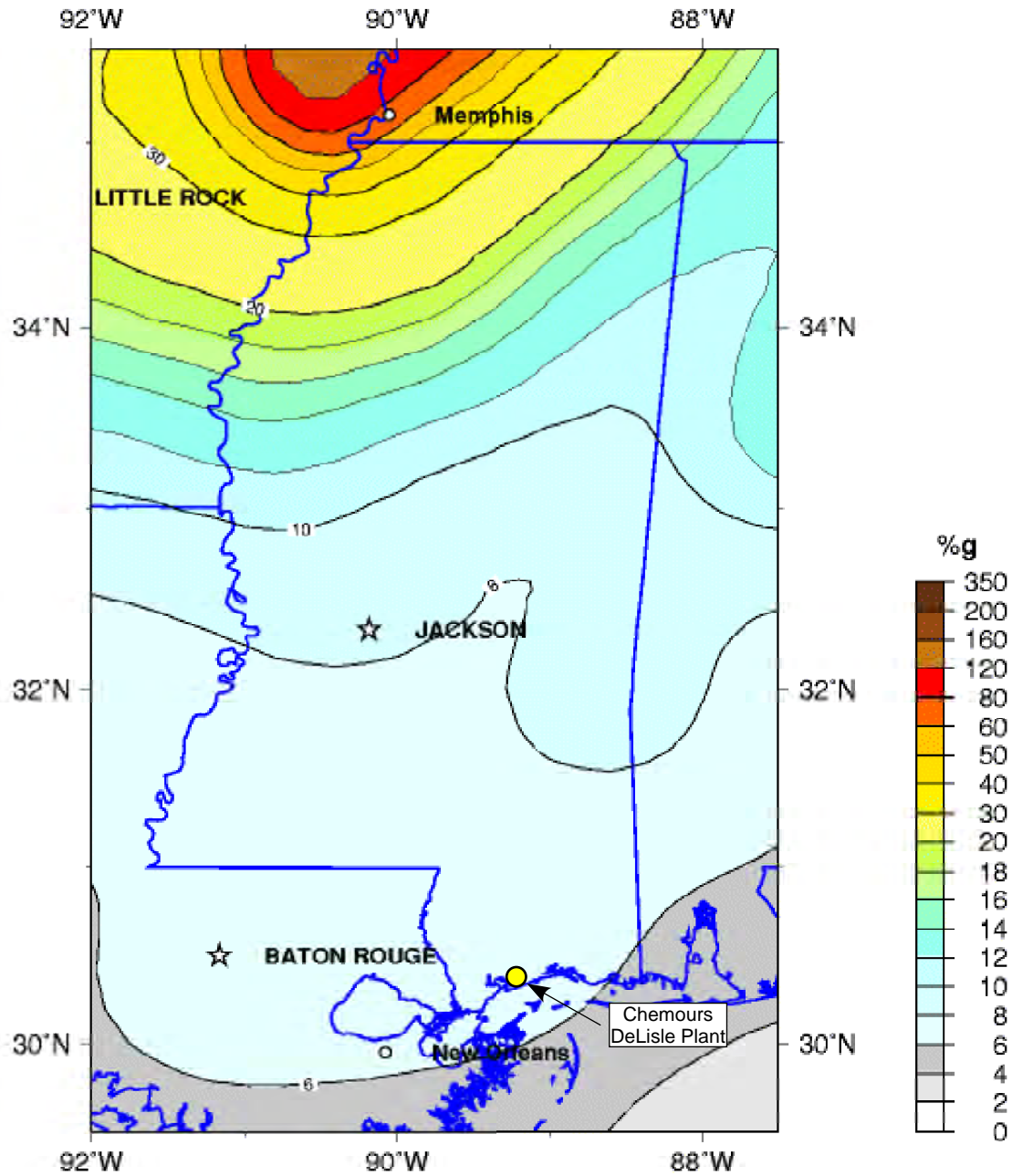
Earthquake locations are from the USGS/NEIC PDE catalog.

adapted from: USGS Earthquake Center NEIC (US Earthquake by State)
adapted by: ESSJ Sandia 8/23/06

source from: <http://earthquake.usgs.gov/regional/states/mississippi/seismicity.php>

Appendix 2-25 1990 -2001 Seismicity of Mississippi

Seismic Hazard Map of Mississippi



**Peak Acceleration (%g) with 2 % Probability of Exceedance in 50 Years
site: NEHRP B-C boundary
National Seismic Hazard Mapping Project**

adapted from: USGS Earthquake Center NEIC (US Earthquake by State Hazard Maps)
adapted by: ESSJ Sandia 9/12/06

source from: <http://earthquake.usgs.gov/regional/states/mississippi/hazards.php>

Appendix 2-26 Seismic Hazard Map of Mississippi

Appendix 2-27
NEIC: Earthquake Search Results for the
State of Mississippi

GSK Project No. DLC160183
September 2016

Date and Time	latitude	longitude	depth	magnitude	id	updated	place	type
2015-08-17T18:00:21.990Z	32.5431	-90.1146	5	2.6	us1000330y	2015-11-17T00:13:33.040Z	9km N of Madison, Mississippi	earthquake
2015-06-29T13:23:01.490Z	32.5614	-90.0744	5	3.2	us10002mc3	2015-09-02T22:37:24.040Z	6km SSW of Canton, Mississippi	earthquake
2015-05-03T01:08:34.860Z	32.5794	-90.1139	5	3	us20002ax8	2015-07-09T22:00:07.040Z	8km WSW of Canton, Mississippi	earthquake
2015-05-03T00:39:23.590Z	32.5571	-90.0759	5	3.2	us20002ax0	2015-07-09T22:00:06.040Z	7km SSW of Canton, Mississippi	earthquake
2008-05-10T17:52:50.000Z	34.35	-88.83	0.1	3.1	usp000g60x	2015-01-28T20:55:44.517Z	Mississippi	earthquake
2002-10-26T20:05:55.930Z	34.029	-90.683	5	3.1	usp000bfe9	2014-11-07T01:16:49.302Z	Mississippi	earthquake
2002-08-11T23:19:46.990Z	34.337	-90.165	5	2.8	usp000b9qv	2014-11-07T01:16:15.112Z	Mississippi	earthquake
1999-02-25T02:11:29.290Z	34.104	-89.869	5	2.9	usp00093ck	2014-11-07T01:07:04.748Z	Mississippi	earthquake
1996-08-11T18:17:49.880Z	33.577	-90.874	10	3.1	usp0007neq	2014-11-07T01:00:58.362Z	Mississippi	earthquake
1996-03-25T14:15:50.550Z	32.131	-88.671	5	3.5	usp0007f9k	2014-11-07T01:00:08.533Z	Mississippi	earthquake
1983-02-05T13:08:19.500Z	34.7	-88.37	2.6	2.9	usp0001sut	2014-11-07T00:32:38.231Z	Mississippi	earthquake
1978-12-11T02:06:48.200Z	31.95	-88.484	5	3.5	usp0000xvs	2014-11-06T23:21:54.860Z	Mississippi	earthquake
1978-06-09T23:15:19.100Z	32.094	-88.58	10	3.3	usp0000uz1	2014-11-06T23:21:49.598Z	Mississippi	earthquake
1977-11-04T11:21:07.000Z	33.833	-89.276	5	3.4	usp0000rca	2014-11-06T23:21:45.077Z	Mississippi	earthquake
1976-10-23T00:40:59.500Z	32.203	-88.726	5	3	usp0000k01	2014-11-06T23:21:37.825Z	Mississippi	earthquake
1975-09-09T11:52:44.100Z	30.662	-89.248	5	2.9	usp0000crj	2014-11-06T23:21:31.897Z	Mississippi	earthquake
1973-01-08T09:11:36.800Z	33.777	-90.625	7	3.5	usp000002m	2014-11-06T23:21:07.452Z	Mississippi	earthquake

Search Performed 2/26/2016
NEIC: Earthquake Search Results
State of Mississippi

Appendix 2-28

Location Sample Service, Inc. Petrographic Core Analysis Report

Monitor Well No. 1 (1974)

MONITOR WELL 1

Location Sample Service Inc.

Unit JACKSON LAB

CORE ANALYSIS REPORT

Date 1-21-74

E. I. DU PONT DE NEMOURS
& COMPANY, INC.

WELL #1 LESTER EARNEST, INC.

FIELD WILDCAT

SIC 4 . 8S R 13W COUNTY HARRISON

STATE MISSISSIPPI

CASE NO 1 FROM 3802 TO 3818 FORMATION

DEPTH	Permeability Millidarcys		Porosity Percent	Formation	REMARKS
	HORIZONTAL	VERTICAL			
3802.5	0	0	7.5		SHALE - PERM & POR ON
3803.5	0	0	8.1		
3804.5	0	0	8.4		
3805.5	0	0	8.4		
3806.5	0	0	8.8		
3807.5	0	0	8.1		
3808.5	0	0	7.6		
3809.5	0	0	8.0		
3810.5	0	0	7.7		
3811.5	0	0	7.9		
3812.5	0	0	8.0		
3813.5	0	0	7.7		
3814.5	0	0	8.7		
3815.5	0	0	8.5		
3816.5	0	0	9.7		
3817.5	0	0	11.0		

011000

Location Sample Service Inc.

CORE ANALYSIS REPORT

Unit JACKSON LAB.

Date 1-21-74

E. I. DU PONT DE
NEMOURS & COMPANY, INC.

WELL #1 LESTER EARNEST, INC.

FIELD WILDCAT

SEC 4 T 8S R 13W

COUNTY HARRISON COUNTY

STATE MISSISSIPPI

CORE NO 2 FROM 3818 TO 3838

FORMATION

Depth Feet	Permeability Millidarcys		Porosity Percent	Res. Sat. Liquid Saturations Oil & Gas		Pressure Pounds	REMARKS
	Horizontal	Vertical		Oil	Gas		
3818.5	0	0	12.2				
3819.5	17.1	22.5	21.7	0	92.4		SHALE - PERM & POR
3820.5	.6	.3	17.6	0	97.2		
3821.5	1.1	1.5	20.0	0	93.8		
3822.5	.5	0	22.9	0	84.5		
3823.5	5.3	4.1	21.7	0	95.6		
3824.5	6.1	3.4	28.0	0	80.4		
3825.5	4.3	5.2	25.4	0	97.6		
3826.5	5.3	4.6	27.2	0	96.2		
3827.5	.7	5.1	17.1	0	91.5		
3828.5	.4	0	17.1	0	94.3		
3829.5	0	0	30.8	0	89.8		
3830.5	0	0	33.9	0	89.2		
3831.5	.4	0	25.0	0	88.6		
3832.5	.2	0	15.6	0	94.8		
3833.5	.1	0	22.0	0	81.7		
3834.5	.3	0	19.5	0	87.4		
3835.5	0	.3	13.3	0	85.2		
3836.5	.4	.3	12.0	0	79.4		

011000

Location Sample Service Inc.

CORE ANALYSIS REPORT

Unit JACKSON LAB.

E. I. DU PONT DE NEMOURS
& COMPANY, INC.

Date 1-25-74

WELL #1 LESTER EARNEST, INC.

FIELD WILDCAT

SEC 4 T 8S R 13W COUNTY HARRISON STATE MISSISSIPPI

CORING NO 6 FROM 4275 TO 4304 FORMATION

Depth	Formation		Porosity Percent	Res. Log		Formation
	Grain Density	Volume		Grain Density	Volume	
4275.5	0	0	8.1	0	81.9	NIL
4276.5	19.5	10.4	15.1	0	85.6	WATER
4277.5	0	0	6.9	0	91.1	NIL
4278.5	.4	1.1	12.9	0	94.6	LOW PERM
4279.5	1.5	1.0	15.0	0	81.0	LOW PERM
4280.5	.4	.4	9.2	0	77.9	LOW PERM
4281.5	1.2	.8	13.2	0	97.9	LOW PERM
4282.5	1.7	1.5	18.9	0	86.4	LOW PERM
4283.5	1.4	4.2	20.8	0	83.8	LOW PERM
4284.5	4.5	1.1	15.3	0	74.7	LOW PERM
4285.5	.4	1.9	13.7	0	80.9	LOW PERM
4286.5	.7	TR	16.4	0	79.7	NIL
4287.5	.7	TR	17.1	0	81.4	NIL
4288.5	2.2	TR	16.7	0	85.6	NIL
4289.5	0	0	10.7	0	84.2	NIL
4290.5	0	0	10.6	0	94.9	NIL
4291.5	0	0	4.8			
4292.5	0	0	5.1			
4293.5	0	0	4.7			
4294.5	0	0	8.6	0	91.3	NIL
4295.5	2.7	0	20.6	0	88.3	NIL
4296.5	0	0	15.0	0	89.9	LOW PERM
4297.5	TR	.6	13.0	0	98.4	NIL
4298.5	TR	0	8.6	0	94.4	NIL
4299.5	1.4	0	12.9	0	85.1	NIL
4300.5	0	0	8.8			
4301.5	0	0	14.1	0	90.6	NIL
4302.5	0	0	9.8	0	80.4	NIL
4303.5	0	0	10.5	0	85.6	NIL

011000

SHALE PERM & FOR ONLY
SHALE PERM & FOR ONLY
SHALE PERM & FOR ONLY

SHALE PERM & FOR ONLY

Location Sample Service Inc.

CORE ANALYSIS REPORT

Unit: JACKSON LAB

Date: 1-25-74

E. I. DU PONT DE NEMOURS

& COMPANY, INC.

WELL #1 LESTER EARNEST, INC.

FIELD WILDCAT

SEC 4 T 8S R 13W

COUNTY HARRISON

STATE MISSISSIPPI

CORE NO 7 FROM 4304 TO 4340

FORMATION

Depth Feet	Permeability Millidarcys		Porosity Percent	Residual Liquid Saturations		Lithology
	Horizontal	Vertical		Oil	Water	
4304.5	TR	0	3.4	0	91.2	NIL
4305.5	TR	TR	8.7	0	85.9	NIL
4306.5	.3	.2	12.5	0	80.0	LOW PERM
4307.5	1.1	1.3	18.6	0	87.7	LOW PERM
4308.5	.3	.3	12.9	0	95.1	LOW PERM
4309.5	0	0	9.5	0	91.8	NIL
4310.5	.8	.7	17.4	0	90.9	LOW PERM
4311.5	.3	.2	13.8	0	92.4	LOW PERM
4312.5	.3	.2	11.7	0	69.4	LOW PERM
4313.5	1.5	TR	13.0	0	87.6	LOW PERM
4314.5	.5	TR	9.6	0	86.3	LOW PERM
4315.5	6.4	0	18.9	0	67.8	WATER
4316.5	1.0	TR	13.1	0	83.5	LOW PERM
4317.5	5.3	TR	18.4	0	98.9	WATER
4318.5	1.5	TR	16.4	0	98.2	LOW PERM
4319.5	4.3	2.1	18.8	0	82.4	LOW PERM
4320.5	1.3	1.0	12.3	0	88.8	LOW PERM
4321.5	1.7	1.3	13.8	0	86.5	LOW PERM
4322.5	1.0	0	6.6	0	92.1	LOW PERM
4323.5	.5	0	10.7	0	73.2	LOW PERM
4324.5	TR	TR	7.1	0	88.1	NIL
4325.5	.4	TR	12.1	0	62.5	LOW PERM
4326.5	2.0	1.6	11.0	0	84.0	LOW PERM
4327.5	3.2	1.1	20.9	0	76.8	LOW PERM

011005

Location Sample Service Inc.

Unit LAUREL LAB.

CORE ANALYSIS REPORT

Date 1-29-74

E. I. DU PONT DE NEMOURS & COMPANY, INC.

WELL #1 LESTER EARNEST, INC.

FIELD WILDCAT

4 T 8S R 13W

COUNTY HARRISON

STATE MISSISSIPPI

CORE NO. 8 FROM 4480 TO 4540

FORMATION

Depth	Permeability		Porosity	Residual Saturation		Formation	REMARKS
	Horizontal	Vertical		Oil	Water		
4480.5	0	0	14.0	0	89.7	NIL	
4481.5	0	0	16.5	0	91.5	NIL	
4482.5	0	0	14.9	0	92.6	NIL	
4483.5	0	0	17.1	0	98.7	NIL	
4484.5	0	0	18.1	0	95.2	NIL	
4485.5	.8	0	11.8	0	96.9	LOW PERM	
4486.5	.5	TR	12.4	0	91.5	LOW PERM	
4487.5	TR	0	13.8	0	98.7	NIL	
4488.5	0	0	13.6	0	96.3	NIL	
4489.5	0	0	15.5	0	94.2	NIL	
4490.5	1.0	0	12.2	0	94.1	LOW PERM	
4491.5	.3	0	12.2	0	90.5	LOW PERM	
4492.5	0	TR	13.1	0	92.8	NIL	
4493.5	.2	0	11.2	0	91.5	LOW PERM	
4494.5	0	0	23.7	0	96.9	NIL	
4495.5	.4	0	11.9	0	98.9	LOW PERM	
4496.5	0	0	13.2	0	91.2	NIL	
4497.5	1.6	0	20.3	0	94.0	LOW PERM	
4498.5	.8	0	11.0	0	91.1	LOW PERM	
4499.5	.3	TR	12.5	0	92.4	LOW PERM	
4500.5	2.2	TR	13.6	0	92.6	LOW PERM	
4501.5	2.1	TR	16.5	0	90.8	LOW PERM	
4502.5	0	0	15.1	0	89.3	NIL	
4503.5	2.2	0	19.7	0	87.6	LOW PERM	
4504.5	.2	0	18.6	0	91.5	LOW PERM	
4505.5	.6	0	11.3	0	96.3	LOW PERM	
4506.5	0	0	14.1	0	86.9	NIL	
4507.5	0	0	12.2	0	95.2	NIL	
4508.5	0	0	8.6	0	97.3	NIL	
4509.5	0	0	9.6	0	98.7	NIL	
4510.5	.8	0	10.5	0	96.9	LOW PERM	
4511.5	1.1	0	9.7	0	99.1	LOW PERM	
4512.5	.9	0	10.1	0	94.2	LOW PERM	
4513.5	.3	0	11.5	0	97.2	LOW PERM	
4514.5	2.7	TR	8.7	0	93.4	LOW PERM	
4515.5	1.3	0	9.6	0	95.1	LOW PERM	
4516.5	3.1	0	7.8	0	97.2	LOW PERM	
4517.5	1.4	0	7.3	0	94.8	LOW PERM	
4518.5	TR	0	8.8	0	88.6	NIL	
4519.5	0	0	6.3	0	91.0	NIL	
4520.5	0	0	9.5	0	92.3	NIL	
4521.5	0	0	6.2	0	98.1	NIL	
4522.5	0	0	8.6	0	93.3	NIL	
4523.5	0	0	7.9	0	94.8	NIL	
4524.5	0	0	8.1	0	95.2	NIL	
4525.5	0	0	7.6	0	96.3	NIL	
4526.5	0	0	5.9	0	95.5	NIL	
4527.5	0	0	8.8	0	97.9	NIL	
4528.5	0	0	11.5	0	96.3	NIL	
4529.5	0	0	11.7	0	94.1	NIL	

01120

CORE ANALYSIS REPORT

Unit _____ Date 2-10-74

E. I. DU PONT DE NEMOURS & COMPANY, INC.

WELL #1 LESTER EARNEST, INC.

FIELD WILDCAT

SECTION 4 T 8S R 13W COUNTY HARRISON

STATE MISSISSIPPI

CORE NO 9 FROM 8666 TO 8716 FORMATION _____

Core No	Diameter (in)		Depth (ft)	Formation		Remarks
	Top	Bottom		Top	Bottom	
8666.5	0	0	3.8			
8667.5	0	0	4.6			
8668.5	0	0	3.8			
8669.5	0	0	4.8			
8670.5	0	0	3.2			
8671.5	0	0	5.0			
8672.5	0	0	4.0			
8673.5	0	0	5.0			
8674.5	0	0	4.1			
8675.5	0	0	4.6			
8676.5	0	0	4.6			
8677.5	0	0	4.6			
8678.5	0	0	3.9			
8679.5	0	0	2.9			
8680.5	0	0	4.8			
8681.5	0	0	2.5			
8682.5	0	0	3.6			
8683.5	0	0	4.6			
8684.5	0	0	4.3			
8685.5	0	0	15.0			
8686.5	0	0	17.7			
8687.5	0	0	4.2			
8688.5	0	0	3.3			
8689.5	0	0	9.4			
8690.5	0	0	12.4			
8691.5	0	0	11.2			
8692.5	0	0	9.1			
8693.5	0	0	12.0			
8694.5	0	0	6.7			
8695.5	0	0	10.0			
8696.5	0	0	9.7			
8697.5	0	0	8.7			
8698.5	0	0	5.0			
8699.5	0	0	4.6			
8700.5	0	0	4.0			
8701.5	0	0	3.9			
8702.5	0	0	2.8			
8703.5	0	0	4.0			
8704.5	0	0	3.2			
8705.5	0	0	2.7			
8706.5	0	0	3.5			
8707.5	0	0	2.4			
8708.5	0	0	2.9			
8709.5	0	0	3.1			
8710.5	0	0	3.5			
8711.5	0	0	4.8			
8712.5	0	0	4.2			
8713.5	0	0	3.3			
8714.5	0	0	2.1			
8715.5	0	0	3.3			

0110025

Location Sample Service Inc.

Unit LAUREL LAB

CORE ANALYSIS REPORT

Date 2-13-74

E. I. DU PONT DE NEMOURS
& COMPANY, INC.

WELL #1 LESTER EARNEST, INC.

FIELD WILDCAT

SEC 4 T 8S R 13W COUNTY HARRISON STATE MISSISSIPPI

CORE NO. 10 FROM 9105 TO 9152 FORMATION

Depth Feet	Permeability Millidarcys		Porosity Percent	Core Loss %	Moisture %	Formation
	Horizontal	Vertical				
9105.5	0	0	7.5			
9106.5	0	0	6.7			
9107.5	0	0	6.9			
9108.5	0	0	7.9			
9109.5	0	0	8.3			
9110.5	0	0	7.7			
9111.5	0	0	5.7			
9112.5	0	0	6.7			
9113.5	17.5	0	7.4	0	89.9	WATER
9114.5	14.4	5.2	17.2	0	94.2	WATER
9115.5	1.2	0	9.6	0	89.8	LOW PERM
9116.5	0	0	14.6	0	91.4	NIL
9117.5	4.9	4.0	15.7	0	90.8	LOW PERM
9118.5	24.7	7.3	14.9	0	87.7	WATER
9119.5	7.2	7.7	18.8	0	86.3	WATER
9120.5	10.1	6.3	14.9	0	86.5	WATER
9121.5	23.4	2.3	22.0	0	82.3	WATER
9122.5	1.7	2.8	13.3	0	88.0	WATER
9123.5	12.8	8.5	17.0	0	91.1	WATER
9124.5	8.7	1.6	16.9	0	86.0	WATER
9125.5	0	0	8.2			
9126.5	0	0	9.7			
9127.5	0	0	8.5			
9128.5	0	0	13.5			
9129.5	0	0	10.0			
9130.5	0	0	13.1			
9131.5	0	0	8.3			
9132.5	0	0	10.2			
9133.5	0	0	8.5			
9134.5	0	0	10.3			
9135.5	0	0	7.7			
9136.5	0	0	10.8			
9137.5	0	0	9.4			
9138.5	0	0	9.5			
9139.5	0	0	15.7	0	90.8	NIL
9140.5	0	5	15.1	0	88.5	LOW PERM
9141.5	0	0	8.1			
9142.5	0	0	4.7			
9143.5	0	0	4.3			
9144.5	0	0	2.4			
9145.5	0	0	12.7			
9146.5	0	0	8.7			
9147.5	0	0	8.8			
9148.5	0	0	9.3			
9149.5	0	0	6.8			
9150.5	0	0	6.3			
9151.5	0	0	9.7			

01100

Location Sample Service Inc.

Unit JACKSON LAB.

CORE ANALYSIS REPORT

Date 2-15-74

E. I. DU PONT DE NEMOURS
& COMPANY, INC.

WELL #1 LESTER EARNEST, INC.

FIELD WILDGAT

4 T 8S R 13W

COUNTY HARRISON

STATE MISSISSIPPI

11 FROM 9286 TO 9317

FORMATION

Sample No.	Moisture (%)	Vol. (%)	Grav. (g)	Grav. (g)	Grav. (g)	Formation
9286.5	0	0	9.7	0	89.9	NIL
9287.5	0	0	7.8	0	96.0	NIL
9288.5	0	0	12.1	0	82.4	NIL
9289.5	0	0	10.5	0	88.4	NIL
9290.5	0	0	9.5	0	92.2	NIL
9291.5	0	0	6.4	0	92.1	NIL
9292.5	0	0	12.4	0	84.3	NIL
9293.5	0	0	12.2	0	82.2	NIL
9294.5	0	0	6.4			
9295.5	0	0	10.9			
9296.5	0	0	4.2			
9297.5	0	0	5.8			
9298.5	0	0	6.7			
9299.5	0	0	6.1			
9300.5	0	0	8.8			
9301.5	0	0	5.8	0	92.1	NIL
9302.5	6.8	.8	12.9	0	83.8	WATER
9303.5	0	.8	13.5	0	85.0	NIL
9304.5	0	0	9.2	0	92.9	NIL
9305.5	0	0	8.2	0	95.3	NIL
9306.5	0	0	7.2	0	96.0	NIL
9307.5	1.1	2.5	14.1	0	77.9	LOW PERM
9308.5	0	0	8.1	0	94.7	NIL
9309.5	.8	0	3.6	0	82.6	LOW PERM
9310.5	0	0	4.7			
9311.5	0	0	4.8			
9312.5	0	0	4.5			
9313.5	0	0	5.1			
9314.5	0	0	3.7			
9315.5	0	0	4.4			
9316.5	0	0	5.0			

01100

Location Sample Service Inc.

CORE ANALYSIS REPORT

Unit JACKSON LAB.

E. I. DU PONT DE NEMOURS & COMPANY, INC.

Date 2-17-74

COMPANY

WELL #1 LESTER EARNEST, INC.

FIELD WILDCAT

S. 4 T. 8S R. 13W COUNTY HARRISON

STATE MISSISSIPPI

CORE NO 12 FROM 9382 TO 9403

FORMATION

Depth Feet	Permeability Millidarcys		Porosity Percent	Plastic Liquid Content		Formation	Remarks
	Horizontal	Vertical		Free	Total		
9382.5	0	0	11.3	0	84.2	NIL	
9383.5	4.1	1.7	20.0	0	78.6	LOW PERM	
9384.5	29.3	14.5	22.2	0	74.1	WATER	
9385.5	14.7	.9	22.2	0	78.4	WATER	
9386.5	8.8	.5	20.5	0	86.9	WATER	
9387.5	1.9	0	18.1	0	91.9	LOW PERM	
9388.5	.1	.4	20.8	0	83.5	LOW PERM	
9389.5	1.5	.4	20.2	0	85.0	LOW PERM	
9390.5	4.8	1.9	21.8	0	84.0	LOW PERM	
9391.5	0	0	7.3				
9392.5	0	0	8.1				
9393.5	1.8	0	15.4	0	85.1	LOW PERM	
9394.5	.8	0	17.6	0	81.3	LOW PERM	

011-511

Location Sample Service Inc.

CORE ANALYSIS REPORT

Unit JACKSON LAB

Date 2-18-74

E. I. DU PONT DE NEMOURS
& COMPANY, INC.

WELL #1 LESTER EARNEST, INC.

FIELD WILDCAT

SEC 4 T 8S R 13W COUNTY HARRISON

STATE MISSISSIPPI

CORE NO 13 FROM 9403 TO 9458 FORMATION

Core No.	Permeability Mudarcas		Porosity Percent	Res. Sat. Initial Saturations % of Pore Space		Pressure Gradient	REMARKS
	Horizontal	Vertical		Gas	Water		
9403.5	1.6	0	19.0	0	91.4	LOW PERM	
9404.5	13.7	5.9	20.9	0	83.9	WATER	
9405.5	91.8	20.3	24.9	0	82.0	WATER	
9406.5	29.6	2.1	20.6	0	88.3	WATER	
9407.5	0	0	6.3				
9408.5	339.0	182.0	22.9	0	89.3	WATER	
9409.5	268.0	377.0	24.2	0	87.2	WATER	
9410.5	192.0	104.0	24.5	0	87.2	WATER	
9411.5	103.0	159.0	25.8	0	84.3	WATER	
9412.5	170.0	103.0	24.4	0	91.1	WATER	
9413.5	38.1	119.0	19.0	0	97.0	WATER	
9414.5	76.1	127.0	20.0	0	88.9	WATER	
9415.5	162.0	315.0	22.9	0	89.4	WATER	
9416.5	209.0	608.0	24.9	0	82.9	WATER	
9417.5	247.0	29.1	21.6	0	93.4	WATER	
9418.5	116.0	278.0	24.4	0	83.6	WATER	
9419.5	50.9	541.0	23.6	0	86.6	WATER	
9420.5	175.0	157.0	25.9	0	84.1	WATER	
9421.5	75.2	58.1	24.0	0	86.9	WATER	
9422.5	86.8	280.0	23.6	0	86.6	WATER	
9423.5	206.0	225.0	23.2	0	90.1	WATER	

011001

Location Sample Service Inc.

CORE ANALYSIS REPORT

Unit JACKSON LAB

Date 2-20-74

E. I. DU PONT DE NEMOURS & COMPANY, INC.

WELL #1 LESTER EARNEST, INC.

FIELD WILDCAT

SEC 4 T 8S R 13W COUNTY HARRISON

STATE MISSISSIPPI

CORE NO 14 FROM 9460 TO 9479 FORMATION

Core No	Depth Feet	Permeability Abundances		Porosity Percent	Moisture Content		Remarks
		Horizontal	Vertical		Free	Total	
9460.5	48.1	66.0	23.6	0	92.6	WATER	
9461.5	93.9	291.0	23.7	0	92.0	WATER	
9462.5	78.4	180.0	25.1	0	88.9	WATER	
9463.5	85.3	86.5	20.4	0	93.8	WATER	
9464.5	19.6	104.0	21.0	0	92.2	WATER	
9465.5	104.0	47.5	20.5	0	90.0	WATER	
9466.5	67.3	71.4	24.7	0	81.0	WATER	
9467.5	0	0	17.7	0	94.9	NIL	
9468.5	0	0	11.2	0	84.8	NIL	
9469.5	0	0	18.1	0	76.9	NIL	
9470.5	0	0	7.9				
9471.5	0	0	6.2				
9472.5	0	0	7.7	0	93.0	NIL	
9473.5	67.3	41.2	19.1	0	89.1	WATER	
9474.5	23.2	14.6	15.7	0	87.9	WATER	
9475.5	0	0	8.9				
9476.5	0	0	8.4				
9477.5	0	0	9.4				

011005

Location Sample Service Inc.

CORE ANALYSIS REPORT

Unit JACKSON LAB.

Date 2-21-74

E. I. DU PONT DE NEMOURS
& COMPANY, INC.

WELL #1 LESTER EARNEST, INC.

FIELD WILDCAT

SECTION 4 T 8S R 13W

COUNTY HARRISON

STATE MISSISSIPPI

CORE NO 15 FROM 9480 TO 9536 FORMATION

Depth	Permeability		Moisture Content	Porosity	Grain Density	Formation	Remarks
	Horizontal	Vertical					
9480.5	103.0	163.0	27.1	0	85.7	WATER	
9481.5	66.2	49.0	25.6	0	86.0	WATER	
9482.5	96.0	46.7	25.7	0	92.1	WATER	
9483.5	0	0	11.8	0	76.5	NIL	
9484.5	0	0	10.3	0	92.7	NIL	
9485.5	66.2	62.4	24.7	0	94.8	WATER	
9486.5	9.3	.7	20.8	0	97.4	WATER	
9487.5	2.6	.4	19.1	0	88.8	LOW PERM	
9488.5	0	.6	20.8	0	90.5	NIL	
9489.5	27.6	24.6	24.2	0	86.4	WATER	
9490.5	31.9	48.1	25.8	0	88.3	WATER	
9491.5	53.8	105.0	24.1	0	82.0	WATER	
9492.5	25.8	17.4	25.8	0	79.2	WATER	
9493.5	37.9	86.4	25.8	0	90.9	WATER	
9494.5	29.3	13.2	22.1	0	91.4	WATER	
9495.5	72.2	162.0	24.2	0	87.5	WATER	
9496.5	49.0	68.8	26.3	0	82.0	WATER	
9497.5	56.7	80.8	21.2	0	92.2	WATER	
9498.5	188.0	312.0	24.7	0	84.8	WATER	
9499.5	52.6	91.8	25.3	0	84.4	WATER	
9500.5	65.2	113.0	25.4	0	84.2	WATER	
9501.5	46.8	83.0	25.0	0	88.2	WATER	
9502.5	79.4	116.0	24.2	0	90.0	WATER	
9503.5	26.1	77.8	23.1	0	90.6	WATER	
9504.5	37.6	4.0	18.8	0	82.4	WATER	
9505.5	46.8	14.1	19.3	0	83.6	WATER	
9506.5	73.3	73.4	24.7	0	92.2	WATER	
9507.5	0	0	4.6	0	90.4	NIL	
9508.5	0	0	5.3	0	87.0	NIL	
9509.5	168.0	197.0	21.8	0	83.4	WATER	
9510.5	262.0	61.5	22.4	0	86.3	WATER	
9511.5	0	0	5.7	0	80.7	NIL	
9512.5	0	0	6.5	0	83.5	NIL	
9513.5	0	0	10.5				
9514.5	0	0	13.6				
9515.5	0	0	12.7				
9516.5	0	0	11.8				
9517.5	0	0	11.0				
9518.5	0	0	11.6				
9519.5	0	0	9.7				
9520.5	0	0	11.4				
9521.5	0	0	14.3	0	96.7	NIL	

0110

Location Sample Service Inc.

CORE ANALYSIS REPORT

Unit JACKSON LAB.

Date 2-22-74

E. I. DU PONT DE NEMOURS
& COMPANY, INC.

WELL #1 LESTER EARNEST, INC.

FIELD WILDCAT

SEC 4 T 8S R 13W COUNTY HARRISON

STATE MISSISSIPPI

CORE NO. 16 FROM 9536 TO 9546 FORMATION:

Core No.	Depth Feet	Permeability (Millidarcys)		Porosity Percent	Residual Oil Content (%)		Remarks
		Horizontal	Vertical		Core	Core	
9536.5		0	0	13.6	0	91.2	NIL
9537.5		0	0	7.2	0	81.9	NIL
9538.5		0	0	9.3			
9539.5		0	0	12.6			
9540.5		0	0	12.2			
9541.5		0	0	13.7			
9542.5		0	0	8.8			
9543.5		0	0	5.4			
9544.5		0	0	8.3			
9545.5		0	0	6.4			

01100

Location Sample Service Inc.

CORE ANALYSIS REPORT

UNIT JACKSON LAB

Date 3-6-74

E. I. DU PONT DE NEMOURS
& COMPANY, INC.

WELL #1 LESTER EARNEST, INC.

FIELD WILDCAT

SE 4 T 8S R 13W COUNTY HARRISON

STATE MISSISSIPPI

DEPTH 17 FROM 9652 TO 9660 FORMATION

DEPTH	GRAVIMETRIC ANALYSIS		Porosity Percent	LOGGING DATA	PHYSICAL PROPERTIES	REMARKS
	Moisture	Grain Density				
9652.5	0	0	3.9			
9653.5	0	0	4.5			
9654.5	0	0	5.1			
9655.5	0	0	5.3			
9656.5	0	0	4.1			
9657.5	0	0	4.1			
9658.5	0	0	3.1			

011

Location Sample Service Inc.

CORE ANALYSIS REPORT

Unit JACKSON LAB.

E. I. DU PONT DE NEMOURS
& COMPANY, INC.

Date 3-6-74

WELL #1 LESTER EARNEST, INC.

FIELD WILDCAT

4 T 8S R 13W COUNTY HARRISON

STATE MISSISSIPPI

18 FROM 9660 TO 9676 FORMATION

DEPTH	PERMEABILITY		POROSITY	SAND	SILT	CLAY	REMARKS
	HORIZONTAL	VERTICAL					
9660.5	0	0	4.7				
9661.5	0	0	4.6				
9662.5	0	0	4.3				
9663.5	0	0	5.0				
9664.5	0	0	5.4				
9665.5	0	0	4.4				
9666.5	0	0	4.4				
9667.5	0	0	4.3				
9668.5	0	0	4.5				
9669.5	0	0	4.3				
9670.5	0	0	4.4				
9671.5	0	0	3.6				
9672.5	0	0	4.8				
9673.5	0	0	4.7				
9674.5	0	0	4.3				
9675.5	0	0	4.7				

01100

Location Sample Service Inc.

CORE ANALYSIS REPORT

Unit JACKSON LAB.

Date 3-6-74

E. I. DU PONT DE NEMOURS
& COMPANY, INC.

WELL #1 LESTER EARNEST, INC.

FIELD WILDCAT

SECTION 4 T 8S R 13W COUNTY HARRISON

STATE MISSISSIPPI

(DEPTH) 19 FROM 9767 TO 9798 FORMATION

DEPTH	Permeability		Porosity	Moisture		FORMATION	REMARKS
	Horizontal	Vertical		Free	Total		
9767.5	1.9	1.0	12.0	0	67.5	LOW PERM	
9768.5	5.9	0	8.0	0	51.5	WATER	
9769.5	Tr	0	13.3	0	71.8	NIL	
9770.5	0	0	4.6				
9771.5	0	0	5.1				
9772.5	0	0	5.1				
9773.5	0	0	4.8				
9774.5	.6	.3	4.1	0	73.2	LOW PERM	
9775.5	0	0	4.1				
9776.5	0	0	4.8				
9777.5	0	0	4.5				
9778.5	0	0	4.3				
9779.5	0	0	3.6				
9780.5	0	0	4.6				
9781.5	0	0	4.2				
9782.5	129.0	144.0	23.0	0	76.4	WATER	
9783.5	272.0	66.8	14.9	0	89.3	WATER	
9784.5	30.5	9.0	19.3	0	96.7	WATER	
9785.5	695.0	350.0	26.4	0	80.0	WATER	
9786.5	467.0	242.0	25.6	0	85.2	WATER	
9787.5	553.0	114.0	24.9	0	80.3	WATER	
9788.5	370.0	115.0	24.4	0	75.6	WATER	
9789.5	539.0	82.7	24.7	0	79.2	WATER	
9790.5	376.0	109.0	25.3	0	80.7	WATER	
9791.5	373.0	132.0	25.4	0	81.3	WATER	
9792.5	442.0	203.0	26.3	0	51.2	WATER	
9793.5	436.0	174.0	24.8	0	79.7	WATER	
9794.5	562.0	381.0	24.9	0	80.3	WATER	
9795.5	290.0	15.4	23.0	0	81.2	WATER	

011000

Location Sample Service Inc.

Unit JACKSON LAB.

CORE ANALYSIS REPORT

Date 3-8-74

E. I. DU PONT DE NEMOURS

PANY & COMPANY, INC.

WELL #1 LESTER EARNEST, INC.

FIELD WILDCAT

SEC 4 T 8S R 13W

COUNTY HARRISON

STATE MISSISSIPPI

CORE NO 20

FROM 9798

9826

FORMATION

DEPTH	GRAVIMETRIC	VOLUMETRIC	WATER	WATER	WATER	REMARKS
FEET	PERCENT	PERCENT	PERCENT	PERCENT	PERCENT	
9798.5	691.0	126.0	23.3	0	24.3	WATER
9799.5	953.0	290.0	23.2	0	85.1	WATER
9800.5	525.0	46.5	25.1	0	75.4	WATER
9801.5	834.0	559.0	20.9	0	85.0	WATER
9802.5	500.0	112.0	23.8	0	80.5	WATER
9803.5	502.0	55.3	23.3	0	97.3	WATER
9804.5	518.0	120.0	22.8	0	82.9	WATER
9805.5	573.0	282.0	22.4	0	72.6	WATER
9806.5	418.0	83.2	22.2	0	89.1	WATER
9807.5	702.0	338.0	21.3	0	87.9	WATER
9808.5	549.0	94.8	22.1	0	85.6	WATER
9809.5	886.0	51.8	22.4	0	84.2	WATER
9810.5	486.0	71.2	22.4	0	84.5	WATER
9811.5	646.0	265.0	24.0	0	86.0	WATER
9812.5	584.0	359.0	23.8	0	84.9	WATER
9813.5	656.0	380.0	24.0	0	82.5	WATER
9814.5	589.0	276.0	24.9	0	88.2	WATER
9815.5	0	0	4.4			
9816.5	0	0	4.4			
9817.5	0	0	4.9			
9818.5	0	0	5.4			
9819.5	26.3	6.2	17.9	0	75.8	WATER
9820.5	22.8	3.6	18.5	0	78.1	WATER
9821.5	2.0	1.1	15.4	0	81.1	LOW PERM
9822.5	333.0	108.0	21.1	0	79.4	WATER
9823.5	266.0	47.7	23.6	0	80.1	WATER
9824.5	454.0	42.4	23.6	0	77.1	WATER
9825.5	0	0	11.4	0	73.0	NIL

011005

Location Sample Service Inc.

Unit JACKSON LAB.

CORE ANALYSIS REPORT

Date 3-8-74

E. I. DU PONT DE NEMOURS
& COMPANY, INC.

WELL #1 LESTER EARNEST, INC.

FIELD WILDCAT

SEC 4 T 8S R 13W COUNTY HARRISON

STATE MISSISSIPPI

CORE NO 21 FROM 9829 TO 9851 FORMATION

DEPTH	PERMEABILITY		TEMPERATURE	PRESSURE	FORMATION	REMARKS
	GRAIN	APPARENT				
9829.5	147.0	16.7	21.3	0	85.4	WATER
9830.5	193.0	281.0	23.9	0	82.9	WATER
9831.5	200.0	49.5	22.2	0	85.3	WATER
9832.5	187.0	23.9	19.8	0	84.0	WATER
9833.5	539.0	323.0	22.0	0	80.0	WATER
9834.5	507.0	253.0	21.7	0	91.9	WATER
9835.5	184.0	74.7	20.3	0	91.0	WATER
9836.5	387.0	96.5	21.4	0	87.0	WATER
9837.5	210.0	12.7	21.3	0	78.3	WATER
9838.5	204.0	73.5	22.5	0	80.9	WATER
9839.5	274.0	37.9	24.3	0	76.0	WATER
9840.5	375.0	146.0	23.9	0	91.3	WATER
9841.5	360.0	61.8	21.1	0	81.3	WATER
9842.5	232.0	103.0	22.0	0	85.9	WATER
9843.5	344.0	206.0	23.2	0	89.0	WATER
9844.5	531.0	161.0	23.8	0	85.9	WATER
9845.5	462.0	62.9	24.0	0	83.2	WATER
9846.5	656.0	178.0	21.4	0	83.1	WATER
9847.5	278.0	253.0	26.2	0	76.4	WATER
9848.5	640.0	219.0	25.6	0	85.0	WATER
9849.5	411.0	272.0	26.0	0	89.0	WATER
9850.5	0	0	5.1			

011005

Location Sample Service Inc.

CORE ANALYSIS REPORT

Unit JACKSON LAB.

Date 3-9-74

E. I. DU PONT DE NEMOURS &
COMPANY, INC.

WELL #1 LESTER EARNEST, INC.

FIELD WILDCAT

SEC 4 T 8S R 13W COUNTY HARRISON

STATE MISSISSIPPI

CORE NO 22 FROM 9857 TO 9917 FORMATION

DEPTH	PERFORATION INCHES	PERFORATION FEET	PERCENT OPEN	PERCENT OPEN	PERCENT OPEN	FORMATION	REMARKS
9857.5	405.0	700.0	26.7	0	72.5	WATER	
9858.5	472.0	82.2	26.6	0	78.5	WATER	
9859.5	386.0	89.2	25.6	0	73.7	WATER	
9860.5	116.0	7.0	24.3	0	76.7	WATER	
9861.5	141.0	5.8	23.0	0	70.7	WATER	
9862.5	102.0	30.3	24.3	0	73.2	WATER	
9863.5	68.0	19.2	22.6	0	78.6	WATER	
9864.5	138.0	18.7	24.1	0	77.4	WATER	
9865.5	161.0	26.5	24.7	0	72.0	WATER	
9866.5	178.0	14.0	23.7	0	74.1	WATER	
9867.5	95.2	37.7	24.2	0	74.3	WATER	
9868.5	197.0	109.0	24.6	0	82.2	WATER	
9869.5	179.0	14.1	22.0	0	77.7	WATER	
9870.5	277.0	154.0	23.9	0	84.7	WATER	
9871.5	226.0	37.5	27.2	0	72.0	WATER	
9872.5	46.0	3.9	21.1	0	65.4	WATER	
9873.5	300.0	100.0	20.5	0	93.2	WATER	
9874.5	134.0	11.7	26.1	0	74.2	WATER	
9875.5	550.0	274.0	22.6	0	79.5	WATER	
9876.5	403.0	447.0	25.0	0	83.6	WATER	
9877.5	509.0	202.0	28.5	0	71.6	WATER	
9878.5	509.0	393.0	24.7	0	81.3	WATER	
9879.5	526.0	246.0	24.2	0	80.0	WATER	
9880.5	412.0	198.0	23.1	0	70.2	WATER	
9881.5	439.0	505.0	23.9	0	70.6	WATER	
9882.5	381.0	32.4	22.9	0	75.7	WATER	
9883.5	132.0	10.8	22.9	0	70.9	WATER	
9884.5	380.0	67.5	23.3	0	76.2	WATER	
9885.5	605.0	385.0	25.3	0	78.9	WATER	
9886.5	573.0	324.0	25.3	0	73.8	WATER	
9887.5	520.0	662.0	26.1	0	71.5	WATER	
9888.5	412.0	272.0	24.9	0	75.0	WATER	
9889.5	379.0	181.0	21.8	0	81.4	WATER	
9890.5	396.0	194.0	24.3	0	81.5	WATER	
9891.5	500.0	313.0	24.9	0	64.2	WATER	
9892.5	531.0	206.0	24.5	0	72.4	WATER	
9893.5	589.0	429.0	26.4	0	75.8	WATER	
9894.5	745.0	703.0	25.4	0	77.8	WATER	
9895.5	791.0	356.0	27.6	0	76.4	WATER	
9896.5	453.0	222.0	24.6	0	85.8	WATER	
9897.5	926.5	386.0	27.5	0	78.9	WATER	
9898.5	550.0	63.7	27.9	0	73.3	WATER	
9899.5	112.0	14.4	22.5	0	93.0	WATER	

01100

Location Sample Service Inc.

CORE ANALYSIS REPORT

Unit JACKSON LAB.

Date 2-25-74

E. I. DU PONT DE NEMOURS
& COMPANY, INC.

WELL #1 LESTER EARNEST, INC.

FIELD WILDCAT

4

8S R 13W

COUNTY HARRISON

STATE MISSISSIPPI

	FROM	TO	SIDEWALLS
3570	0	0	9.1
3572	0	0	8.7
3575	0	0	7.9
3577	0	0	8.1
3582	0	0	8.6
3590	0	0	7.8
3592	0	0	9.6
3595	0	0	9.4
3597	0	0	8.9
3600	0	0	9.4
3602	0	0	10.6
3605	0	0	11.9
3607	0	0	8.4
3610	0	0	7.9
3612	0	0	7.6
3615	0	0	7.3
3617	0	0	8.9
3622	0	0	6.9
3625	0	0	7.2
3627	0	0	7.0
3630	0	0	6.8
3632	0	0	7.1
3635	0	0	6.8
3637	0	0	7.4
3640	0	0	7.8
3642	0	0	7.6
3645	0	0	7.5
3647	0	0	6.5
3650	0	0	7.2
3660	0	0	6.7
3662	0	0	7.0

011000

CORE ANALYSIS REPORT

E. I. DU PONT DE NEMOURS &
COMPANY, INC.

WELL #1 LESTER EARNEST, INC.

FIELD WILDCAT

4 T 8S R 13W

COUNTY HARRISON

STATE MISSISSIPPI

CORE NO	FROM		TO	FORMATION		SIDEWALLS	REMARKS
	PERMEABILITY MILLIDARCS	WATER CONTENT		WATER CONTENT	WATER CONTENT		
4171	112.0	86.9	22.8	0	85.2	WATER	
4366	10.1	TR	18.1	0	91.6	WATER	
4378	169.0	186.0	24.4	0	94.7	WATER	
4391	28.4	0	17.9	0	89.3	WATER	
4404	65.5	18.4	19.3	0	91.6	WATER	
4410	41.1	52.8	26.3	0	94.3	WATER	
4423	24.2	13.6	21.8	0	87.7	WATER	
9578	342.0	218.0	28.0	0	94.2	WATER	
9580	114.0	40.8	26.2	0	90.8	WATER	
9582	248.0	214.0	26.8	0	91.5	WATER	
9584	420.0	269.0	27.2	0	95.8	WATER	
9586	144.0	48.3	28.8	0	91.9	WATER	
9588	369.0	312.0	26.7	0	90.3	WATER	
9590	287.0	111.0	26.6	0	95.8	WATER	
9592	300.0	368.0	26.9	0	90.2	WATER	
9594	366.0	418.0	26.3	0	88.7	WATER	
9596	414.0	329.0	29.1	0	91.1	WATER	
9598	400.0	374.0	28.4	0	91.3	WATER	
9600	368.0	388.0	27.7	0	85.8	WATER	
9602	281.0	149.0	26.8	0	90.0	WATER	
9604	380.0	161.0	27.4	0	91.8	WATER	
9606	462.0	322.0	28.4	0	92.1	WATER	
9608	964.0	812.0	27.9	0	90.5	WATER	
9610	875.0	960.0	27.7	0	92.8	WATER	
9612	740.0	710.0	26.1	0	87.2	WATER	
9614	680.0	412.0	26.0	0	85.5	WATER	
9616	547.0	610.0	24.9	0	88.6	WATER	
9618	710.0	610.0	27.2	0	85.9	WATER	
9620	674.0	408.0	26.6	0	87.7	WATER	
9622	218.0	140.0	24.4	0	89.8	WATER	
9624	840.0	316.0	27.3	0	85.4	WATER	
9626	628.0	492.0	28.6	0	86.7	WATER	
9628	962.0	680.0	27.9	0	85.1	WATER	
9630	1060.0	810.0	28.1	0	91.2	WATER	
9932	64.1	49.8	23.8	0	90.2	WATER	
9934	83.7	28.9	22.9	0	88.9	WATER	
9936	28.9	4.1	22.1	0	91.3	WATER	
9938	189.0	110.0	24.2	0	89.9	WATER	
9940	210.0	160.0	25.8	0	90.1	WATER	
9942	269.0	141.0	26.0	0	86.3	WATER	
9944	352.0	184.0	26.1	0	85.7	WATER	
9946	210.0	48.0	24.6	0	87.5	WATER	

01100

Location Sample Service Inc.

CORE ANALYSIS REPORT

Unit JACKSON LAB

Date 1-24-74

E. I. DU PONT DE NEMOURS

& COMPANY, INC.

WELL #1 LESTER EARNEST, INC.

FIELD WILDCAT

SEC 4 T 8S R 13W

COUNTY HARRISON

STATE MISSISSIPPI

CORE NO	FROM	TO	GRAVITY	WATER	WATER	FORMATION	SIDEWALLS
3745	4650.0	4490.0	38.4	0	89.5	WATER	
3753	3910.0	3800.0	36.8	0	93.0	WATER	
3757	5100.0	5190.0	37.6	0	93.7	WATER	
3765	3220.0	1610.0	34.5	0	95.2	WATER	
3767	4280.0	3610.0	37.8	0	97.1	WATER	
3771	212.0	84.0	27.1	0	90.6	WATER	
3774	10.0	0	9.3	0	91.7	WATER	
3777	2580.0	2140.0	36.2	0	92.7	WATER	
3785	3250.0	3380.0	37.7	0	93.6	WATER	
3788	4600.0	3990.0	38.5	0	93.0	WATER	
3835	84.6	75.9	26.3	0	95.8	WATER	
3836	15.8	12.2	18.1	0	94.1	WATER	
3844	TR	0	14.3	0	92.3	NIL	
3860	2960.0	1900.0	34.8	0	92.7	WATER	011065
3863	0	0	11.9	0	89.6	NIL	
3866	14.9	3.6	18.8	0	94.1	WATER	
3869	1820.0	8.6	23.6	0	94.0	WATER	
3883	87.9	65.3	26.7	0	90.9	WATER	
3895	3940.0	3280.0	35.6	0	92.6	WATER	
3904	INSUFFICIENT SAMPLE FOR ANALYSIS						
3924	INSUFFICIENT SAMPLE FOR ANALYSIS						
3925	INSUFFICIENT SAMPLE FOR ANALYSIS						
3933	4200.0	4310.0	37.4	0	95.1	WATER	
3936	INSUFFICIENT SAMPLE FOR ANALYSIS						
3946	3840.0	240.0	37.7	0	90.7	WATER	
3948	3630.0	3410.0	37.1	0	93.6	WATER	
3975	0	0	6.5				SHALE - PERM & POR ON
3983	INSUFFICIENT SAMPLE FOR ANALYSIS						
3986	TR	0	11.8	0	92.6	NIL	

Appendix 2-29

Location Sample Service, Inc. Petrographic Core Analysis Report

Well No. 2 Original Borehole (1979)

PLANT WELL 2

Location Sample Service Inc.

Unit JACKSON LAB

IMPACT _____

CORE ANALYSIS REPORT

WELL 7 0 70

SEC. _____ T. _____ R. _____ COUNTY HARRISON

STATE MISSISSIPPI

CORE NO 4 FROM 9900 TO 9955 FORMATION _____

Sample No	Depth Feet	Permeability Millidarcys		Porosity Percent	Residual Liquid Saturations % of Pore Space		Probable Production	REMARKS
		Horizontal	Vertical		Oil	Total Water		
9906.5	57.5			22.7	0	76.5	WATER	
9907.5	224.0			22.8	0	76.2	WATER	
9908.5	250.0			23.0	0	87.8	WATER	
9909.5	400.0			25.0	0	59.3	WATER	
9910.5	67.4			23.2	0	75.0	WATER	
9911.5	223.0			22.0	0	81.6	WATER	
9912.5	314.0			23.7	0	82.2	WATER	
9913.5	196.0			23.0	0	92.6	WATER	
9914.5	103.0			20.1	0	97.8	WATER	
9915.5	89.0			22.3	0	86.2	WATER	
9916.5	239.0			23.4	0	90.1	WATER	
9917.5	158.0			21.0	0	93.3	WATER	
9919.5	98.4			21.1	0	74.1	WATER	
9920.5	169.0			22.0	0	77.1	WATER	
9921.5	162.0			21.0	0	91.7	WATER	
9922.5	333.0			25.9	0	71.9	WATER	
9923.5	248.0			23.9	0	75.6	WATER	
9924.5	378.0			21.8	0	82.9	WATER	
9925.5	137.0			20.1	0	87.0	WATER	
9926.5	220.0			24.8	0	71.4	WATER	
9927.5	170.0			24.9	0	62.9	WATER	
9928.5	24.9			17.6	0	91.7	WATER	
9929.5	129.0			20.6	0	85.9	WATER	
9930.5	407.0			24.6	0	80.8	WATER	
9931.5	397.0			25.8	0	78.6	WATER	
9932.5	387.0			23.5	0	87.3	WATER	
9933.5	254.0			24.1	0	83.7	WATER	
9934.5	259.0			23.4	0	83.7	WATER	
9935.5	386.0			26.2	0	76.1	WATER	
9937.5	606.0			23.3	0	82.3	WATER	
9938.5	423.0			25.1	0	88.8	WATER	
9939.5	328.0			27.7	0	81.8	WATER	
9940.5	253.0			24.2	0	92.1	WATER	
9941.5	476.0			25.2	0	73.3	WATER	
9942.5	135.0			22.7	0	86.3	WATER	
9943.5	430.0			23.6	0	72.0	WATER	
9944.5	449.0			23.6	0	83.1	WATER	
9945.5	153.0			23.5	0	64.1	WATER	
9946.5	.9			7.4	0	81.6	WATER	
9947.5	.4			12.5	0	54.9	WATER	
9948.5	.5			8.6	0	63.0	WATER	
9949.5	.5			7.7	0	54.9	WATER	
9950.5	TR			6.6	0	85.2	NIL	
9951.5	TR			11.0	0	80.2	NIL	
9952.5	684.0			21.5	0	89.1	WATER	
9953.5	492.0			22.6	0	91.0	WATER	
9954.5	516.0			23.3	0	94.3	WATER	

Location Sample Service Inc.

CORE ANALYSIS REPORT

Unit JAC 41960
Date 2-9-79

COMPANY DUPONT WELL DISPOSAL WELL NO. 2 FIELD _____

SEC. _____ T. _____ R. _____ COUNTY HARRISON STATE MISS.

CORE NO. 5 FROM 9985 TO 10045 FORMATION _____

Sample No	Depth Feet	Permeability Millidarcys		Porosity Percent	Residual Liquid Saturations % of Pore Space		Probable Production	REMARKS
		Horizontal	Vertical		Oil	Total Water		
9985.5	240.0			24.1	0	80.2	WATER	
9986.5	36.0			25.4	0	76.2	WATER	
9988.5	377.0			25.2	0	74.1	WATER	
9989.5	124.0			19.7	0	88.1	WATER	
9990.5	394.0			25.3	0	78.2	WATER	
9991.5	259.0			24.5	0	77.8	WATER	
9992.5	371.0			27.7	0	80.3	WATER	
9993.5	122.0			20.1	0	71.7	WATER	
9994.5	314.0			24.0	0	82.9	WATER	
9995.5	374.0			23.8	0	79.4	WATER	
9996.5	404.0			22.7	0	87.5	WATER	
9997.5	116.0			19.0	0	81.0	WATER	
9998.5	260.0			25.6	0	72.4	WATER	
9999.5	318.0			23.0	0	84.9	WATER	
10000.5	201.0			21.4	0	93.0	WATER	
10001.5	896.0			24.4	0	72.6	WATER	
10002.5	637.0			24.9	0	81.9	WATER	
10003.5	366.0			24.1	0	76.4	WATER	
10004.5	659.0			27.2	0	77.5	WATER	
10006.5	541.0			23.8	0	83.4	WATER	
10007.5	651.0			26.2	0	71.5	WATER	
10008.5	642.0			24.7	0	82.1	WATER	
10009.5	799.0			25.8	0	75.4	WATER	
10010.5	584.0			26.2	0	72.4	WATER	
10011.5	581.0			23.8	0	77.7	WATER	
10012.5	361.0			22.8	0	89.6	WATER	
10013.5	908.0			26.3	0	72.9	WATER	
10014.5	868.0			26.2	0	73.3	WATER	
10015.5	1056.0			27.1	0	75.5	WATER	
10016.5	924.0			26.1	0	81.5	WATER	
10017.5	1152.0			25.1	0	82.7	WATER	
10018.5	857.0			26.8	0	79.7	WATER	
10019.5	126.0			24.9	0	69.7	WATER	
10020.5	594.0			26.9	0	74.6	WATER	
10021.5	701.0			23.4	0	71.7	WATER	
10022.5	773.0			28.3	0	76.7	WATER	
10023.5	748.0			27.4	0	76.5	WATER	
10024.5	170.0			26.8	0	76.5	WATER	
10026.5	353.0			20.8	0	89.3	WATER	
10027.5	202.0			25.1	0	77.8	WATER	
10028.5	206.0			26.7	0	67.7	WATER	
10035.5	0			6.9	0	39.1	NIL	
10036.5	0			4.7	0	85.8	NIL	
10037.5	1.4			15.4	0	64.7	LOW PERM	
10038.5	41.0			17.1	0	54.3	WATER	
10039.5	62.7			23.9	0	67.7	WATER	

Location Sample Service, Inc.

JACKSON, MISSISSIPPI

CORE RECORD

010360

UNIT JACKSON LAB
 DATE 2-9-79
 FROM 9985 TO 100
 CUT 60 FT
 RECOVERED 59 1/2
 ANALYZED 51 FT

COMPANY DUPONT

WELL DISPOSAL WELL NO.2

LOCATION HARRISON COUNTY, MISS.

FORMATION NAME TUSCALOOSA

Core No.	DEPTH	Min/Ft.	DESCRIPTION OF RECOVERY
			CORE NO. 5 9985-10045
			CUT: 60 FT.
			REC: 59 1/2 FT.
			9985-10029 44 FT. SAND, TAN, MG WELL SORTED, FAIR/GOOD P&P, SLI GLAUC, OCC THIN MICA PARTINGS, SOME HEAVY MINERAL GRAINS VISIBLE, NO APPARENT SHOW
			10029-10035 6 FT SHALE, MED/DK GRAY, SLI, MOTTLED, SILTY, MICA
			10035-10037 2 FT. LIMESTONE, LT/DK GRAY, DNS ARGILL FOSS, SANDY WITH ABUNDANT GREENISH GRAY CLAY NODULES, OCC TWISTED MICA PARTINGS, PARTLY CARB, V TITE, NO SHOW
			10037-10039 2 FT. SAND, LT GRAY, VFG/FG, ABUNDANT MICA PARTINGS, TITE, SOME SHALE LAMINATIONS, NO SHOW
			10039-10042 3 FT. SAND, GREENISH GRAY, FG/MG, CLEANER THAN ABOVE WITH FNLY DISS GLAUC, POOR-FAIR P&P, NO SHOW
			10042-10044 2 1/2 FT. SHALE, MED/DK GRAY, MOTTLED, SILTY, FIRM PARTLY RINGTAILED MICA

Appendix 2-30

Omni Laboratories, Inc. Petrographic Study Final Report

Well No. 2 Sidetrack #1 (1996)

**-FINAL REPORT-
PETROGRAPHIC STUDY
FOR
DUPONT ENVIRONMENTAL
DELISLE NO. 2, S/T NO. 1 WELL
DUPONT DELISLE PLANT
HARRISON COUNTY, MISSISSIPPI**

March 22, 1996

Mr. Phillip Papadeas
DuPont Environmental Remediation Services
140 Cypress Station, Suite 240
Houston, Texas 77090

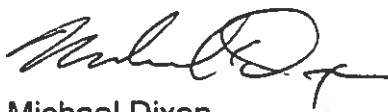
SUBJECT: Final Report - Petrographic Study
Delisle No. 2, S/T No. 1
Dupont Delisle Plant
Harrison County, Mississippi
File No. GN-3402

Dear Mr. Papadeas,

Twenty-seven (27) rotary (drilled) sidewall core samples from the above referenced well were submitted for X-ray diffraction (XRD) analysis. Nineteen (19) of these samples were analyzed by thin section petrography, and sixteen (16) were analyzed by scanning electron microscopy (SEM). This final report includes all data, interpretations, and photomicrographs associated with these analyses. Eight (8) copies of this report are provided.

It has been a pleasure to provide this study for DuPont Environmental Remediation Services. Please feel free to contact us if you have any questions concerning this report or if we can be of further service.

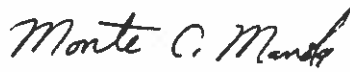
Sincerely,
OMNI LABORATORIES, INC.



Michael Dixon
Manager, Geologic Services



Raymond Bruce
Geologist



Monte C. Manske
Senior Geologist

SUMMARY OF RESULTS

Twenty-seven rotary sidewall core samples from the referenced well were submitted for petrographic analysis, which includes X-ray diffraction (XRD), thin section petrography, and scanning electron microscopy (SEM). Based on these results, the samples display a range of porosity development from poor (9796', 9852', and 9896'), to moderate (9921'), to good (remaining samples).

The samples with good porosity development are massive, poor to well sorted, fine- to medium-grained sandstones. These sands are typically quite quartzose, providing a chemically stable framework for these sandstones. Primary intergranular porosity (13%-24%) is the dominant porosity type. Porosity is generally open and evenly distributed, but is occasionally blocked by secondary cements. The most common cements are quartz overgrowths, kaolinite, pyrite, siderite, and iron oxides. Low amounts of secondary dissolution porosity (1%-3%) augment the primary pores and were formed by the partial to complete leaching of relatively unstable framework grains, such as feldspars and lithic fragments. The upper sandstones (especially from 9802' to 9843') also contain a titanium-rich material with minor iron which partially fills and encrusts some pores. This material is often found associated with authigenic clays, and is one of the last components to precipitate in the pore system of these sandstones. The composition of this titanium material was characterized by the X-ray Energy Dispersive Spectrometer (EDS) detector attached to the SEM. This detector can qualitatively identify elements with an atomic number of 11 (sodium) to 92 (uranium). Another constituent found during thin section point count is an iron-rich component observed "flowing" into some pores and partially filling them. This iron-rich component is found primarily in the lower samples, especially from 9902' to 9990'. Halite is found in some samples in trace amounts (by weight from XRD) and is believed to be a precipitate from the formation brine associated with these zones.

The samples with poor to fair porosity development (9796', 9852', 9896', and 9921), are shaly to very shaly and should act as significant barriers to vertical permeability. The shale is clay-rich as can be seen on XRD analysis (6%-49%), and is composed of a variety of clay types.

Petrographic and core analysis results are summarized in Table 1 shown below.

TABLE 1
SUMMARY OF PETROGRAPHY AND CORE ANALYSIS RESULTS

Sample Depth	Core Perm. (md)	Core Porosity (%)	Avg. Grain Size (mm)	Fabric	Matrix (%)	Cement (%)	Reservoir Quality
9473.0	650.0	24.5	0.23	Massive	2	3	Good
9505.0	498.0	24.0	0.22	Massive	3	3	Good
9562.0	1488.0	25.1	0.32	Massive	2	5	Good
9796.0	<0.01	3.9	0.14	Massive	1	16	Poor
9800.0	462.0	23.4	0.39	Massive	0	8	Good
9802.0	682.0	24.1	0.31	Massive	2	9	Good
9810.0	460.0	12.9	0.43	Massive	1	20	Good
9820.0	1133.0	21.4	0.40	Massive	Tr	15	Good
9843.0	230.0	18.1	0.33	Massive	Tr	23	Good
9850.0	264.0	24.1	0.44	Massive	8	7	Good
9852.0	*	*	0.13	Massive	57	1	Poor
9896.0	0.02	4.1	0.07	Laminated	39	4	Poor
9902.0	222.0	21.3	0.24	Massive	2	4	Good
9921.0	1.90	12.7	0.16	Laminated	8	6	Moderate
9928.0	274.0	24.0	0.28	Massive	4	8	Good
9934.0	*	21.9	0.33	Massive	3	11	Good
9962.0	449.0	23.0	0.27	Massive	2	7	Good
9970.0	324.0	23.5	0.29	Massive	1	10	Good
9990.0	466.0	20.9	0.22	Massive	1	9	Good

* No data available

INTRODUCTION

X-ray diffraction (XRD) analysis, thin section petrography, and scanning electron microscopy (SEM) were performed on core samples from the referenced well (see Appendices B through D, respectively). Table 1 below outlines the sample depths and the analyses performed.

TABLE 1
SAMPLE DEPTHS AND ANALYSES PERFORMED

<u>SAMPLE DEPTH</u> <u>(feet)</u>	<u>THIN SECTION</u> <u>PETROGRAPHY</u>	<u>SEM</u>	<u>XRD</u>
9473	X	X	X
9505	X	X	X
9562	X	X	X
9755			X
9794			X
9796	X	X	X
9800	X	X	X
9802	X	X	X
9810	X	X	X
9820	X	X	X
9832			X
9843	X	X	X
9850	X		X
9852	X	X	X
9858			X
9896	X	X	X
9902	X	X	X
9912			X
9921	X	X	X
9928	X		X
9934	X	X	X
9947			X
9962	X		X
9970	X	X	X
9975			X
9990	X	X	X
10012			X

The objectives of these analyses were to: 1) characterize the texture and mineralogy; 2) examine porosity development and determine controls on porosity and permeability; and 3) identify any materials introduced into the formation, if present.

PETROGRAPHIC RESULTS

The following sections briefly characterize the sand intervals with respect to sedimentary texture, composition, porosity development, and the effects of mineralogy on log response. Specific information on individual samples is included in the Appendices.

Sedimentary Texture

The nineteen samples examined by thin section (see Appendix C) are medium-grained (eleven samples), fine-grained (six samples), and very fine-grained (one sample) sandstones. The sample at 9852' is described as a mudstone (shale). The average grain size ranges from 0.07 mm (9896') to 0.51 mm (9850'). Most samples are generally massive, and poor to well sorted, depending on the grain size distribution and amount of fine matrix material present. The samples at 9896' and 9921' contain common shale laminations. Slight bioturbation is observed in the sample at 9896'. Bioturbation refers to the reworking of sediment by organisms shortly after deposition. The framework grains in each sample analyzed range from subangular to subrounded, with subangular grains being most common. Compositionally, the sandstones are classified as feldspathic litharenites and sublitharenites, based on the classification scheme of Folk, 1980.

Framework Grains

Monocrystalline quartz (32%-59%) is the dominant framework grain in the sandstones analyzed in thin section (Appendix C). Other common framework constituents include polycrystalline quartz (4%-11%), plagioclase feldspar (trace-5%), potassium (K-) feldspar (trace-3%), and various lithic fragments (2%-13% total lithics). The most common lithic types are volcanic (2%-11%) and metamorphic rock fragments (0%-5%). Minor constituents present in these samples include organic material, glauconite, calcareous fossil fragments, muscovite, biotite, tourmaline, and zircon. The presence of glauconite indicates marine depositional influence.

Secondary Constituents

The nineteen samples analyzed by thin section (Appendix C) have associated secondary constituents. The secondary constituents found are quartz overgrowths (trace-8%), kaolinite (0%-1%), calcite (trace-10%), and dolomite (0%-1%). Minor cementing agents in these samples include pyrite (0%-1%), siderite (0%-2%), and iron oxides (0%-trace). Pyrite occurs as scattered framboidal forms, microcrystalline aggregates, and as a grain replacement. The clays are discussed further in the

following section on "Clay Mineralogy". Siderite is found as scattered patches of pore-filling microcrystals. Iron oxides are typically found as grain-coatings.

Two components appear to have been introduced into the formation, having precipitated directly within the pore system or on adjacent mineral surfaces. A titanium-dominant material with minor iron is seen partially filling and encrusting the pores of some samples. The titanium-dominant material is found primarily in the shallower samples, especially from 9802' to 9843'. This material is found associated with authigenic clays, as well as other fines and micropores found within these rocks. The composition of this material was characterized by the X-ray Energy Dispersive Spectrometer (EDS) detector attached to the SEM. This detector can qualitatively identify elements with an atomic number of 11 (sodium) to 92 (uranium). Lesser amounts of iron and in some cases chlorine, are detected in the titanium-rich material. Another constituent found during thin section point count is an iron-rich component observed "flowing" into some pores and partially filling them. This iron-rich component is found primarily in the lower samples, especially from 9902' to 9990'. Halite is found in some samples in trace amounts (by weight from XRD) and is believed to be a precipitate from the formation brine associated with these zones.

Clay Mineralogy

X-ray diffraction (XRD) analyses (Appendix B) of twenty-seven total samples reveal that the total clay content ranges from 1% (several samples) to 57% (9755'), and averages 8%. Mixed-layer illite/smectite (0%-19%), illite (trace-20%), chlorite (trace-18%), and kaolinite (0%-15%) are the clay types present.

Scanning electron microscope (SEM) analyses (Appendix D) of sixteen samples show that the clays present vary with each sample and no one clay is dominant overall. These clays have three modes of occurrence 1) as a patchy pore-filling matrix; 2) as an authigenic grain-coating constituent; and 3) in association with lithic fragments. The patchy clay matrix in these samples has an erratic distribution. Some of this matrix may actually be "pseudomatrix" derived from the insitu breakdown of selective lithic fragments. Authigenic kaolinite commonly occurs as aggregates of stacked platelets, or booklets, with erratically fill-selective pores. Authigenic chlorite is also observed in many of the samples analyzed, and occurs as face-to-edge platelets along pore walls and grain surfaces. Authigenic illite/smectite is also a fairly common grain-coating, but these coatings are thin and discontinuous. Other clay types are variable in abundance, depositional in origin, and occur as minor constituents of the matrix and lithic fragments. Illite and kaolinite also occur as alteration products of feldspars.

Mineralogic Influences on Log Response

The following section discusses the effects on log response of the mineralogy and associated porosity types found in these samples.

1. Resistivity Logs: The main components which may cause low resistivity in these intervals are dispersed clay and shale laminations. Sands containing a relative abundance of these clay types may exhibit suppressed resistivity due to associated bound, or irreducible water.

2. Density Logs: The sandstones examined contain generally low amounts of high density minerals such as carbonate minerals and pyrite, except at 9794', 9858', and 9947', which are carbonate-rich. Appropriate density values should be used in intervals which contain minerals with anomalously high or low density.

3. Gamma-Ray Log: Gamma-ray logs respond to radioactive isotopes. The clay minerals chlorite (trace-18% by weight from XRD) and kaolinite (0%-15% by weight from XRD) will not be detected by gamma-ray logs due to the absence of potassium in these minerals. Conversely, the mineral K-feldspar (0%-6% by weight from XRD) will be detected as "clay" by gamma-ray logs due to the presence of potassium in this mineral.

APPENDIX A

PETROGRAPHIC ANALYTICAL PROCEDURES

X-ray Diffraction (XRD) Analysis

A representative portion of each sample was dried, extracted if necessary, and then ground in a Brinkman MM-2 Retsch Mill to a fine powder. This ground sample was next loaded into an aluminum sample holder. This "bulk" sample mount was scanned with a Philips X-ray diffractometer using nickel-filtered copper K-alpha radiation at standard scanning parameters. Computer analysis of the diffractograms provide qualitative identification of mineral phases and semiquantitative analysis of the relative abundance (in weight percent) of the various mineral phases. It should also be noted that X-ray diffraction **does not** allow the detection and identification of non-crystalline (amorphous) material, such as organic material.

An oriented clay fraction mount was also prepared for each sample from the ground powder. The samples were further size fractionated by centrifuge to separate the <4 micron fraction. Ultrasonic treatment was used to suspend the material, then a dispersant was used to prevent flocculation when noted. The solution containing the clay fraction was then passed through a Fisher filter membrane apparatus allowing the solids to be collected on a cellulose membrane filter. These solids were then mounted on a glass slide, dried, and scanned with the Philips diffractometer. The oriented clay mount was then glycolated and another diffractogram prepared to identify the expandable, water sensitive minerals. When necessary, the patterns were deconvoluted, or the samples heat treated, to aid in distinguishing kaolinite and chlorite.

Scanning Electron Microscopy (SEM) Analysis

Samples selected for scanning electron microscopy analysis were first broken, or split, to expose fresh surfaces. The samples were then mounted on sample holders with a conductive carbon paste and coated with gold in a "cool" sputter coater to prevent heat damage to sensitive clay minerals or friable samples. The samples were analyzed with a Model SX-40 International Scientific Instruments (ISI) Scanning Electron Microscope and PGT Energy Dispersive Spectrometer (EDS).

Thin Section Petrographic Analysis

Samples selected for thin section analysis were prepared by first vacuum impregnating with blue-dyed epoxy. The samples were then mounted on an optical glass slide and cut and lapped in water to a thickness of 0.03 mm. The prepared sections were then covered with index oil and temporary cover slips, and then analyzed using standard petrographic techniques.

APPENDIX B

X-RAY DIFFRACTION DATA

OMNI LABORATORIES, INC.
X-RAY DIFFRACTION
(WEIGHT %)

Client: DUPONT ENVIRONMENTAL
Well: DELISLE NO. 2, S/T NO. 1 WELL (HARRISON CO., MISSISSIPPI)

File No: N-3402
Date: 12/7/95

Sample Depth	CLAYS				CARBONATES				OTHER MINERALS							TOTALS		
	Chlorite	Kaolinite	Illite	Ill./Smec.	Calcite	Dolomite*	Siderite	Quartz	Flag.	K-Spar	Halite	Fe Oxide**	Pyrite	Clays	Carb.	Other		
9473'	1	TR	TR	0	TR	0	0	94	4	1	TR	0	0	1	TR	99		
9505'	2	TR	2	0	0	TR	0	93	1	1	1	0	TR	4	TR	96		
9562'	2	TR	TR	TR	1	0	0	96	1	TR	TR	0	0	2	1	97		
9755'	9	15	20	13	1	0	2	35	3	1	0	0	1	57	3	40		
9794'	1	2	2	TR	1	27	0	58	6	1	0	0	2	5	28	67		
9796'	TR	3	3	TR	7	0	0	79	6	2	0	0	TR	6	7	87		
9800'	6	2	4	TR	0	0	0	82	2	4	0	0	0	12	0	88		
9802'	1	0	1	TR	TR	0	0	97	1	TR	0	TR	0	2	TR	98		
9810'	2	0	1	0	0	0	0	95	2	TR	0	TR	0	3	0	97		
9820'	1	0	TR	TR	0	0	0	98	1	TR	TR	0	0	1	0	99		
9832'	1	TR	2	TR	0	0	0	95	1	0	1	0	TR	3	0	97		
9843'	TR	TR	1	0	0	0	0	99	TR	TR	TR	TR	0	1	0	99		
9850'	1	0	TR	TR	TR	0	0	98	TR	0	0	TR	1	1	TR	99		
9852'	9	7	14	19	1	TR	0	48	2	TR	0	0	TR	49	1	50		
9858'	3	2	2	TR	26	0	0	58	6	3	0	0	0	7	26	67		
9896'	18	0	11	0	TR	TR	1	55	12	2	0	0	1	29	1	70		
9902'	1	TR	1	1	TR	0	0	86	8	3	0	0	0	3	TR	97		
9912'	TR	1	1	0	0	0	0	93	5	TR	0	TR	TR	2	0	98		
9921'	1	4	1	TR	0	1	2	74	11	6	TR	0	0	6	3	91		
9928'	TR	TR	1	0	TR	TR	0	99	TR	TR	TR	TR	0	1	TR	99		
9934'	4	0	3	TR	0	0	0	93	TR	TR	0	0	0	7	0	93		
9947'	2	0	1	0	65	0	0	27	4	1	0	TR	0	3	65	32		
9962'	TR	2	2	0	0	0	1	84	8	3	TR	0	0	4	1	95		
9970'	2	TR	1	TR	0	1	0	90	5	1	TR	TR	0	3	1	96		
9975'	TR	1	1	0	0	0	TR	93	4	1	TR	TR	0	2	TR	98		
9990'	TR	2	1	0	0	0	5	84	7	1	0	TR	0	3	5	92		
10012'	2	0	TR	0	0	0	5	88	4	1	0	0	TR	2	5	93		
AVERAGE	2	2	3	1	4	1	1	81	4	1	TR	TR	TR	8	6	86		

*Some may be an iron rich variety (ankerite).

**XRD methods cannot quantify amorphous components; limonite (a common Fe oxide) was detected in this section in greater abundance than indicated here.

APPENDIX C

**THIN SECTION ANALYSES
AND
THIN SECTION PHOTOMICROGRAPHS**

THIN SECTION MODAL ANALYSIS

Dupont Environmental
 Delisle No. 2, S/T No. 1
 Dupont Delisle Plant
 Harrison County, Mississippi

DEPTH	9473'	9505'	9562'	9796'
Grain Size Avg. (mm):	0.23	0.22	0.32	0.14
Grain Size Range (mm):	0.07-0.44	0.09-0.40	0.12-0.60	0.04-0.26
Sorting:	Moderately well	Moderately well	Well	Moderate
Rock Name (Folk):	Sublitharenite	Sublitharenite	Sublitharenite	Sublitharenite
FRAMEWORK GRAINS				
<i>Quartz</i>	<u>55</u>	<u>59</u>	<u>60</u>	<u>64</u>
Monocrystalline	48	51	53	59
Polycrystalline	7	8	7	5
<i>Feldspar</i>	<u>6</u>	<u>3</u>	<u>2</u>	<u>3</u>
K-Feldspar	2	1	1	2
Plagioclase	4	2	1	1
<i>Lithic Fragments</i>	<u>10</u>	<u>7</u>	<u>7</u>	<u>11</u>
Plutonic	0	0	0	0
Volcanic	8	4	6	9
Metamorphic	2	3	1	2
Chert	0	0	tr	0
Mudstone	0	0	0	0
ACCESSORY GRAINS				
Muscovite	tr	tr	tr	1
Biotite	0	0	0	0
Heavy Minerals*	tr	tr	0	0
ENVIRON. INDICATORS				
Plant Fragments	tr	0	0	0
Glaucinite	0	0	0	0
Fossil Fragments	0	tr	0	0
CLAY MATRIX				
	<u>2</u>	<u>3</u>	<u>2</u>	<u>1</u>
AUTHIGENIC CEMENT				
	<u>3</u>	<u>3</u>	<u>5</u>	<u>16</u>
Pore-lining clay	0	0	0	0
Kaolinite	tr	tr	tr	1
Quartz overgrowths	2	2	3	5
Calcite	0	0	0	10
Dolomite	1	1	tr	0
Ankerite	0	0	0	0
Siderite	0	0	0	0
Pyrite	tr	tr	0	tr
Fe/Ti Oxides	0	0	0	0
Iron Component	0	0	0	0
Halite	0	tr	0	0
Titanium Component	0	0	2	0
POROSITY				
	<u>24</u>	<u>25</u>	<u>24</u>	<u>4</u>
Primary	23	24	23	3
Secondary	1	1	1	1
Microscopic	0	0	0	tr
TOTALS:	100	100	100	100

* Tourmaline, zircon

THIN SECTION MODAL ANALYSIS

Dupont Environmental
 Delisle No. 2, S/T No. 1
 Dupont Delisle Plant
 Harrison County, Mississippi

DEPTH	9800'	9802'	9810'	9820'
Grain Size Avg. (mm):	0.39	0.31	0.43	0.40
Grain Size Range (mm):	0.16-0.65	0.08-0.75	0.16-0.84	0.10-0.88
Sorting:	Moderately Well	Moderately Well	Moderately Well	Moderately Well
Rock Name (Folk):	Feld. Litharenite	Sublitharenite	Sublitharenite	Sublitharenite
FRAMEWORK GRAINS				
<i>Quartz:</i>	<u>51</u>	<u>53</u>	<u>52</u>	<u>52</u>
Monocrystalline	45	46	44	44
Polycrystalline	6	7	8	8
<i>Feldspar</i>	<u>5</u>	<u>4</u>	<u>2</u>	<u>3</u>
K-Feldspar	3	3	1	2
Plagioclase	2	1	1	1
<i>Lithic Fragments</i>	<u>13</u>	<u>10</u>	<u>8</u>	<u>13</u>
Plutonic	0	0	0	0
Volcanic	9	8	5	11
Metamorphic	4	2	3	2
Chert	0	0	0	0
Mudstone	0	0	0	0
ACCESSORY GRAINS	<u>1</u>	<u>tr</u>	<u>2</u>	<u>tr</u>
Muscovite	1	tr	2	tr
Biotite	0	0	0	0
Heavy Minerals*	0	tr	0	0
ENVIRON. INDICATORS	<u>0</u>	<u>0</u>	<u>0</u>	<u>0</u>
Plant Fragments	0	0	0	0
Glaucanite	0	0	0	0
Fossil Fragments	0	0	0	0
CLAY MATRIX	<u>0</u>	<u>2</u>	<u>1</u>	<u>tr</u>
AUTHIGENIC CEMENT	<u>8</u>	<u>2</u>	<u>20</u>	<u>15</u>
Pore-lining clay	0	0	0	0
Kaolinite	1	0	0	0
Quartz overgrowths	7	6	8	6
Calcite	0	0	0	0
Dolomite	0	0	0	0
Ankerite	0	0	0	0
Siderite	0	0	0	tr
Pyrite	0	0	0	0
Fe/Ti Oxides	0	tr	0	tr
Iron Component	0	0	0	0
Halite	0	0	0	0
Titanium Component	tr	3	12	9
POROSITY	<u>22</u>	<u>22</u>	<u>15</u>	<u>17</u>
Primary	20	20	14	16
Secondary	2	2	1	1
Microscopic	tr	0	0	0
TOTALS:	<u>100</u>	<u>100</u>	<u>100</u>	<u>100</u>

* Tourmaline, zircon

THIN SECTION MODAL ANALYSIS

Dupont Environmental
 Delisle No. 2, S/T No. 1
 Dupont Delisle Plant
 Harrison County, Mississippi

DEPTH	9843'	9850'	9852'	9896'
Grain Size Avg. (mm):	0.33	0.44	0.13	0.07
Grain Size Range (mm):	0.06-0.58	<0.01-0.89	<0.01-0.52	<0.01-0.26
Sorting:	Moderately Well	Poor	Poor	Moderately Poor
Rock Name (Folk):	Sublitharenite	Sublitharenite	Mudstone	Feld. Litharenite
FRAMEWORK GRAINS				
<i>Quartz</i>	<u>50</u>	<u>51</u>	<u>36</u>	<u>36</u>
Monocrystalline	45	42	29	32
Polycrystalline	5	9	7	4
<i>Feldspar</i>	<u>3</u>	<u>3</u>	<u>1</u>	<u>6</u>
K-Feldspar	2	3	tr	1
Plagioclase	1	tr	1	5
<i>Lithic Fragments</i>	<u>9</u>	<u>11</u>	<u>2</u>	<u>10</u>
Plutonic	0	0	0	0
Volcanic	8	8	2	8
Metamorphic	1	3	0	2
Chert	0	0	0	0
Mudstone	0	0	0	tr
ACCESSORY GRAINS				
	<u>tr</u>	<u>tr</u>	<u>tr</u>	<u>tr</u>
Muscovite	tr	tr	0	tr
Biotite	tr	tr	tr	tr
Heavy Minerals*	tr	0	0	0
ENVIRON. INDICATORS				
	<u>0</u>	<u>1</u>	<u>1</u>	<u>2</u>
Plant Fragments	0	1	1	2
Glauconite	0	0	0	0
Fossil Fragments	0	tr	tr	0
CLAY MATRIX				
	<u>tr</u>	<u>8</u>	<u>57</u>	<u>39</u>
AUTHIGENIC CEMENT				
	<u>23</u>	<u>7</u>	<u>1</u>	<u>4</u>
Pore-lining clay	0	0	0	0
Kaolinite	0	1	0	0
Quartz overgrowths	7	6	tr	2
Calcite	0	0	0	0
Dolomite	tr	0	0	0
Ankerite	0	0	0	0
Siderite	0	0	tr	1
Pyrite	0	tr	1	1
Fe/Ti Oxides	0	tr	0	0
Iron Component	0	0	0	0
Halite	0	0	0	0
Titanium Component	16	tr	0	0
POROSITY				
	<u>15</u>	<u>19</u>	<u>2</u>	<u>3</u>
Primary	13	18	0	1
Secondary	2	1	0	0
Microscopic	0	tr	2	2
TOTALS:	100	100	100	100

* Tourmaline, zircon

THIN SECTION MODAL ANALYSIS

Dupont Environmental
 Delisle No. 2, S/T No. 1
 Dupont Delisle Plant
 Harrison County, Mississippi

DEPTH	9902'	9921'	9928'	9934'
Grain Size Avg. (mm):	0.24	0.16	0.28	0.33
Grain Size Range (mm):	0.07-0.48	<0.01-0.38	0.13-0.59	0.07-0.52
Sorting:	Moderate	Moderate	Moderately Well	Moderate
Rock Name (Folk):	Feld. Litharenite	Sublitharenite	Sublitharenite	Sublitharenite
FRAMEWORK GRAINS				
<i>Quartz</i>	<u>53</u>	<u>57</u>	<u>53</u>	<u>57</u>
Monocrystalline	45	52	42	48
Polycrystalline	8	5	11	9
<i>Feldspar</i>	<u>7</u>	<u>7</u>	<u>1</u>	<u>1</u>
K-Feldspar	2	2	tr	tr
Plagioclase	5	5	1	1
<i>Lithic Fragments</i>	<u>13</u>	<u>8</u>	<u>9</u>	<u>9</u>
Plutonic	0	0	0	0
Volcanic	8	6	6	7
Metamorphic	5	2	3	2
Chert	0	0	0	0
Mudstone	0	0	0	0
ACCESSORY GRAINS	<u>2</u>	<u>2</u>	<u>1</u>	<u>tr</u>
Muscovite	2	2	1	tr
Biotite	tr	tr	tr	tr
Heavy Minerals*	tr	tr	tr	tr
ENVIRON. INDICATORS	<u>1</u>	<u>tr</u>	<u>tr</u>	<u>tr</u>
Plant Fragments	1	tr	tr	tr
Glauconite	0	tr	0	0
Fossil Fragments	0	tr	0	tr
CLAY MATRIX	<u>2</u>	<u>8</u>	<u>4</u>	<u>3</u>
AUTHIGENIC CEMENT	<u>4</u>	<u>6</u>	<u>8</u>	<u>11</u>
Pore-lining clay	0	0	0	0
Kaolinite	tr	tr	0	0
Quartz overgrowths	4	4	8	6
Calcite	0	tr	0	0
Dolomite	0	tr	tr	tr
Ankerite	0	tr	0	0
Siderite	0	1	tr	0
Pyrite	tr	tr	tr	tr
Fe/Ti Oxides	0	0	tr	tr
Iron Component	tr	1	tr	5
Halite	0	0	0	0
Titanium Component	0	0	0	0
POROSITY	<u>18</u>	<u>12</u>	<u>24</u>	<u>19</u>
Primary	17	11	22	16
Secondary	1	1	2	3
Microscopic	0	tr	0	0
TOTALS:	100	100	100	100

* Tourmaline, zircon

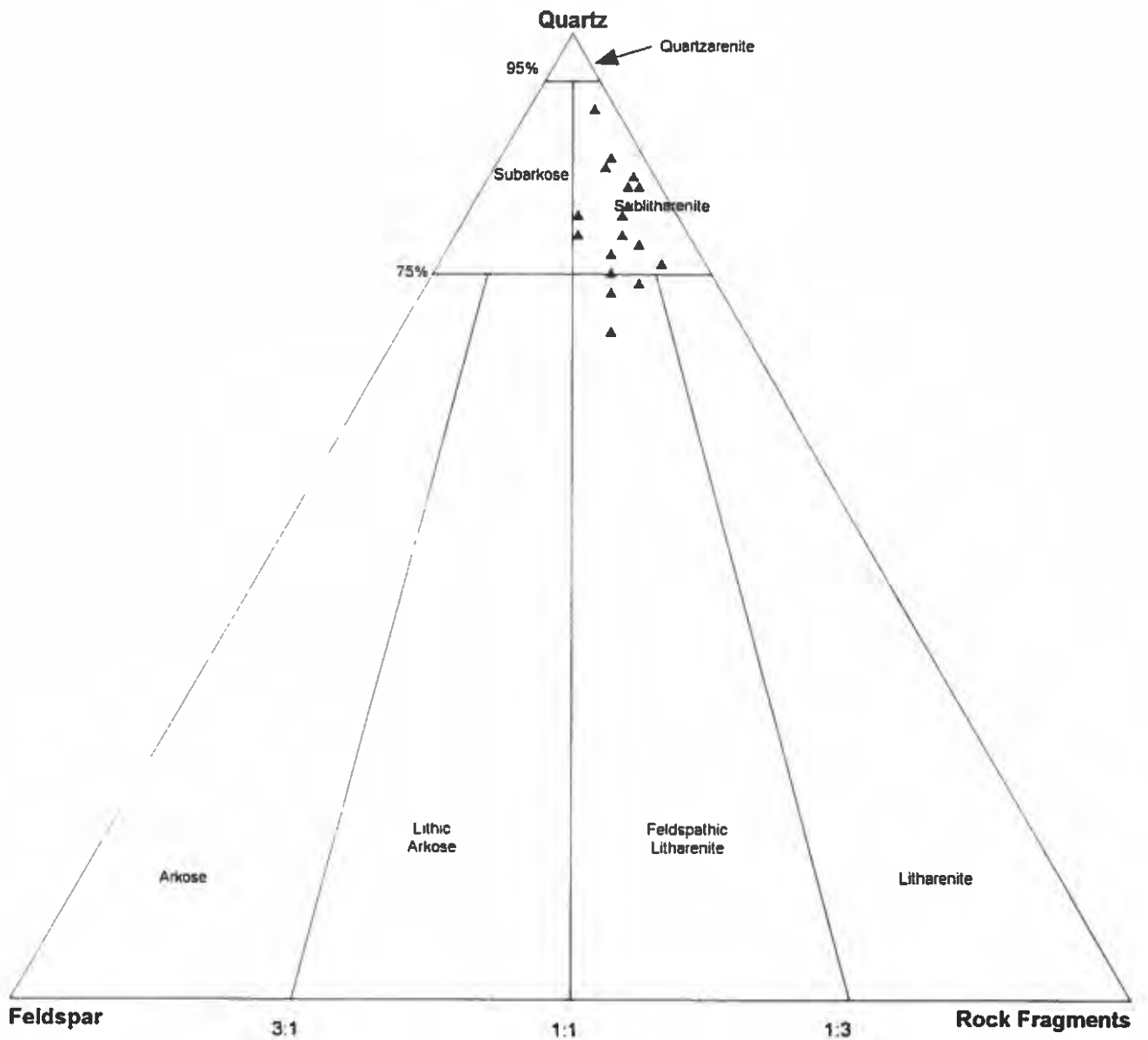
THIN SECTION MODAL ANALYSIS

Dupont Environmental
 Delisle No. 2, S/T No. 1
 Dupont Delisle Plant
 Harrison County, Mississippi

DEPTH	9962'	9970'	9990'	
Grain Size Avg. (mm):	0.27	0.29	0.22	
Grain Size Range (mm):	0.10-0.57	0.08-0.46	0.07-0.45	
Sorting:	Moderately Well	Moderately Well	Moderately Well	
Rock Name (Folk):	Sublitharenite	Sublitharenite	Sublitharenite	
FRAMEWORK GRAINS				
Quartz	<u>51</u>	<u>54</u>	<u>52</u>	
Monocrystalline	45	48	47	
Polycrystalline	6	6	5	
Feldspar	<u>7</u>	<u>6</u>	<u>6</u>	
K-Feldspar	2	2	2	
Plagioclase	5	4	4	
Lithic Fragments	<u>12</u>	<u>7</u>	<u>11</u>	
Plutonic	0	0	0	
Volcanic	10	6	10	
Metamorphic	2	1	1	
Chert	0	0	0	
Mudstone	0	0	0	
ACCESSORY GRAINS	<u>1</u>	<u>tr</u>	<u>tr</u>	
Muscovite	1	tr	tr	
Biotite	tr	0	0	
Heavy Minerals*	tr	tr	tr	
ENVIRON. INDICATORS	<u>0</u>	<u>1</u>	<u>tr</u>	
Plant Fragments	0	1	tr	
Glauconite	tr	0	tr	
Fossil Fragments	0	0	0	
CLAY MATRIX	<u>2</u>	<u>1</u>	<u>1</u>	
AUTHIGENIC CEMENT	<u>7</u>	<u>10</u>	<u>9</u>	
Pore-lining clay	0	0	0	
Kaolinite	tr	1	1	
Quartz overgrowths	7	7	5	
Calcite	0	0	0	
Dolomite	0	tr	tr	
Ankerite	0	0	0	
Siderite	tr	0	2	
Pyrite	tr	tr	tr	
Fe/Ti Oxides	0	0	0	
Iron Component	tr	2	1	
Halite	0	0	0	
Titanium Component	0	0	0	
POROSITY	<u>20</u>	<u>21</u>	<u>21</u>	
Primary	19	20	20	
Secondary	1	1	1	
Microscopic	0	tr	tr	
TOTALS:	<u>100</u>	<u>100</u>	<u>100</u>	

* Tourmaline, zircon

COMPOSITION



Feldspar / Rock Fragment Ratio

**Delisle No. 2, S/T No. 1
Dupont Delisle Plant
Harrison County, Mississippi**

Dupont Environmental
Delisle No. 2, Stk No. 1
Harrison County, Mississippi

File No. GN-3402

SAMPLE DEPTH: 9473 FEET

PLATE 1A

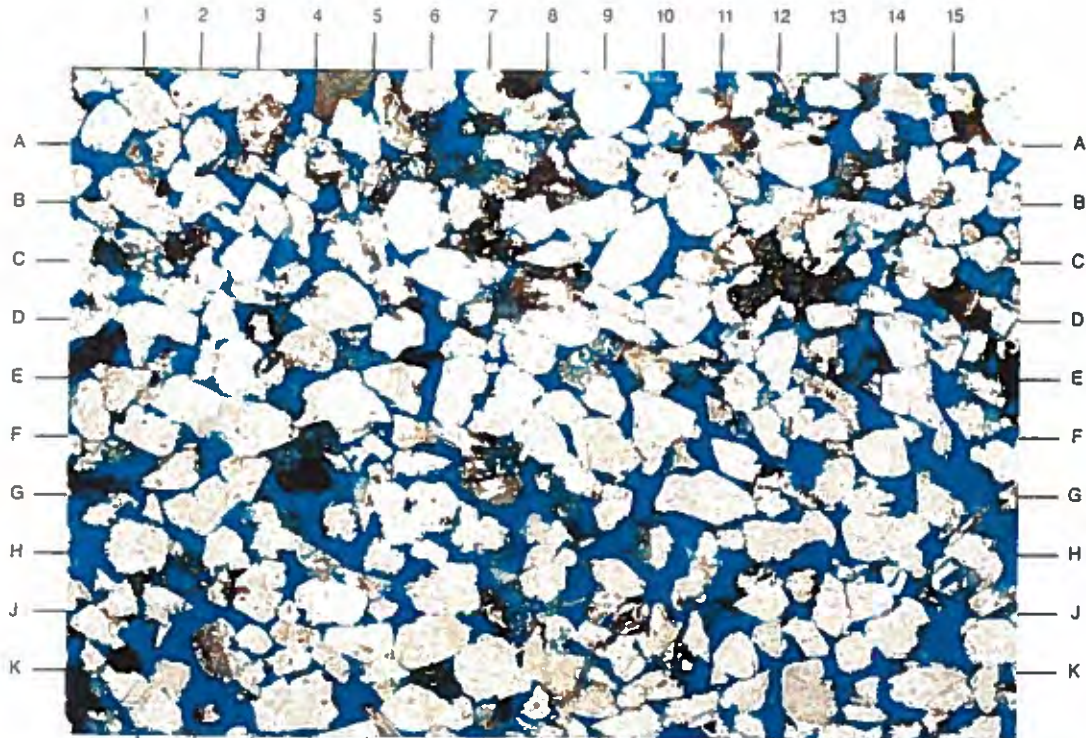
The low magnification survey photomicrograph shows the good reservoir quality in the sandstone taken from 9473'. The sandstone is moderately well sorted and fine-grained with an average grain size of 0.23mm. Intergranular porosity (blue) is abundant and well interconnected. Note the secondary dolomite cement at C-D12.

Magnification: 40X

PLATE 1B

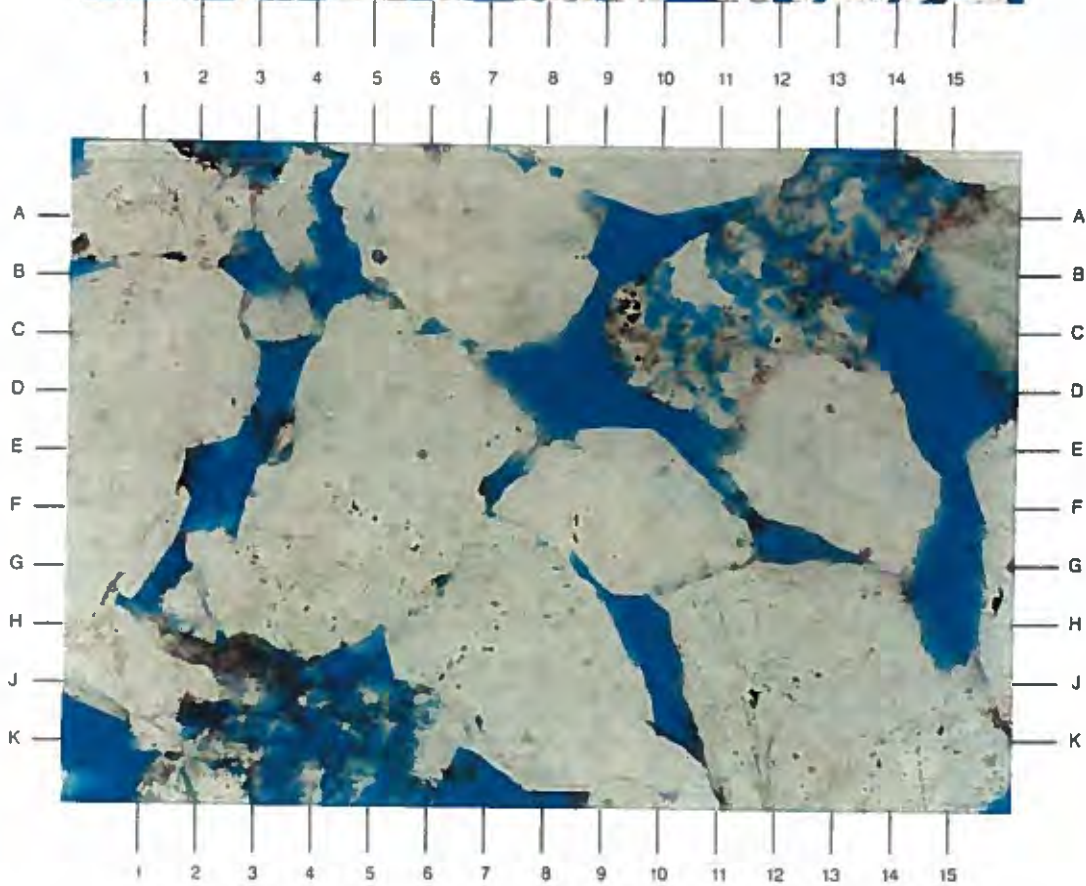
The high magnification view of the area near E8 in Plate 1A depicts the pore types found in the sample. Good intergranular porosity (D8.5,H10,D15) is found between framework grains. Secondary intragranular porosity (A13,C11) is seen in partially dissolved lithic fragments and feldspars.

Magnification: 200X



A

0.25 mm



B

0.05 mm

SAMPLE DEPTH: 9505 FEET

PLATE 2A

The low magnification survey photomicrograph illustrates the abundance of intergranular pores and oversize dissolution pores (blue) found in the sandstone taken from 9505'. The litharenite (Folk, 1980) is moderately well sorted, massive, and fine-grained. Framework grains tend to be subangular. Visible cementation is low, with siderite (E5.5) and dolomite (J9) observed.

Magnification: 40X

PLATE 2B

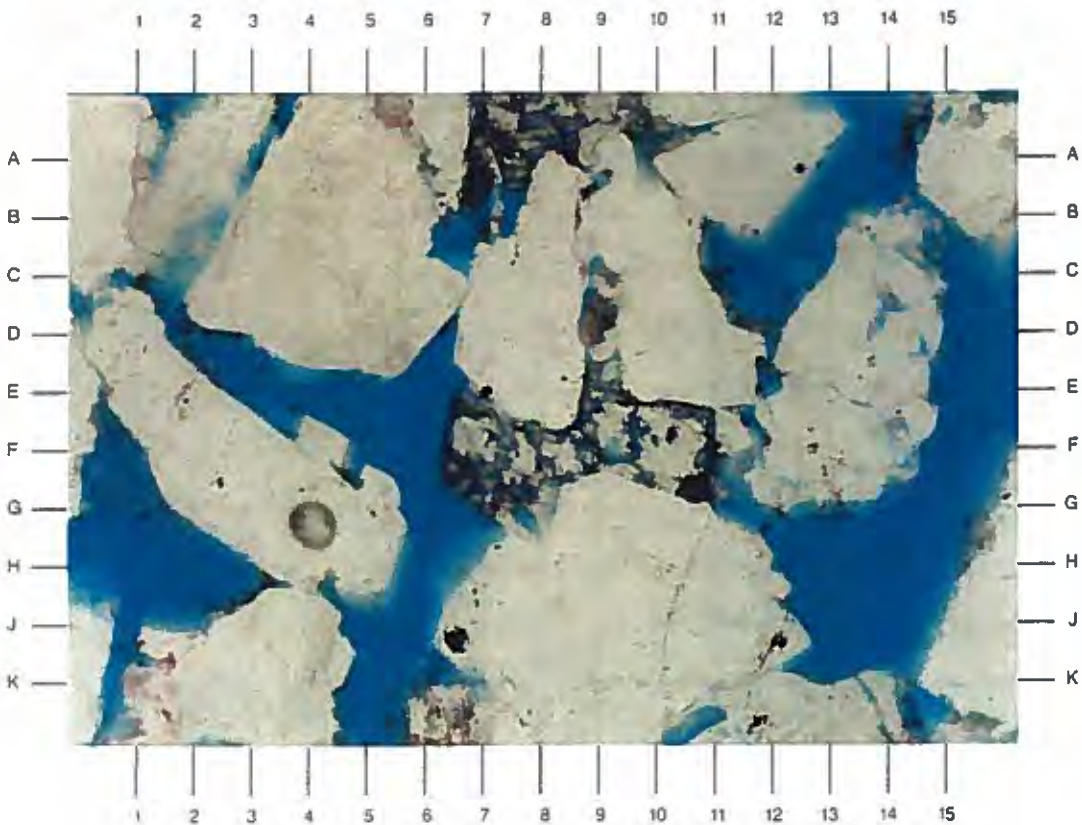
The high magnification view of the area near E8 in Plate 2A documents the subangular nature of the framework grains (B5,J9,D10). Overall cementation is low, and includes quartz overgrowths (C2.5,J12) and dolomite (A8,F8). Note the secondary intragranular porosity at C-D14.

Magnification: 200X



A

0.25 mm



B

0.05 mm

SAMPLE DEPTH: 9562 FEET

PLATE 3A

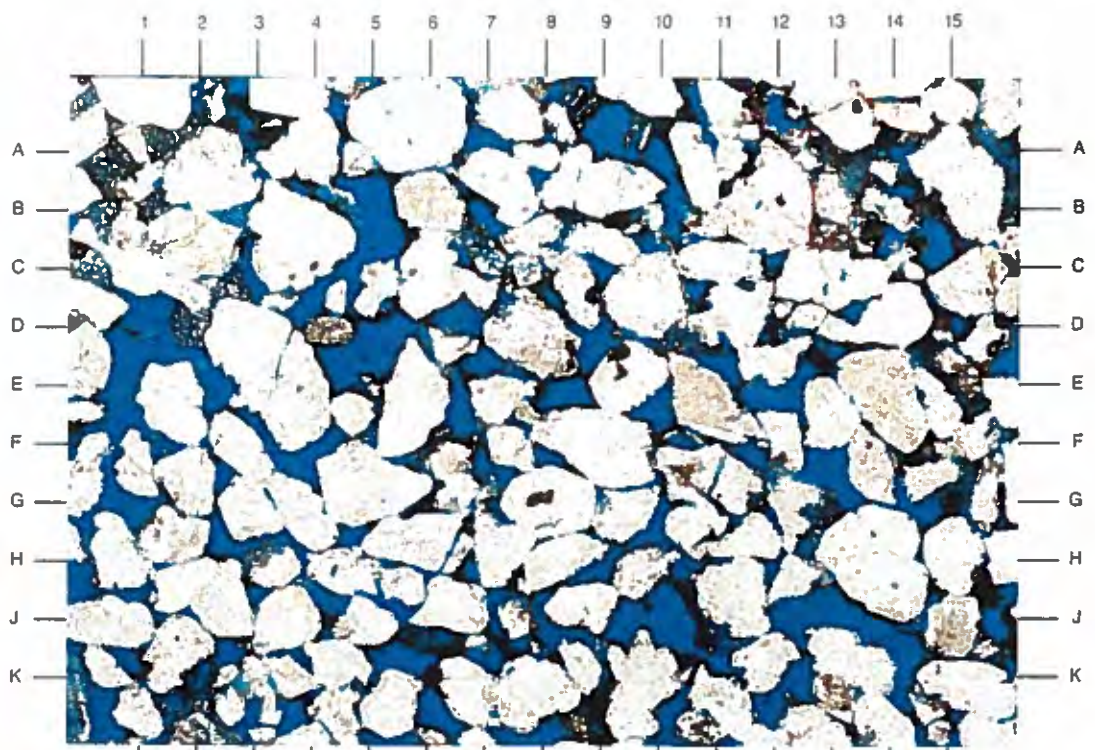
The massive, medium-grained sandstone shown in the low magnification photomicrograph on the facing page is well sorted. Reservoir quality is excellent due to abundant, well interconnected intergranular porosity (blue), which is occasionally enhanced by secondary dissolution (C7.5,C13). Note the random dolomite cement (A1.5,A-B0.5) occluding some pores.

Magnification: 40X

PLATE 3B

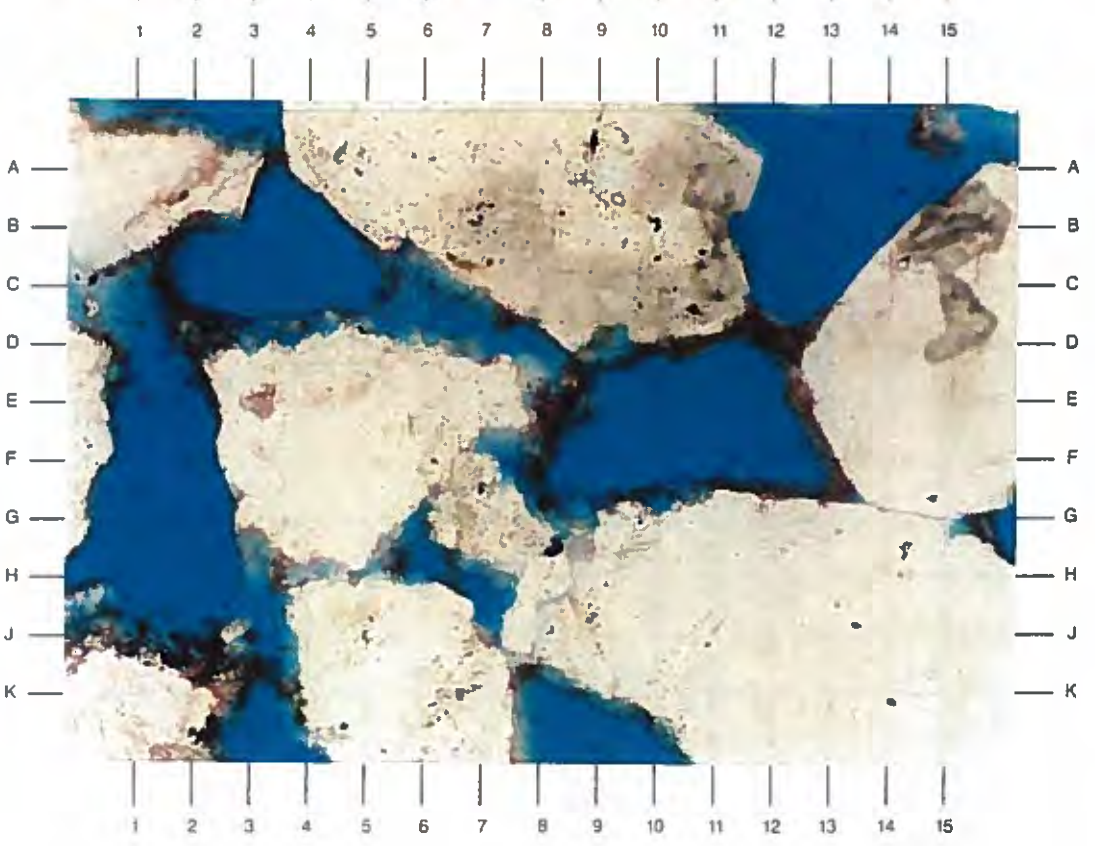
The high magnification view of the center of Plate 3A depicts a titanium component (C1.5,E8.5,C-D12) that has left "rims" in pores. Framework grains are loosely connected, allowing for good reservoir porosity and permeability. Note the silt grain (G7) partially occluding a pore.

Magnification: 200X



A

0.25 mm



B

0.05 mm

SAMPLE DEPTH: 9796 FEET

PLATE 4A

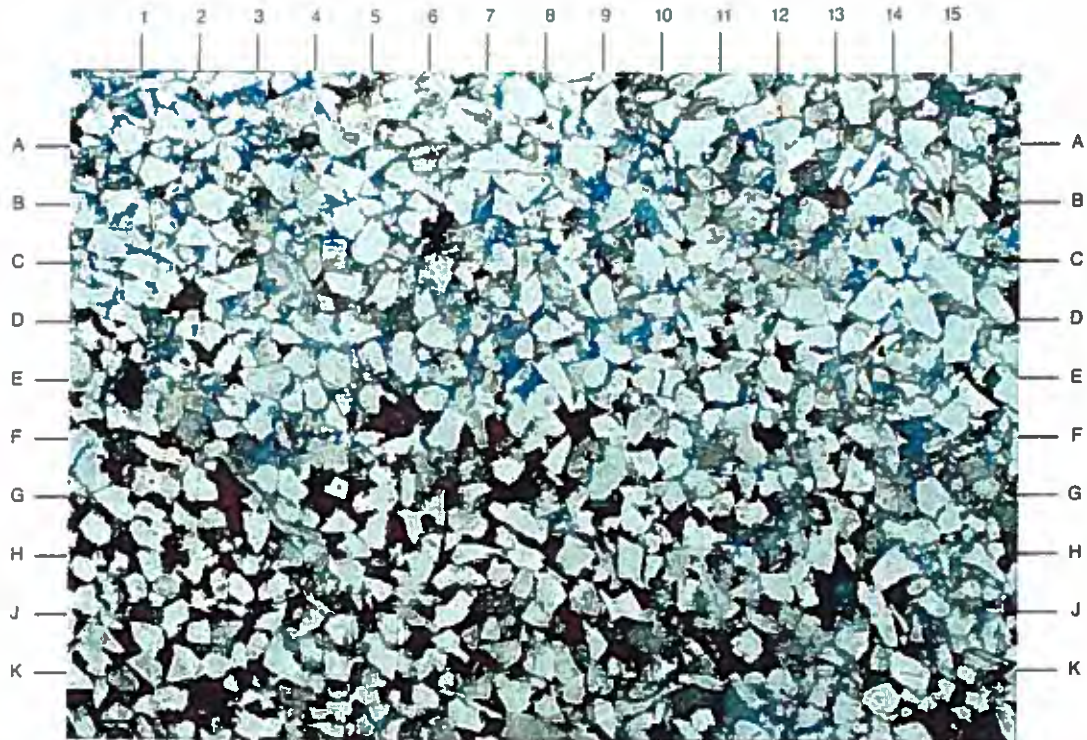
The low magnification photomicrograph on the facing page depicts a moderately sorted sandstone that is partially cemented by calcite (red-stained in lower half of photo). This fine-grained sandstone shows signs of compaction (see contorted mica fragment at G3). Remaining intergranular porosity (blue, upper half) is reduced by compaction.

Magnification: 40X

PLATE 4B

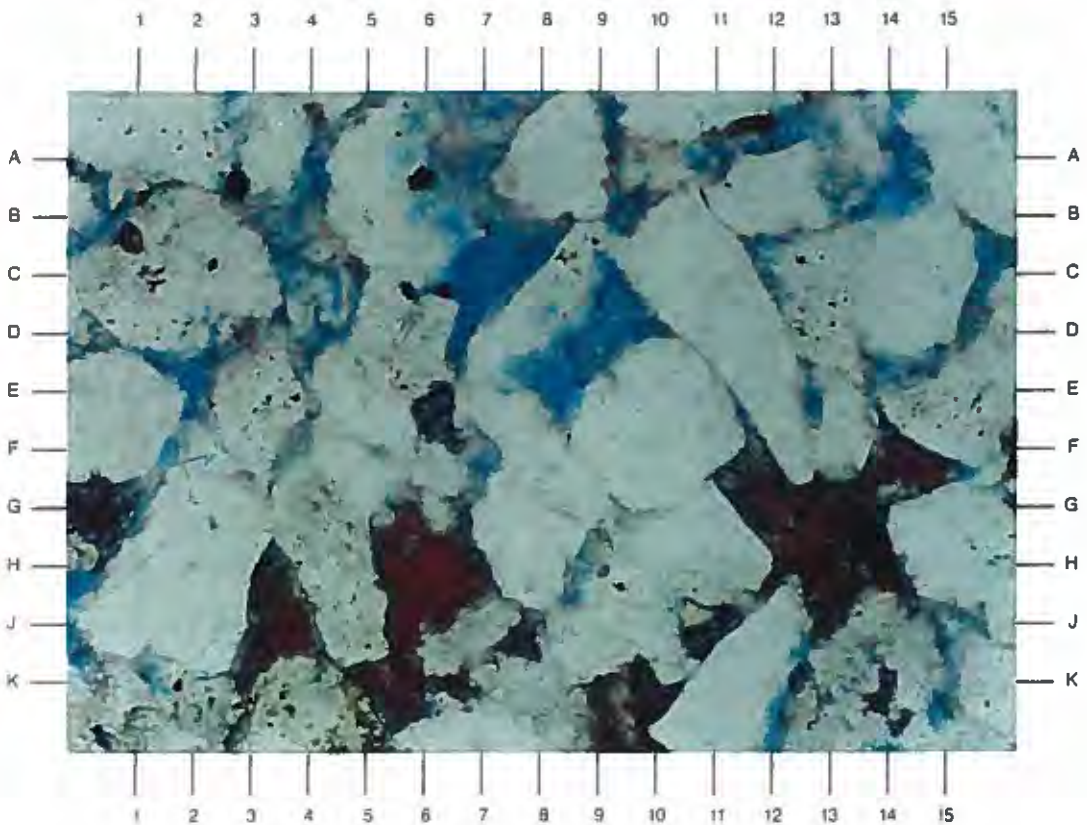
The high magnification view of the area near E8 in Plate 4A shows the nearly complete occlusion of porosity in the area filled by calcite cement (red). Note the reduction in intergranular pore size (blue) compared to the previous sample described from 9562' (Plate 3B).

Magnification: 200X



A

0.25 mm



B

0.05 mm

SAMPLE DEPTH: 9800 FEET

PLATE 5A

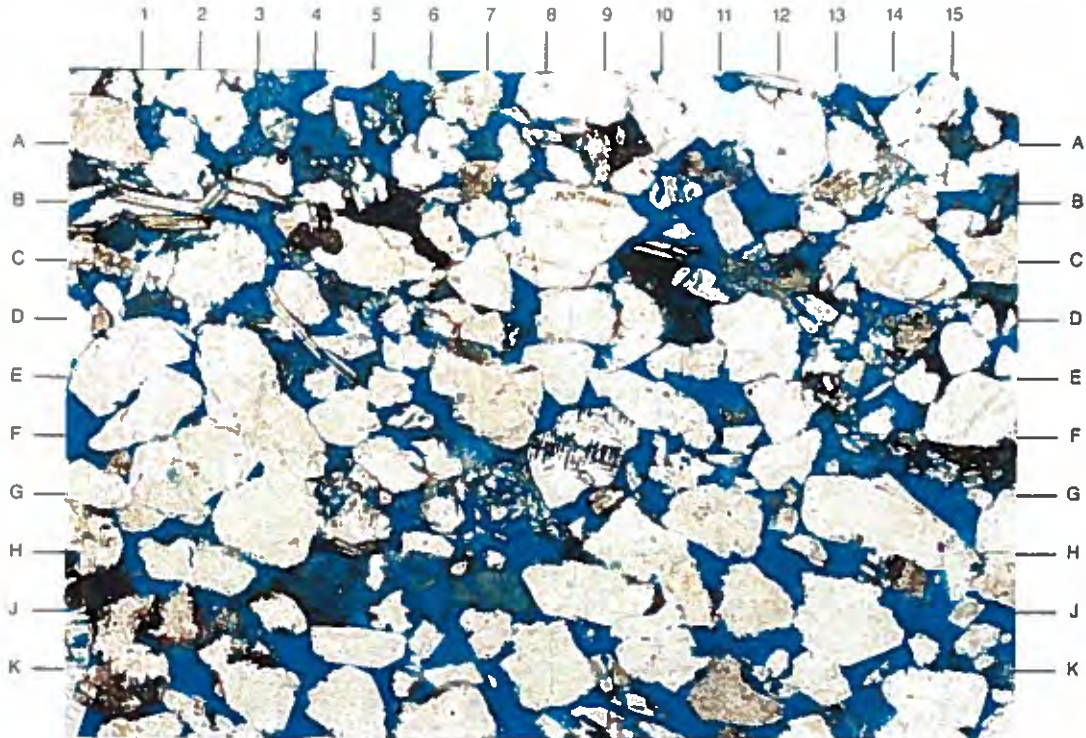
The low magnification survey photomicrograph taken from 9800' shows a moderately well sorted, medium-grained sandstone with abundant intergranular porosity. This feldspathic litharenite (Folk, 1980) contains silty zones (D-E13.5,G-H7). Note the compaction effects on the mica fragment at B2 and quartz overgrowths (A11.5,C7.5) present.

Magnification: 40X

PLATE 5B

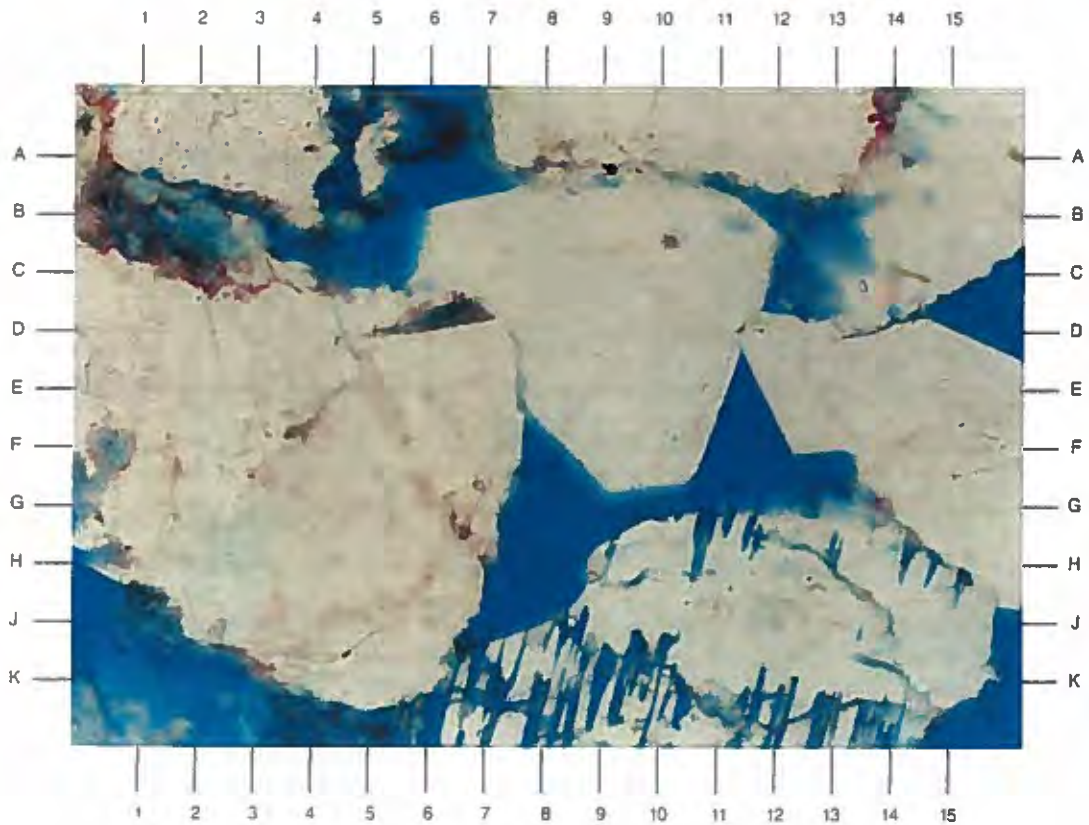
The high magnification view of the area near E8 in Plate 5A shows the pore types found in the sandstone. Intergranular porosity (H8,F11.5,C-D15.5) is abundant and well interconnected. Intragranular porosity is observed in partially leached feldspar (K7-K14). Note the detrital silt at A5 and quartz overgrowths at E12.5.

Magnification: 200X



A

0.25 mm



B

0.05 mm

SAMPLE DEPTH: 9802 FEET

PLATE 6A

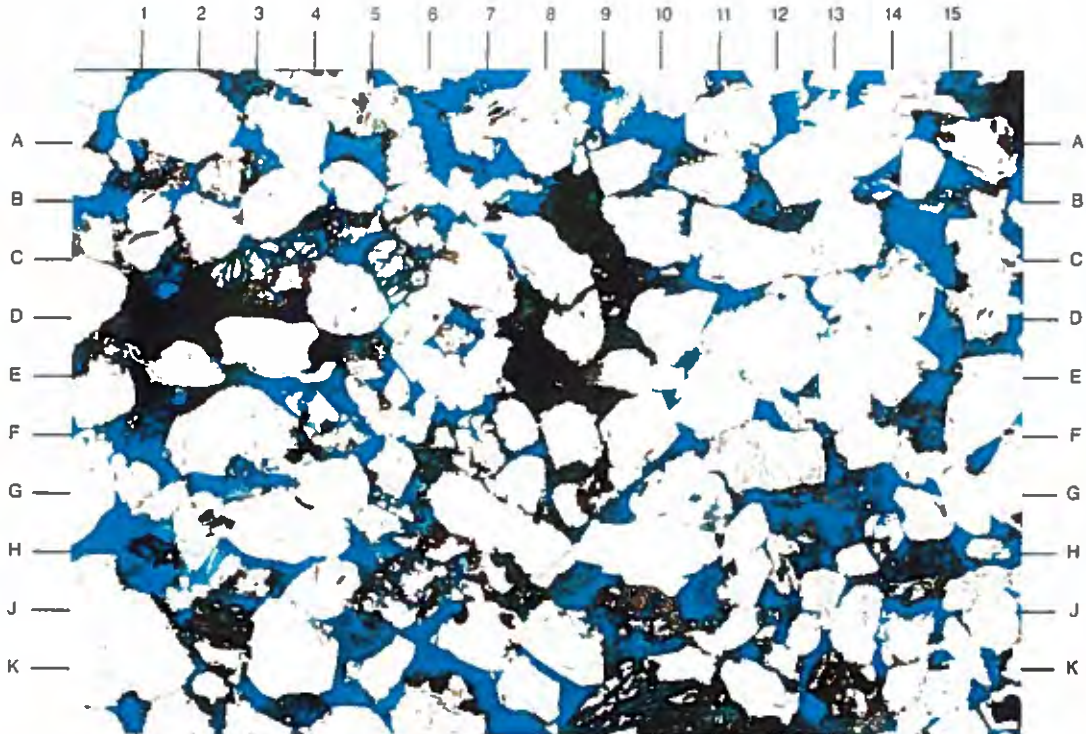
The moderately well sorted, medium-grained sandstone taken from 9802' is shown on the facing page under low magnification. The primary pore type is intergranular porosity (A6,C-D11,K6), although intragranular pores (H14.5,G11) are found in partially leached lithics and feldspar. Note the presence of a titanium component that is iron-rich (D2,B8.5,E8) found in some pores.

Magnification: 40X

PLATE 6B

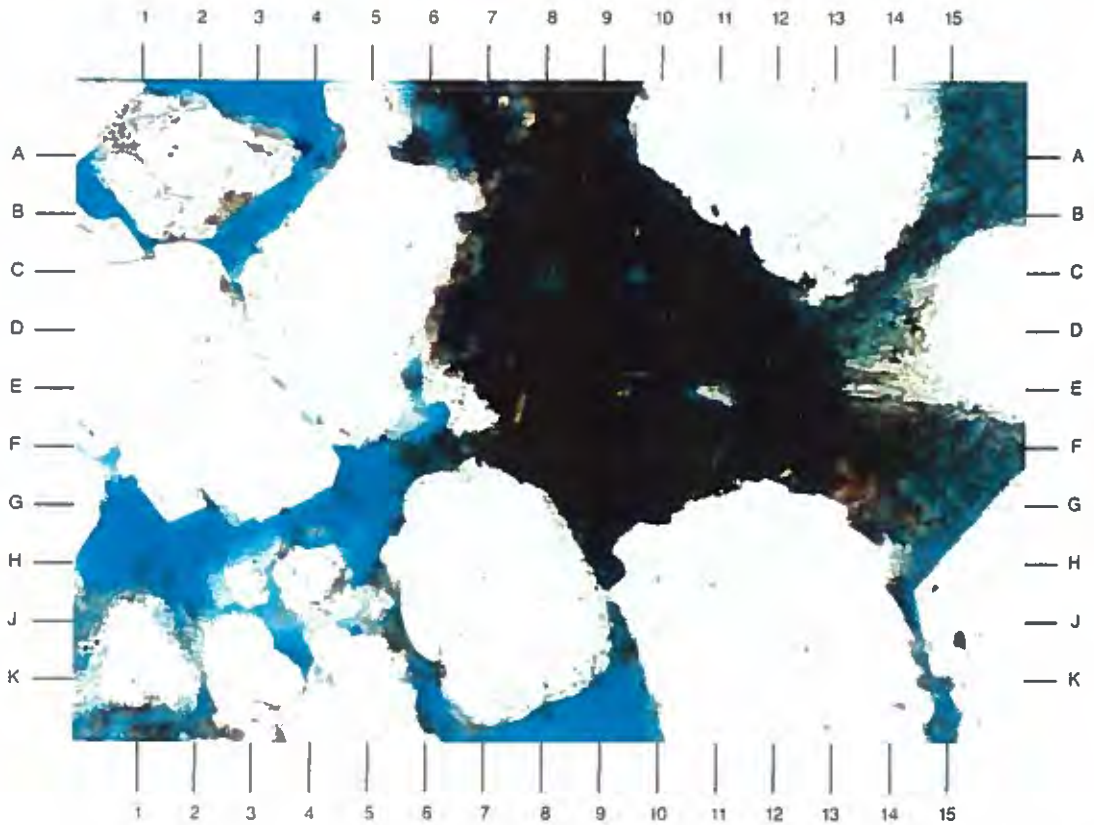
The high magnification view of the area near E8 in Plate 6A shows the presence of a titanium component (black) filling an intergranular pore. Other pore-reducing components found are quartz overgrowths (H8.5,J15), detrital silt (H-J4), and pseudomatrix (A15.5), possibly composed of chlorite.

Magnification: 200X



A

0.25 mm



B

0.05 mm

Dupont Environmental
Delisle No. 2, Stk No. 1
Harrison County, Mississippi

File No. GN-3402

SAMPLE DEPTH: 9810 FEET

PLATE 7A

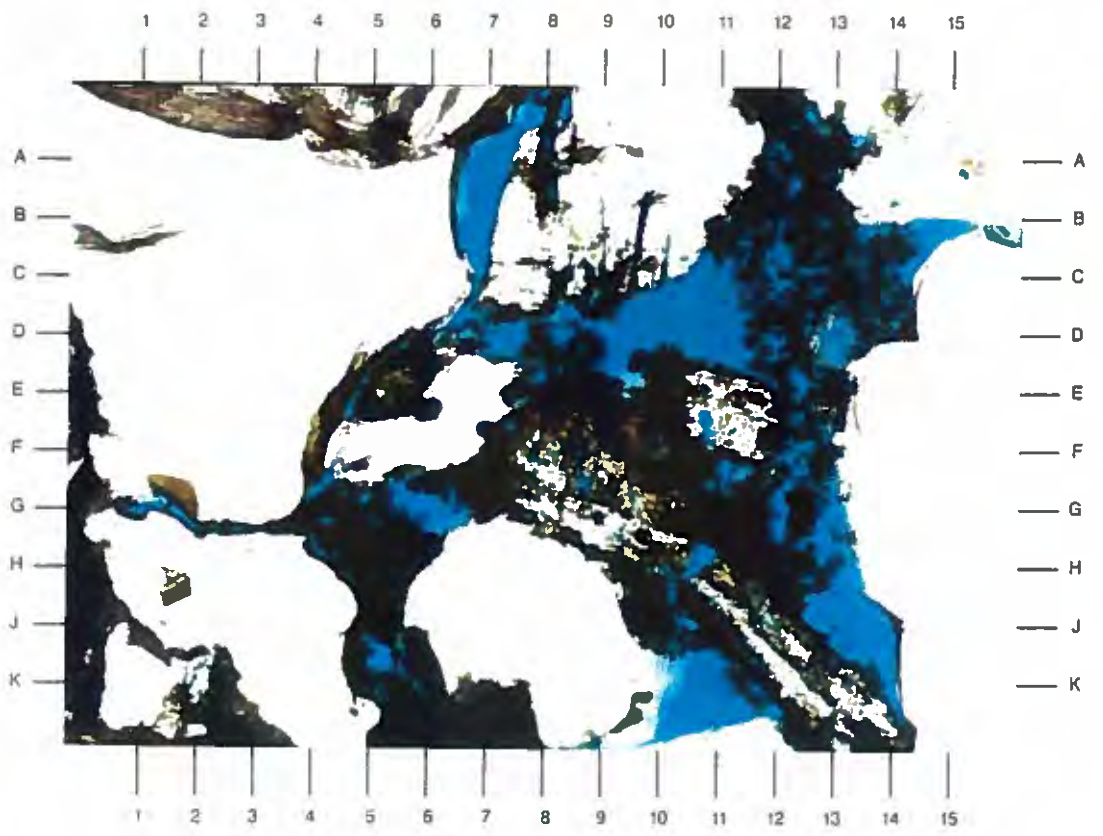
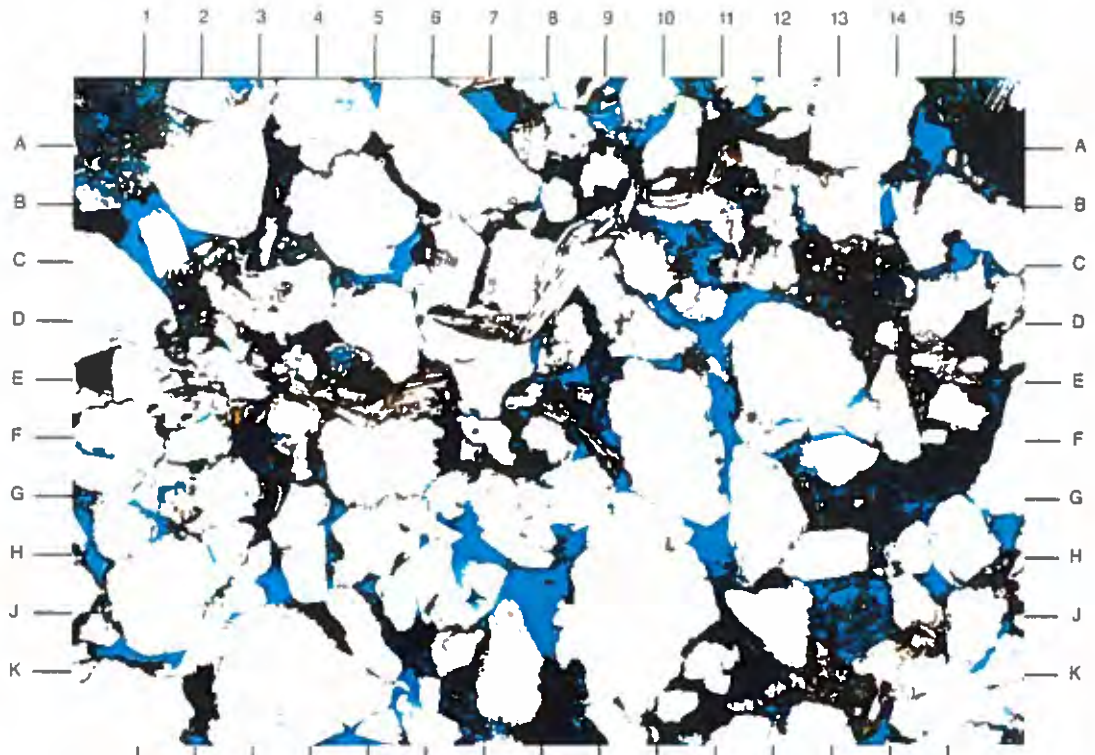
The low magnification survey photomicrograph on the facing page shows an abundance of a titanium component (black) occluding some pores. This component accounts for 12% of the sample (by thin section point count). Intergranular porosity (blue) is abundant and well interconnected, even though some compaction is evident by contortion of ductile mica fragments (E-F5,C8).

Magnification: 40X

PLATE 7B

The high magnification view of the area near E8 in Plate 7A shows the pervasive, titanium component (black) flooding pores and pore throats. Intragranular porosity (A-B8,F-G9) is only partially filled with the precipitate, accounting for their poor connection to intergranular porosity. Note the slight reduction in pore size by quartz overgrowths (D6.5,C14.5).

Magnification: 200X



Dupont Environmental
Delisle No. 2, Stk No. 1
Harrison County, Mississippi

File No. GN-3402

SAMPLE DEPTH: 9820 FEET

PLATE 8A

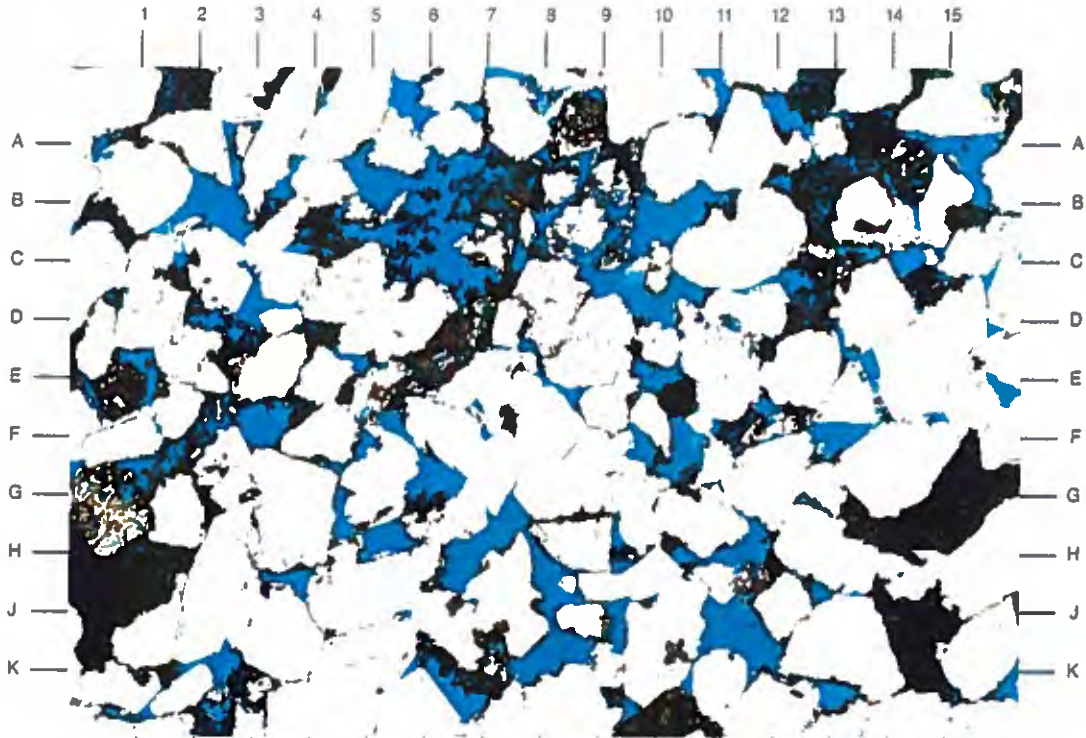
The low magnification survey photomicrograph is similar to the previous sample described at 9810' (Plate 7A). Abundant, well interconnected intergranular porosity and some dissolution pores (blue) are partially filled with a titanium component (black).

Magnification: 40X

PLATE 8B

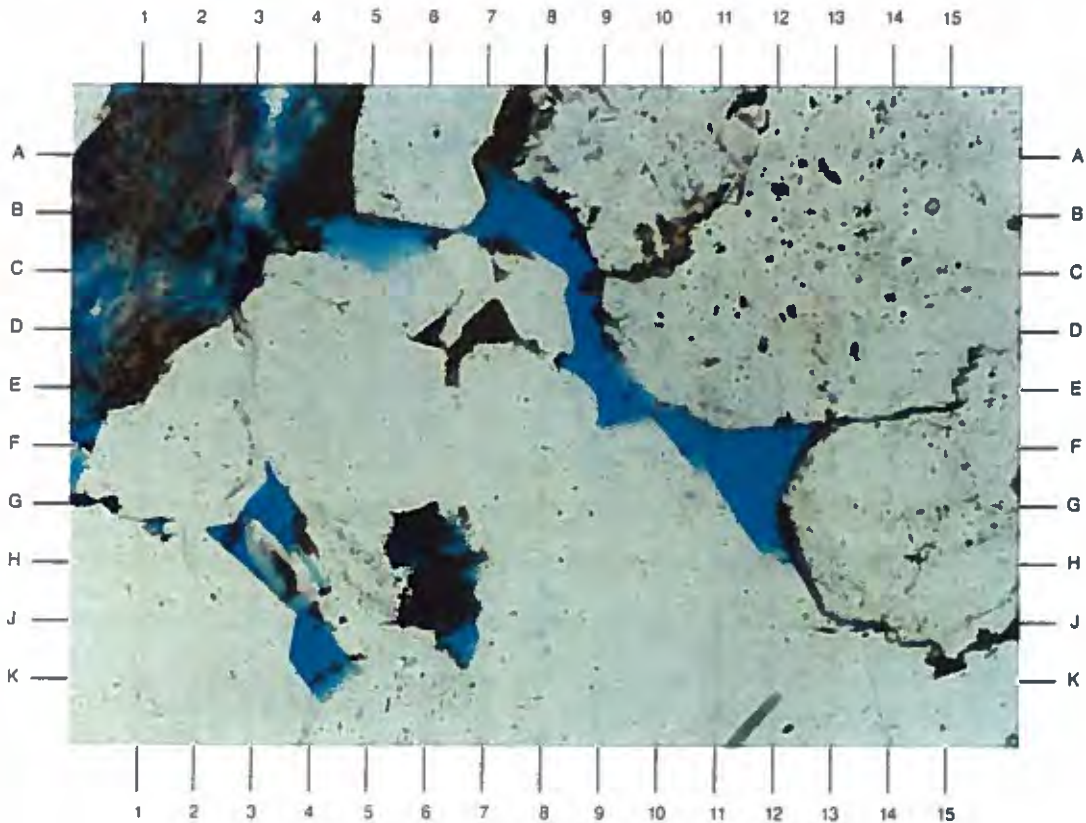
The high magnification view of the area near E8 in Plate 8A documents the cementation present in this sample. Quartz overgrowths (G3,J3,E-F10) are locally abundant and are seen reducing pore and pore throat size. A titanium component is observed partially filling pores at B4 and A7.5. Note the partial dissolution of a lithic fragment at B1.5.

Magnification: 200X



A

0.25 mm



B

0.05 mm

Dupont Environmental
Delisle No. 2, Stk No. 1
Harrison County, Mississippi

File No. GN-3402

SAMPLE DEPTH: 9843 FEET

PLATE 9A

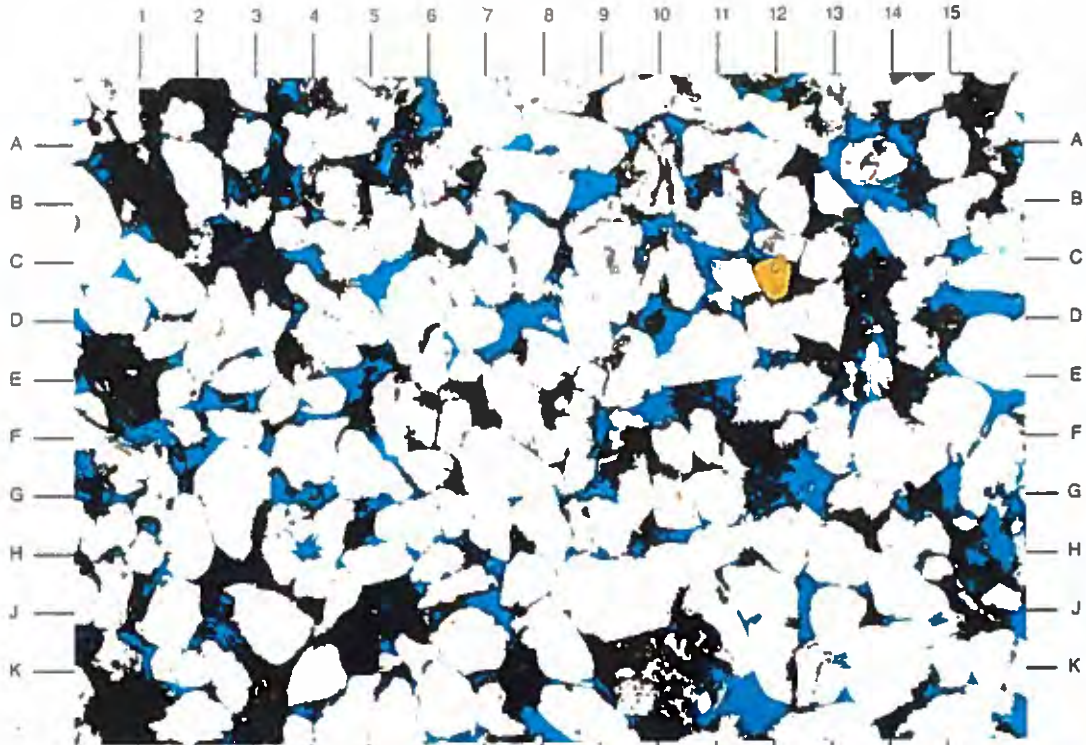
The massive, moderately well sorted, medium-grained sandstone shown in the low magnification photomicrograph illustrates the pervasive pore-filling titanium component (black) found in the sample. Note the tourmaline grain seen at C12.

Magnification: 40X

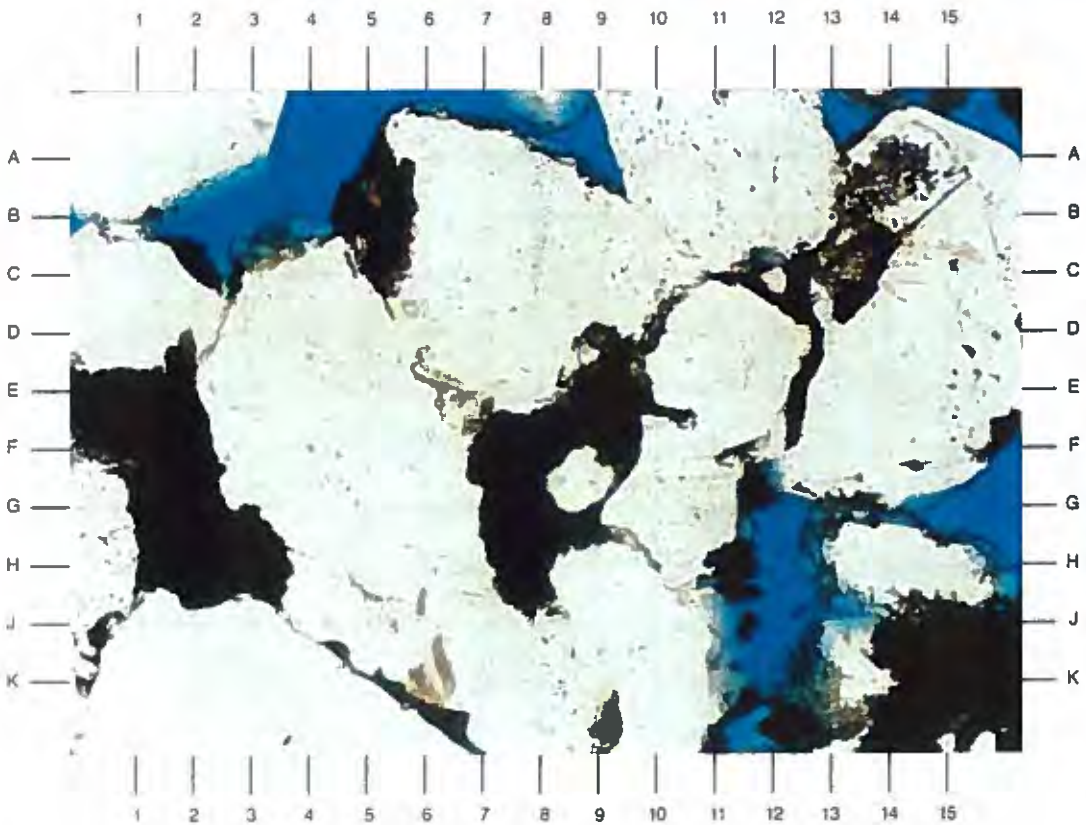
PLATE 9B

The high magnification view of the center of Plate 9A shows the complete occlusion of some pores (G2,F8) by the titanium component while others remain open (A4,H12). Quartz overgrowths (A8,F12) and detrital silt (F-G9) are observed slightly reducing intergranular pores.

Magnification: 200X



A



B

SAMPLE DEPTH: 9850 FEET

PLATE 10A

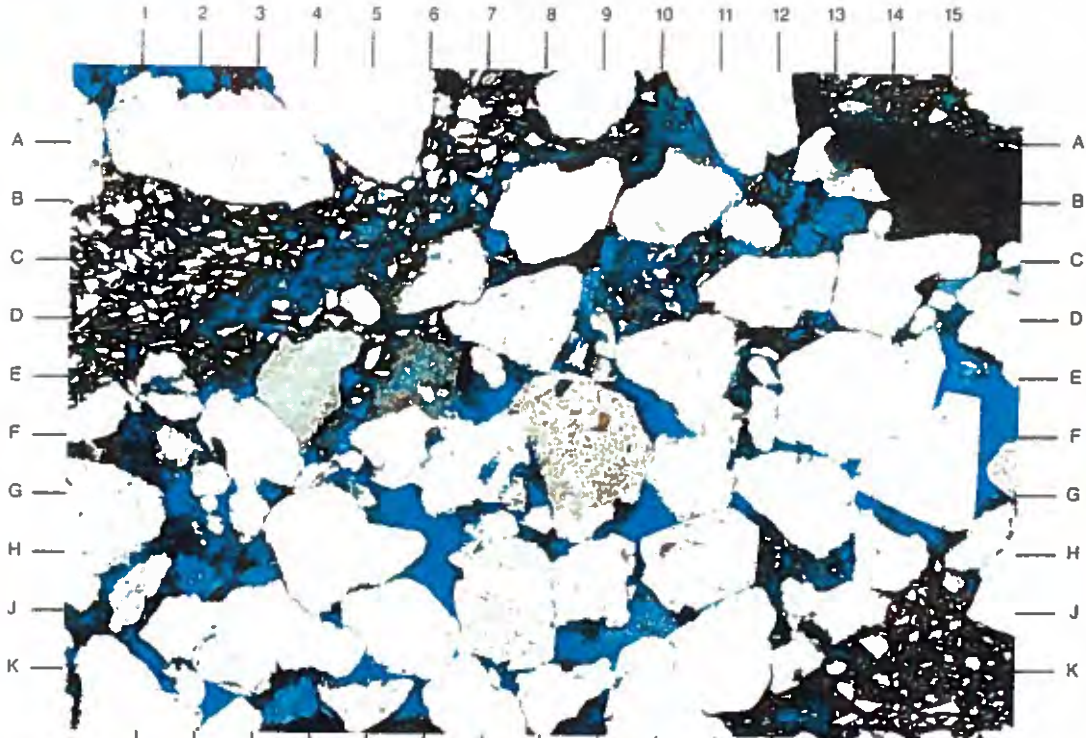
The low magnification photomicrograph on the facing page depicts an upper medium-grained sandstone with abundant intergranular porosity (blue). Thin, silty, organic-rich lenses (C1-A8,K15) are present in the sample described and are discontinuous in the sample. Some pores are restricted by a titanium component (below K3.5,F-G1) and "pseudomatrix" created by insitu breakdown of lithic fragments (E6,H12.5).

Magnification: 40X

PLATE 10B

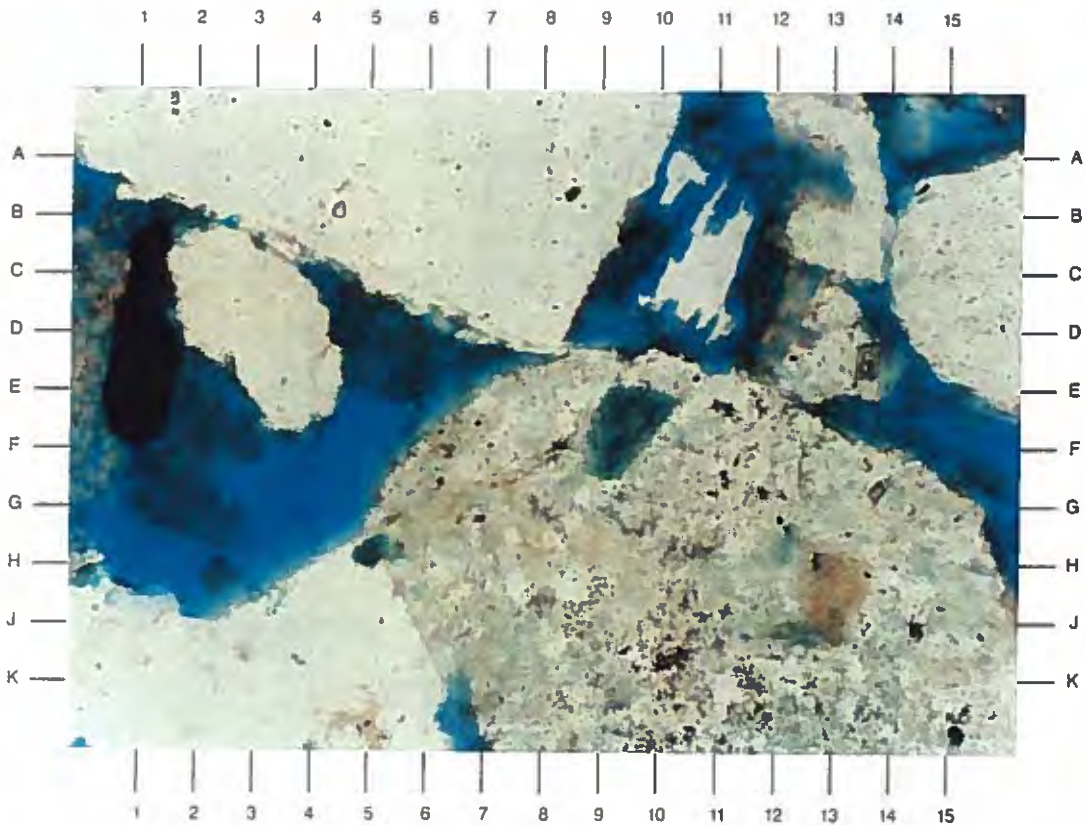
The high magnification view of the area near E8 in Plate 10A shows components present in the sample that are pore-reducing. A titanium component (D1), "pseudomatrix" (E2-G2,D5) created from lithic fragment breakdown, and quartz overgrowths (C5,J5) are seen as occupying pore space. Note the presence of intragranular porosity at B11 and A-B12.5.

Magnification: 200X



A

0.25 mm



B

0.05 mm

Dupont Environmental
Delisle No. 2, Stk No. 1
Harrison County, Mississippi

File No. GN-3402

SAMPLE DEPTH: 9852 FEET

PLATE 11A

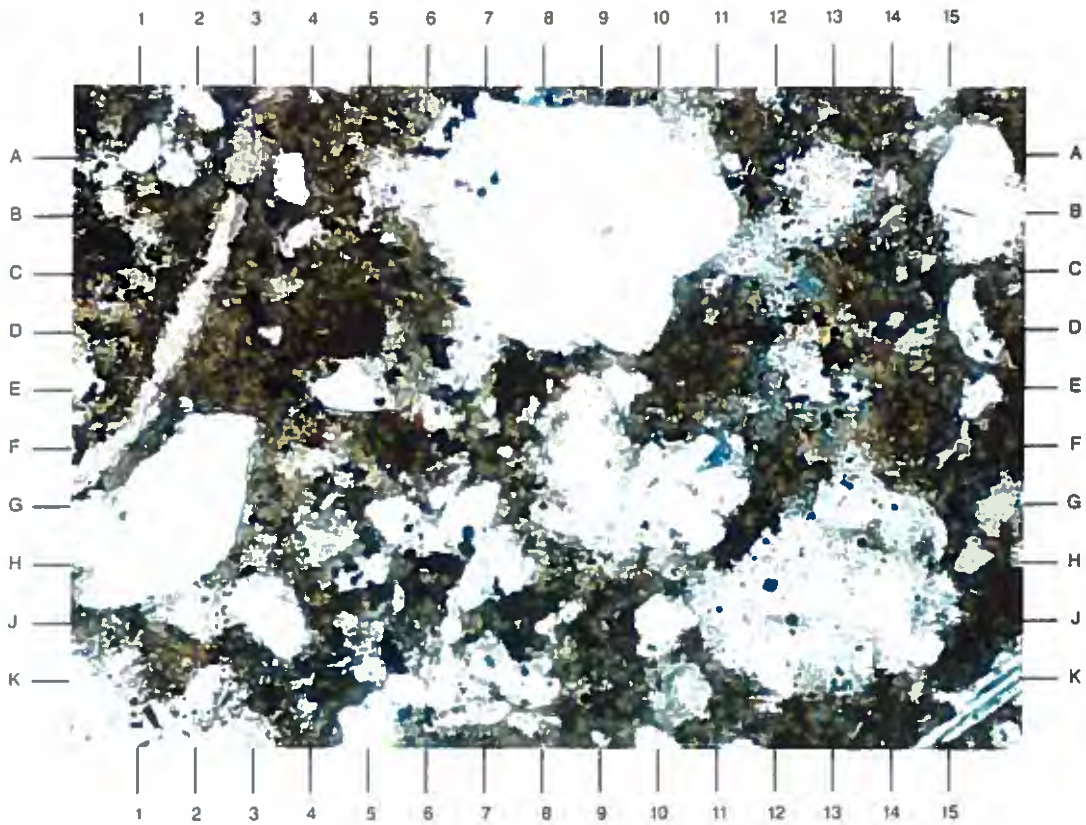
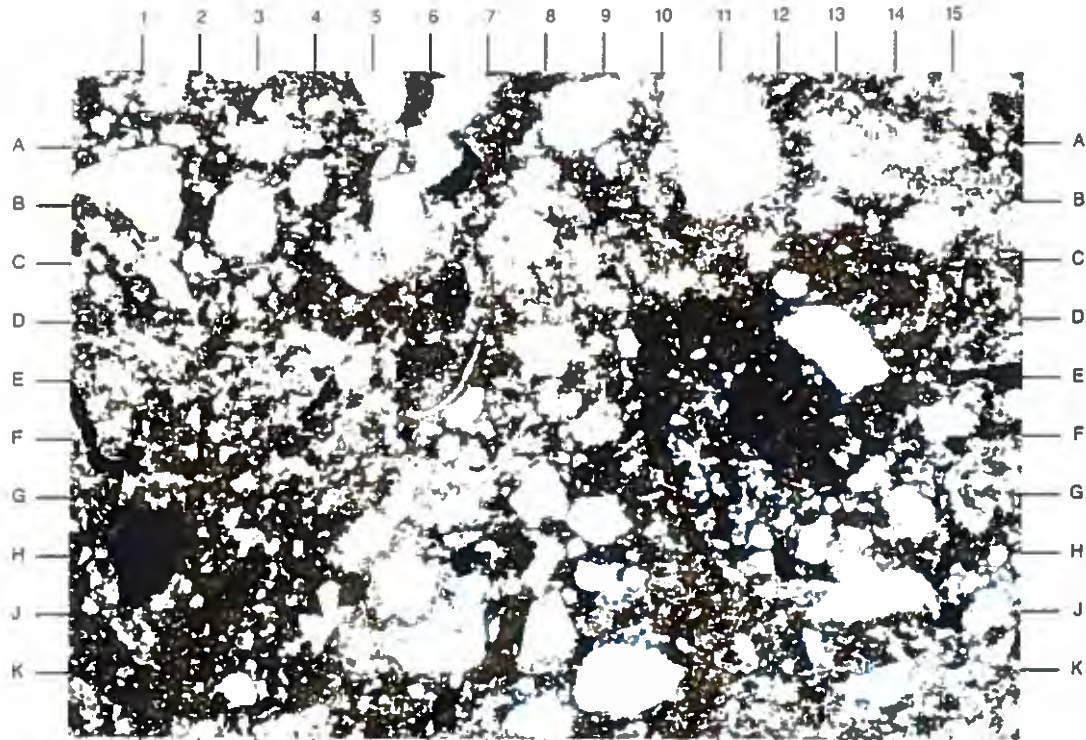
Nearly total occlusion of porosity (lack of blue epoxy) is depicted in the low magnification photomicrograph shown on the facing page. This mudstone (shale) is sand/silt-rich. The matrix (brown) is composed primarily of illite and illite/smectite (33% by weight from XRD). Note the pyrite (black) and fossil fragment (E6.5) present.

Magnification: 40X

PLATE 11B

The high magnification view of the area near E8 in Plate 11A shows minor microscopic porosity (F11,C12.5) remaining in the shale. The poorly sorted nature of the shale is evident at this magnification. Note the pyrite "specks" (black) randomly distributed.

Magnification: 200X



Dupont Environmental
Delisle No. 2, Stk No. 1
Harrison County, Mississippi

File No. GN-3402

SAMPLE DEPTH: 9896 FEET

PLATE 12A

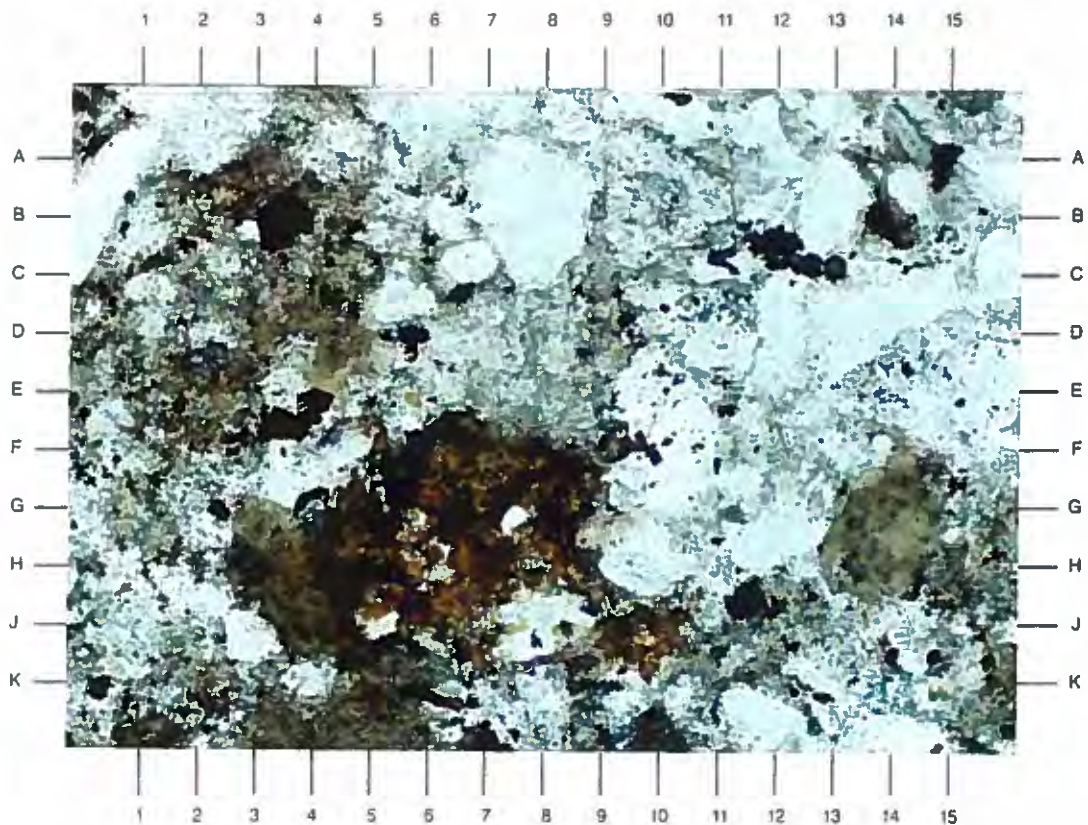
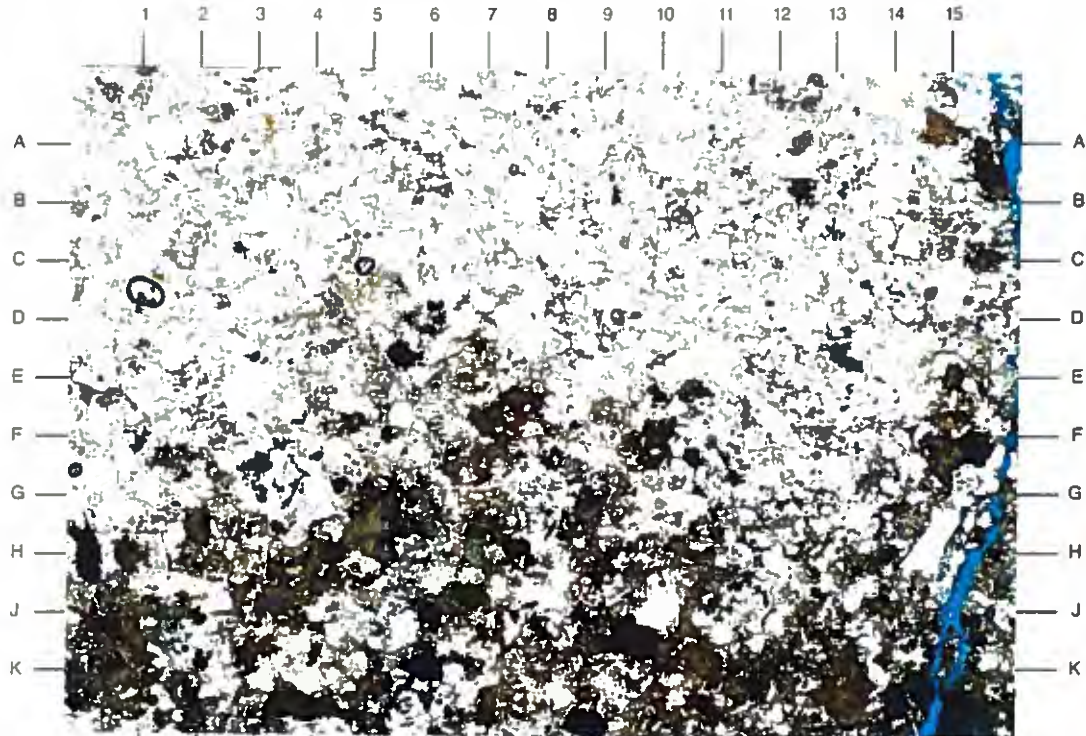
The low magnification survey photomicrograph depicted on the facing page shows a moderately poorly sorted, variably shaly laminated, very fine-grained sandstone. Primary intergranular pore space is occluded by detrital clay and silt. Plant fragments and secondary pyrite (black) are seen in the shaly portion of the sample.

Magnification: 40X

PLATE 12B

The high magnification view of the area near E8 in Plate 12A shows the occlusion of porosity by silt and clay. Siderite (dark brown at G7) also is seen filling pores. Note the random distribution of pyrite (black) in the photo.

Magnification: 200X



Dupont Environmental
Delisle No. 2, Stk No. 1
Harrison County, Mississippi

File No. GN-3402

SAMPLE DEPTH: 9902 FEET

PLATE 13A

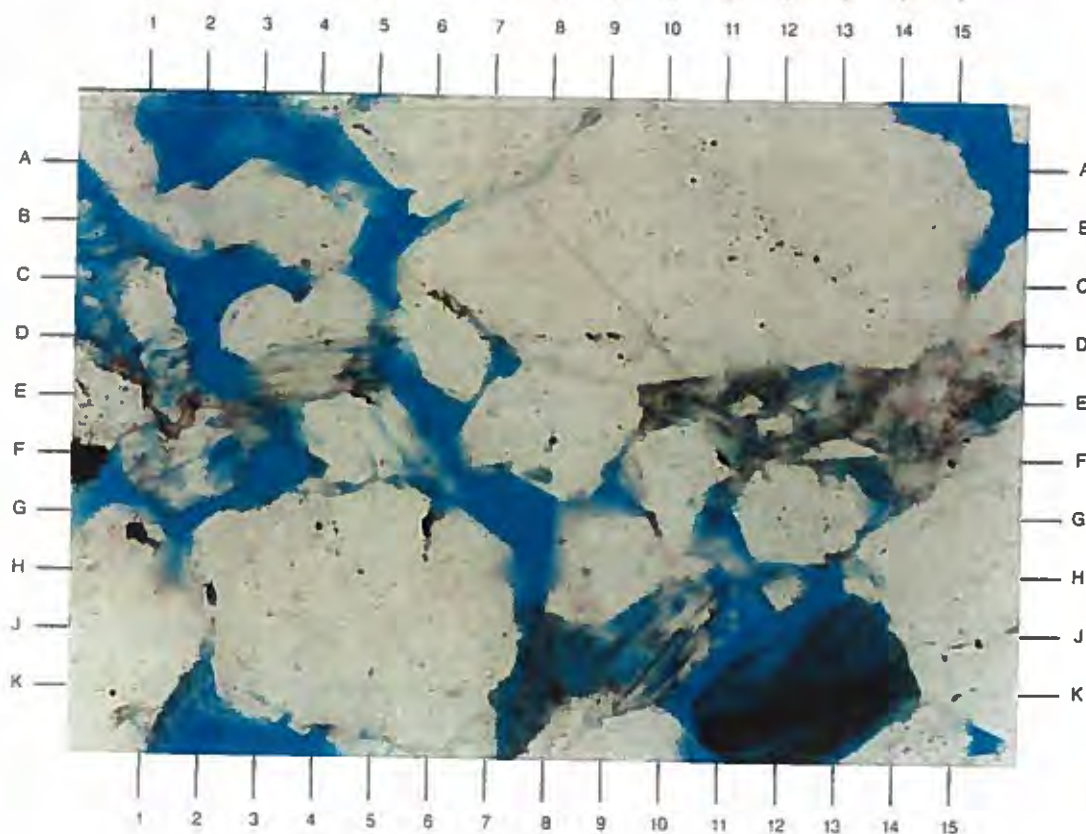
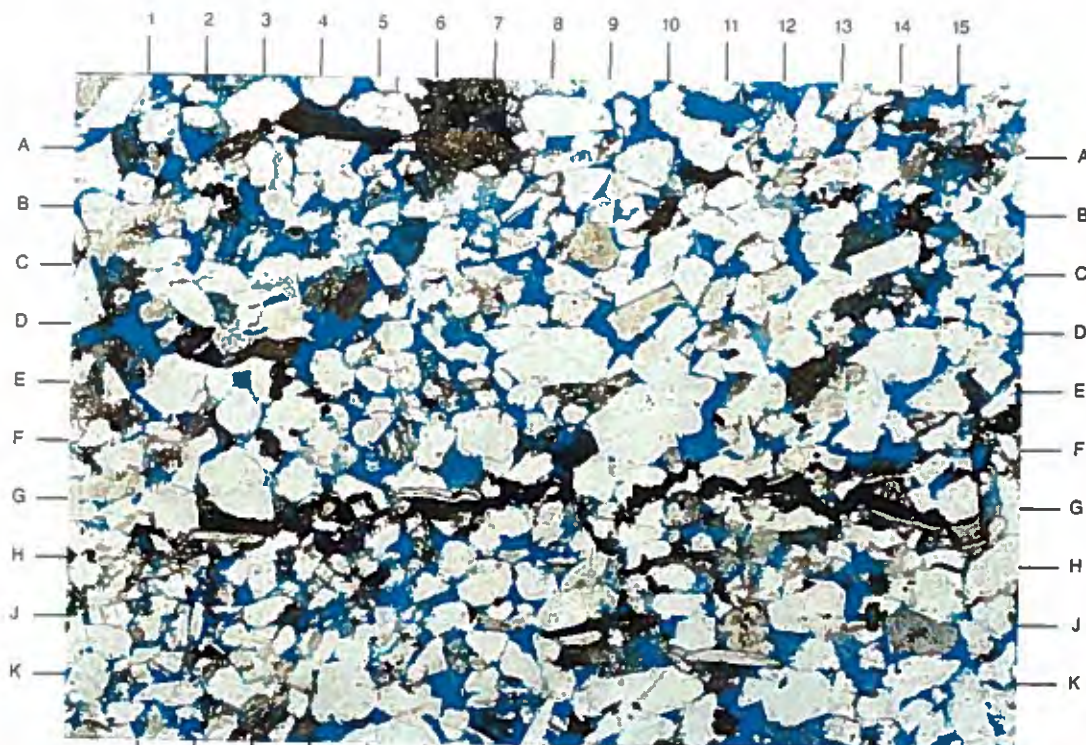
The low magnification survey photomicrograph illustrates a moderately sorted, massive, fine-grained sandstone taken from 9902'. Intergranular porosity (blue) is abundant and well developed. Carbonaceous material (probably plant fragments) is observed from G2.5-G14.5. Note the low compaction seen on the mica fragments (G6,J-K11,G-H14).

Magnification: 40X

PLATE 13B

The high magnification view of the area near E8 in Plate 13A documents the abundant intergranular porosity (blue) seen in this sample. The lithic fragment at J12-K13 is partially leached by secondary dissolution. Note the quartz overgrowths seen at A5, E6, and G7.

Magnification: 200X



Dupont Environmental
Delisle No. 2, Stk No. 1
Harrison County, Mississippi

File No. GN-3402

SAMPLE DEPTH: 9928 FEET

PLATE 14A

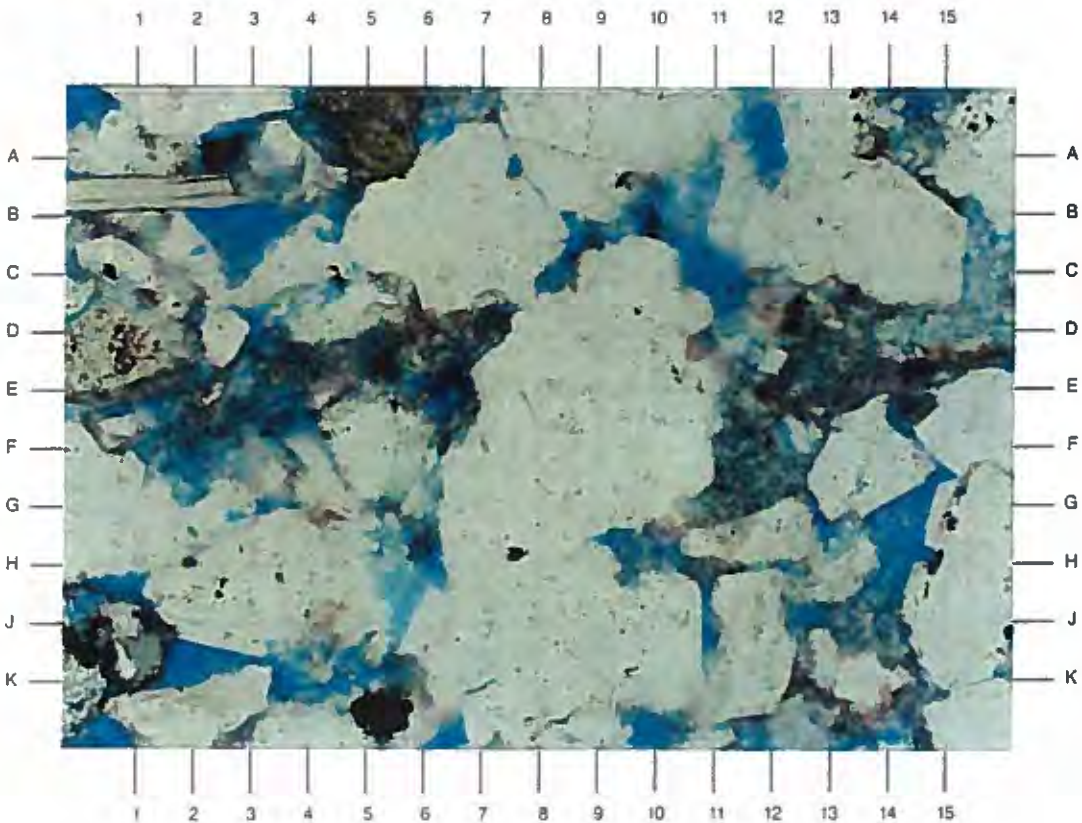
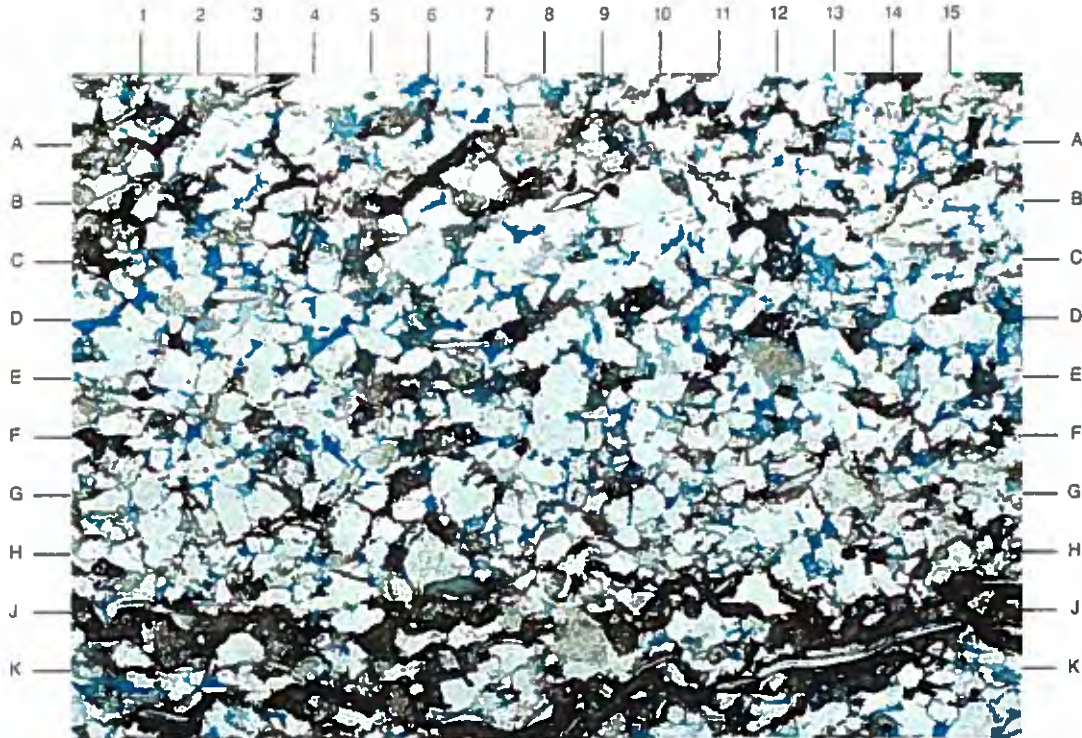
The massive, moderately well sorted, medium-grained sandstone shown in the low magnification photomicrograph shows abundant, well developed intergranular porosity (D0.5,F4.5,H11) throughout. Overall porosity is enhanced by secondary intragranular porosity found in partially dissolved lithic fragments and feldspars (C4,D9,A-B14.5).

Magnification: 40X

PLATE 14B

The high magnification view of the center of Plate 14A shows the two pore types observed in the sample. Intergranular porosity (K1,G6,K15.5) and intragranular porosity (E1,B11) are seen. Note the quartz overgrowths (C6,G-H8,H6).

Magnification: 200X



SAMPLE DEPTH: 9934 FEET

PLATE 15A

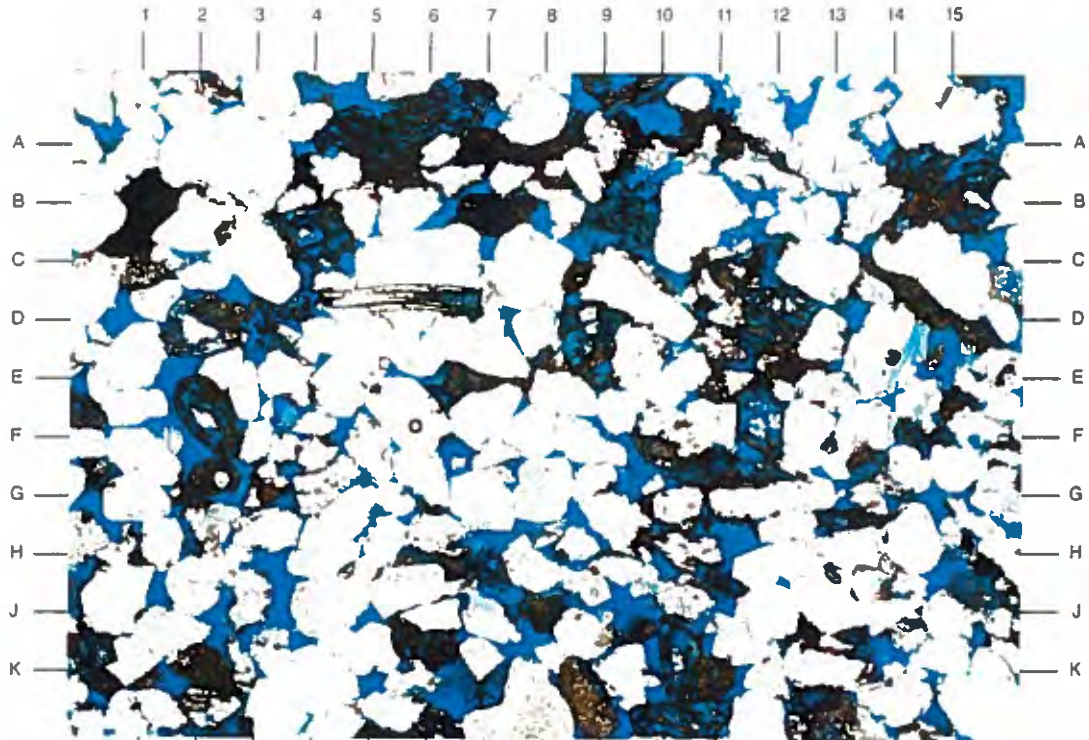
The low magnification photomicrograph on the facing page depicts a sandstone similar to the sample described at 9928' (Plate 14A). Both intergranular porosity (E1.5,G7) and secondary intragranular porosity (E5,E13) are observed. Overall porosity, however, is not as abundant as seen in the previous sample. Note the iron-rich component (B-C2.5,C10.5,B-C15.5) partially occluding some pores.

Magnification: 40X

PLATE 15B

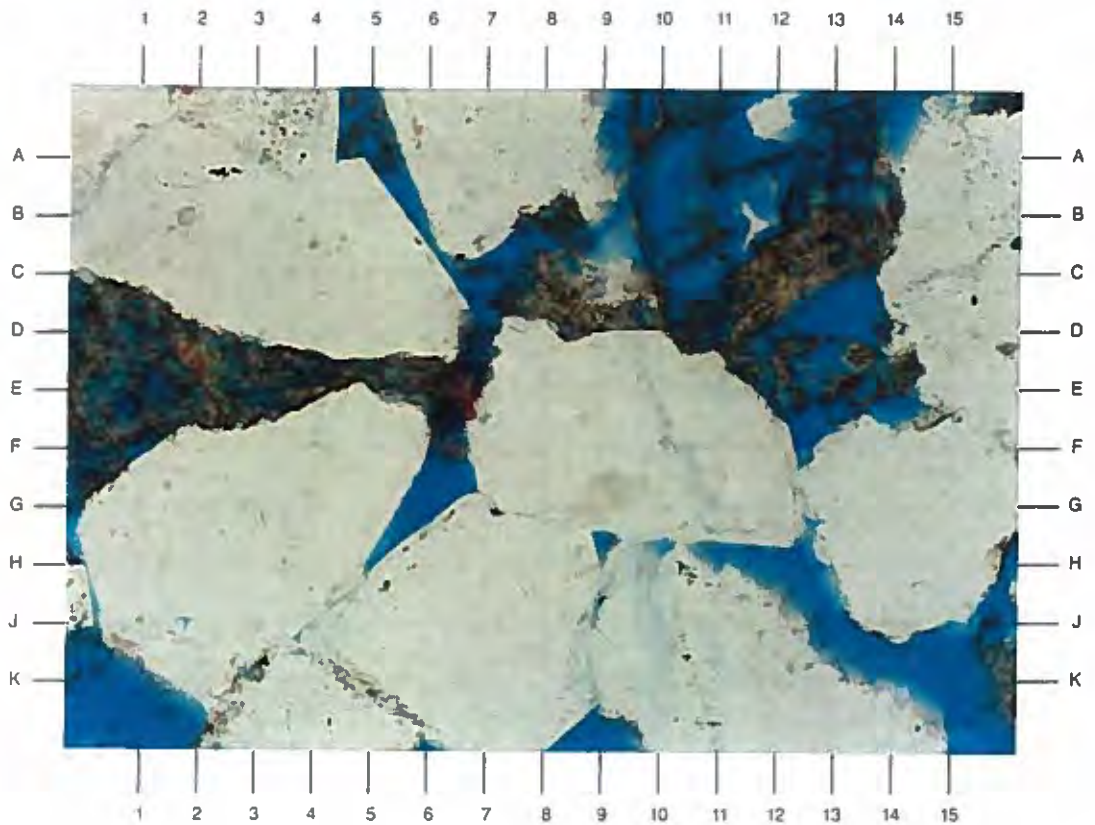
The high magnification view of the area near E8 in Plate 15A shows the occlusion of pore throats surrounding framework grains by an iron-rich component or precipitate (dark material in upper half of photo). Some intergranular porosity (G10.5,K4) and intragranular porosity (E13,K0.5) remain open.

Magnification: 200X



0.25 mm

A



0.05 mm

B

SAMPLE DEPTH: 9921 FEET

PLATE 16A

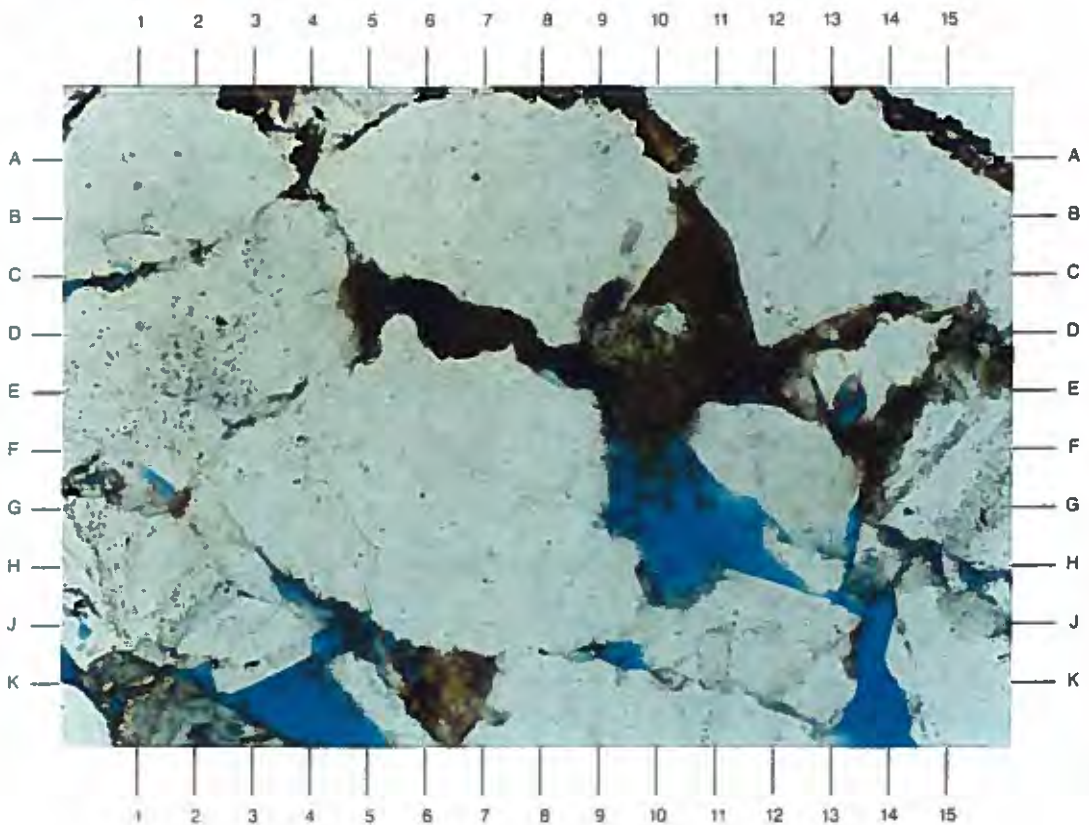
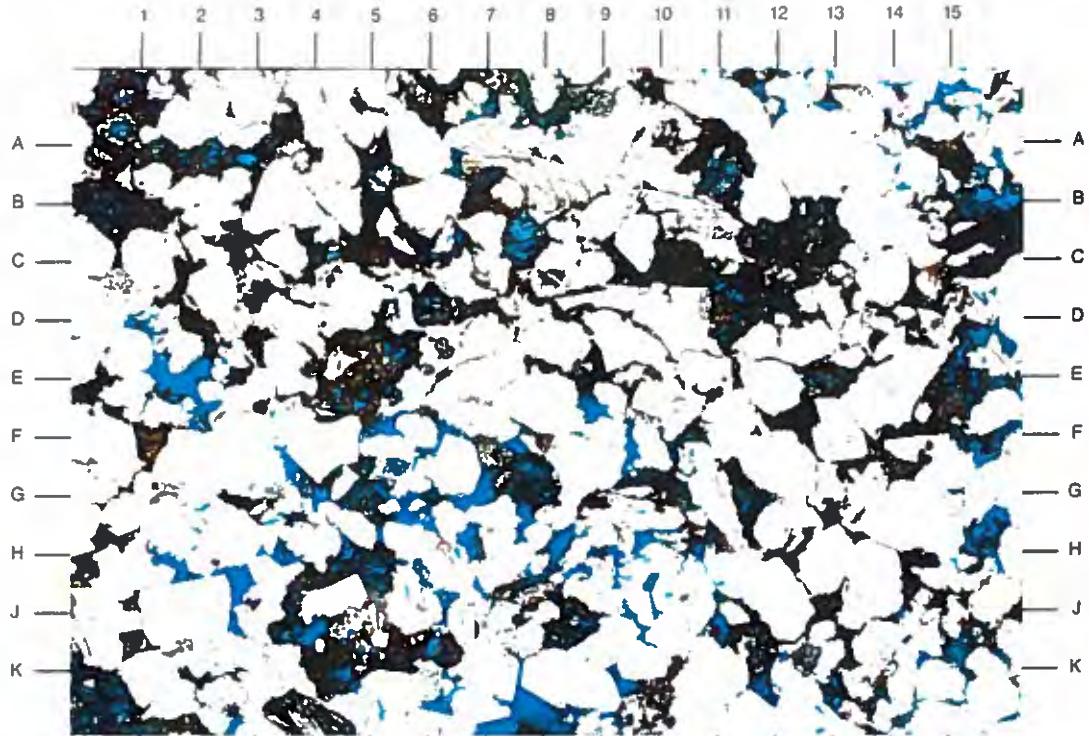
The low magnification survey photomicrograph taken from 9921' shows a laminated, moderately sorted, fine-grained sandstone with an average grain size of 0.16mm. Intergranular porosity (blue) is reduced in both pore size and amount compared to the previous sample at 9902'. Shale laminae observed are thin and discontinuous (K1-J15).

Magnification: 40X

PLATE 16B

The high magnification view of the area near E8 in Plate 16A shows the remaining intergranular porosity observed in this sample. Pore-reducing cements seen are quartz overgrowths (A7.5,G15), kaolinite (C15.5), clay matrix (F11.5,D-E13), and secondary pyrite (below K5,J0.5).

Magnification: 200X



SAMPLE DEPTH: 9962 FEET

PLATE 17A

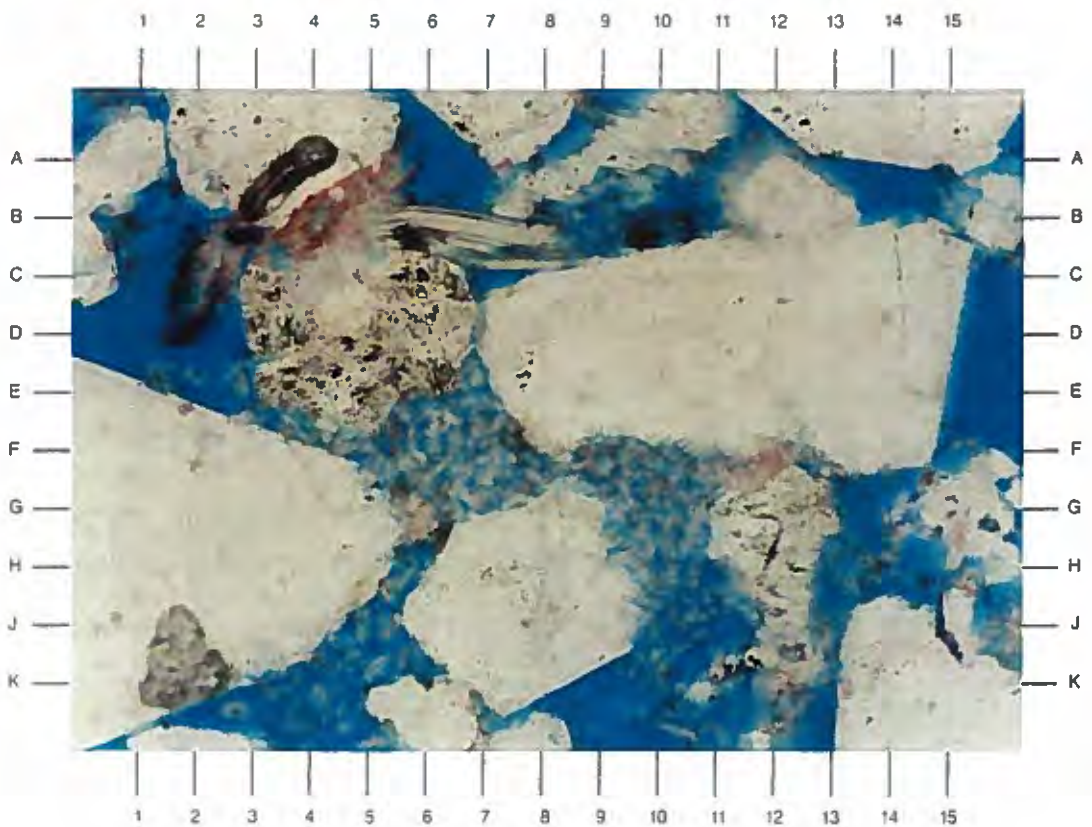
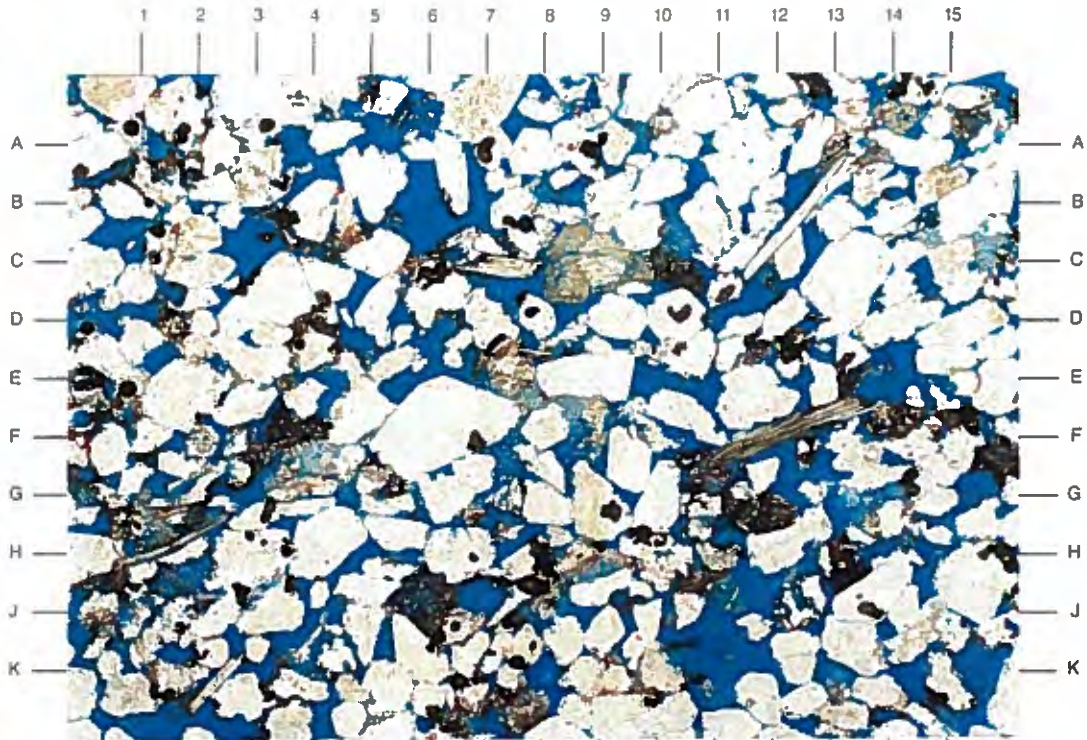
The massive sandstone taken from 9962' is shown on the facing page under low magnification. Low compaction is evident in the sample as seen in the uncontorted or slightly contorted mica fragments (H1.5,B13,E-F12.5). Intergranular porosity (blue) is abundant and well interconnected. The sublitharenite (Folk, 1980) is moderately well sorted and lower medium-grained sand-sized.

Magnification: 40X

PLATE 17B

The high magnification view of the area near E8 in Plate 17A depicts the partial occlusion of intergranular porosity due to kaolinite (F6.5,G10). Quartz overgrowths (A12,E8,E-F4) are also seen slightly reducing pore size. Note the slightly contorted mica flakes seen at B-C6.5.

Magnification: 200X



Dupont Environmental
Delisle No. 2, Stk No. 1
Harrison County, Mississippi

File No. GN-3402

SAMPLE DEPTH: 9970 FEET

PLATE 18A

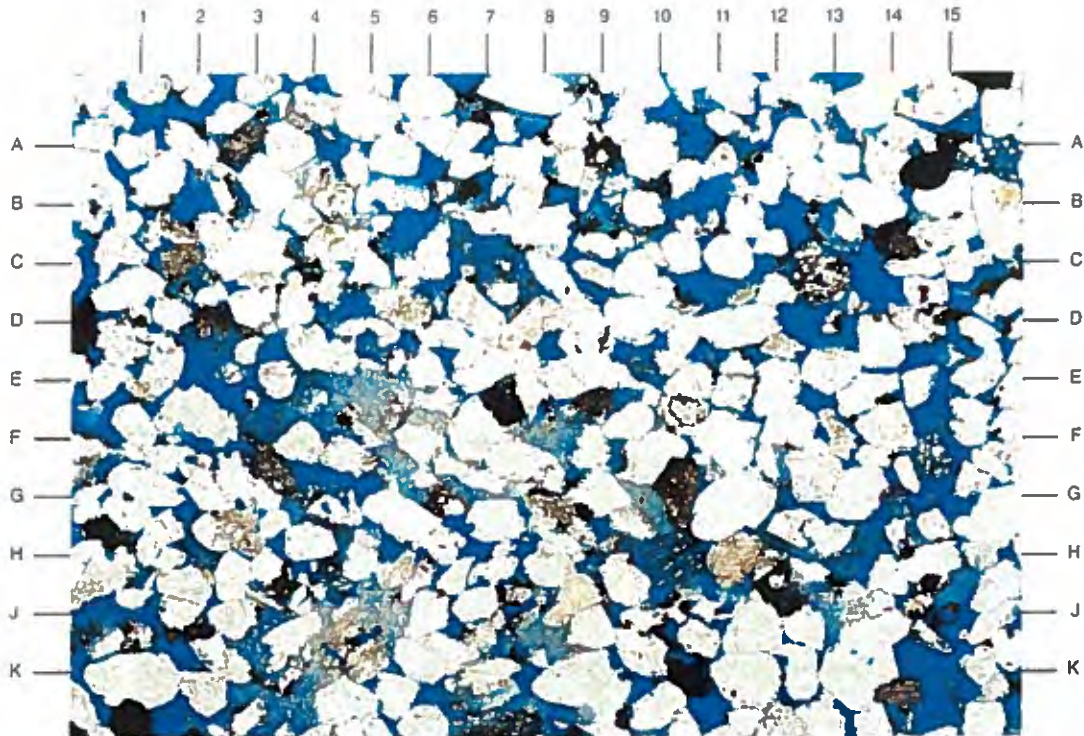
The low magnification survey photomicrograph on the facing page, taken from 9970', is similar to the previous sample described from 9962'. Abundant intergranular porosity (blue) is evenly distributed in this medium-grained massive sandstone. Note the patches of kaolinite clay (E-F5,F8.5,J-K8).

Magnification: 40X

PLATE 18B

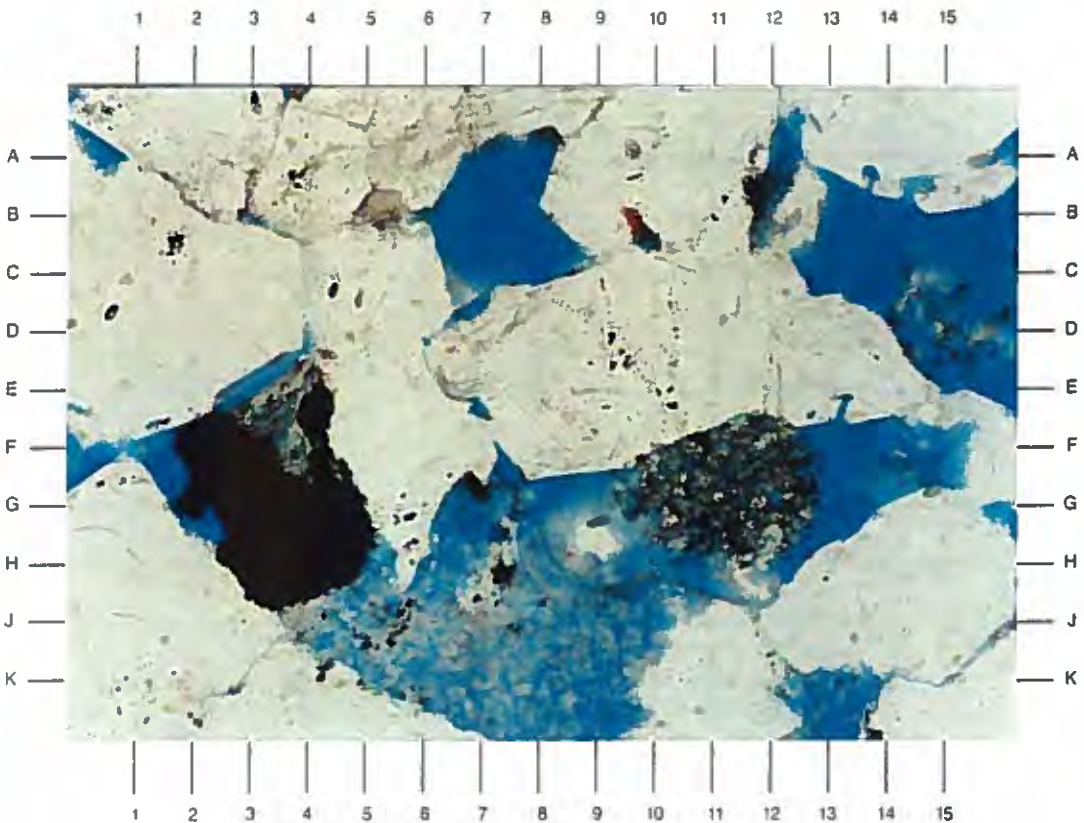
The high magnification view of the area near E8 in Plate 18A shows the pore types present in this sample. Intergranular porosity (B7.5,C14.5,F13.5) is the primary pore type. Intragranular porosity (G12) is seen in partially dissolved lithics. Secondary pyrite (G-H3.5) and kaolinite (J8) are observed partially filling pores.

Magnification: 200X



A

0.25 mm



B

0.05 mm

Dupont Environmental
Delisle No. 2, Stk No. 1
Harrison County, Mississippi

File No. GN-3402

SAMPLE DEPTH: 9990 FEET

PLATE 19A

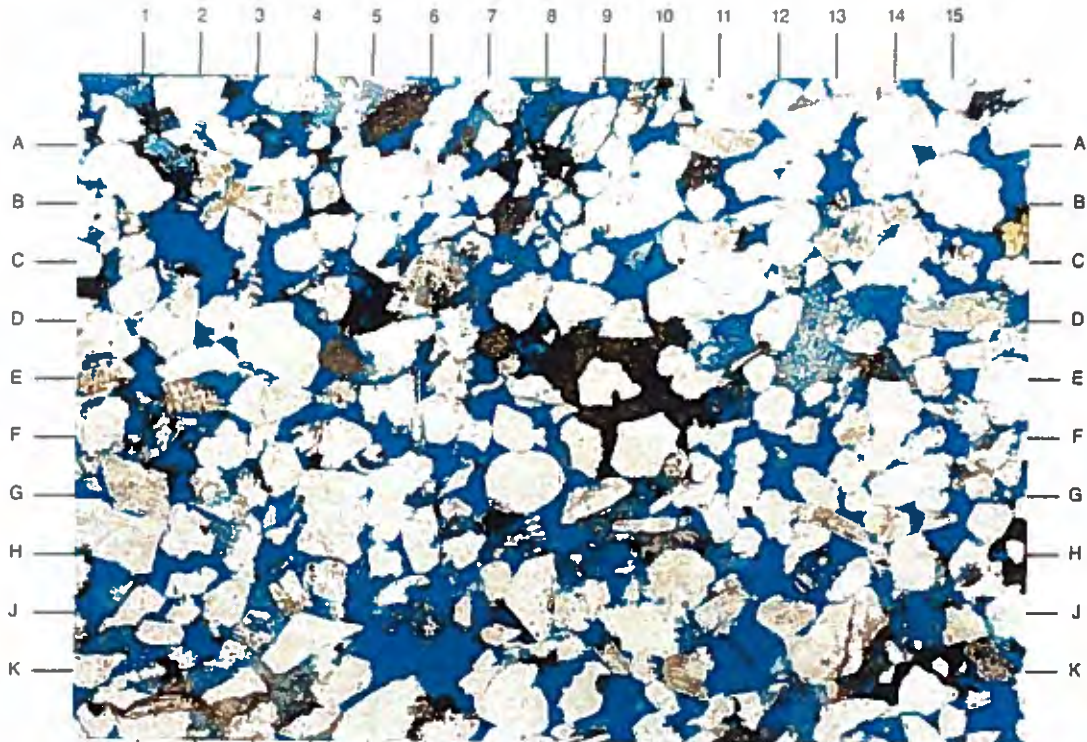
The low magnification survey photomicrograph illustrates a moderately well sorted, upper fine-grained sandstone with abundant intergranular porosity (blue). Like the previous samples described at 9962' and 9970' (Plates 17A and 18A), kaolinite (D-E13) is seen occluding some pores. Other pore-occluding components are dolomite (E9) and an iron-rich component (C-D5).

Magnification: 40X

PLATE 19B

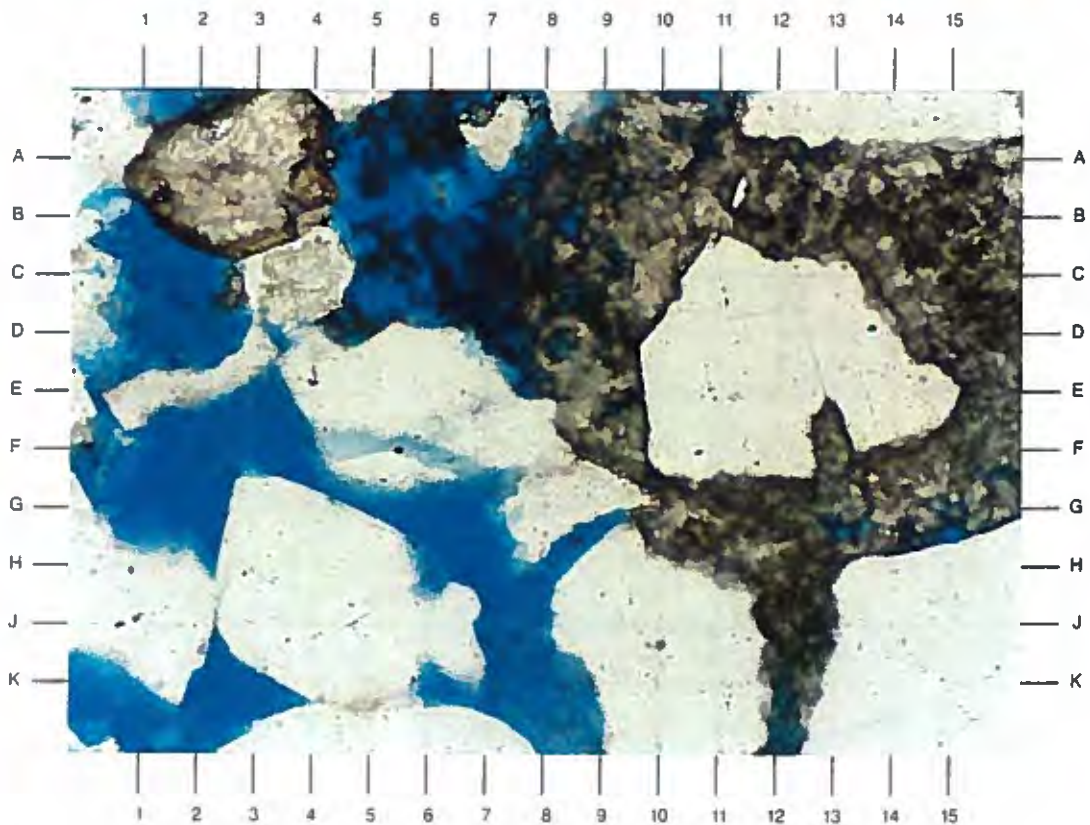
The high magnification view of the area near E8 in Plate 19A documents the occlusion of some porosity by dolomite (surrounding framework grain at D12). Remaining intergranular porosity is large and well interconnected. Note the quartz overgrowths seen at H2.5 and G4.5.

Magnification: 200X



A

┌
└ 0.25 mm



B

┌
└ 0.05 mm

APPENDIX D

**SCANNING ELECTRON MICROSCOPE
PHOTOMICROGRAPHS AND DESCRIPTIONS**

(Note the micron bar at the lower right portion of each photomicrograph for scale)

Dupont Environmental
Delisle No. 2, S/T No. 1
Harrison County, Mississippi

File No. GN-3402

SAMPLE DEPTH: 9473 FEET

PLATE 20A

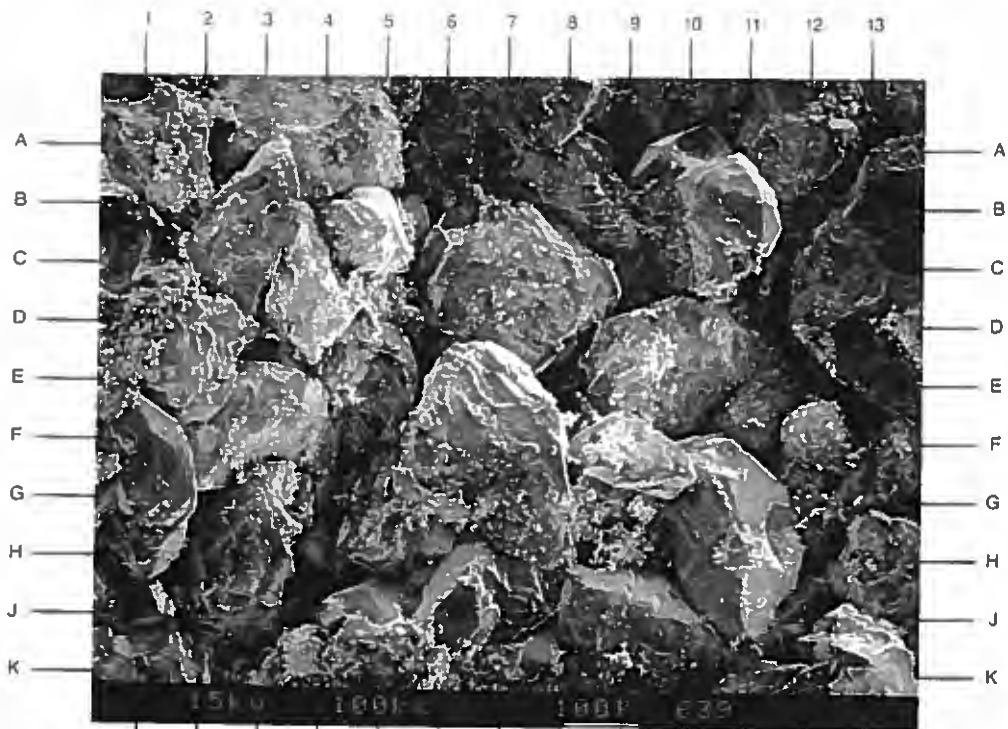
The low magnification survey photomicrograph shown on the opposite page illustrates the good, but variable, intergranular porosity in this sample. Local pores are partially blocked by secondary quartz overgrowths (A9.5,J5) and patchy authigenic kaolinite (D-E1,G-H9).

Magnification: 100X

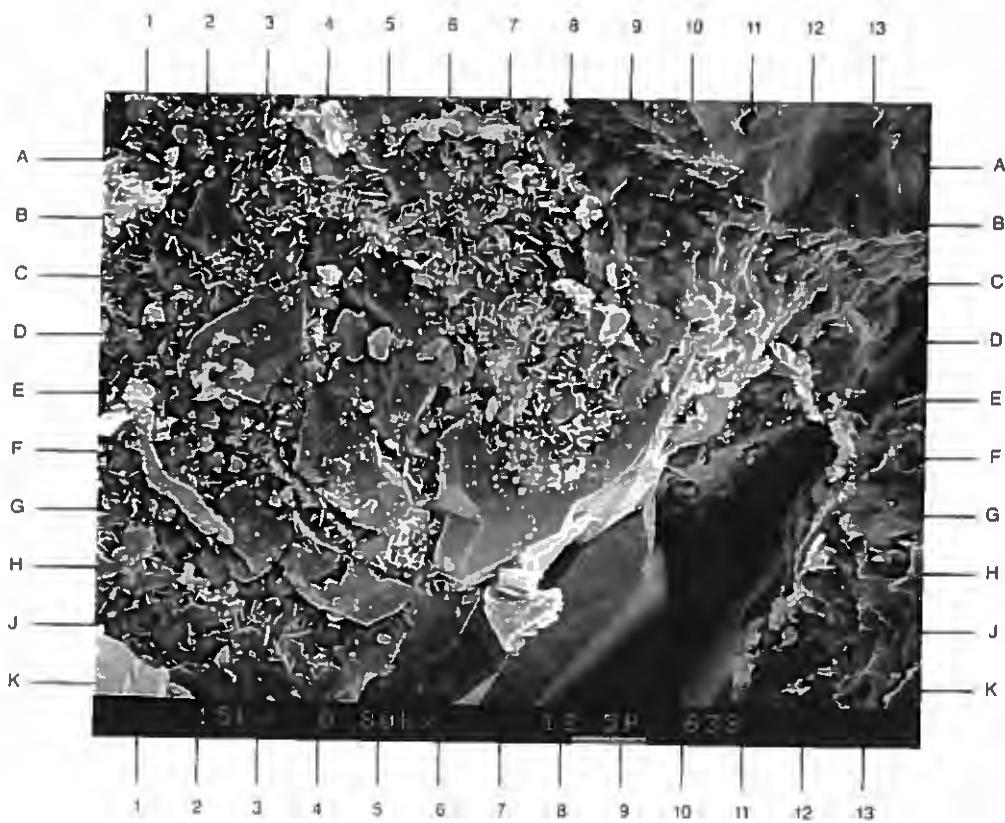
PLATE 20B

The high magnification view of the area near D8 in Plate 20A depicts a quartz framework grain with a coating of authigenic chlorite (B4-E8) and variable quartz overgrowth cement (D3,G7). The authigenic chlorite platelets have a characteristic face-to-edge orientation. Note the trace of illite in the pore throat at E12.

Magnification: 800X



A



B

SAMPLE DEPTH: 9473 FEET

PLATE 21A

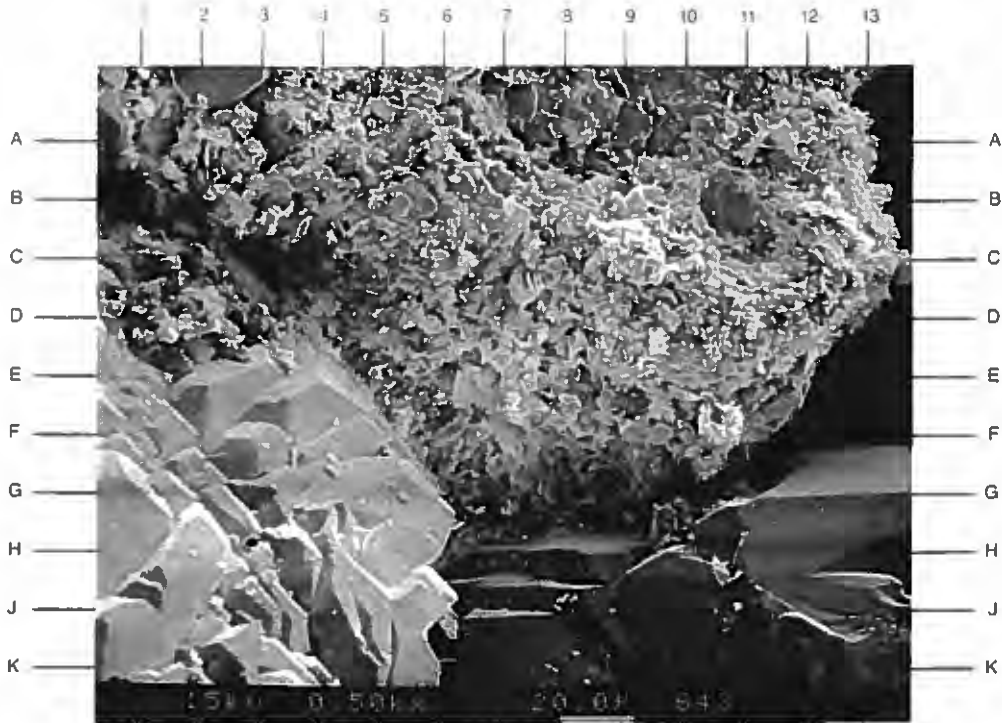
The high magnification photomicrograph illustrates a lithic grain (top and center) that is composed of quartz, chlorite, illite (minor), and encrusted with halite (NaCl). Note the well developed quartz overgrowths (lower third of photo) surrounding the lithic grain.

Magnification: 500X

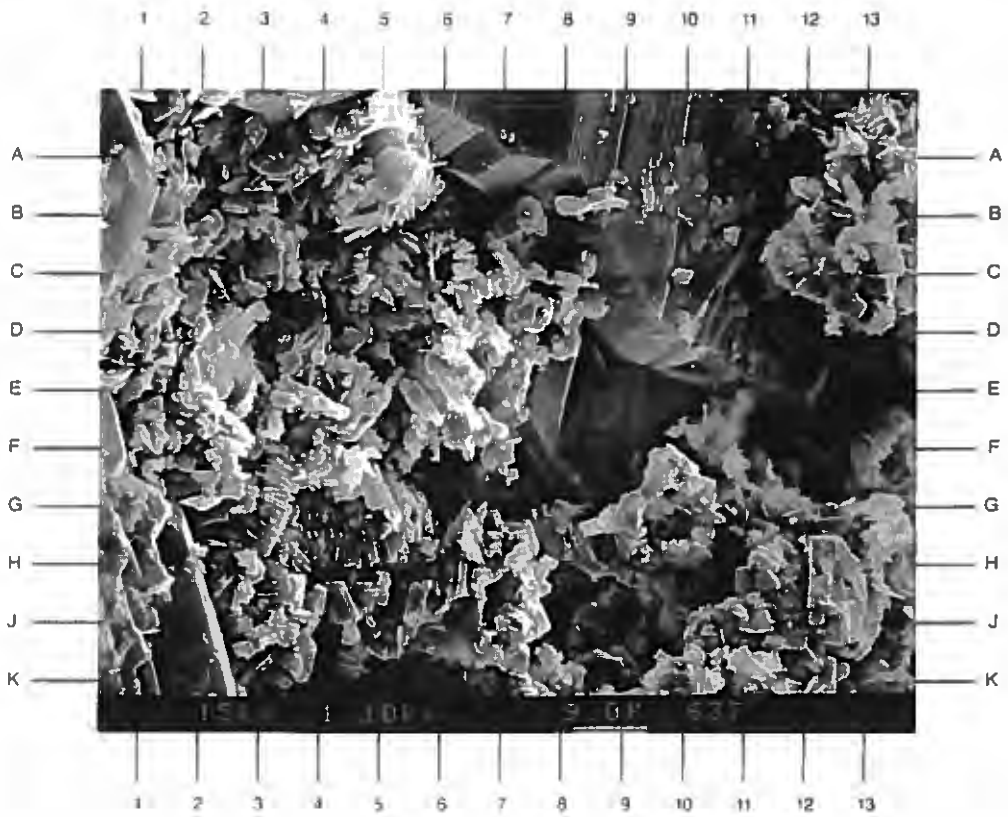
PLATE 21B

The high magnification view documents authigenic kaolinite as a patchy, pore-filling component. The typical vermicular booklets (G-H4) of this clay has high associated microporosity. Minor illite is observed intermixed with the kaolinite.

Magnification: 1,100X



A



B

SAMPLE DEPTH: 9505 FEET

PLATE 22A

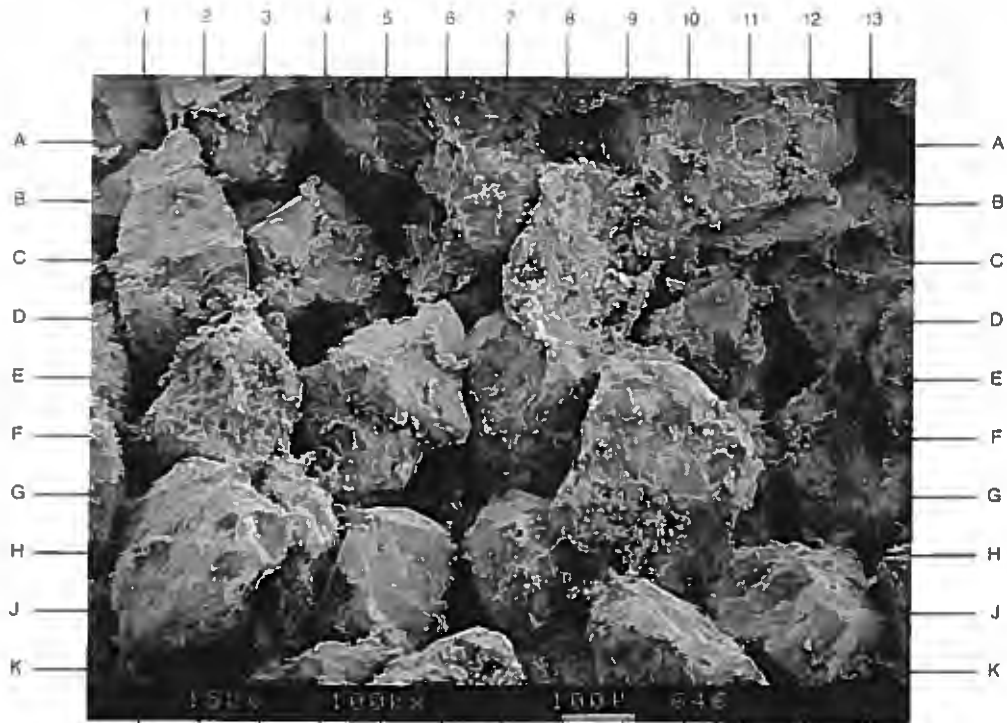
The massive, fine-grained sandstone shown in the low magnification photomicrograph identifies the fairly evenly distributed primary intergranular porosity that is enhanced by secondary dissolution (C9). Quartz overgrowths (D-E6,G-H5) is the primary cement observed.

Magnification: 100X

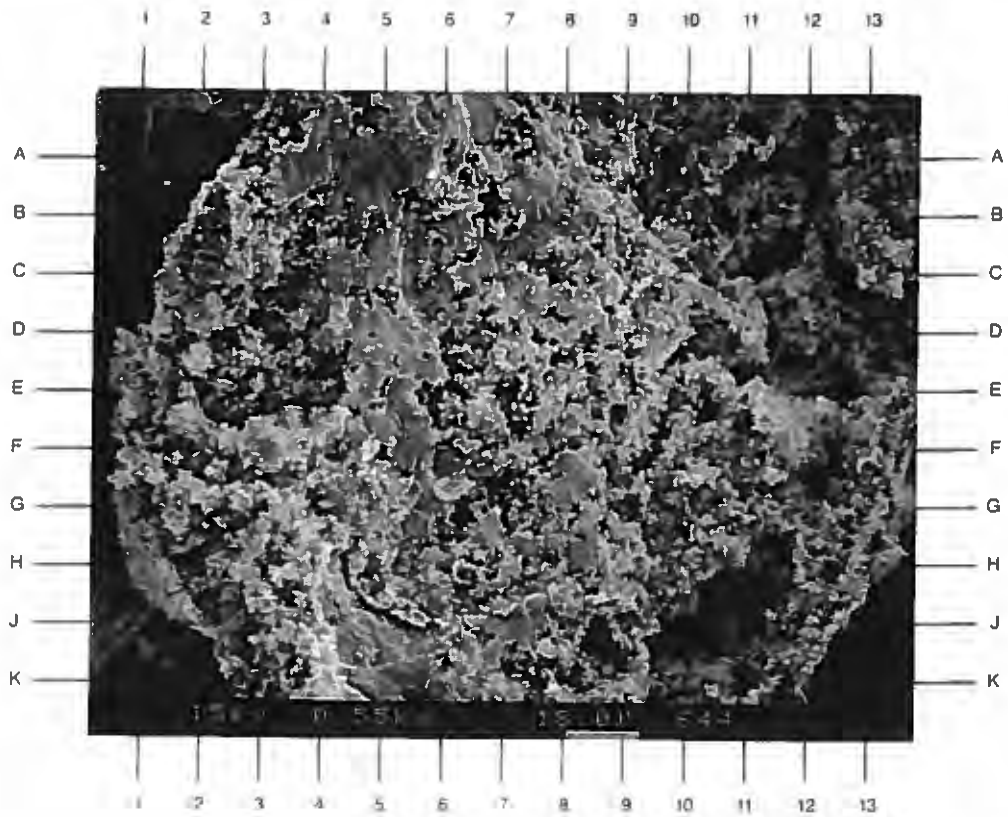
PLATE 22B

The high magnification view of Plate 22A near C8 shows a lithic fragment that is strongly leached by secondary dissolution. Note the intragranular porosity (microporosity) associated with this lithic. Internal secondary clays (F1-K4) of illite and kaolinite are also observed.

Magnification: 550X



A



B

Dupont Environmental
Delisle No. 2, S/T No. 1
Harrison County, Mississippi

File No. GN-3402

SAMPLE DEPTH: 9505 FEET

PLATE 23A

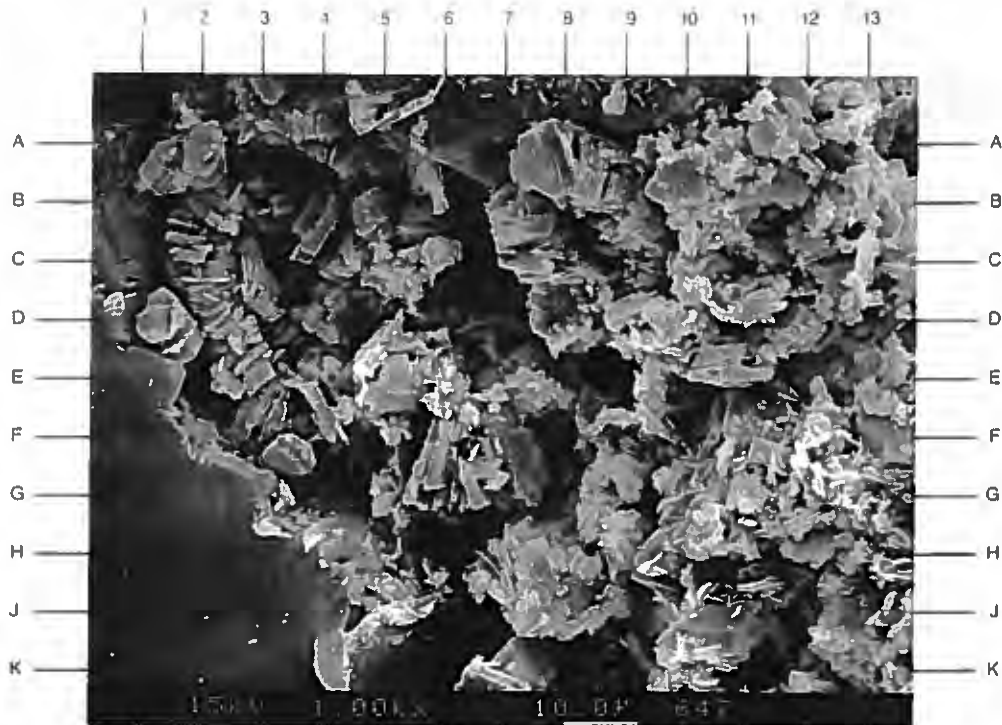
The high magnification photomicrograph on the facing page depicts aggregates of authigenic kaolinite booklets (C2,A8,F3) that are seen loosely filling selective pores. Illite is observed intermixed with kaolinite on the right side of the photo.

Magnification: 1,000X

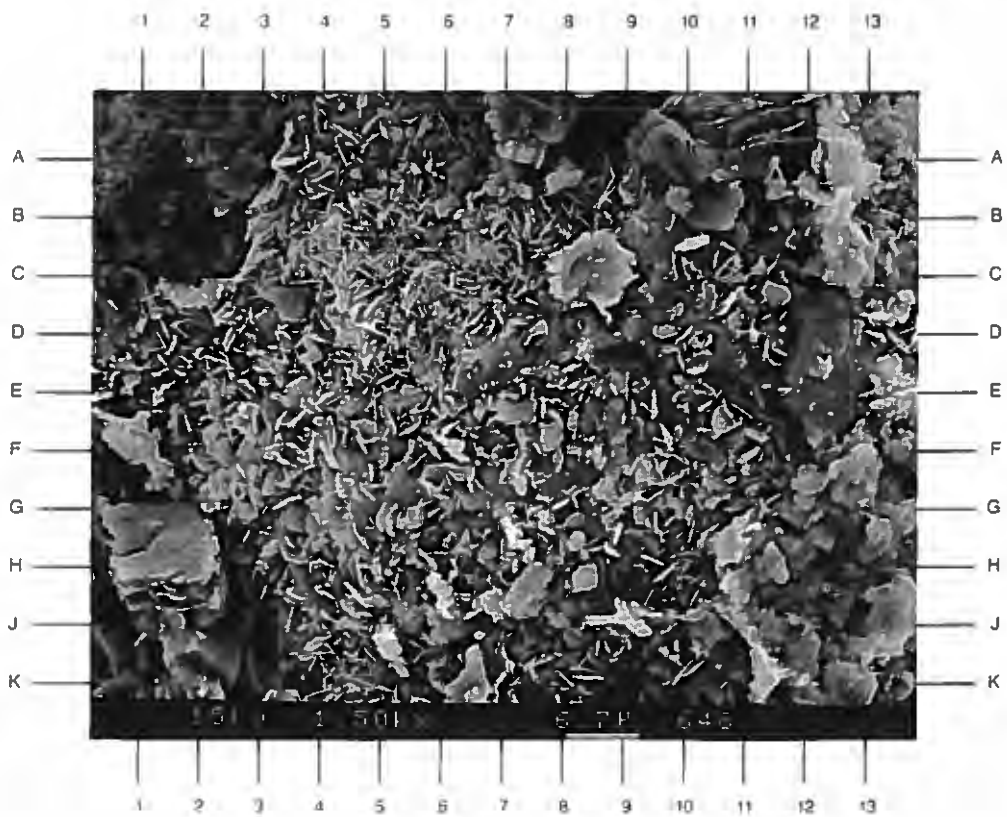
PLATE 23B

The high magnification view shown here depicts authigenic chlorite coating quartz sand grains. The chlorite platelets show face-to-edge, or card-house arrangement on the grain surfaces. Note the quartz overgrowth at D-E12.

Magnification: 1,500X



A



B

SAMPLE DEPTH: 9562 FEET

PLATE 24A

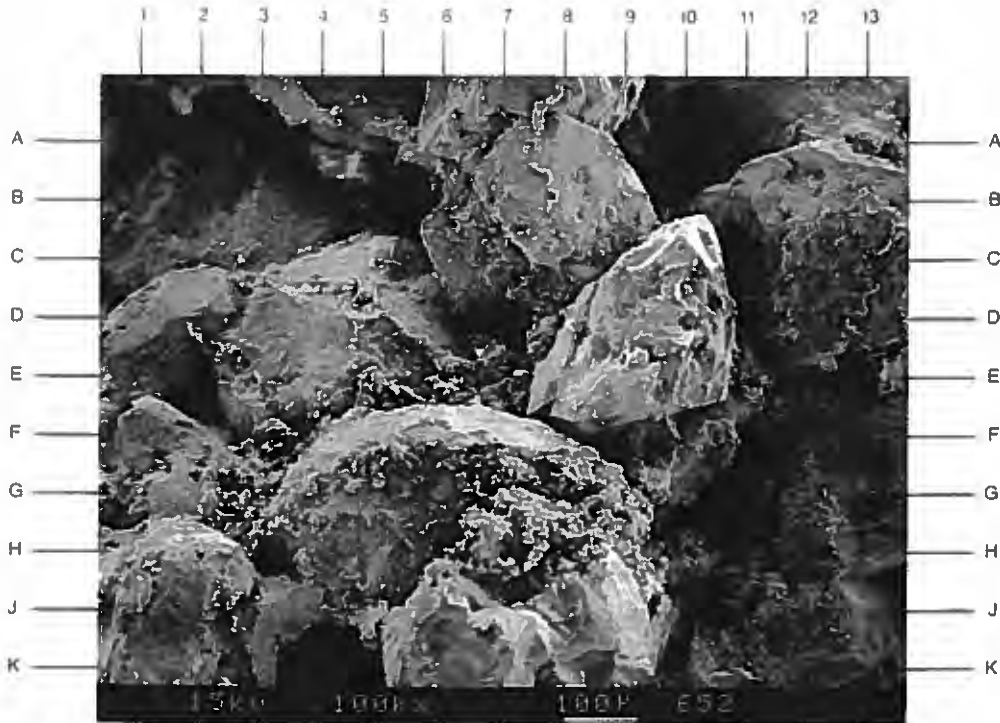
The low magnification survey photomicrograph taken from 9562' shows a coarser grain size in this sample than in the previous samples (see Plate 20A and 22A) described. Large, intergranular pores (B5,A10,G11) are evenly distributed and slightly enhanced by secondary dissolution (K4). Note the quartz overgrowths (E8,K6.5) and pore-filling clay (G3,G-H7).

Magnification: 100X

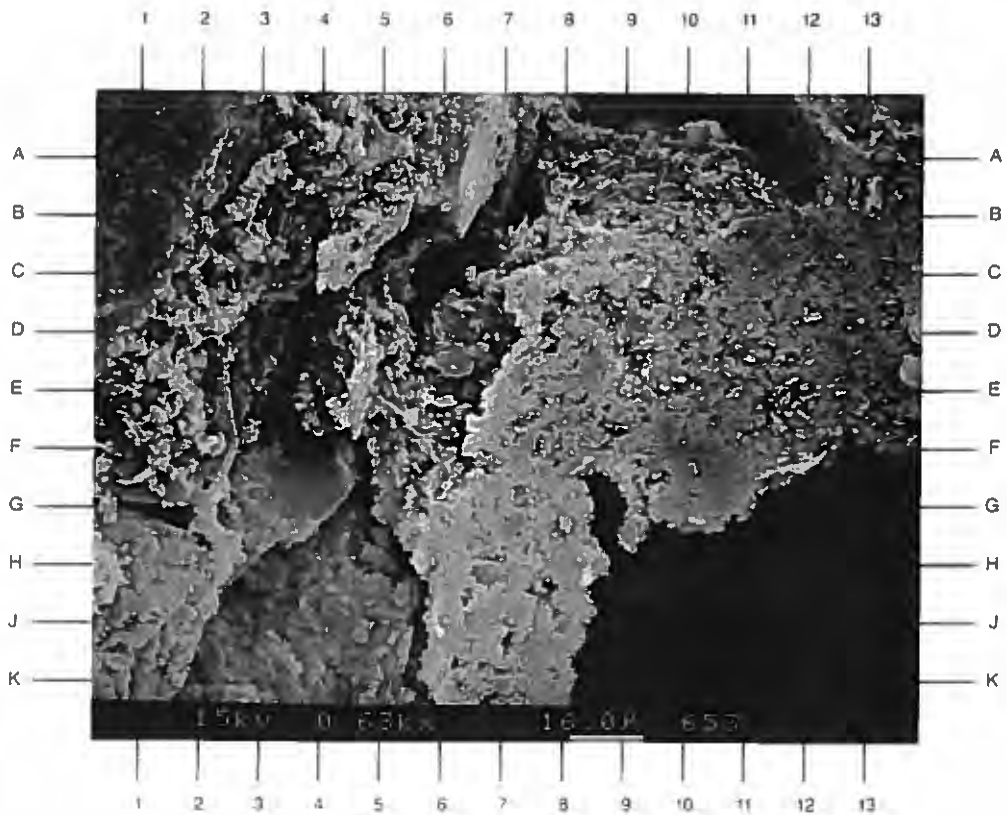
PLATE 24B

The high magnification view of the area near J3 in Plate 24A shows a possible plagioclase remnant grain rim (E13-K8) after secondary dissolution and the resulting grain moldic porosity (J12). These remnant rims are occasionally iron-rich due to possible iron-oxide staining. Note the authigenic kaolinite booklets at B3.

Magnification: 630X



A



B

Dupont Environmental
Delisle No. 2, S/T No. 1
Harrison County, Mississippi

File No. GN-3402

SAMPLE DEPTH: 9562 FEET

PLATE 25A

The sandstone taken from 9562' is shown on the facing page having clean, open, intergranular pores (A7-E7,F3). The feldspar grain (right side of photo) is partially leached, but not significantly altered to clay. Note the quartz overgrowths at B6.5 and J-K2.

Magnification: 200X

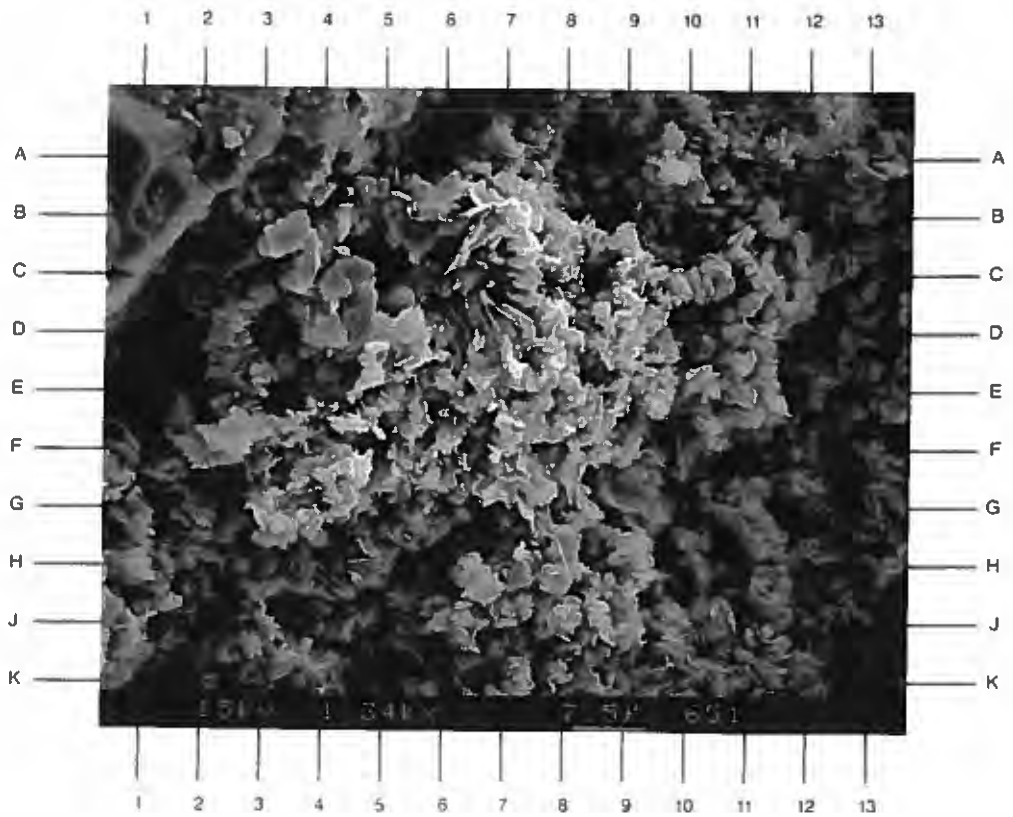
PLATE 25B

The high magnification view pictured here show the patches of authigenic, pore-filling clay that is occasionally found in this sample. This clay is composed of a fine intermixture of authigenic kaolinite (books and plates) and illite (wispy component).

Magnification: 1,340X



A



B

SAMPLE DEPTH: 9796 FEET

PLATE 26A

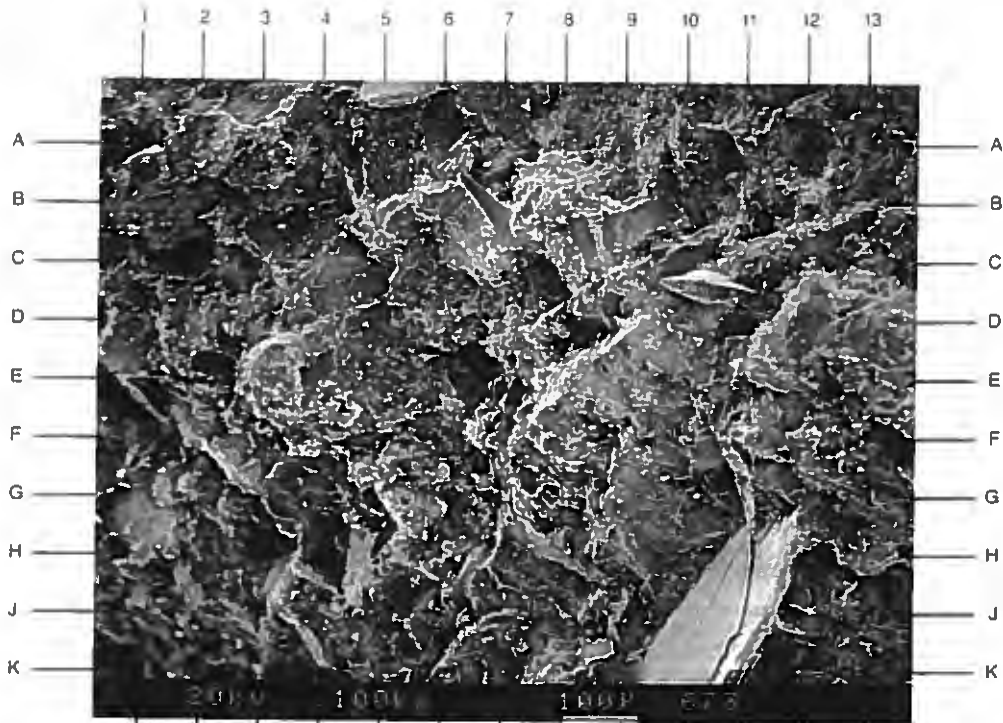
The low magnification survey photomicrograph shown here documents the poor reservoir quality of the sandstone. Visible porosity (C2,E6.5,A12) is severely reduced by quartz overgrowths and calcite cementation. Intergranular porosity and dissolution porosity is widely scattered and discontinuous. Note the mica at J11, showing minor deformation.

Magnification: 100X

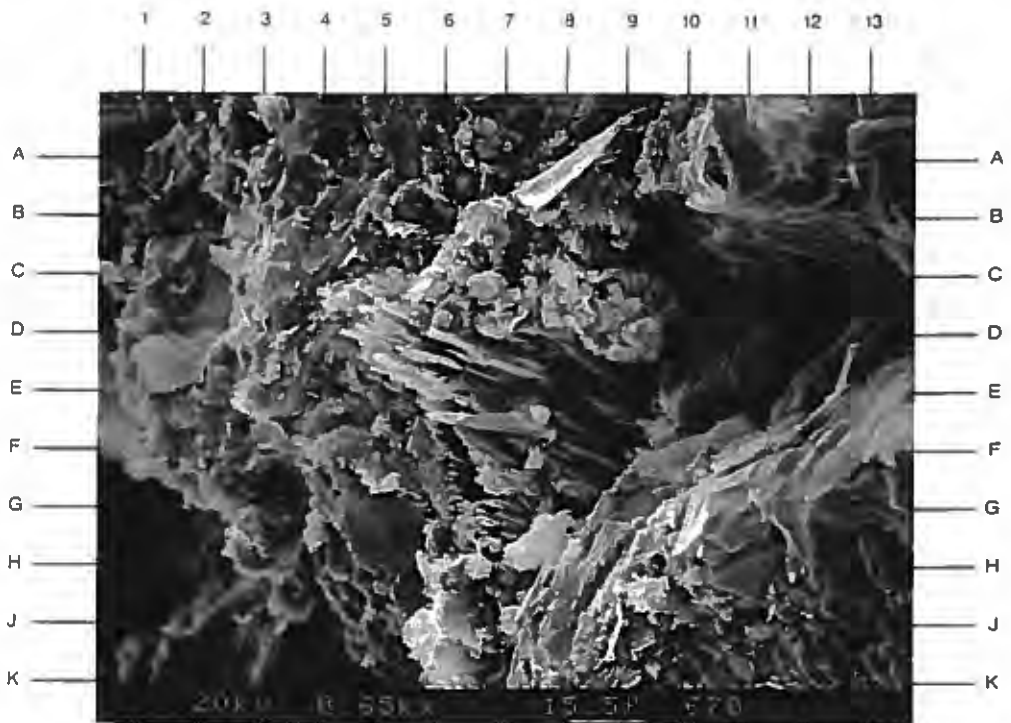
PLATE 26B

The high magnification view of the area near D8 in Plate 26A shows secondary dissolution porosity that is associated with a strongly leached plagioclase feldspar grain. Note the dense, well-cemented sandstone surrounding the leached grain.

Magnification: 650X



A



B

SAMPLE DEPTH: 9796 FEET

PLATE 27A

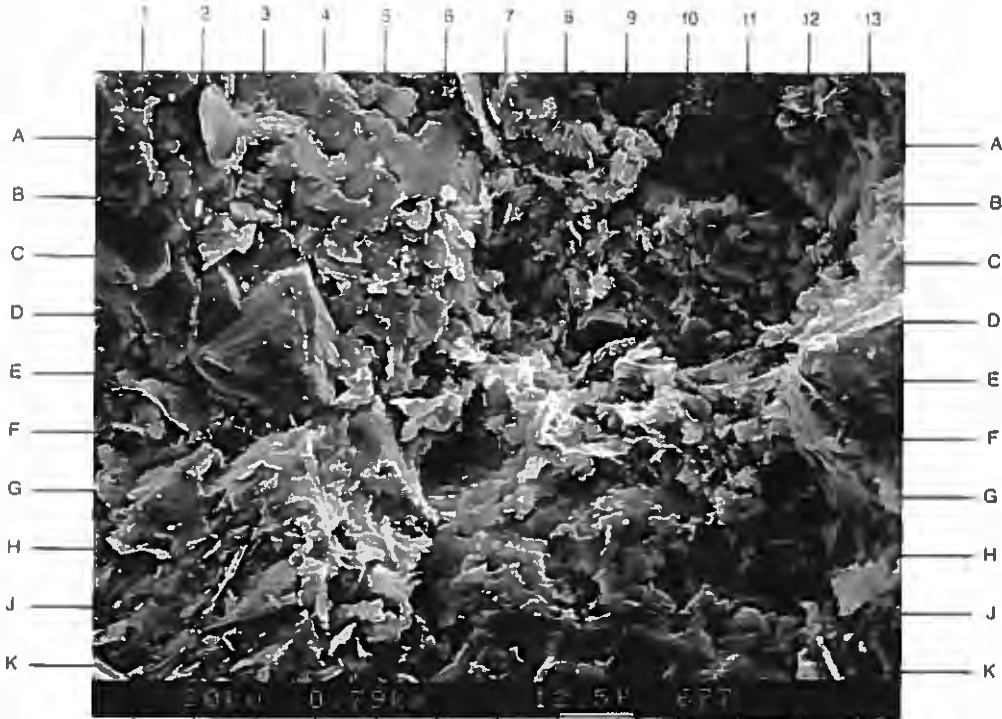
The high magnification photomicrograph illustrates patches of detrital matrix, or pseudomatrix, which is largely composed of illite that may have been recrystallized. Note the authigenic kaolinite booklets at A8 and calcite cement as a pore-fill at G3.

Magnification: 790X

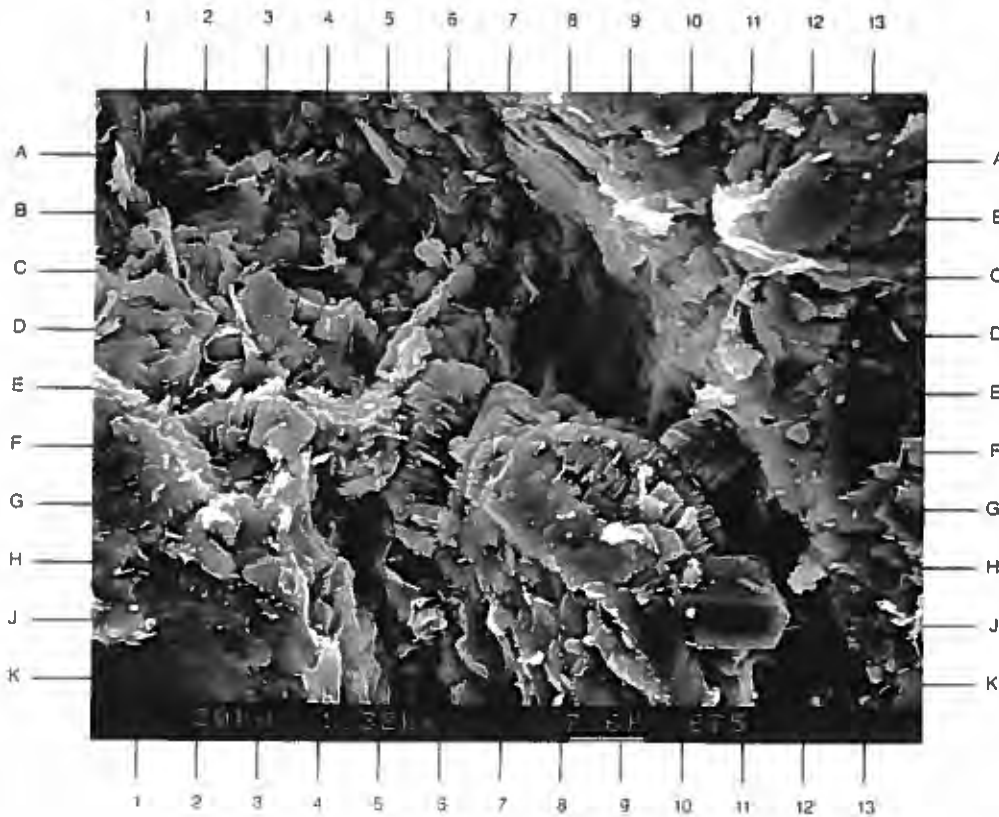
PLATE 27B

The high magnification view documents an intergranular pore that is enlarged by secondary dissolution. The pore is partially infilled by booklets of authigenic kaolinite. Note the quartz overgrowths at J11.

Magnification: 1,320X



A



B

Dupont Environmental
Delisle No. 2, S/T No. 1
Harrison County, Mississippi

File No. GN-3402

SAMPLE DEPTH: 9800 FEET

PLATE 28A

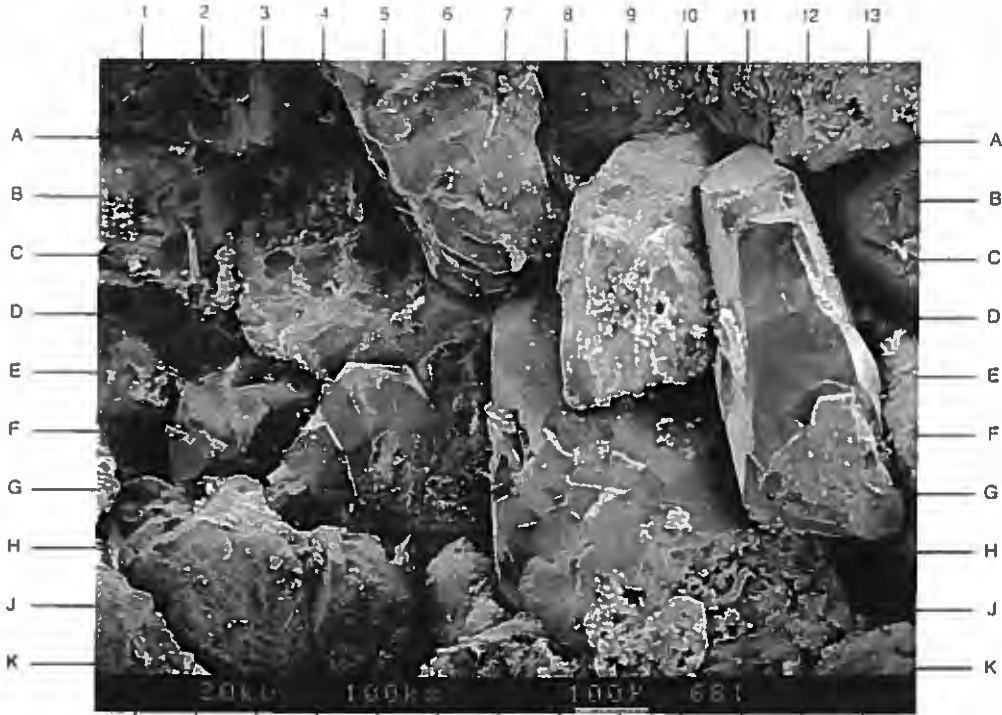
The medium-grained sandstone shown in the low magnification survey photomicrograph has very good reservoir quality. Primary intergranular porosity (A4,A8,H13) is dominant with moderate to minor secondary dissolution porosity (H11) observed. Quartz overgrowths (E-F5,B13) are the primary cement type.

Magnification: 100X

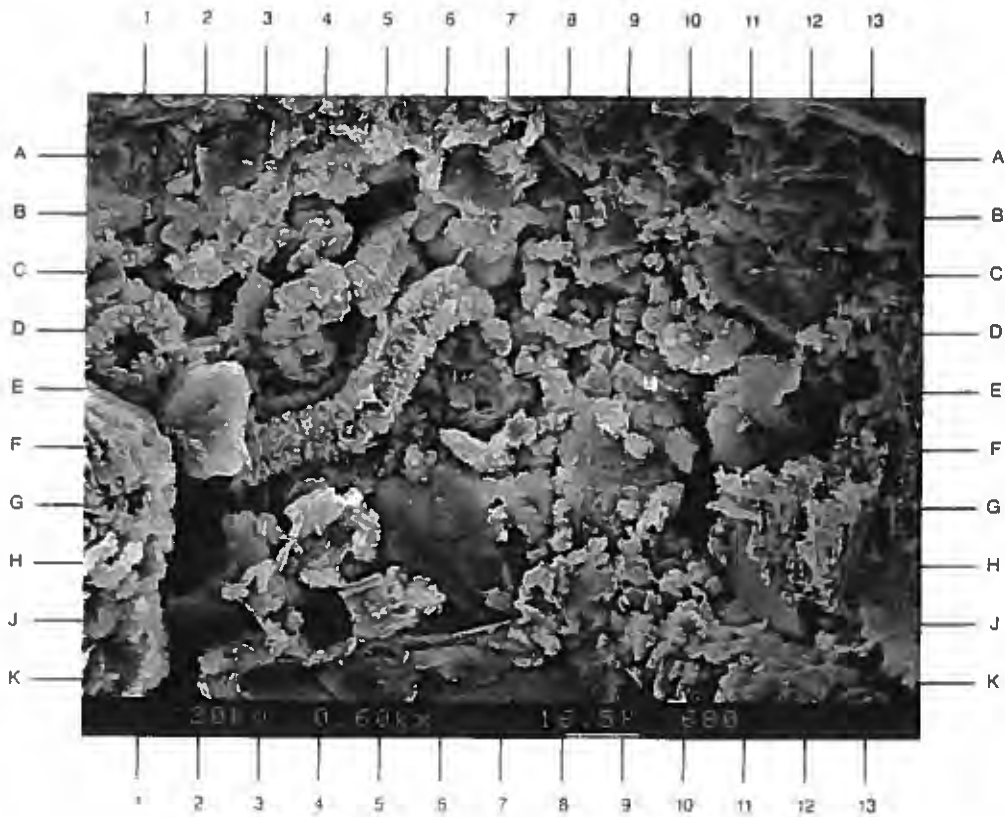
PLATE 28B

The high magnification view near J11 of Plate 28A shows authigenic kaolinite occurring as vermicular (worm-like) booklets in a loose pore-filling aggregate. Note the dissolved feldspar (G12) and intermixed illite (A7,B-C2) present.

Magnification: 600X



A



B

Dupont Environmental
Delisle No. 2, S/T No. 1
Harrison County, Mississippi

File No. GN-3402

SAMPLE DEPTH: 9800 FEET

PLATE 29A

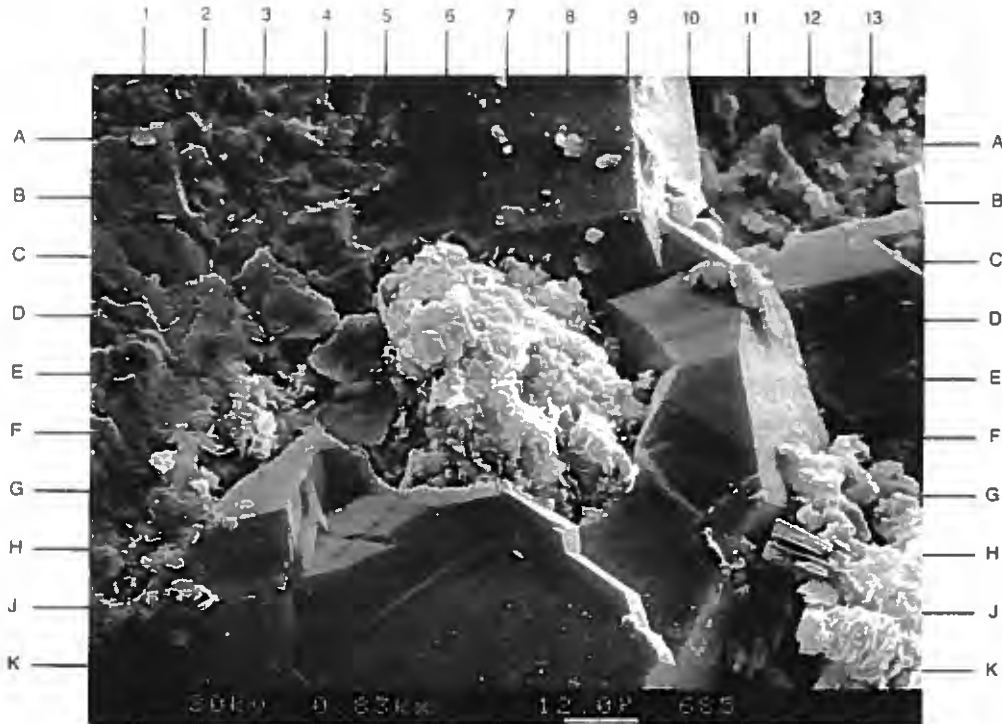
As seen in the photomicrograph on the facing page, salt (Halite;NaCl) tends to precipitate (D5-F8) on grain surfaces coated by authigenic chlorite (C7,D8,F-G6). Quartz overgrowth crystal surfaces (H2-H11,E10) are not coated by halite. Note the authigenic kaolinite booklets at H12.

Magnification: 830X

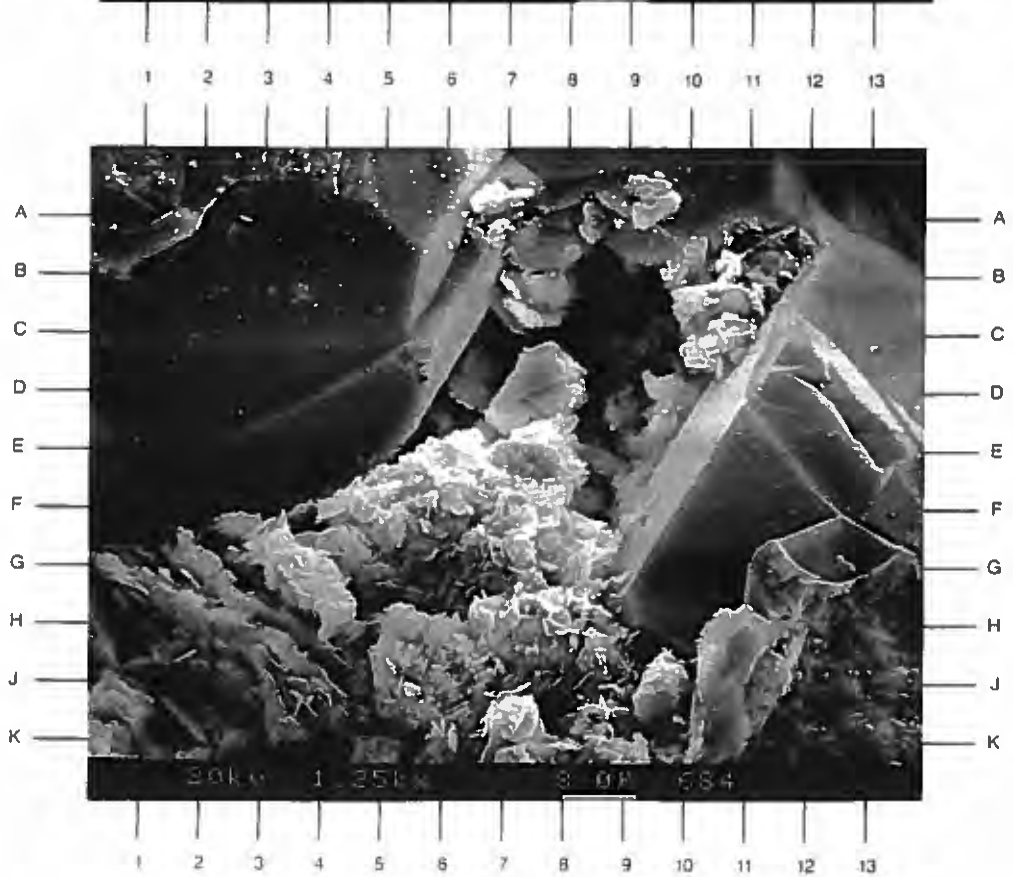
PLATE 29B

The high magnification view of an intergranular pore shows quartz overgrowths (C6,E12) pore fill and grain coating authigenic chlorite (G7). Authigenic kaolinite (B7.5) is also observed. Note the high surface area of chlorite and its associated microporosity.

Magnification: 1,250X



A



B

SAMPLE DEPTH: 9802 FEET

PLATE 30A

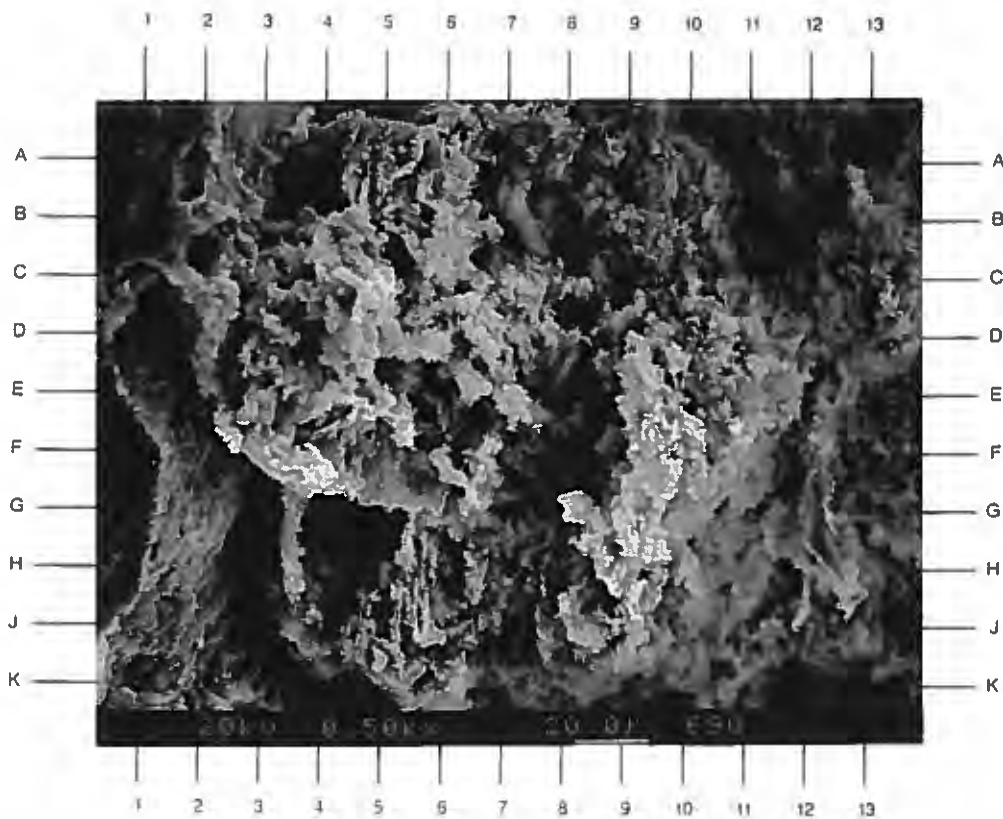
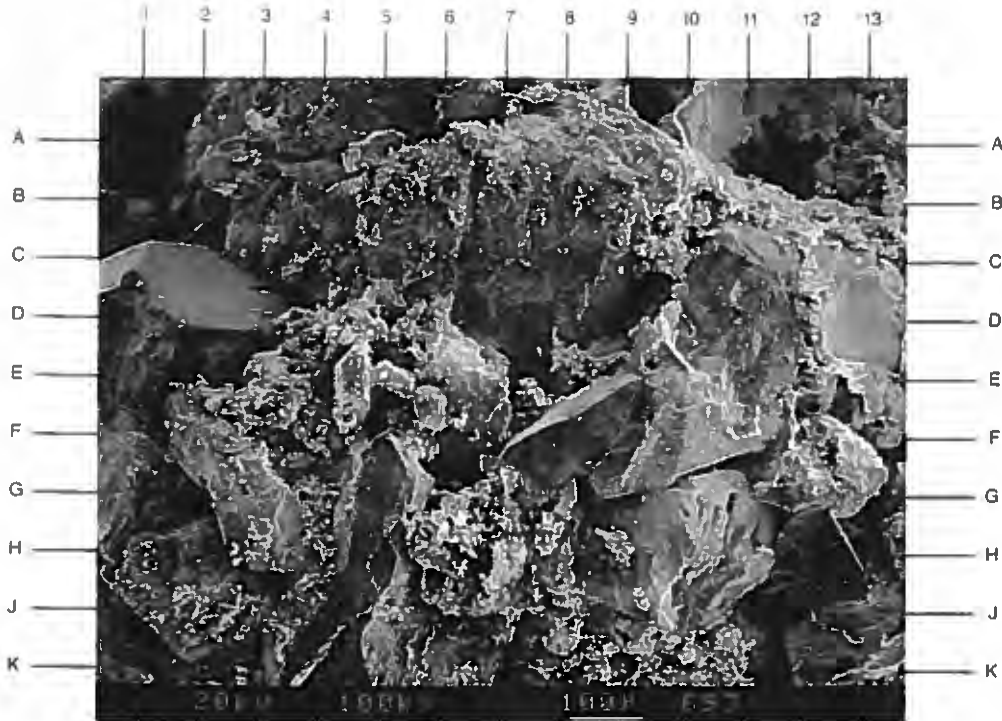
The massive sandstone taken from 9802' is shown on the facing page under low magnification. Clusters (or zones) of intergranular porosity, some of which are partially blocked by a titanium (minor iron) precipitate (E3,H6.5), are observed. Note the quartz overgrowths (G5,F8) present.

Magnification: 100X

PLATE 30B

The high magnification view of the area near H7 in Plate 30A shows a corroded sand grain (or feldspar) which contains abundant microporosity with high associated surface area. These areas appear to serve as sites for precipitation of the titanium (minor iron) precipitate.

Magnification: 500X



Dupont Environmental
Delisle No. 2, S/T No. 1
Harrison County, Mississippi

File No. GN-3402

SAMPLE DEPTH: 9802 FEET

PLATE 31A

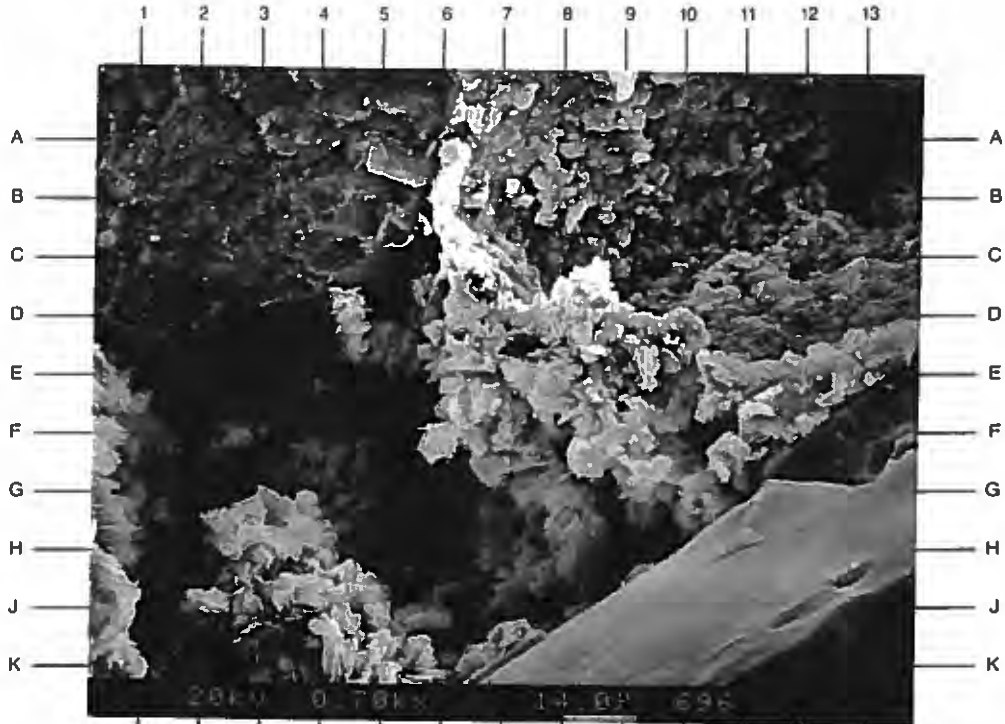
The high magnification survey photomicrograph seen on the opposite page identifies illite (C6-E11) occurring as a patchy matrix clay and vague authigenic kaolinite (G0.5,G7). The titanium phase precipitate (D8,D4.5) is commonly associated with the clays present in the sample.

Magnification: 700X

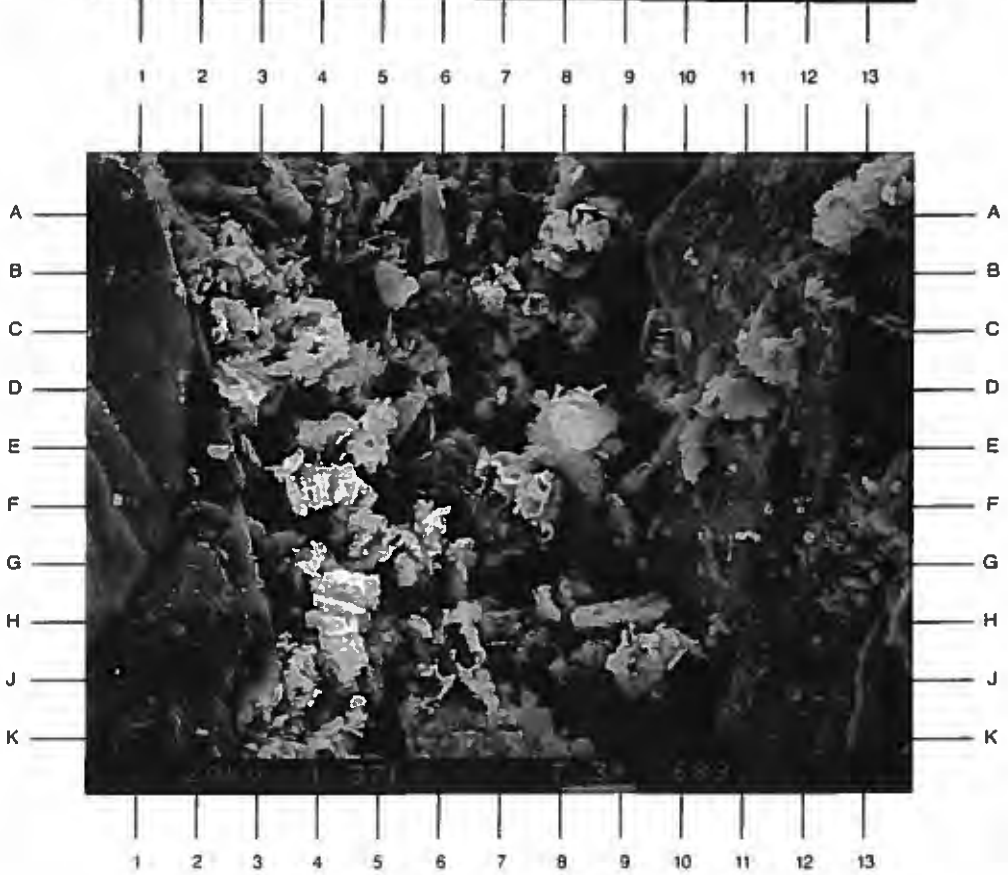
PLATE 31B

A high magnification view of the titanium (minor iron) precipitate (C3.5,D-E8,H4.5) is pictured in the photomicrograph. The precipitate tends to nucleate/precipitate on high surface area matrix fines, as seen here. It is also commonly observed in association with partially leached lithics (not pictured).

Magnification: 1,370X



A



B

SAMPLE DEPTH: 9810 FEET

PLATE 32A

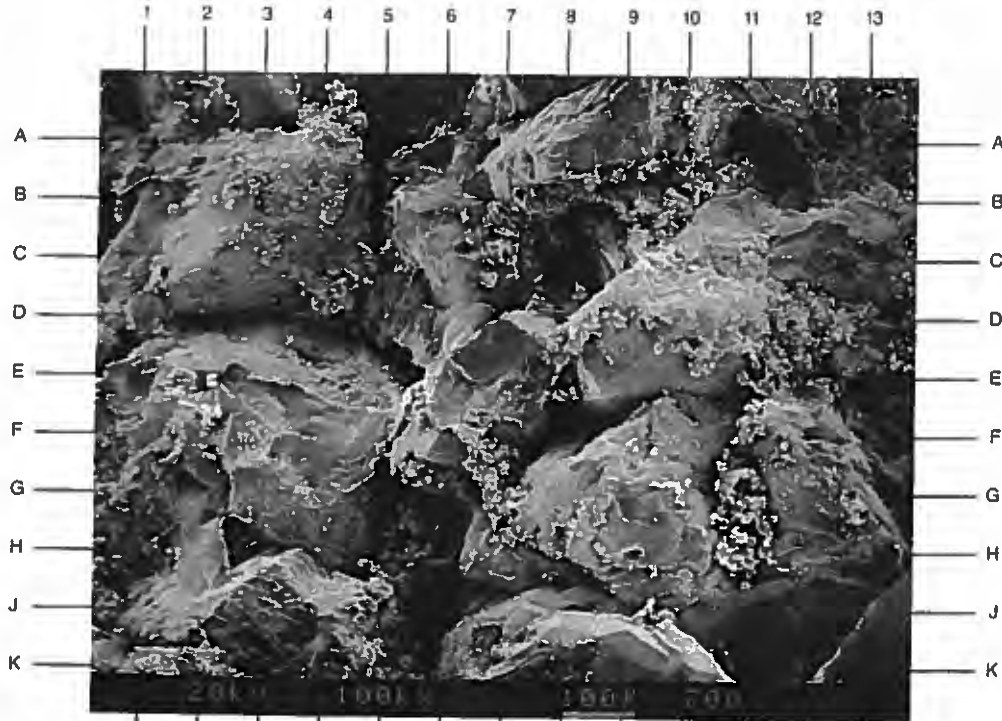
The low magnification survey photomicrograph illustrates fairly good porosity development in this quartz overgrowth-cemented sandstone. Intergranular porosity (A5) is the predominant pore type. Secondary pores (C8) are also noted. Abundant titanium precipitate (B10,D12,G-H11) is observed in the pores.

Magnification: 100X

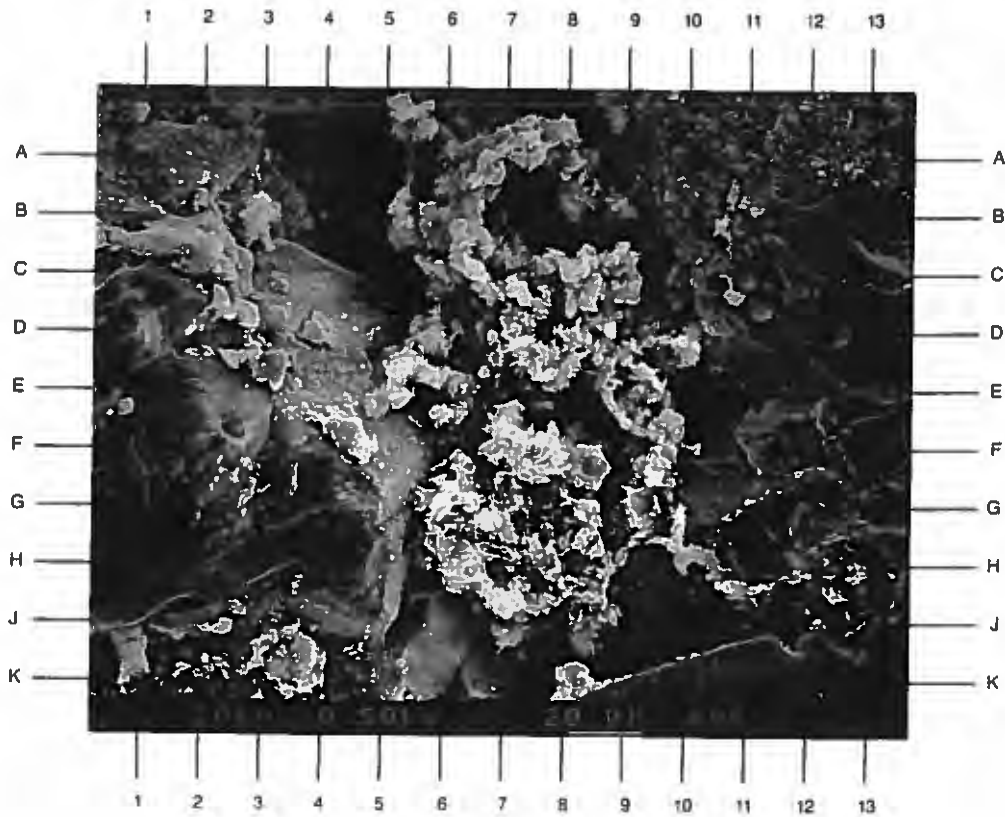
PLATE 32B

The high magnification view of the area near H11 in Plate 32A documents a highly microporous lithic fragment extensively leached by secondary dissolution. This dissolution aids in communication of the two intergranular pores (A5,H10) in the field of view. Minor coating by a titanium component (E5,F7) is seen.

Magnification: 500X



A



B

Dupont Environmental
Delisle No. 2, S/T No. 1
Harrison County, Mississippi

File No. GN-3402

SAMPLE DEPTH: 9810 FEET

PLATE 33A

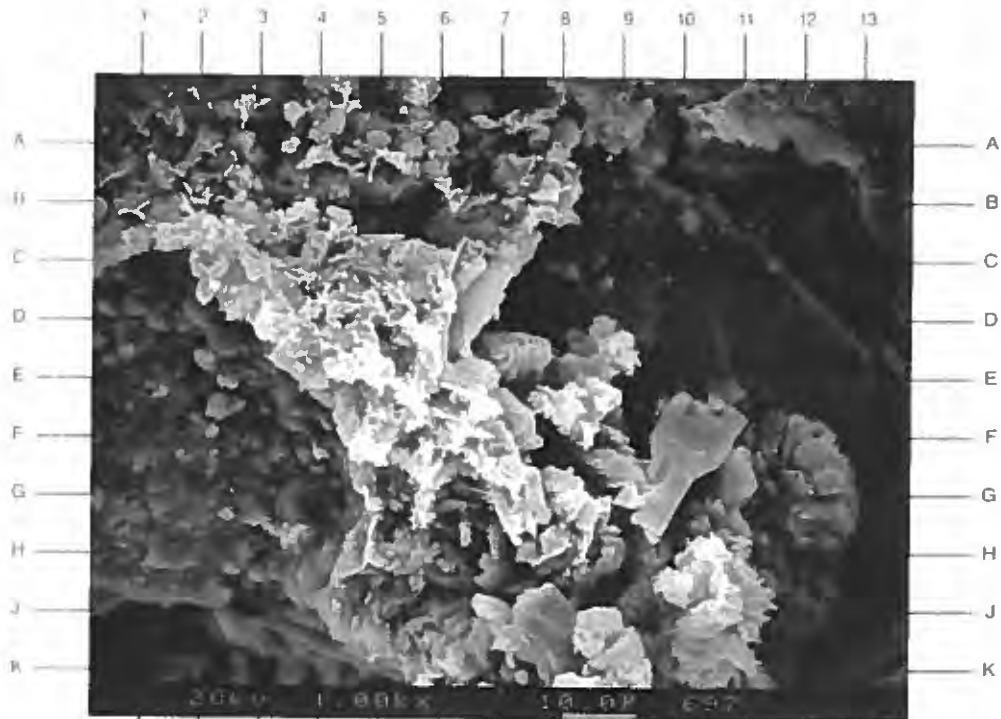
A patch of illitic clay (B2-D5) is seen partially infilling an intergranular pore. Titanium precipitate (D-E5,F5.5,H-J10) is observed coating this illitic clay, as well as some pore walls (E2.5).

Magnification: 1,000X

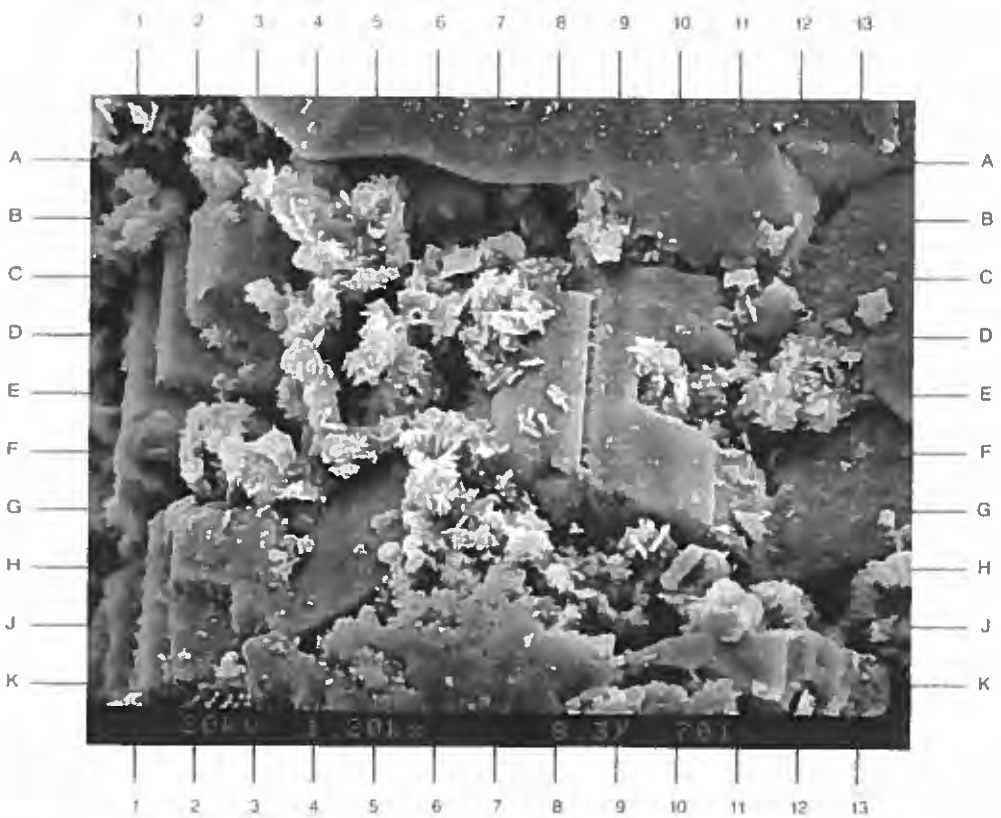
PLATE 33B

The high magnification view in the photomicrograph on the opposite page shows a close-up of authigenic, grain-coating chlorite plates (C4,F3,G6) coated by a titanium precipitate. This chlorite clay has formed between quartz overgrowths (C2,H2,F9,A11).

Magnification: 1,200X



A



B

SAMPLE DEPTH: 9820 FEET

PLATE 34A

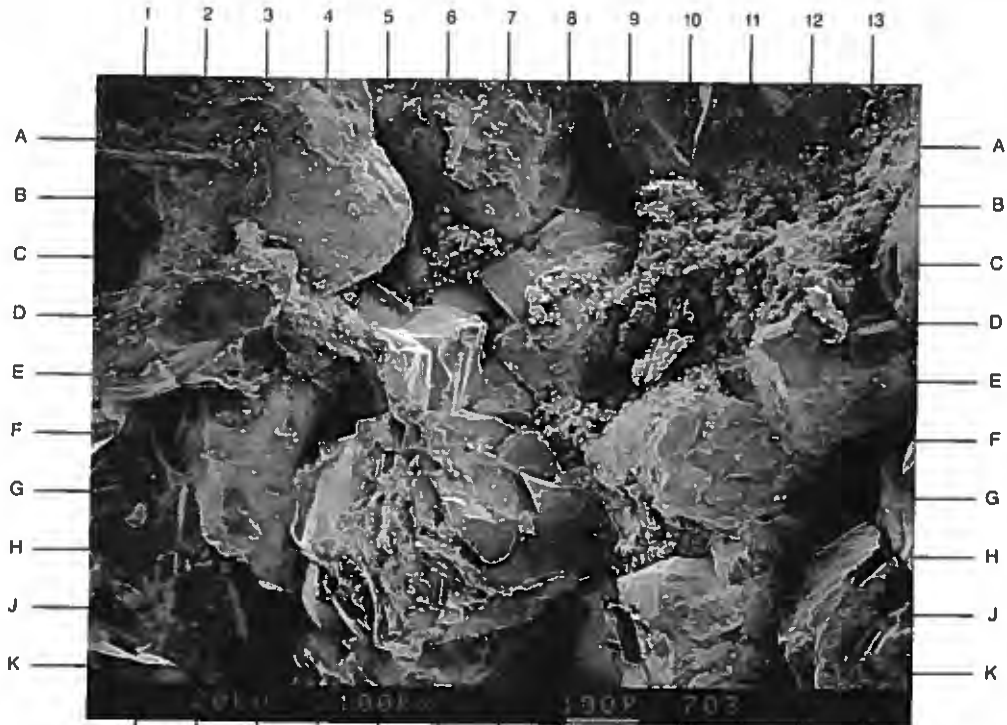
The low magnification photomicrograph on the facing page depicts a medium-grained sandstone with very good reservoir quality. Intergranular porosity (C1,B8.5,K8) is well developed, with local, minor pore blockage by natural clays (C10,B12.5), titanium precipitate (D-E10), and quartz overgrowths (D13,D-E6).

Magnification: 100X

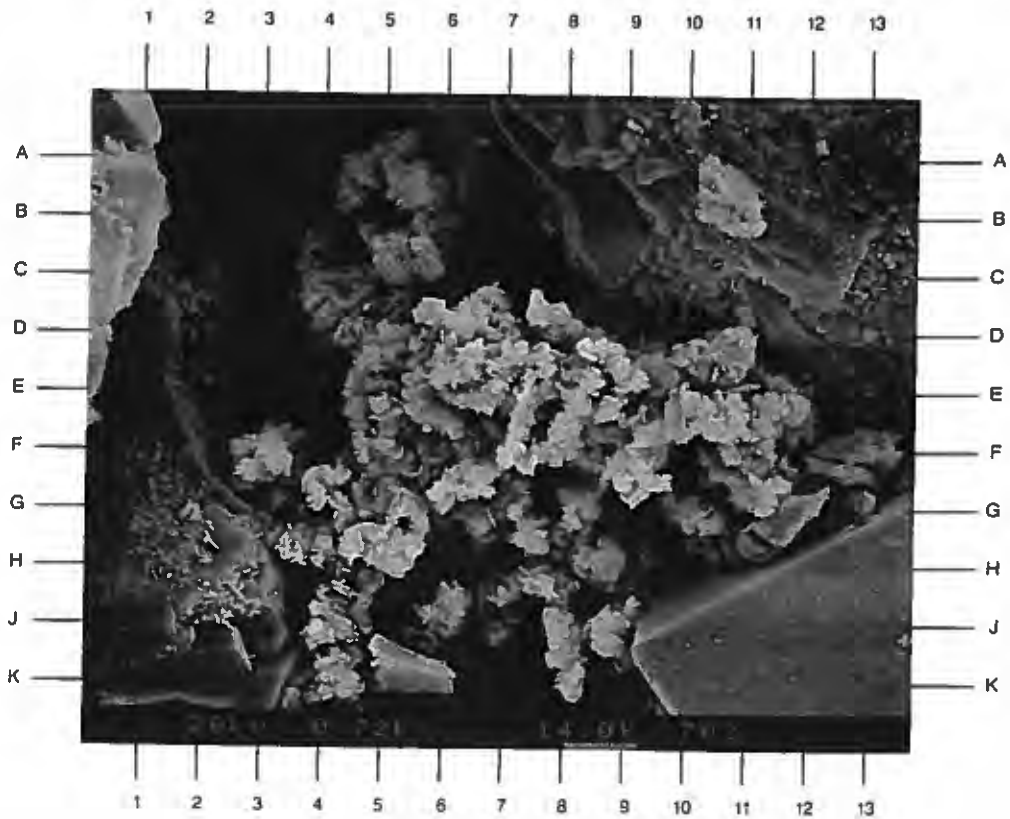
PLATE 34B

The high magnification view of the area near C6 in Plate 34A shows a late-enplaced titanium (oxide?) phase coating an aggregate of unknown fines in an intergranular pore. Fines appear to be both illitic and intermixed authigenic kaolenite. Note the quartz overgrowths (A6.5,J10) present.

Magnification: 720X



A



B

SAMPLE DEPTH: 9820 FEET

PLATE 35A

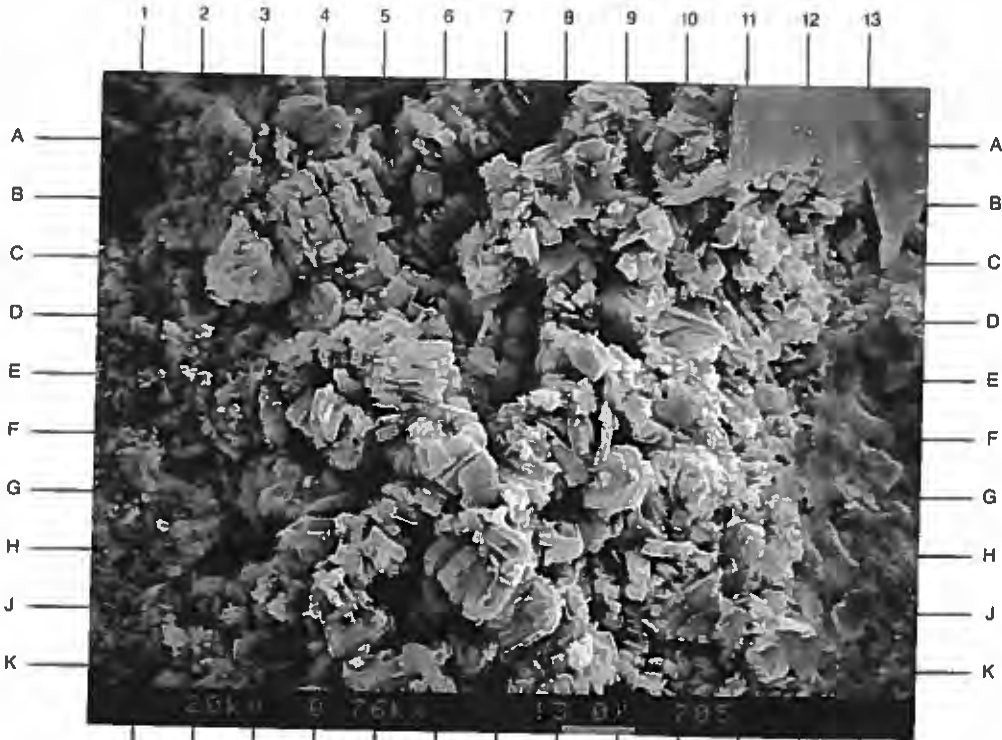
An uncommon patch of authigenic kaolinite is seen in this sandstone in the photomicrograph on the facing page. This clay is displayed in typical booklet form (E5.5,F4) and occurs in loose, pore-filling aggregates. Note the microporosity associated with the clay.

Magnification: 760X

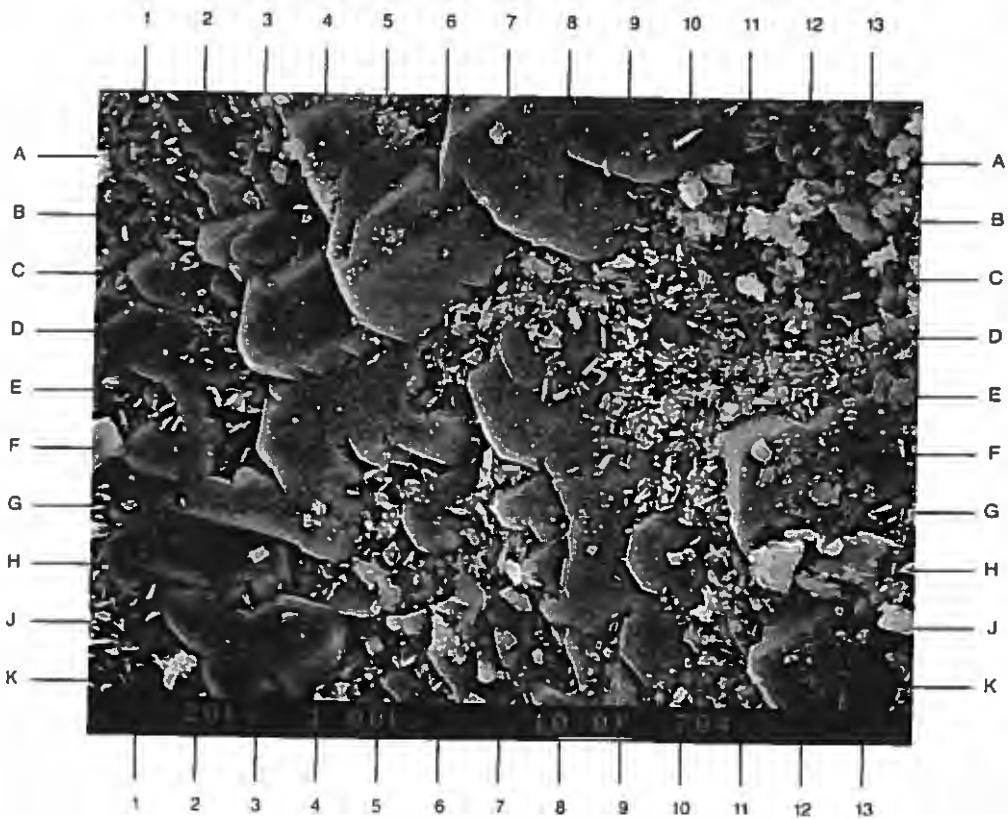
PLATE 35B

This high magnification view shows a close-up of a quartz sand grain surface containing a light coating of authigenic chlorite (A1,E9,D12) occurring between quartz overgrowth crystal faces (C4,E7). The individual chlorite platelets have been "thickened" by titanium coatings.

Magnification: 1,000X



A



B

SAMPLE DEPTH: 9843 FEET

PLATE 36A

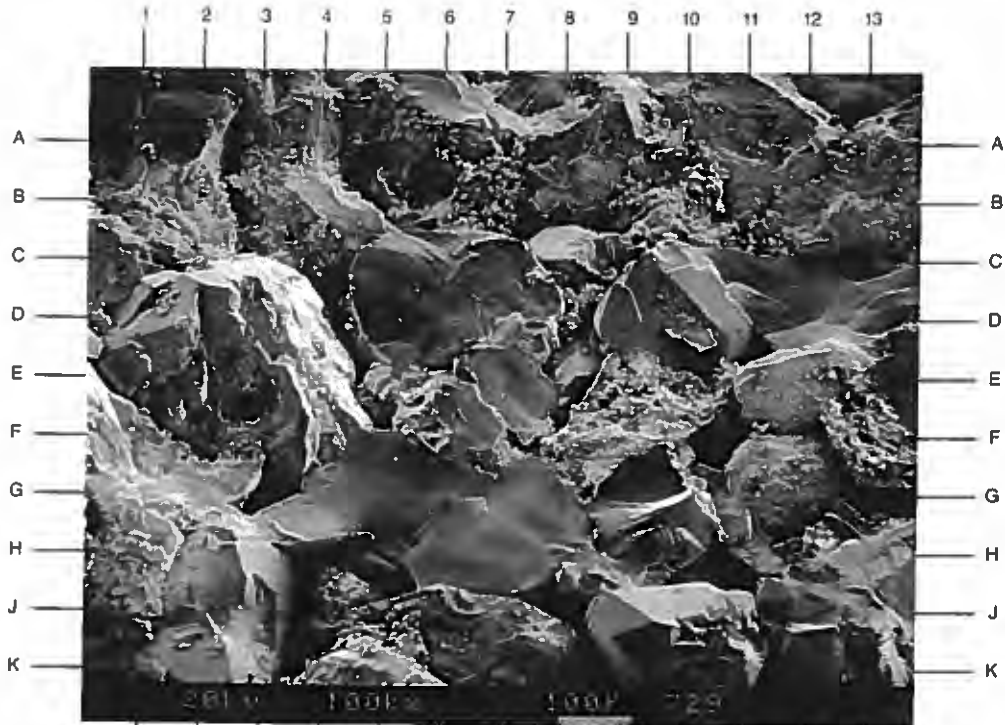
The medium-grained sandstone taken from 9843' is shown on the facing page under low magnification. Regions of fairly well connected, open intergranular porosity (C4,H-J5,H-J10.5) are contrasted with areas cemented by quartz overgrowths (D12,G-H6.5) and kaolinite (B7). The fines are typically coated by a titanium precipitate.

Magnification: 100X

PLATE 36B

The high magnification view of the area near B7 in Plate 36A shows a titanium-rich precipitate coating "fines". These fines, or the precipitate itself, have a vague, blocky shape which may represent authigenic kaolinite remnant forms. Note the quartz overgrowths (B1,A3) present.

Magnification: 760X



A



B

SAMPLE DEPTH: 9843 FEET

PLATE 37A

In this relatively tight portion of the sample two feldspar sand grains (E4,J12) are partially leached. Resultant intragranular porosity is largely ineffective, but can enhance the permeability in the zone in areas where more intergranular porosity is present. Leaching of grains, however, also contributes to the overall fines load of the pore system.

Magnification: 400X

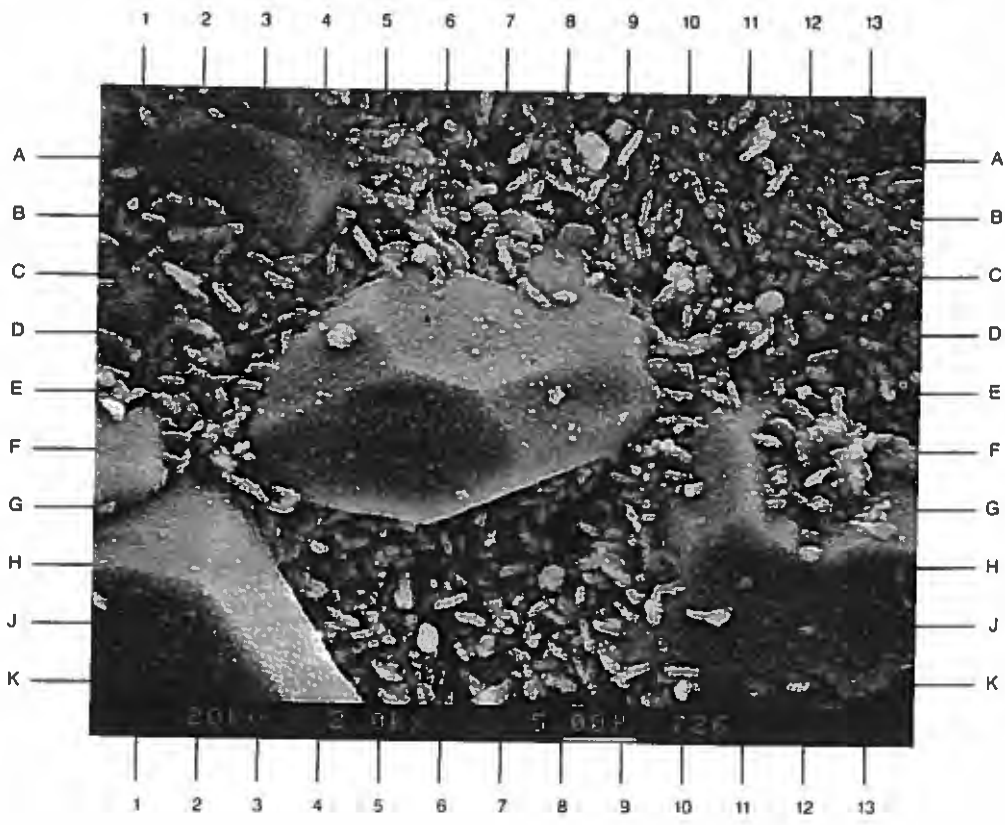
PLATE 37B

A close-up of a sand grain surface shows the micro-granular coating of a titanium-rich material on both authigenic chlorite flakes (B6,C10,H7) and quartz overgrowths (E6,J2,H12). This coating is more evident as a thickening of chlorite plates, but the fine, "bumpy" texture is noted throughout the sample.

Magnification: 2,000X



A



B

Dupont Environmental
Delisle No. 2, S/T No. 1
Harrison County, Mississippi

File No. GN-3402

SAMPLE DEPTH: 9852 FEET

PLATE 38A

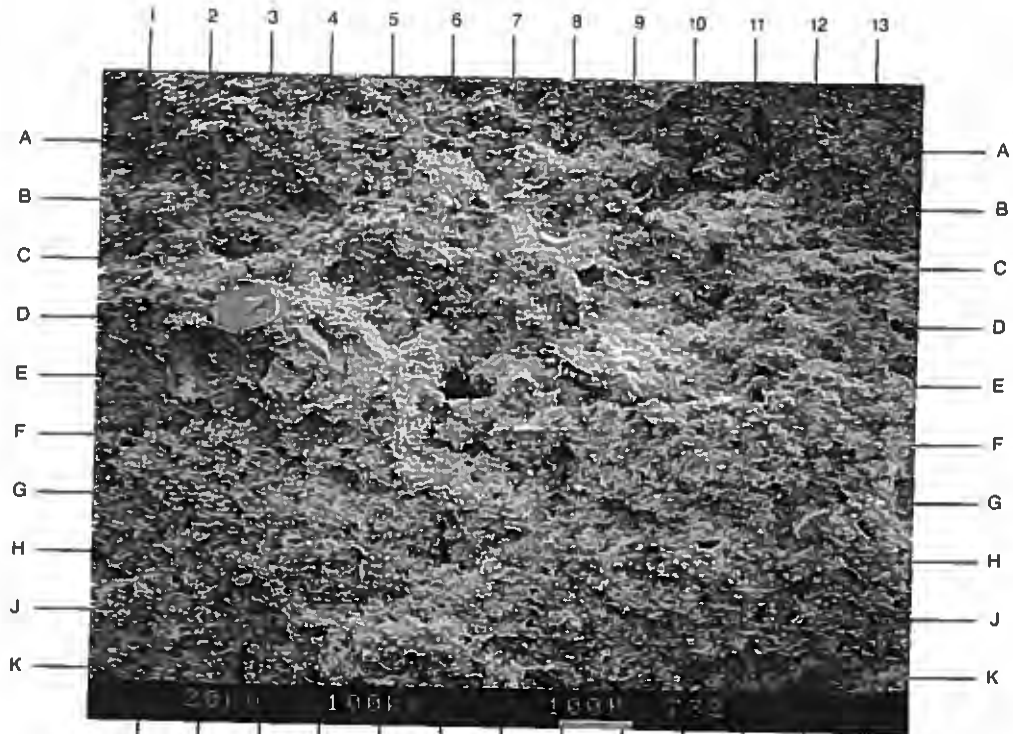
The low magnification survey photomicrograph illustrates a dense shale composed largely of detrital illite, illite/smectite, and quartz sand. Almost all primary intergranular porosity is infilled by illitic depositional clay.

Magnification: 100X

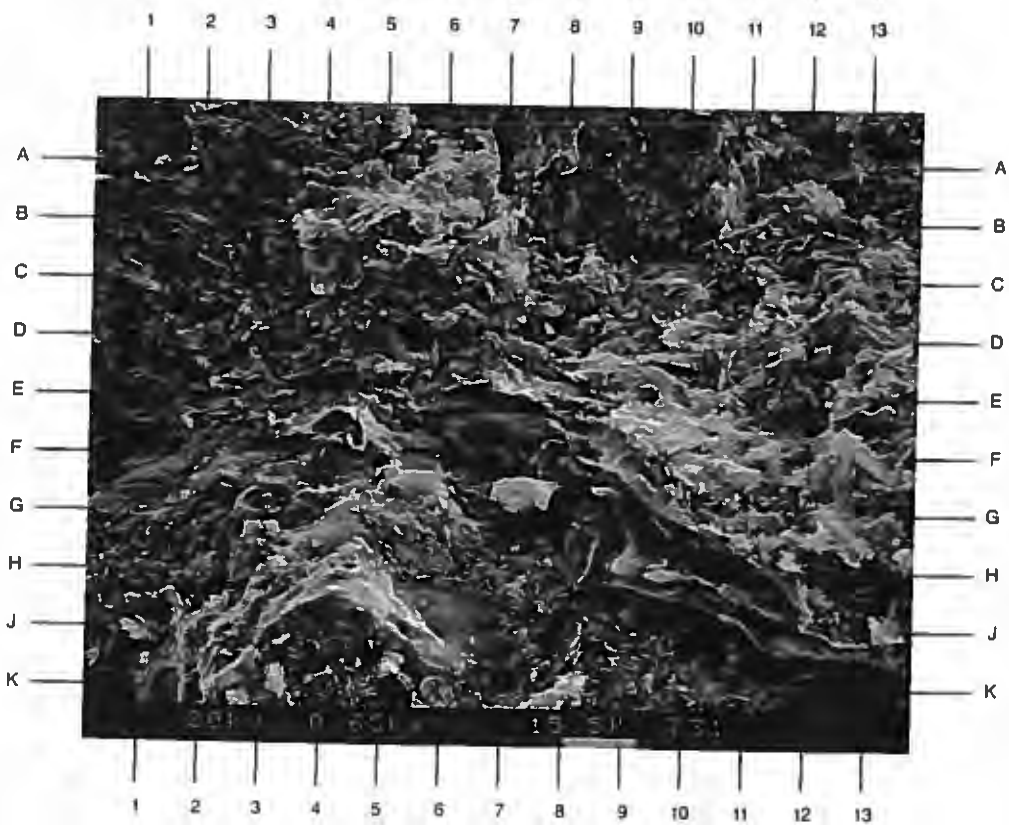
PLATE 38B

The high magnification view of the area near E8 in Plate 38A documents the clay types that compose this shale. Illite and illite/smectite typically occur as flat to curved (crenulated) sheets (E2-E8,H10) which display a subparallel orientation. This clay network seriously impedes vertical permeability.

Magnification: 650X



A



B

Dupont Environmental
Delisle No. 2, S/T No. 1
Harrison County, Mississippi

File No. GN-3402

SAMPLE DEPTH: 9852 FEET

PLATE 39A

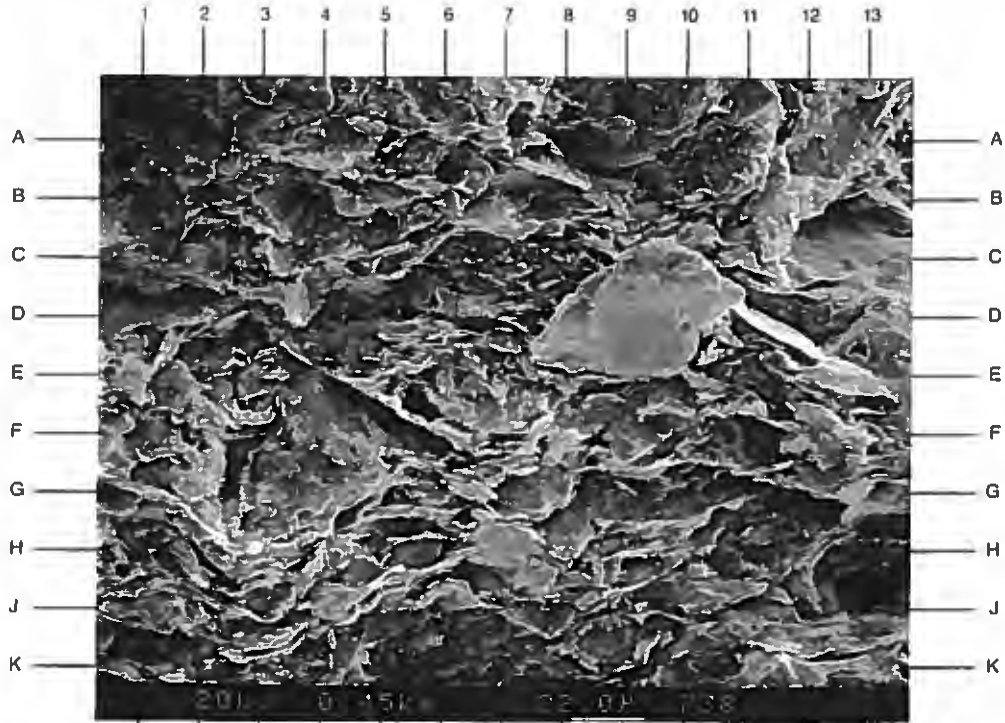
Some laminations in this shale are micaceous (D9,D11.5). As with clays, micas show subparallel orientation. The contortion seen from C1-B7 and H-J2 is due to compaction of the sample. High local microporosity is usually associated with gaps between discrete clay particles.

Magnification: 450X

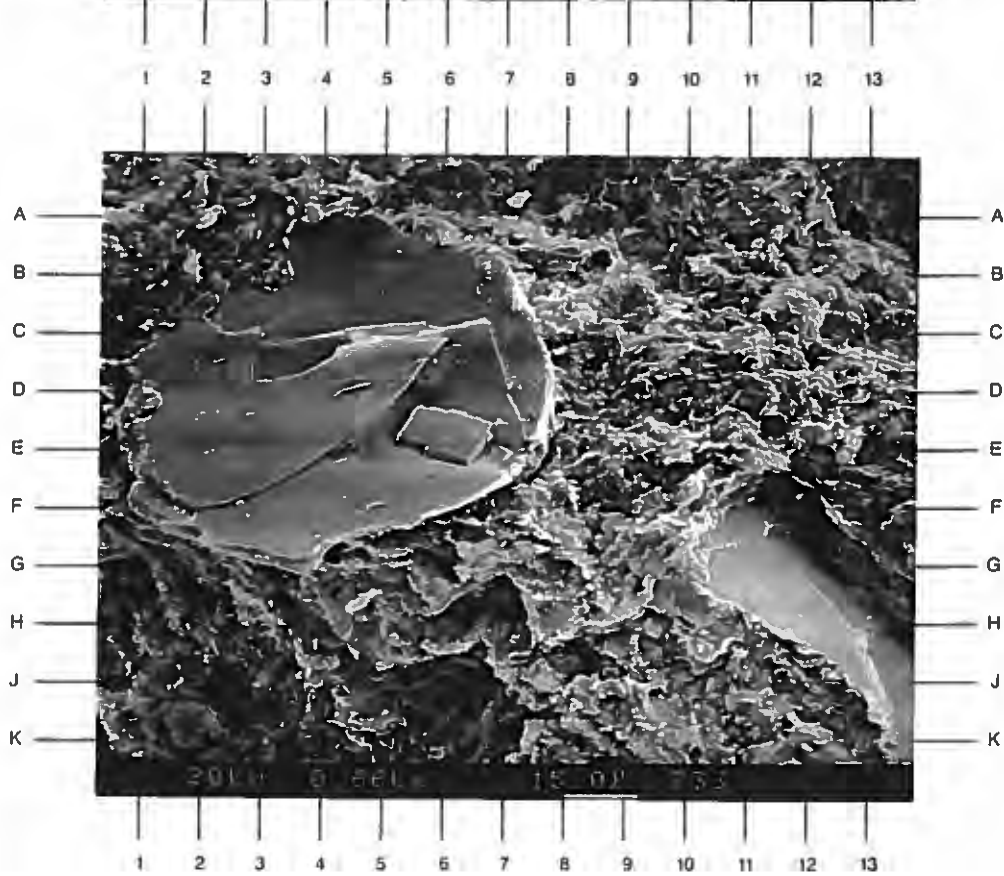
PLATE 39B

The high magnification view near D3 of Plate 38A shows rounded to subrounded quartz sand grains (D4,H12) floating in a matrix consisting locally of illite, illite/smectite, and minor chlorite. Note the calcite crystal (D-E6) seen on the quartz grain.

Magnification: 660X



A



B

SAMPLE DEPTH: 9896 FEET

PLATE 40A

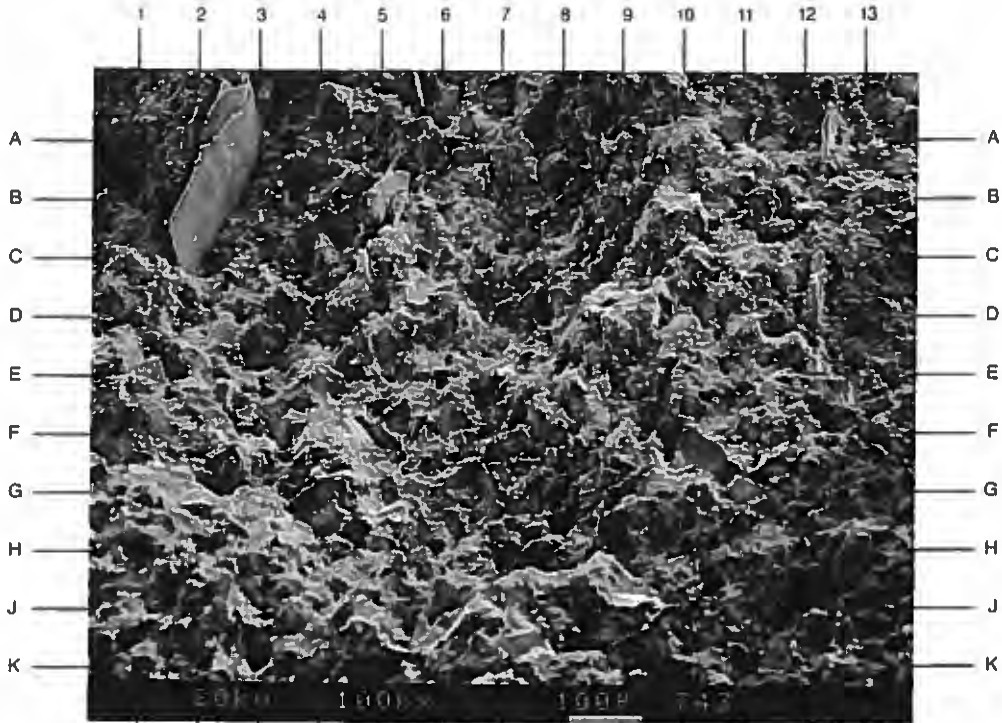
The low magnification photomicrograph on the facing page depicts a poor reservoir quality sandstone infilled with common illite and chlorite. A few, fairly isolated primary intergranular pores (A8,G2.5) are preserved, but microporosity associated with the matrix remains the dominant pore type.

Magnification: 100X

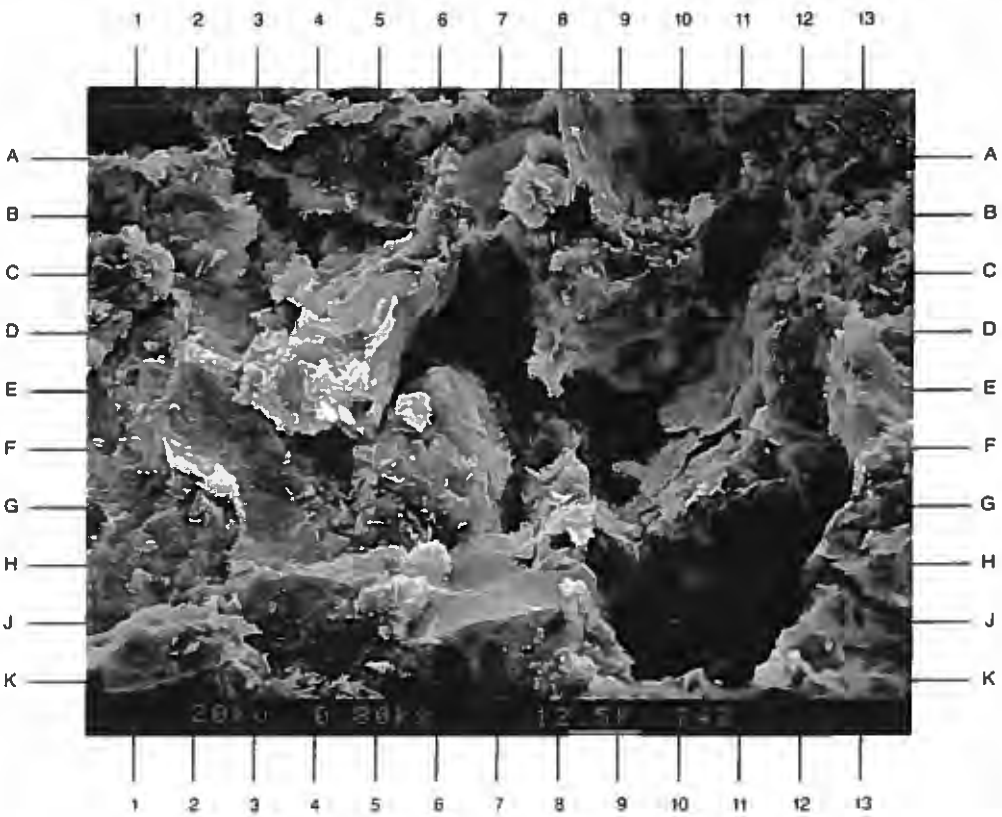
PLATE 40B

The high magnification view of the area near G7 in Plate 40A shows a close-up of uncommon primary intergranular pores (D7,H11). Detrital clays (A2,A8,G8) viewed are composed of illite and minor chlorite. Note the grain-coating chlorite seen at G4.5.

Magnification: 800X



A



B

Dupont Environmental
Delisle No. 2, S/T No. 1
Harrison County, Mississippi

File No. GN-3402

SAMPLE DEPTH: 9896 FEET

PLATE 41A

The low magnification survey photomicrograph taken from 9896' shows a large mica (muscovite) flake (K1-C7) encased by a dense, detrital clay matrix composed largely of illite. Observed microporosity is locally low and some matrix clay is recrystallized (J-K8,G8).

Magnification: 750X

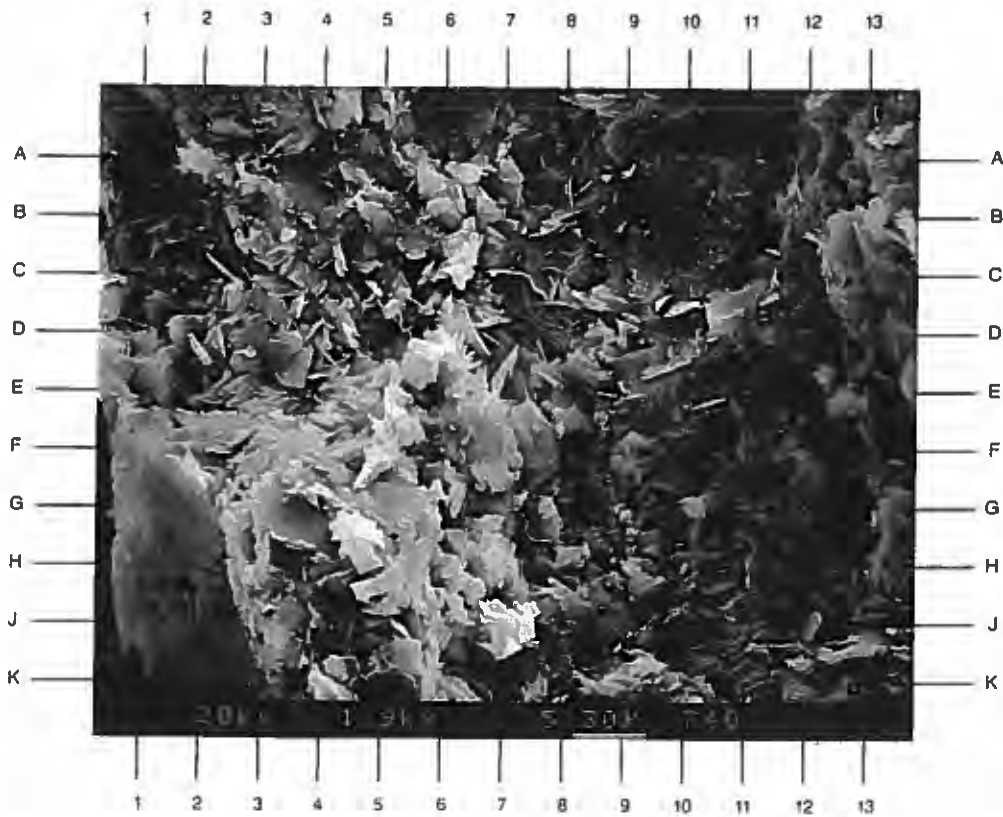
PLATE 41B

In small areas where primary pores are preserved, well developed authigenic chlorite (C-D7,G9.5,D4) can be found. This clay forms in open pore space during diagenesis, and displays a characteristic face-to-edge orientation of platelets. As is observed, this clay is very microporous.

Magnification: 1,900X



A



B

SAMPLE DEPTH: 9902 FEET

PLATE 42A

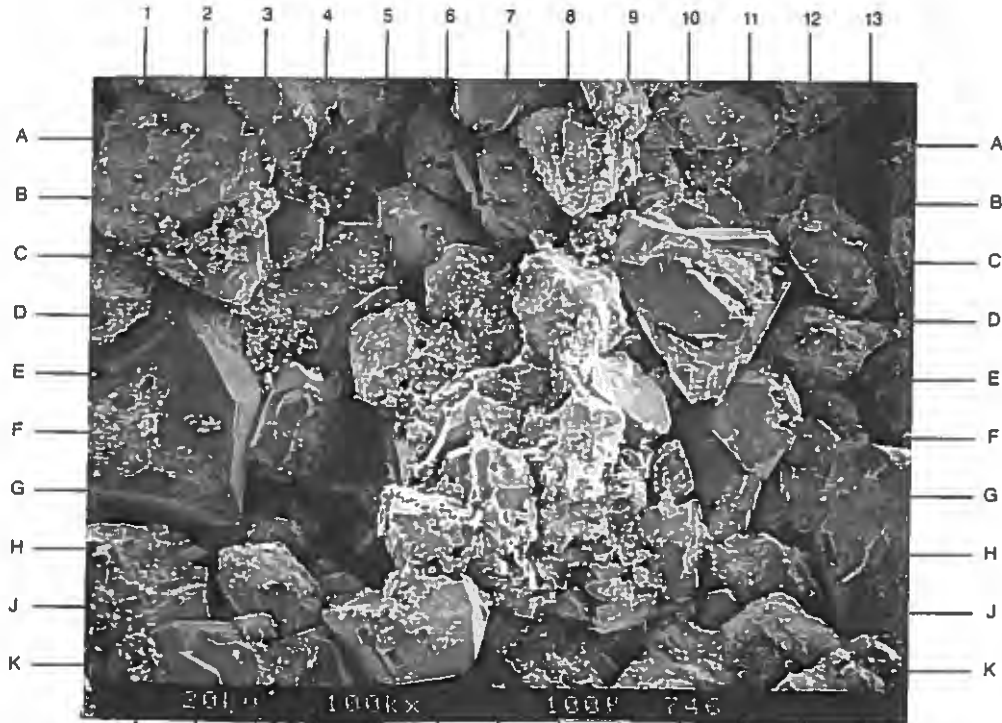
Generally good, but variable porosity distribution is shown on the facing page under low magnification from the sample taken from 9902'. Intergranular pores (E12.5,A13) are most common, with enhancement by secondary dissolution evident. Note the oversized pore at G4 which is secondary in origin. Iron titanium precipitates are rare in this sample.

Magnification: 100X

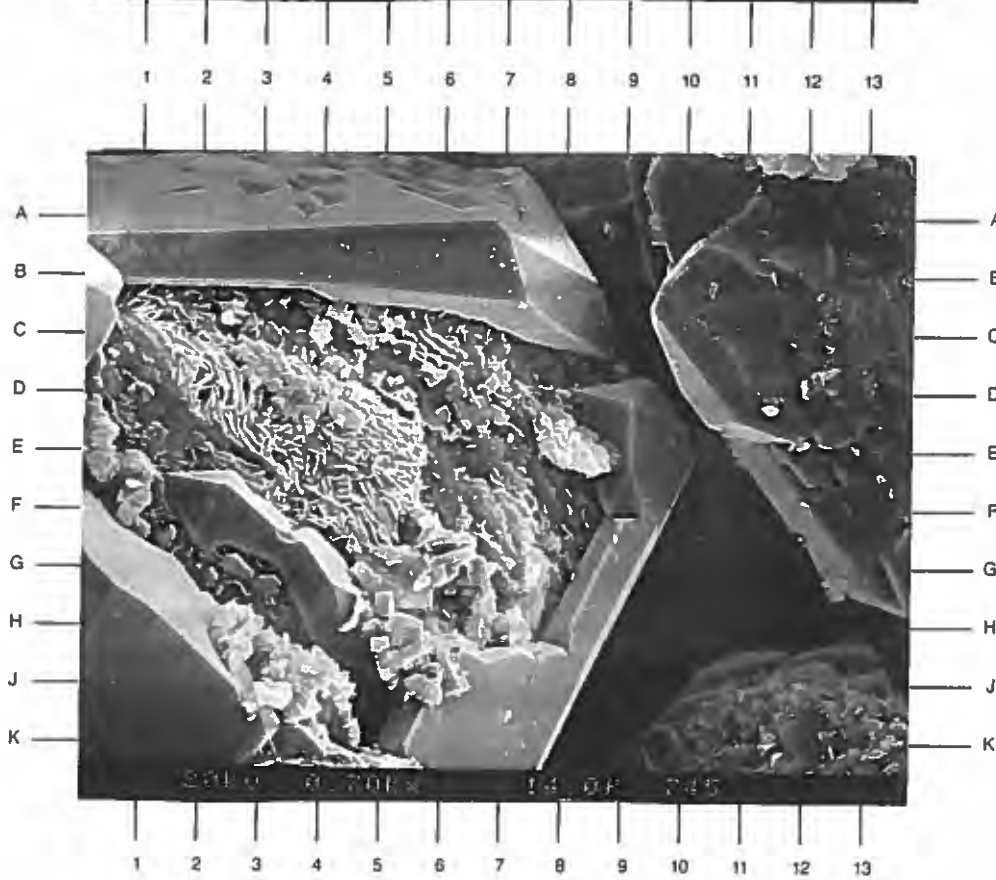
PLATE 42B

The high magnification view of the area near C11 in Plate 42A shows well developed quartz overgrowth cement and authigenic chlorite. Chlorite occurs as fairly discontinuous grain-coating, and is found where quartz overgrowths do not locally form. Note the open pore-throat at D9.5.

Magnification: 700X



A



B

SAMPLE DEPTH: 9902 FEET

PLATE 43A

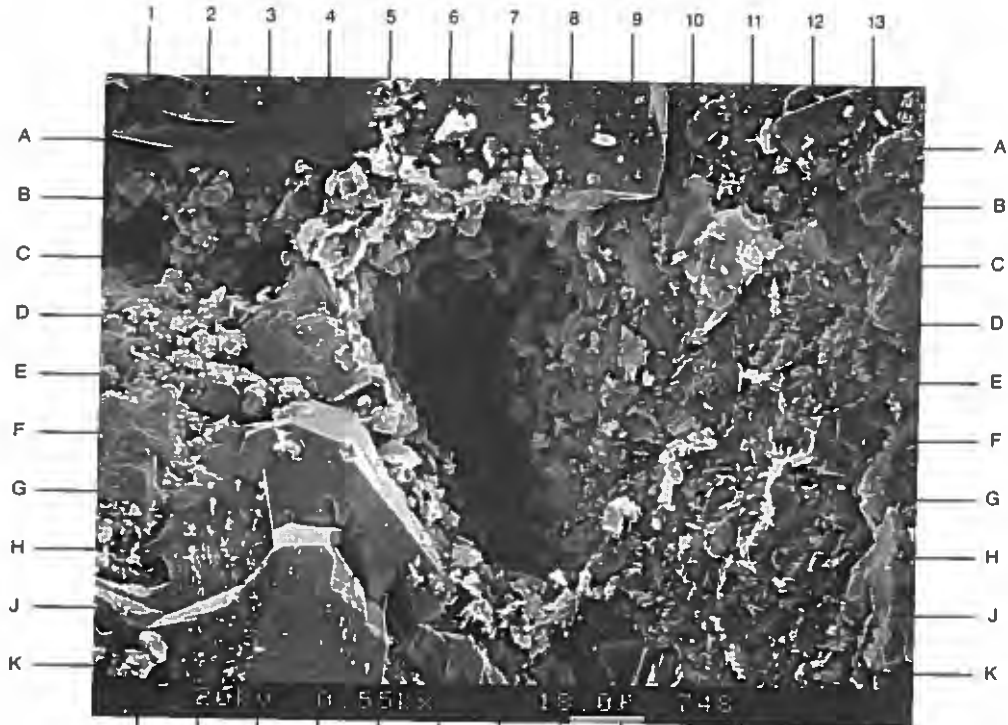
The secondary grain-moldic pore (F7) shown in the photomicrograph on the facing page is fairly isolated, but improves intergranular pore connectivity. Secondary clays are typically not found in association with secondary pores, suggesting dissolution post-dates most clay mineral precipitation events.

Magnification: 550X

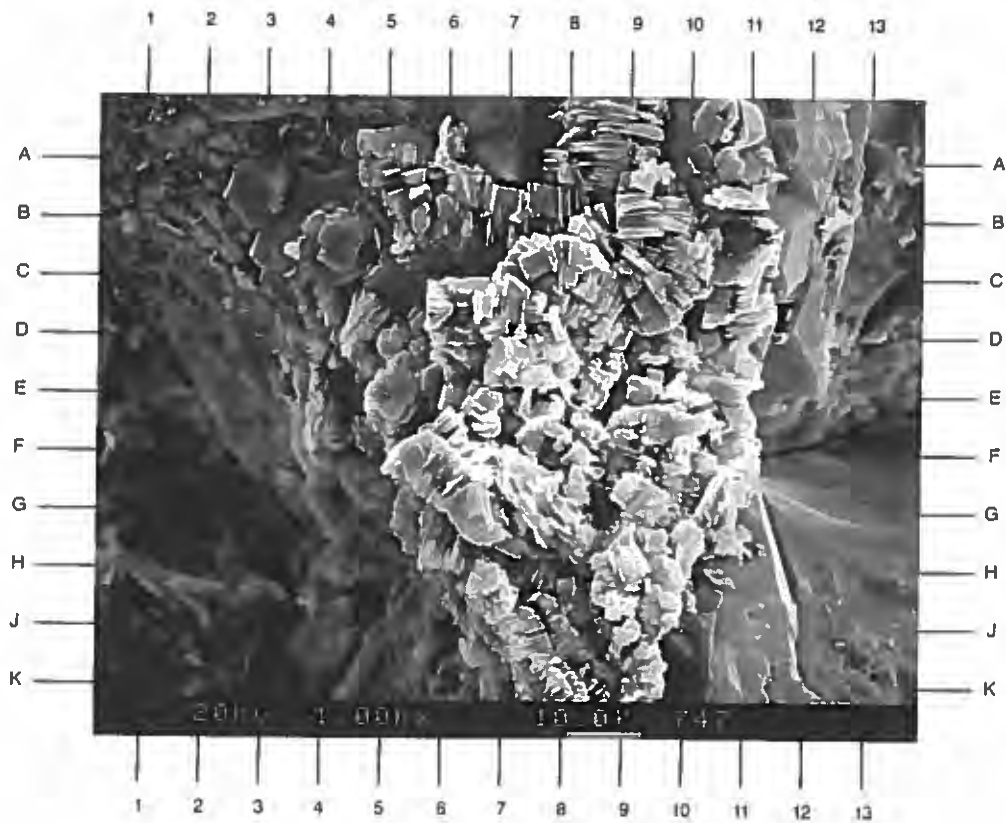
PLATE 43B

The high magnification view of the area near E8 in Plate 42A shows authigenic kaolinite as a pore-fill. This clay is found here as loose aggregates of booklets and is very microporous.

Magnification: 1,000X



A



B

Dupont Environmental
Delisle No. 2, S/T No. 1
Harrison County, Mississippi

File No. GN-3402

SAMPLE DEPTH: 9921 FEET

PLATE 44A

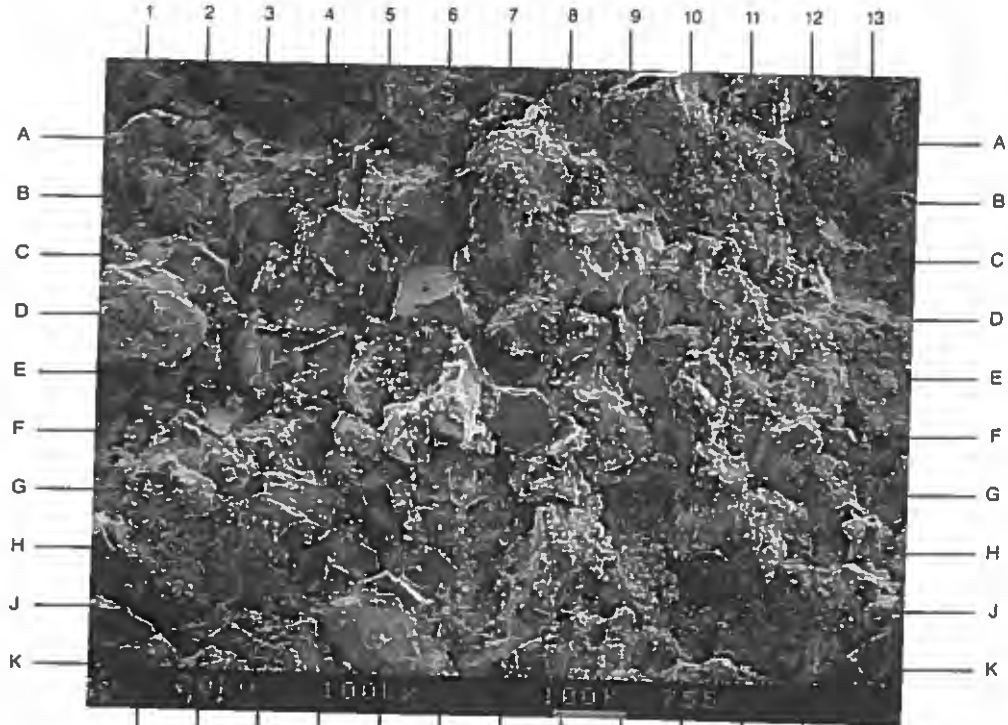
The low magnification survey photomicrograph illustrates the relatively low reservoir quality of this sample. The sandstone is well cemented and authigenic kaolinite is observed as an erratic pore filling throughout. Minor carbonate cements are also present.

Magnification: 100X

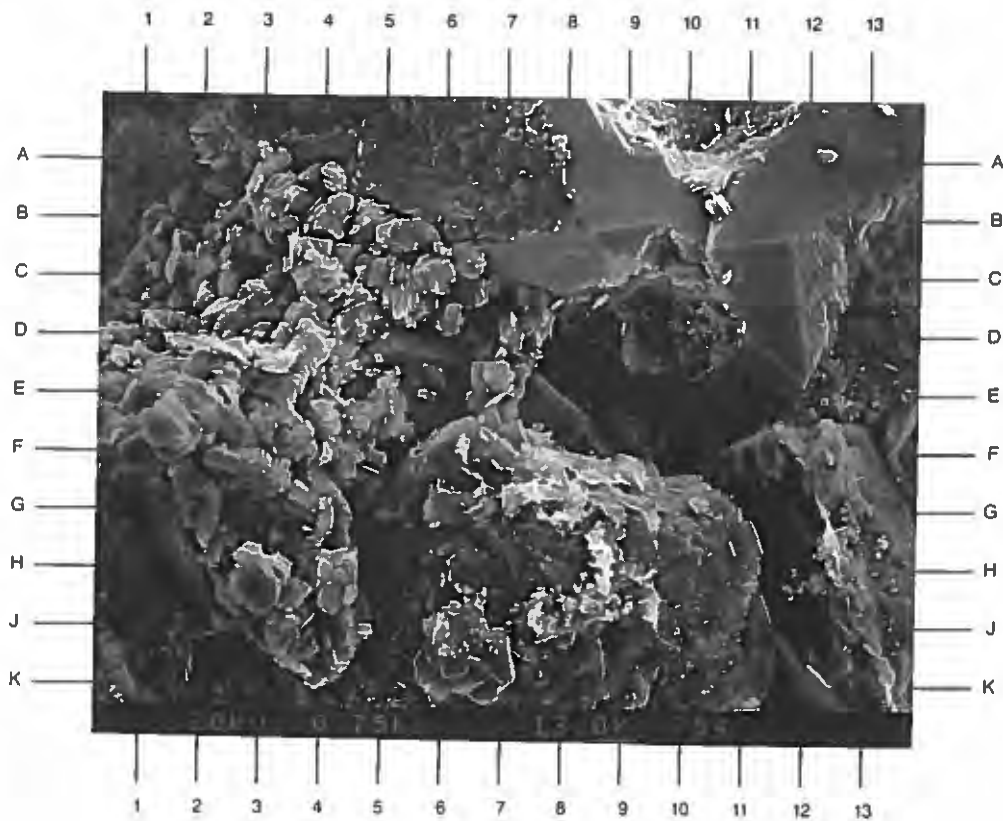
PLATE 44B

Two clay types are seen in this high magnification view taken from 9921'. Authigenic kaolinite (B3-J4) is seen infilling pores and pore throats. Illite (H9,F-G8) occurs as a discontinuous grain-coating. Note the quartz overgrowths (C11).

Magnification: 750X



A



B

Dupont Environmental
Delisle No. 2, S/T No. 1
Harrison County, Mississippi

File No. GN-3402

SAMPLE DEPTH: 9921 FEET

PLATE 45A

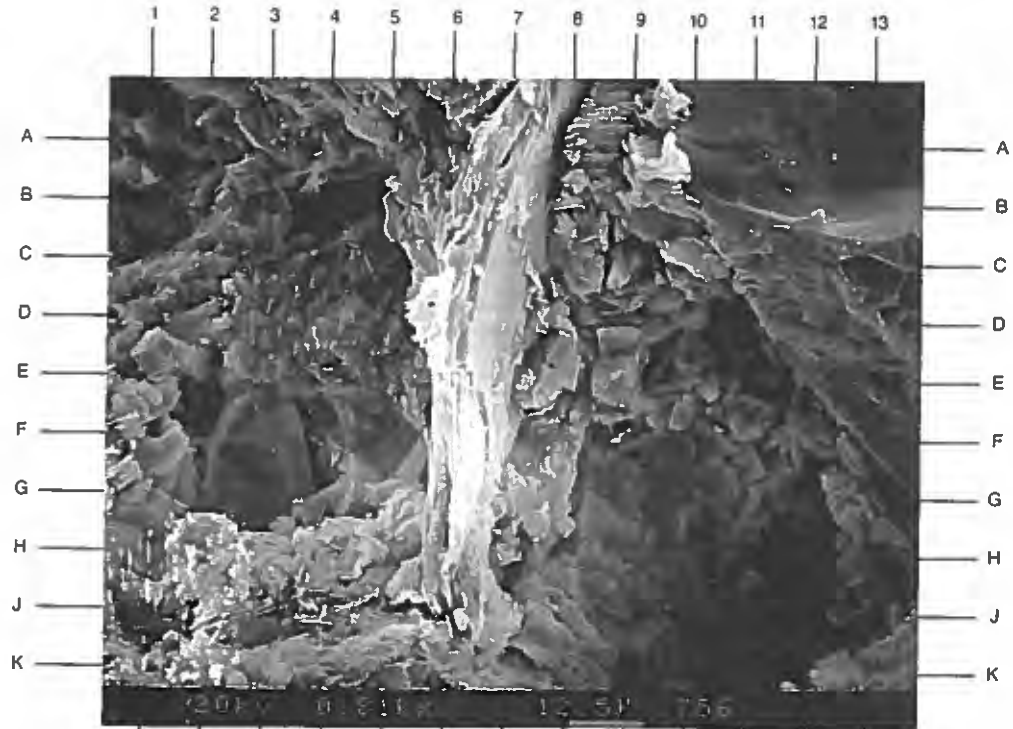
The mica flake observed from A7 to J6.5 is unaffected by compaction. A large grain-moldic dissolution pore is seen at H11. Authigenic chlorite (H-J4) is found as discontinuous grain-coatings.

Magnification: 810X

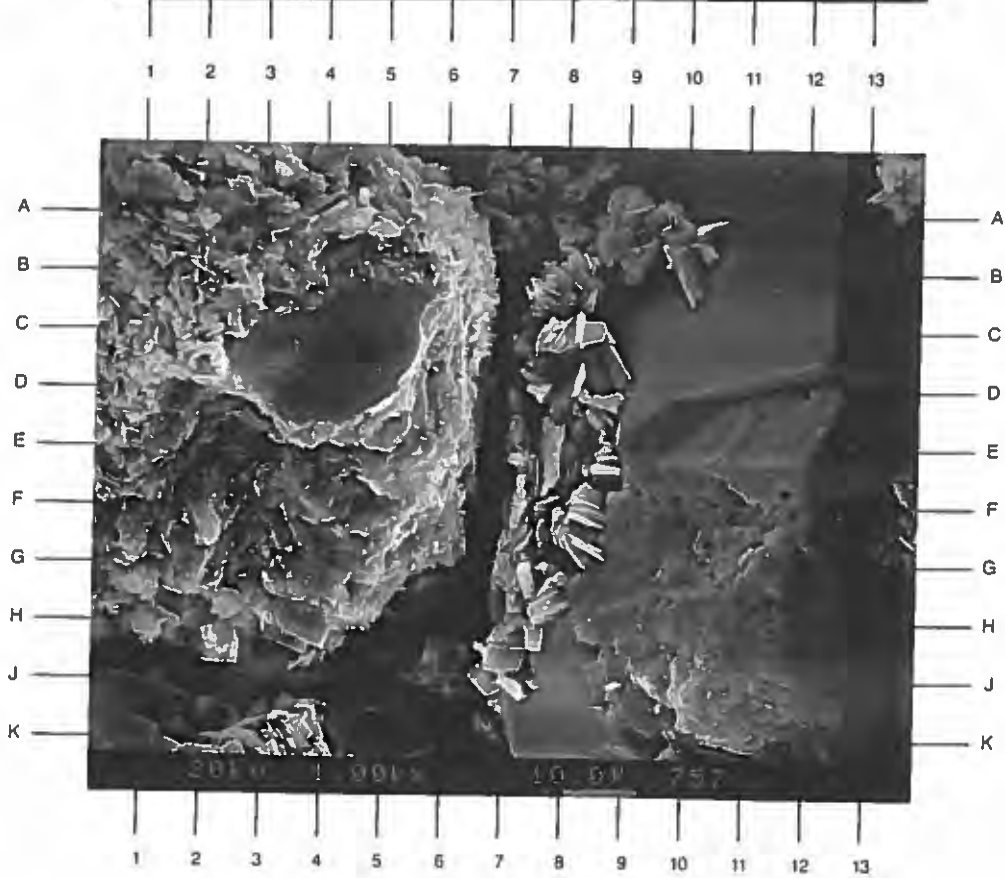
PLATE 45B

A pore throat (B7-G6.5) is seen here partially occluded by quartz overgrowths (C10,K8) and authigenic kaolinite(A8-J7). Note how the quartz overgrowths partially entrap the kaolinite booklets, suggesting the kaolinite formed contemporaneous with, or before, the quartz overgrowths.

Magnification: 1,000X



A



B

Dupont Environmental
Delisle No. 2, S/T No. 1
Harrison County, Mississippi

File No. GN-3402

SAMPLE DEPTH: 9934 FEET

PLATE 46A

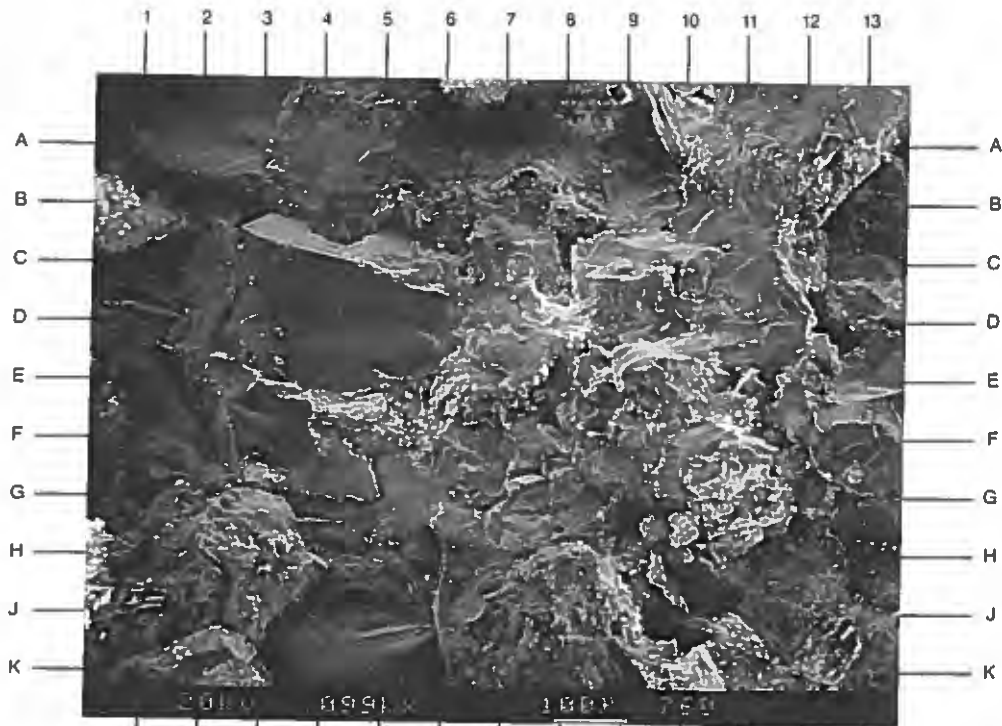
The low magnification photomicrograph on the facing page depicts erratically distributed intergranular porosity development in this sample. Cementation found here is erratic and generally composed of quartz overgrowths (B-C4,B10).

Magnification: 99X

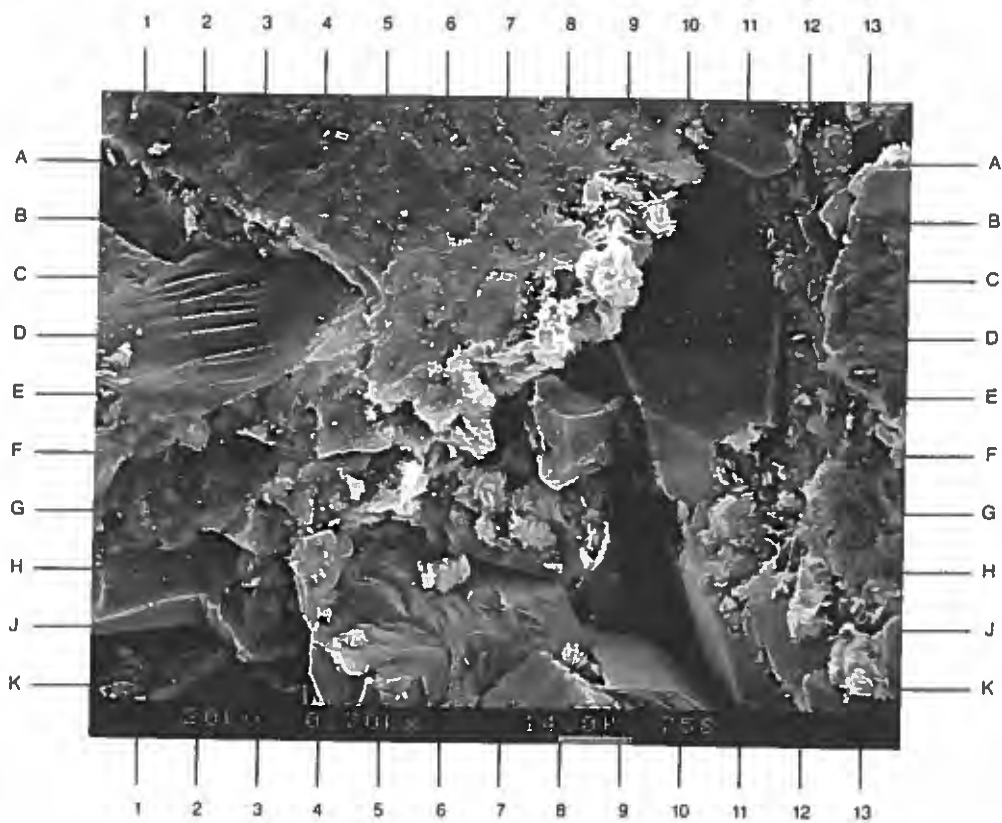
PLATE 46B

The high magnification view of the area near E8 in Plate 46A shows an intergranular pore (H-J9.5) bound mostly by flat quartz overgrowth crystal faces (J7,E10) as well as by authigenic chlorite (B9-D8). Note the densely cemented regions at B2 and E-F2.5.

Magnification: 700X



A



B

Dupont Environmental
Delisle No. 2, S/T No. 1
Harrison County, Mississippi

File No. GN-3402

SAMPLE DEPTH: 9934 FEET

PLATE 47A

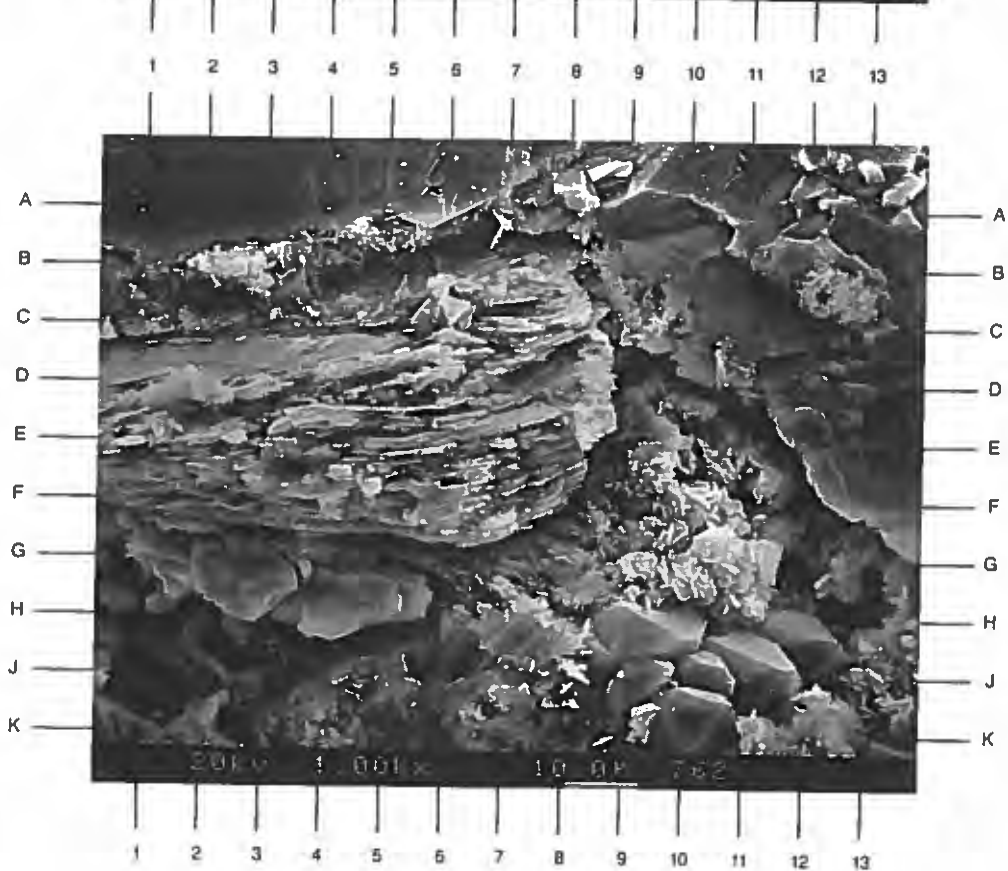
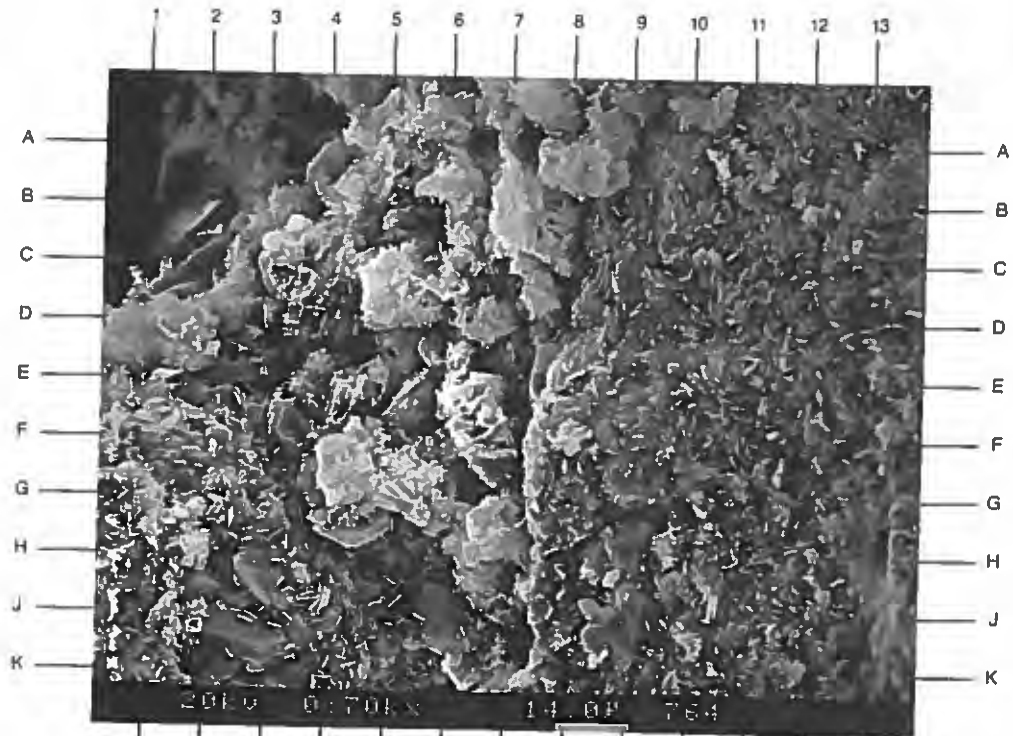
The high magnification view in the photomicrograph on the facing page shows several clay types. A clay-filled pore (A6-H7) is observed. This pore-fill is composed of authigenic kaolinite (D4) and finely mixed illite (E-F6,C-D5). Authigenic grain-coating chlorite is seen on the sand grain at the right of the photo.

Magnification: 700X

PLATE 47B

The book of detrital mica (E1-D8) observed is not affected by compaction. Authigenic chlorite (G10) is found lining pores and pore throats, and on grain surfaces where quartz overgrowths (J10.5) are absent.

Magnification: 1,000X



Dupont Environmental
Delisle No. 2, S/T No. 1
Harrison County, Mississippi

File No. GN-3402

SAMPLE DEPTH: 9970 FEET

PLATE 48A

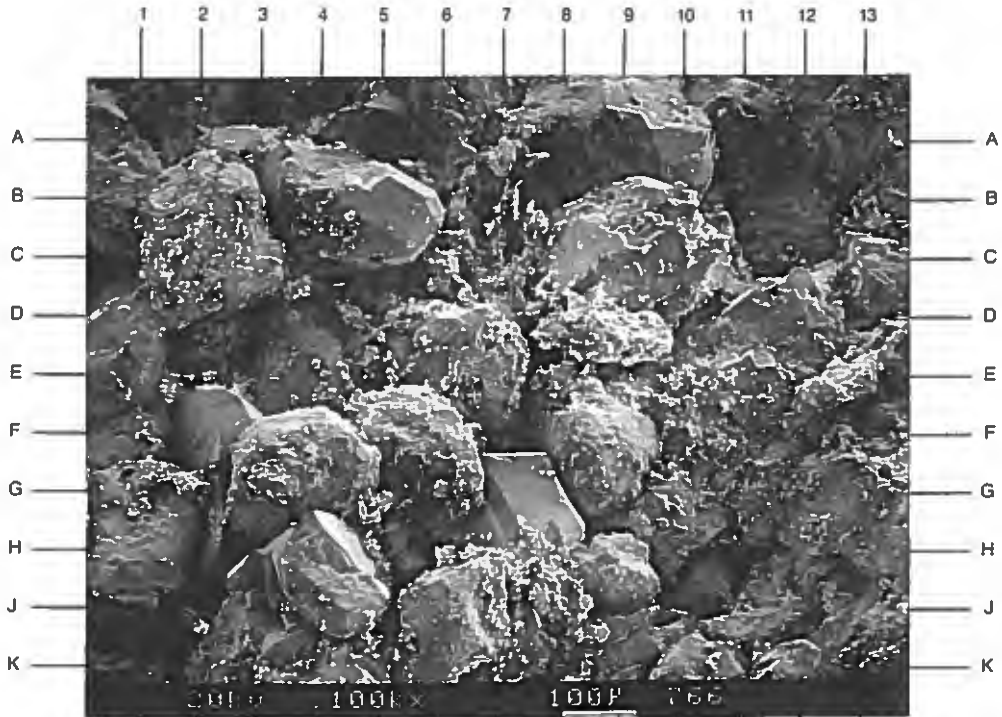
The fine-grained sandstone taken from 9970' shown on the facing page under low magnification has good overall reservoir quality. Intergranular porosity ranges from relatively open (left half of photo) to blocked by secondary cements and clays (right half of photo).

Magnification: 100X

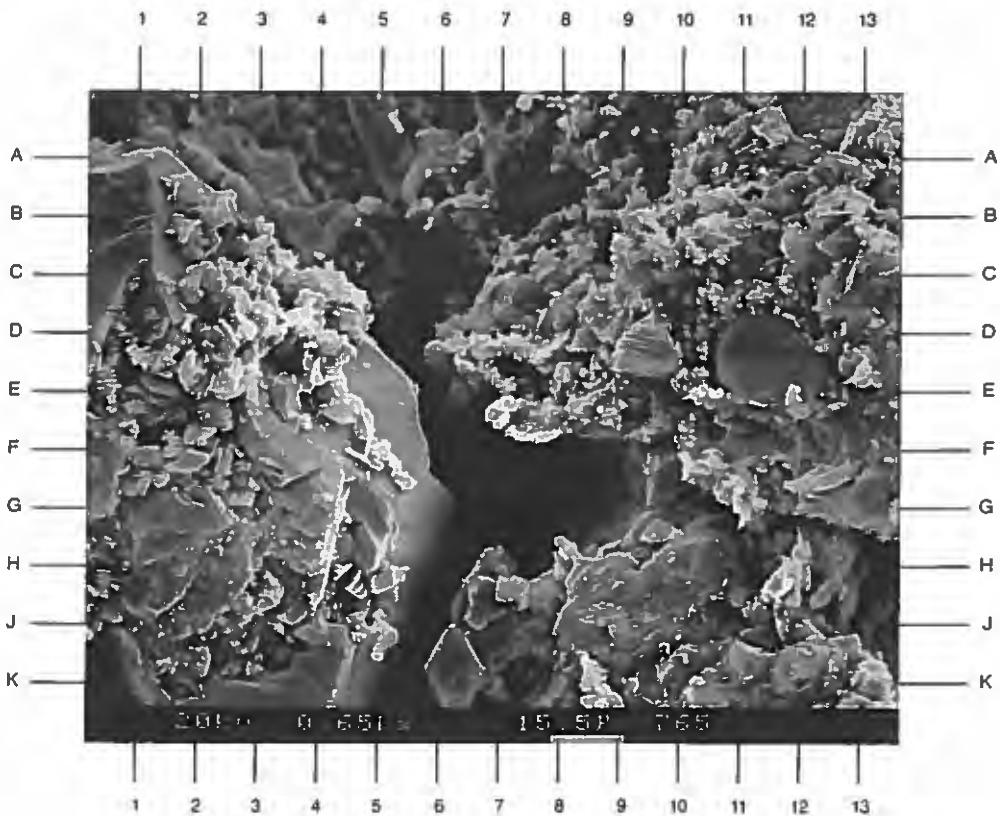
PLATE 48B

The high magnification view of the area near D7 in Plate 48A shows an open intergranular pore (F7). The lithic fragment to the upper right of the pore is illitic in composition. Iron oxides (below C11,D10,B-C8) seen replacing the lithic. The quartz grain to the left of the pore has well developed quartz overgrowths (B1,E5,G4) and associated authigenic kaolinite books (E2).

Magnification: 650X



A



B

Dupont Environmental
Delisle No. 2, S/T No. 1
Harrison County, Mississippi

File No. GN-3402

SAMPLE DEPTH: 9970 FEET

PLATE 49A

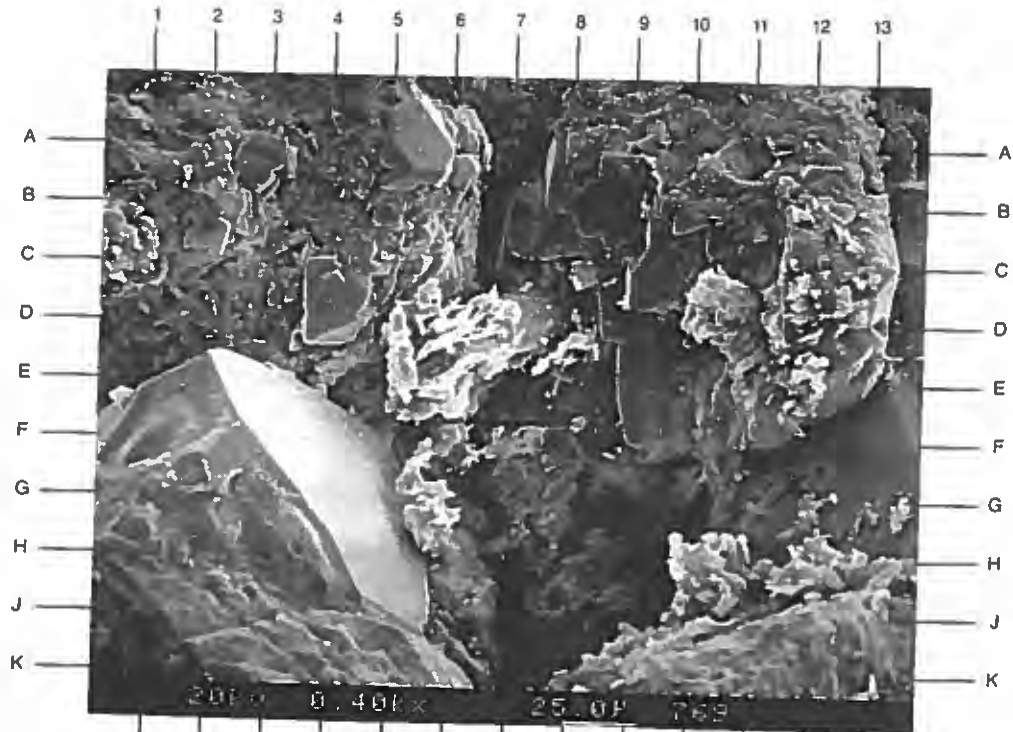
The high magnification survey photomicrograph on the facing page depicts a dissolution pore (H8) containing fine remnant material. These pores improve overall reservoir quality, but also add to the fines load of the pore system.

Magnification: 400X

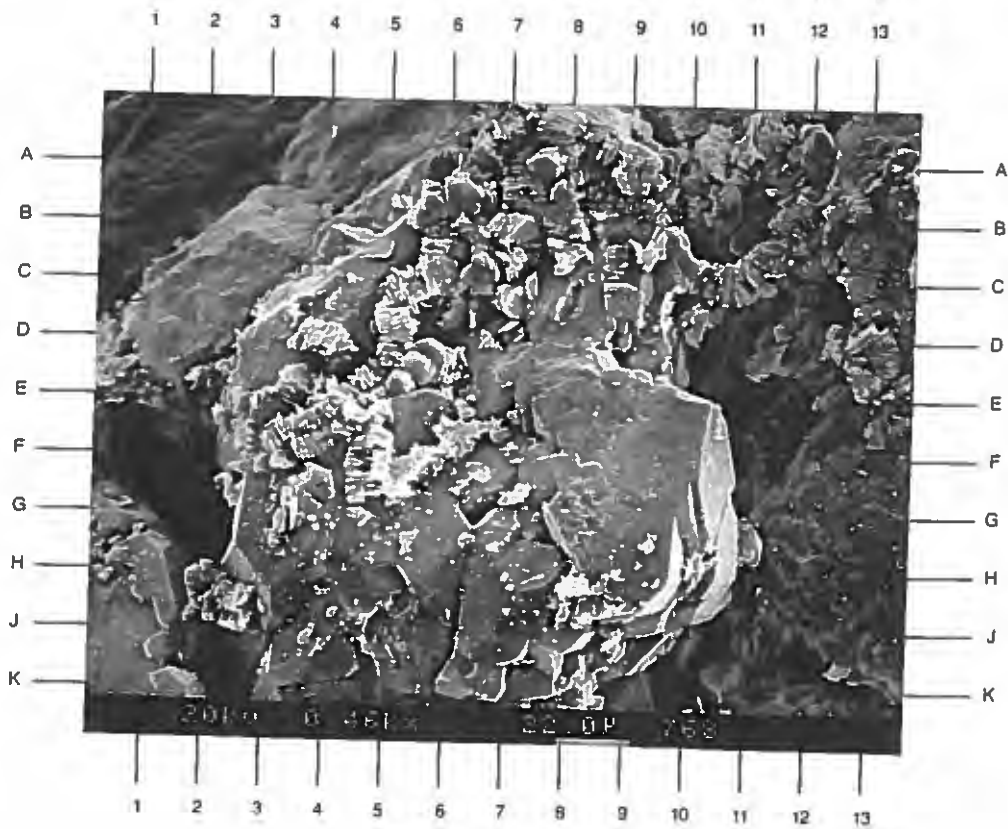
PLATE 49B

Vermiform (worm-like) booklets of authigenic kaolinite (E-F4,C10) are seen loosely attached to pore walls. Note the kaolinite (H-J2.5) found within a pore throat. The kaolinite seen here is partly intergrown with the quartz overgrowths (H1,C4.5).

Magnification: 460X



A



B

SAMPLE DEPTH: 9990 FEET

PLATE 50A

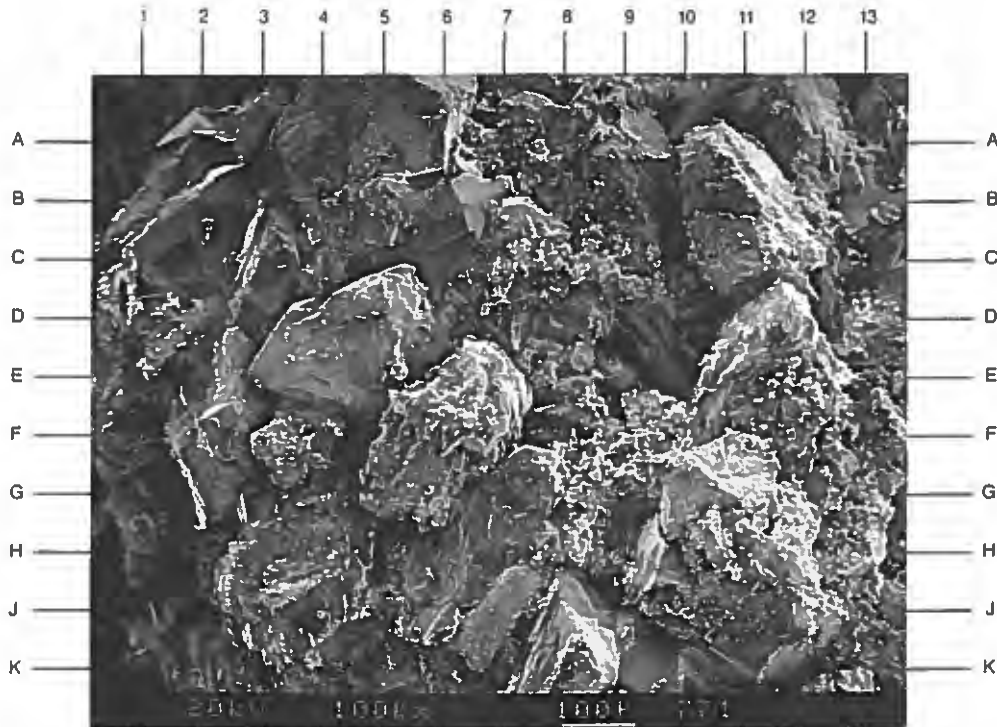
The low magnification survey photomicrograph on the facing page shows the good overall reservoir quality of the sample taken from 9990'. Quartz overgrowth cement (C3,B-C6,K11.5) is common, but variable. Relatively large secondary pores (D10) are seen augmenting primary intergranular porosity.

Magnification: 100X

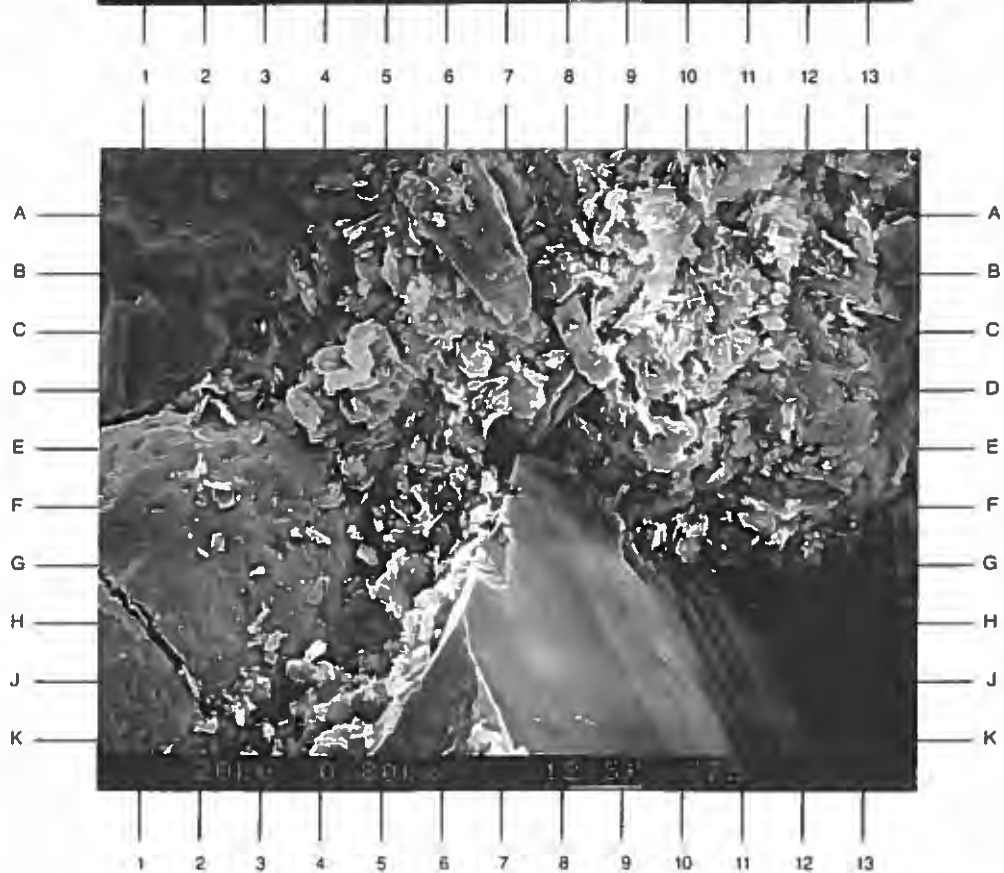
PLATE 50B

The high magnification view of the area near H8 in Plate 50A identifies rare areas of grain-coating authigenic chlorite (C10,B12) found in this sample. Authigenic kaolinite and intermixed illite can be seen as pore-fill (E5.5). This pore-fill is highly microporous.

Magnification: 800X



A



B

Dupont Environmental
Delisle No. 2, S/T No. 1
Harrison County, Mississippi

File No. GN-3402

SAMPLE DEPTH: 9990 FEET

PLATE 51A

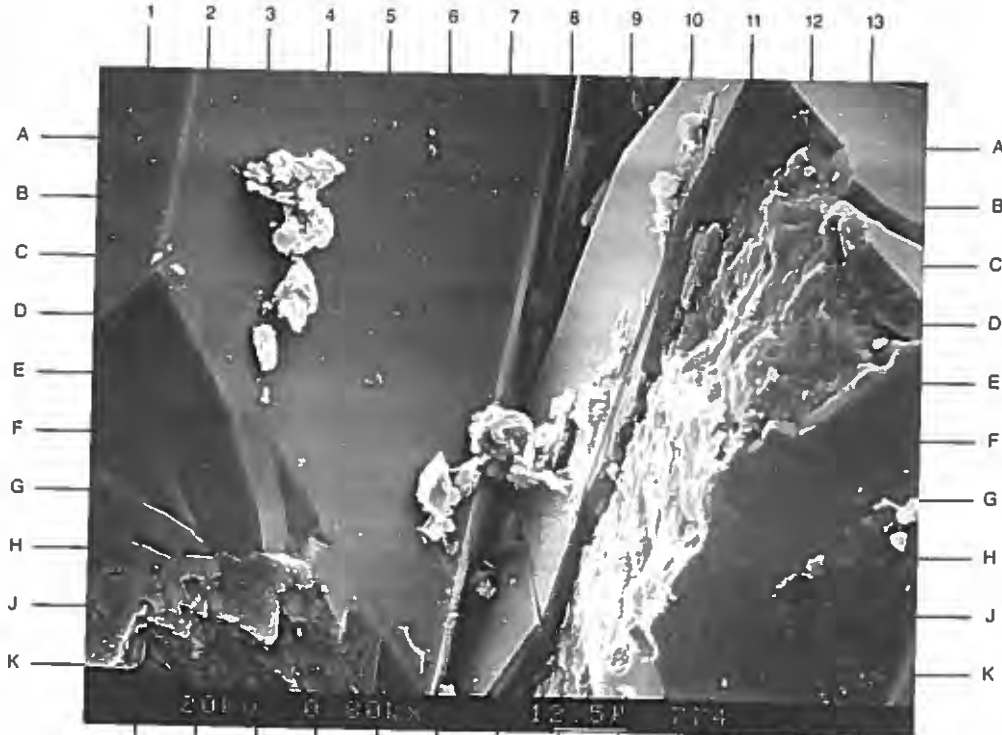
The high magnification survey photomicrograph on the facing page illustrates a narrow pore throat (A8.5-K6.5) bounded by quartz overgrowth crystal faces. The kaolinite and illite particles (F7.5) are fairly large compared to the pore throat, and may prevent flow.

Magnification: 800X

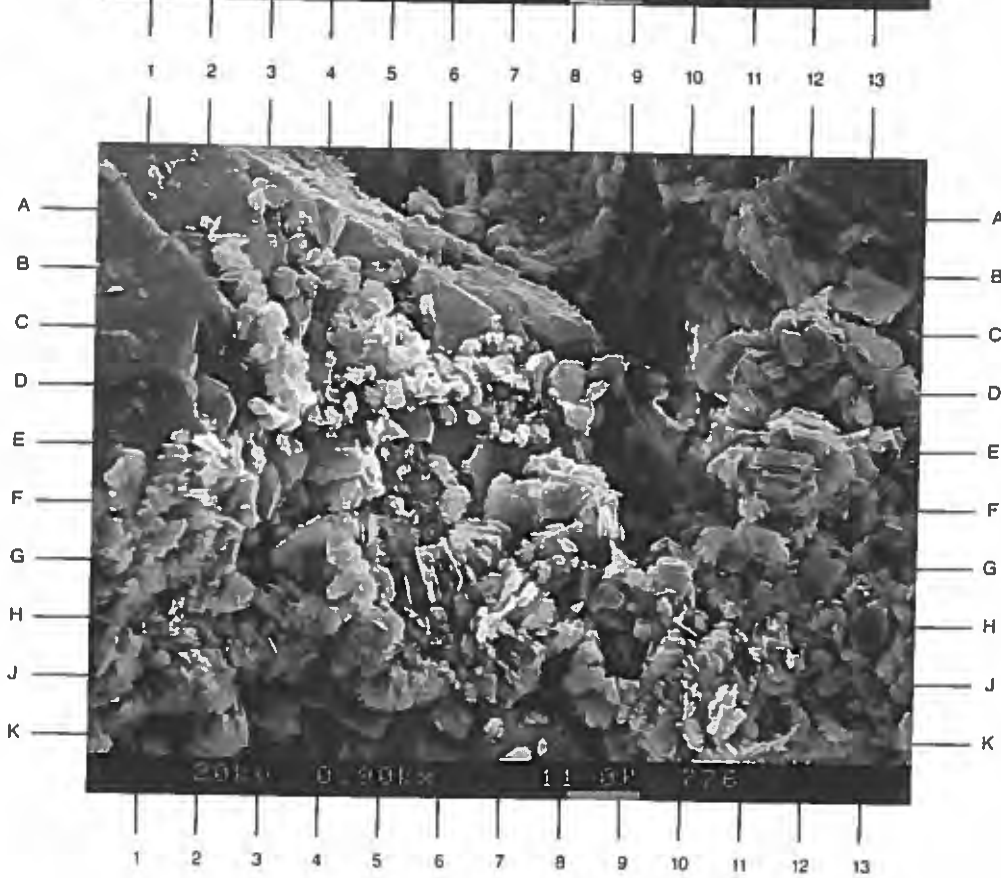
PLATE 51B

Authigenic kaolinite (G2,G7,J10) and finely mixed illite (H7,H11.5) are observed coating grains and partially filling a pore in the high magnification photomicrograph on the facing page. Note the quartz overgrowths seen at C2 and C7.5.

Magnification: 900X



A



B

CORE PHOTOGRAPHS

FOR

**DUPONT ENVIRONMENTAL REMEDIATION SERVICES
DELISLE NO. 2 S/T NO. 1
DUPONT DELISLE PLANT
HARRISON COUNTY, MISSISSIPPI**

DUPONT ENVIRONMENTAL REMEDIATION SERVICES
 DELISLE NO. 2, S/T NO. 1
 DUPONT DELISLE PLANT
 HARRISON COUNTY, MISSISSIPPI



FILE NO.: N-3402
 ANALYST: CHILEK/COTTON
 DATE: 23-NOV-95
 CORES: SCHLUMBERGER

ROTARY SIDEWALL CORE REPORT

Inches Rec.	Sample Number	Sample Depth feet	Permeability		Porosity Helium %	Grain Density gm/cc	Formation Description
			Horizontal Kair md				
0.1	1	8155.0			7.5	2.71	Ls lt gry vfxln min flu
		9372.0			*		Empty bottle
1.2	2	9473.0	650.00		24.5	2.66	Sd lt gry vf-fg sity no flu
1.3	3	9505.0	498.00		24.0	2.66	Sd lt gry vf-fg sity no flu
1.4	4	9562.0	1488.00		25.1	2.65	Sd lt gry fg sity no flu
0.5	5	9755.0					Shale dk gry no flu
1.3	6	9794.0	< 0.01		8.1	2.74	Sd gry vf-fg sity sshy mott scalc spts min flu
1.2	7	9796.0	< 0.01		3.9	2.68	Sd lt gry vfg vsity pyr calc no flu
1.2	8	9800.0	462.00		23.4	2.65	Sd lt tan f-vfg sity no flu
1.0	9	9802.0	682.00		24.1	2.62	Sd lt tan f-vfg sity no flu
1.3	10	9810.0	460.00		12.9	2.65	Sd lt tan f-vfg sity no flu
1.3	11	9820.0	1133.00		21.4	2.66	Sd lt tan f-vfg sity no flu
1.5	12	9832.0	643.00		23.3	2.63	Sd lt tan f-vfg sity no flu
1.3	13	9843.0	230.00		18.1	2.68	Sd lt tan vf-fg sity no flu
1.2	14	9850.0	264.00		24.1	2.61	Sd gry-brn f-mg carb lam no flu
0.8	15	9852.0					Shale dk gry-black no flu
1.2	16	9858.0	< 0.01		4.2	2.71	Sd gry-gm vfg vsity lmy no flu
		9890.0					Empty bottle
1.3	17	9896.0	0.02		4.1	2.69	Sd dk gry vfg sity vshy lam mica no flu
1.2	18	9902.0	222.00		21.3	2.65	Sd gry-gm f-vfg sity scarb mica no flu
1.2	19	9912.0	52.00		21.0	2.66	Sd red-brn f-vfg sity mica no flu
0.8	20	9921.0	1.90		12.7	2.69	Sd gry vf-fg sity sshy lam mica no flu
1.3	21	9928.0	274.00		24.0	2.60	Sd lt tan f-vfg sity carb lam no flu
0.4	22	9934.0			21.9	2.61	Sd lt tan f-vfg sity no flu
0.3	23	9947.0			6.9	2.78	Sd gry-brn f-vfg vsity pyr w/peb vlmv spts min flu
1.2	24	9962.0	449.00		23.0	2.65	Sd lt gry vf-fg sity no flu
1.2	25	9970.0	324.00		23.5	2.68	Sd gry-brn f-vfg sity no flu
1.2	26	9975.0	412.00		22.8	2.65	Sd gry f-vfg sity no flu

DUPONT ENVIRONMENTAL REMEDIATION SERVICES
 DELISLE NO. 2, S/T NO. 1
 DUPONT DELISLE PLANT
 HARRISON COUNTY, MISSISSIPPI



ROTARY SIDEWALL CORE REPORT

FILE NO.: N-3402
 ANALYST: CHILEK/COTTON
 DATE: 23-NOV-95
 CORES: SCHLUMBERGER

Inches Rec.	Sample Number	Sample Depth feet	Permeability		Porosity Helium %	Grain Density gm/cc	Formation Description
			Horizontal	Kair md			

1.2	27	9990.0	466.00	23.2	2.68	Sd gry f-vfg sity no flu
0.8	28	10012.0		20.9	2.68	Sd gry fg sity no flu

* Broken core, small pieces - Data may be questionable - No permeability measurement possible







9802.



9810.

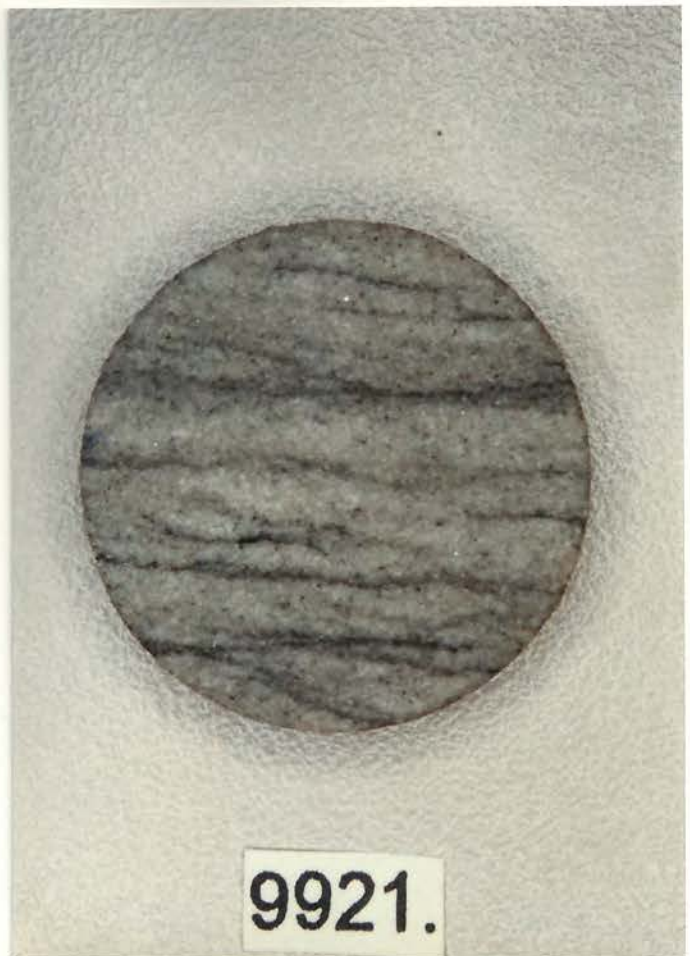


9820.



9832.









Appendix 2-31

Omni Laboratories, Inc. Petrographic Study Final Report

Well No. 3 Sidetrack #1 (1999)

**-FINAL REPORT-
PETROGRAPHIC STUDY
FOR
DU PONT
INJECTION WELL NO. 3 S/T
DU PONT DELISLE PLANT
HARRISON COUNTY, MISSISSIPPI**



April 1, 1999

Mr. Phil Papadeas
Sandia Technologies
140 Cypress Station Drive
Suite 130
Houston, Texas 77090

SUBJECT: *Final Report- Petrographic Study*
Injection Well No. 3 S/T
DuPont Delisle Plant
Harrison County, Mississippi
OMNI File No. GN-4474

Dear Mr. Papadeas:

Twenty-five (25) rotary sidewall core samples from the above referenced well were submitted for complete Petrographic Analysis, which includes X-ray diffraction (XRD), detailed thin section petrography, and scanning electron microscopy (SEM). Four (4) additional samples were submitted for XRD data only, and one (1) sample was submitted for detailed thin section analysis only. This final report includes all data, interpretations, and photomicrographs associated with these analyses. Three (3) copies of this report were prepared. Additional report copies can be made upon request.

It has been a pleasure to provide this study for Sandia Technologies. Please contact us if you have any questions concerning these results.

Sincerely,
OMNI LABORATORIES, INC.

A handwritten signature in black ink, appearing to read "Michael Dixon".

Michael Dixon
Manager, Geologic Services

A handwritten signature in black ink, appearing to read "Raymond Bruce".

Raymond Bruce
Geologist

A handwritten signature in black ink, appearing to read "Jilin Zhang".

Jilin Zhang
Geologist

PETROGRAPHIC ANALYSIS

X-ray diffraction (XRD) analysis, detailed thin section petrography, and scanning electron microscopy (SEM) were performed on twenty-five (25) rotary sidewall core samples from the well. An additional four (4) samples were selected for XRD data only, and one (1) additional sample was selected for thin section analysis only (see Appendices B through D, respectively). Table 1 (below) shows the sample depths and the analyses performed.

TABLE 1

SAMPLE DEPTHS AND ANALYSES PERFORMED

<u>SAMPLE DEPTH</u> (feet)	<u>THIN SECTION</u> <u>PETROGRAPHY</u>	<u>SEM</u>	<u>XRD</u>
9432.0	X	X	X
9493.0			X
9520.0			X
9536.0	X	X	X
9572.0			X
9588.0	X	X	X
9822.0	X	X	X
9826.0	X	X	X
9844.0	X	X	X
9848.0	X	X	X
9856.0	X		
9861.0	X	X	X
9866.0	X	X	X
9871.0	X	X	X
9876.0			X
9887.0	X	X	X
9899.0	X	X	X
9904.0	X	X	X
9916.0	X	X	X
9929.0	X	X	X
9938.0	X	X	X
9952.0	X	X	X
9962.0	X	X	X
9970.0	X	X	X
9992.0	X	X	X
9996.0	X	X	X
10008.0	X	X	X
10016.0	X	X	X
10023.0	X	X	X
10032.0	X	X	X

The objectives of these analyses were to: 1) characterize the sample quality, texture, and mineralogy; 2) examine porosity development and determine controls on porosity and permeability; and 3) determine the effects of mineralogy on log response.

Summary Of Petrographic Results

X-ray diffraction (XRD) analysis, detailed thin section petrography, and scanning electron microscopy (SEM) were performed on twenty-five (25) rotary sidewall core samples from the well. An additional four (4) samples were selected for XRD data only, and one (1) additional sample was selected for thin section analysis only. Quartz is the dominant framework grain type, with lesser amounts of feldspars and lithic fragments also present. Reservoir quality ranges from poor to good in the samples analyzed and is strongly controlled by the amount and distribution of remaining effective porosity. Porosity distribution is influenced by 1) cementation, especially by quartz overgrowths and carbonate cements; 2) secondary dissolution, and to a lesser extent; 3) sediment compaction; and 4) detrital pore-filling and authigenic grain-coating clays. Most samples analyzed have moderate to good reservoir quality. Samples with poor reservoir quality are high in either shaly matrix or carbonate cements. Primary intergranular porosity (trace-17%), secondary dissolution porosity (2%-8%), and microporosity (0%-2%) are the porosity types present in these sandstone samples. Primary intergranular porosity is variably to evenly distributed and generally open. Occasional occlusion by naturally occurring cements and detrital clays is observed in some samples. Cements include quartz overgrowths, siderite, dolomite, calcite, and pyrite. Residual waste material is observed in several samples as a pore-reducing component and is noted in thin section analysis as part of iron/titanium oxides and other opaques. These waste components tend to attach to microporous areas, such as are associated with siderite, quartz, and kaolinite microcrystals. This waste components can also be seen attached to irregular surfaces of sand grains. Secondary dissolution pores are seen erratically distributed in all samples and were formed by partial (intragranular) to complete (grain-moldic) dissolution of less stable framework grains, such as feldspars and lithics. Microporosity is associated with authigenic and detrital clays, as well as intragranular porosity. This porosity type is considered to be ineffective. X-ray diffraction (XRD) analysis of the sandstone samples reveals a total clay content ranging from 3%-14%, by weight. The clay types present are chlorite (average 2%), kaolinite (average 2%), illite (average 2%), and mixed-layer illite/smectite (average 1%). SEM analysis shows that illite and mixed-layer illite/smectite are finely intermixed and occur largely as a detrital pore-filling matrix component with a patchy distribution, or occur as the main components of discontinuous shale laminations. Minor amounts of authigenic illitic clays are also present. Authigenic secondary chlorite occurs as flat platelets with a face-to edge orientation and is found as a discontinuous grain-coating clay. Authigenic kaolinite is the most commonly observed secondary clay mineral, and is found as patchy pore fillings in the form of aggregates of booklets. All clay types are also found in association with certain lithic fragment types.

Thin section results are summarized in Table 1 shown below.

TABLE 1
SUMMARY OF THIN SECTION RESULTS

Sample Depth	Grain Size Avg. (mm)	Resistivity Suppression	Fabric	Matrix (%)	Secondary Cement (%)	Porosity Development
9432'	0.38	None	Massive	Trace	19	Good
9536'	0.28	None	Massive	1	15	Good
9588'	0.36	None	Massive	Trace	19	Good
9822'	0.20	Strong	Sl. Shaly	6	21	Poor
9826'	0.32	Slight	Gr. Bed	4	16	Moderate
9838'	0.45	Slight	Massive	1	12	Good
9844'	0.42	None	Massive	Trace	21	Good
9848'	0.42	Slight	Massive	Trace	18	Good
9856'	0.47	None	Massive	1	18	Good
9861'	0.48	None	Massive	1	19	Good
9866'	0.55	None	Massive	Trace	41	Poor
9871'	0.22	Strong	Shaly	22	37	Poor
9887'	0.20	Slight	Massive	3	33	Moderate
9899'	0.36	Slight	Massive	2	25	Good
9904'	0.20	Slight	Massive	Trace	20	Good
9916'	0.34	Slight	Massive	4	16	Good
9929'	0.32	Slight	Massive	2	20	Good
9938'	0.30	Slight	Massive	Trace	27	Good
9952'	0.20	None	Massive	0	37	Poor
9962'	0.23	Slight	Massive	Trace	32	Moderate
9970'	0.18	None	Massive	0	27	Moderate
9992'	0.17	None	Massive	Trace	23	Moderate
9996'	0.15	Slight	Laminated	3	17	Moderate
10008'	0.14	Moderate	Laminated	10	21	Poor
10016'	0.27	Slight	Massive	1	20	Good
10023'	0.28	Slight	Massive	Trace	18	Good
10032'	0.33	Slight	Massive	Trace	15	Good

PETROGRAPHIC RESULTS

Sedimentary Fabric and Texture

The samples analyzed by thin section (Appendix C) range from poor (9866') to moderately well sorted (several samples), very fine- to lower coarse-grained sandstones. The average grain size of each sample ranges from 0.14mm to 0.55mm. These sandstones contain occasional discontinuous faint laminations (9996' and 10008') or are massive in fabric, except at 9826' and 9871'. The sample taken from 9826' exhibits graded bedding and the sample from 9871' is shaly. In general, the angularity of the grains ranges from angular to subrounded, with most grains being subangular.

Framework Grain Mineralogy

The most common framework grain type in the sandstone samples is monocrystalline quartz (17%-51%). Other common components include various lithic fragments (1%-11% total lithics; mainly metamorphic with lesser chert), plagioclase feldspar (1%-4%), K-feldspar (trace-2%), and polycrystalline quartz (2%-11%). Accessory grains are seen in minor amounts and include muscovite mica, biotite mica (3% at 10008') and the mature heavy minerals garnet, tourmaline and zircon. Low amounts of environmental indicators include calcareous fossil fragments, glauconite, and organic material (plant fragments). Glauconite is an indicator of marine depositional influence. Compositionally, these sandstones are similar and are classified by the Folk (1980) method as either subarkoses or sublitharenites.

Cementation

The dominant cement in these samples is secondary quartz overgrowths (2%-22%). These overgrowths form as nucleations on host quartz sand grains, reducing adjacent intergranular pore space and pore throats. Quartz microcrystals are also common in these sandstones. Other cements found in lesser amounts are pore-lining clay, pyrite, calcite, dolomite, siderite, and kaolinite. Pyrite occurs as aggregates of pore-filling microcrystals, as well as a replacement product of organic material. The carbonate minerals (dolomite, siderite, and calcite) occur as a patchy pore-filling. Calcite cement is especially common at 9866' and 9871'. Dolomite is also common at 9887'. Siderite is seen in greater amounts at 9938', 9962', and 9970'. Clays are discussed in the following section on "Clay Mineralogy".

Unknown components that appear as possible iron/titanium oxides or other opaques under cementation in the thin section point-count data account for 0%-6% (total components) of the sample volume. These components are likely remnants of the

waste material which has been introduced into these zones. These components tend to attach to microporous areas associated with siderite, quartz, and kaolinite microcrystals. This waste components can also be seen attached to irregular surfaces of sand grains.

Clay Mineralogy

X-ray diffraction (XRD) analysis (Appendix B) of the sandstone samples reveals a total clay content ranging from 3%-14%, by weight. The clay types present are chlorite (average 2%), kaolinite (average 2%), illite (average 2%), and mixed-layer illite/smectite (average 1%). SEM analysis shows that illite and mixed-layer illite/smectite are finely intermixed and occur largely as a detrital pore-filling matrix component with a patchy distribution, or occur as the main components of discontinuous shale laminations. Minor amounts of authigenic illitic clays are also present. Authigenic secondary chlorite occurs as flat platelets with a face-to-edge orientation, and is found as a discontinuous grain-coating clay. Authigenic kaolinite is the most commonly observed secondary clay mineral, and is found as patchy pore-fillings in the form of aggregates of booklets. All clay types are also found in association with certain lithic fragment types. It should be noted that XRD analysis cannot quantify amorphous components. Waste remnant material may be amorphous, as indicated by the presence in thin section and SEM examination, but not in XRD.

Porosity Development

Primary intergranular porosity (trace-17%), secondary dissolution porosity (2%-8%), and microporosity (0%-2%) are the porosity types present in these sandstone samples. Primary intergranular porosity is variably to evenly distributed and generally open. Occasional occlusion by naturally occurring cements and detrital clays is observed in some samples. Cements include quartz overgrowths, siderite, dolomite, calcite, and pyrite. Residual waste material is observed in several samples as a pore-reducing component, and is noted in thin section analysis as part of iron/titanium oxides and other opaques. Secondary dissolution pores are seen erratically distributed in all samples and were formed by partial (intragranular) to complete (grain-moldic) dissolution of less stable framework grains, such as feldspars and lithics. Microporosity is associated with authigenic and detrital clays, and intragranular porosity. This porosity type is considered to be ineffective.

Reservoir quality ranges from poor to good in the samples analyzed and is strongly controlled by the amount and distribution of remaining effective porosity. Porosity distribution is influenced by 1) cementation, especially by quartz overgrowths and carbonate cements; 2) secondary dissolution, and, to a lesser extent; 3) sediment compaction; and 4) detrital pore-filling and authigenic grain-coating clays. Most samples analyzed have moderate to good reservoir quality. Samples with poor

APPENDIX A

PETROGRAPHIC ANALYTICAL PROCEDURES

X-ray Diffraction (XRD) Analysis

A representative portion of each sample was dried, extracted if necessary, and then ground in a Brinkman MM-2 Retsch Mill to a fine powder. This ground sample was next loaded into an aluminum sample holder. This "bulk" sample mount was scanned with a Philips X-ray diffractometer using nickel-filtered copper K-alpha radiation at standard scanning parameters. Computer analysis of the diffractograms provide qualitative identification of mineral phases and semiquantitative analysis of the relative abundance (in weight percent) of the various mineral phases. It should also be noted that X-ray diffraction **does not** allow the detection and identification of non-crystalline (amorphous) material, such as organic material.

An oriented clay fraction mount was prepared for each sample from the ground powder. The samples were further size fractionated by centrifuge to separate the <4 micron fraction. Ultrasonic treatment was used to suspend the material, then a dispersant was used to prevent flocculation when noted. The solution containing the clay fraction was then passed through a Fisher filter membrane apparatus allowing the solids to be collected on a cellulose membrane filter. These solids were then mounted on a glass slide, dried, and scanned with the Philips diffractometer. The oriented clay mount was glycolated and another diffractogram prepared to identify the expandable, water sensitive minerals. The samples were also heat treated, to aid in distinguishing kaolinite and chlorite.

Thin Section Petrographic Analysis

Samples selected for thin section analysis were prepared by first vacuum impregnating with blue-dyed epoxy. The samples were then mounted on an optical glass slide and cut and lapped in water to a thickness of 0.03 mm. The prepared sections were then covered with index oil and temporary cover slips, and then analyzed using standard petrographic techniques.

Scanning Electron Microscopy (SEM) Analysis

Samples selected for scanning electron microscopy analysis were first broken, or split, to expose fresh surfaces. The samples were then mounted on sample holders with a conductive carbon paste and coated with gold in a "cool" sputter coater to prevent heat damage to sensitive clay minerals or friable samples. The samples were analyzed with a SM-3000 Topcon Digital Scanning Electron Microscope and Tracor Northern Energy Dispersive Spectrometer (EDS).

reservoir quality are also high in either shaly matrix or carbonate cements. These samples are 9822', 9866', 9871', 9952', and 10008'.

Mineralogic Influences on Log Response

The following section discusses the effects on log response of the mineralogy and associated porosity types found in these samples.

1. Resistivity Logs: The main factors that may suppress resistivity in these intervals are "water bound" microporosity associated with pore-filling kaolinite and occasional, thin, clay-rich laminations, except at 9822' and 9871'. These two samples contain variable amounts of pore-filling detrital matrix clays that are microporous. Resistivity suppression within the analyzed zones is expected to be variable (see Table 1).

2. Density Logs: Thin section analysis indicates that some of the sandstones analyzed from this well contain the high density minerals dolomite (0%-10%), calcite (0%-36%), siderite (0%-15%), and pyrite (trace-4%). Core analysis data indicates that measured grain density ranges from 2.62 gm/cc to 2.79 gm/cc. Grain densities higher than 2.64 gm/cc have variable amounts of these higher-density minerals. Appropriate density values should be used in intervals which contain minerals with anomalously high or low density.

3. Gamma-Ray Log: Gamma-ray logs respond to radioactive isotopes. The clay minerals kaolinite (2% by weight from XRD) and chlorite (2% by weight from XRD) will not be detected by gamma-ray logs due to the absence of potassium in these minerals. Conversely, the mineral K-feldspar (2% by weight from XRD) will be detected as "clay" by gamma-ray logs due to the presence of potassium in this mineral.

APPENDIX B

X-RAY DIFFRACTION DATA

OMNI LABORATORIES, INC.
X-RAY DIFFRACTION
(WEIGHT %)

Client: Sandia Technologies, LLC **File No: N-4474**
Well: Dupont Injection Well No. 3 S/T 1 (Harrison County, MS) **Date: 03/02/99**

Sample Depth	CLAYS				CARBONATES				OTHER MINERALS							TOTALS		
	Chlorite	Kaolinite	Illite	/S or S	Calcite	Dolomite	Siderite	Quartz	K-spar	Plag.	Pyrite	Halite	Barite	Clays	Carb.	Other		
9432.00'	2	1	Tr	1	Tr	1	Tr	93	1	1	Tr	0	0	4	1	95		
9493.00'	3	1	Tr	Tr	Tr	Tr	Tr	91	2	3	Tr	0	0	4	Tr	96		
9520.00'	3	1	1	Tr	Tr	1	Tr	91	1	2	Tr	0	0	5	1	94		
9536.00'	2	2	0	Tr	Tr	1	Tr	90	2	3	Tr	0	0	4	1	95		
9572.00'	2	1	1	0	Tr	Tr	Tr	92	1	3	Tr	0	0	4	Tr	96		
9588.00'	2	1	Tr	0	1	Tr	1	94	Tr	1	Tr	0	0	3	2	95		
9822.00'	Tr	4	Tr	3	0	0	Tr	88	1	3	1	0	0	7	Tr	93		
9826.00'	2	4	4	2	0	Tr	Tr	82	2	3	1	0	0	12	Tr	88		
9844.00'	3	Tr	0	Tr	Tr	0	Tr	92	1	4	Tr	0	0	3	Tr	97		
9848.00'	1	2	0	Tr	Tr	0	Tr	95	Tr	2	Tr	0	0	3	Tr	97		
9861.00'	2	2	1	Tr	0	Tr	Tr	90	2	3	Tr	0	0	5	Tr	95		
9866.00'	2	1	2	2	41	Tr	8	40	Tr	2	2	0	0	7	49	44		
9871.00'	1	2	2	2	22	Tr	Tr	63	2	2	4	0	0	7	22	71		
9876.00'	2	17	19	22	0	0	Tr	34	5	1	Tr	0	0	60	Tr	40		
9887.00'	4	1	2	Tr	Tr	8	Tr	78	2	5	Tr	0	0	7	8	85		
9899.00'	3	2	1	0	Tr	0	Tr	89	1	4	Tr	0	0	6	Tr	94		
9904.00'	1	2	1	0	Tr	Tr	Tr	92	1	3	Tr	0	0	4	Tr	96		
9916.00'	3	2	2	0	0	Tr	Tr	89	1	3	Tr	0	0	7	Tr	93		
9929.00'	1	4	2	0	Tr	Tr	Tr	84	2	7	Tr	0	0	7	Tr	93		
9938.00'	1	3	1	Tr	1	Tr	6	85	1	2	Tr	0	0	5	7	88		
9952.00'	5	Tr	1	0	38	Tr	Tr	53	1	2	Tr	0	0	6	38	56		
9962.00'	2	2	Tr	0	Tr	0	11	80	2	3	Tr	0	0	4	11	85		
9970.00'	1	2	1	0	0	Tr	18	68	3	7	Tr	0	0	4	18	78		
9992.00'	1	3	3	Tr	5	2	Tr	75	3	8	Tr	0	0	7	7	86		
9996.00'	1	3	2	0	Tr	3	Tr	78	4	9	Tr	0	0	6	3	91		
10008.00'	1	6	7	Tr	Tr	Tr	Tr	70	3	8	5	0	0	14	Tr	86		
10016.00'	Tr	4	1	0	0	0	Tr	90	1	4	Tr	0	0	5	Tr	95		
10023.00'	Tr	4	Tr	0	Tr	Tr	Tr	91	1	4	Tr	0	0	4	Tr	96		
10032.00'	Tr	3	Tr	0	Tr	0	Tr	92	1	4	Tr	0	0	3	Tr	97		
AVERAGE	2	2	2	1	4	Tr	2	81	2	4	Tr	0	0	7	6	87		

* expandable mixed-layer illite/smectite or smectite

APPENDIX C

**THIN SECTION ANALYSIS RESULTS
AND
THIN SECTION PHOTOMICROGRAPHS**

THIN SECTION MODAL ANALYSIS

DuPont
Injection Well No. 3 S/T
Harrison County, Mississippi

DEPTH	9432'	9536'	9588'	9822'
Grain Size Avg. (mm):	0.38	0.28	0.36	0.20
Grain Size Range (mm):	0.10-0.60	0.10-0.45	0.10-0.64	0.03-0.48
Sorting:	Moderately Well	Moderately Well	Moderately Well	Moderate
Rock Name (Folk):	Subarkose	Subarkose	Subarkose	Subarkose
FRAMEWORK GRAINS				
<i>Quartz</i>	<u>55</u>	<u>56</u>	<u>53</u>	<u>48</u>
Monocrystalline	50	50	46	43
Polycrystalline	5	6	7	5
<i>Feldspar</i>	<u>3</u>	<u>4</u>	<u>4</u>	<u>6</u>
K-Feldspar	1	1	1	2
Plagioclase	2	3	3	4
<i>Lithic Fragments</i>	<u>2</u>	<u>3</u>	<u>1</u>	<u>4</u>
Carbonate Grains	0	0	0	0
Volcanic	tr	1	tr	tr
Metamorphic	2	2	1	2
Chert	tr	tr	tr	2
Mudstone	tr	0	0	0
ACCESSORY GRAINS	<u>tr</u>	<u>1</u>	<u>tr</u>	<u>2</u>
Muscovite	tr	1	tr	2
Biotite	0	0	0	0
Heavy Minerals*	tr	tr	tr	tr
ENVIRON. INDICATORS	<u>tr</u>	<u>tr</u>	<u>tr</u>	<u>3</u>
Organics (Plant Fragments)	tr	tr	tr	3
Glauconite	tr	0	0	0
Fossil Fragments	0	0	tr	0
CLAY MATRIX	<u>tr</u>	<u>1</u>	<u>tr</u>	<u>6</u>
AUTHIGENIC CEMENT	<u>19</u>	<u>15</u>	<u>19</u>	<u>21</u>
Pore-lining Clay	0	0	0	3
Kaolinite	tr	tr	tr	6
Quartz Overgrowths	12	11	12	10
Calcite	0	0	0	0
Dolomite	2	1	1	0
Ankerite	0	0	0	0
Siderite	tr	tr	tr	tr
Pyrite	tr	tr	tr	2
Fe/Ti Oxides**	4	3	4	0
Barite	0	0	0	0
Other opaques**	1	tr	2	0
Analcime	0	0	0	0
POROSITY	<u>21</u>	<u>20</u>	<u>23</u>	<u>10</u>
Primary	14	13	16	4
Secondary	7	7	7	4
Microscopic	tr	tr	tr	2
TOTALS:	100	100	100	100

* Garnet, tourmaline, zircon

THIN SECTION MODAL ANALYSIS

**DuPont
Injection Well No. 3 S/T
Harrison County, Mississippi**

DEPTH	9826'	9838'	9844'	9848'
Grain Size Avg. (mm):	0.22	0.45	0.42	0.42
Grain Size Range (mm):	0.02-0.70	0.05-1.04	0.05-0.98	0.05-0.83
Sorting:	Moderate	Moderate	Moderate	Moderate
Rock Name (Folk):	Subarkose	Subarkose	Subarkose	Subarkose
FRAMEWORK GRAINS				
<i>Quartz</i>	<u>51</u>	<u>57</u>	<u>56</u>	<u>51</u>
Monocrystalline	46	50	47	44
Polycrystalline	5	7	9	7
<i>Feldspar</i>	<u>6</u>	<u>6</u>	<u>2</u>	<u>6</u>
K-Feldspar	2	2	tr	2
Plagioclase	4	4	2	4
<i>Lithic Fragments</i>	<u>4</u>	<u>5</u>	<u>1</u>	<u>4</u>
Carbonate Grains	0	0	0	0
Volcanic	tr	tr	tr	tr
Metamorphic	2	2	tr	1
Chert	2	3	1	3
Mudstone	0	0	tr	0
ACCESSORY GRAINS	<u>3</u>	<u>tr</u>	<u>tr</u>	<u>tr</u>
Muscovite	3	tr	tr	tr
Biotite	0	0	0	0
Heavy Minerals*	tr	tr	tr	tr
ENVIRON. INDICATORS	<u>2</u>	<u>tr</u>	<u>tr</u>	<u>tr</u>
Organics (Plant Fragments)	2	tr	tr	tr
Glauconite	0	0	0	0
Fossil Fragments	0	0	0	0
CLAY MATRIX	<u>4</u>	<u>1</u>	<u>tr</u>	<u>tr</u>
AUTHIGENIC CEMENT	<u>16</u>	<u>12</u>	<u>21</u>	<u>18</u>
Pore-lining Clay	0	0	0	0
Kaolinite	2	tr	tr	1
Quartz Overgrowths	10	8	16	12
Calcite	0	0	0	0
Dolomite	0	0	0	0
Ankerite	0	0	0	0
Siderite	tr	0	0	0
Pyrite	2	tr	tr	tr
Fe/Ti Oxides**	0	2	3	4
Barite	0	0	0	0
Other Opaques**	2	2	2	1
Analcime	0	0	0	0
POROSITY	<u>14</u>	<u>19</u>	<u>20</u>	<u>21</u>
Primary	6	13	16	16
Secondary	8	6	4	5
Microscopic	tr	tr	tr	tr
TOTALS:	<u>100</u>	<u>100</u>	<u>100</u>	<u>100</u>

* Garnet, tourmaline, zircon

THIN SECTION MODAL ANALYSIS

DuPont
Injection Well No. 3 S/T
Harrison County, Mississippi

DEPTH	9856'	9861'	9866'	9871'
Grain Size Avg. (mm):	0.47	0.48	0.55	0.22
Grain Size Range (mm):	0.05-0.85	0.08-1.04	0.06-1.49	<0.01-0.70
Sorting:	Moderate	Moderately Poor	Poor	Moderate
Rock Name (Folk):	Subarkose	Subarkose	Sublitharenite	Subarkose
FRAMEWORK GRAINS				
<i>Quartz</i>	<u>57</u>	<u>52</u>	<u>42</u>	<u>21</u>
Monocrystalline	46	46	35	17
Polycrystalline	11	6	7	4
<i>Feldspar</i>	<u>1</u>	<u>2</u>	<u>4</u>	<u>5</u>
K-Feldspar	tr	tr	2	2
Plagioclase	1	2	2	3
<i>Lithic Fragments</i>	<u>2</u>	<u>3</u>	<u>7</u>	<u>1</u>
Carbonate Grains	0	0	0	0
Volcanic	tr	0	0	0
Metamorphic	tr	1	tr	tr
Chert	2	2	2	1
Mudstone	0	0	5	0
ACCESSORY GRAINS				
Muscovite	tr	1	0	tr
Biotite	0	0	0	0
Heavy Minerals*	tr	tr	tr	0
ENVIRON. INDICATORS				
Organics (Plant Fragments)	tr	tr	1	7
Glauconite	0	0	0	0
Fossil Fragments	0	0	0	4
CLAY MATRIX				
AUTHIGENIC CEMENT				
Pore-lining Clay	0	0	0	0
Kaolinite	tr	tr	tr	0
Quartz Overgrowths	15	14	2	5
Calcite	0	0	36	28
Dolomite	0	0	0	0
Ankerite	0	0	0	0
Siderite	0	0	0	0
Pyrite	tr	tr	2	4
Fe/Ti Oxides**	tr	4	0	0
Barite	0	0	0	0
Other Opaques**	3	1	0	0
Analcime	0	0	0	0
POROSITY				
Primary	17	17	1	1
Secondary	4	5	4	2
Microscopic	tr	tr	tr	2
TOTALS:	100	100	100	100

* Garnet, tourmaline, zircon

THIN SECTION MODAL ANALYSIS

**DuPont
Injection Well No. 3 S/T
Harrison County, Mississippi**

DEPTH	9887'	9899'	9904'	9916'
Grain Size Avg. (mm):	0.20	0.26	0.28	0.30
Grain Size Range (mm):	0.06-0.49	0.05-0.70	0.03-0.53	0.04-0.85
Sorting:	Moderately Well	Moderate	Moderately Well	Moderate
Rock Name (Folk):	Sublitharenite	Sublitharenite	Sublitharenite	Sublitharenite
<i>FRAMEWORK GRAINS</i>				
<i>Quartz</i>	<u>34</u>	<u>43</u>	<u>49</u>	<u>43</u>
Monocrystalline	30	35	40	38
Polycrystalline	4	8	9	5
<i>Feldspar</i>	<u>4</u>	<u>4</u>	<u>4</u>	<u>3</u>
K-Feldspar	1	1	1	1
Plagioclase	3	3	3	2
<i>Lithic Fragments</i>	<u>7</u>	<u>6</u>	<u>6</u>	<u>7</u>
Carbonate Grains	0	0	0	0
Volcanic	1	0	tr	tr
Metamorphic	4	2	4	5
Chert	2	4	2	2
Mudstone	0	0	0	tr
<i>ACCESSORY GRAINS</i>	<u>tr</u>	<u>tr</u>	<u>tr</u>	<u>1</u>
Muscovite	tr	tr	tr	1
Biotite	0	0	0	0
Heavy Minerals*	0	tr	tr	tr
<i>ENVIRON. INDICATORS</i>	<u>3</u>	<u>1</u>	<u>0</u>	<u>1</u>
Organics (Plant Fragments)	3	1	0	1
Glauconite	0	0	0	tr
Fossil Fragments	0	0	0	0
<i>CLAY MATRIX</i>	<u>3</u>	<u>2</u>	<u>tr</u>	<u>4</u>
<i>AUTHIGENIC CEMENT</i>	<u>33</u>	<u>25</u>	<u>20</u>	<u>19</u>
Pore-lining Clay	0	0	0	tr
Kaolinite	tr	tr	1	1
Quartz Overgrowths	18	22	16	11
Calcite	tr	0	0	0
Dolomite	10	0	0	0
Ankerite	0	0	0	0
Siderite	0	0	0	1
Pyrite	1	tr	tr	tr
Fe/Ti Oxides**	0	0	0	3
Barite	0	0	0	0
Other Opaques**	4	3	3	tr
Analcime	0	0	0	0
<i>POROSITY</i>	<u>16</u>	<u>19</u>	<u>21</u>	<u>22</u>
Primary	12	16	17	17
Secondary	4	3	4	5
Microscopic	tr	tr	tr	tr
TOTALS:	<u>100</u>	<u>100</u>	<u>100</u>	<u>100</u>

* Garnet, tourmaline, zircon

THIN SECTION MODAL ANALYSIS

DuPont
Injection Well No. 3 S/T
Harrison County, Mississippi

DEPTH	9929'	9938'	9952'	9962'
Grain Size Avg. (mm):	0.28	0.30	0.20	0.26
Grain Size Range (mm):	0.10-0.55	0.07-0.50	0.03-0.48	0.08-0.48
Sorting:	Moderately Well	Moderately Well	Moderately Well	Moderately Well
Rock Name (Folk):	Sublitharenite	Sublitharenite	Sublitharenite	Sublitharenite
FRAMEWORK GRAINS				
<i>Quartz</i>	<u>45</u>	<u>45</u>	<u>43</u>	<u>37</u>
Monocrystalline	37	41	41	32
Polycrystalline	8	4	2	5
<i>Feldspar</i>	<u>4</u>	<u>2</u>	<u>3</u>	<u>4</u>
K-Feldspar	1	tr	1	1
Plagioclase	3	2	2	3
<i>Lithic Fragments</i>	<u>7</u>	<u>5</u>	<u>11</u>	<u>7</u>
Carbonate Grains	0	0	5	0
Volcanic	tr	0	0	tr
Metamorphic	5	4	4	5
Chert	2	1	2	2
Mudstone	0	0	0	0
ACCESSORY GRAINS	<u>2</u>	<u>1</u>	<u>3</u>	<u>2</u>
Muscovite	2	1	3	2
Biotite	0	0	0	0
Heavy Minerals*	tr	tr	tr	tr
ENVIRON. INDICATORS	<u>tr</u>	<u>1</u>	<u>1</u>	<u>tr</u>
Organics (Plant Fragments)	tr	1	1	tr
Glauconite	0	0	0	0
Fossil Fragments	0	0	0	0
CLAY MATRIX	<u>2</u>	<u>tr</u>	<u>0</u>	<u>tr</u>
AUTHIGENIC CEMENT	<u>20</u>	<u>27</u>	<u>37</u>	<u>32</u>
Pore-lining Clay	0	0	0	0
Kaolinite	2	1	0	2
Quartz Overgrowths	14	12	2	14
Calcite	0	0	32	0
Dolomite	0	0	0	0
Ankerite	0	0	0	0
Siderite	0	10	0	12
Pyrite	tr	1	3	1
Fe/Ti Oxides**	4	0	0	0
Barite	0	0	0	0
Other Opaques**	tr	3	0	3
Analcime	0	0	0	0
POROSITY	<u>20</u>	<u>19</u>	<u>2</u>	<u>18</u>
Primary	14	15	tr	11
Secondary	6	4	2	7
Microscopic	tr	tr	0	tr
TOTALS:	100	100	100	100

* Garnet, tourmaline, zircon

THIN SECTION MODAL ANALYSIS

**DuPont
Injection Well No. 3 S/T
Harrison County, Mississippi**

DEPTH	9970'	9992'	9996'	10008'
Grain Size Avg. (mm):	0.21	0.17	0.15	0.14
Grain Size Range (mm):	0.04-0.38	0.03-0.28	0.04-0.45	<0.01-0.42
Sorting:	Moderately Well	Moderately Well	Moderately Well	Moderate
Rock Name (Folk):	Subarkose	Subarkose	Subarkose	Subarkose
FRAMEWORK GRAINS				
<i>Quartz</i>	<u>48</u>	<u>49</u>	<u>46</u>	<u>35</u>
Monocrystalline	43	42	40	30
Polycrystalline	5	7	6	5
<i>Feldspar</i>	<u>5</u>	<u>5</u>	<u>6</u>	<u>4</u>
K-Feldspar	2	2	2	1
Plagioclase	3	3	4	3
<i>Lithic Fragments</i>	<u>4</u>	<u>4</u>	<u>4</u>	<u>3</u>
Carbonate Grains	0	0	0	0
Volcanic	tr	0	tr	tr
Metamorphic	3	3	3	2
Chert	1	1	1	1
Mudstone	0	tr	0	0
ACCESSORY GRAINS	<u>1</u>	<u>2</u>	<u>3</u>	<u>9</u>
Muscovite	1	1	3	6
Biotite	0	0	0	3
Heavy Minerals*	tr	1	tr	tr
ENVIRON. INDICATORS	<u>tr</u>	<u>2</u>	<u>2</u>	<u>8</u>
Organics (Plant Fragments)	tr	2	2	8
Glauconite	0	tr	0	tr
Fossil Fragments	0	0	0	0
CLAY MATRIX	<u>0</u>	<u>tr</u>	<u>3</u>	<u>10</u>
AUTHIGENIC CEMENT	<u>27</u>	<u>23</u>	<u>17</u>	<u>21</u>
Pore-lining Clay	0	0	0	0
Kaolinite	tr	tr	tr	5
Quartz Overgrowths	11	13	11	12
Calcite	0	4	1	tr
Dolomite	0	5	3	1
Ankerite	0	0	0	0
Siderite	15	tr	tr	0
Pyrite	tr	1	1	3
Fe/Ti Oxides**	tr	0	0	0
Barite	0	0	0	0
Other Opaques**	1	0	1	0
Analcime	0	0	0	0
POROSITY	<u>15</u>	<u>15</u>	<u>19</u>	<u>10</u>
Primary	12	11	15	7
Secondary	3	4	4	2
Microscopic	tr	tr	tr	1
TOTALS:	<u>100</u>	<u>100</u>	<u>100</u>	<u>100</u>

* Garnet, tourmaline, zircon

THIN SECTION MODAL ANALYSIS

**DuPont
Injection Well No. 3 S/T
Harrison County, Mississippi**

DEPTH	10016'	10023'	10032'	
Grain Size Avg. (mm):	0.27	0.28	0.33	
Grain Size Range (mm):	0.05-0.52	0.08-0.55	0.05-0.48	
Sorting:	Moderately Well	Moderately Well	Moderately Well	
Rock Name (Folk):	Sublitharenite	Sublitharenite	Sublitharenite	
<i>FRAMEWORK GRAINS</i>				
<i>Quartz</i>	<u>47</u>	<u>54</u>	<u>57</u>	
Monocrystalline	41	51	51	
Polycrystalline	6	3	6	
<i>Feldspar</i>	<u>3</u>	<u>3</u>	<u>3</u>	
K-Feldspar	1	tr	tr	
Plagioclase	2	3	3	
<i>Lithic Fragments</i>	<u>5</u>	<u>4</u>	<u>3</u>	
Carbonate Grains	0	0	0	
Volcanic	0	0	tr	
Metamorphic	3	3	2	
Chert	2	1	1	
Mudstone	0	0	0	
<i>ACCESSORY GRAINS</i>	<u>1</u>	<u>tr</u>	<u>tr</u>	
Muscovite	1	tr	tr	
Biotite	0	0	0	
Heavy Minerals*	tr	tr	tr	
<i>ENVIRON. INDICATORS</i>	<u>4</u>	<u>1</u>	<u>tr</u>	
Organics (Plant Fragments)	4	1	tr	
Glauconite	tr	0	0	
Fossil Fragments	0	0	0	
<i>CLAY MATRIX</i>	<u>1</u>	<u>tr</u>	<u>tr</u>	
<i>AUTHIGENIC CEMENT</i>	<u>20</u>	<u>18</u>	<u>15</u>	
Pore-lining Clay	0	0	0	
Kaolinite	tr	1	1	
Quartz Overgrowths	16	16	14	
Calcite	0	0	0	
Dolomite	0	0	0	
Ankerite	0	0	0	
Siderite	tr	0	0	
Pyrite	1	tr	tr	
Fe/Ti Oxides**	1	0	0	
Barite	0	0	0	
Other Opaques**	2	1	tr	
Analcime	0	0	0	
<i>POROSITY</i>	<u>19</u>	<u>20</u>	<u>22</u>	
Primary	14	14	16	
Secondary	5	4	6	
Microscopic	tr	2	tr	
TOTALS:	100	100	100	

* Garnet, tourmaline, zircon

**Dupont
Injection Well No. 3 S/T
Harrison County, Mississippi**

File No. GN-4474

SAMPLE DEPTH: 9432 FEET

PLATE 1A

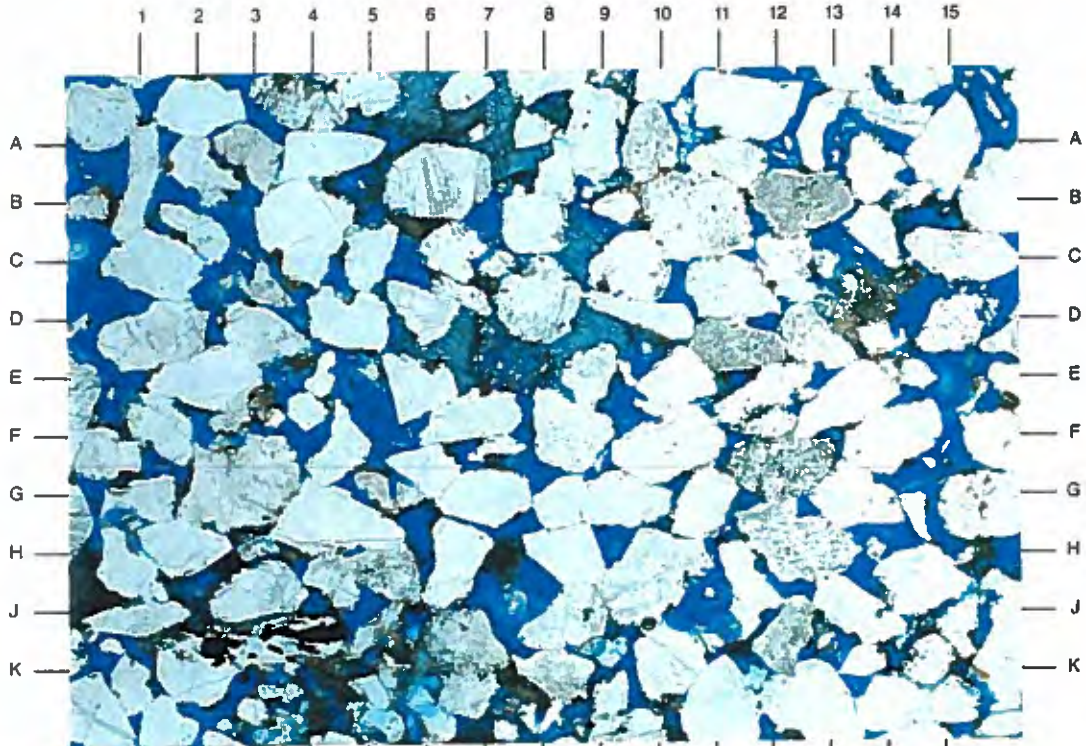
The low magnification photomicrograph shows a coarse-grained sandstone that has fairly abundant and evenly distributed visible porosity (blue). Visible pore types include both primary intergranular (E-F11.5,G10) and secondary dissolution (E7,F5) types. Secondary porosity includes both grain-moldic (F5,J7.5) and intragranular (E7) pore types. Note the dolomite cement (A6,C8.5) found as a patchy pore filling.

Magnification: 40X

PLATE 1B

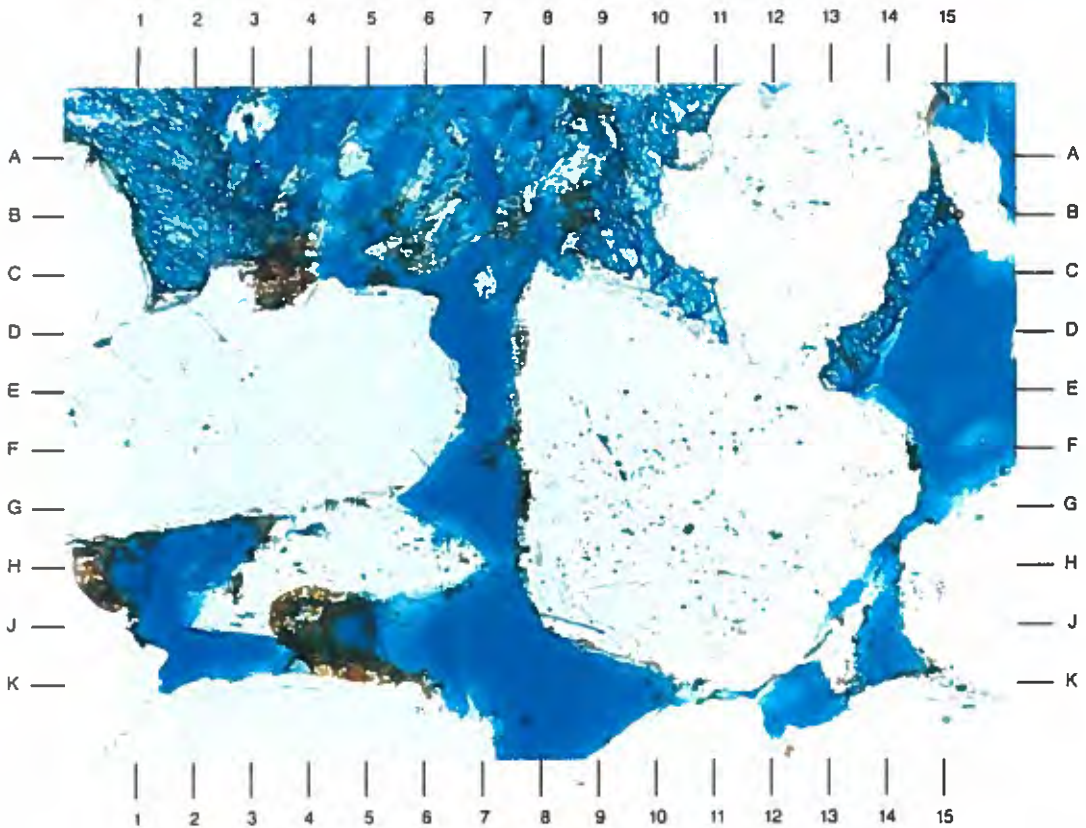
The high magnification photomicrograph details the area of E8 in Plate 1A. Overall cementation in this sample is moderate and accounts for 19% of the sample (thin section analysis). Quartz overgrowths (E12,G-H4) form flat to pseudo-hexagonal crystal faces that nucleate on host quartz sand grains. Dolomite cement (A1,A10) is a patchy pore filling and is iron-rich.

Magnification: 200X



A

0.25 mm



B

0.05 mm

**Dupont
Injection Well No. 3 S/T
Harrison County, Mississippi**

File No. GN-4474

SAMPLE DEPTH: 9536 FEET

PLATE 2A

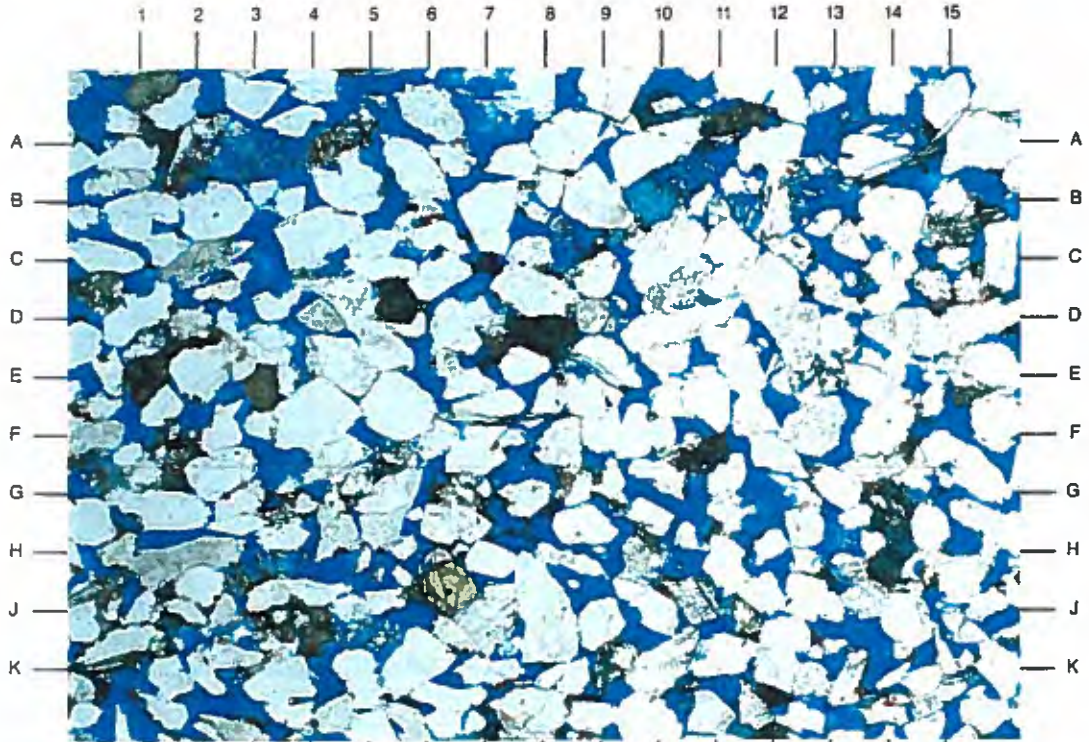
This low magnification photomicrograph shows another sandstone that has good effective porosity development. These pores include both primary intergranular (E8,E-F12) and secondary dissolution (A-B3,H7.5) pore types. This sandstone is quartz-rich and is classified as a subarkose (Folk, 1980). Low amounts of feldspars (J10.5) and lithics (E-F3) are also noted.

Magnification: 40X

PLATE 2B

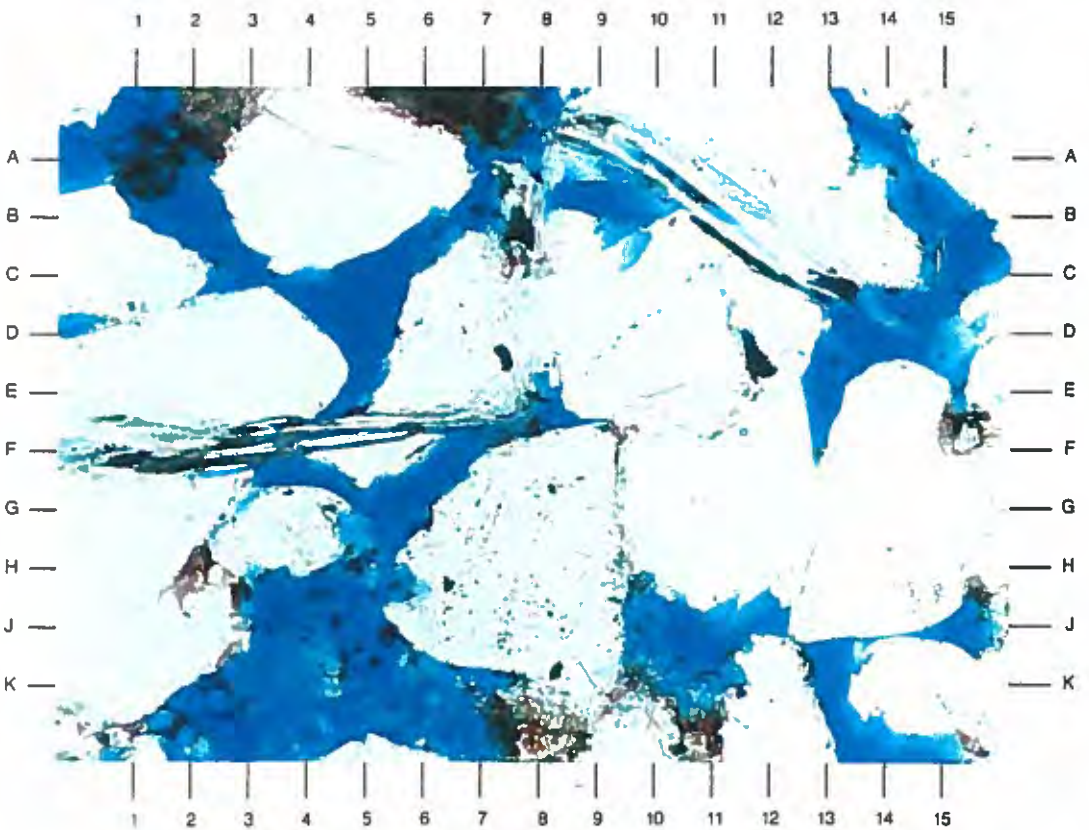
The high magnification view details the area of E8 in Plate 2A. Both primary (C5) and secondary (K5) pores are intermixed in this sample. These pores are interconnected by mostly open pore throats (B-C6,G6). Some pore throats, however, are occluded by quartz overgrowths (G9.5,H12.5). Note the slightly contorted ductile mica fragments (B11,F2).

Magnification: 200X



A

0.25 mm



B

0.05 mm

**Dupont
Injection Well No. 3 S/T
Harrison County, Mississippi**

File No. GN-4474

SAMPLE DEPTH: 9588 FEET

PLATE 3A

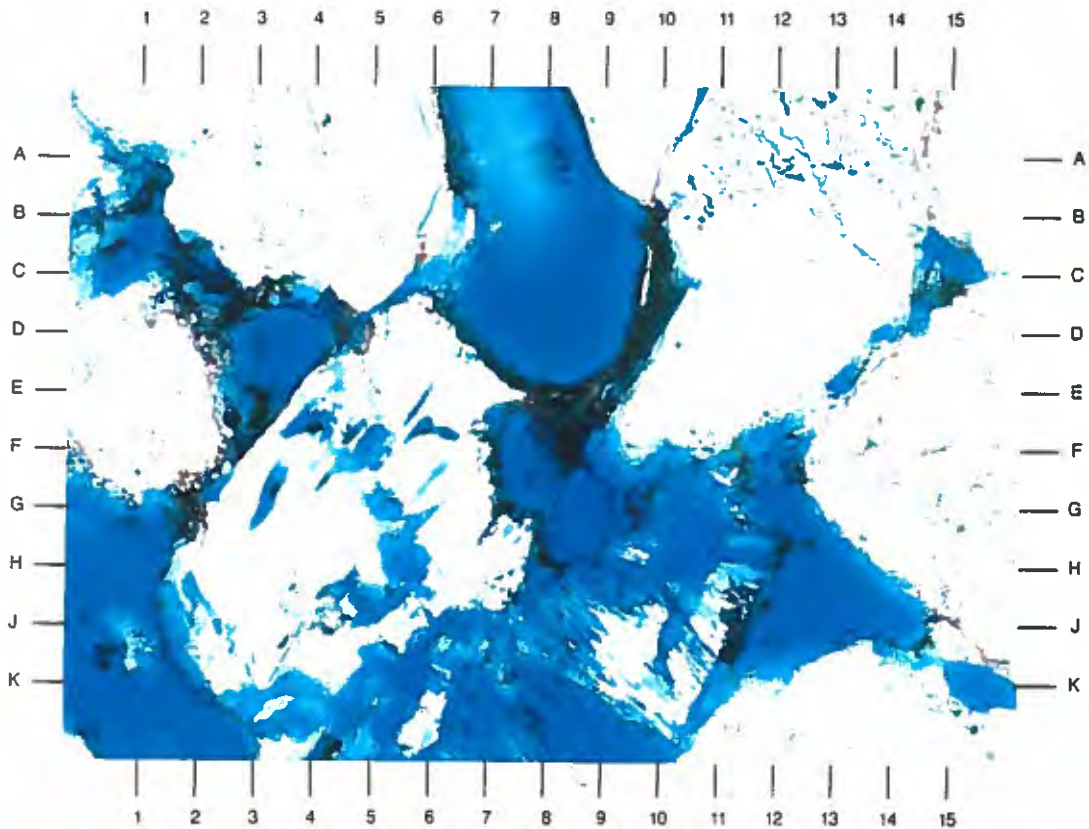
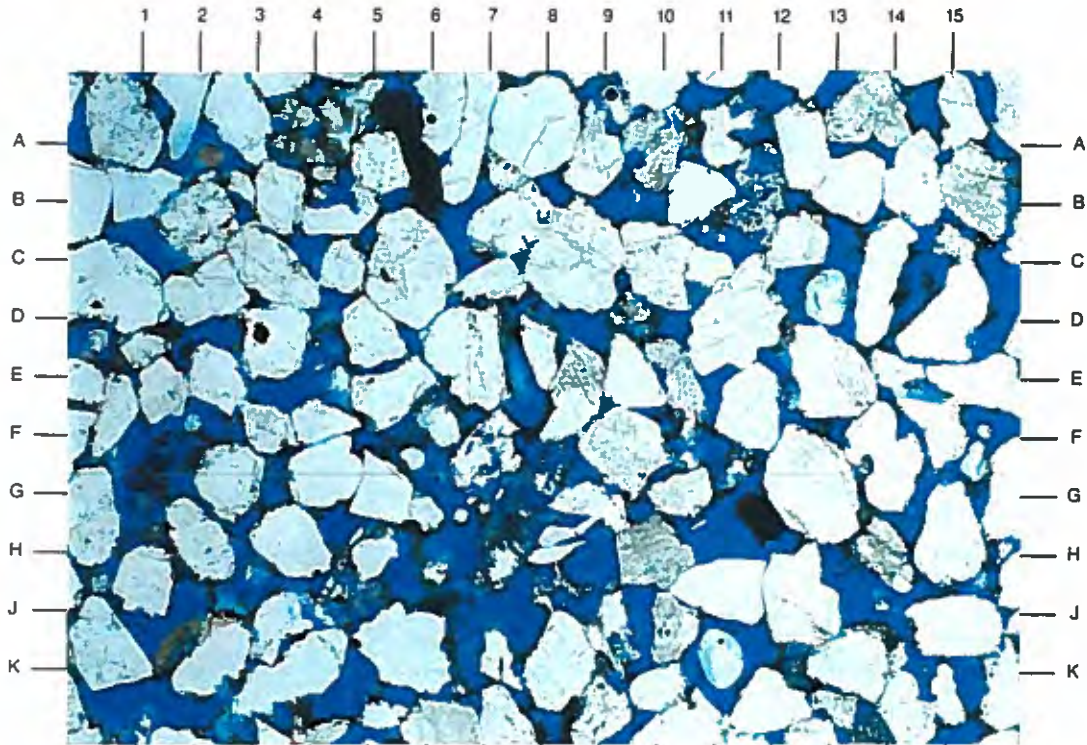
Sample 16398 feet is a moderately well sorted, medium-grained sandstone (average grain size is 0.36mm). Both intergranular (B8,E11) and dissolution (B11.5,J7) pores (blue) are abundant in this view and appear to be well interconnected. The dark material that infills some pores (A5.5) and lines pore walls (F8,F11) is residual quantities of waste material that has been introduced into the zone.

Magnification: 40X

PLATE 3B

This high magnification photomicrograph details the area of E8 in Plate 3A. Many pore walls in this sandstone are lined with residual waste (C2,D10) that has been introduced into this sandstone. This material clings to the irregular surfaces of sand grains. Secondary porosity is well developed in this sample and includes both grain-moldic (B7) and intragranular (G5) pore types.

Magnification: 200X



Dupont
Injection Well No. 3 S/T
Harrison County, Mississippi

File No. GN-4474

SAMPLE DEPTH: 9822 FEET

PLATE 4A

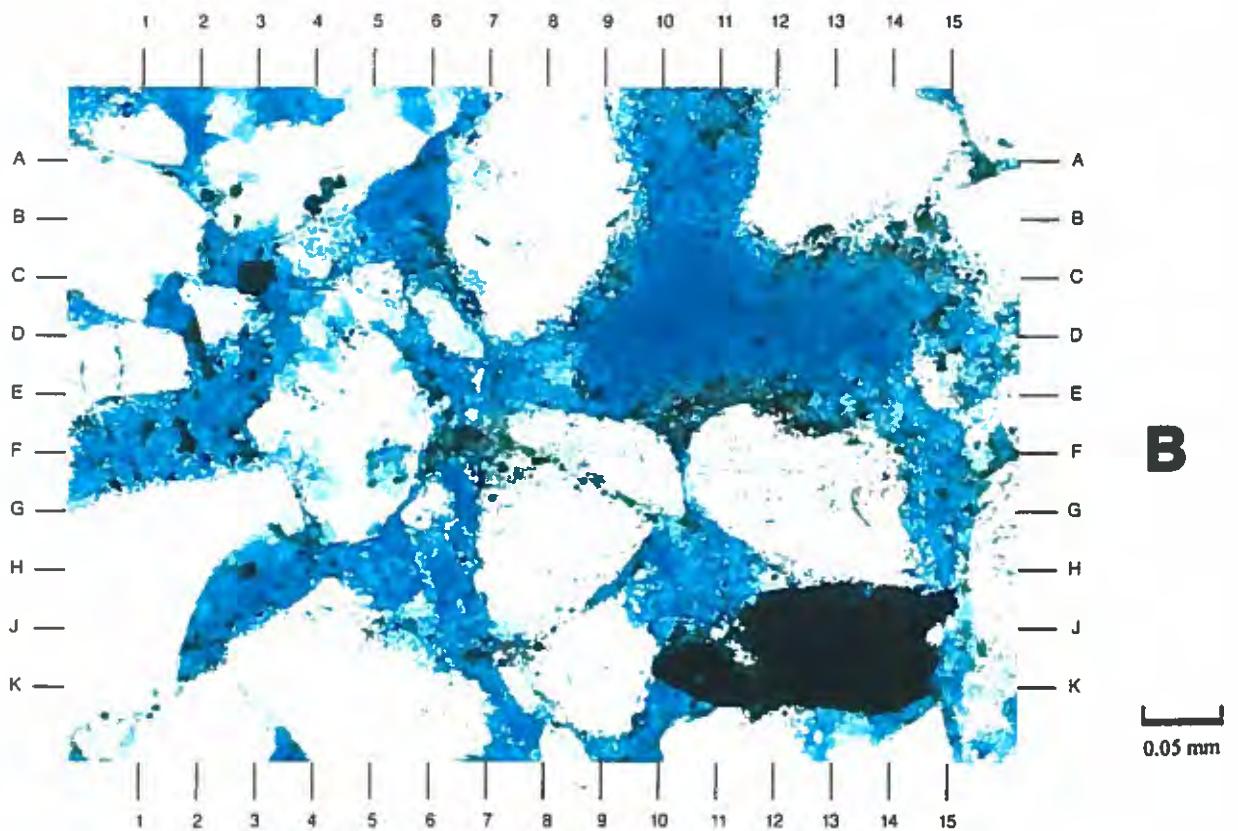
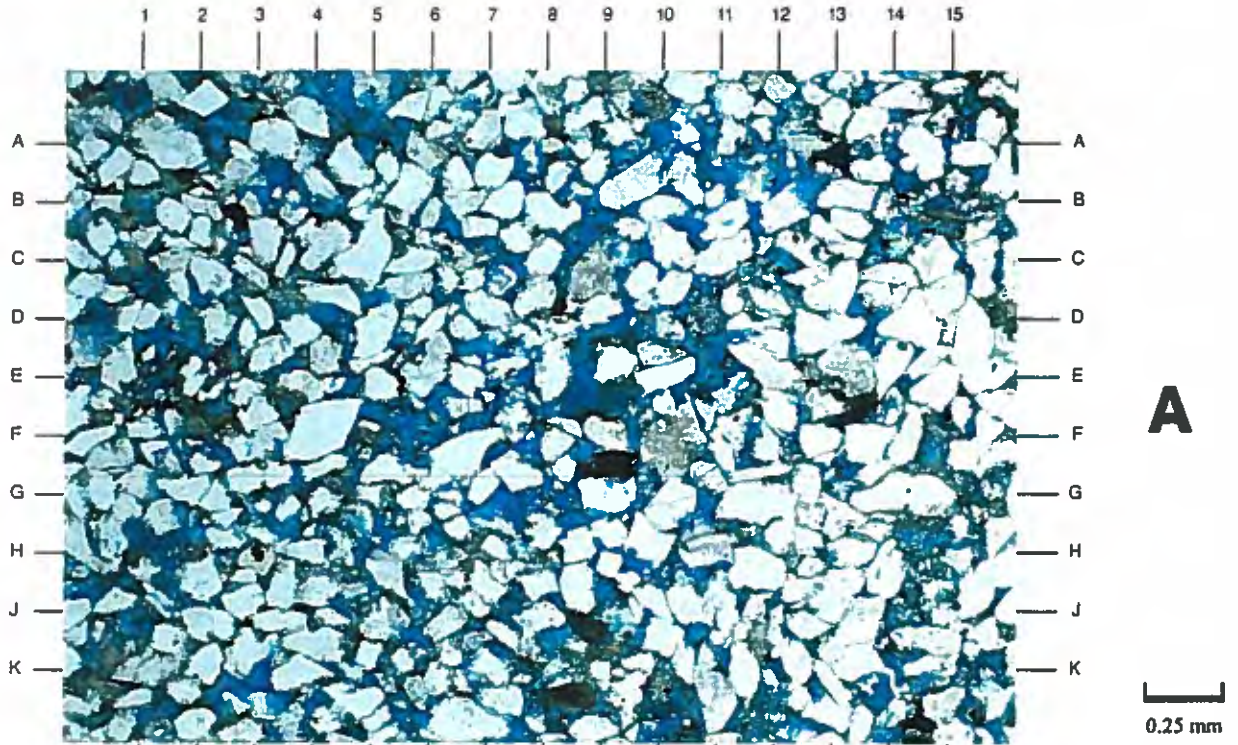
A fine-grained sandstone is observed in the sample taken from 9822'. This sandstone is moderately well sorted and massive in fabric. Occasional fragments of organic material (black) are scattered throughout the sample. Although most visible pores appear to be well interconnected, most pore throats are reduced by the presence of authigenic kaolinite.

Magnification: 40X

PLATE 4B

This high magnification photomicrograph details the area of F8 in Plate 4A. Authigenic kaolinite (A10,F1,H11) is seen infilling pores and lining pore walls. This clay type forms as aggregates of booklets that are loosely bound to pore walls and can block pore throats. Quartz overgrowths (A15,K1.5) are also seen occluding pore throats.

Magnification: 200X



Dupont
Injection Well No. 3 S/T
Harrison County, Mississippi

File No. GN-4474

SAMPLE DEPTH: 9826 FEET

PLATE 5A

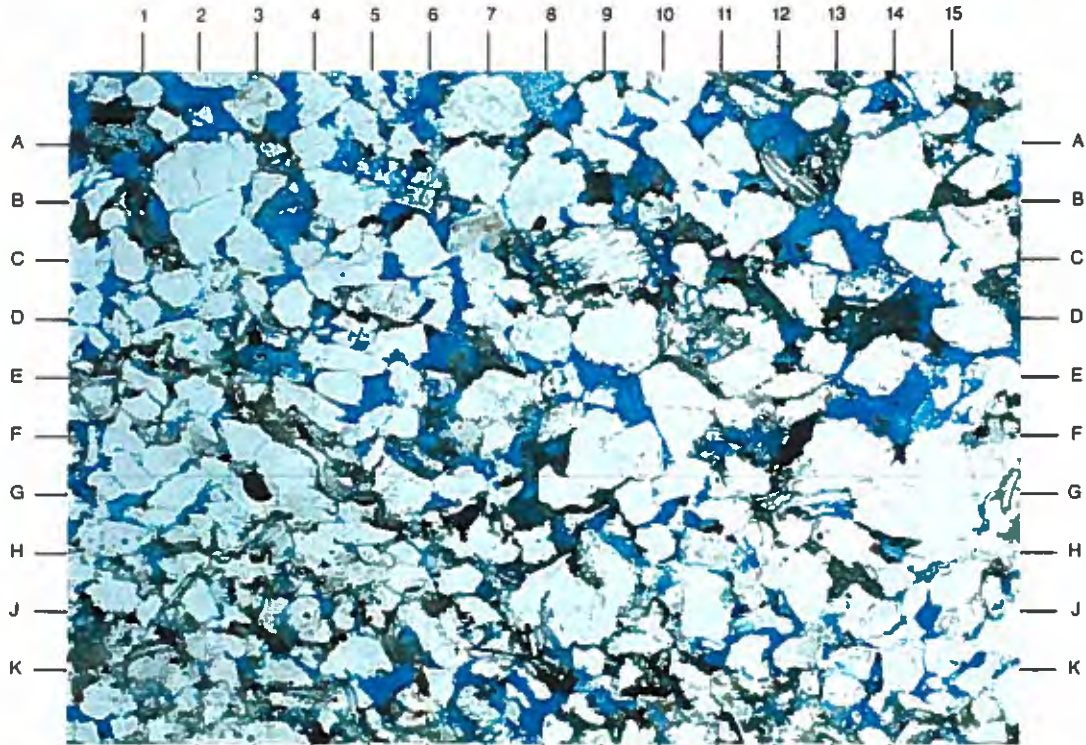
This low magnification photomicrograph shows that the sample taken from 9826' is a moderately sorted medium-grained sandstone (average grain size is 0.32mm). Visible porosity (blue) is more erratically distributed in this sandstone than seen in previous samples, thereby creating a more tortuous flow path. Slightly contorted mica fragments (G4) indicate some sediment compaction has occurred.

Magnification: 40X

PLATE 5B

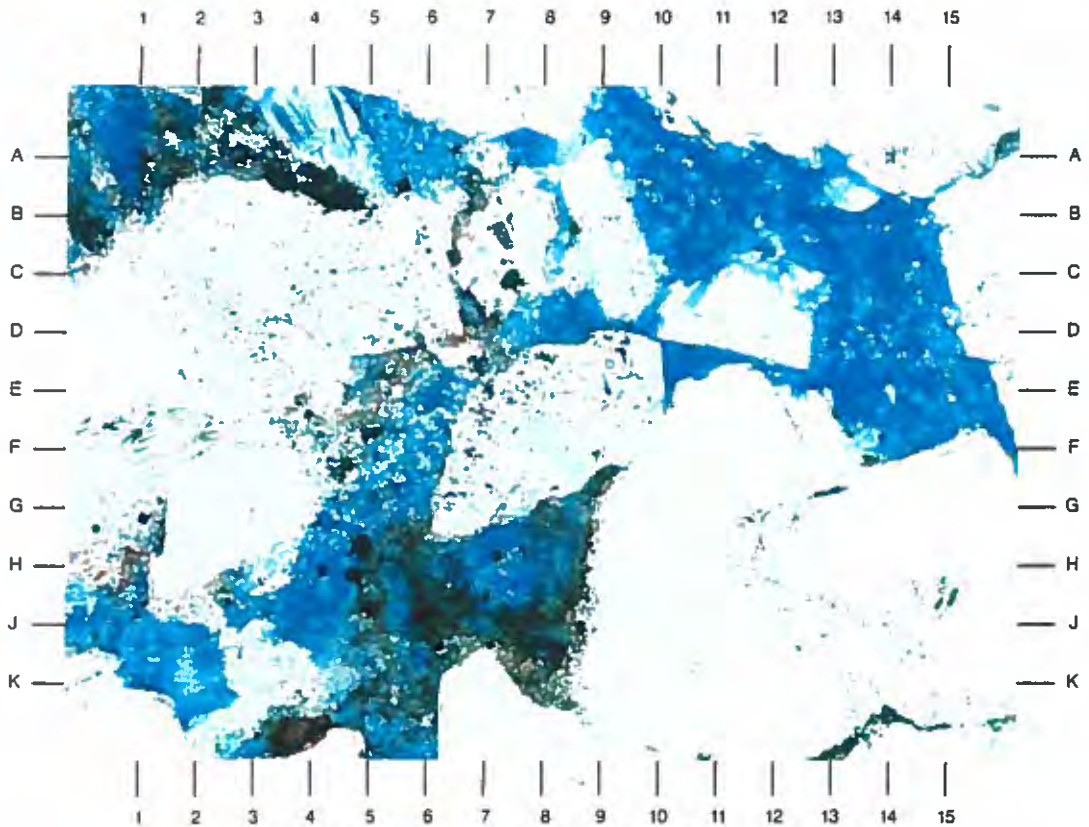
This high magnification photomicrograph details the area of E7 in Plate 5A. The visible pores (blue) that appear here are not well interconnected. Quartz overgrowth cementation (F9.5,J2.5) restrict adjoining pore throats. Authigenic kaolinite (A6,F5.5) also reduces the effectiveness of these pores.

Magnification: 200X



A

0.25 mm



B

0.05 mm

Dupont
Injection Well No. 3 S/T
Harrison County, Mississippi

File No. GN-4474

SAMPLE DEPTH: 9844 FEET

PLATE 6A

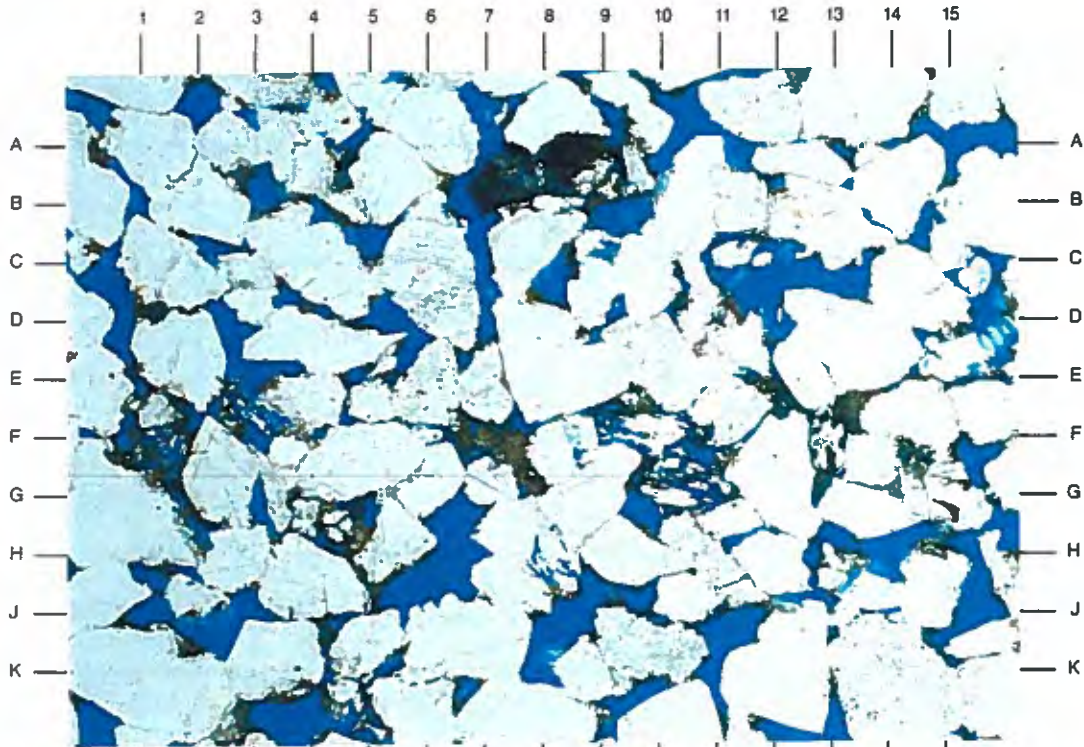
The coarse-grained sandstone taken from 9844' is massive in fabric and has a well developed pore system (blue). These pores are well interconnected, as documented by the remaining residual waste material (brown) found in interconnecting pore throats. This sandstone is quartz-rich and classified as a subarkose (Folk, 1980).

Magnification: 40X

PLATE 6B

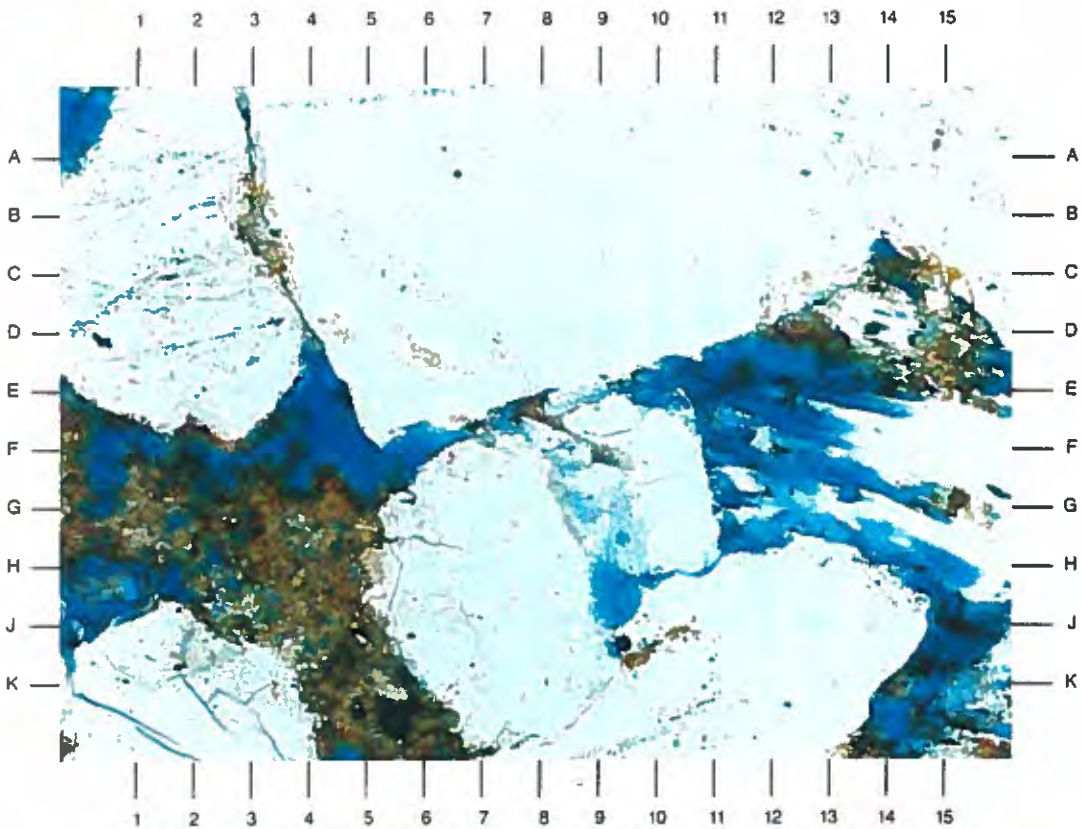
This high magnification photomicrograph details the area of E8 in Plate 6A. Waste material (brown) that has been introduced into the zone is observed as pore filling or lining pore walls and pore throats. Some pore throats, however, are reduced by quartz overgrowths (B3,G8). Note the partially dissolved feldspar grain at F14.

Magnification: 200X



A

0.25 mm



B

0.05 mm

**Dupont
Injection Well No. 3 S/T
Harrison County, Mississippi**

File No. GN-4474

SAMPLE DEPTH: 9848 FEET

PLATE 7A

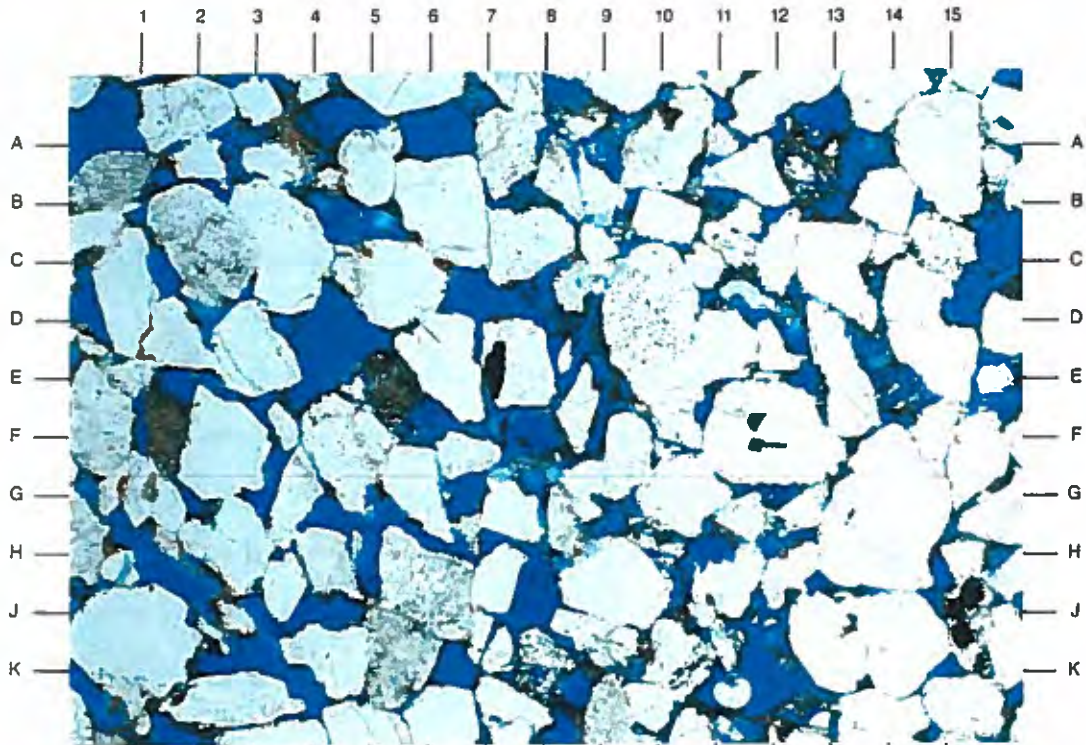
This sample is similar to the previous sample described (see Plate 7A). This coarse-grained sandstone (average grain is size 0.42mm) is massive in fabric and moderately sorted. Visible pores (blue) are abundant and appear well interconnected. Many pore walls are lined by waste material, indicating these pores are well interconnected.

Magnification: 40X

PLATE 7B

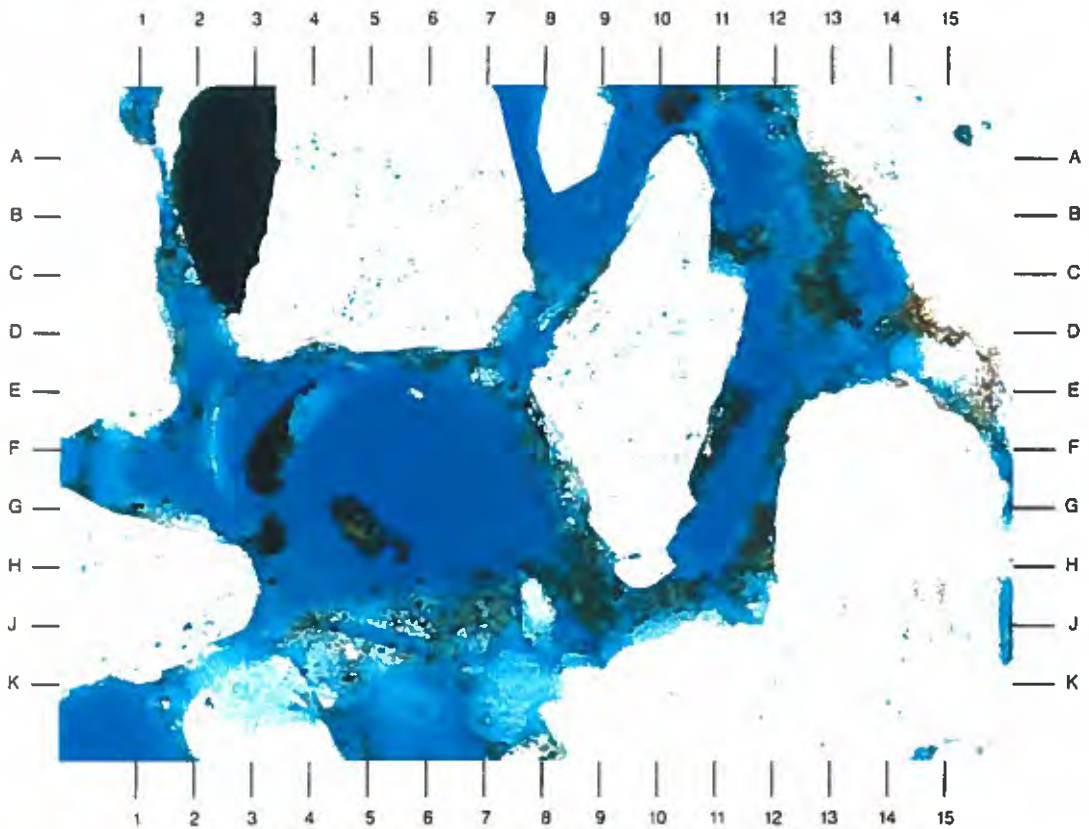
This high magnification photomicrograph details the area of E8 in Plate 7A. Pore-lining material (C1.5,J9,C13) is noted and reduces apparent pore-throat interconnection. The irregular surfaces of many sand grains allows this material to cling to sand grain surfaces.

Magnification: 200X



A

0.25 mm



B

0.05 mm

**Dupont
Injection Well No. 3 S/T
Harrison County, Mississippi**

File No. GN-4474

SAMPLE DEPTH: 9856 FEET

PLATE 8A

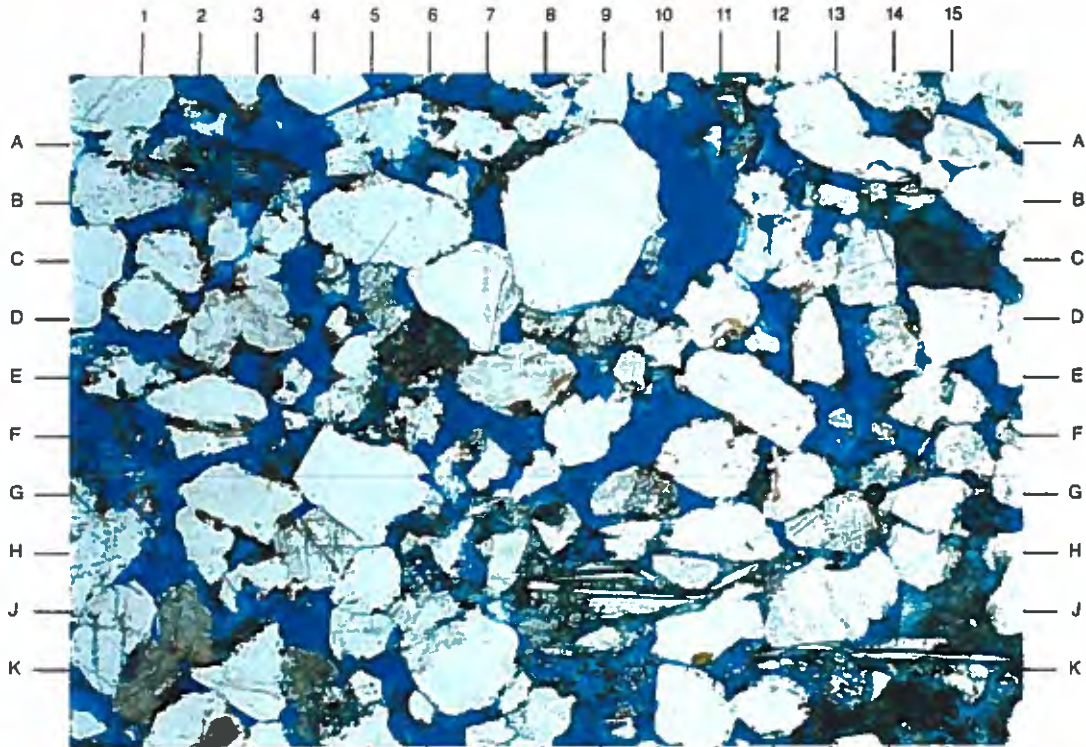
The thin section sample from 9856' consists of a massive, coarse-grained sandstone that is quartz-rich. This sandstone is classified as a quartzarenite (Folk, 1980). Less stable grains (A3,C7,B10) composed of feldspar and lithic fragments appear partially dissolved by secondary dissolution. This secondary porosity accounts for 4% of the sample. Primary intergranular porosity (E-F4,F-G13) was determined by thin section analysis to be 17%.

Magnification: 40X

PLATE 8B

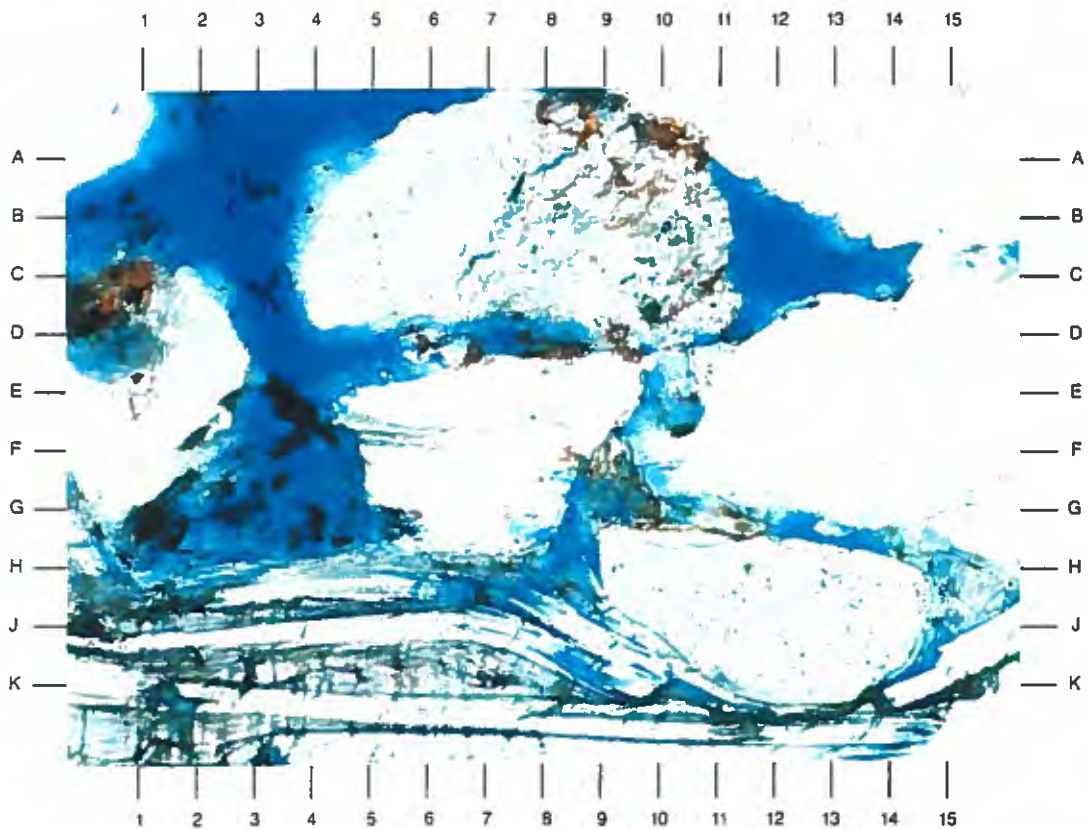
This high magnification photomicrograph shows the area of E8 in Plate 8A. Partial pore occlusion by booklets of authigenic kaolinite (E11,C4) is noted. Quartz overgrowths (B-C3.5,G2,K5) also act as a pore-reducing component. Quartz grains are common in this quartzarenite and consist of both monocrystalline (A1,A15) and polycrystalline (A7) varieties.

Magnification: 200X



A

0.25 mm



B

0.05 mm

SAMPLE DEPTH: 9861 FEET

PLATE 9A

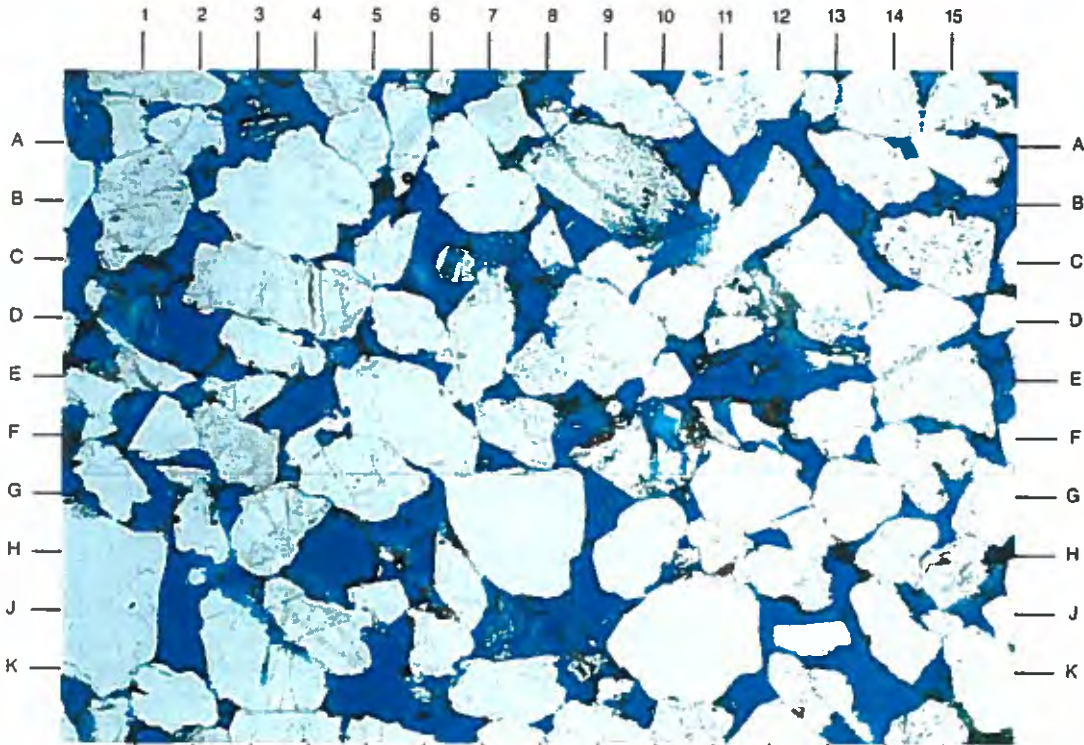
The low magnification of the sample taken from 9861' shows that this upper medium-grained sandstone (average grain size is 0.48mm) is moderately poorly sorted. Framework grains range in size from 0.08mm to 1.04mm. Remnants of waste material (light brown) are seen clinging to the irregular surfaces of sand grains, as evidence of a well interconnected pore system.

Magnification: 40X

PLATE 9B

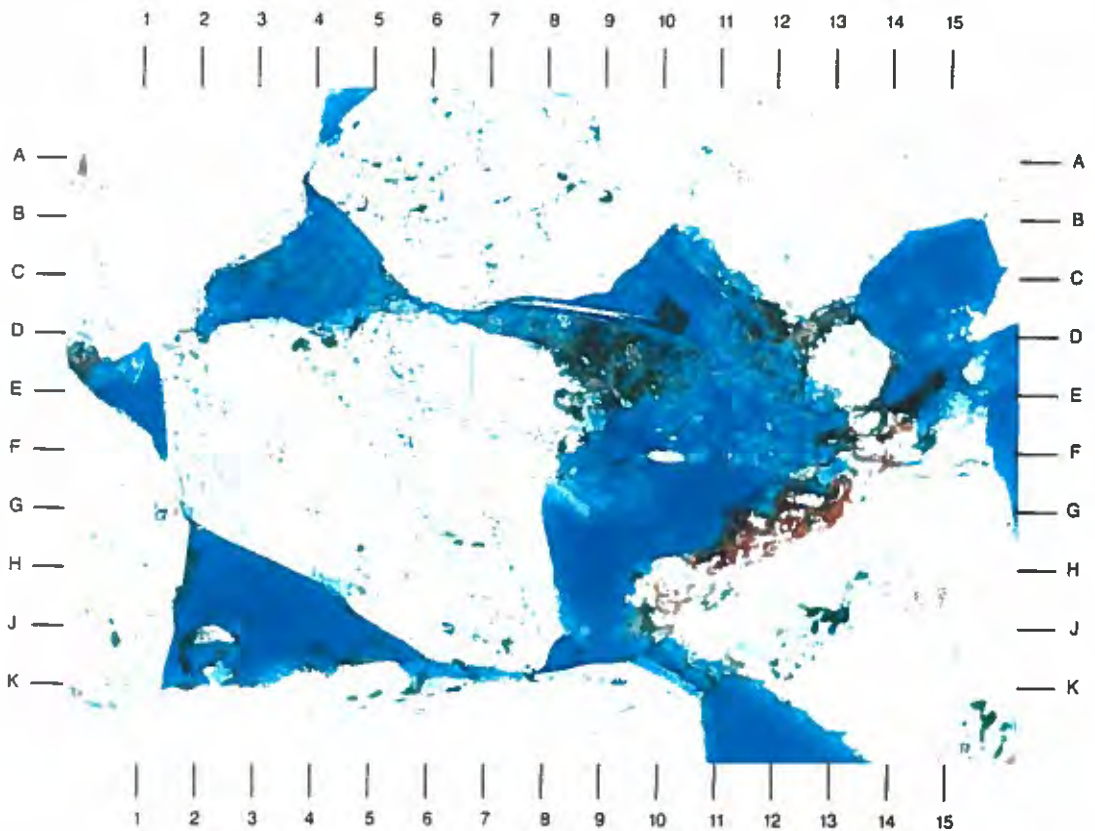
This high magnification photomicrograph details the area of G10 in Plate 9A. Remnants of waste material that have passed through the pore system is indicated by light brown staining. Irregular sand grain surfaces are created by the presence of quartz overgrowth crystals that nucleate on the host grains. Note the slight deformation of a ductile mica fragment by a sand grain (K12) during sediment compaction.

Magnification: 200X



A

0.25 mm



B

0.05 mm

Dupont
Injection Well No. 3 S/T
Harrison County, Mississippi

File No. GN-4474

SAMPLE DEPTH: 9866' FEET

PLATE 10A

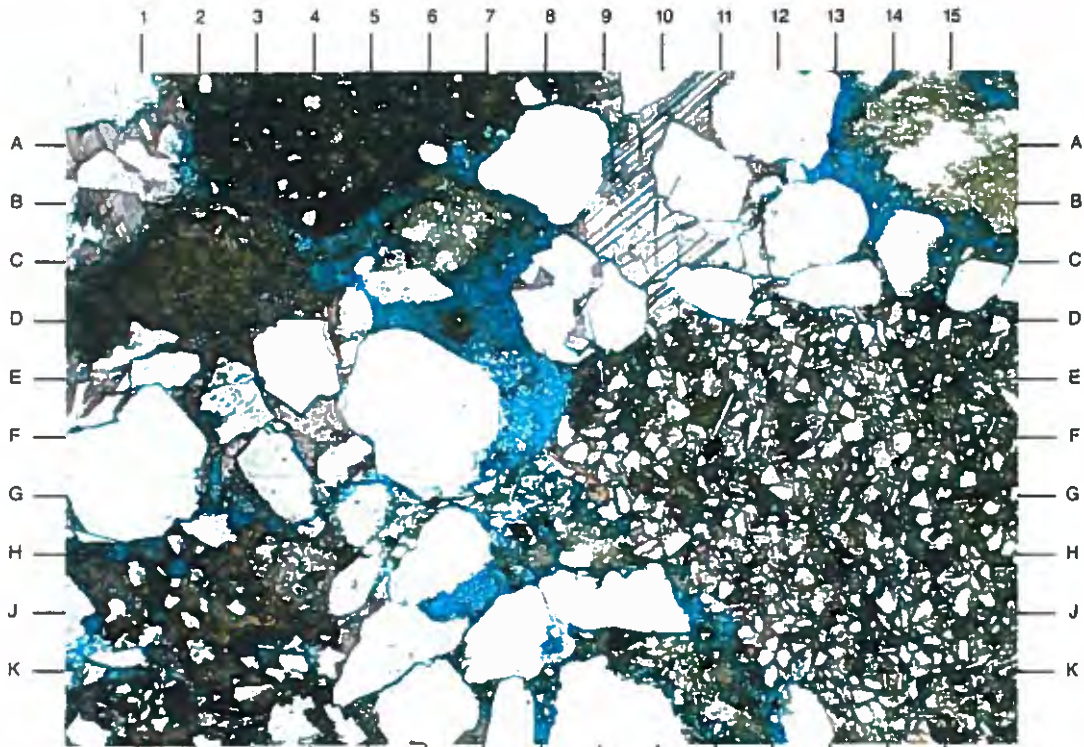
The low magnification photomicrograph shows that the sample from 9866' has a complex diagenetic history. This poorly sorted sandstone consists of assorted quartz sand grains (white) intermixed with larger shale- and siderite-rich clasts (A4,C2). A large calcite-cemented clast (G13) is also noted. Most intergranular areas are infilled with calcite cement (red). Nearly all remaining visible porosity (blue) is secondary.

Magnification: 40X

PLATE 10B

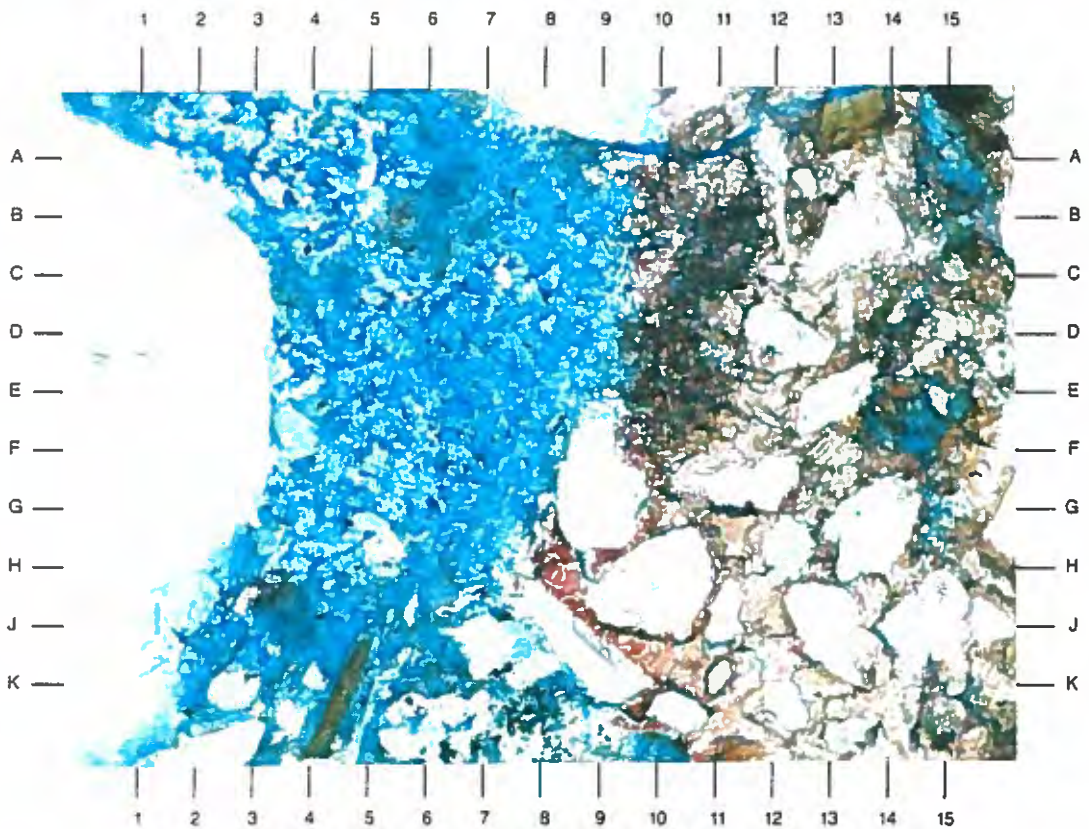
This high magnification photomicrograph details the area of E8 in Plate 10A. A large secondary pore (blue) is infilled with authigenic kaolinite. Adjacent to this pore are a large quartz sand grain (E1) and a portion of a clast. Calcite cement is seen completely surrounding sand grains in this clast, effectively occluding primary porosity. Only rare secondary pores (A15,E-F15) are seen.

Magnification: 200X



A

0.25 mm



B

0.05 mm

Dupont
Injection Well No. 3 S/T
Harrison County, Mississippi

File No. GN-4474

SAMPLE DEPTH: 9871 FEET

PLATE 11A

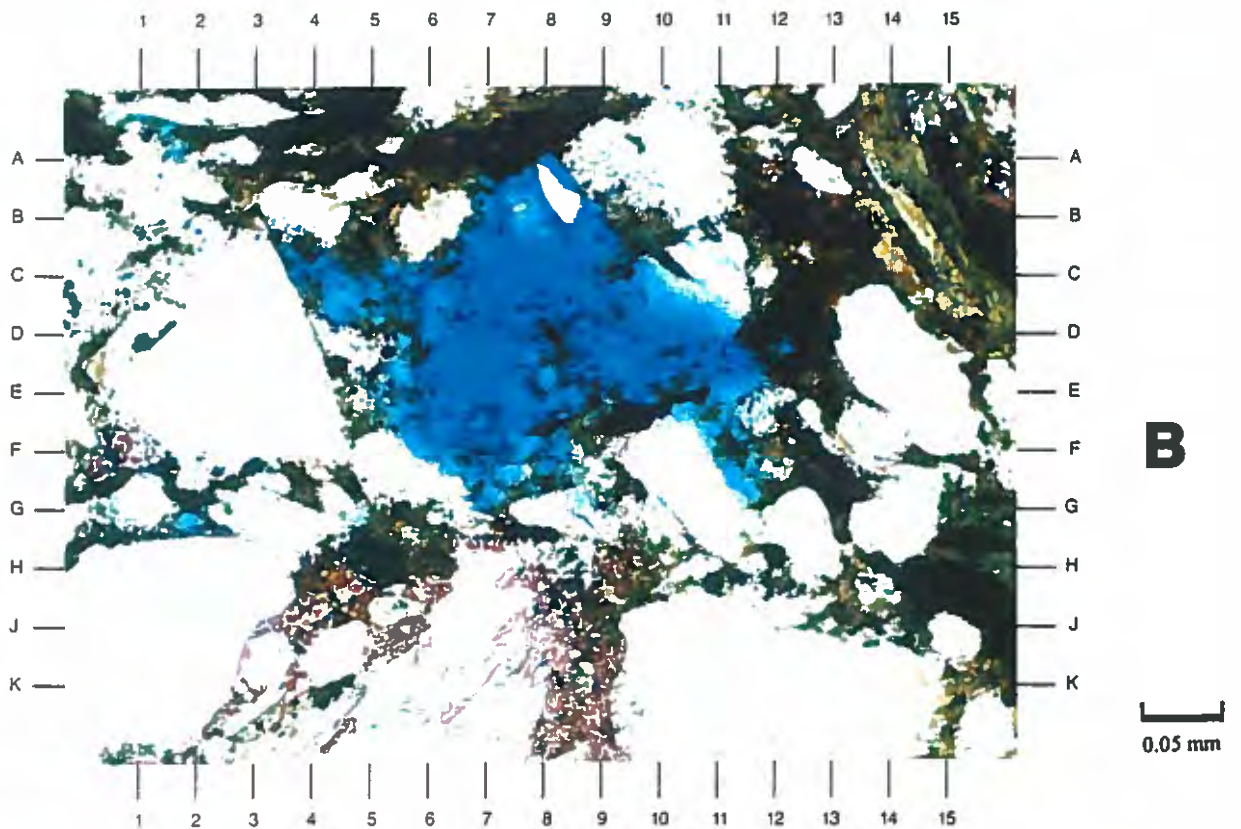
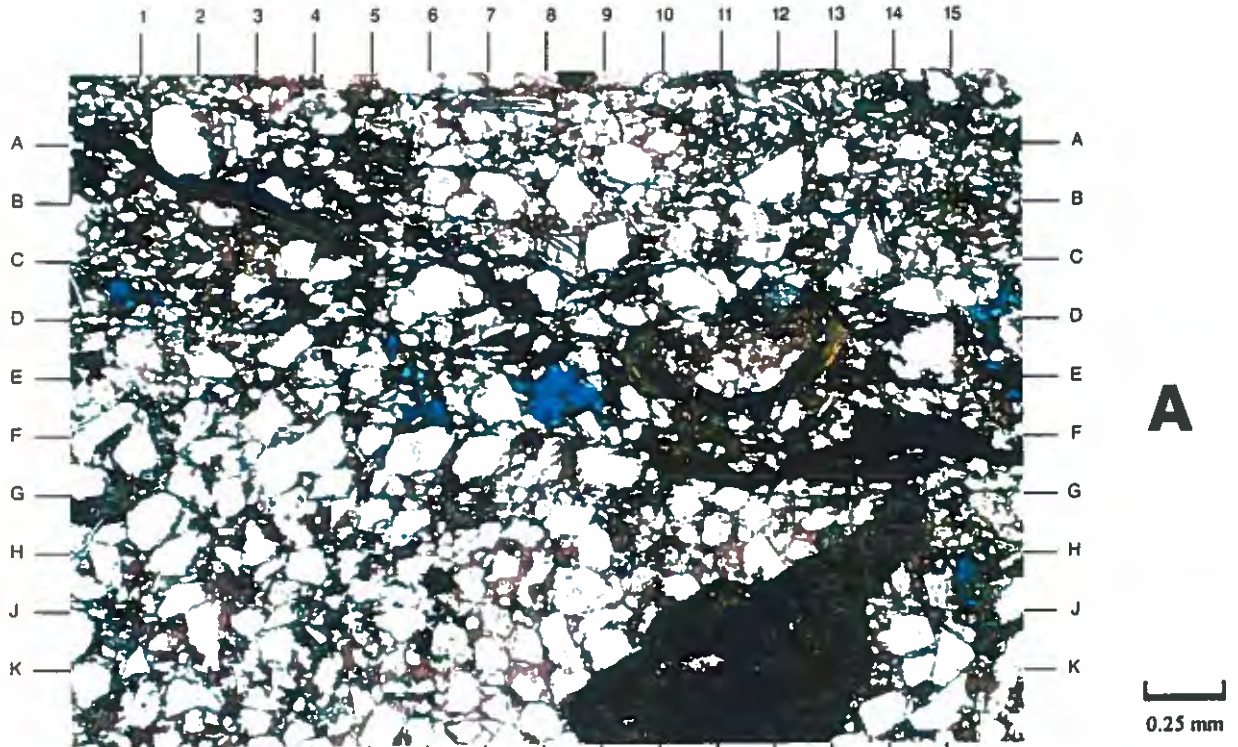
A shaly, fine-grained sandstone is found at this depth. Detrital matrix (brown) is seen infilling numerous intergranular pores. Abundant calcite cementation (red) is also noted in most intergranular areas. This combination of pore-filling components results in a severe reduction in visible porosity. Remaining visible porosity (blue) is isolated. Occasional calcareous fossil fragments (E12) are observed in this sandstone.

Magnification: 40X

PLATE 11B

This high magnification photomicrograph details the area of E8 in Plate 11A. The secondary pore in this view is surrounded by calcite cement (red) and detrital matrix (dark brown). This detrital material appears organic-rich. Organic material is also partially pyritized.

Magnification: 200X



**Dupont
Injection Well No. 3 S/T
Harrison County, Mississippi**

File No. GN-4474

SAMPLE DEPTH: 9887 FEET

PLATE 12A

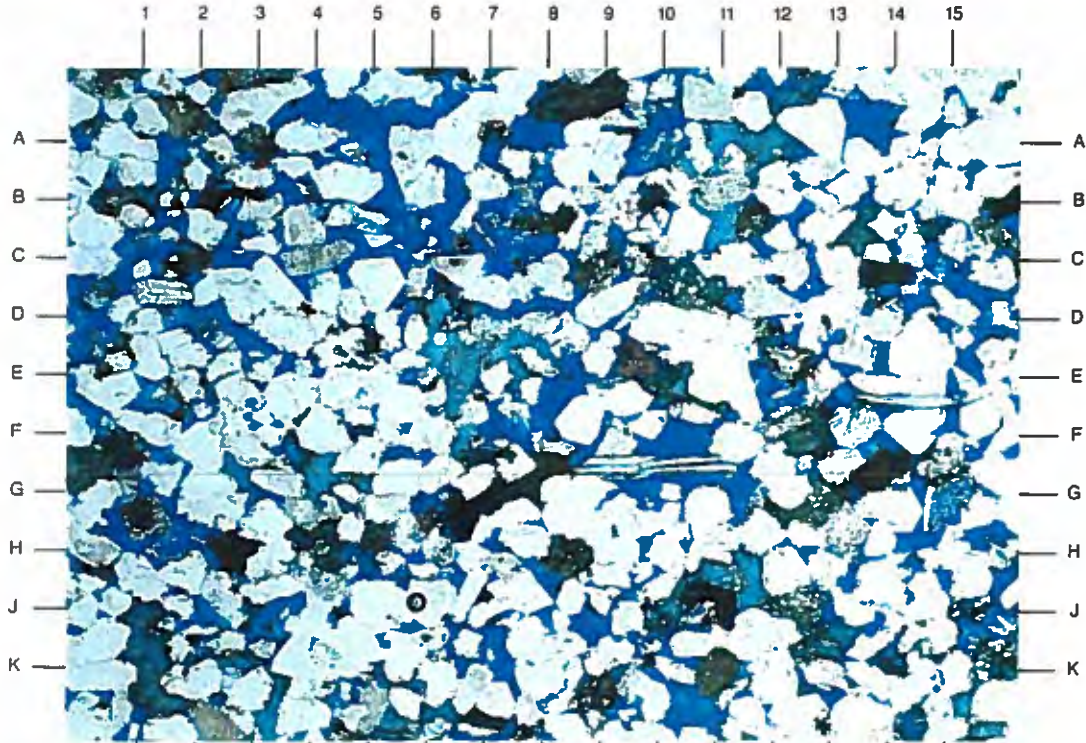
The low magnification photomicrograph shows a massive sandstone that is moderately well sorted and fine-grained. The effective pore system (blue) is well developed, with both primary intergranular (C5,B-C12.5) and secondary dissolution (C7,H1.5) observed. Carbonate cement is noted as a patchy pore filling and includes dolomite (E6.5,H-J11.5) and calcite (D-E9.5).

Magnification: 40X

PLATE 12B

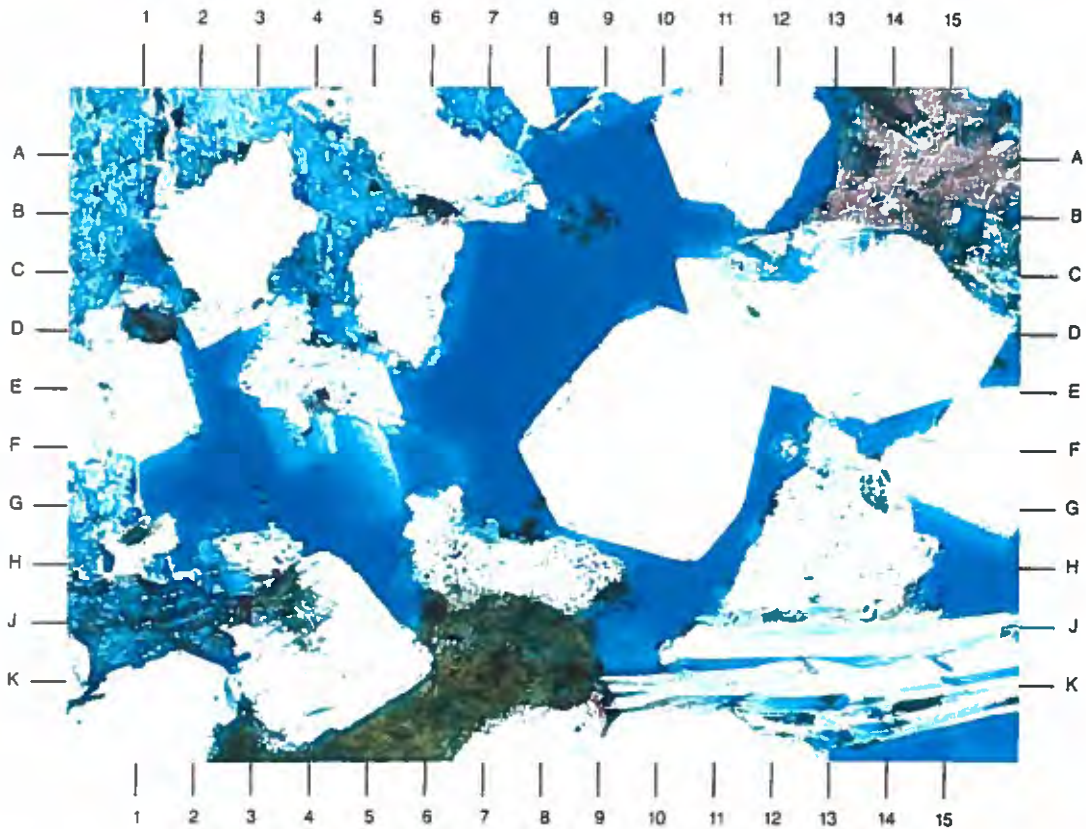
The high magnification photomicrograph details the area of E8 in Plate 12A. Erratically distributed pore-reducing components include dolomite (A1,G0.5) and calcite (A15) cements, quartz overgrowths (F8,B11.5,D-E11), and detrital matrix (K7). The dolomite cement in this sample is iron-rich. Note the lack of deformation in ductile mica fragments at K13.

Magnification: 200X



A

0.25 mm



B

0.05 mm

**Dupont
Injection Well No. 3 S/T
Harrison County, Mississippi**

File No. GN-4474

SAMPLE DEPTH: 9899 FEET

PLATE 13A

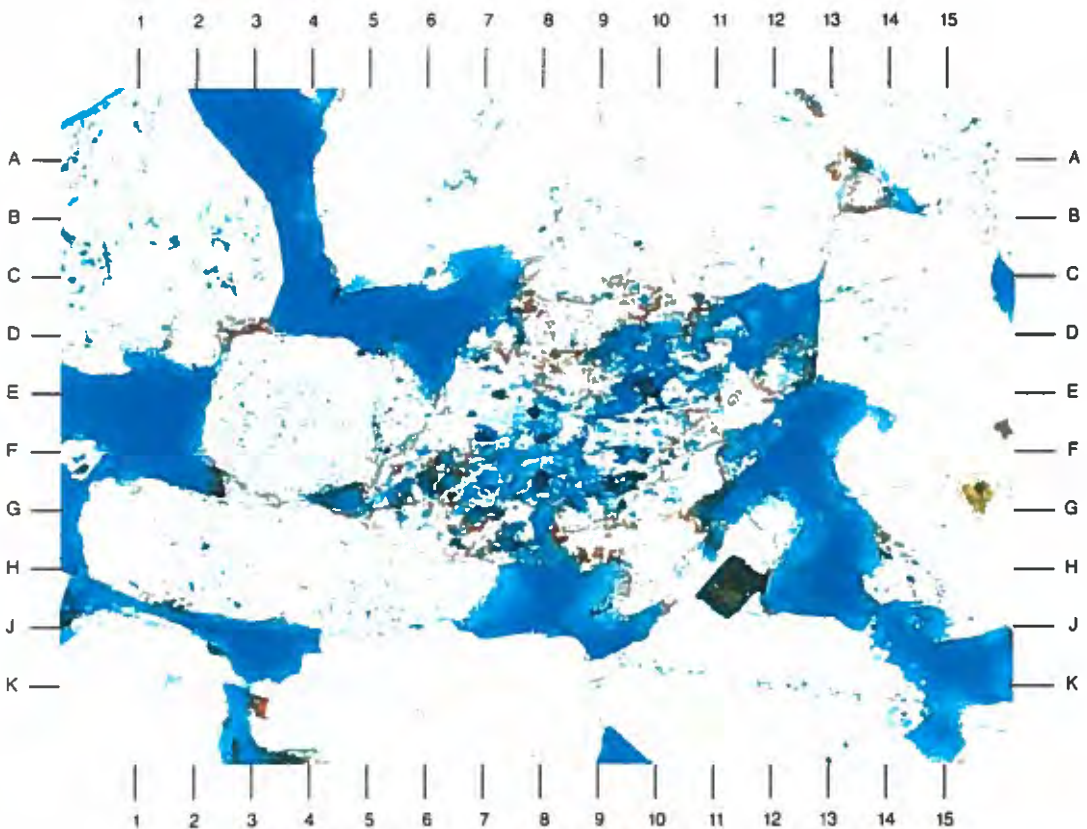
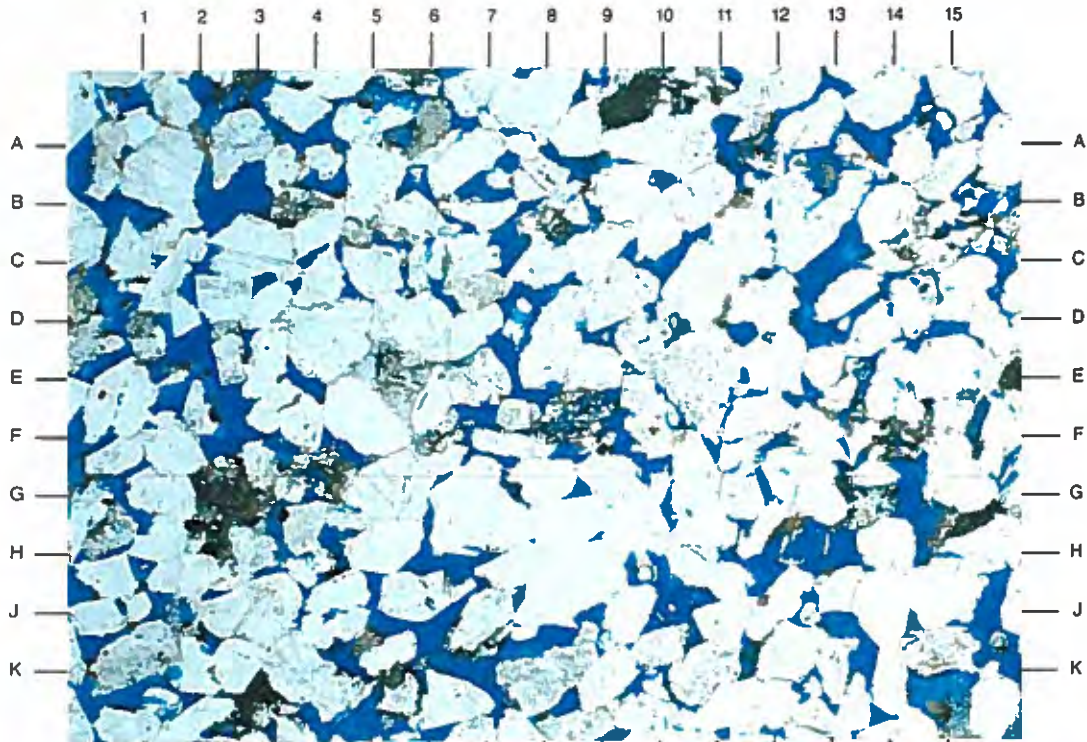
This low magnification photomicrograph shows the fairly even porosity distribution (blue) seen in this massive sandstone. Total effective porosity (by thin section analysis) is 19%. These pores are well interconnected as evidenced by measured core analysis permeability of 509.0 md. Remnants of waste material is seen as light brown staining (D11,G-H12.5) along pore walls.

Magnification: 40X

PLATE 13B

The high magnification view details the area of E8 in Plate 13A. Remnant waste material is seen as light brown traces along the irregular surfaces of pore walls and pore throats. The secondary porosity found in a partially dissolved lithic fragment (center of photo) is partially infilled with this waste material. Although most pores (blue) are well interconnected, quartz overgrowths (F-G3.5,J-K5,K9) can occlude some pore throats.

Magnification: 200X



**Dupont
Injection Well No. 3 S/T
Harrison County, Mississippi**

File No. GN-4474

SAMPLE DEPTH: 9904 FEET

PLATE 14A

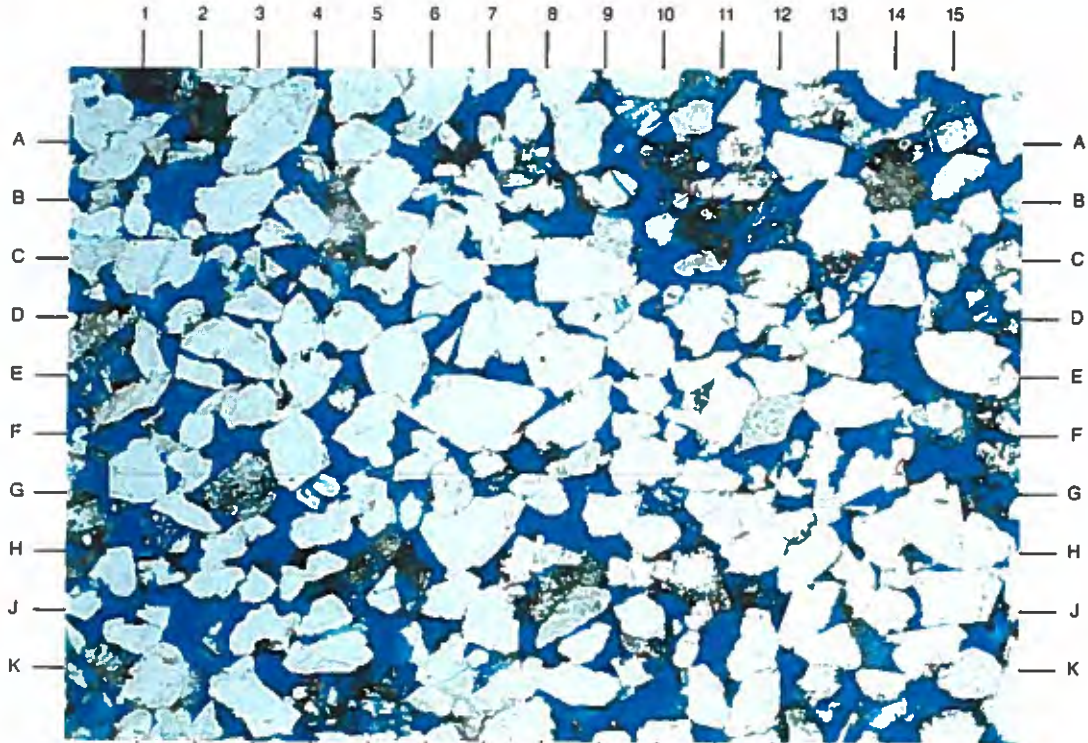
This sandstone is similar to previous samples described. It is massive in fabric and effective porosity (blue) is evenly distributed and well interconnected. The Folk Classification (1980) categorizes this sandstone a sublitharenite. Low amounts of lithics (A-B14,G3) and feldspars (above A9.5,C-D15.5) are found in this otherwise quartz-rich sandstone. Note the traces of pore-filling authigenic kaolinite (J-K14).

Magnification: 40X

PLATE 14B

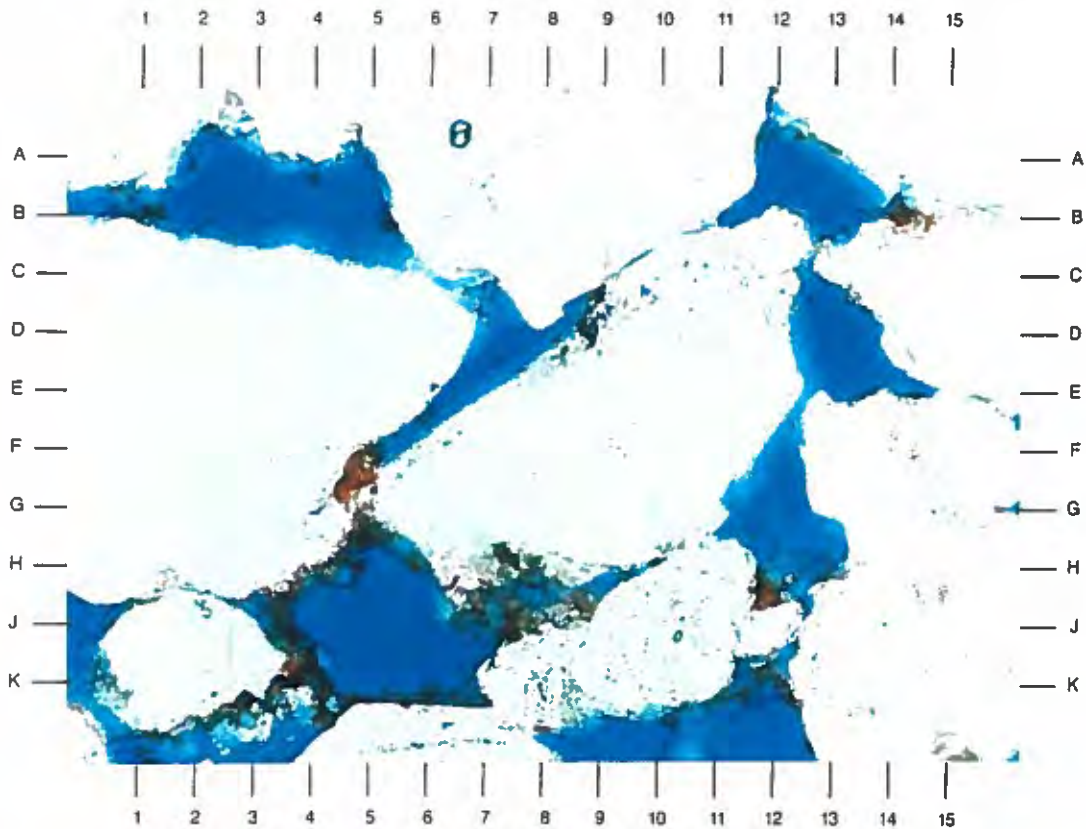
This high magnification photomicrograph details the area of E8 in Plate 14A. The main cementing component in this sandstone is quartz overgrowths (B-C10,B15,G15). Quartz overgrowths form as flat to pseudo-hexagonal crystal faces that nucleate on host quartz sand grains. This cement effectively binds these grains and occasionally occludes interconnecting pore throats. Note the evidence of waste material (light brown) that clings to grain surfaces.

Magnification: 200X



A

0.25 mm



B

0.05 mm

**Dupont
Injection Well No. 3 S/T
Harrison County, Mississippi**

File No. GN-4474

SAMPLE DEPTH: 9916 FEET

PLATE 15A

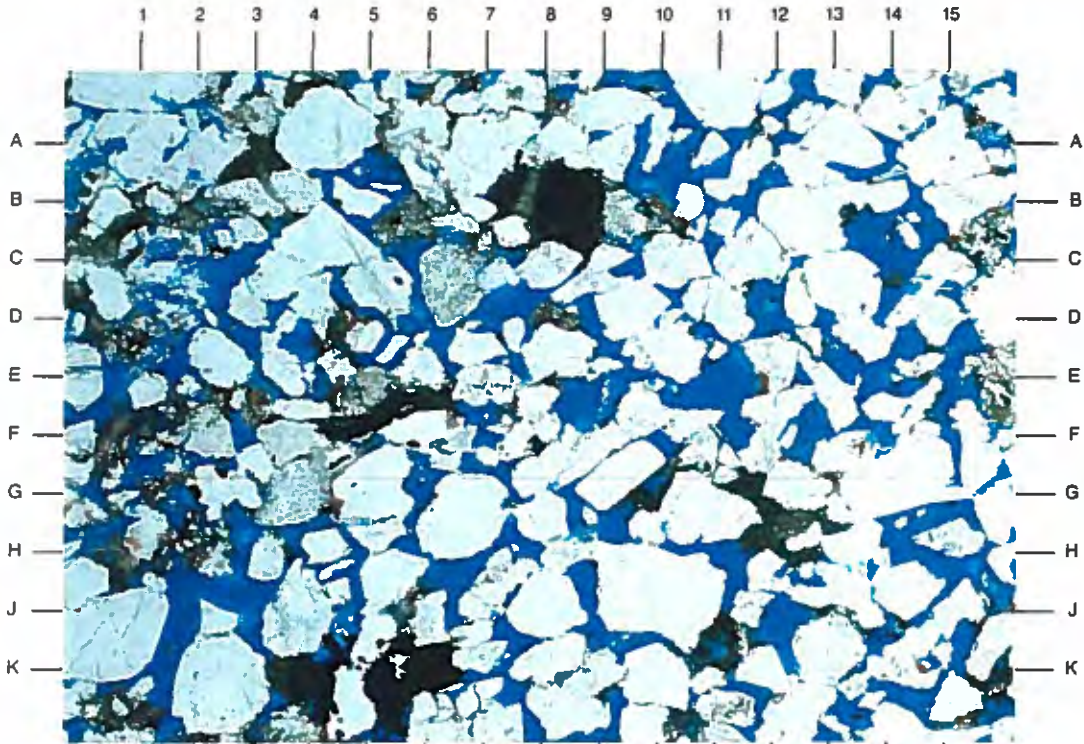
Most effective porosity in the sample taken from 9916' is primary intergranular (D7.5,J9,B12) in type. However, secondary dissolution porosity is seen as both grain-moldic (B10,E11) and intragranular (C1.5,D1.5) pores. The most common cement type found is quartz overgrowths. However, low amounts of siderite (B8,G12) are also seen.

Magnification: 40X

PLATE 15B

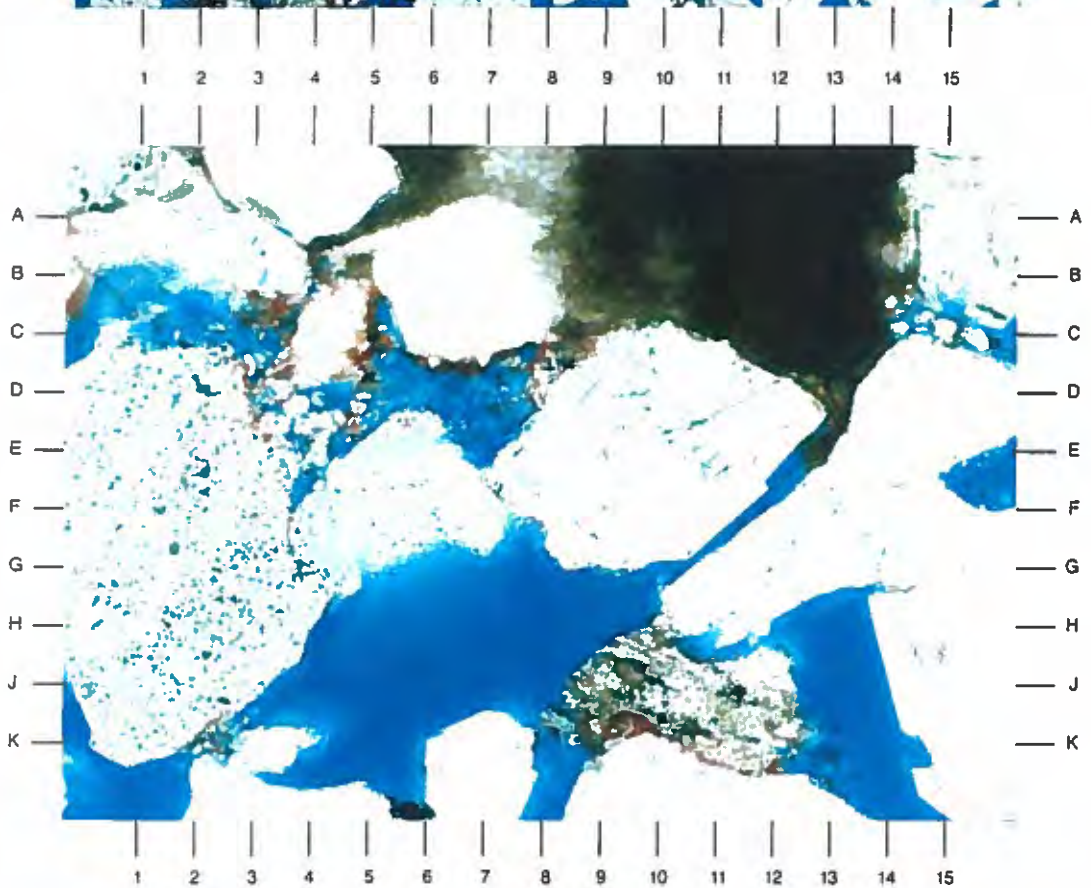
This high magnification photomicrograph details the area of C8 in Plate 15A. This sublitharenite (Folk, 1980) contains low amounts of lithic fragments (J11) which are mostly metamorphic in origin. Note the secondary pore that is infilled with sideritic cement (A12).

Magnification: 200X



A

0.25 mm



B

0.05 mm

**Dupont
Injection Well No. 3 S/T
Harrison County, Mississippi**

File No. GN-4474

SAMPLE DEPTH: 9929 FEET

PLATE 16A

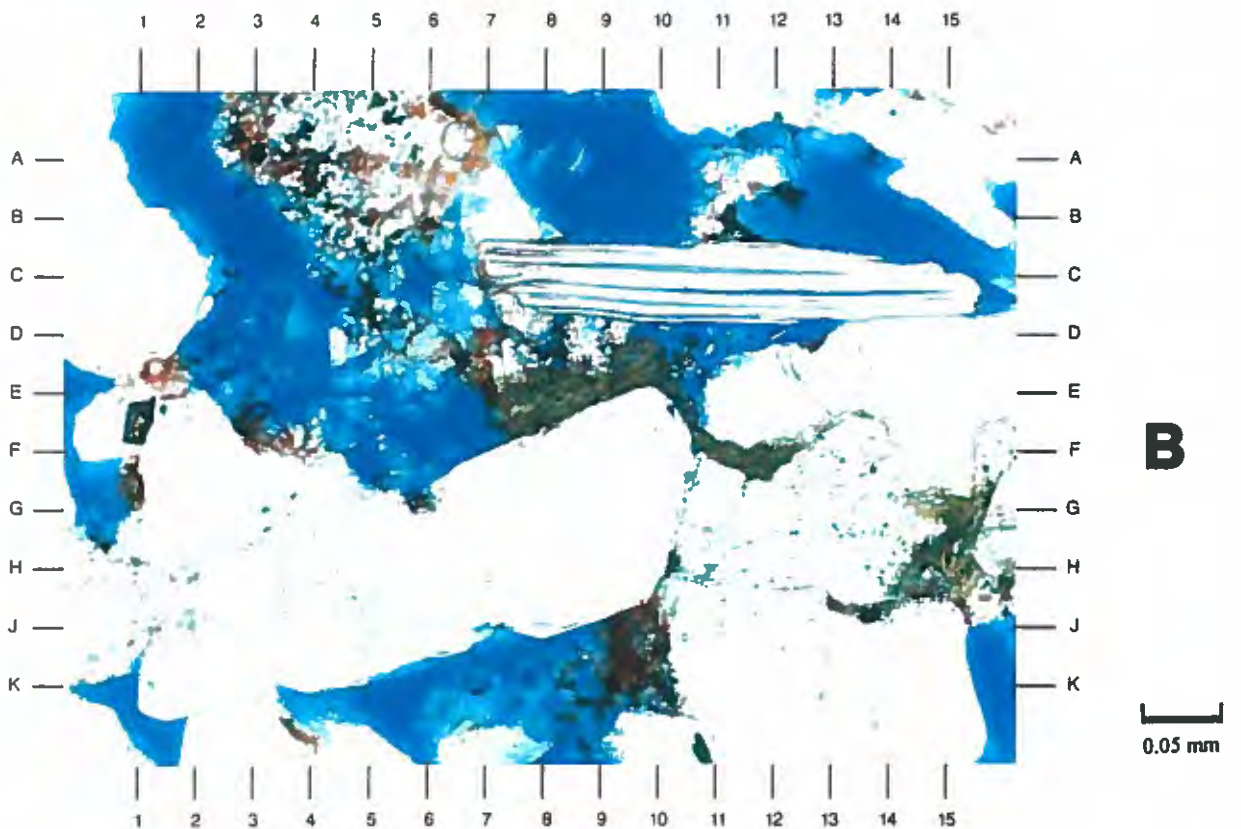
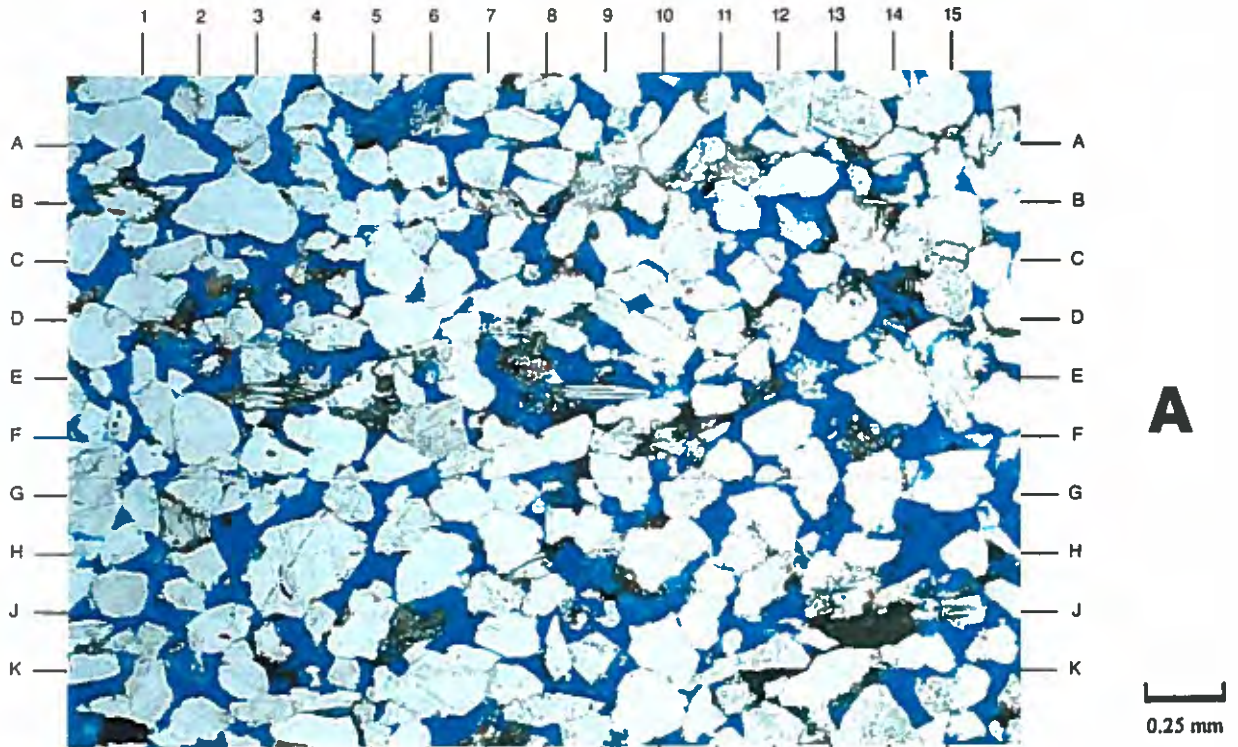
This low magnification photomicrograph shows that the sample taken from 9929' is an upper fine-grained sandstone (average grain size 0.22mm). While most porous areas in the sample are intergranular (A3.5,B-C6.5,G-H11) in type, some dissolution porosity (D14,H14.5,J9) is also present. Total effective porosity by thin section analysis is 20%.

Magnification: 40X

PLATE 16B

This high magnification photomicrograph details the area of E8 in Plate 16A. Remnants of waste material (light brown) is seen clinging to irregular surfaces of sand grains in this view. Minor amounts of detrital matrix (E-F8,F11) is also noted. The ductile mica fragment at C12 is undeformed, indicating less sediment compaction.

Magnification: 200X



**Dupont
Injection Well No. 3 S/T
Harrison County, Mississippi**

File No. GN-4474

SAMPLE DEPTH: 9938 FEET

PLATE 17A

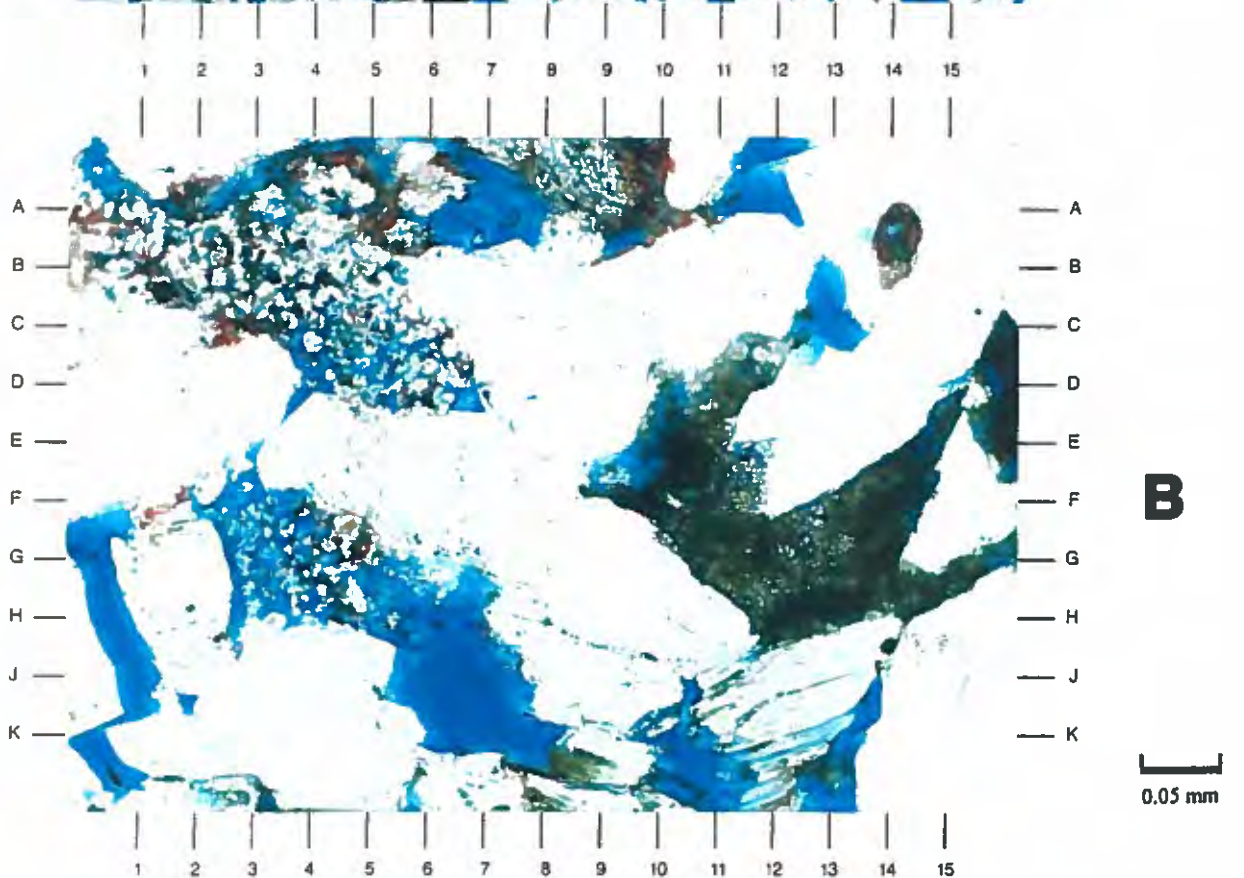
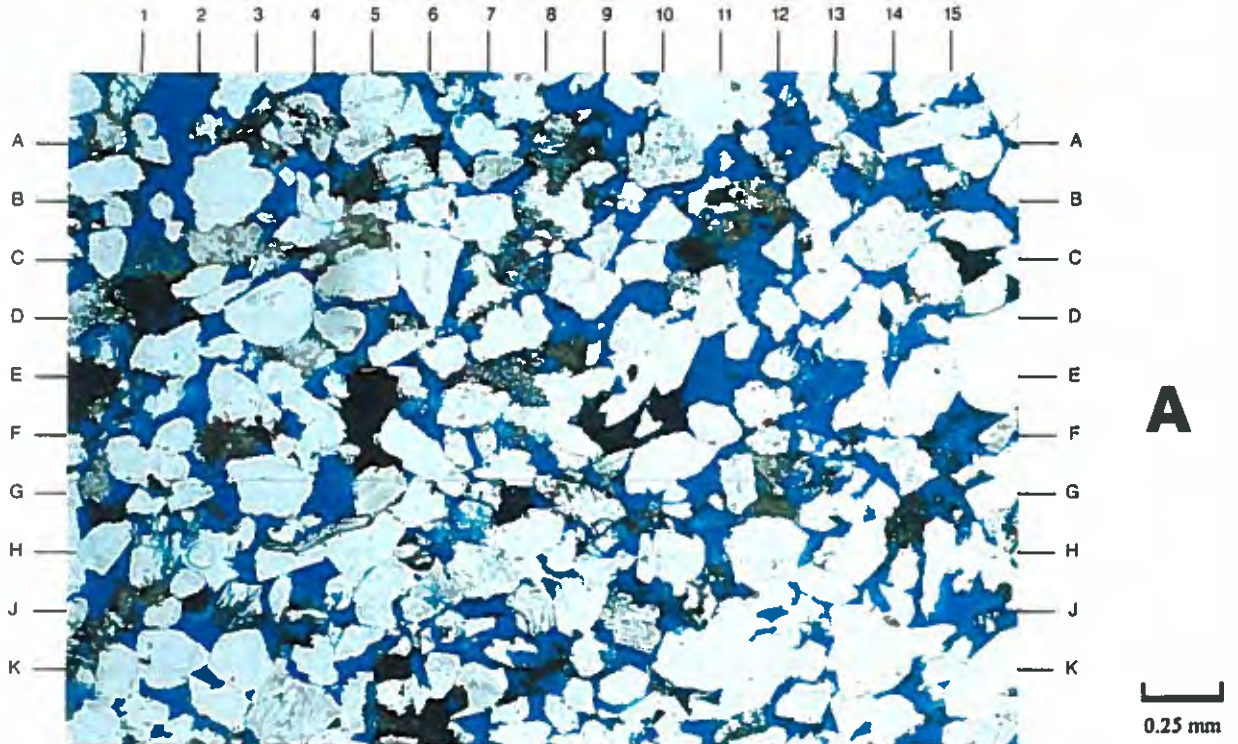
This sample is a massive sandstone that is medium-grained. Dark patches of siderite cement (E-F5,F10) are seen infilling several pores. This carbonate cement forms as small microcrystals and appears to "trap" remnants of waste material that have been introduced in the zone. Thin section analysis indicates that 10% (by volume) of siderite is present in the sample.

Magnification: 40X

PLATE 17B

This high magnification photomicrograph details the area of E8 in Plate 17A. Pore-reducing constituents seen here include siderite (G13), authigenic kaolinite (C4,G3), and quartz overgrowths (J2,B7). Both siderite and authigenic kaolinite are microscopic components that "trap" residual waste material. The aggregates of booklets of kaolinite are also loosely bound to pore walls and may migrate during waste flow in the zone. This migrating clay can become trapped into smaller pore throats, thereby reducing the effectiveness of the zone.

Magnification: 200X



Dupont
Injection Well No. 3 S/T
Harrison County, Mississippi

File No. GN-4474

SAMPLE DEPTH: 9952 FEET

PLATE 18A

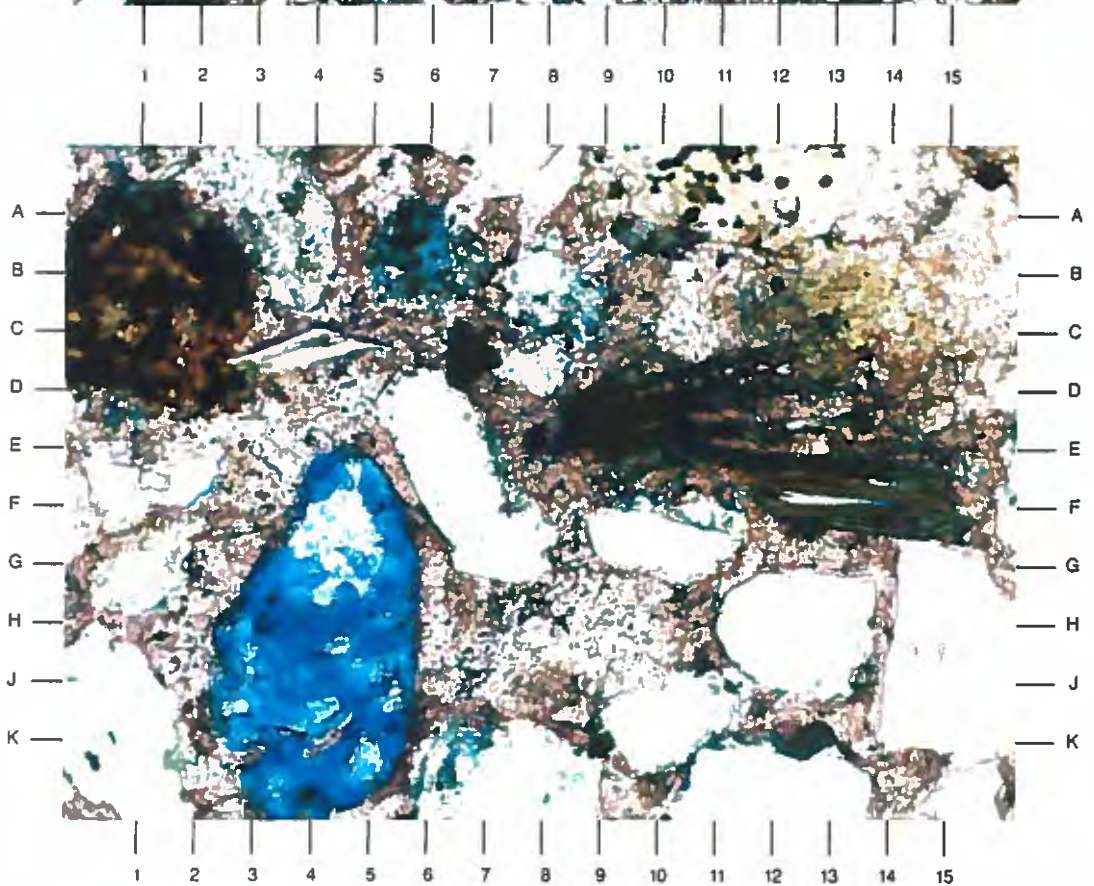
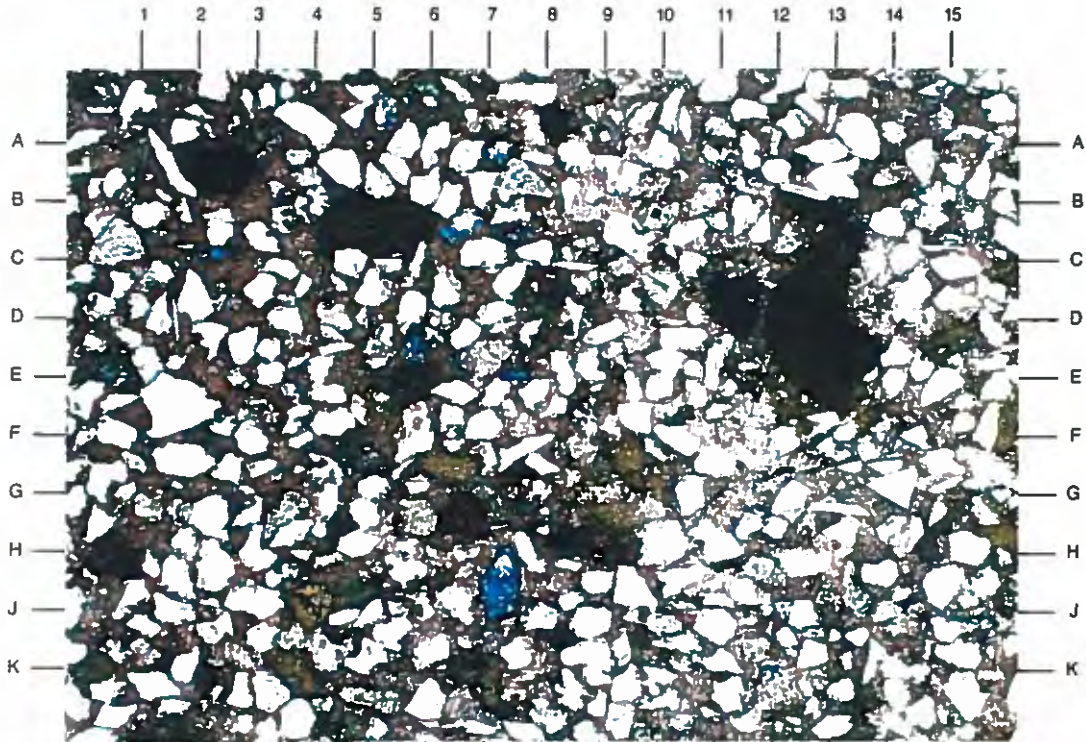
Primary intergranular porosity is nearly totally occluded in this sample due to the introduction of calcite cement (red). This carbonate cement surrounds most framework grains and accounts for 32% of the sample (by volume from thin section analysis). Rare secondary pores (blue) are present, but are isolated and ineffective.

Magnification: 40X

PLATE 18B

This high magnification photomicrograph details the area of H8 in Plate 18A. Pervasive calcite cement (red) is seen infilling intergranular areas of this sample. The secondary pores at J4 and A-B5.5 are effectively isolated by surrounding calcite. Note the presence of small secondary pyrite framboids (black specks) scattered throughout the sample.

Magnification: 200X



Dupont
Injection Well No. 3 S/T
Harrison County, Mississippi

File No. GN-4474

SAMPLE DEPTH: 9962 FEET

PLATE 19A

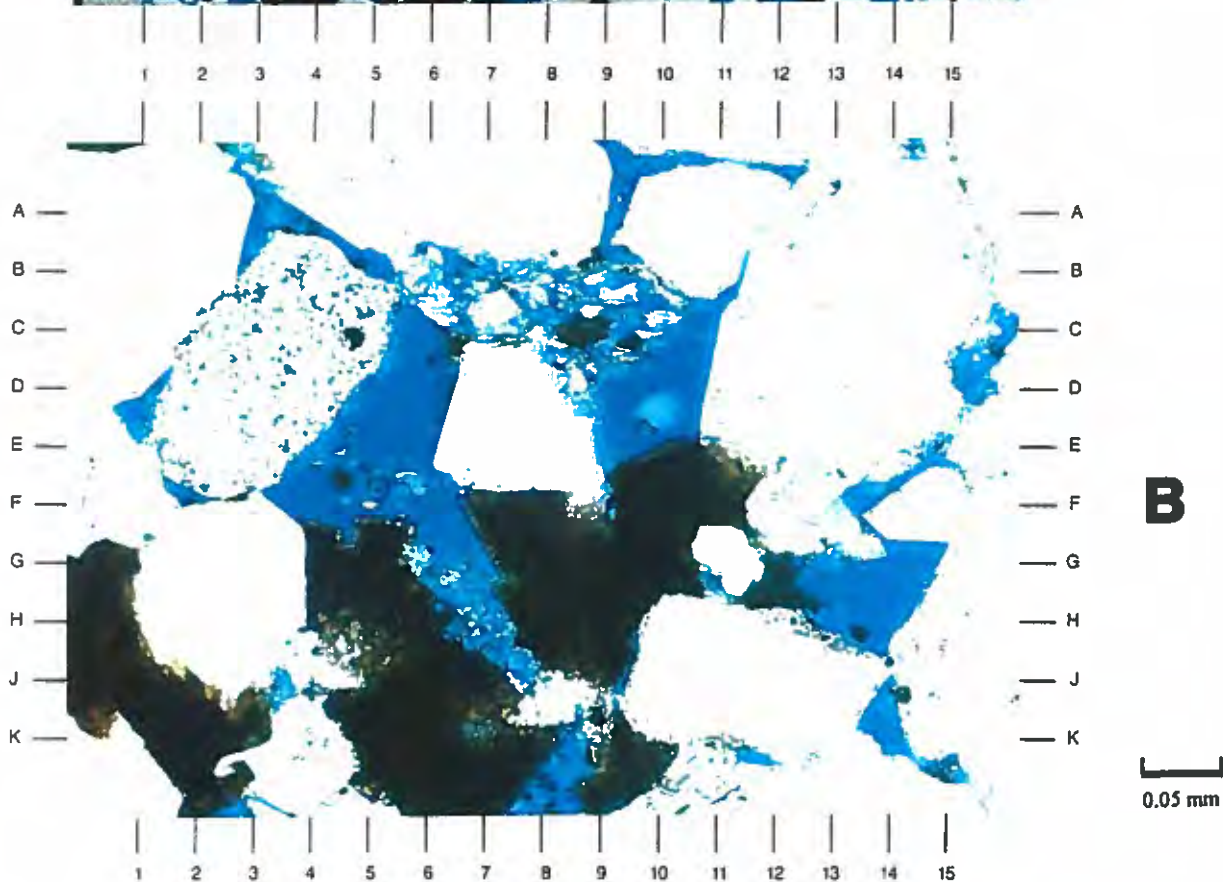
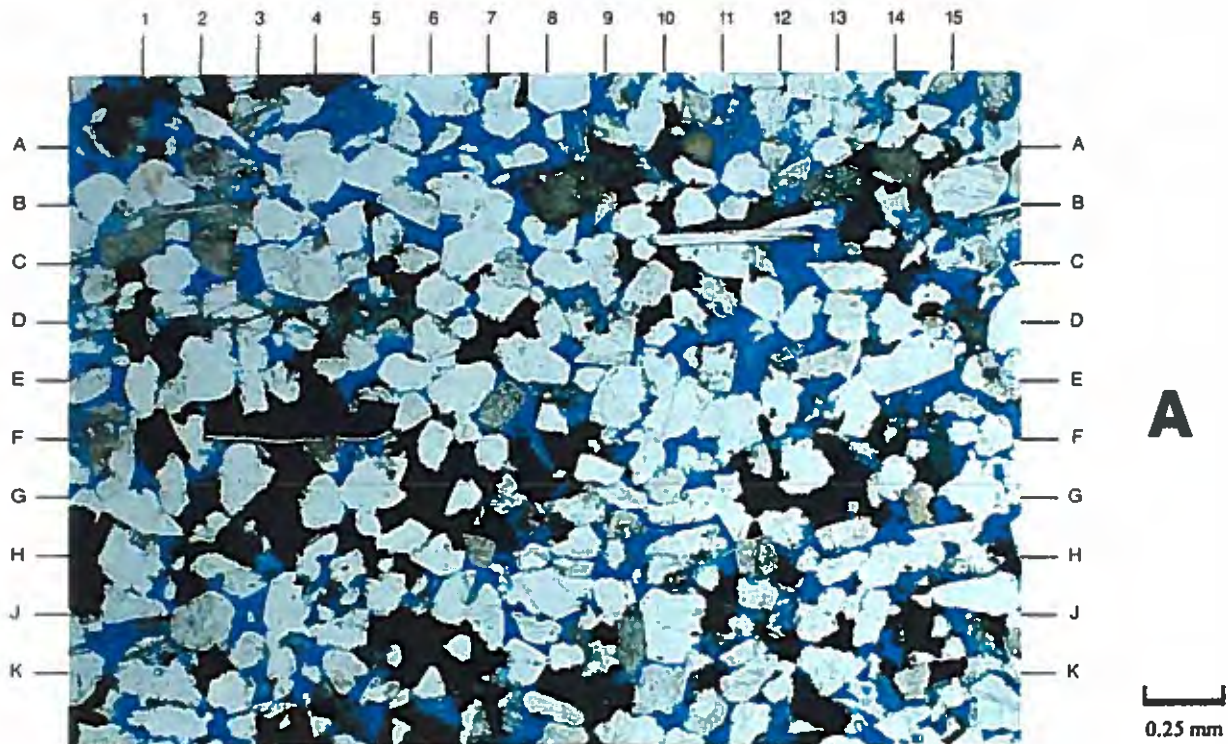
Common siderite cement is seen as a dark pore-filling material in this low magnification view. Normally siderite cement does not appear nearly black as shown here; however, microcrystals of this carbonate cement have "trapped" residual waste that was previously introduced into the zone. Note that ductile mica fragments (B-C12,F4,B2) are not contorted, indicating sediment compaction is low.

Magnification: 40X

PLATE 19B

This high magnification photomicrograph details the area of F8 in Plate 19A. Siderite cement is seen as small microcrystals that partially (H6) to totally (H0.5) infill primary and secondary pores. This cement is darkened by the entrapment of waste material in microporosity between microcrystals. Quartz overgrowth cementation (B11.5,F15,F1.5) is another pore-reducing component that is observed.

Magnification: 200X



Dupont
Injection Well No. 3 S/T
Harrison County, Mississippi

File No. GN-4474

SAMPLE DEPTH: 9970 FEET

PLATE 20A

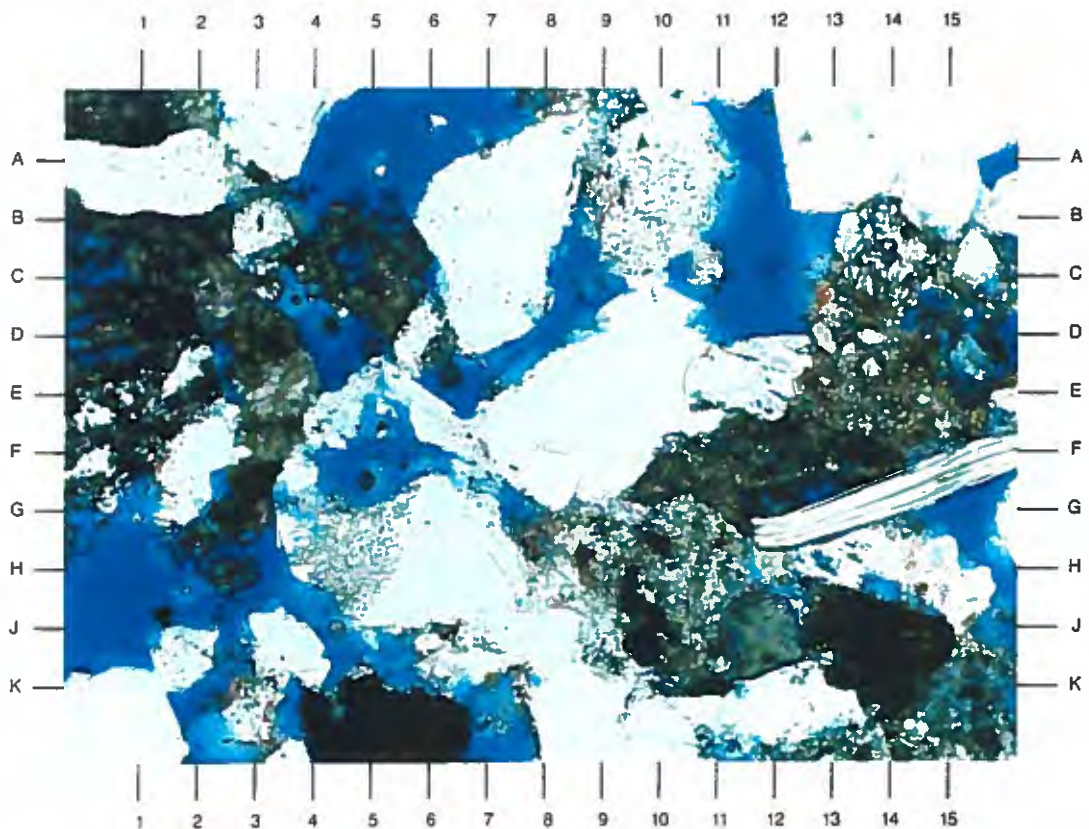
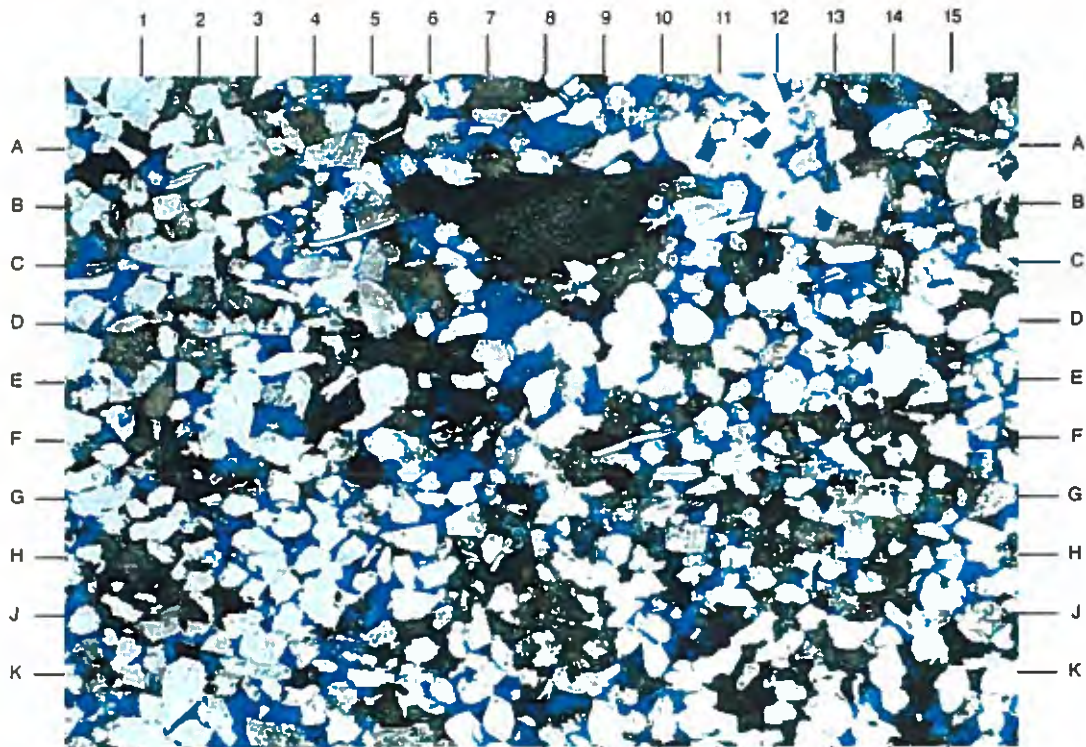
The thin section sample from 9970' consists of a fine-grained sandstone that is moderately well sorted and well cemented. Common cements include quartz overgrowths (A3,J-K3,D9.5; 11% by volume from thin section analysis) and siderite (D-E6,J8,F-G8.5,B8; 16% by volume from thin section analysis). Much of the siderite cement is darkened by introduction of waste material in the zone.

Magnification: 40X

PLATE 20B

This high magnification photomicrograph shows the area of E8 in Plate 20A. Although effective porosity (blue) accounts for 15% (by volume from thin section analysis) of the sample, a large component of pores are infilled with siderite cement (B-C2,F-G11). Quartz overgrowths (A3.5,E10) are seen reducing numerous remaining pores.

Magnification: 200X



Dupont
Injection Well No. 3 S/T
Harrison County, Mississippi

File No. GN-4474

SAMPLE DEPTH: 9992 FEET

PLATE 21A

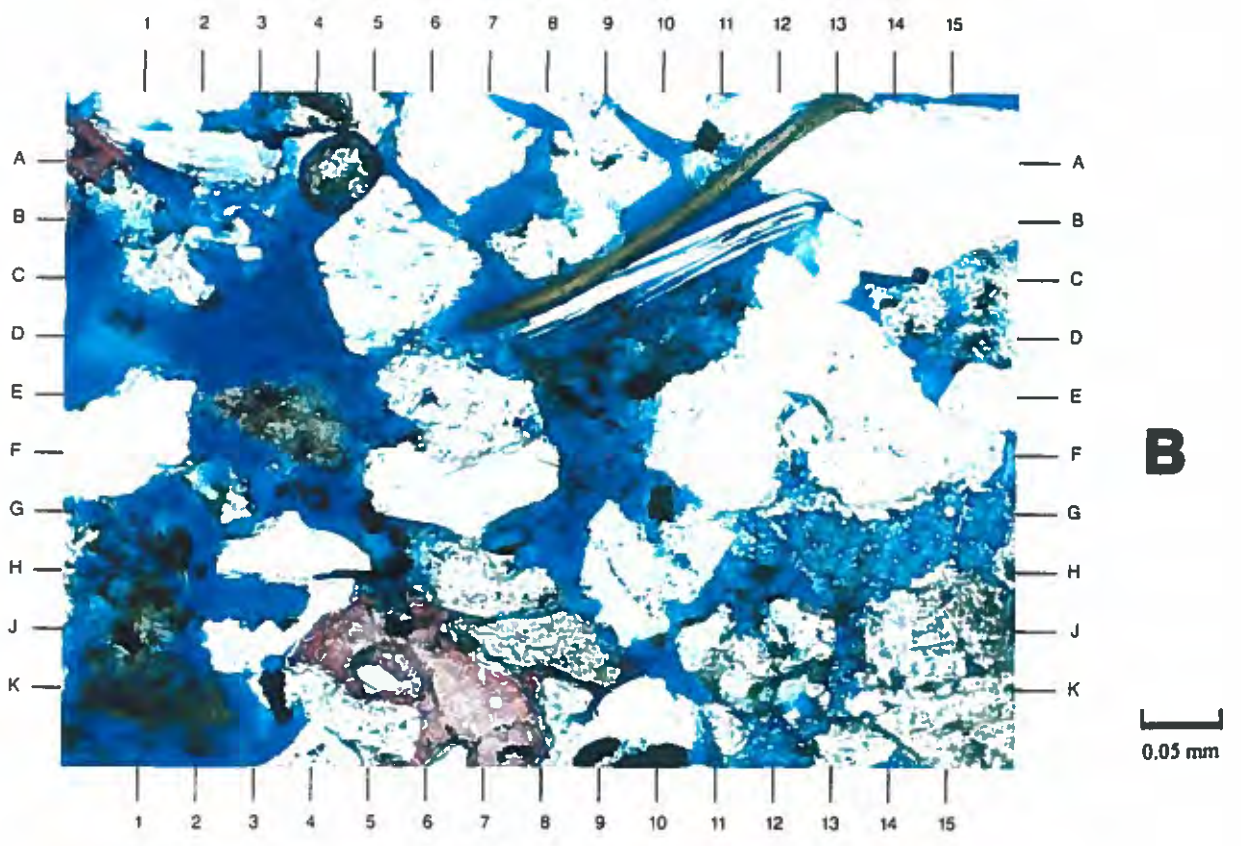
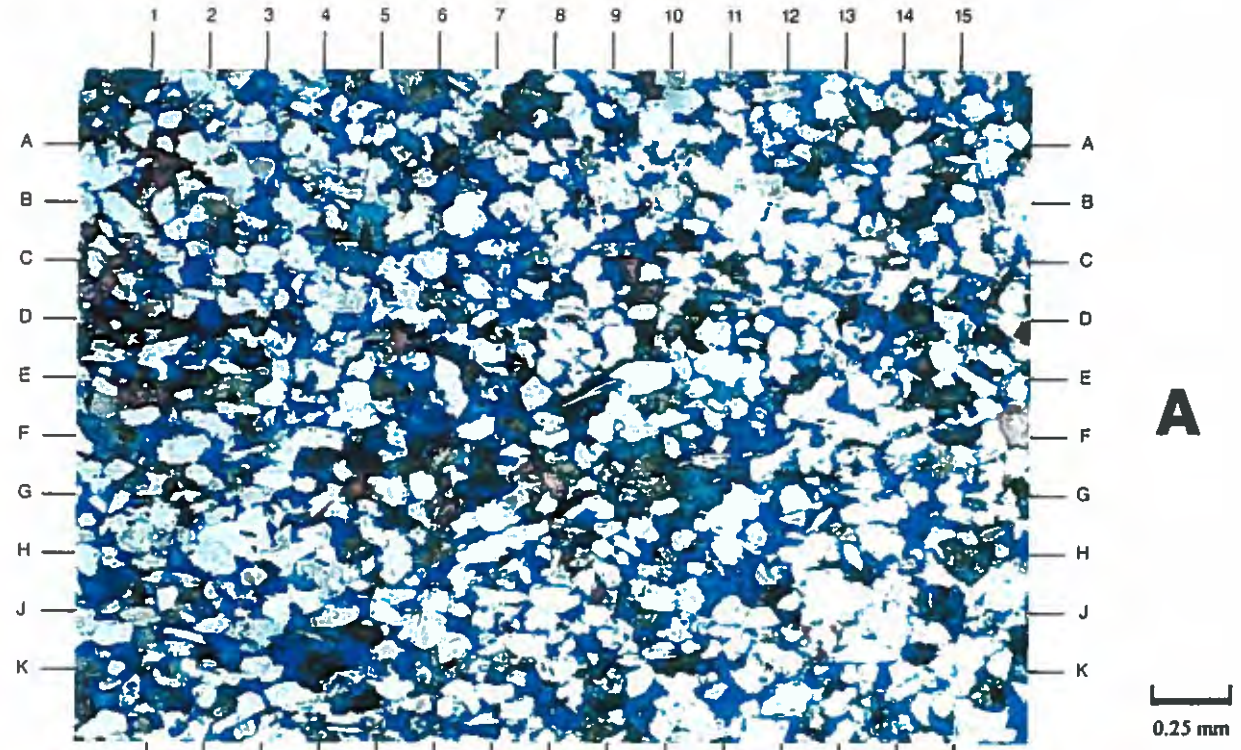
The low magnification shows that this sample is a fine-grained sandstone (average grain size 0.17mm) that has a massive fabric. Intergranular pores are common (A3,D4.5,E-F13) and appear to be moderately well interconnected. Lesser amounts of secondary dissolution pores (F5.5,G10.5,J-K4) are also noted. Evenly distributed effective porosity is interrupted by erratically distributed cementation. Cements include quartz overgrowths (B11,J13.5), calcite (red), and dolomite (B-C5,G11).

Magnification: 40X

PLATE 21B

This high magnification photomicrograph details the area of E8 in Plate 21A. Both primary intergranular (B7.5,D15,G5) and secondary dissolution (D3,F9) pore types are found in this sandstone and account for 15% (by volume from thin section analysis) of the sample. Carbonate cement is seen as calcite (K7) and dolomite (G-H14) and makes up 9% (by volume from thin section analysis) of the sample.

Magnification: 200X



**Dupont
Injection Well No. 3 S/T
Harrison County, Mississippi**

File No. GN-4474

SAMPLE DEPTH: 9996 FEET

PLATE 22A

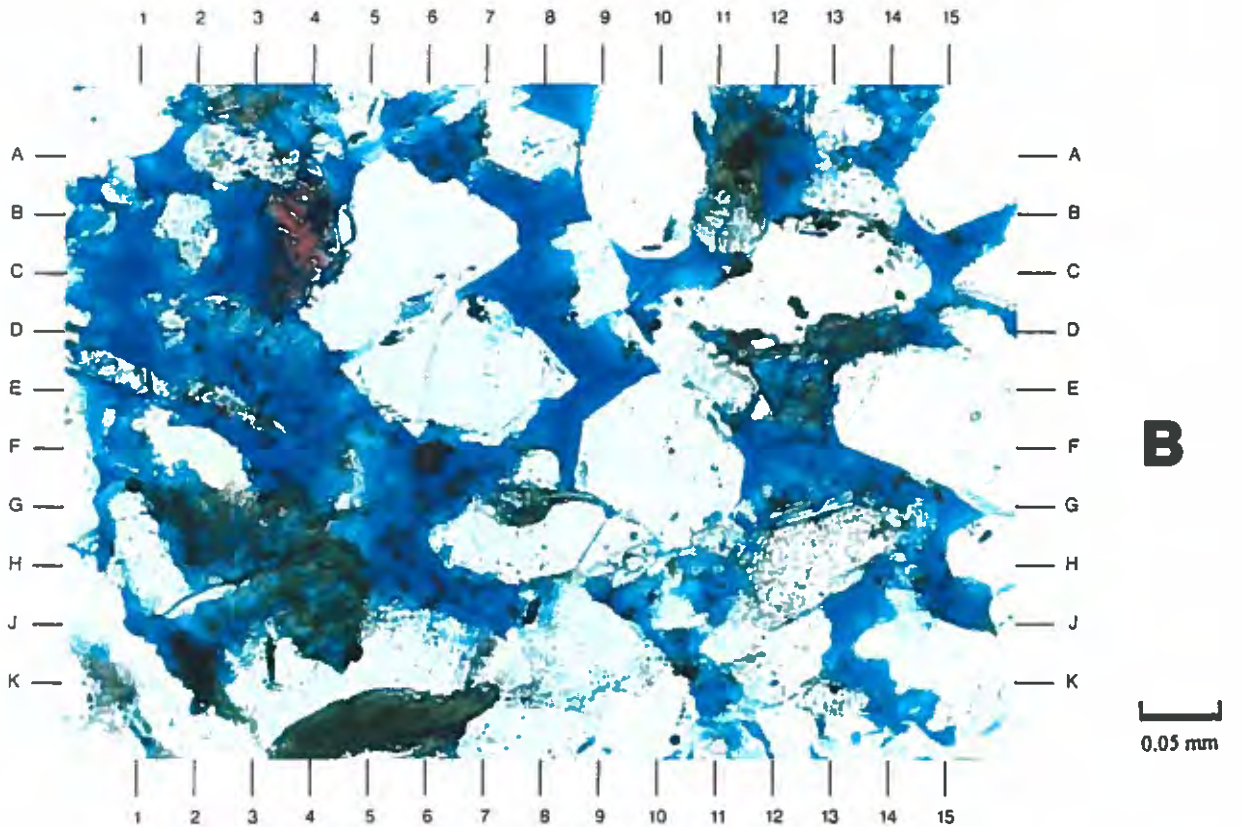
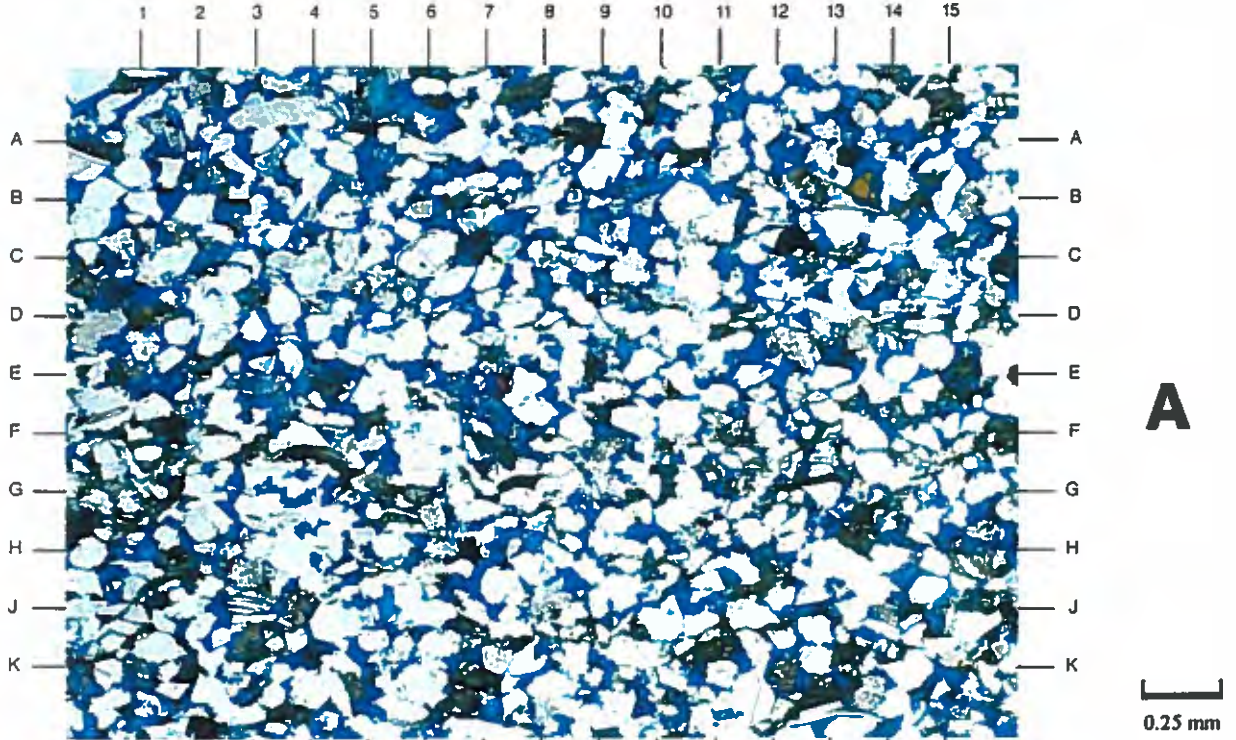
The low magnification photomicrograph shows a fine-grained massive sandstone that is classified as a subarkose (Folk, 1980). The effective pore system (blue) is mainly intergranular (A3,C4,E12) with enhancement by secondary dissolution (A6,E-F7). Some ductile mica fragments are slightly contorted (below K13,F-G4) due to sediment compaction.

Magnification: 40X

PLATE 22B

This high magnification photomicrograph details the area of E8 in Plate 22A. Visible pores (blue) appear moderately interconnected and core analysis indicates that permeability is 47 md. Pore throat obstruction due to cementation is observed. Cements observed include quartz overgrowths (D6,H1), dolomite (D-E12.5), calcite (B4), and pyrite (B-C11.5,D11.5,K2).

Magnification: 200X



Dupont
Injection Well No. 3 S/T
Harrison County, Mississippi

File No. GN-4474

SAMPLE DEPTH: 10008 FEET

PLATE 23A

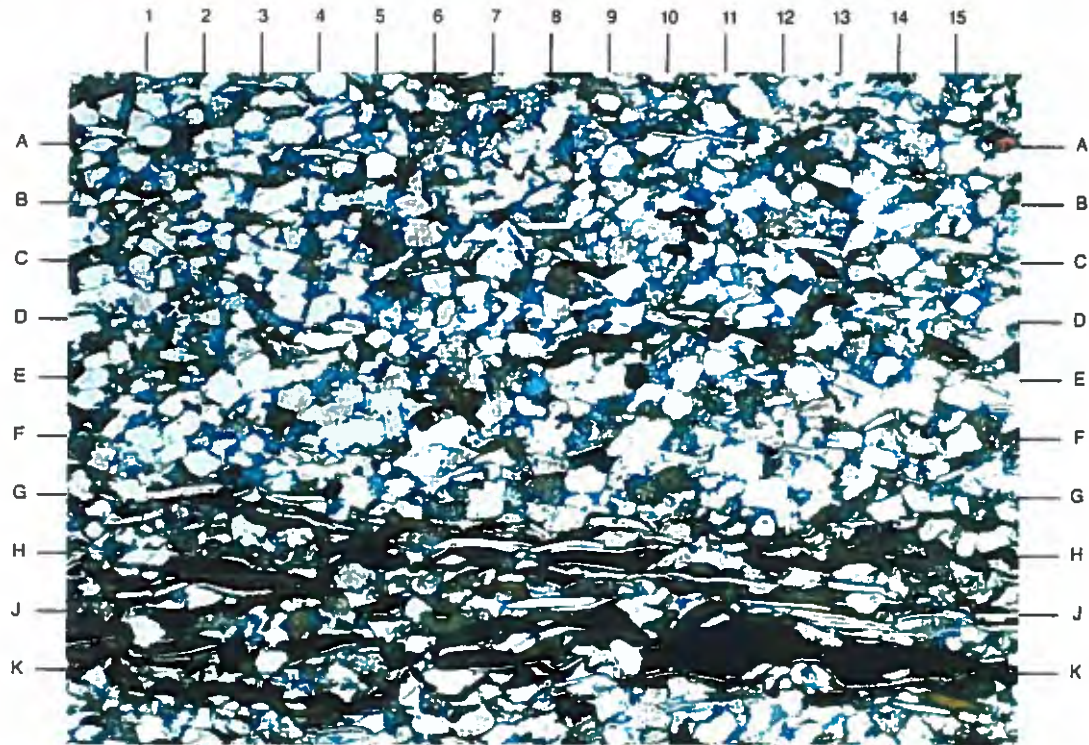
A lamination (H1-J15) rich in mica fragments and organic material is seen under low magnification. These components are concentrated in distinct laminae and account for 6% and 8% (by volume from thin section analysis) of the sample, respectively. This lower fine-grained sandstone has reduced visible porosity due to common pore-filling authigenic kaolinite.

Magnification: 40X

PLATE 23B

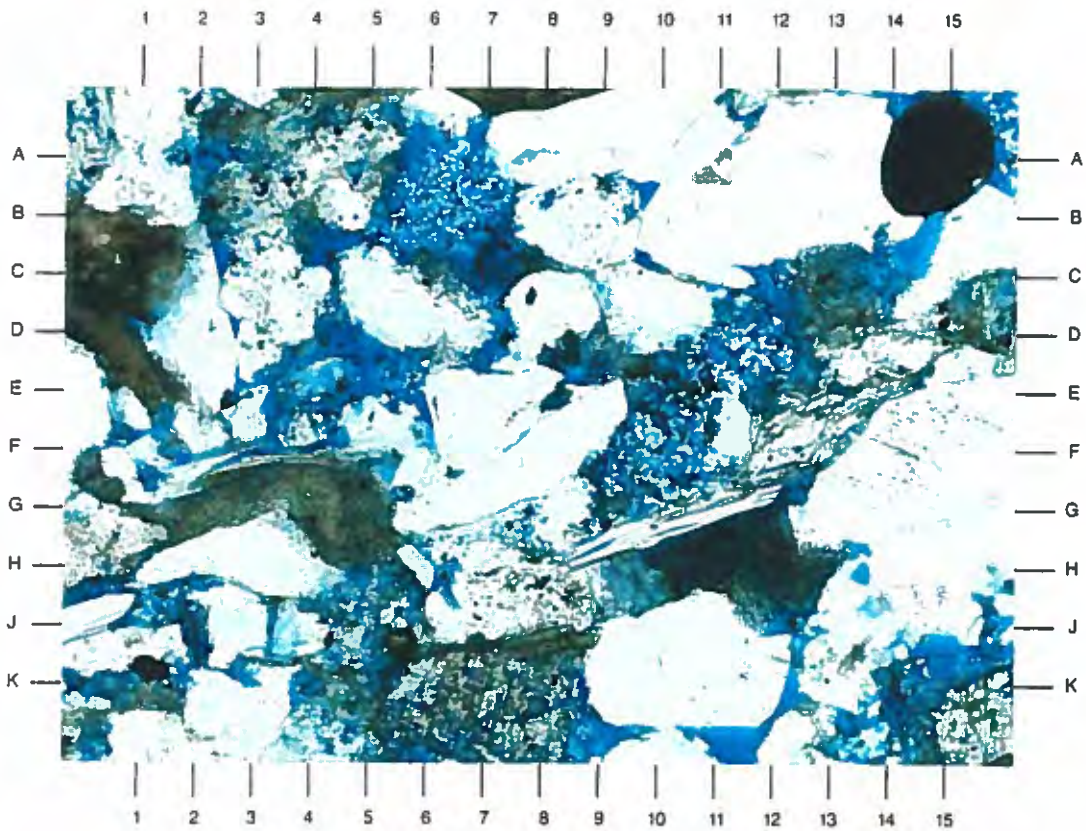
This high magnification photomicrograph details the area of F8 in Plate 23A. Authigenic kaolinite (B6,F10,J5) is found in nearly every visible pore of this sample. This clay mineral forms as aggregates of booklets that are loosely bound to pore walls and may be prone to fines migration. High associated microporosity is also noted with this clay type.

Magnification: 200X



A

0.25 mm



B

0.05 mm

**Dupont
Injection Well No. 3 S/T
Harrison County, Mississippi**

File No. GN-4474

SAMPLE DEPTH: 10016 FEET

PLATE 24A

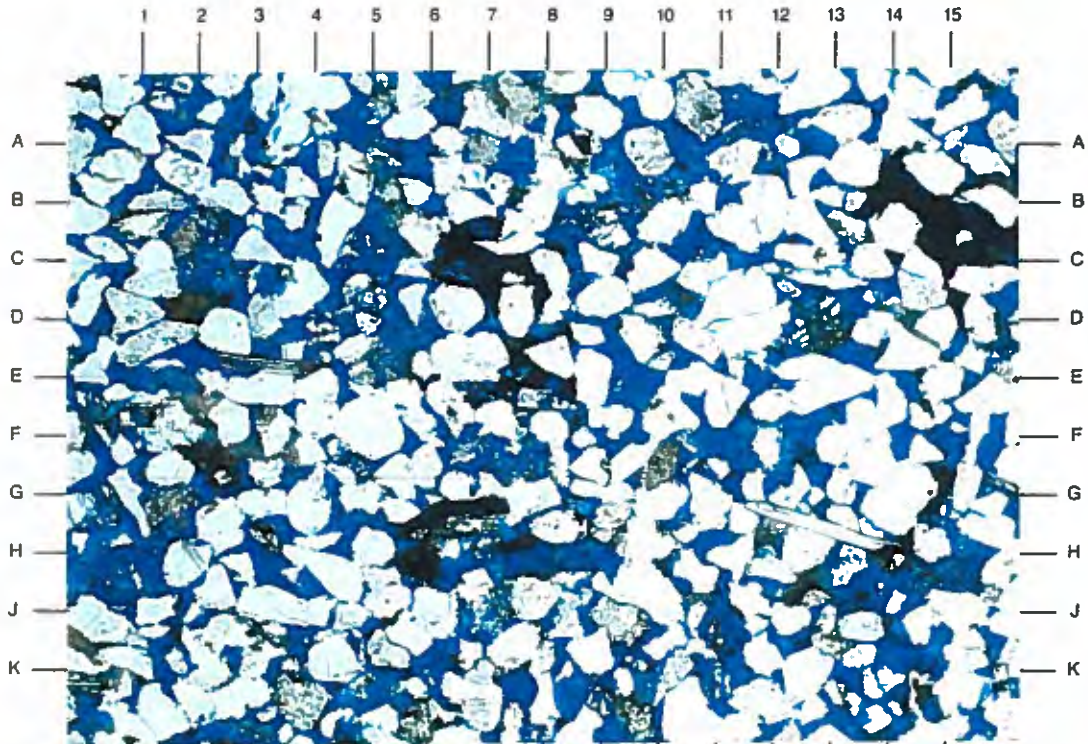
A lower medium-grained sandstone is classified as a sublitharenite (Folk, 1980) because of low amounts of lithics (D2,G10) and feldspars (A10.5,J0.5), combined with abundant quartz sand grains (white grains). Common effective porosity (blue) is well developed and evenly distributed. Organic material (C7,B-C15) is noted in this sandstone and is partially pyritized.

Magnification: 40X

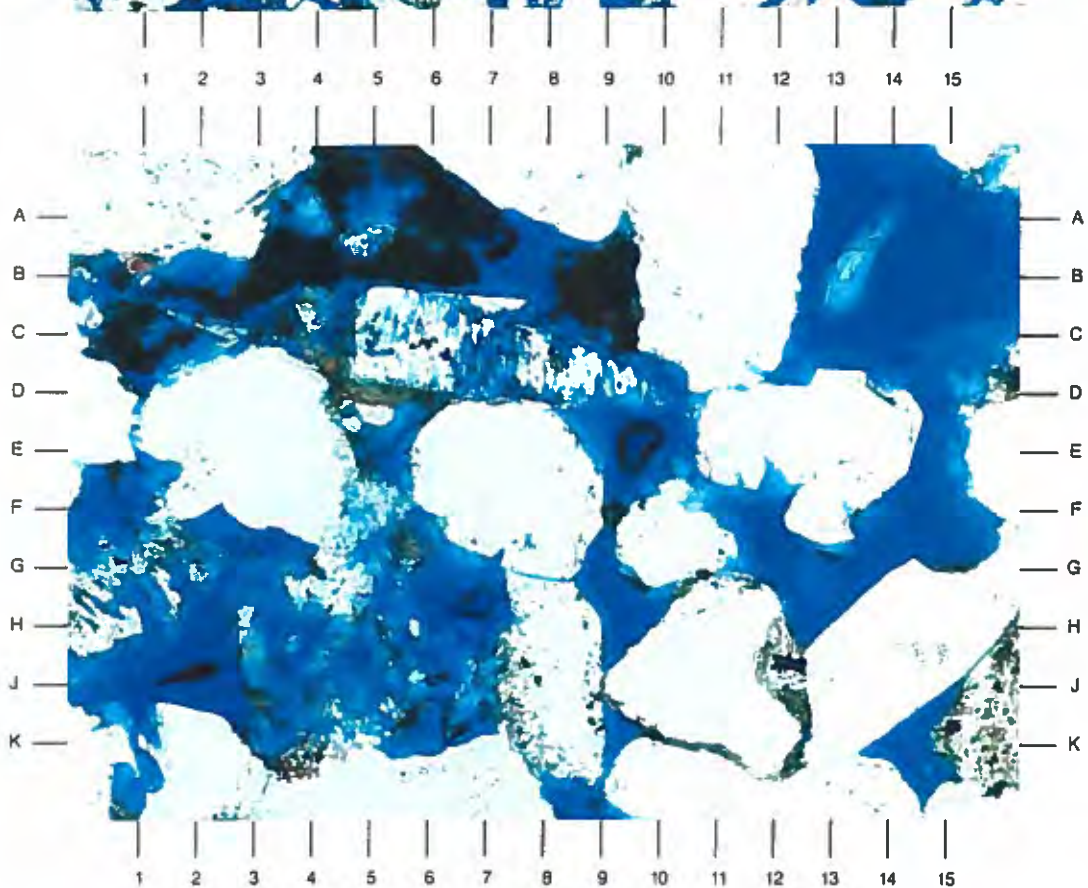
PLATE 24B

This high magnification photomicrograph details the area of E8 in Plate 24A. Both primary and secondary pore types are noted in this view. Intergranular porosity (E9,G9.5) is intermixed with dissolution pores. Dissolution pores include both grain-moldic (H2) and intragranular (C7) varieties. Note the partially pyritized organic material (black) that partially infills a pore.

Magnification: 200X



A



B

**Dupont
Injection Well No. 3 S/T
Harrison County, Mississippi**

File No. GN-4474

SAMPLE DEPTH: 10023 FEET

PLATE 25A

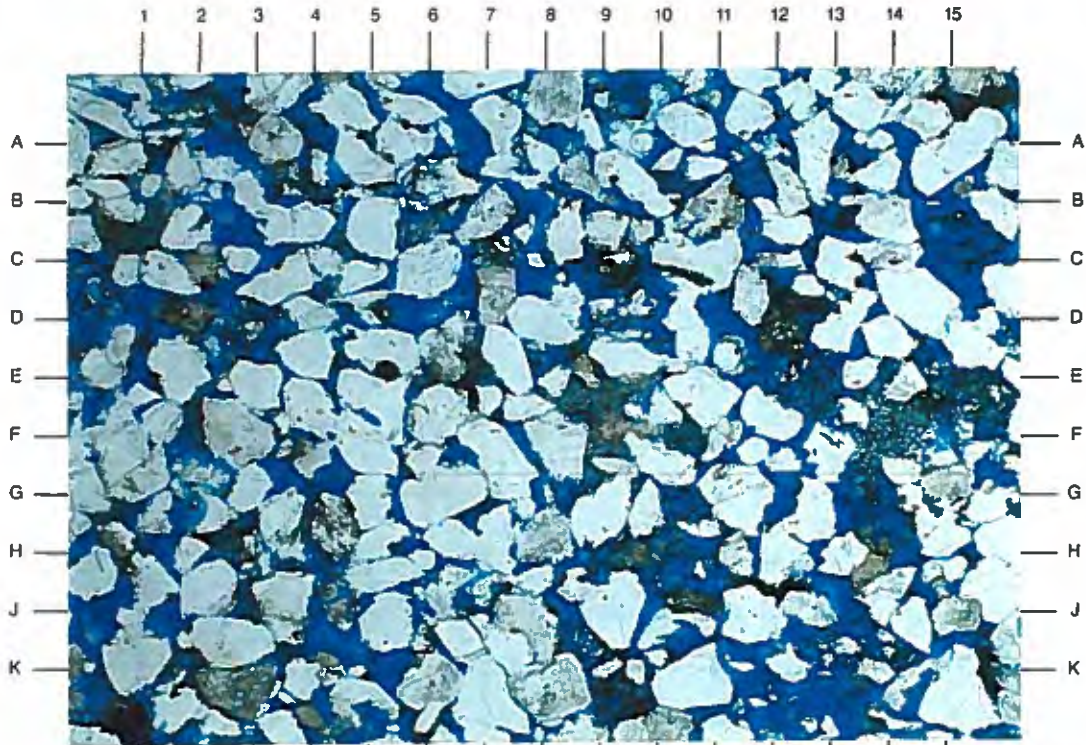
This low magnification photograph of the sample taken from 10023' indicates that this lower medium-grained sandstone is massive in fabric. As seen in some previous samples this sandstone has good effective porosity (blue) that appears well interconnected. Core analysis permeability is measured at 508 md, confirming the interconnectability of this pore system. Both primary (A8,A13.5,F-G6) and secondary (D0.5,H10.5) pores are noted.

Magnification: 40X

PLATE 25B

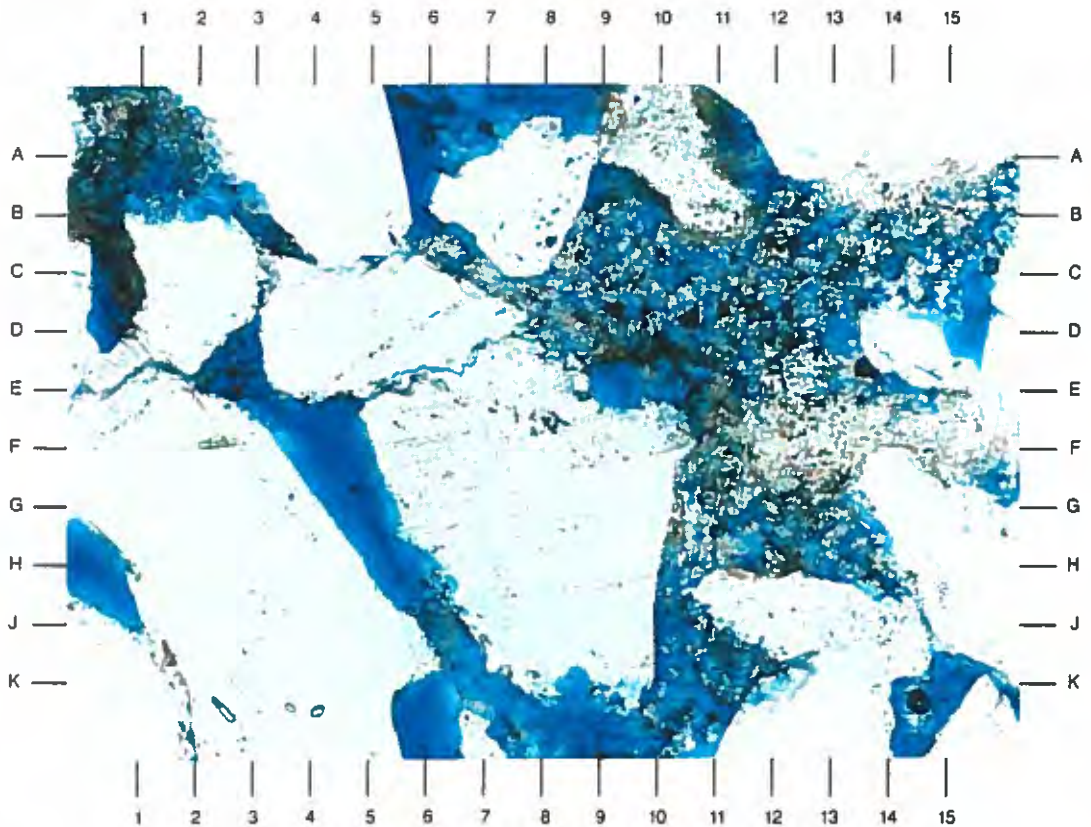
This high magnification photomicrograph details the area of E8 in Plate 25A. This view shows primary and secondary pores that are both open and partially infilled. Authigenic kaolinite (C9-B15,H13) is seen infilling an intergranular pore and a grain-moldic pore, indicating this clay infilled these pores late diagenetically. Other pores in the area are restricted by smaller pore throats which may have prevented the larger kaolinite booklets to migrate into them.

Magnification: 200X



A

0.25 mm



B

0.05 mm

**Dupont
Injection Well No. 3 S/T
Harrison County, Mississippi**

File No. GN-4474

SAMPLE DEPTH: 10032 FEET

PLATE 26A

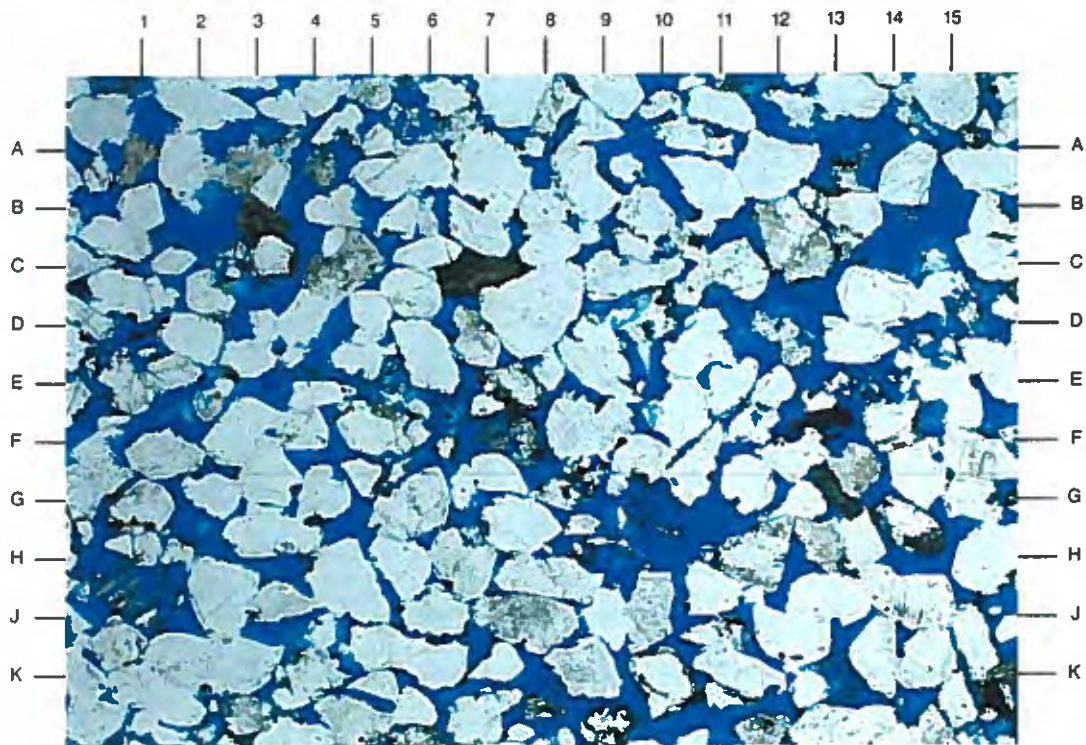
The sample taken from 10032' is similar to the previous sample described. This medium-grained massive sandstone has a well developed effective pore system (blue) that is well interconnected. This sandstone is classified as a sublitharenite (Folk, 1980). Quartz overgrowth cementation (B7.5,A-B11,J12.5) accounts for 14% (by volume from thin section analysis) of the sample.

Magnification: 40X

PLATE 26B

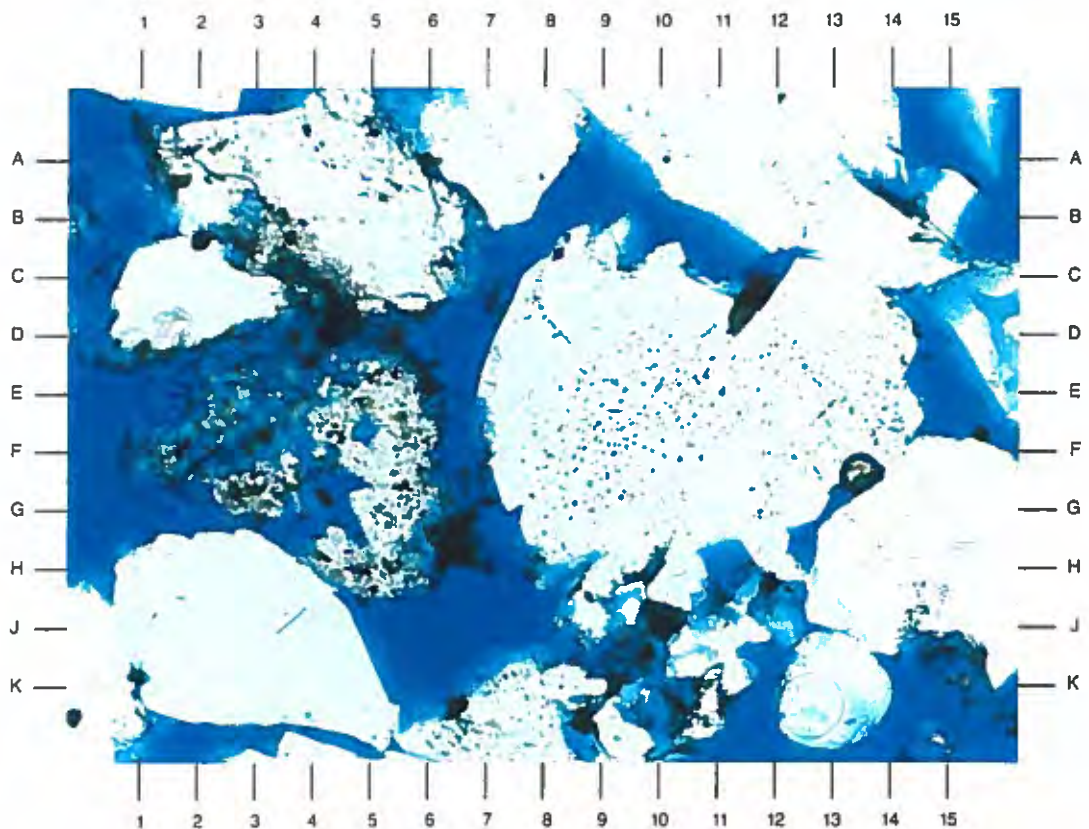
This high magnification photomicrograph details the area of E8 in Plate 26A. Both primary and secondary pore types are noted in this view. Intergranular porosity (B9,E15) is intermixed with grain-moldic (K15) and intragranular (F4) dissolution pores. The presence of quartz overgrowths on the sand grain at F10 accounts for its irregular surface.

Magnification: 200X



A

0.25 mm



B

0.05 mm

APPENDIX D

SCANNING ELECTRON MICROSCOPE PHOTOMICROGRAPHS AND DESCRIPTIONS

(Note the micron bar at the lower portion of each photomicrograph for scale)

**DuPont
Injection Well No. 3 S/T
Harrison County, Mississippi**

File No. GN-4474

SAMPLE DEPTH: 9432 FEET

PLATE 27A

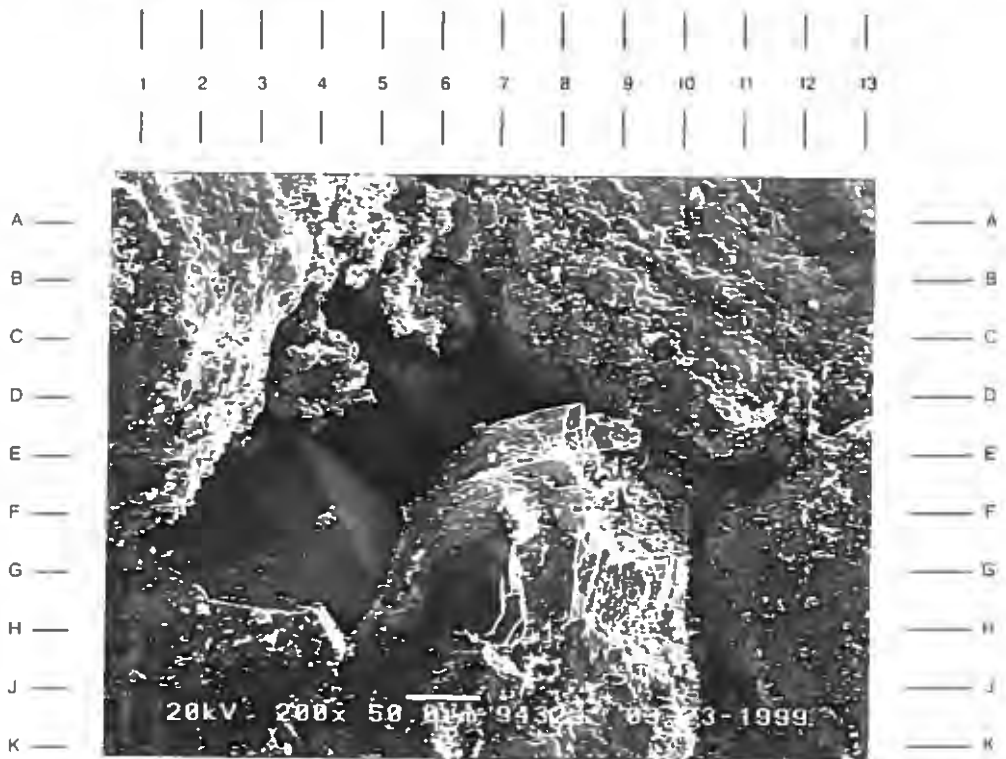
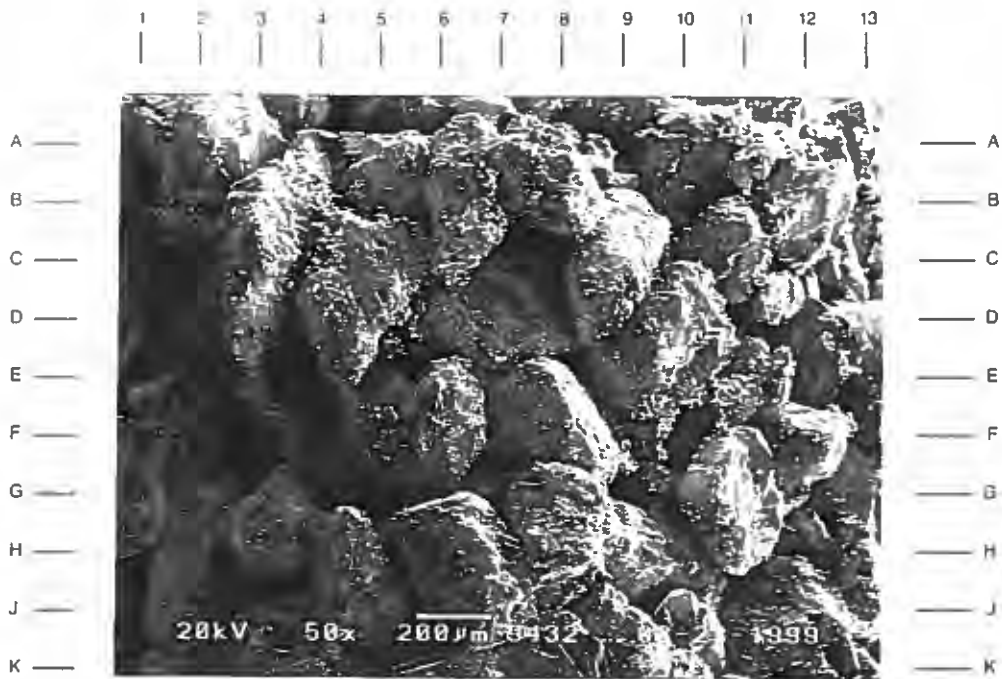
The low magnification survey photomicrograph of a clean, massive, medium-grained sandstone is seen here. Primary intergranular porosity (C7.5,G6.5) is evenly distributed and well interconnected. Most sand grain surfaces are clean; however, some discontinuous grain coatings of clay (C3.5,E-F6,E11) are noted.

Magnification: 50X

PLATE 27B

The high magnification view of the area near D6 in Plate 27A shows a secondary pore (G2-C6) that has been created by the partial dissolution of a less stable lithic fragment. Note the growth of quartz (F4,D5.5) on nearby sand grains. Quartz overgrowths are common in these sandstones and form flat to pseudo-hexagonal crystal faces that nucleate on host quartz sand grains.

Magnification: 200X



**DuPont
Injection Well No. 3 S/T
Harrison County, Mississippi**

File No. GN-4474

SAMPLE DEPTH: 9432 FEET

PLATE 28A

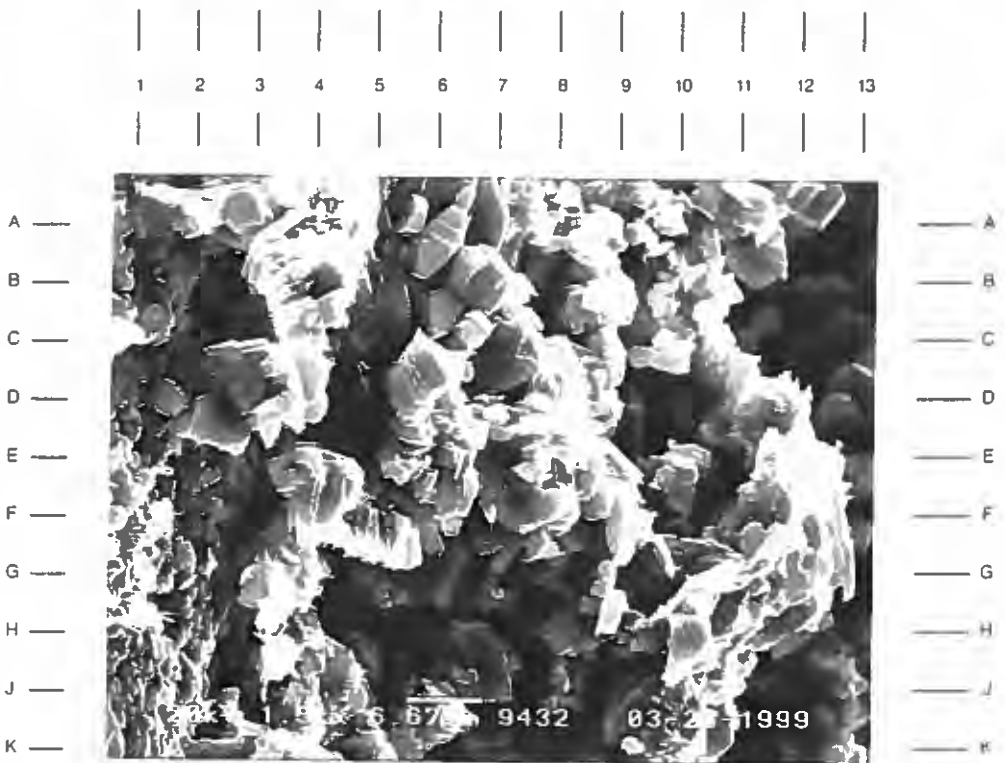
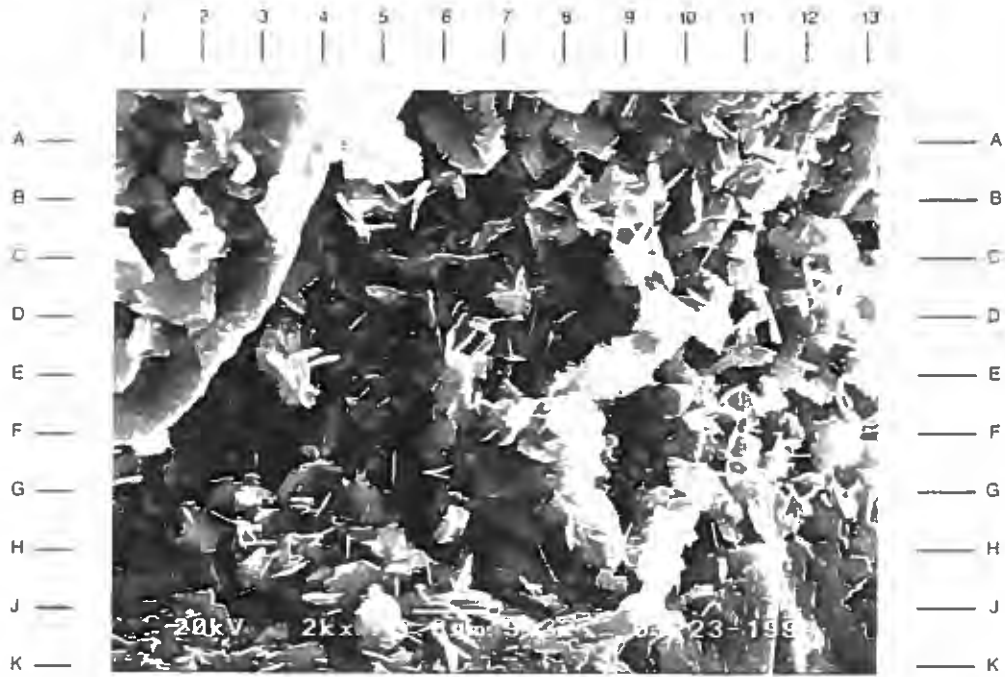
The high magnification photomicrograph illustrates a rarely seen grain coating of authigenic chlorite. Authigenic chlorite forms flat crystals that have a face-to-edge orientation. Note the associated microporosity of this authigenic clay type. X-ray diffraction (XRD) data indicates that 2% (by weight) of the sample is chlorite.

Magnification: 2,000X

PLATE 28B

This high magnification view documents another authigenic clay type found in this sandstone. Authigenic kaolinite acts as a pore filling, as shown here, and forms aggregates of booklets that are loosely bound to the pore walls. This loosely bound clay can be a migration concern when found in sufficient quantities or during changes in rock wettability.

Magnification: 1,500X



**DuPont
Injection Well No. 3 S/T
Harrison County, Mississippi**

File No. GN-4474

SAMPLE DEPTH: 9536 FEET

PLATE 29A

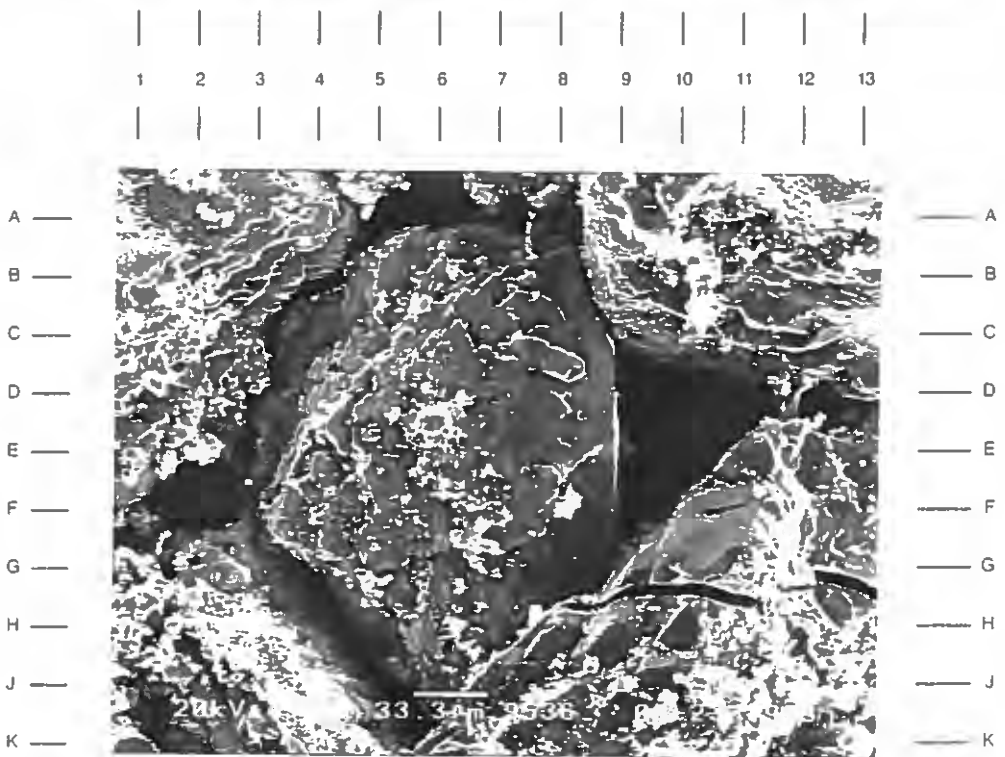
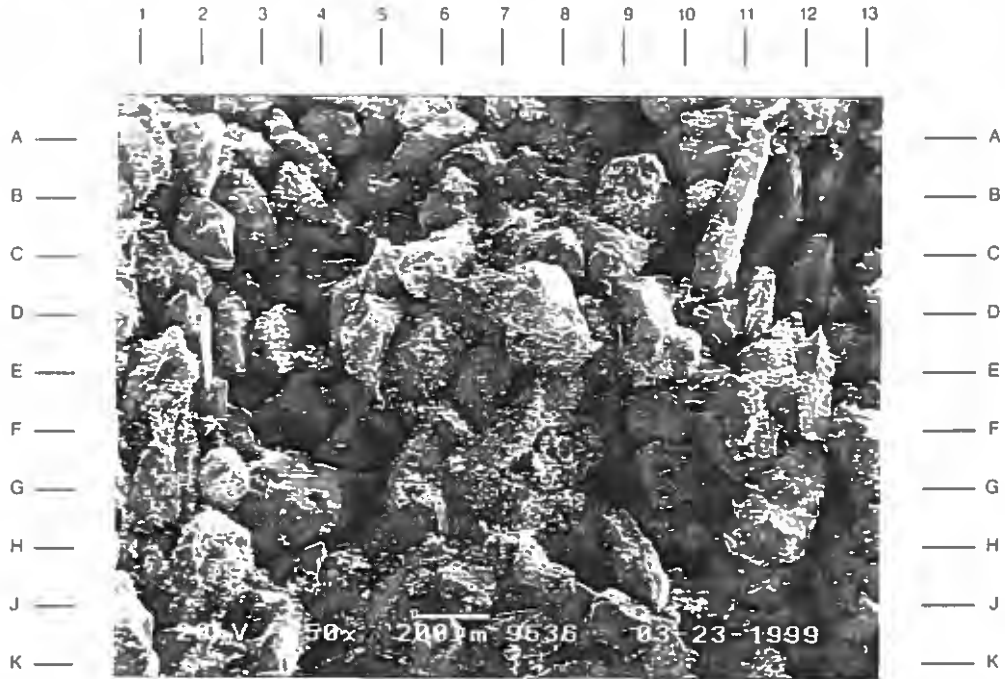
A low magnification survey photograph of the sample taken from 9536' is seen here. This lower medium-grained sandstone has a well developed intergranular pore system (A9.5,D4,E7) that has lesser amounts of secondary dissolution porosity (F-G7.5,G9). The framework grains in this sample appear to be moderately well sorted and generally subangular.

Magnification: 50X

PLATE 29B

The high magnification view of the center of Plate 29A shows a sand grain that is surrounded by small intergranular pores (A6,E10,F3). These primary pores are open and connected by small, but unrestricted pore throats (C3.5,H8). Incipient coatings of quartz overgrowths (C12,F11,E4.5) are noted on the grain surfaces.

Magnification: 300X



**DuPont
Injection Well No. 3 S/T
Harrison County, Mississippi**

File No. GN-4474

SAMPLE DEPTH: 9536 FEET

PLATE 30A

The high magnification photomicrograph depicts an area of a grain surface where quartz overgrowths (F2-J10) have been inhibited by the presence of grain-coating authigenic chlorite (E6). Note the nearby growth of feldspar (A1-A8) on an adjacent sand grain. Micas (D11) are also observed in these samples.

Magnification: 2,000X

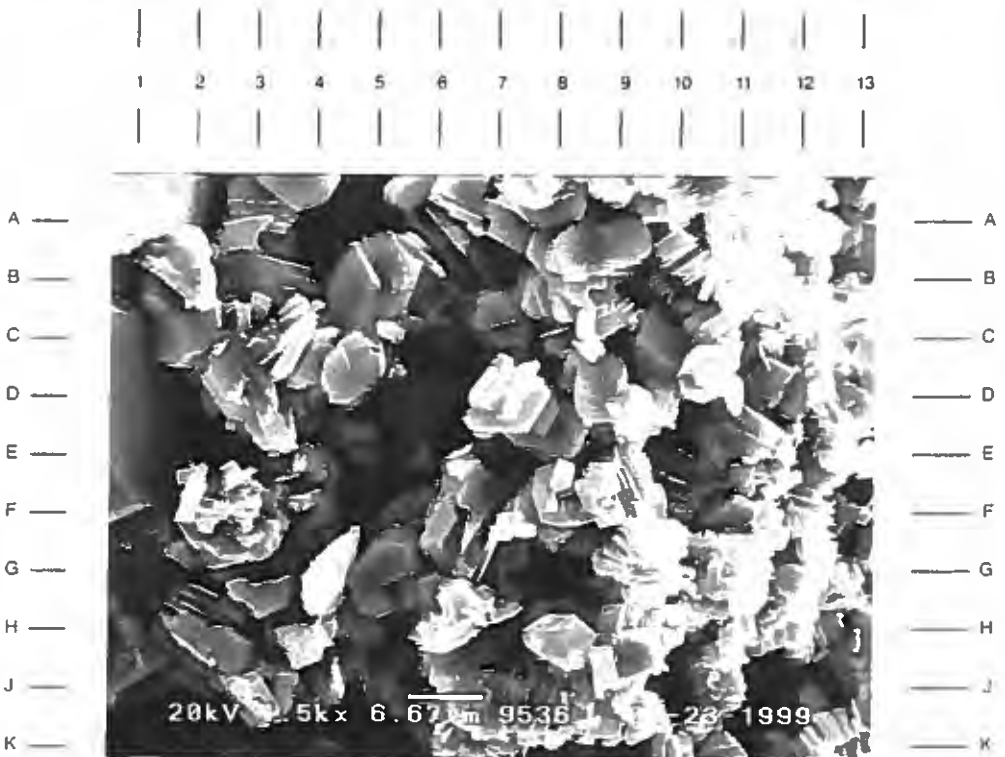
PLATE 30B

This high magnification view shows aggregates of blocky booklets of authigenic kaolinite. This authigenic clay is seen as a pore filling and is highly microporous. XRD data indicates that 2% (by weight) of the sample is composed of kaolinite. Kaolinite may also be found as a detrital clay; however, detrital clays are not common in most of these sandstone samples.

Magnification: 1,500X



A



B

**DuPont
Injection Well No. 3 S/T
Harrison County, Mississippi**

File No. GN-4474

SAMPLE DEPTH: 9588 FEET

PLATE 31A

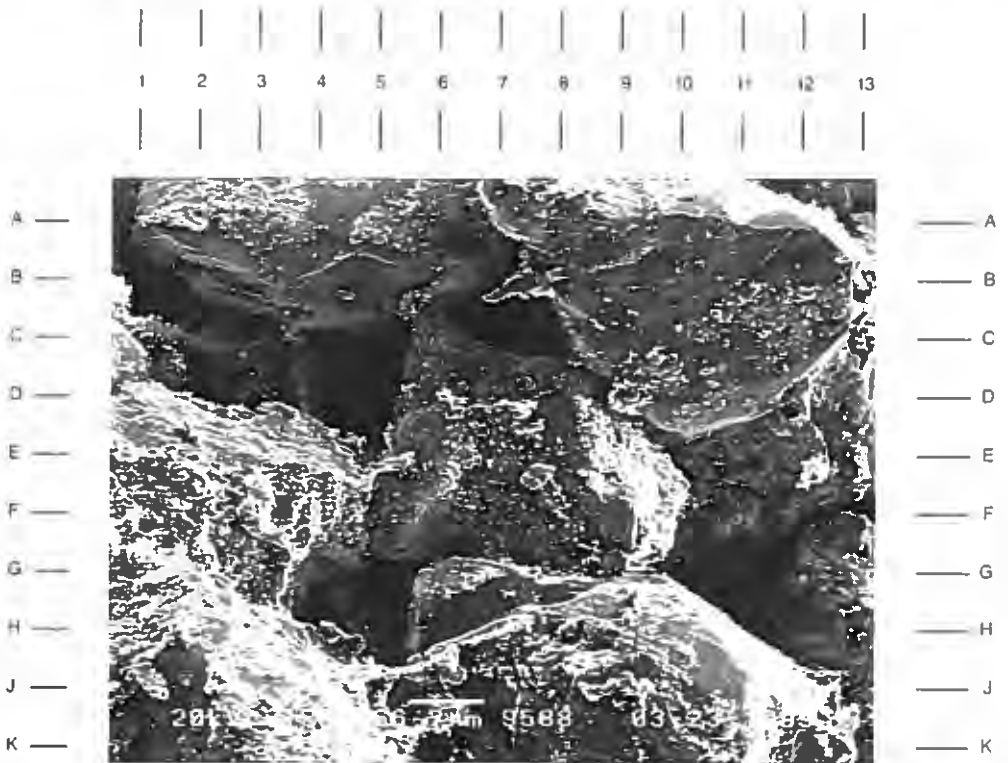
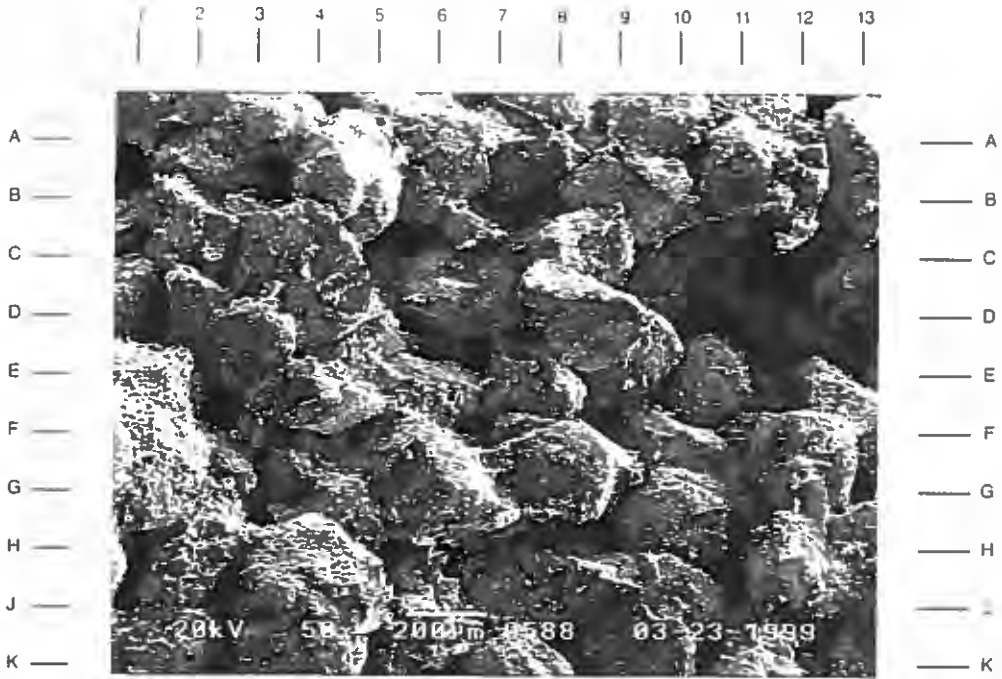
The low magnification survey photomicrograph taken from 9588' shows a medium-grained sandstone that has good porosity development. Primary intergranular porosity (C5,F8.5,H8) is open and evenly distributed. Secondary dissolution porosity (C-D12) is occasionally seen scattered throughout the sample. Note the clay (or dust) rim (B-C10) that was left behind after a less stable grain was dissolved to form this secondary pore.

Magnification: 50X

PLATE 31B

Quartz overgrowth development is an important feature of these sandstones. The high magnification view of the area near E8 in Plate 31A shows that these sand grains have a discontinuous coating of quartz, in the form of overgrowths (A-B12,H6) and as microcrystals (F2,F7). Secondary quartz growth tends to reduce nearby pore throats (D9,G8,C6), thus restricting flow.

Magnification: 150X



**DuPont
Injection Well No. 3 S/T
Harrison County, Mississippi**

File No. GN-4474

SAMPLE DEPTH: 9588 FEET

PLATE 32A

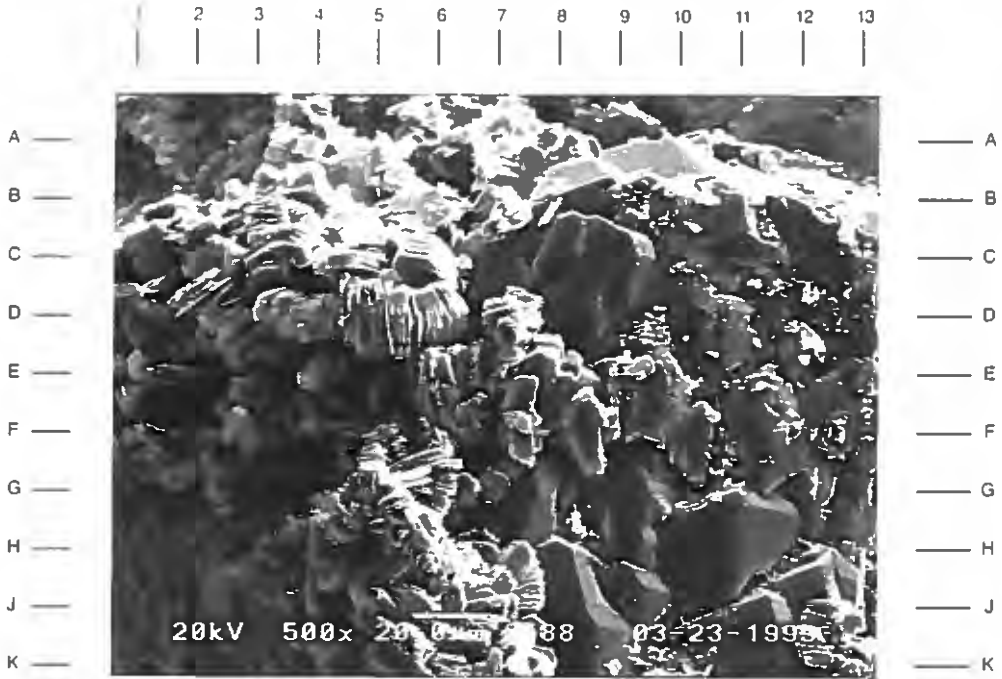
As seen in this high magnification view, authigenic kaolinite (D4,H5) appears as aggregates of booklets that cling loosely to pore walls. This pore-filling authigenic clay also contains microporosity that may suppress well log resistivity. Note the quartz overgrowths (H11,C8.5) that have formed on an adjacent sand grain.

Magnification: 500X

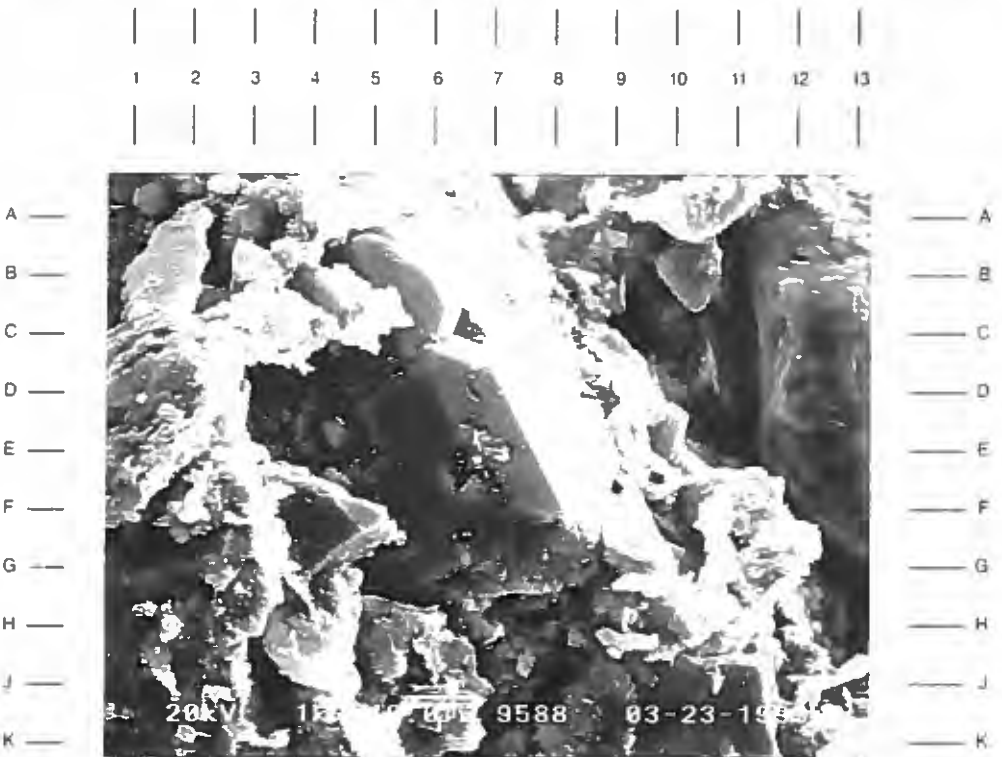
PLATE 32B

This high magnification view shows the well-developed nature of quartz overgrowths (E7) in these sandstones. Quartz overgrowths form flat to pseudo-hexagonal crystal faces that nucleate on host quartz sand grains. Another form of quartz growth is microcrystals (A1.5) that are attached to grain surfaces.

Magnification: 1,000X



A



B

**DuPont
Injection Well No. 3 S/T
Harrison County, Mississippi**

File No. GN-4474

SAMPLE DEPTH: 9822 FEET

PLATE 33A

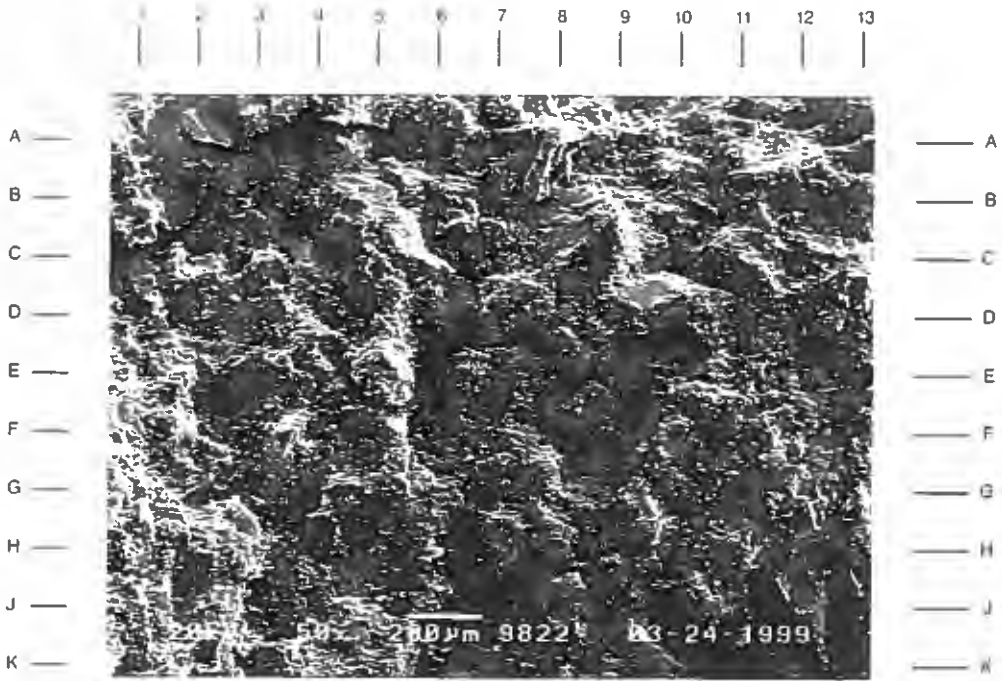
The low magnification survey photomicrograph shows that most porosity in this sandstone is coated, or masked, by authigenic kaolinite. This clay is seen attached to most pore walls, thereby restricting flow through nearby pore throats. Resulting porosity development is poor.

Magnification: 50X

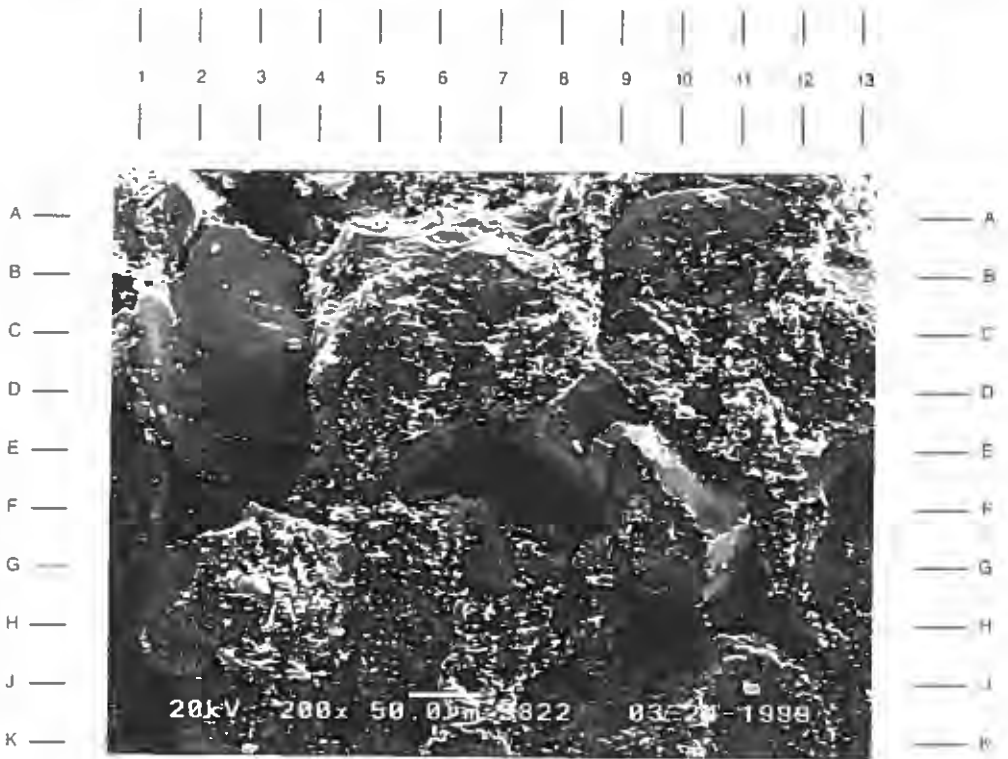
PLATE 33B

The high magnification view of the area near D7 in Plate 33A shows a closer view of framework grains that appear coated with a mixture of authigenic kaolinite and quartz microcrystals. Some pores (F7) are generally open, but connecting pore throats (F4,G9) are blocked.

Magnification: 200X



A



B



**DuPont
Injection Well No. 3 S/T
Harrison County, Mississippi**

File No. GN-4474

SAMPLE DEPTH: 9822 FEET

PLATE 34A

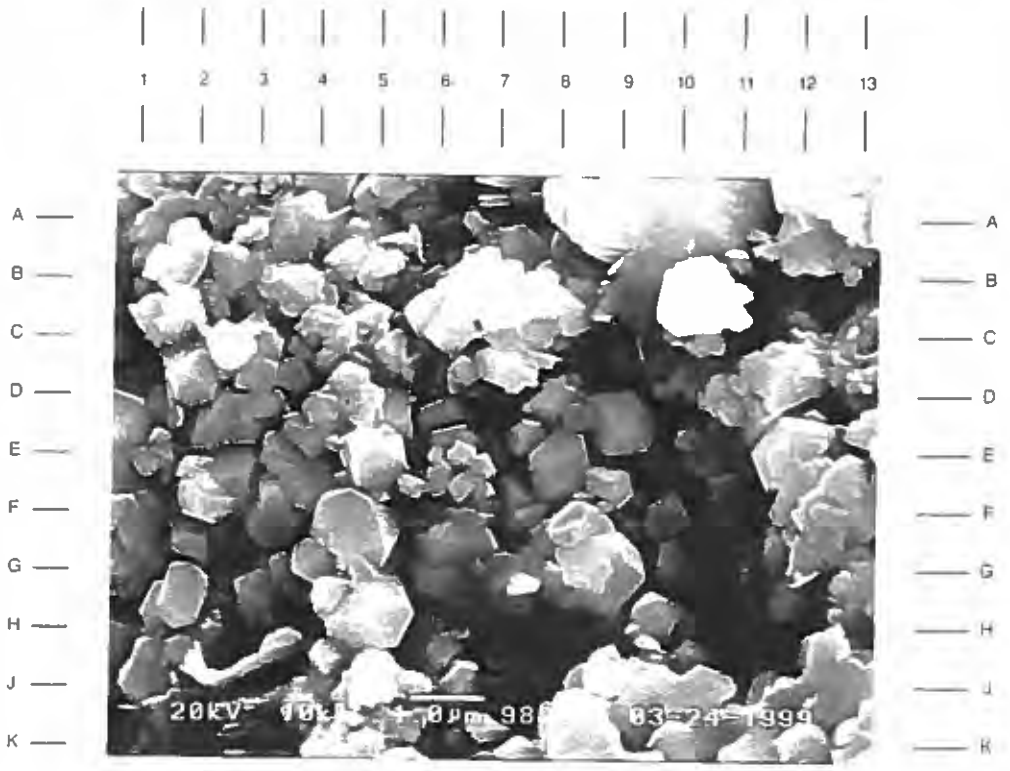
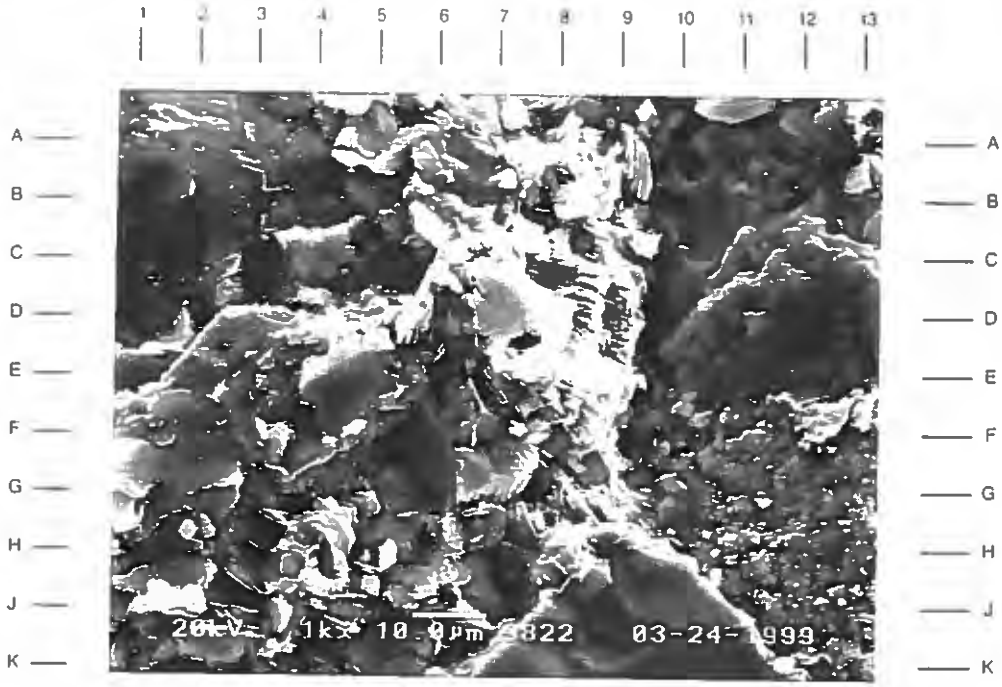
The high magnification photomicrograph taken near C8 of Plate 33B illustrates the pore-filling habit of authigenic kaolinite in this sample. These aggregates of blocky crystals tend to infill pores and restrict flow through nearby pore throats. Development of quartz as overgrowths (H5,J7) also appear in this view.

Magnification: 1,000X

PLATE 34B

This very high magnification view of the area near H12 in Plate 34A documents the presence of quartz microcrystals as a grain coating on quartz sand grains. Note the microporosity found between these microcrystals, which will contribute to well log resistivity suppression.

Magnification: 10,000X



**DuPont
Injection Well No. 3 S/T
Harrison County, Mississippi**

File No. GN-4474

SAMPLE DEPTH: 9826 FEET

PLATE 35A

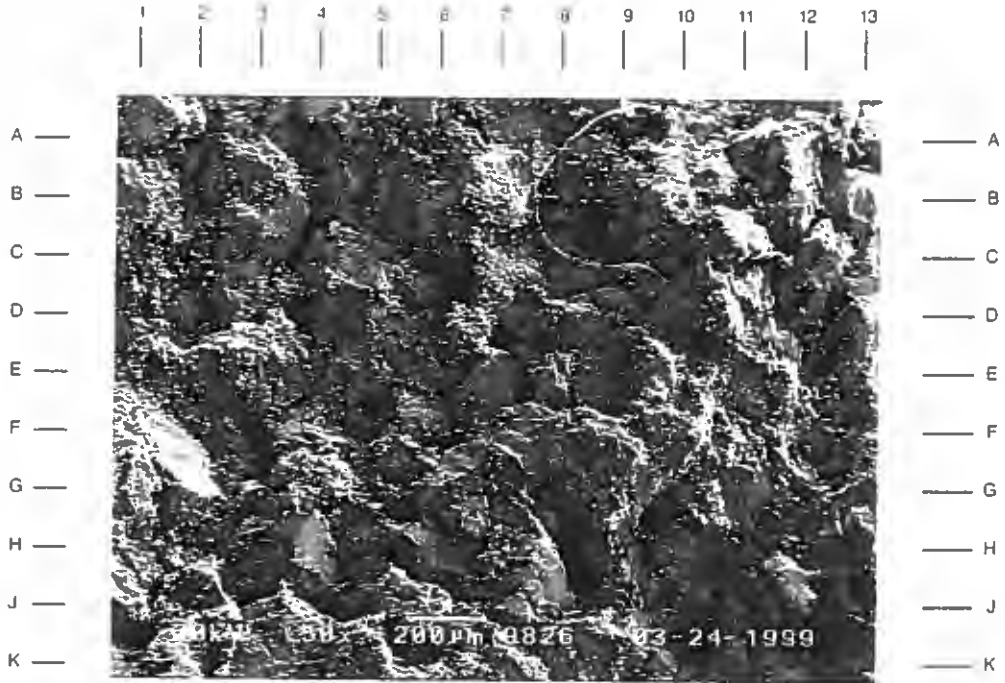
Primary intergranular porosity (C3.5,C-D6,F3) is scattered throughout the sandstone taken from 9826'. Quartz overgrowths (B6,D10,J7.5) are common as a pore-reducing component. These overgrowths are also observed restricting pore throats. A scattering of possible waste material (B7,G4,E12) clinging to the surface of sand grains is also noted.

Magnification: 50X

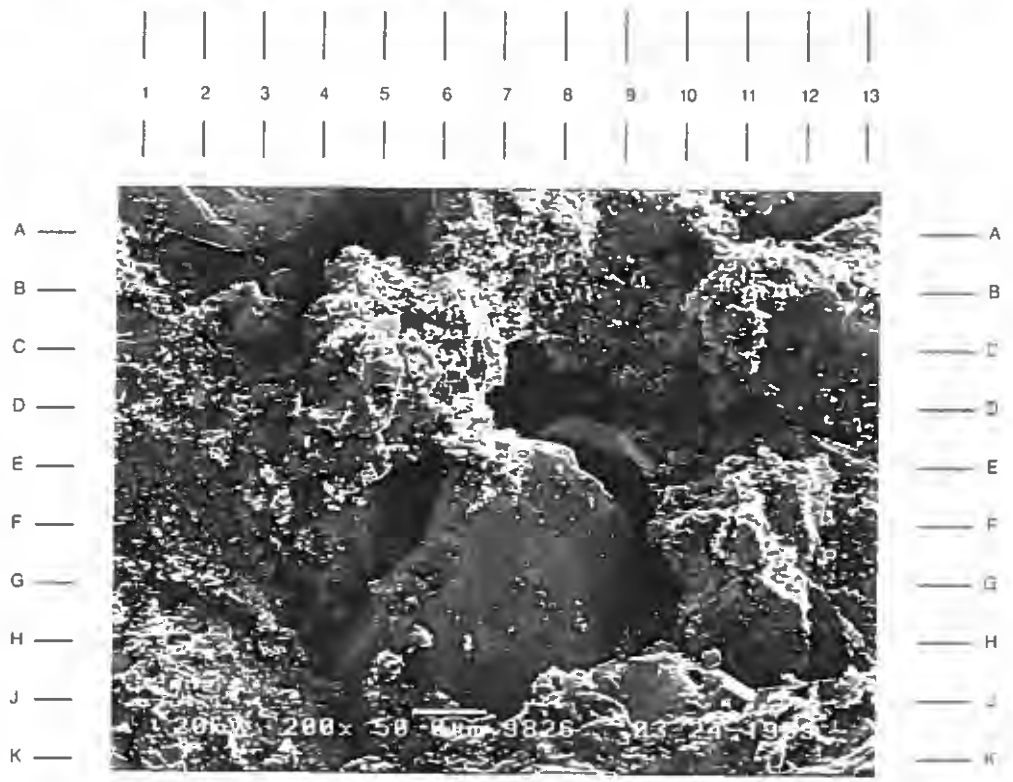
PLATE 35B

The high magnification view of the center of Plate 35A shows how most sand grains appear to be discontinuously coated with possible waste material (B8,J2). The end result is for grains to appear "etched" or "pitted". Crystal faces of quartz overgrowths (A3.5,E8) are seen protruding into open pore bodies.

Magnification: 200X



A



B



**DuPont
Injection Well No. 3 S/T
Harrison County, Mississippi**

File No. GN-4474

SAMPLE DEPTH: 9826 FEET

PLATE 36A

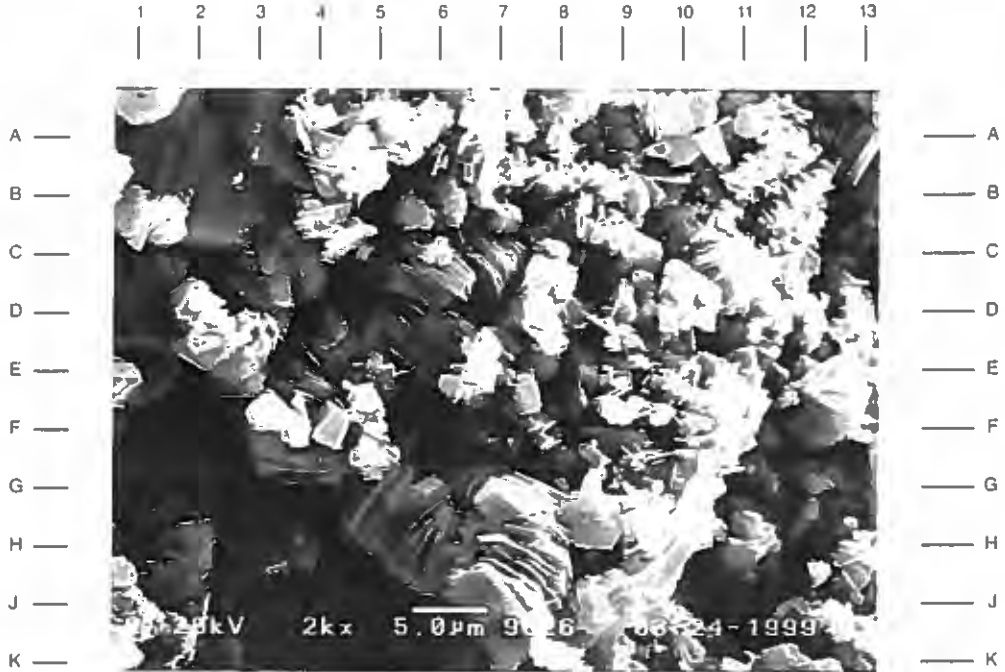
This high magnification photomicrograph depicts authigenic kaolinite (D6,H6) as a pore filling. These aggregates of booklets are intermixed with small particles (<5.0 microns) of suspected waste material. Quartz overgrowths (A3,D1) can be seen on a nearby sand grain.

Magnification: 2,000X

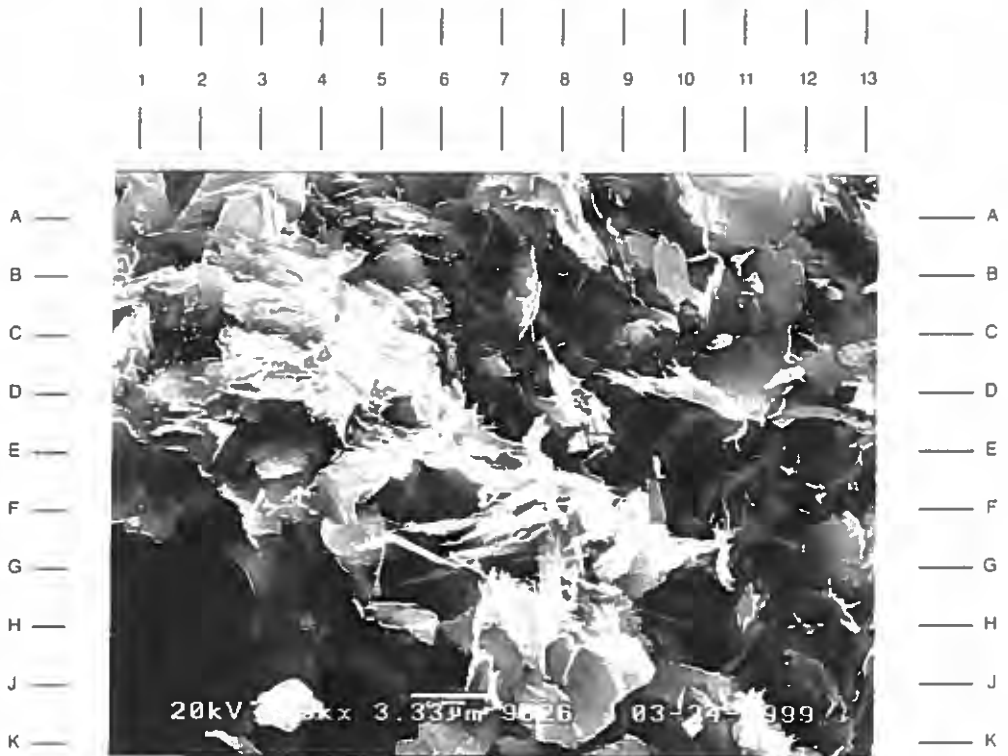
PLATE 36B

The high magnification view of chloritic clay is seen here. This clay type is typically authigenic in these samples and is found as a discontinuous grain coating. This clay forms as flat platelets that can have a face-to-edge orientation. Note the increase in microporosity due to this plate orientation.

Magnification: 3,000X



A



B

**DuPont
Injection Well No. 3 S/T
Harrison County, Mississippi**

File No. GN-4474

SAMPLE DEPTH: 9844 FEET

PLATE 37A

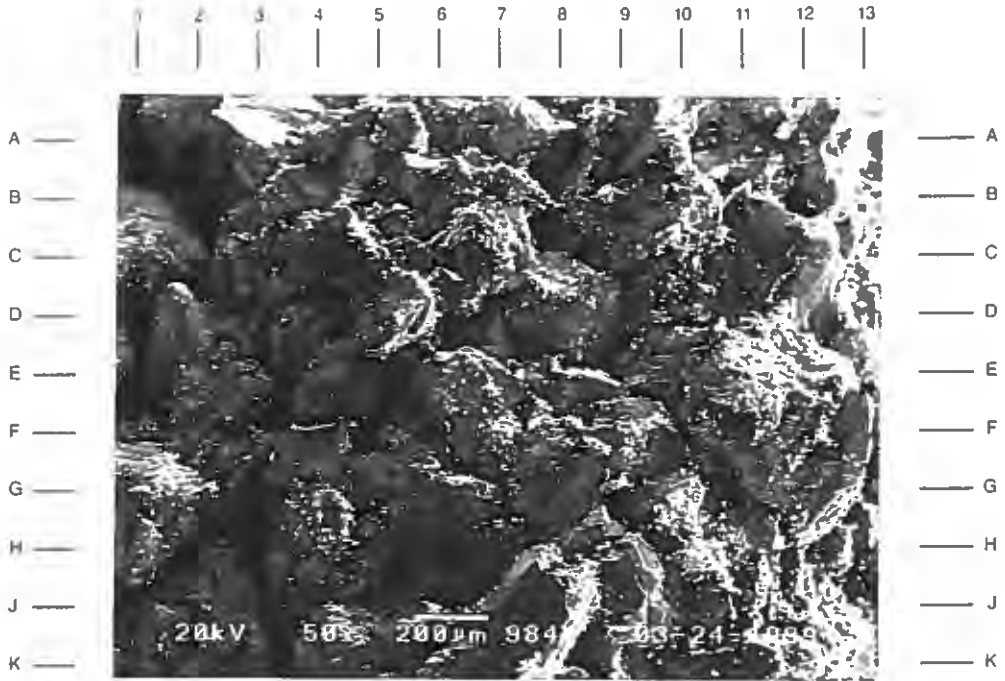
This low magnification view of the SEM subsample taken from 9844' shows that the effective pore system is well developed. Primary intergranular porosity (C8,D-E6,G9) is evenly distributed. Occasional secondary dissolution pores (A-B1.5) are seen scattered throughout the sample.

Magnification: 50X

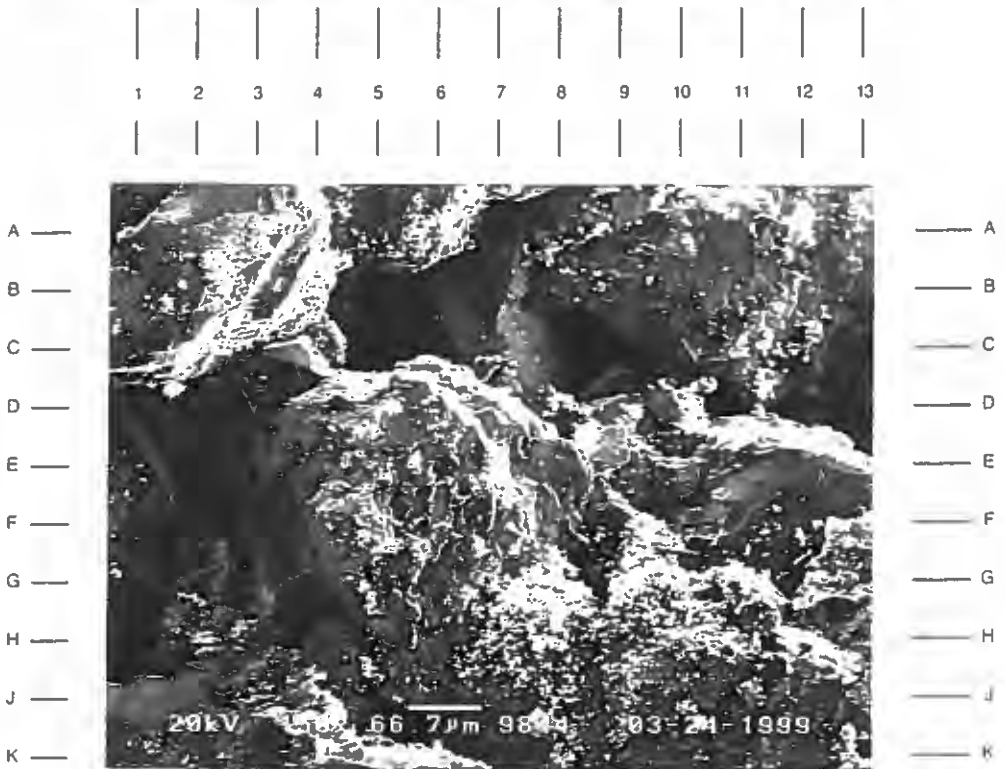
PLATE 37B

The high magnification view of the area near E7 in Plate 37A shows most intergranular pores (C5,C8,D13) are open. Contamination by waste material (H8,H10.5) is seen in the form of grain coatings. Quartz overgrowths (C7,E2) are well developed and reduce some pores and pore throats.

Magnification: 150X



A



B

**DuPont
Injection Well No. 3 S/T
Harrison County, Mississippi**

File No. GN-4474

SAMPLE DEPTH: 9844 FEET

PLATE 38A

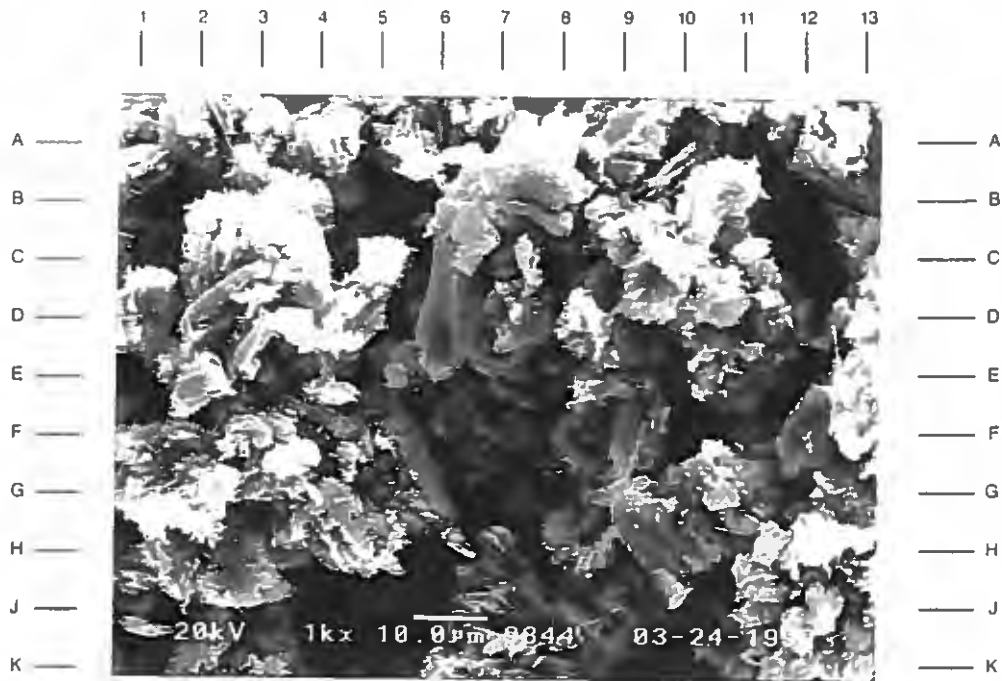
Another view of authigenic kaolinite is seen under high magnification in this photomicrograph. Aggregates of these stacked platelets (B10,G4,H10) can be seen in this pore-filling material. A scattering of probable waste material (B-C3,G2,H12) is also noted clinging to these booklets of kaolinite.

Magnification: 1,000X

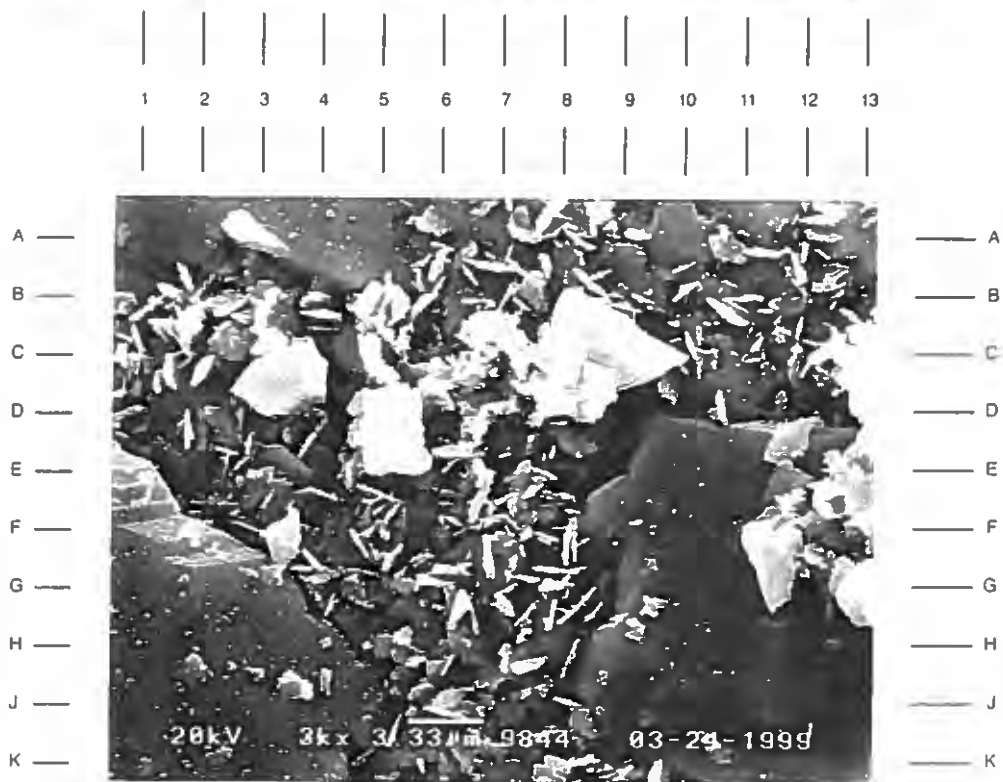
PLATE 38B

This high magnification view shows flat platelets of authigenic chlorite that are embedded on a sand grain surface. Note the face-to-edge orientation of several platelets. Irregularly-shaped particle (D5,B-C9,F-G11.5) are likely waste material that has been introduced into the zone. Note the growth of quartz (G2,F10) around this chloritic clay. Grain coatings of clay will inhibit the growth of quartz.

Magnification: 3,000X



A



B



**DuPont
Injection Well No. 3 S/T
Harrison County, Mississippi**

File No. GN-4474

SAMPLE DEPTH: 9848 FEET

PLATE 39A

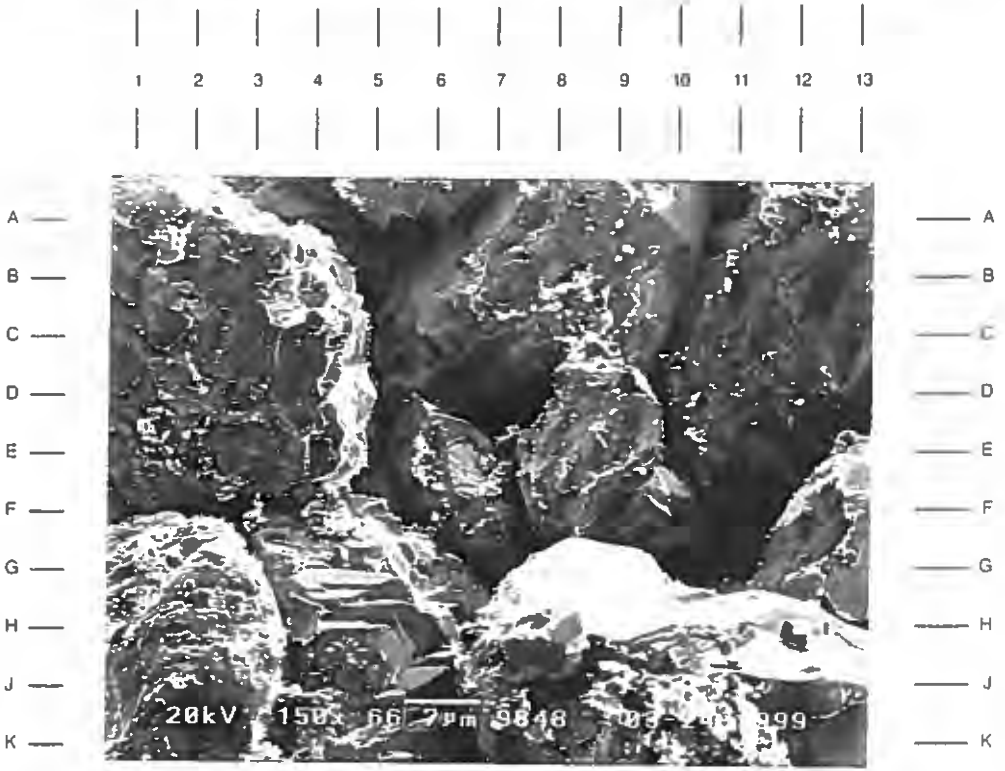
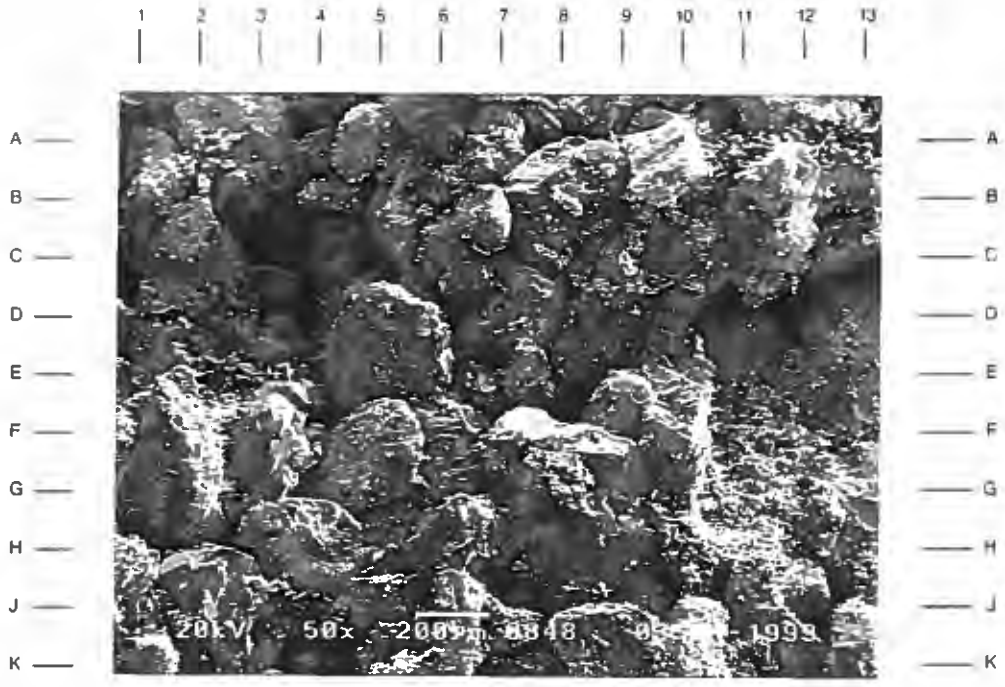
The low magnification survey photomicrograph indicates that a mixture of primary and secondary pores exist in the sandstone taken from 9848'. Intergranular porosity (E-F8,A3.5) appears to be open and well interconnected. Dissolution porosity (K4,J7) that is secondary is scattered in the sample.

Magnification: 50X

PLATE 39B

The high magnification view of the area near E7 in Plate 39A documents the well interconnected nature of the primary intergranular porosity (B5,D7,G11) seen in this medium-grained sandstone. Although some pore throats are reduced by quartz overgrowths (F4,F-G8.5), other appear to be open (B10.5,H3.5). Core analysis data indicates that permeability in this sample is 2502.0 md.

Magnification: 150X



1 2 3 4 5 6 7 8 9 10 11 12 13

**DuPont
Injection Well No. 3 S/T
Harrison County, Mississippi**

File No. GN-4474

SAMPLE DEPTH: 9848 FEET

PLATE 40A

The high magnification photomicrograph of this SEM subsample shows that authigenic kaolinite is present, as seen in previous samples. This authigenic clay is seen in its characteristic form of aggregates of booklets and appears as a pore filling. Note the microporosity associated with this clay type.

Magnification: 1,500X

PLATE 40B

This high magnification view of a sand grain surface identifies a cluster of quartz microcrystals (C2,D12,H8). Note the pseudo-hexagonal crystal structure typical of this mineral type. The presence of these small crystals creates an irregular grain surface and small particles of injected waste (D10,E7,G11) can become "attached", as is seen here.

Magnification: 2,000X



**DuPont
Injection Well No. 3 S/T
Harrison County, Mississippi**

File No. GN-4474

SAMPLE DEPTH: 9861 FEET

PLATE 41A

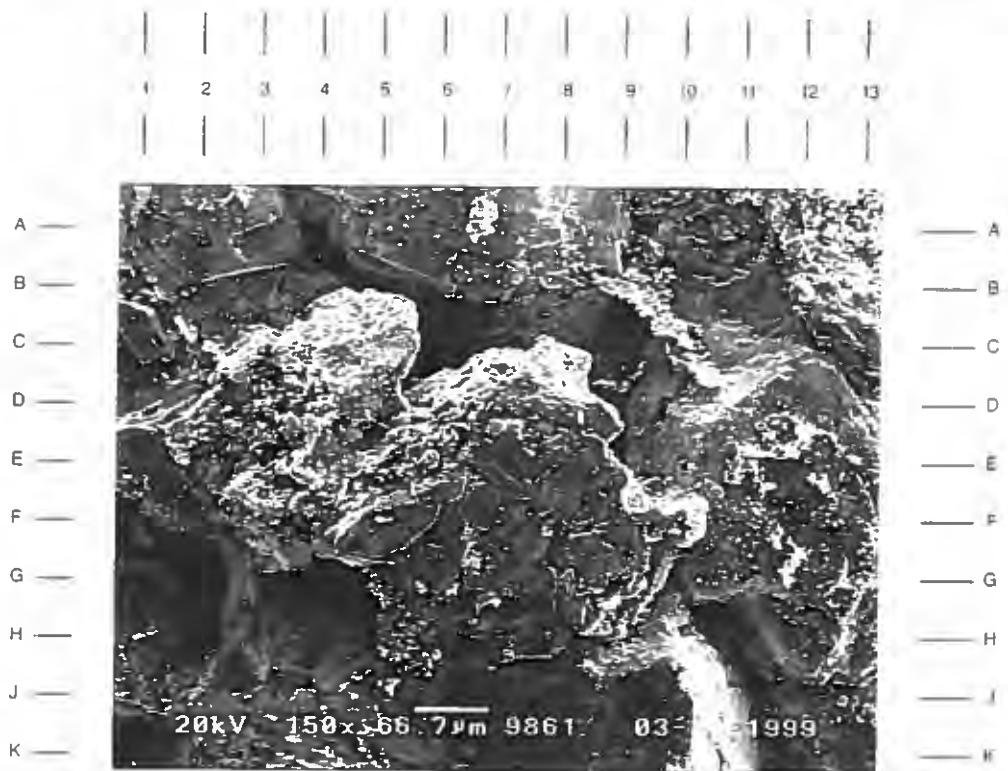
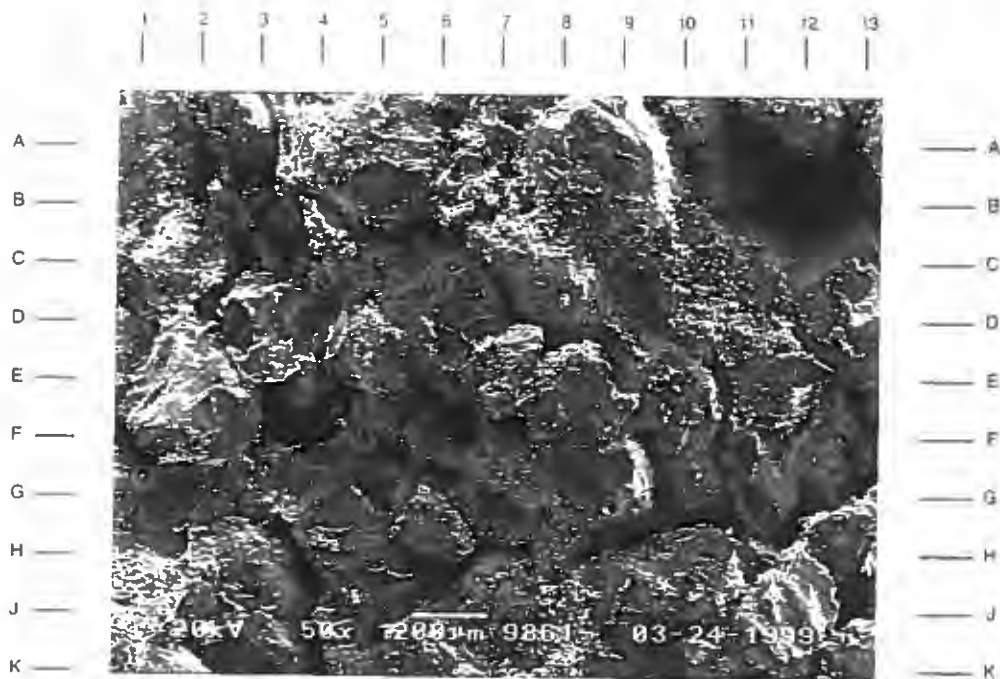
The low magnification survey photomicrograph illustrates a sandstone that has rather large grains. This sample is an upper medium-grained sandstone (average grain size is 0.48mm) and has moderately poor sorting. Visible pores (B12,E-F3.5) between grains are rather large and contribute to good porosity development.

Magnification: 50X

PLATE 41B

The high magnification view of the area near E8 in Plate 41A documents the presence of secondary dissolution. Less stable framework grains (D4) are observed as partially dissolved and contain intragranular microporosity. The pore-bridging component at B-C10 is either clay or waste material.

Magnification: 150X



**DuPont
Injection Well No. 3 S/T
Harrison County, Mississippi**

File No. GN-4474

SAMPLE DEPTH: 9861 FEET

PLATE 42A

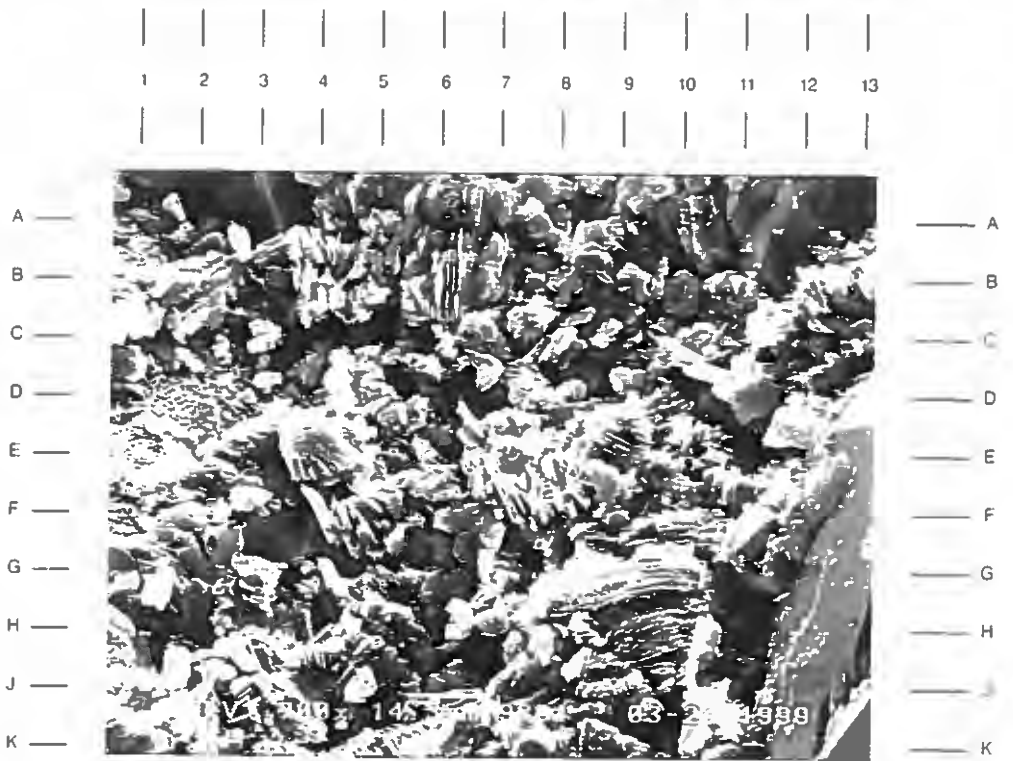
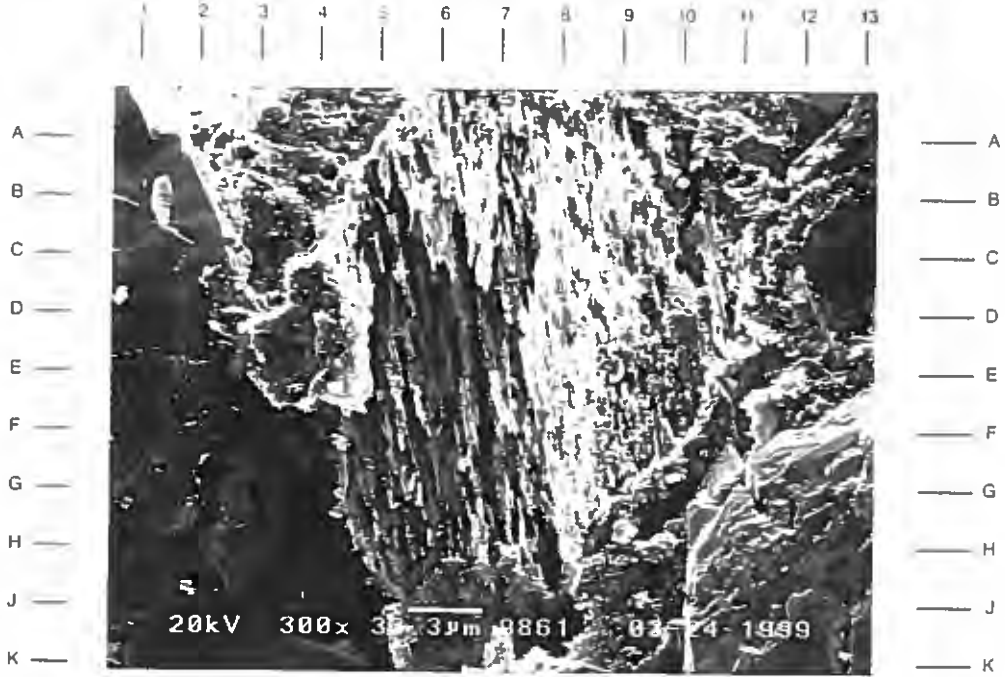
A partially dissolved plagioclase feldspar sand grain is seen under high magnification. Note the triclinic crystal morphology suggested by the resistive (to leaching) crystal remnants. Good intragranular microporosity is noted within this grain. Plagioclase grains account for only 2% of the sample; however some grain-moldic pores seen in this sandstone were likely derived from the complete dissolution of feldspar grains.

Magnification: 300X

PLATE 42B

An intergranular pore is shown under high magnification in this view, and is infilled with authigenic kaolinite. These flat platelets of clay are attached as aggregates and are typically loosely bound to pore walls. XRD data indicates that 2% (by weight) of the sample is composed of kaolinite. Note the quartz overgrowths (D13-K13) on a nearby sand grain.

Magnification: 700X



**DuPont
Injection Well No. 3 S/T
Harrison County, Mississippi**

File No. GN-4474

SAMPLE DEPTH: 9866 FEET

PLATE 43A

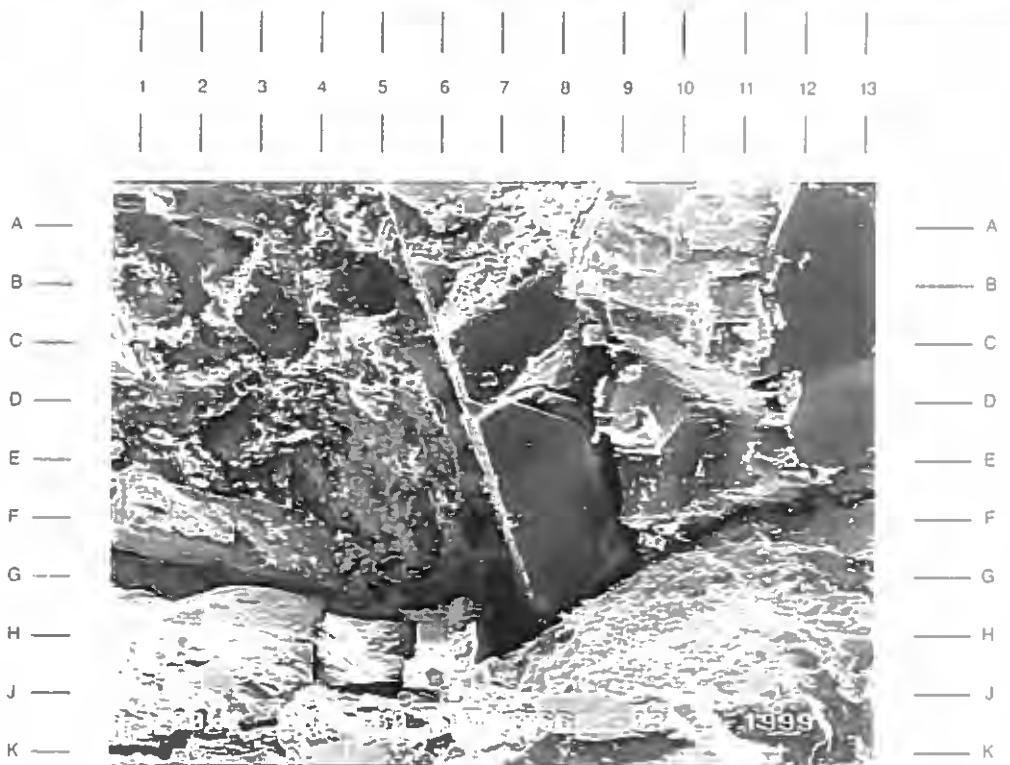
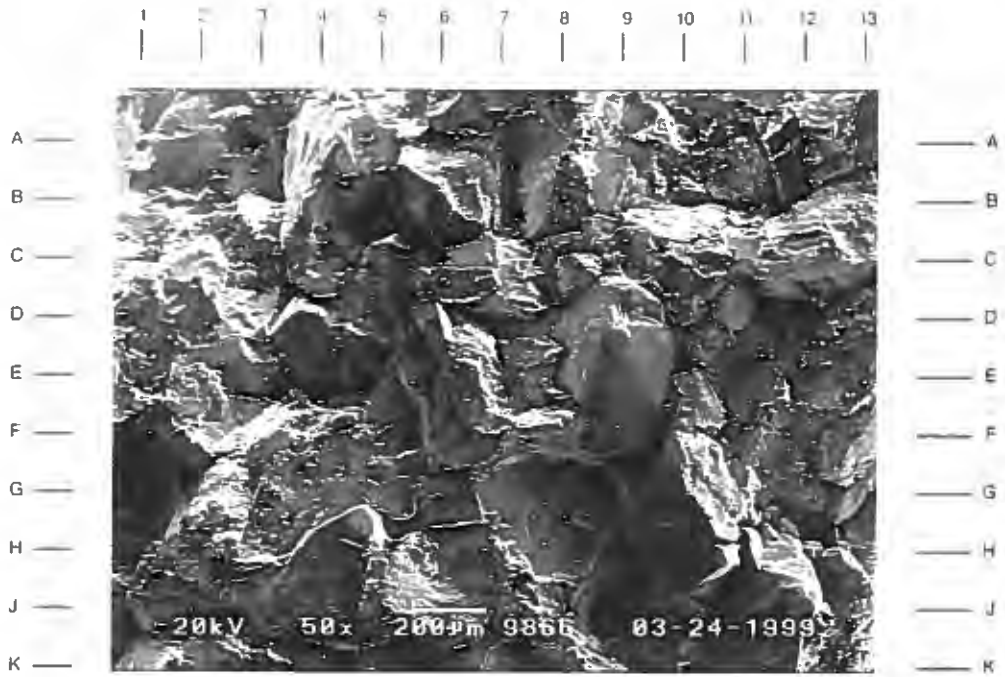
The low magnification photomicrograph on the facing page depicts a well cemented sandstone that lacks effective porosity. Intergranular areas (B3,E7.5,F11.5) are infilled with calcite cement. This carbonate cement is seen as a patchy pore filling and is quite common, accounting for 36% of the sample (by thin section analysis).

Magnification: 50X

PLATE 43B

The high magnification view of the area near A12 in Plate 43A shows blocky crystals of calcite that appear as a cement in intergranular areas of the sample. Note the severe reduction of this intergranular pore (H7). Remaining intergranular porosity in this sample is reduced to 1% (by thin section analysis).

Magnification: 200X



**DuPont
Injection Well No. 3 S/T
Harrison County, Mississippi**

File No. GN-4474

SAMPLE DEPTH: 9866 FEET

PLATE 44A

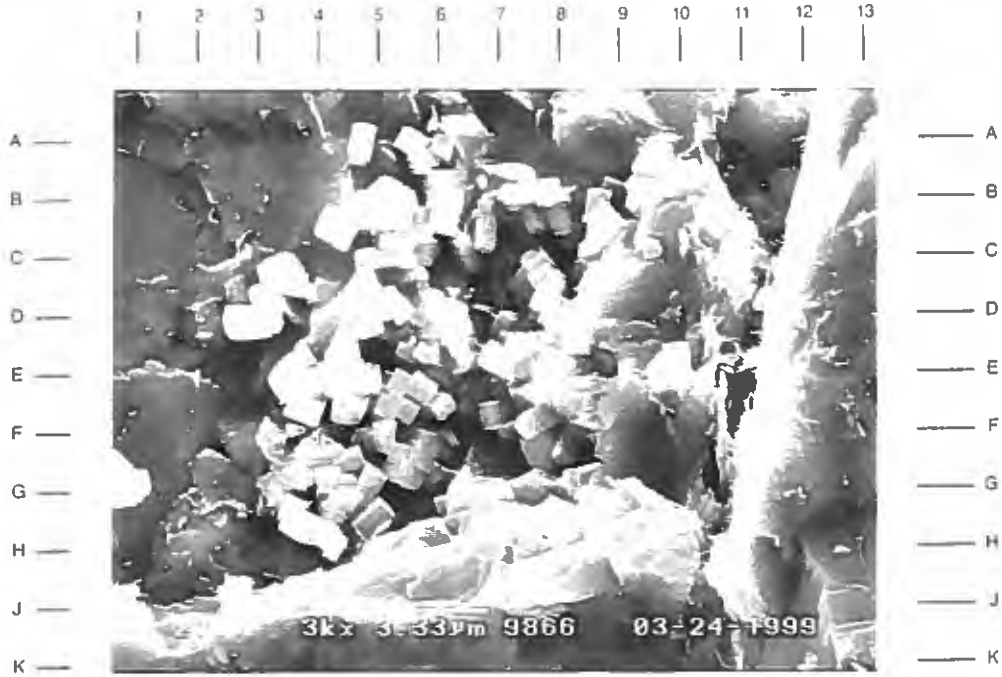
The high magnification photomicrograph was taken of the SEM subsample from 9866'. Small individual crystals of probable pyrite are found attached to a sand grain surface. Note the cubic structure that are occasionally interlinked (D5,G5.5). Small fibers of illitic clay (C11,E11.5) are intermixed with chloritic clay (J-K10.5) in this view.

Magnification: 3,000X

PLATE 44B

This high magnification view shows an intermix of two authigenic clay types found in these sandstones. Authigenic kaolinite (G3,J6) forms stacks of loosely attached booklets. Authigenic chlorite (D-E5.5,D10) is seen as flat platelets that occasionally have a face-to-edge orientation. Both clay types contain high amounts of microporosity.

Magnification: 3,000X



A



B



**DuPont
Injection Well No. 3 S/T
Harrison County, Mississippi**

File No. GN-4474

SAMPLE DEPTH: 9871 FEET

PLATE 45A

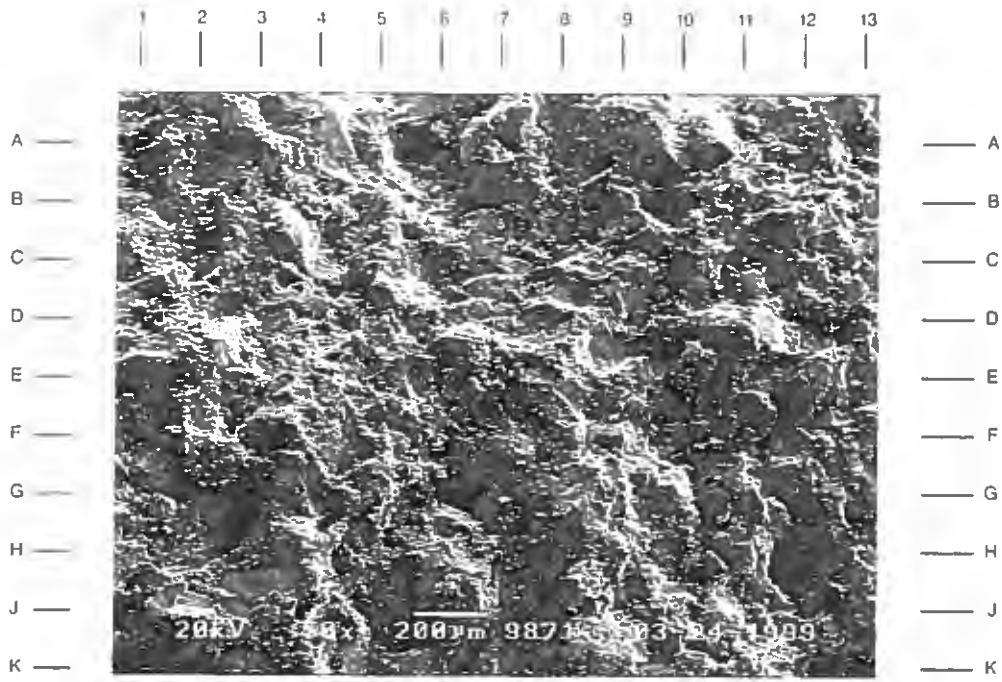
Poor porosity development is noted in the fine-grained sandstone taken from 9871'. Intergranular areas (B4,B10.5,H5.5) are infilled with calcite cement and detrital (clay-rich) matrix. Occasional primary (B2,G-H4) and secondary (J3.5,H-J12) pores are found erratically distributed and poorly connected.

Magnification: 50X

PLATE 45B

The high magnification view of the area near E7 in Plate 45A shows pore-filling material in an intergranular pore. This material consists of detrital matrix and silt grains. The dense matrix material is clay-rich and mostly illitic in composition. Both illite and mixed-layer illite/smectite are detected in XRD analysis.

Magnification: 500X



**DuPont
Injection Well No. 3 S/T
Harrison County, Mississippi**

File No. GN-4474

SAMPLE DEPTH: 9871 FEET

PLATE 46A

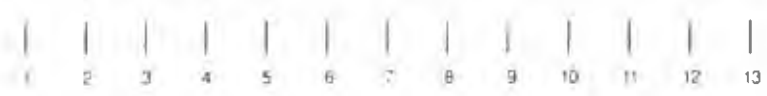
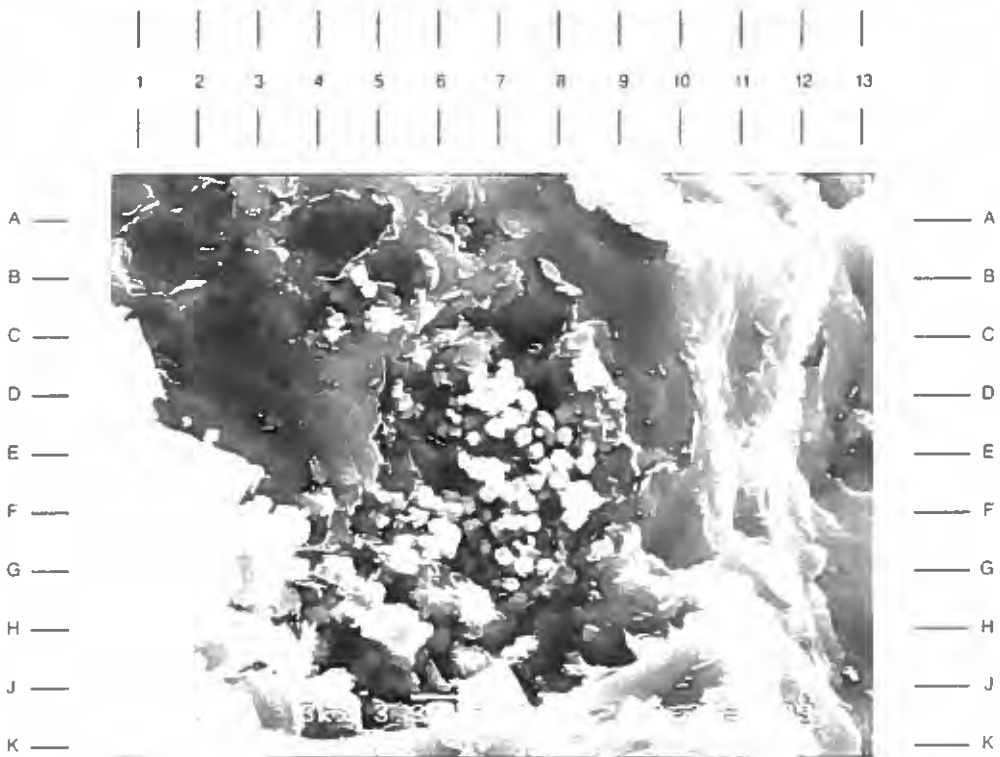
The high magnification photomicrograph of a filled intergranular pore is shown here. Pore-filling components include detrital matrix (F6,G-H7.5), pyrite (D-E7.5), and silt (C9). The detrital matrix is composed of illitic clays and chlorite (G5). Note the relatively clean surface of a nearby sand grain (right side of photo).

Magnification: 3,000X

PLATE 46B

This high magnification view shows a concentration of pyrite crystals in a small secondary pore. Secondary pyrite is found as a replacement product of organic material or as a pore filling, as shown here. Small flakes of illitic and/or chloritic clay (A3.5,B-C8,F-G4) are noted in this photo.

Magnification: 3,000X



**DuPont
Injection Well No. 3 S/T
Harrison County, Mississippi**

File No. GN-4474

SAMPLE DEPTH: 9887 FEET

PLATE 47A

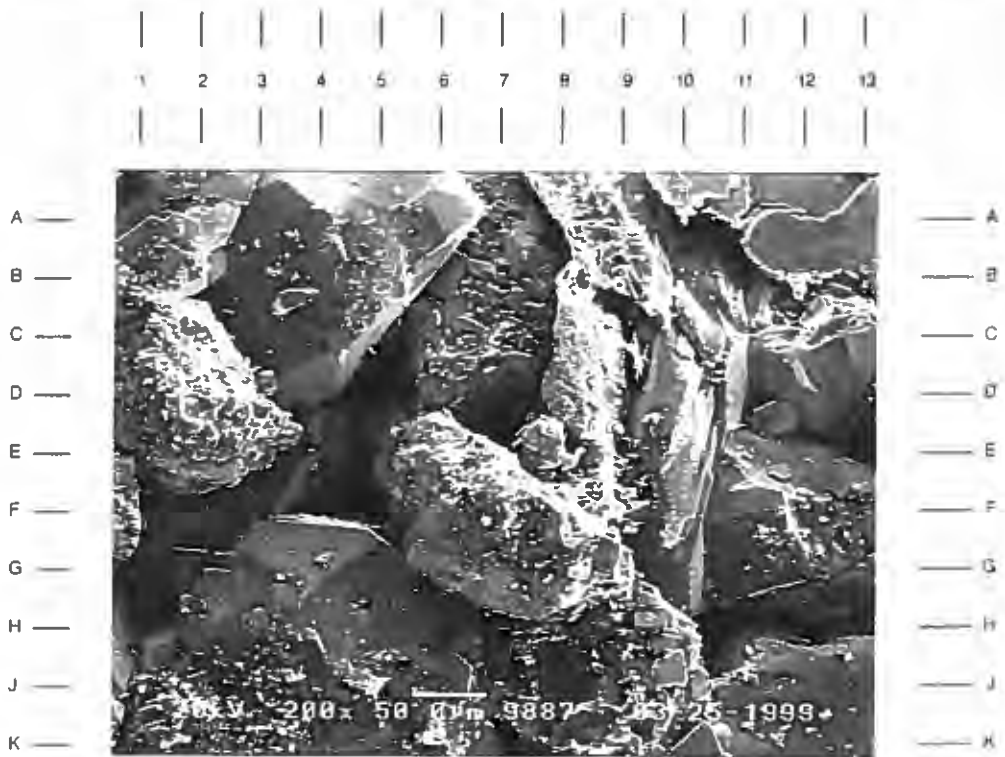
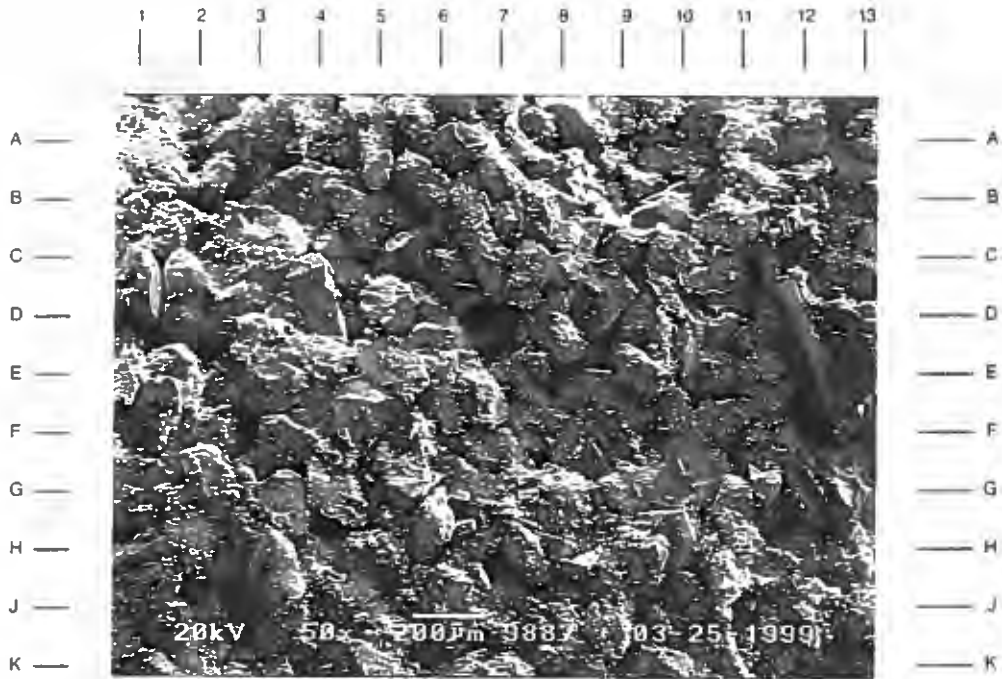
The low magnification survey photomicrograph illustrates a finer grained sandstone than seen in previous samples. This fine-grained sandstone has reduced porosity development due to the presence of common cementation. Primary cements include quartz overgrowths (D2,E5,H8) and dolomite (E6,H2). Note the relatively unaltered mica fragment at D12.

Magnification: 50X

PLATE 47B

The high magnification view of the area near D9 in Plate 47A documents locally good remaining intergranular porosity (D5,H1,H11) found within this sandstone. However, these pore and adjoining pore throats are restricted by quartz overgrowths (G2,G-H13,E4) and dolomite (D10).

Magnification: 200X



**DuPont
Injection Well No. 3 S/T
Harrison County, Mississippi**

File No. GN-4474

SAMPLE DEPTH: 9887 FEET

PLATE 48A

Secondary porosity accounts for 4% (by volume from thin section analysis) of the sample taken from 9887'. These pores are seen as both grain-moldic and intragranular pore types. This high magnification view is of a plagioclase feldspar sand grains (center of photo) that has been partially leached by dissolution, resulting in the creation of intragranular microporosity. Note the nearby quartz overgrowths (B1,J8,B12) protruding from quartz sand grains and into the open pore.

Magnification: 700X

PLATE 48B

The high magnification view of a small cluster of authigenic chlorite (center of photo) is seen here. Chlorite is the more common clay type (4% by weight from XRD data) found in this sandstone. The face-to-edge orientation is characteristic of the authigenic form of this clay mineral.

Magnification: 3,000X



A



B



**DuPont
Injection Well No. 3 S/T
Harrison County, Mississippi**

File No. GN-4474

SAMPLE DEPTH: 9899 FEET

PLATE 49A

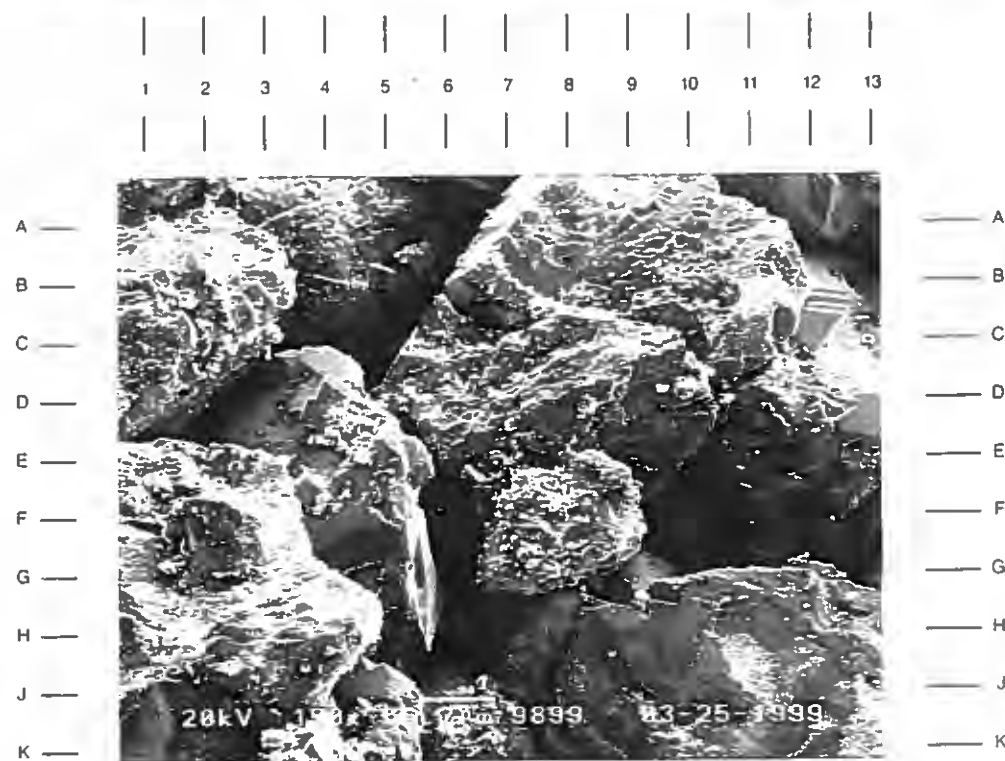
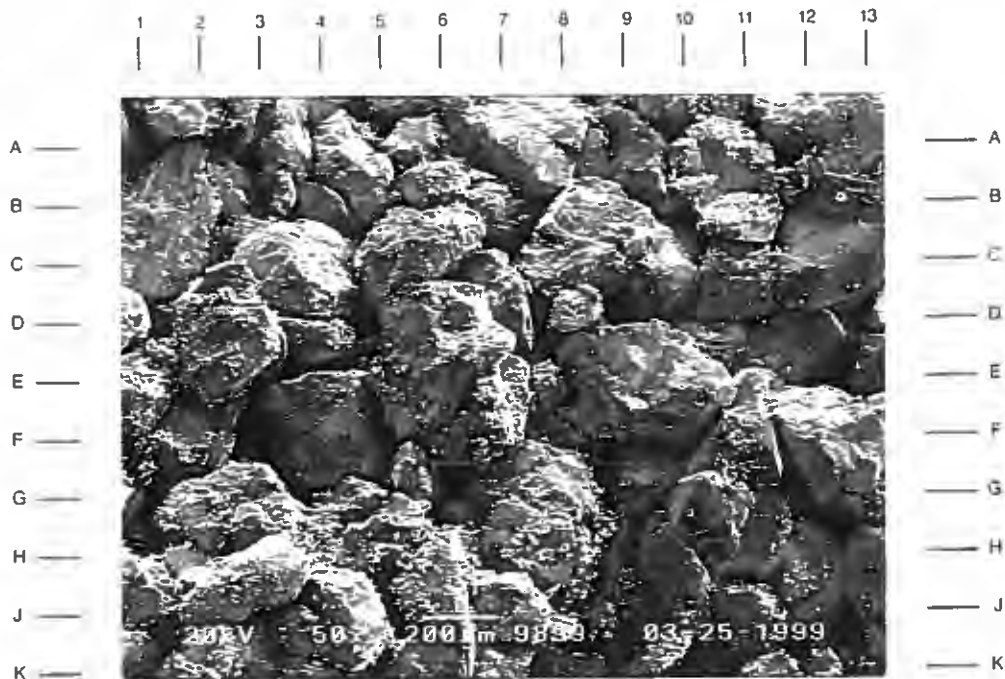
The low magnification photomicrograph on the facing page depicts a medium-grained sandstone that has a fairly well developed, evenly distributed intergranular pore system. Primary intergranular porosity (D4.5,D9,G8.5) accounts for 16% of the sample (by thin section analysis). Quartz overgrowths (C4.5,C10,G11) are the main constraints to the pore system.

Magnification: 50X

PLATE 49B

The high magnification view of the area near D8 in Plate 49A shows the typical growth of quartz (B-C12,H5.5,H8.5) as flat to pseudo-hexagonal crystal faces that nucleate on host quartz sand grains. Remaining intergranular porosity (A6,F10,H7) is relatively open; however some pore throat restrictions (D11,J5) are evident.

Magnification: 150X



**DuPont
Injection Well No. 3 S/T
Harrison County, Mississippi**

File No. GN-4474

SAMPLE DEPTH: 9899 FEET

PLATE 50A

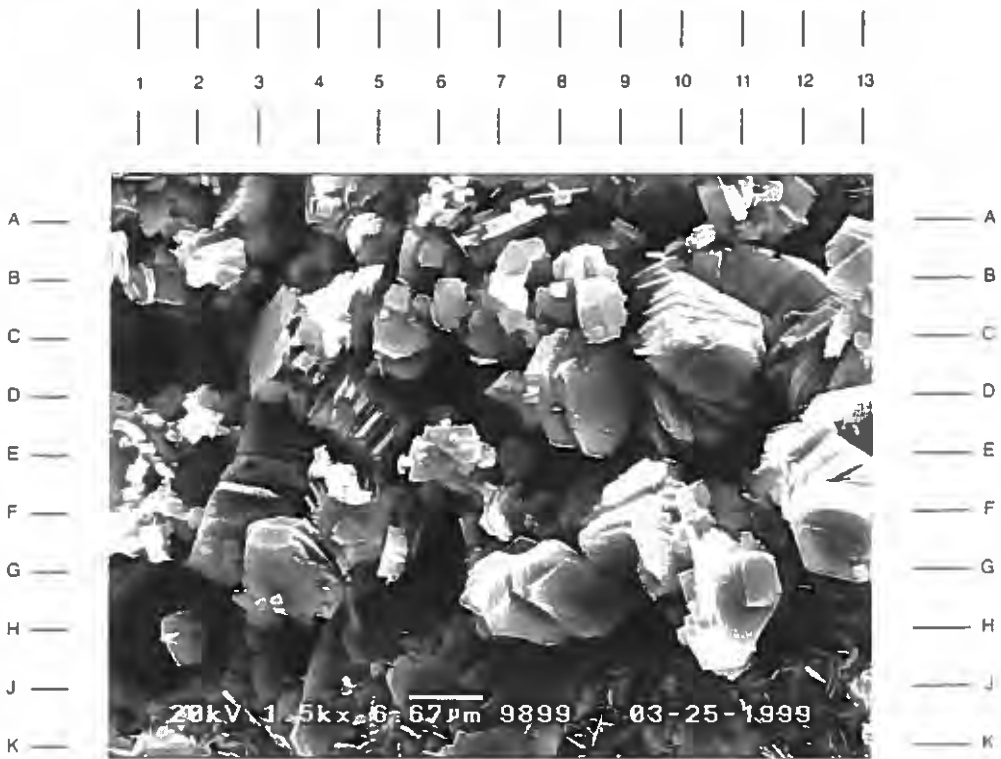
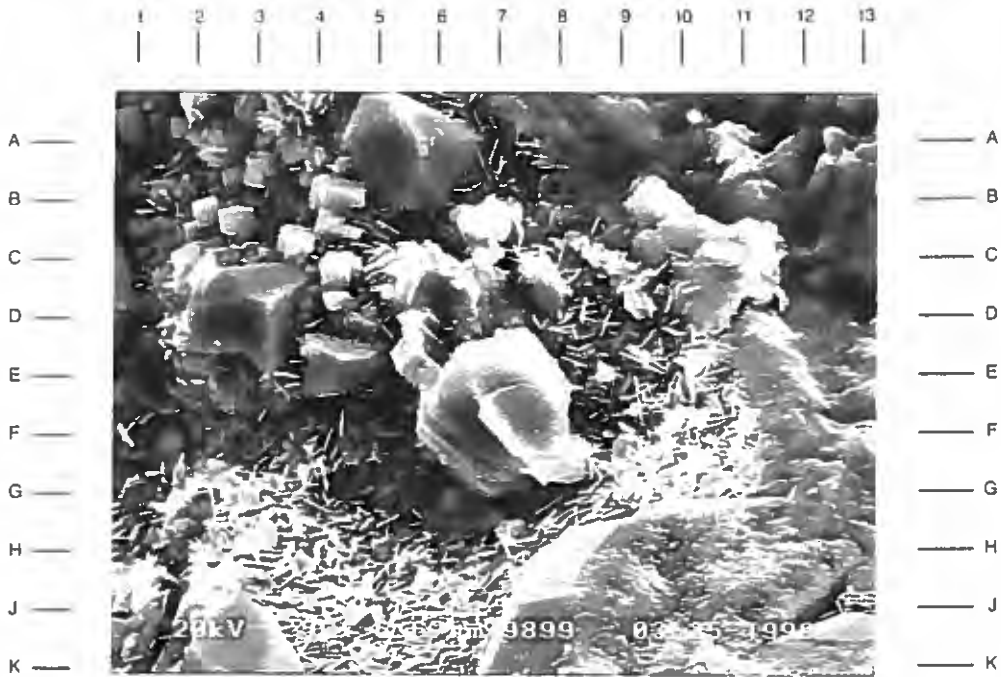
Grain-coating material on the sand grains found in this sample are uncommon. However, low amounts of authigenic clays are seen deposited discontinuously. Authigenic kaolinite (F7) can be found in a few intergranular areas as a pore filling and is loosely attached to pore walls. Authigenic chlorite (E9,J5) is also discontinuous and usually is found as flat platelets with a face-to-edge orientation. Quartz overgrowths are most common on sand grains and are only inhibited by the presence of grain-coating clay.

Magnification: 1,500X

PLATE 50B

The high magnification view of authigenic kaolinite as a pore-filling component is seen in this photo. This authigenic clay is seen here in association with small crystals (A6,E1) of either pyrite or halite. Halite would be derived from the precipitation of salt from formation water during core retrieval. Note the mixture of authigenic chlorite and quartz overgrowths at the base of this photo.

Magnification: 1,500X



**DuPont
Injection Well No. 3 S/T
Harrison County, Mississippi**

File No. GN-4474

SAMPLE DEPTH: 9904 FEET

PLATE 51A

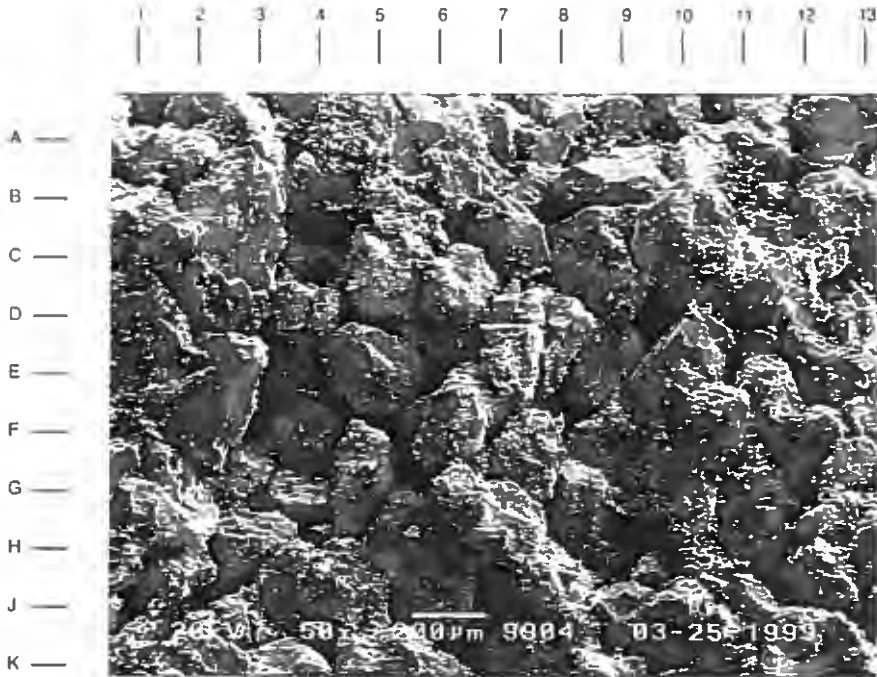
The low magnification survey photomicrograph of a fine-grained sandstone indicates that primary intergranular porosity (B8,D9.5,F5) is fairly common. Secondary dissolution porosity (H9.5) enhances the effective pore system. These pores appear to be open and framework sand grain surfaces are relatively clean.

Magnification: 50X

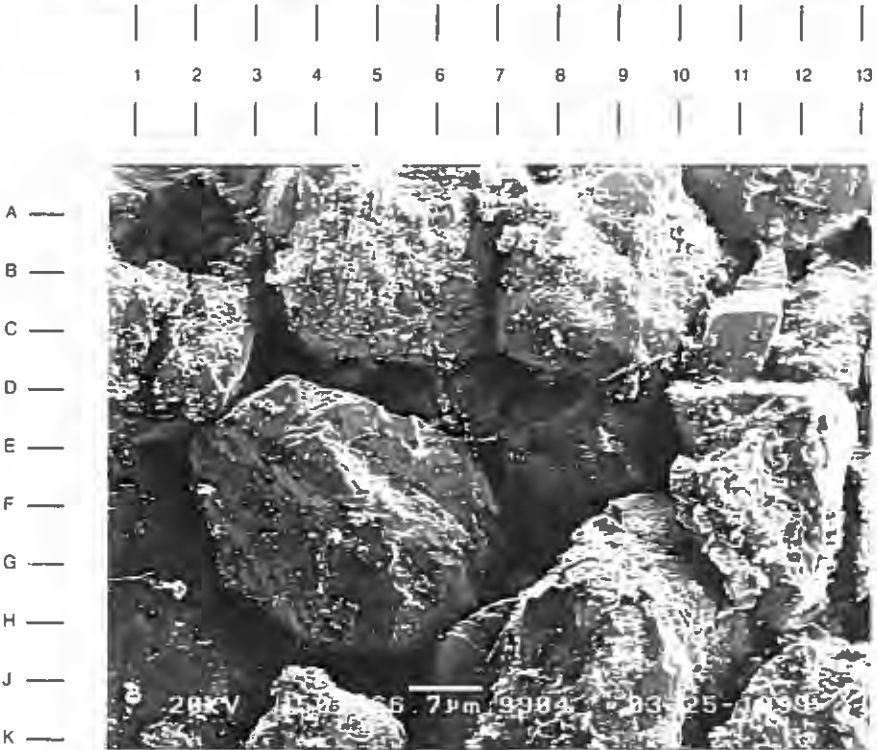
PLATE 51B

The high magnification view of the area near E6 in Plate 51A shows that pore throats (B7,D-E2.5,H6.5) which connect intergranular pores are generally open. Core analysis measurement of permeability (618 md) confirms that these pores are well interconnected. Quartz overgrowths (C-D3,C-D9) that appear on sand grain surfaces are not well developed.

Magnification: 150X



A



B

**DuPont
Injection Well No. 3 S/T
Harrison County, Mississippi**

File No. GN-4474

SAMPLE DEPTH: 9904 FEET

PLATE 52A

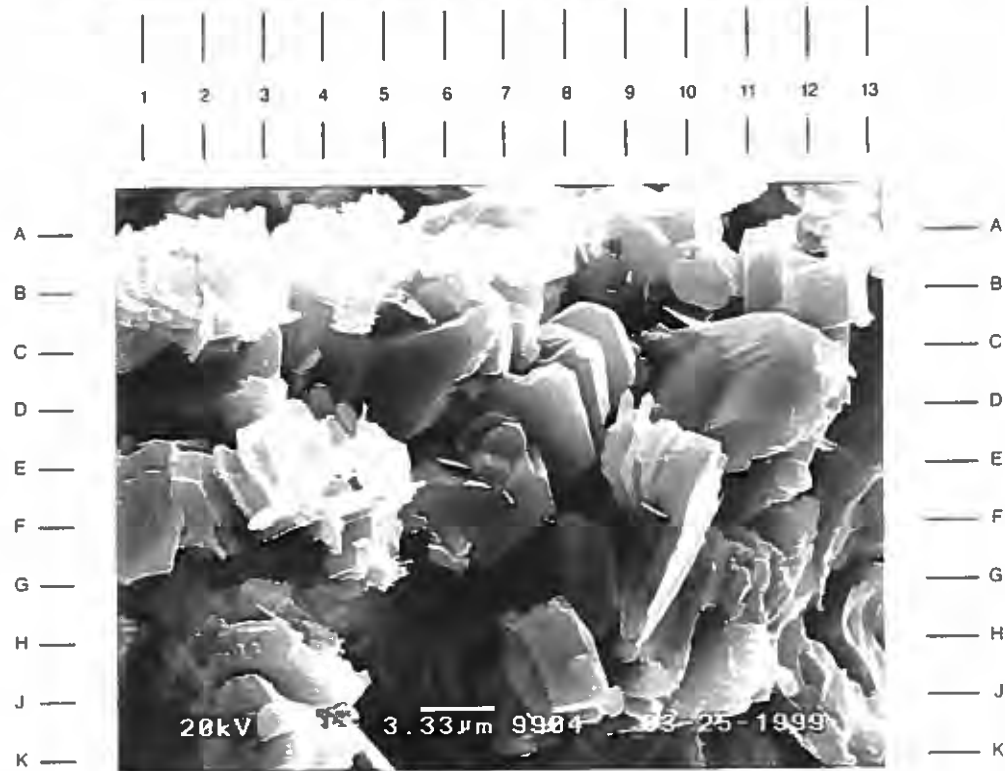
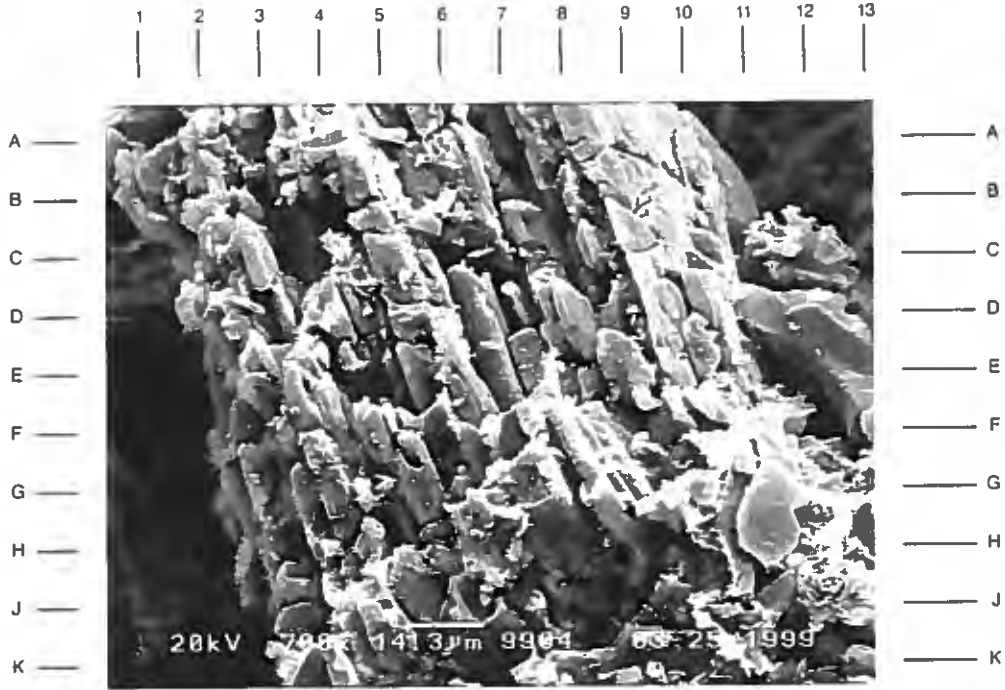
The high magnification photomicrograph shown here illustrates a feldspar sand grain that appears to be partially dissolved by secondary dissolution. Secondary dissolution has occurred in all samples (as indicated by the presence of secondary porosity); however, less stable grains that are capable of being dissolved are found in low amounts, which limit the volume of dissolution pores. Note the intragranular microporosity found between the crystal lattices of this grain.

Magnification: 700X

PLATE 52B

This high magnification view shows blocky and platey forms of authigenic kaolinite. Some plates form aggregates (J7) while other platelets are singular. This loose attachment allows this authigenic clay to easily migrate during well flow. Authigenic kaolinite is found in low amounts in nearly all samples of this study.

Magnification: 3,000X



**DuPont
Injection Well No. 3 S/T
Harrison County, Mississippi**

File No. GN-4474

SAMPLE DEPTH: 9916 FEET

PLATE 53A

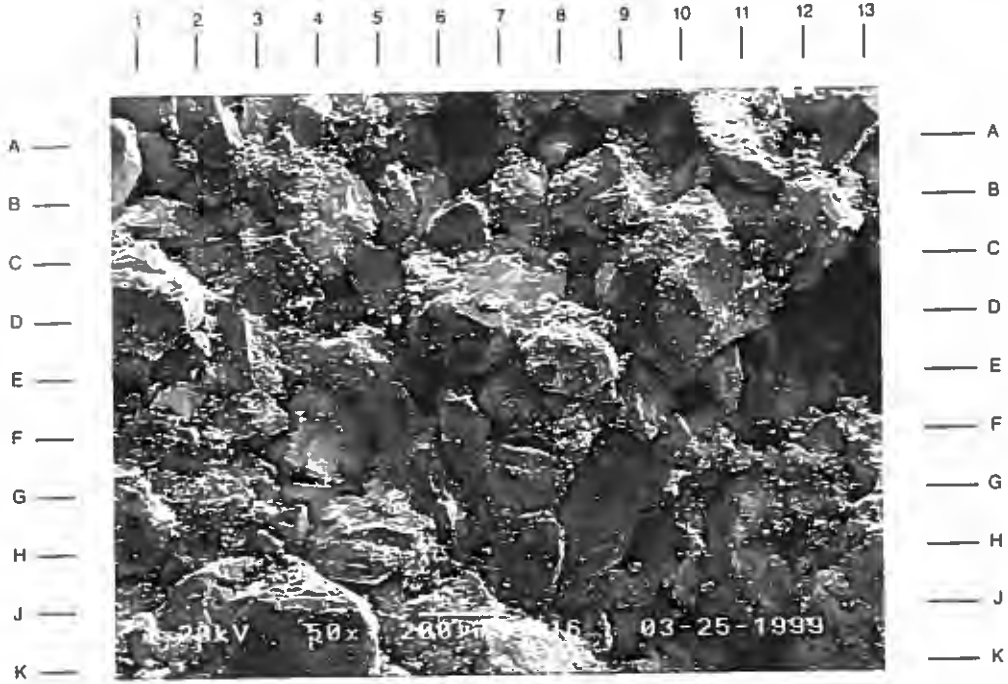
The low magnification survey photomicrograph of the SEM subsample taken from 9916' indicates that overall effective porosity is reduced by the presence of quartz overgrowths (C8,E5,F10) and residual waste material (A4.5,G2,F8). Compaction of the sediment has also contributed to porosity reduction. Thin section analysis indicates that total porosity comprises 22% (by volume) of the sample.

Magnification: 50X

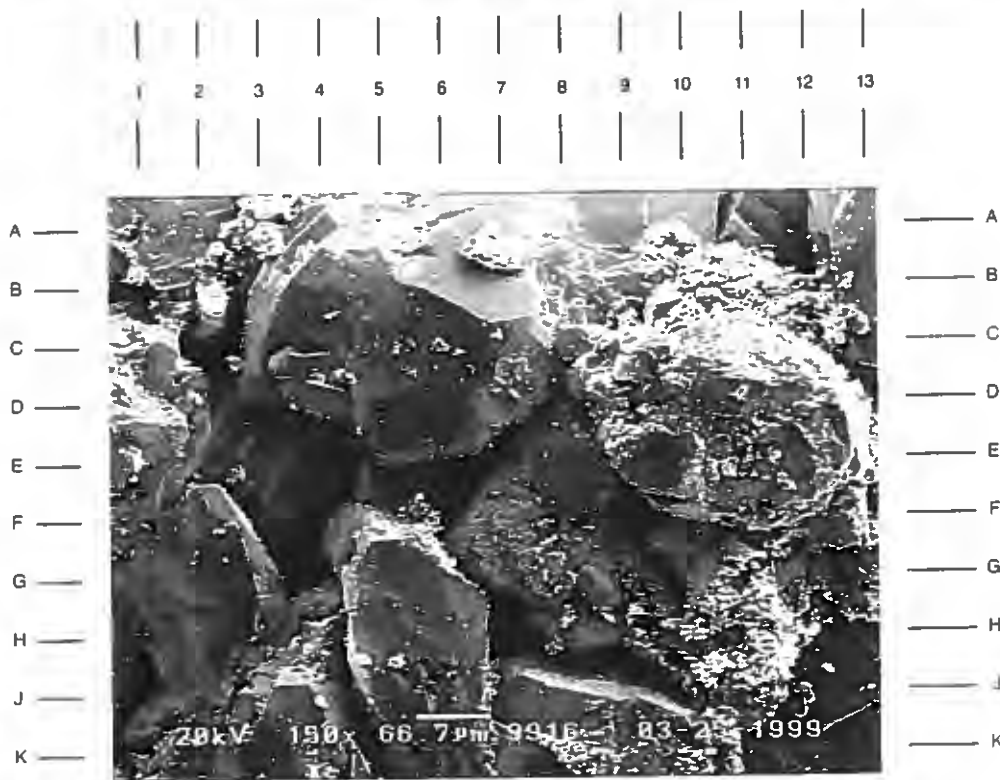
PLATE 53B

The high magnification view of the area near E7 in Plate 53A shows quartz overgrowths (C-D3,F2,D6) nucleating from host sand grains slightly protrude into open pores, thus reducing pore volume. Remnants of waste material (B11,H11) is seen infilling other pore bodies.

Magnification: 150X



A



B

**DuPont
Injection Well No. 3 S/T
Harrison County, Mississippi**

File No. GN-4474

SAMPLE DEPTH: 9916 FEET

PLATE 54A

This high magnification photomicrograph of pore-filling material indicates that authigenic kaolinite is the major component. This authigenic clay has formed flat to blocky booklets that collect as aggregates to infill this pore body. Minor amounts of probable remnant waste material (A6,G-H3) has attached itself to kaolinite.

Magnification: 1,500X

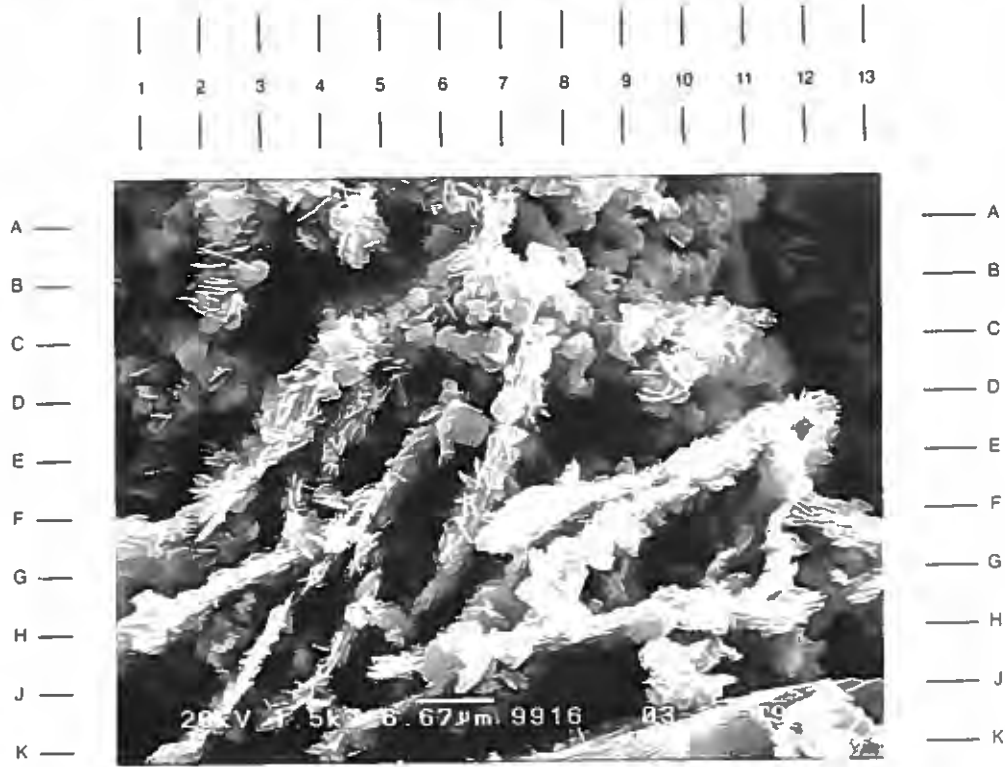
PLATE 54B

A partially dissolved feldspar grain (probably plagioclase) is shown in this high magnification photomicrograph. The remnants of this grain is coated with authigenic chlorite that has formed flat platelets which occasionally show face-to-edge orientation. The presence of this clay may have prevented further dissolution of this grain. Note the intragranular porosity (D-E9,F6,J8.5).

Magnification: 1,500X



A



B

**DuPont
Injection Well No. 3 S/T
Harrison County, Mississippi**

File No. GN-4474

SAMPLE DEPTH: 9929 FEET

PLATE 55A

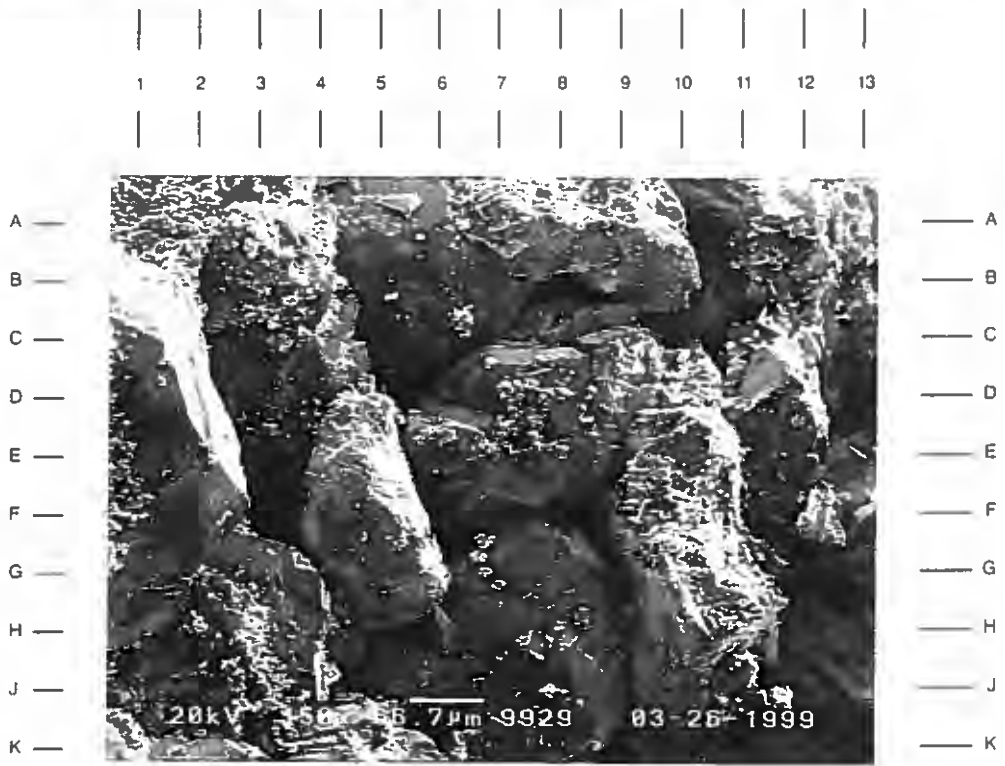
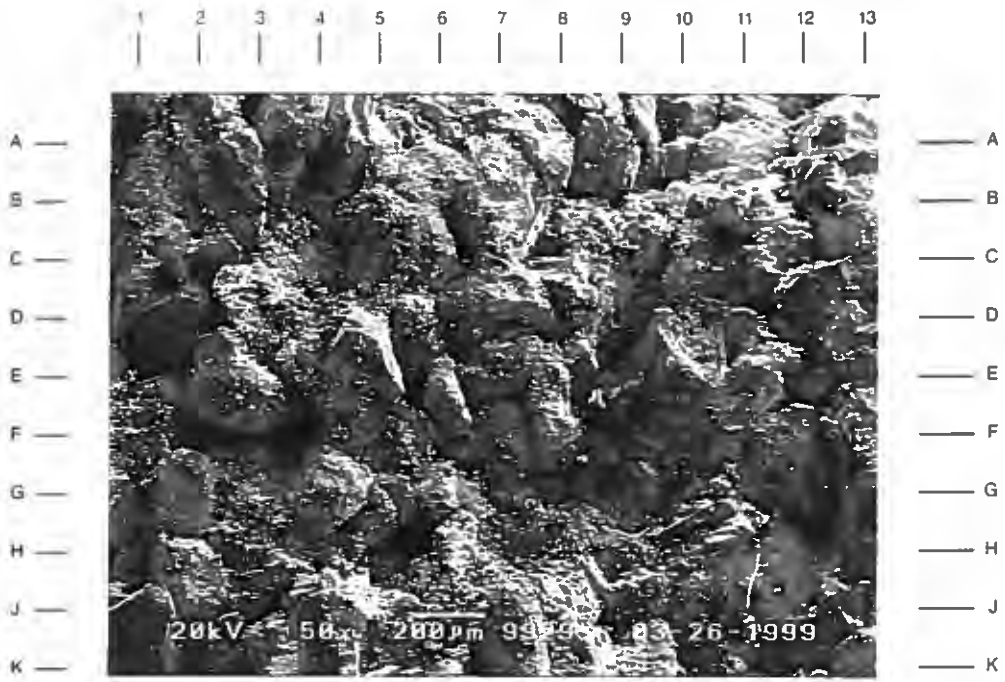
As seen in previous samples, this fine-grained sandstone has common intergranular porosity (C-D1.5,B-C10.5,E-F5.5) with lesser secondary dissolution porosity (H5.5) also present. Total effective porosity, by volume from thin section analysis, is 20%. Measured permeability of 419 md indicates that these pores are well interconnected.

Magnification: 50X

PLATE 55B

The high magnification view of the center of Plate 55A shows the moderately well sorting of framework grains found at this depth. Pores (F3,F8,D13), created by these intersecting grains, are primarily intergranular in type, and are connected by open pore throats (B-C8,F8,H9). Discontinuous coatings (A-B3.5,F10) on sand grains are likely contaminants from introduced waste material.

Magnification: 150X



**DuPont
Injection Well No. 3 S/T
Harrison County, Mississippi**

File No. GN-4474

SAMPLE DEPTH: 9929 FEET

PLATE 56A

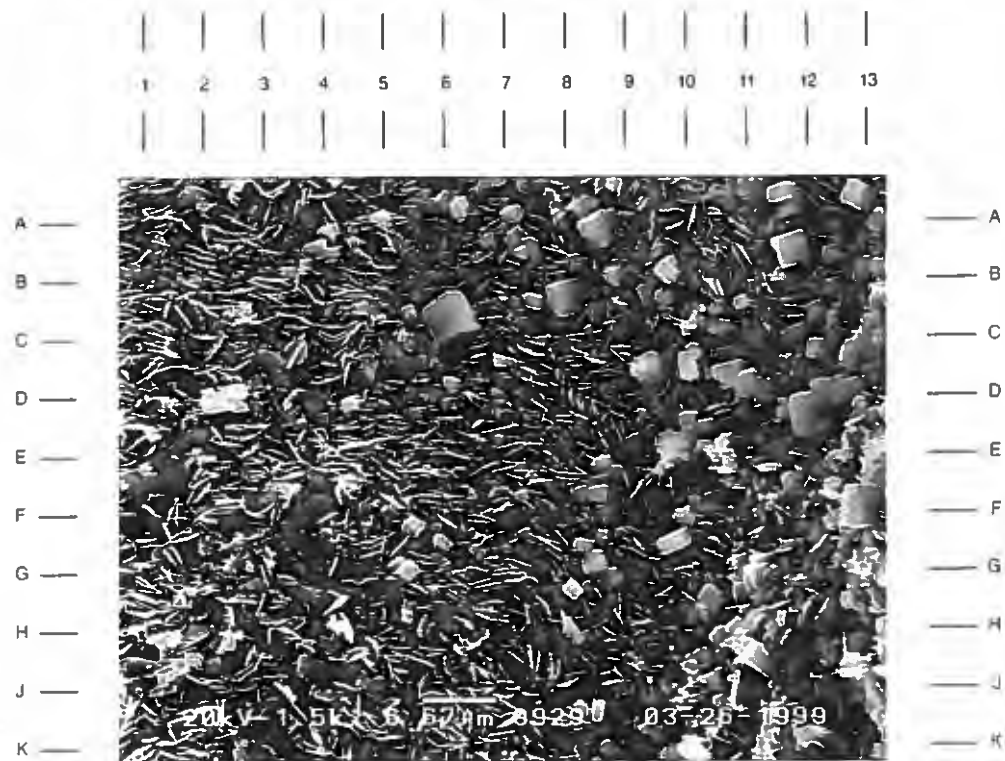
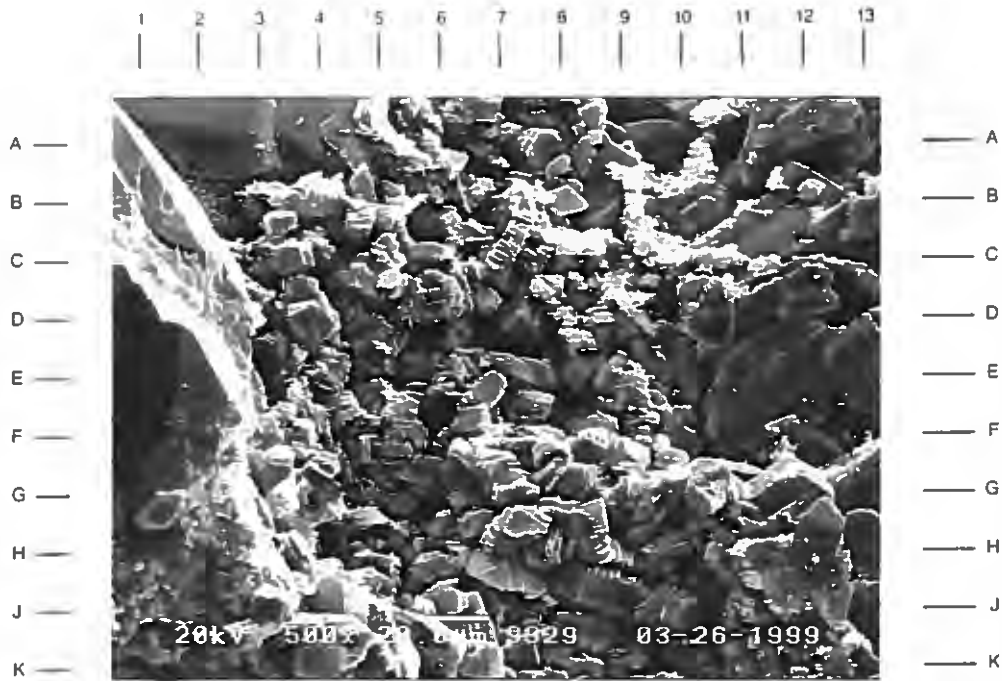
The high magnification photomicrograph on the facing page depicts an intergranular pore that has been infilled with authigenic kaolinite. These aggregates of booklets are loosely bound to the pore walls and can be prone to migration during well flow. Note the presence of quartz overgrowths (A4,E12) on adjacent grain surfaces.

Magnification: 500X

PLATE 56B

This high magnification view shows a grain surface that is locally coated with flat platelets of authigenic chlorite. Note the microporosity associated with this authigenic clay. Intermixed with this clay are small cubic crystals of either halite (from formation water precipitation) or pyrite.

Magnification: 1,500X



**DuPont
Injection Well No. 3 S/T
Harrison County, Mississippi**

File No. GN-4474

SAMPLE DEPTH: 9938 FEET

PLATE 57A

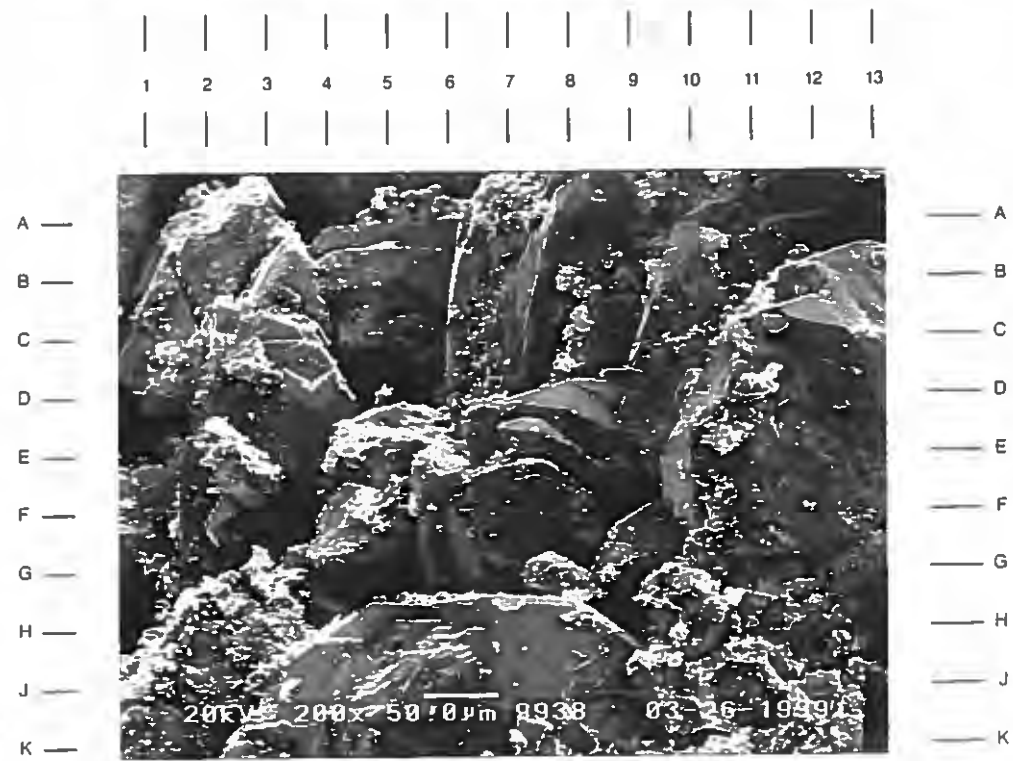
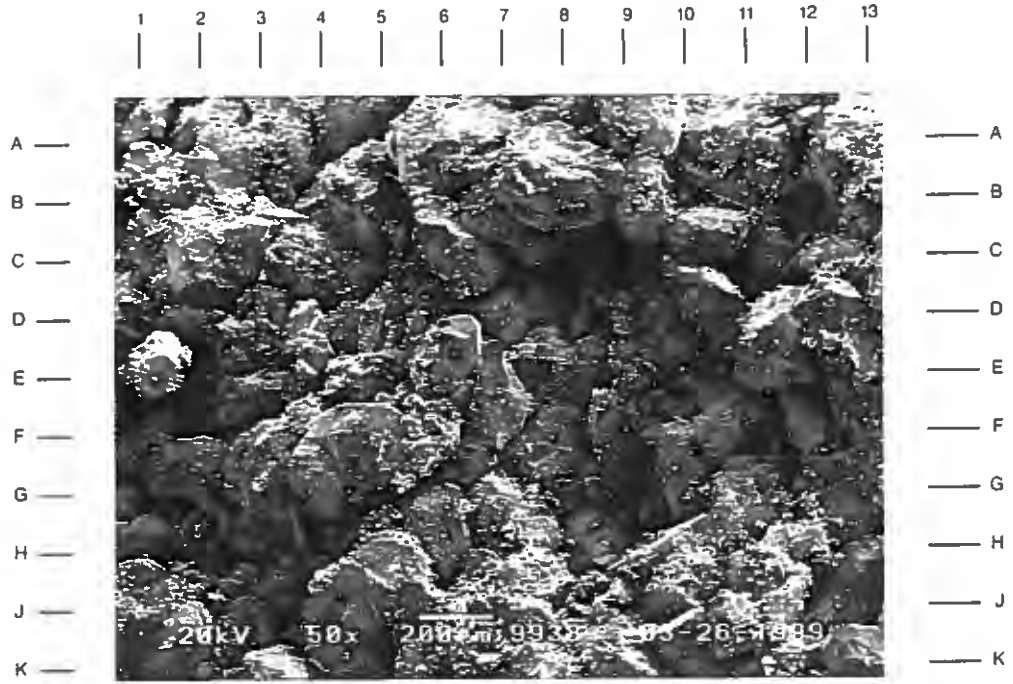
A moderately sorted, medium-grained sandstone is seen under low magnification here. Overall porosity development is good and intergranular pores (C11,F-G11.5,H4) are the dominant pore type. Quartz overgrowths (A6,F9.5,G-H3.5) are a common pore-reducing constituent.

Magnification: 50X

PLATE 57B

The high magnification view of the area near D5 in Plate 57A shows that quartz overgrowths (C12,H5,C9) are well developed and form flat to pseudo-hexagonal crystal faces on sand grain surfaces. Siderite is also common as a pore-filling cement, but is not seen in this view.

Magnification: 200X



**DuPont
Injection Well No. 3 S/T
Harrison County, Mississippi**

File No. GN-4474

SAMPLE DEPTH: 9938 FEET

PLATE 58A

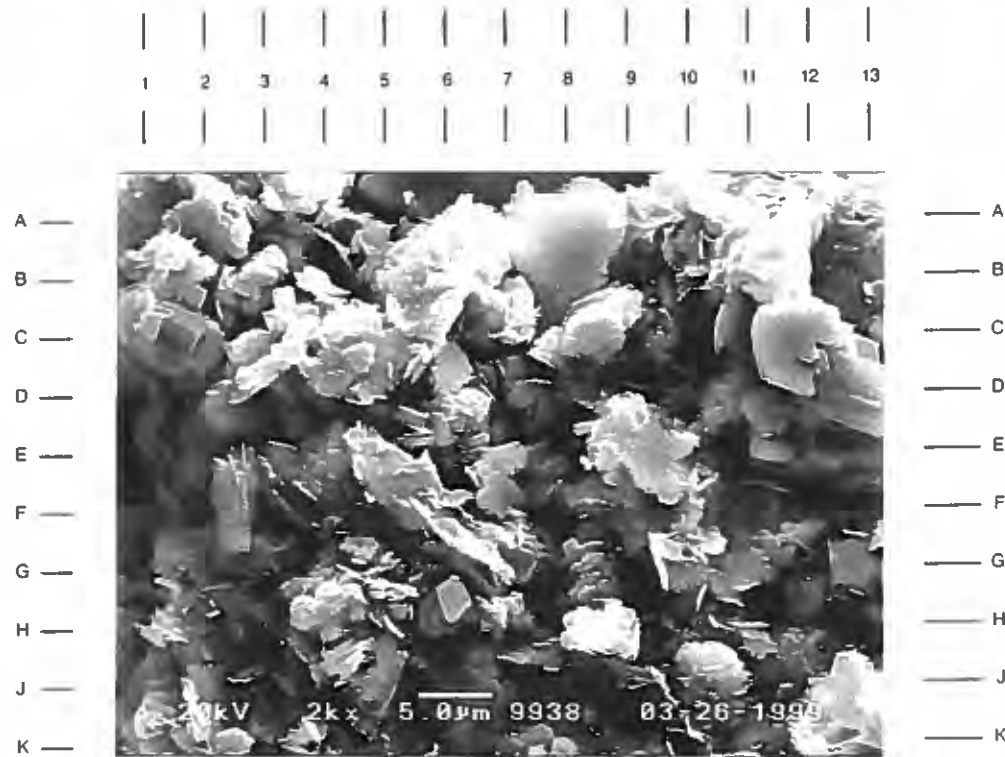
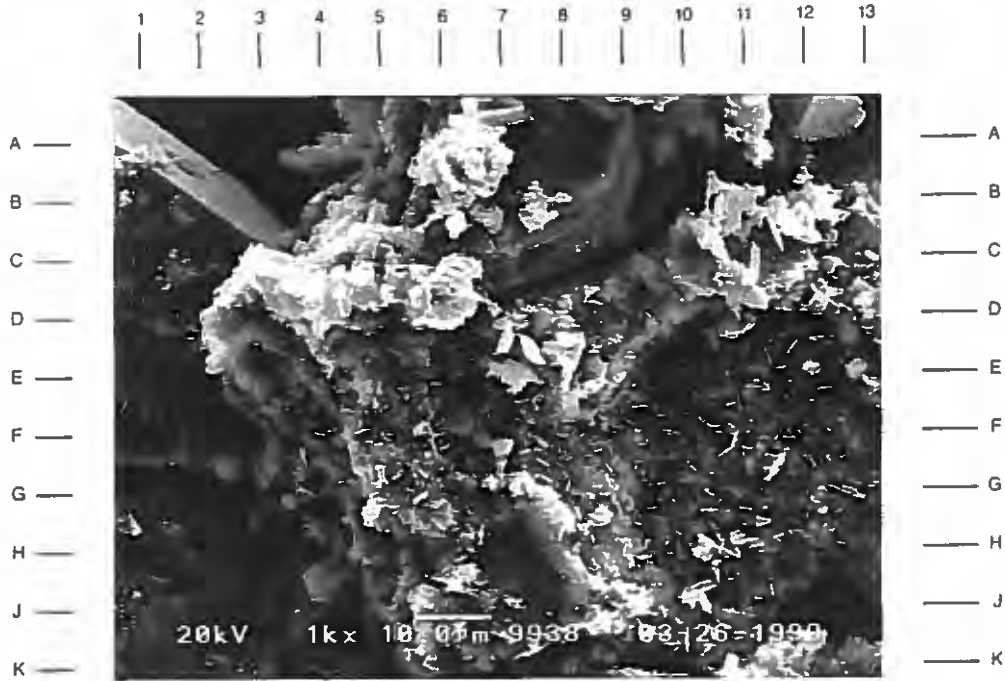
The high magnification photomicrograph shows a variety of features. Authigenic chlorite (G5,G11) is seen as a discontinuous grain coating on a sand grain surface. Pore-filling material at C-D4 is indeterminate by SEM examination, but is likely residual remnants of waste material. Quartz overgrowths (B2,B8.5) on adjacent sand grains are well developed.

Magnification: 1,000X

PLATE 58B

The high magnification view here shows another intergranular pore that has been infilled with authigenic kaolinite. Note the poor development of kaolinite aggregates. Most of this clay is seen as individual plates that exhibit poor orientation. Associated microporosity is good, but ineffective.

Magnification: 2,000X



**DuPont
Injection Well No. 3 S/T
Harrison County, Mississippi**

File No. GN-4474

SAMPLE DEPTH: 9952 FEET

PLATE 59A

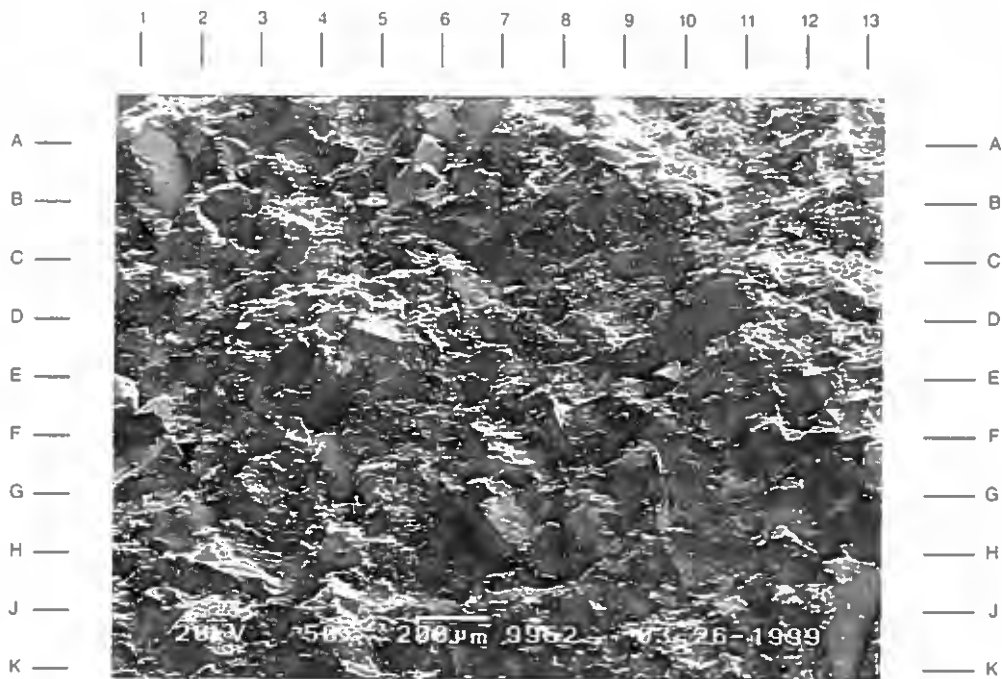
The low magnification survey photomicrograph indicates that this sandstone is distinctly different from the previous samples described. Most intergranular areas (B4,D8,F6) are completely occluded by the presence of calcite cement. Thin section analysis indicates that 32% of the sample is composed of calcite cement. Remaining visible porosity only represents 2% of the rock.

Magnification: 50X

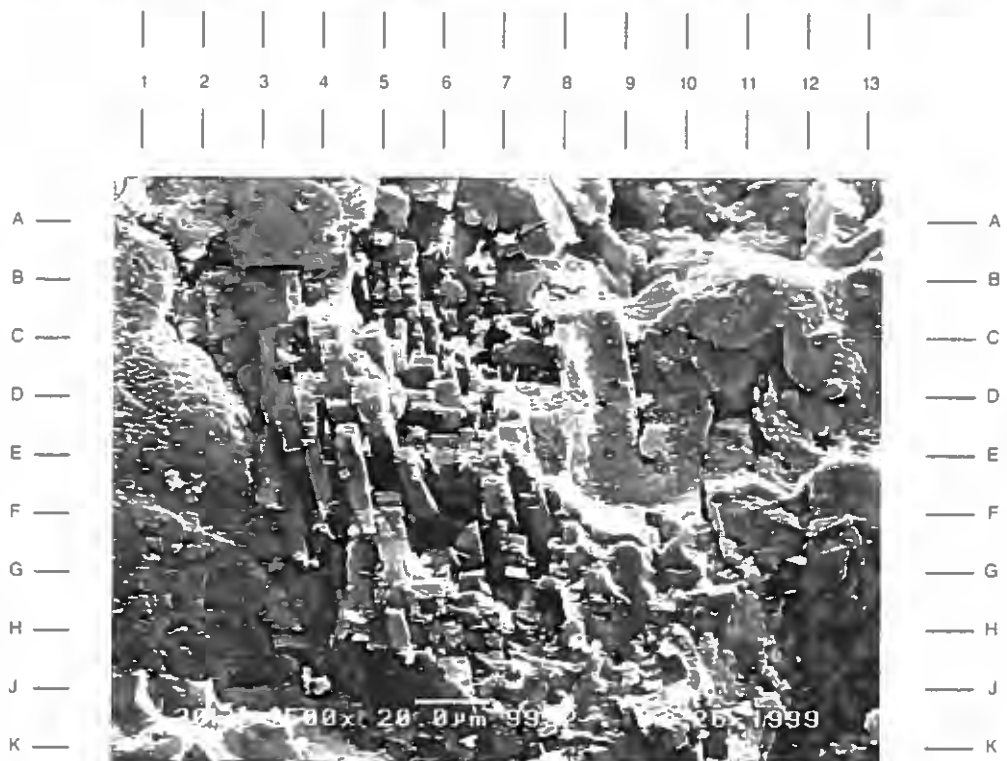
PLATE 59B

The high magnification view of the SEM subsample from 9952' shows an intergranular area that has been infilled with calcite cement. The cement is attached tightly to an adjacent sand grain (A1-J4). Partial dissolution of the cement is seen in the center of the photo, creating some intragranular porosity. Otherwise, this blocky (D9) cement is nonporous.

Magnification: 500X



A



B



**DuPont
Injection Well No. 3 S/T
Harrison County, Mississippi**

File No. GN-4474

SAMPLE DEPTH: 9952 FEET

PLATE 60A

The high magnification photomicrograph shows a typical form of calcite cement. This carbonate cement forms blocky (C4,G4) to indistinct shapes and is found infilling pores and pore throats. Small pores (E4,H5,G-H9.5) can be seen within this calcite structure; however, these pores are microscopic and ineffective.

Magnification: 2,000X

PLATE 60B

This high magnification view shows a sand grain surface that is locally coated with authigenic chlorite (E8,H10) and possible authigenic kaolinite (H-J8). The adjacent pore is nearly totally infilled with calcite cement (upper right of photo), thereby reducing its effectiveness.

Magnification: 2,000X



**DuPont
Injection Well No. 3 S/T
Harrison County, Mississippi**

File No. GN-4474

SAMPLE DEPTH: 9962 FEET

PLATE 61A

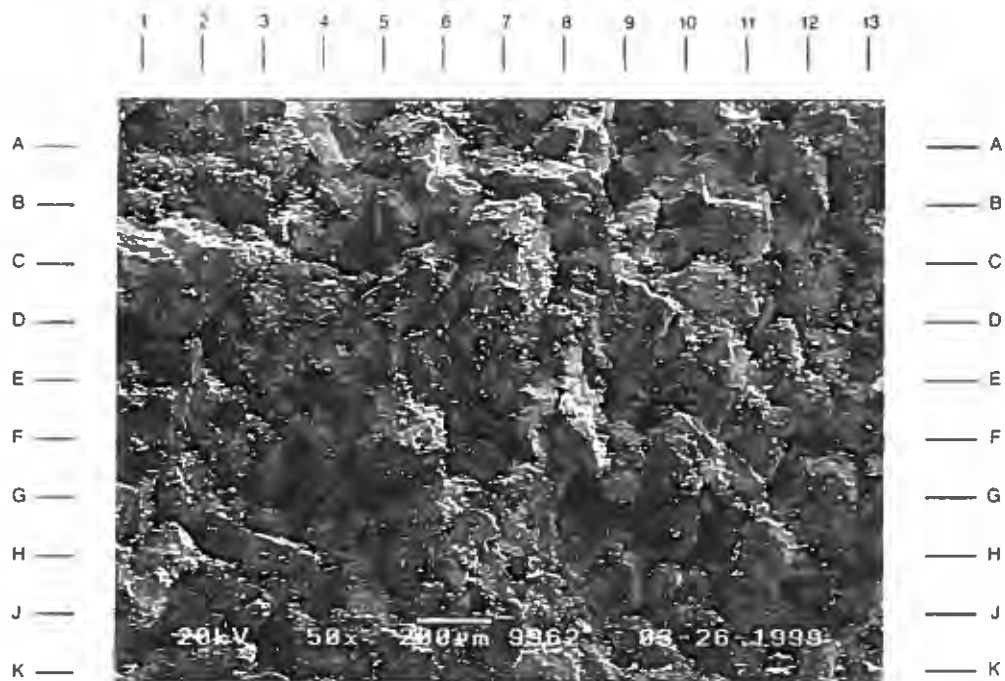
The low magnification survey photomicrograph illustrates an upper fine-grained sandstone that has reduced porosity due to cementation. Dominant cements include quartz overgrowths (B5,B10.5,H3) and siderite (C3,F5.5). These cementing agents comprise 14% and 15%, respectively, of the sample. The erratic distribution of these cements creates a tortuous flow system, and measured permeability is reduced to 39.0 md.

Magnification: 50X

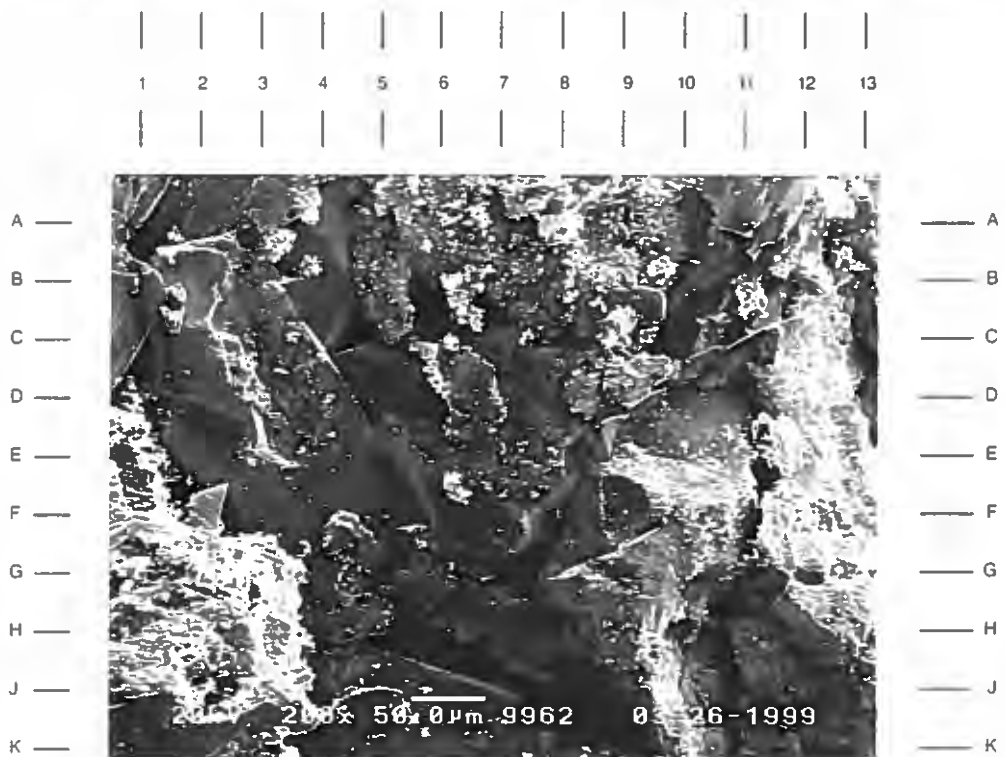
PLATE 61B

The high magnification view of the area near E7 in Plate 61A documents the pore-reducing components found in this sandstone. Quartz overgrowths (B4,C10) form flat to pseudohexagonal crystal faces that nucleate on host sand grain surfaces. Siderite (H2) is seen as a microcrystalline pore filling. These agents combine to reduce both pores and pore throats.

Magnification: 200X



A



B

**DuPont
Injection Well No. 3 S/T
Harrison County, Mississippi**

File No. GN-4474

SAMPLE DEPTH: 9962 FEET

PLATE 62A

Residual waste material that has been introduced into this zone appears to "cling" to microscopic pores, microscopic components, and irregular grain surfaces. A mixture of authigenic kaolinite and waste material is seen as a pore filling in this photomicrograph. Note the well developed quartz overgrowths on the adjacent sand grain surface (G-H12).

Magnification: 1,000X

PLATE 62B

The high magnification view of a sand grain surface indicates that authigenic chlorite (flat platelets) is intermixed with possible quartz microcrystals (H4). Small particles of remnant waste material are also noted as it becomes "trapped" in microporosity associated with the chloritic clay and quartz microcrystals.

Magnification: 3,000X



1 2 3 4 5 6 7 8 9 10 11 12 13

**DuPont
Injection Well No. 3 S/T
Harrison County, Mississippi**

File No. GN-4474

SAMPLE DEPTH: 9970 FEET

PLATE 63A

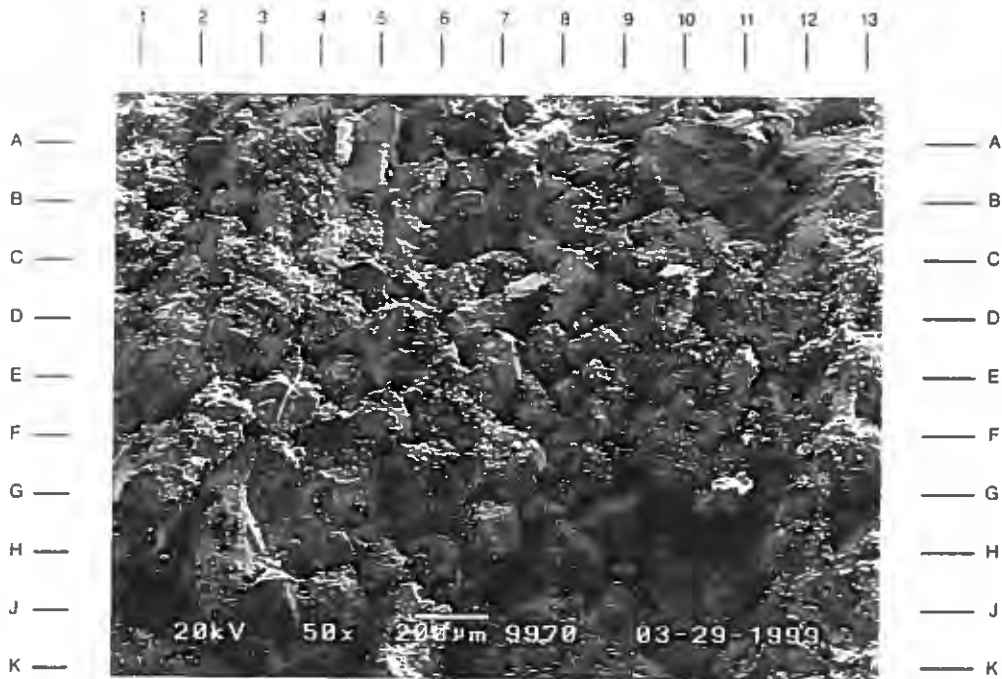
The low magnification photomicrograph on the facing page depicts a fine-grained sandstone that is similar to the previous sample described (see Plate 61A). This sandstone has reduced reservoir quality because of the presence of quartz overgrowths (A5,E7,G-H9) and siderite cement (C-D4,F6). Waste material masks much of the siderite that appears in microcrystalline form.

Magnification: 50X

PLATE 63B

The high magnification view of the area near E7 in Plate 63A shows porosity reduction by the presence of quartz overgrowths (B10,D-E9,J10) and waste material (J2,F10.5). The remnant waste shown here is likely attached to microcrystals of siderite cement that forms as a patchy pore filling. Remaining intergranular porosity (C5.5,J5) are restricted by the adjoining reduced pore throats.

Magnification: 200X



**DuPont
Injection Well No. 3 S/T
Harrison County, Mississippi**

File No. GN-4474

SAMPLE DEPTH: 9970 FEET

PLATE 64A

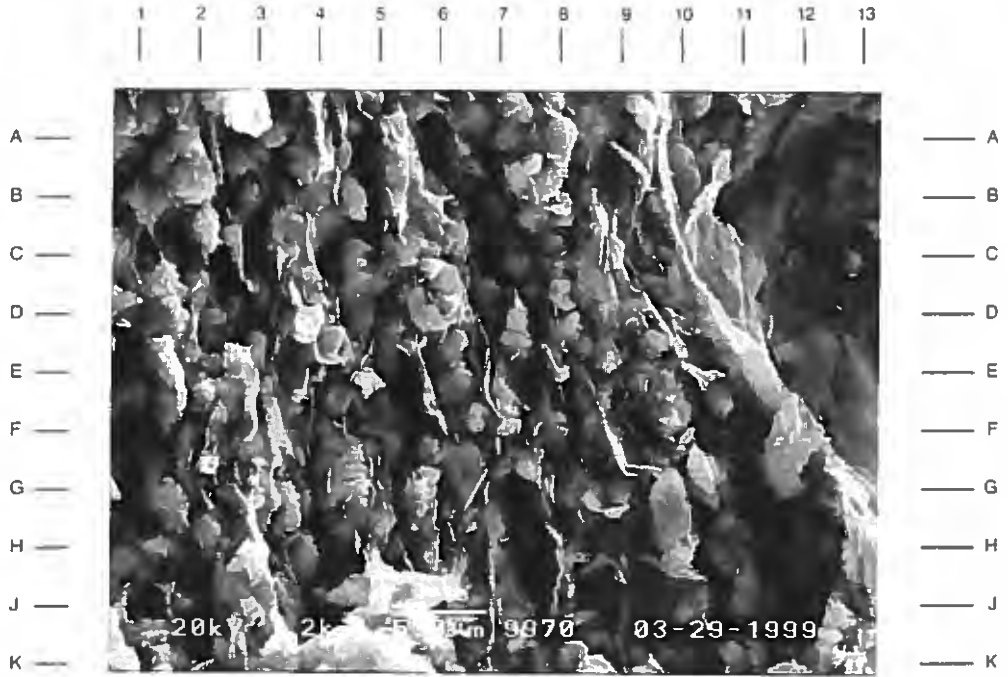
The high magnification photomicrograph taken of the SEM subsample from 9970' shows wavy, or crenulated, sheets of illitic clay on a sand grain surface. This illitic clay accounts for only 1% (by weight from XRD) of the sample. Note the stratified orientation of this clay type. Small microcrystals of possible quartz (C7,E6,H2) are also noted on this grain surface.

Magnification: 2,000X

PLATE 64B

Authigenic kaolinite appears as a pore filling in this photomicrograph. These aggregates of booklets contain fairly abundant microporosity and are prone to fines migration. Possible pore throat blockage by this loosely bound clay is a concern in many of these intervals.

Magnification: 2,000X



**DuPont
Injection Well No. 3 S/T
Harrison County, Mississippi**

File No. GN-4474

SAMPLE DEPTH: 9992 FEET

PLATE 65A

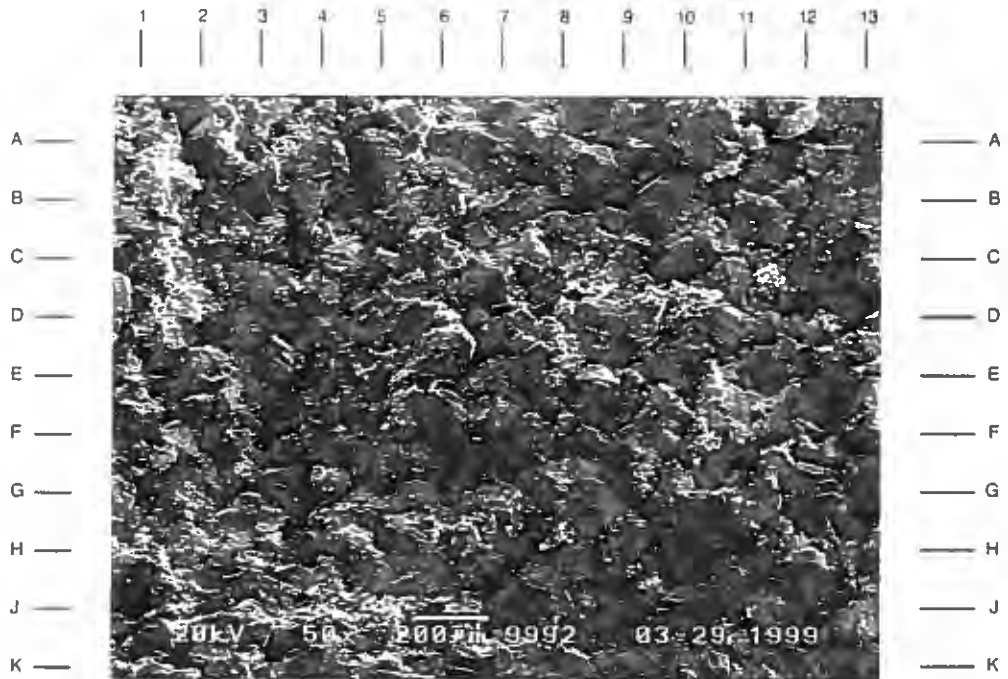
Reservoir quality is only moderate at this depth, primarily due to erratic distribution of cementation by quartz overgrowths and carbonates. Quartz overgrowths (F7,B2.5,B9) form flat to pseudo-hexagonal crystal faces that nucleate on host sand grains. The carbonate cements (A9,H-J4) calcite and dolomite are patchy pore filling components.

Magnification: 50X

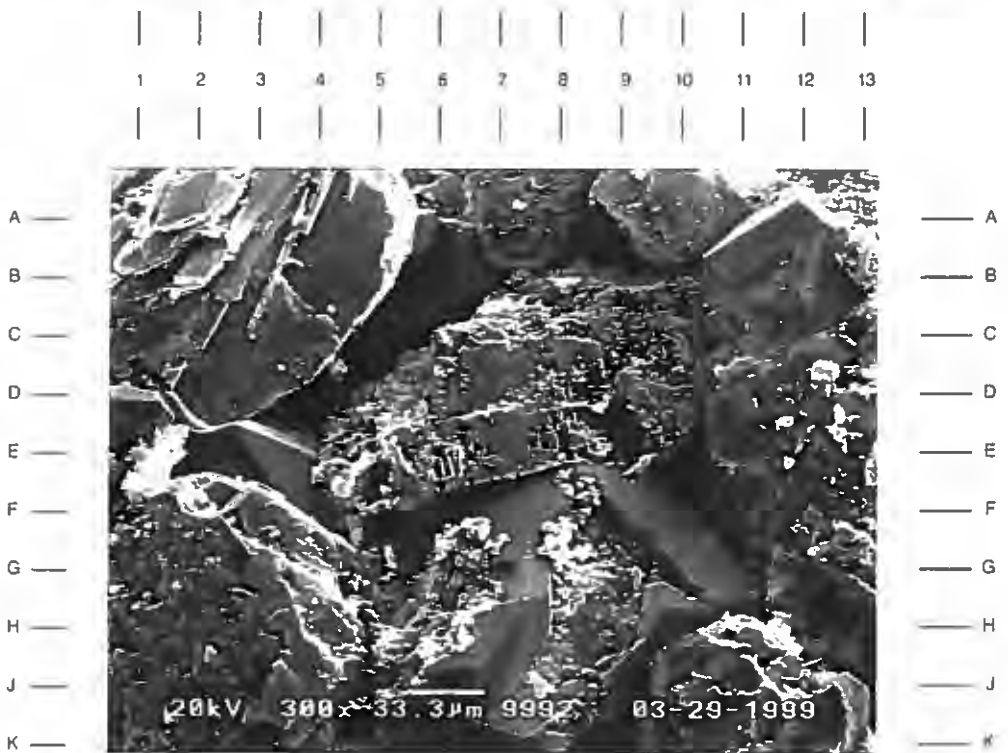
PLATE 65B

The high magnification view of the area near E7 in Plate 65A shows a potassium feldspar grain (D8) that has undergone secondary dissolution, resulting in the development of intragranular porosity. Secondary porosity (4% by volume from thin section analysis) enhances the overall pore system. Primary intergranular porosity (A-B8.5,D4,E-F10.5) accounts for 11% (by volume from thin section analysis) of the sample.

Magnification: 300X



A



B

**DuPont
Injection Well No. 3 S/T
Harrison County, Mississippi**

File No. GN-4474

SAMPLE DEPTH: 9992 FEET

PLATE 66A

The high magnification photomicrograph shown here identifies authigenic chlorite (H8,A2,E7) as a grain-coating clay on the surface of this sand grain. This clay type forms as flat platelets that are occasionally oriented face-to-edge. Microcrystals of quartz (A7.5,E-F5.5) are erratically scattered in this grain-coated area. A fine example of quartz twinning is noted at B-C4.

Magnification: 3,000X

PLATE 66B

This high magnification view shows blocky crystals of authigenic kaolinite (center of photo) that have infilled a micropore found on a grain surface. XRD data indicates that 3% (by weight) of the sample is kaolinite. This authigenic clay type is surrounded by well-developed quartz overgrowths. Quartz overgrowths account for 13% (by thin section analysis) of the sample and represent the main cementing agent in this sandstone.

Magnification: 3,000X



A



B

**DuPont
Injection Well No. 3 S/T
Harrison County, Mississippi**

File No. GN-4474

SAMPLE DEPTH: 9996 FEET

PLATE 67A

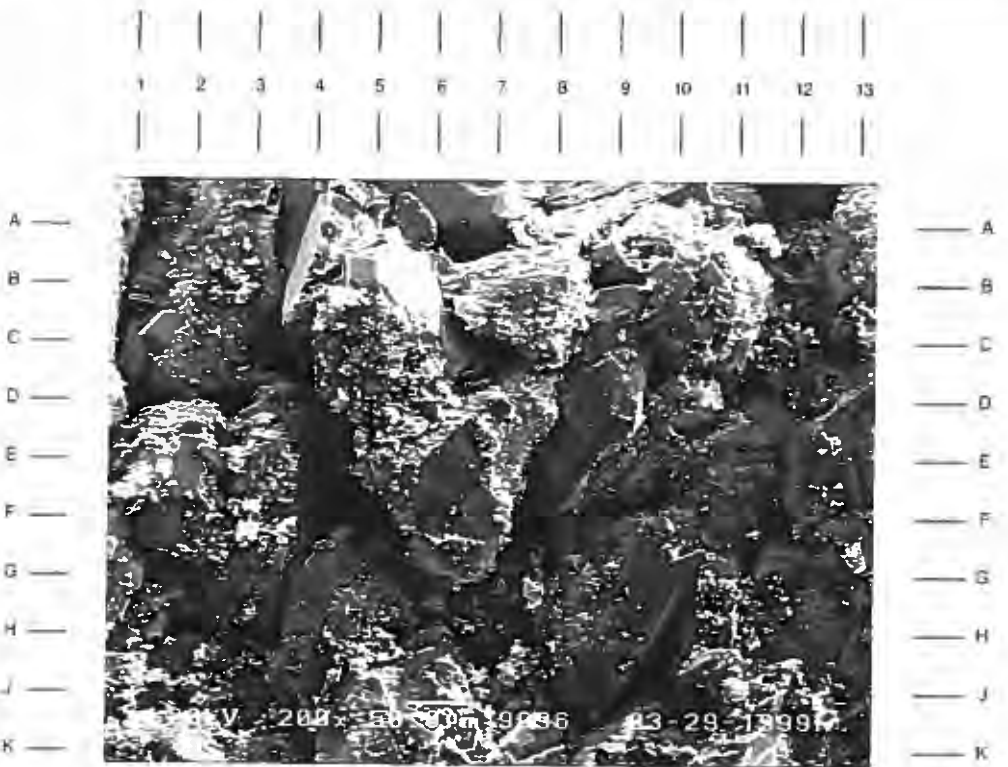
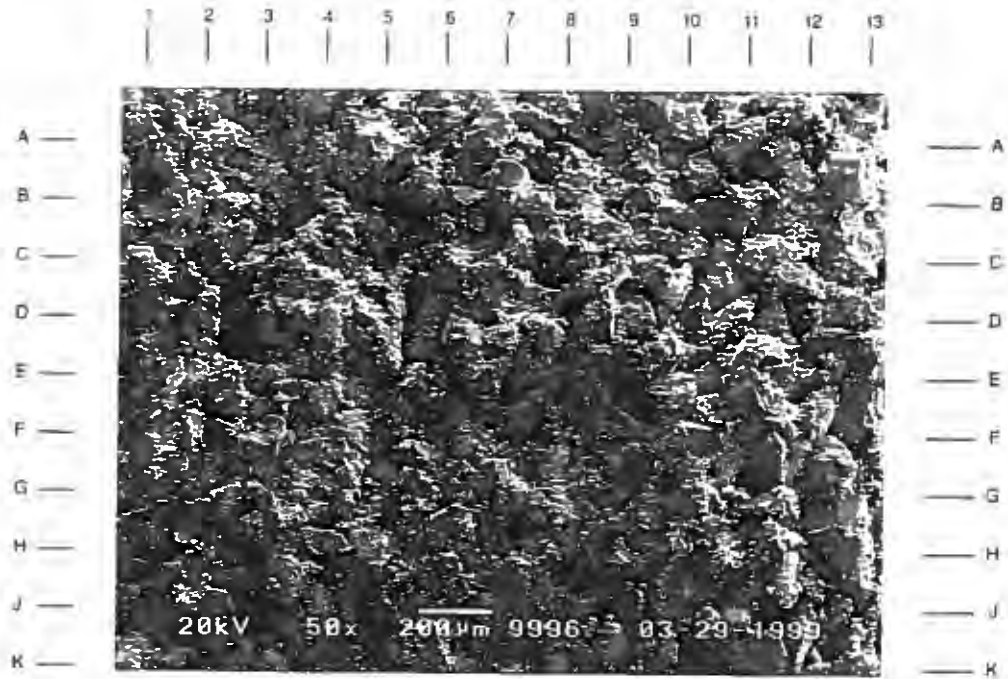
The low magnification survey photomicrograph illustrates a fine-grained sandstone that is moderately well sorted. Although visible porosity (B-C3,D-E2.5,D8) is common (19% by volume of the sample from thin section analysis) reservoir quality is only moderate. This reduction in reservoir quality is due to the reduced size of intergranular pores and pore-reducing cement.

Magnification: 50X

PLATE 67B

The high magnification view of the area near E7 in Plate 67A documents the reduced size of intergranular pores (C3,F4,E-F9.5) because of the smaller grain size (average is 0.15mm) found in this sandstone. A resulting reduction in permeability (47.0 md, by core analysis) is also noted. Remnants of probable waste material (D5.H11.5) are seen infilling some pores.

Magnification: 200X



**DuPont
Injection Well No. 3 S/T
Harrison County, Mississippi**

File No. GN-4474

SAMPLE DEPTH: 9996 FEET

PLATE 68A

A partially dissolved plagioclase feldspar grain is seen in the center of this photomicrograph. Note the resulting intragranular porosity found within this grain. Adjacent pores (C10,H10.5) are partially infilled with illitic clay.

Magnification: 700X

PLATE 68B

A high magnification view of pore-filling components is seen here. These components include authigenic kaolinite (D9,F7) and illitic clay (C2.5,H-J8). Authigenic kaolinite forms its characteristic aggregates of booklets that are loosely attached to pore walls. Illite is seen as crenulated, or wavy, sheets. Authigenic chlorite (J11.5) is also noted here as a grain coating.

Magnification: 1,500X



A



B



**DuPont
Injection Well No. 3 S/T
Harrison County, Mississippi**

File No. GN-4474

SAMPLE DEPTH: 10008 FEET

PLATE 69A

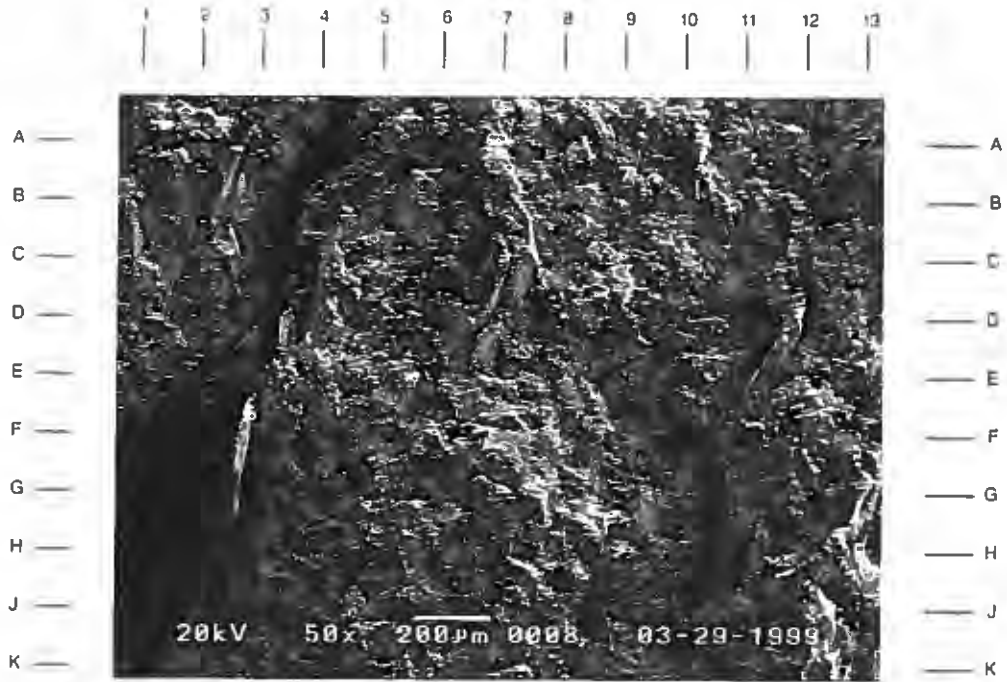
The low magnification photomicrograph on the facing page depicts a shaly sandstone that has poor reservoir quality. Detrital matrix is seen as both a pore-filling component and as clay-rich laminations. Evidence of laminar bedding is seen by the parallel orientation of numerous mica fragments (G3,D7,D11.5).

Magnification: 50X

PLATE 69B

The high magnification view of the area near E6 in Plate 69A shows that remaining intergranular porosity (D10.5,D-E6.5,J4) is poorly interconnected due to the presence of pore-filling detrital matrix (D2,D8,G5). This matrix is composed mainly of kaolinite and illite, based on XRD data.

Magnification: 200X



A



B

**DuPont
Injection Well No. 3 S/T
Harrison County, Mississippi**

File No. GN-4474

SAMPLE DEPTH: 10008 FEET

PLATE 70A

Another clay found in this sample as a pore-filling component is chlorite. This clay type forms flat platelets that occasionally exhibit a face-to-edge orientation and may be recrystallized. Note the microporosity found between platelets. Small booklets at F-G4 may be authigenic kaolinite.

Magnification: 3,000X

PLATE 70B

This high magnification view of the SEM subsample taken from 10008' shows a mixture of grain-coating components found on the surface of a sand grain. Authigenic clays chlorite (C10,E11) and kaolinite (F4) are seen intermixed with occasional quartz microcrystals (E-F6).

Magnification: 3,000X



**DuPont
Injection Well No. 3 S/T
Harrison County, Mississippi**

File No. GN-4474

SAMPLE DEPTH: 10016 FEET

PLATE 71A

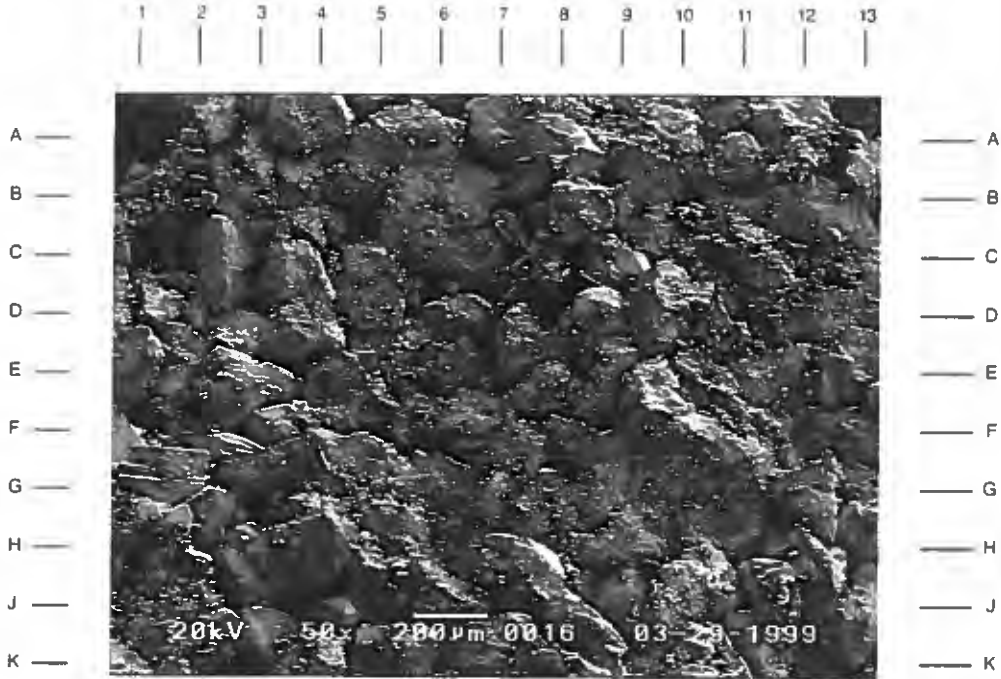
The low magnification survey photomicrograph indicates that the lower medium-grained sandstone taken from 10016' has good reservoir quality with common, evenly distributed visible porosity (B-C4.5,C-D6,J4.5). Some pores (C12.5,G-H5,H8) are partially infilled with probable waste material that reduces apparent effective porosity.

Magnification: 50X

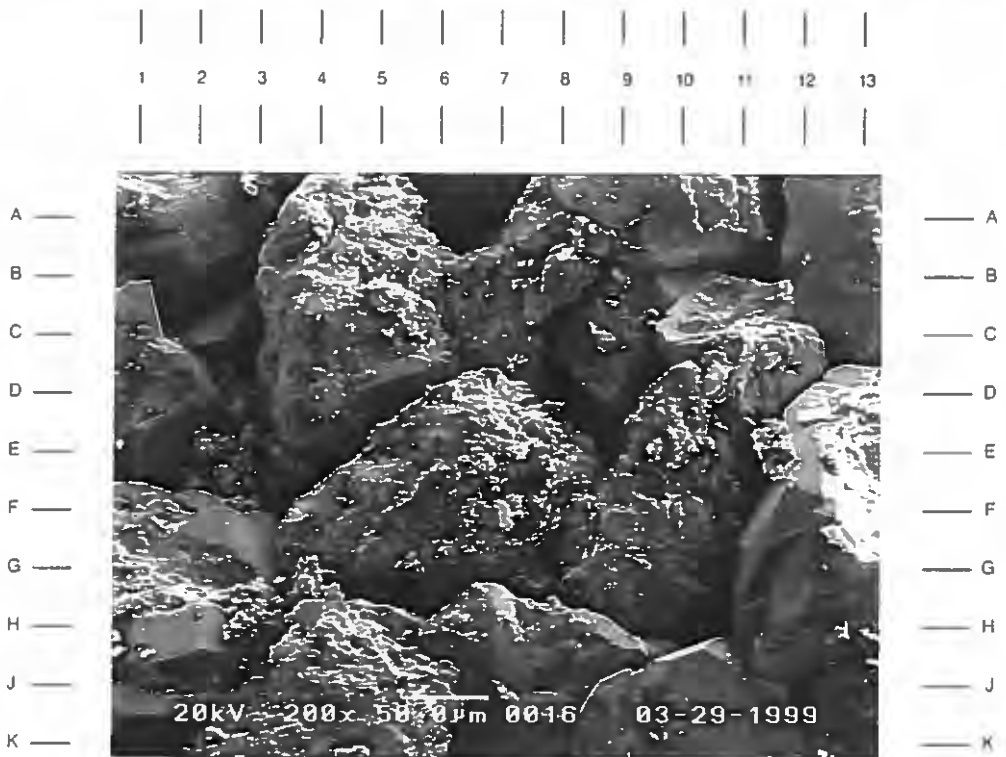
PLATE 71B

The high magnification view of the area near E7 in Plate 71A shows that primary intergranular porosity (D8,G-H6,H10.5) is common and appears well interconnected by open pore throats (B10,G11,E4.5). The grain in the center of the photo has been partially dissolved and contains intragranular porosity (E-F7). Note the presence of quartz overgrowths (C2.5,H2,H11) on host sand grains.

Magnification: 200X



A



B

**DuPont
Injection Well No. 3 S/T
Harrison County, Mississippi**

File No. GN-4474

SAMPLE DEPTH: 10016 FEET

PLATE 72A

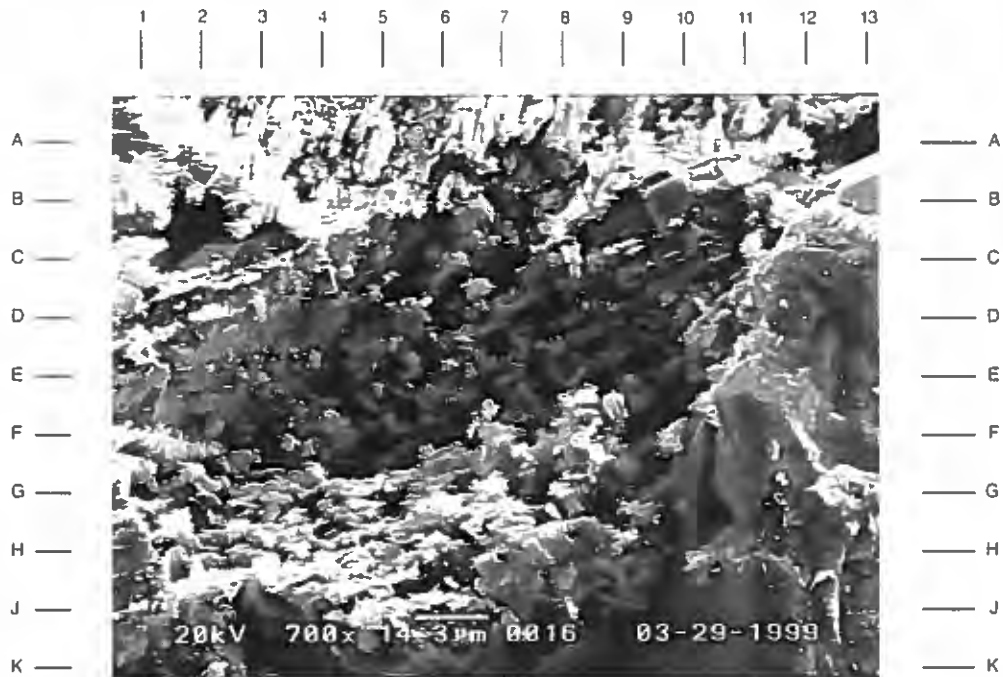
The low magnification survey photomicrograph illustrates a partially dissolved framework grain (center of photo) that contain abundant intragranular microporosity. This grain is composed of feldspar, although it is unclear whether it is potassium or plagioclase.

Magnification: 700X

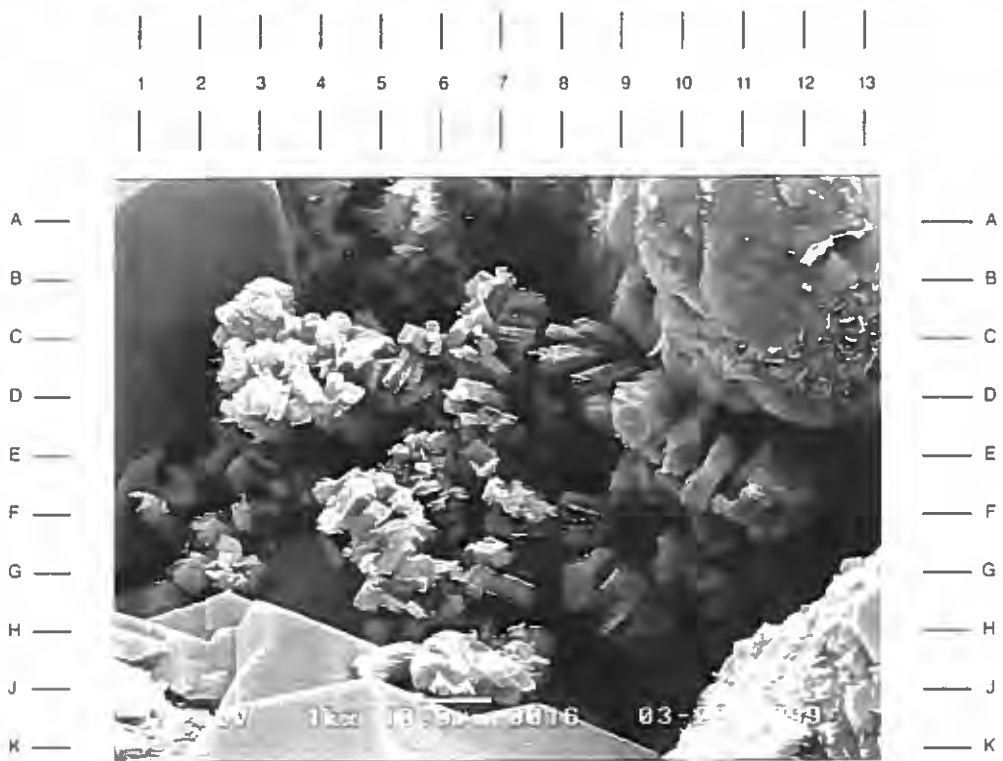
PLATE 72B

The high magnification view of the area near E3 in Plate 71B indicates that the pore-filling component found in this intergranular pore is composed of blocky crystals of authigenic kaolinite. Adjacent grains contain discontinuous grain coatings of authigenic chlorite (C13) and illite (A5.5). Quartz overgrowths (H3) are also noted.

Magnification: 1,000X



A



B

1 2 3 4 5 6 7 8 9 10 11 12 13

**DuPont
Injection Well No. 3 S/T
Harrison County, Mississippi**

File No. GN-4474

SAMPLE DEPTH: 10023 FEET

PLATE 73A

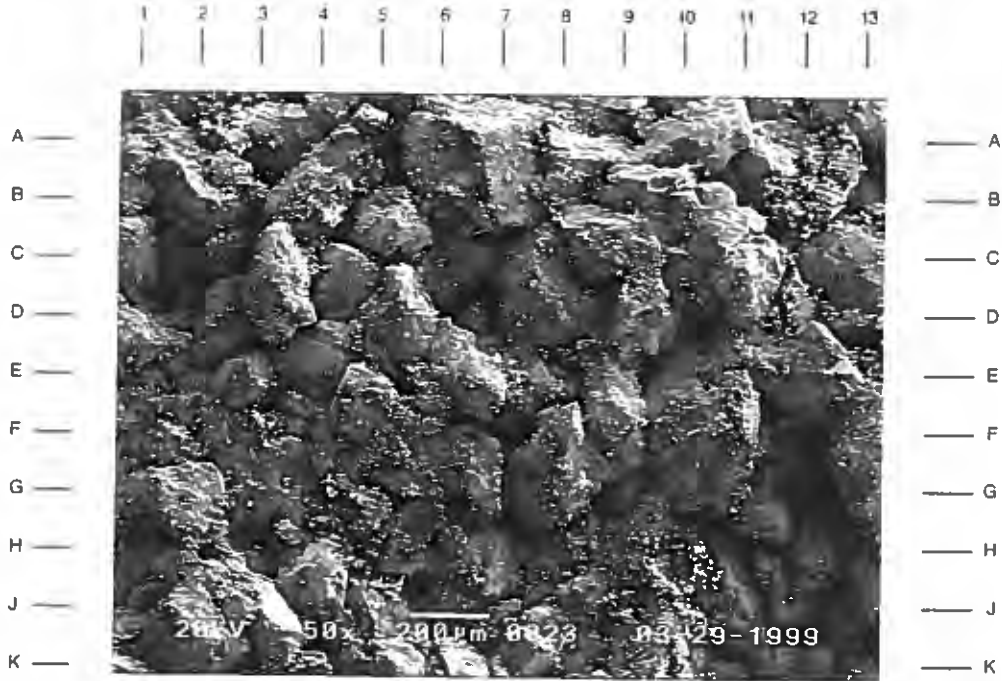
The low magnification photomicrograph on the facing page depicts a moderately well sorted, medium-grained sandstone that has good reservoir quality, similar to the previous sample described (see Plate 71A). Intergranular porosity (A-B5,D6.5,H11) is the primary pore type found and accounts for 14% (by volume from thin section analysis) of the sample. Core analysis permeability (508 md) indicates these pores are well interconnected.

Magnification: 50X

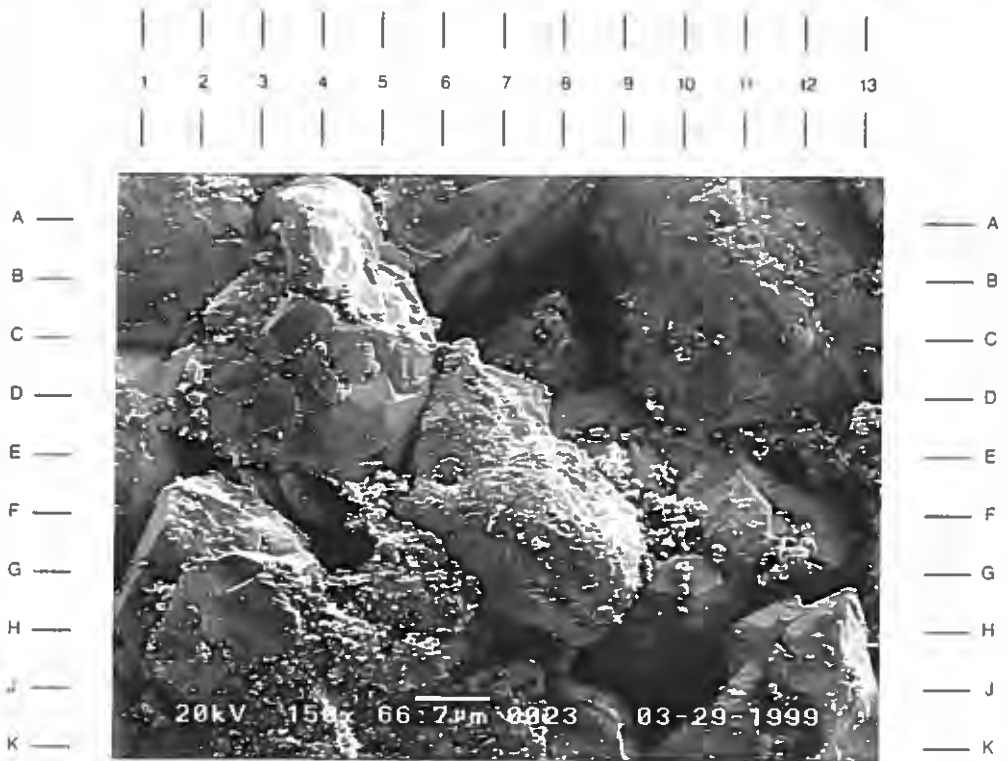
PLATE 73B

The high magnification view of the area near E7 in Plate 73A shows that several pore throats are reduced by natural quartz overgrowths (D-E5.5,H11.5) and artificial waste material components (F5,F9). Partial pore filling is seen by the probable waste material (H4,E12).

Magnification: 150X



A



B

**DuPont
Injection Well No. 3 S/T
Harrison County, Mississippi**

File No. GN-4474

SAMPLE DEPTH: 10023 FEET

PLATE 74A

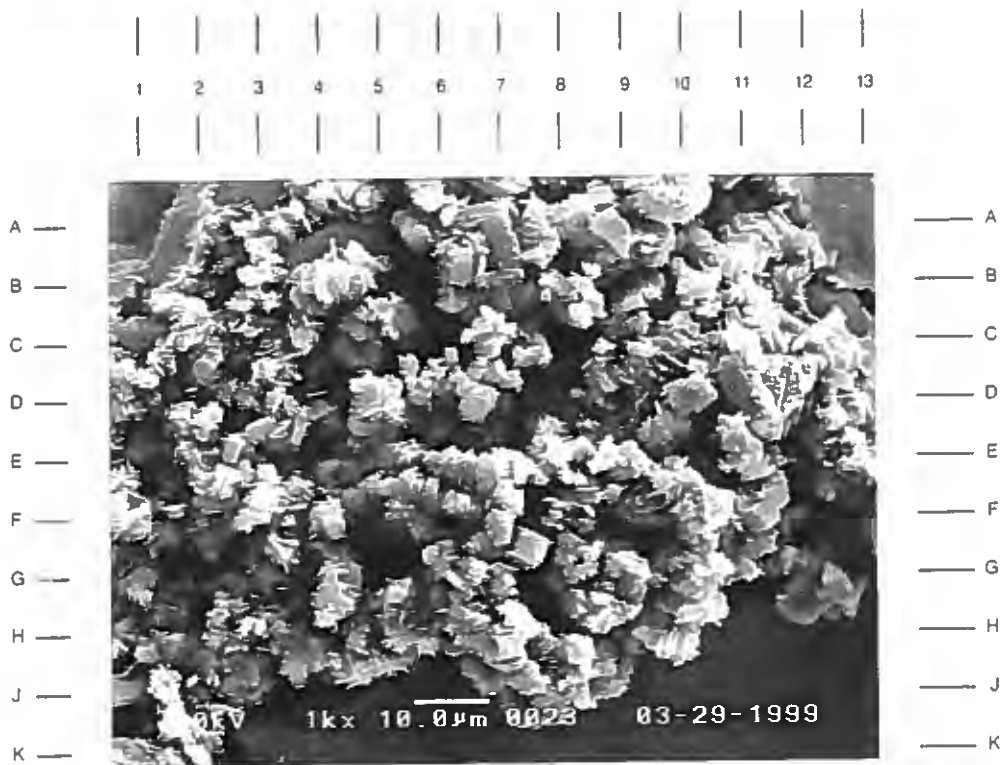
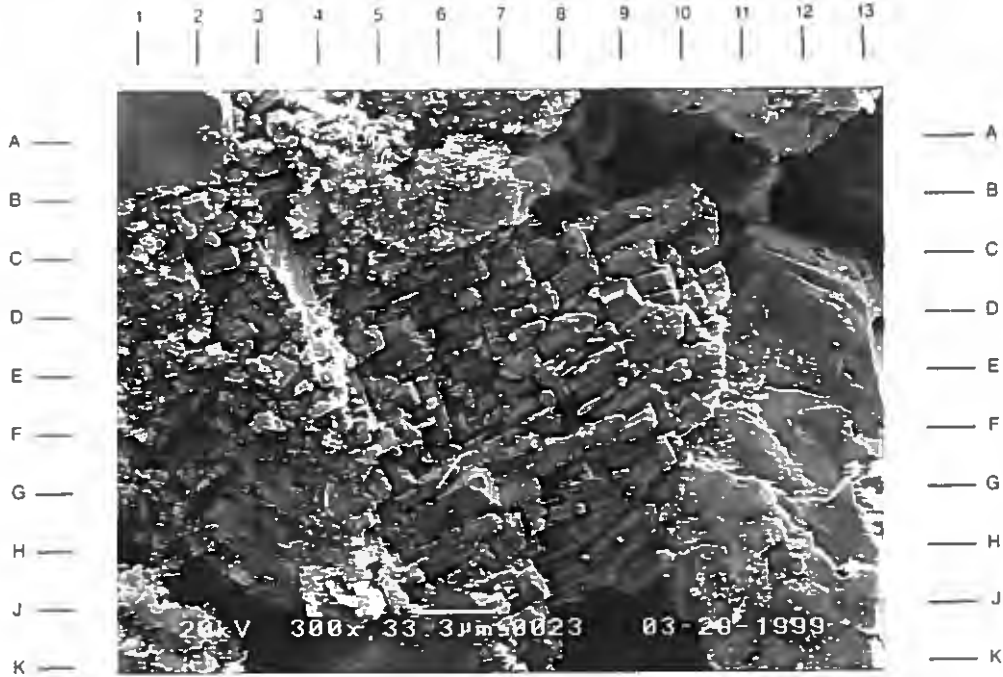
The low magnification survey photomicrograph taken of the SEM subsample from 10023' shows that secondary dissolution affects less stable sand grains, such as lithics and feldspars. The feldspar grain in the center of this photo contains some leaching from dissolution. Note that grain contacts seen here indicate a moderate degree of compaction.

Magnification: 300X

PLATE 74B

This high magnification view of a pore filling indicates that this material is composed of small aggregates of booklets of authigenic kaolinite. This authigenic clay is typically loosely bound to the pore walls and is prone to fines migration.

Magnification: 1,000X



**DuPont
Injection Well No. 3 S/T
Harrison County, Mississippi**

File No. GN-4474

SAMPLE DEPTH: 10032 FEET

PLATE 75A

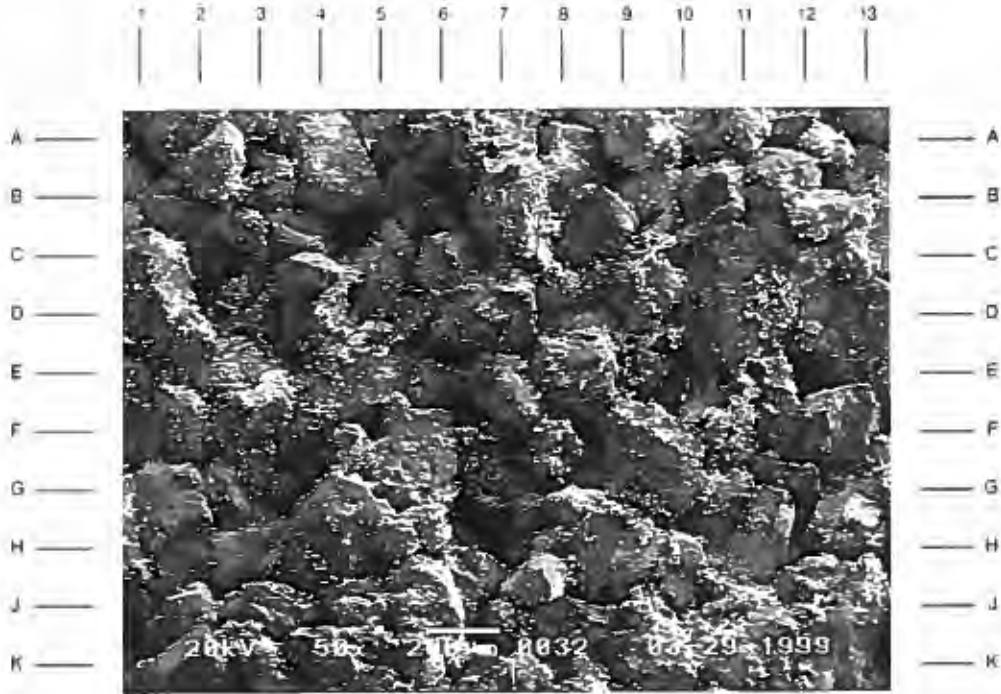
The medium-grained sandstone seen here contains a well developed effective pore system. Both primary intergranular (B-C4.5,F6,E12) and secondary dissolution (H6.5) pore varieties are evenly distributed in this massive sandstone. Traces of probable waste material (C9,F11) are found "clinging" to irregular surfaces of sand grains and pore walls.

Magnification: 50X

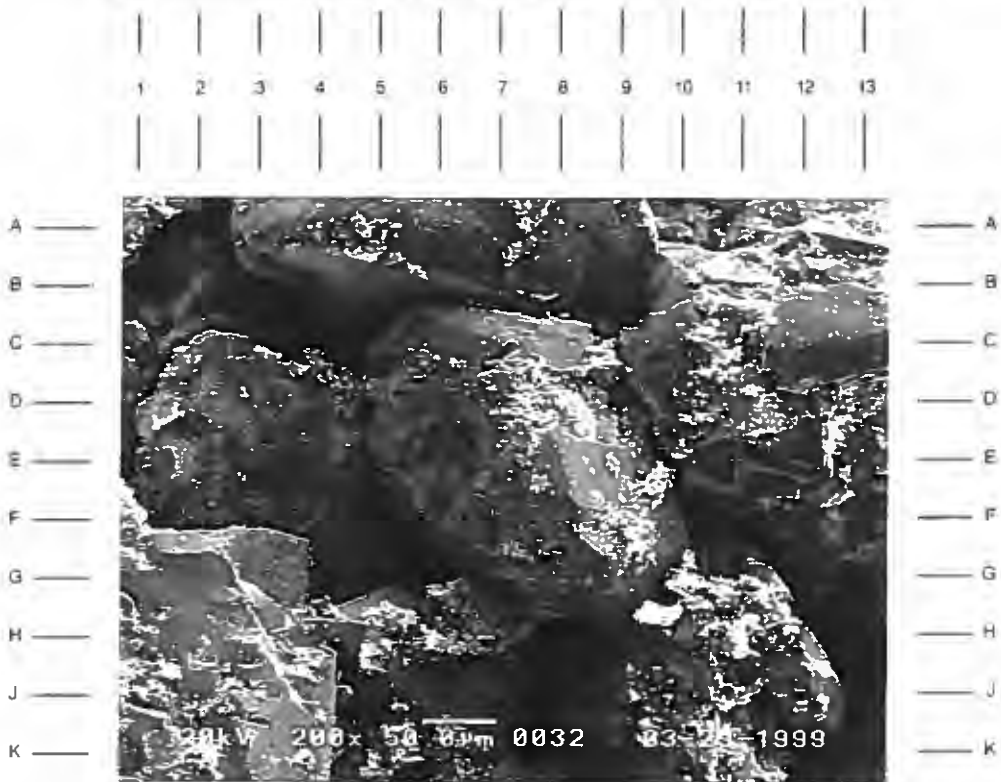
PLATE 75B

The high magnification view of the area near E7 in Plate 75A shows that intergranular porosity (C3,G5.5,H13) is well developed and well interconnected. Adjourning pore throats (B-C7,J8,E4.5) are open and fairly clean, except for residual waste material.

Magnification: 200X



A



B

**DuPont
Injection Well No. 3 S/T
Harrison County, Mississippi**

File No. GN-4474

SAMPLE DEPTH: 10032 FEET

PLATE 76A

The high magnification photomicrograph of a partially developed secondary pore is seen here. Incomplete dissolution of a probable feldspar grain is noted. Nearby authigenic kaolinite (B11) may be the result of this dissolution process. Poorly developed quartz overgrowths (D2) are seen at the edge of a grain and slightly protruding into an open pore.

Magnification: 500X

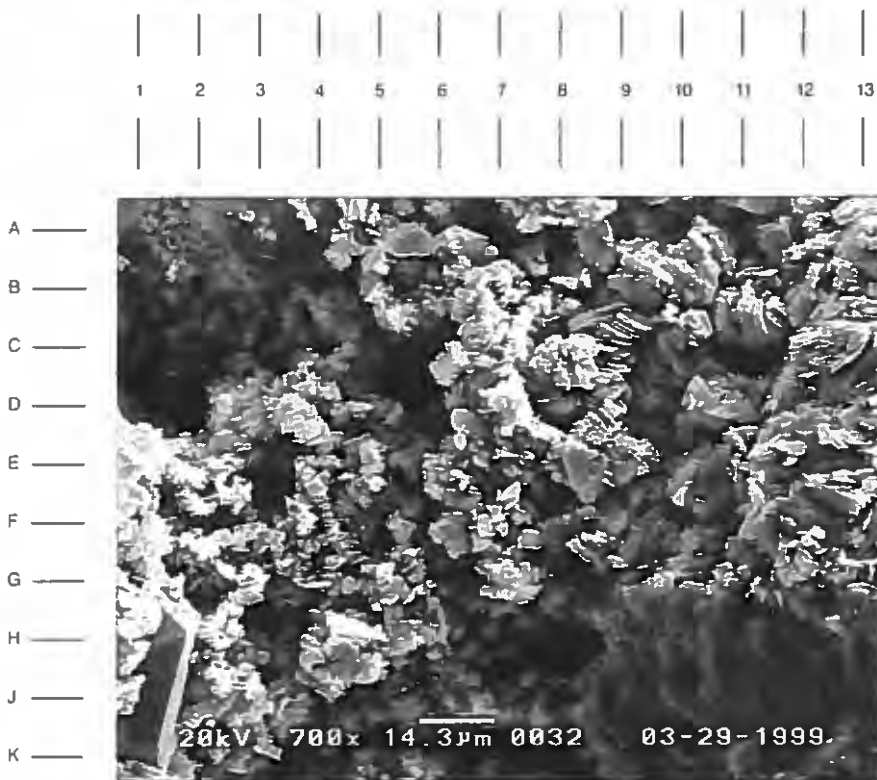
PLATE 76B

This high magnification view identifies this pore-filling material as authigenic kaolinite. Kaolinite is seen in nearly all samples in this study and is generally authigenic in origin. XRD data indicates that kaolinite accounts for 3% (by weight of the sample). Note the quartz overgrowth (J1.5) on a nearby sand grain.

Magnification: 700X



A



B

COMPILATION REPORT

for

DUPONT

Injection Well No. 3, S/T No. 1
Delisle, MS Plant
Harrison County, Mississippi

Dupont
Injection Well No. 3 S/T 1
Delisle, MS Plant
Harrison County, MS



FILE NO.: N-4474
ANALYST: Chilek / Cotton
DATE: 19-Jan-99
CORES: Schlumberger

ROTARY SIDEWALL CORE ANALYSIS

Sample Number	In. Rec.	Sample Depth feet	Permeability	Porosity Helium %	Grain Density gm/cc	Formation Description
			Horizontal Kair 400 psi md			
1	1.5	8184.0				Shale dk gy calc
2	0.4	9016.0				Shale dk gy calc
3	1.2	9212.0				Shale dk gy calc
4	1.7	9418.0	108.00	20.4	2.66	Sd lt-gy vf-fg vsilty w/scarb lams glauc
5	1.4	9432.0	2543.00	28.5	2.63	Sd lt-gy f-mg ssilty
6	0.8	9444.0	231.00	21.1	2.64	Sd lt-gy vf-fg slty
7	0.5	9455.0	**	22.8	2.62	Sd lt-gy fg slty
8	1.6	9493.0	331.00	25.3	2.64	Sd lt-gy vf-fg slty-vsilty w/scarb lams
9	0.5	9506.0	* 420.00	21.8	2.63	Sd lt-gy fg slty
10	1.4	9520.0	698.00	22.1	2.64	Sd lt-gy fg slty
11	1.3	9536.0	855.00	22.0	2.63	Sd lt-gy fg slty
12	1.1	9572.0	603.00	21.1	2.64	Sd lt-gy fg w/scarb lams
13	1.5	9588.0	* 1751.00	24.2	2.63	Sd lt-gy f-mg ssilty
14	0.5	9663.0				Shale dk gy
15	0.5	9724.0				Shale dk gy
16	0.4	9804.0				Shale dk gy
17	1.5	9822.0	0.09	9.2	2.66	Sd lt-gy vfg slty
18	0.9	9826.0	12.00	13.5	2.65	Sd lt-gy f-vfg slty w/scarb lams
19	1.6	9830.0	186.00	20.1	2.63	Sd lt-gy fg slty
20	1.1	9838.0	1087.00	20.3	2.63	Sd lt-gy-brn mg ssilty
21	1.5	9844.0	2042.00	21.6	2.62	Sd lt-gy-brn mg ssilty
22	1.7	9848.0	2502.00	22.6	2.63	Sd lt-gy-brn mg ssilty
23	1.3	9856.0	1247.00	22.1	2.63	Sd lt-gy-brn mg ssilty
24	1.7	9861.0	824.00	22.6	2.62	Sd lt-gy mg slty
25	1.7	9866.0	* 0.52	7.7	2.71	Sd lt-gy vf-mg slty w/clay clasts vcalc
26	1.3	9871.0	0.01	5.1	2.69	Sd gy vfg vsilty shy calc
27	0.3	9876.0				Shale dk gy
28	1.8	9887.0	90.00	17.0	2.67	Sd lt-gy vf-fg slty scalc
29	1.9	9899.0	509.00	19.5	2.63	Sd lt-gy f-vfg slty w/scarb lams
30	1.5	9904.0	618.00	20.3	2.63	Sd lt-gy vf-fg slty
31	1.4	9916.0	* 391.00	20.3	2.64	Sd lt-gy vf-fg slty
32	1.5	9929.0	419.00	19.7	2.63	Sd lt-gy f-vfg slty w/scarb lams
33	1.5	9938.0	400.00	20.9	2.68	Sd lt-gy f-vfg slty
34	1.2	9952.0	0.01	4.3	2.70	Sd lt-gy vf-fg vsilty vcalc
35	1.6	9962.0	39.00	17.7	2.72	Sd lt-gy vf-fg slty
36	1.6	9970.0	35.00	14.7	2.79	Sd lt-gy vfg slty

Dupont
 Injection Well No. 3 S/T 1
 Delisle, MS Plant
 Harrison County, MS



FILE NO.: N-4474
 ANALYST: Chilek / Cotton
 DATE: 19-Jan-99
 CORES: Schlumberger

ROTARY SIDEWALL CORE ANALYSIS

Sample Number	In. Rec.	Sample Depth feet	Permeability	Porosity Helium %	Grain Density gm/cc	Formation Description
			Horizontal Kair 400 psi md			

37	1.7	9992.0	18.00	14.1	2.67	Sd lt-gy vfg vsity calc
38	1.7	9996.0	47.00	17.8	2.66	Sd lt-gy sity
39	1.4	10008.0	0.14	10.4	2.69	Sd gy vfg slty w/carb lams spyr mica
40	1.1	10016.0	259.00	20.2	2.63	Sd lt-gy f-vfg slty
41	0.8	10023.0	508.00	20.4	2.63	Sd lt-gy f-vfg slty
42	1.0	10032.0	1121.00	23.4	2.62	Sd lt-gy fg slty

- * Permeability may be less accurate due to short length of plug
- ** Plug unacceptable for permeability measurements

Dupont
 Injection Well # 3, S/T # 1
 Delisle, MS Plant

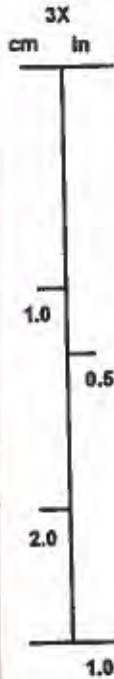
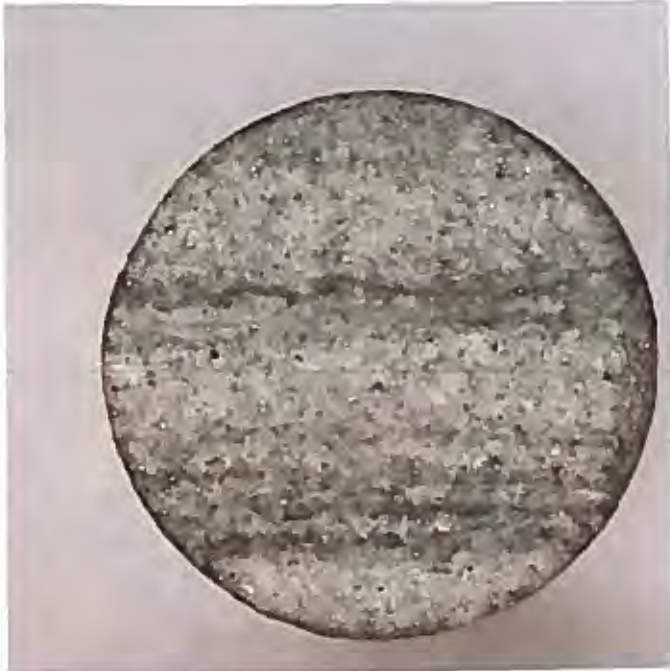


N-4474
 27-Jan-99
 Harrison Co., MS

DEPTH ft	PERM (mD)	POR (%)	OIL% (pore)	WTR% (pore)	GAS% (vol)	PROB PROD	GRAIN DENSITY	LITHOLOGY
9418.0	108.0	20.4					2.66	Sd lt-gy vf-fg vsity w/scarb lams glauc

Visible Light

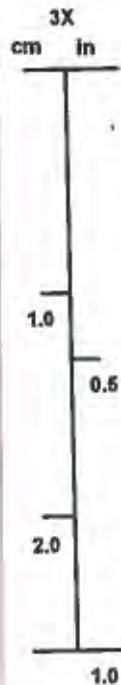
Ultraviolet Light



DEPTH ft	PERM (mD)	POR (%)	OIL% (pore)	WTR% (pore)	GAS% (vol)	PROB PROD	GRAIN DENSITY	LITHOLOGY
9432.0	2543.0	28.5					2.63	Sd lt-gy f-mg ssily

Visible Light

Ultraviolet Light



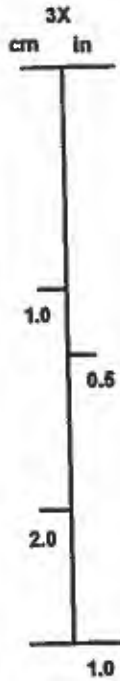
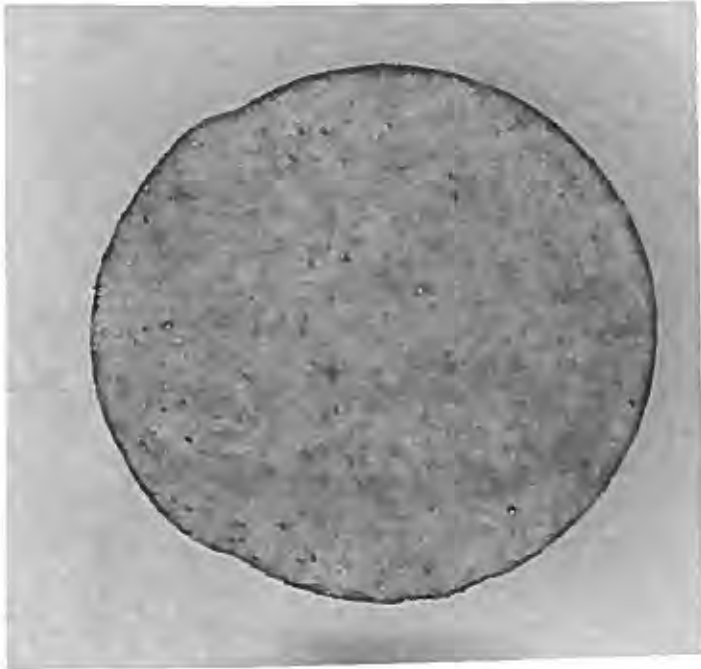
Dupont
 Injection Well # 3, S/T # 1
 Delisle, MS Plant



N-4474
 27-Jan-99
 Harrison Co., MS

DEPTH ft	PERM (mD)	POR (%)	OIL% (pore)	WTR% (pore)	GAS% (vol)	PROB PROD	GRAIN DENSITY	LITHOLOGY
9444.0	231.0	21.1					2.64	Sd lt-gy vf-fg slty

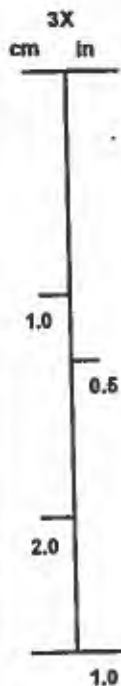
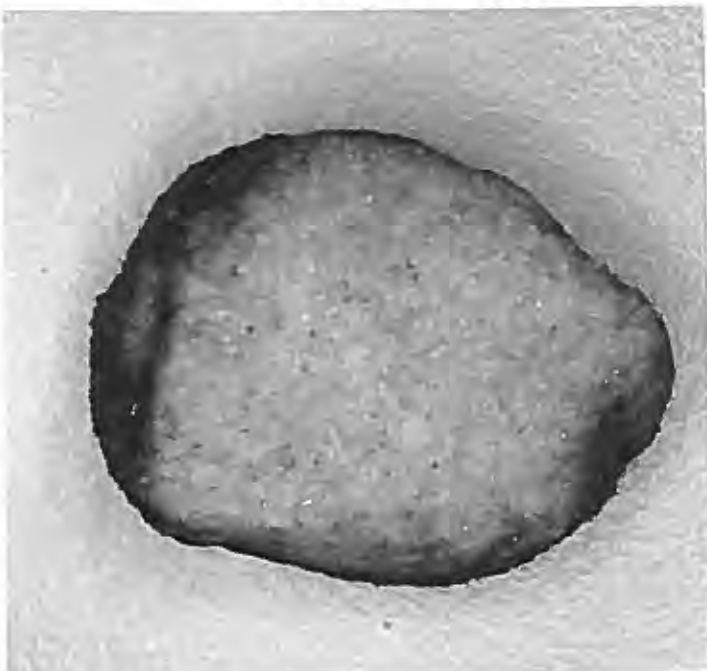
Visible Light



Ultraviolet Light

DEPTH ft	PERM (mD)	POR (%)	OIL% (pore)	WTR% (pore)	GAS% (vol)	PROB PROD	GRAIN DENSITY	LITHOLOGY
9455.0	**	22.8					2.62	Sd lt-gy fg slty

Visible Light



Ultraviolet Light

Dupont
 Injection Well # 3, S/T # 1
 Delisle, MS Plant



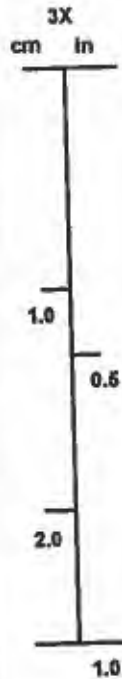
N-4474
 27-Jan-99
 Harrison Co., MS

DEPTH ft	PERM (mD)	POR (%)	OIL% (pore)	WTR% (pore)	GAS% (vol)	PROB PROD	GRAIN DENSITY	LITHOLOGY
9493.0	331.0	25.3					2.64	Sd lt-gy vf-fg slty-vsity w/scarb lams

Visible Light

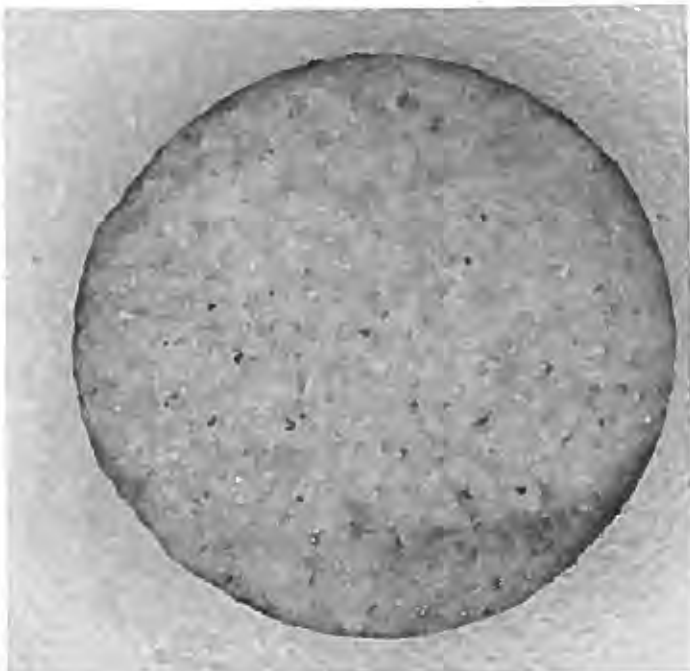


Ultraviolet Light

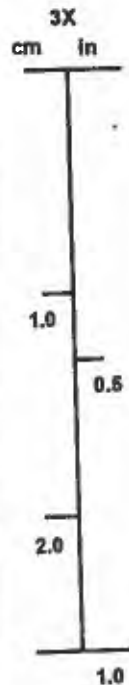


DEPTH ft	PERM (mD)	POR (%)	OIL% (pore)	WTR% (pore)	GAS% (vol)	PROB PROD	GRAIN DENSITY	LITHOLOGY
9506.0	420.0	21.8					2.63	Sd lt-gy fg slty

Visible Light



Ultraviolet Light



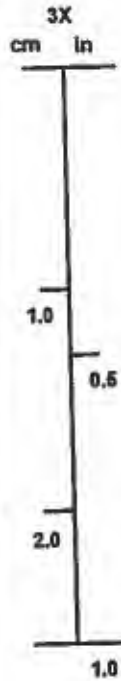
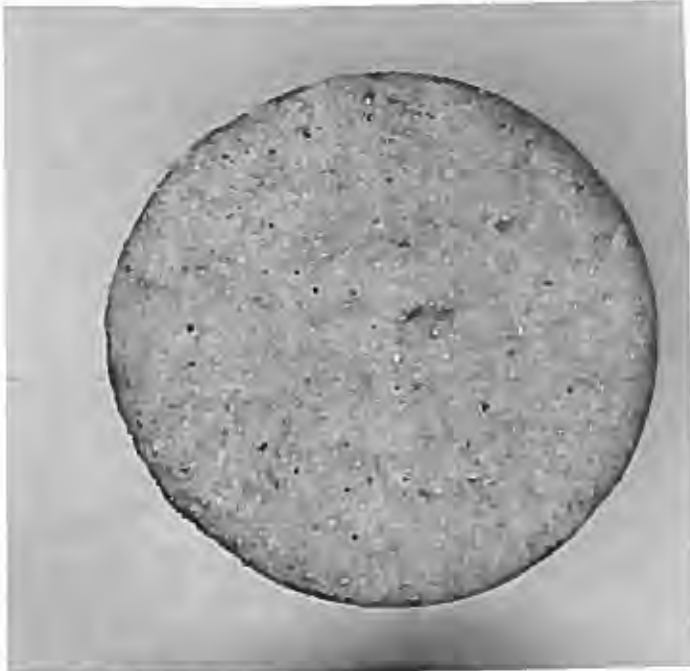
Dupont
 Injection Well # 3, S/T # 1
 Delisle, MS Plant



N-4474
 27-Jan-99
 Harrison Co., MS

DEPTH ft	PERM (mD)	POR (%)	OIL% (pore)	WTR% (pore)	GAS% (vol)	PROB PROD	GRAIN DENSITY	LITHOLOGY
9520.0	698.0	22.1					2.64	Sd lt-gy fg slty

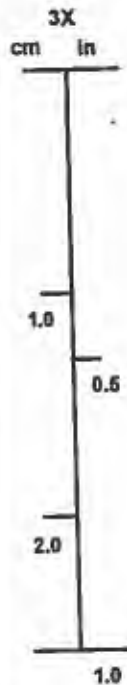
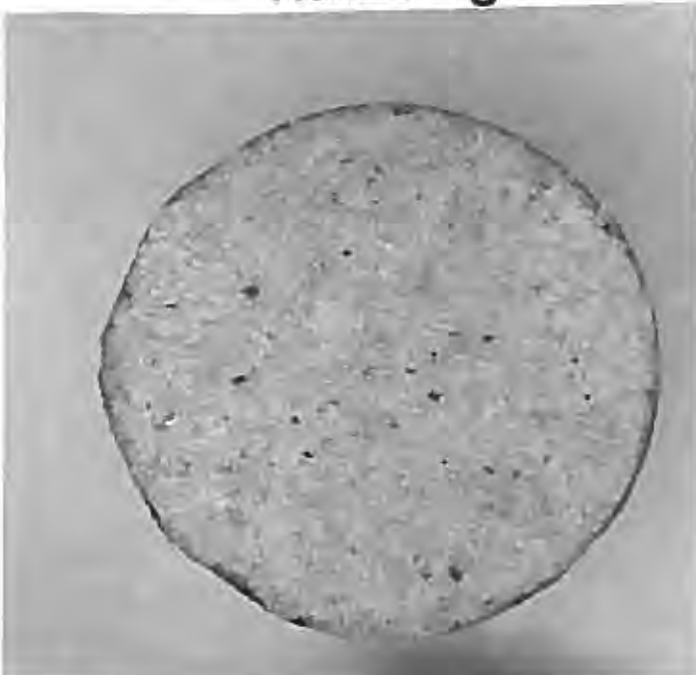
Visible Light



Ultraviolet Light

DEPTH ft	PERM (mD)	POR (%)	OIL% (pore)	WTR% (pore)	GAS% (vol)	PROB PROD	GRAIN DENSITY	LITHOLOGY
9536.0	855.0	22.0					2.63	Sd lt-gy fg slty

Visible Light



Ultraviolet Light

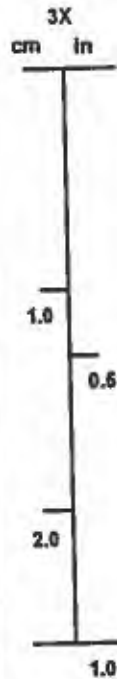
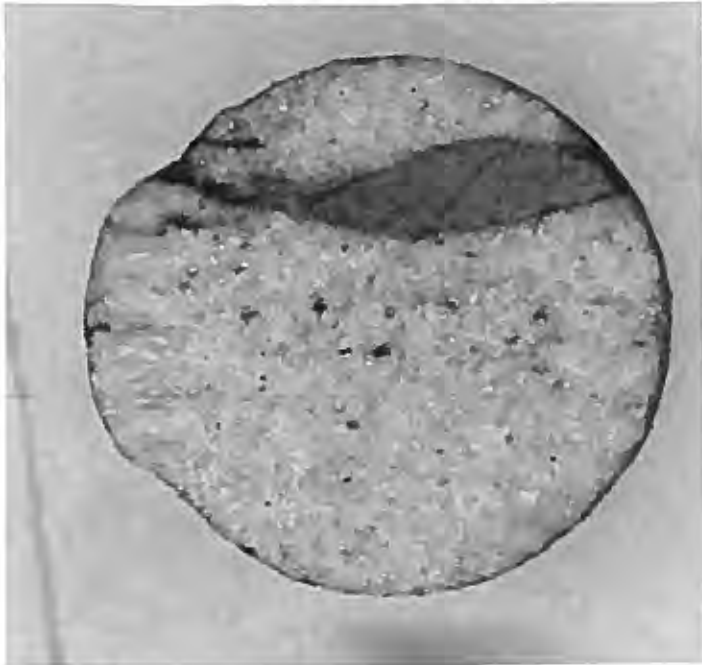
Dupont
 Injection Well # 3, S/T # 1
 Delisle, MS Plant



N-4474
 27-Jan-99
 Harrison Co., MS

DEPTH ft	PERM (mD)	POR (%)	OIL% (pore)	WTR% (pore)	GAS% (vol)	PROB PROD	GRAIN DENSITY	LITHOLOGY
9572.0	603.0	21.1					2.64	Sd lt-gy fg w/scarb lams

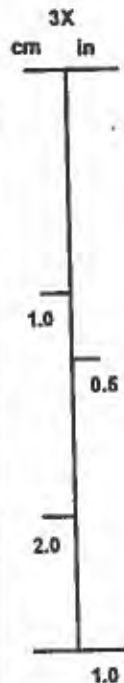
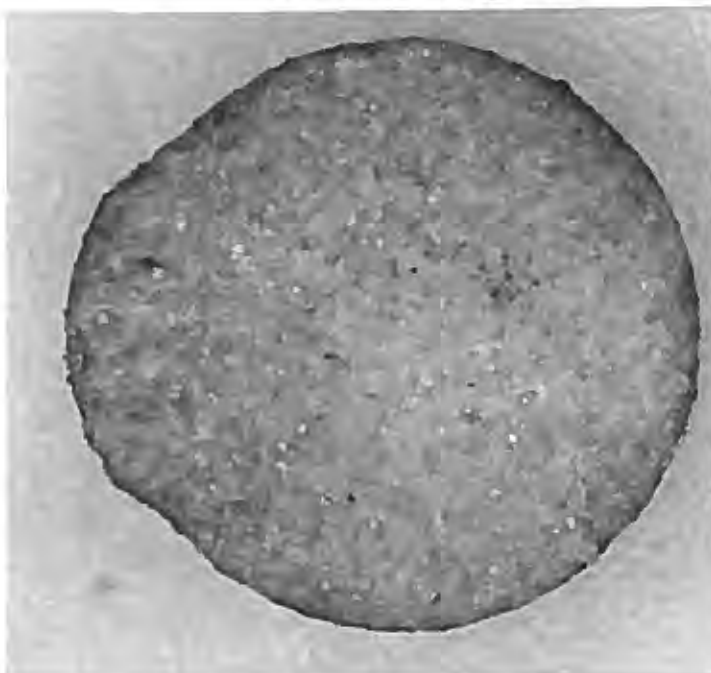
Visible Light



Ultraviolet Light

DEPTH ft	PERM (mD)	POR (%)	OIL% (pore)	WTR% (pore)	GAS% (vol)	PROB PROD	GRAIN DENSITY	LITHOLOGY
9588.0	1751.0	24.2					2.63	Sd lt-gy f-mg ssily

Visible Light



Ultraviolet Light

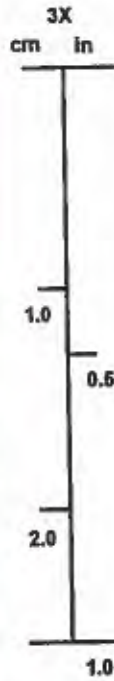
Dupont
 Injection Well # 3, S/T # 1
 Delisle, MS Plant



N-4474
 27-Jan-99
 Harrison Co., MS

DEPTH ft	PERM (mD)	POR (%)	OIL% (pore)	WTR% (pore)	GAS% (vol)	PROB PROD	GRAIN DENSITY	LITHOLOGY
9822.0	0.09	9.2					2.66	Sd lt-gy vfg slty

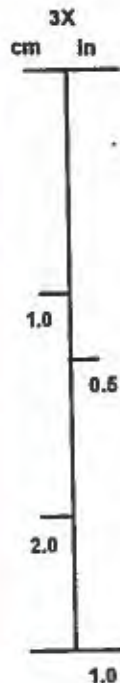
Visible Light



Ultraviolet Light

DEPTH ft	PERM (mD)	POR (%)	OIL% (pore)	WTR% (pore)	GAS% (vol)	PROB PROD	GRAIN DENSITY	LITHOLOGY
9826.0	11.9	13.5					2.65	Sd lt-gy f-vfg slty w/scarb lams

Visible Light



Ultraviolet Light

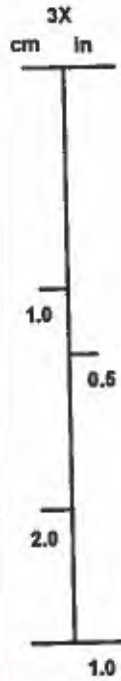
Dupont
 Injection Well # 3, S/T # 1
 Delisle, MS Plant



N-4474
 27-Jan-99
 Harrison Co., MS

DEPTH ft	PERM (mD)	POR (%)	OIL% (pore)	WTR% (pore)	GAS% (vol)	PROB PROD	GRAIN DENSITY	LITHOLOGY
9830.0	186.0	20.1					2.63	Sd lt-gy fg slty

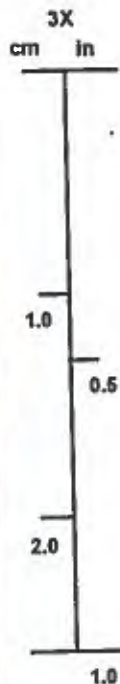
Visible Light



Ultraviolet Light

DEPTH ft	PERM (mD)	POR (%)	OIL% (pore)	WTR% (pore)	GAS% (vol)	PROB PROD	GRAIN DENSITY	LITHOLOGY
9838.0	1087.0	20.3					2.63	Sd lt-gy-brn mg ssly

Visible Light



Ultraviolet Light

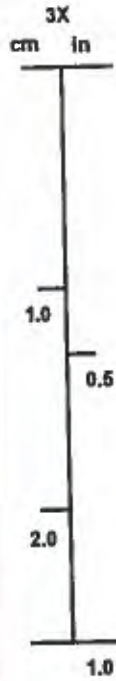
Dupont
 Injection Well # 3, S/T # 1
 Delisle, MS Plant



N-4474
 27-Jan-99
 Harrison Co., MS

DEPTH ft	PERM (mD)	POR (%)	OIL% (pore)	WTR% (pore)	GAS% (vol)	PROB PROD	GRAIN DENSITY	LITHOLOGY
9844.0	2042.0	21.6					2.62	Sd lt-gy-brn mg ssly

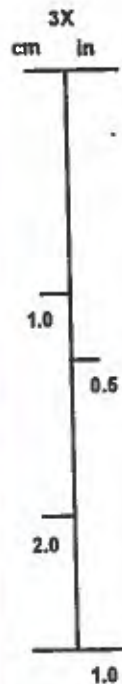
Visible Light



Ultraviolet Light

DEPTH ft	PERM (mD)	POR (%)	OIL% (pore)	WTR% (pore)	GAS% (vol)	PROB PROD	GRAIN DENSITY	LITHOLOGY
9848.0	2502.0	22.6					2.63	Sd lt-gy-brn mg ssly

Visible Light



Ultraviolet Light

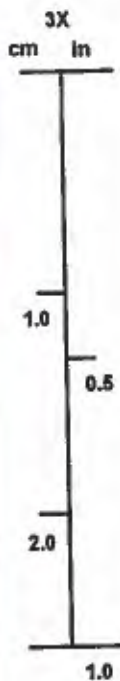
DuPont
 Injection Well # 3, S/T # 1
 Delisle, MS Plant



N-4474
 27-Jan-99
 Harrison Co., MS

DEPTH ft	PERM (mD)	POR (%)	OIL% (pure)	WTR% (pore)	GAS% (vol)	PROB PROD	GRAIN DENSITY	LITHOLOGY
9856.0	1247.0	22.1					2.63	Sd lt-gy-brn mg ssly

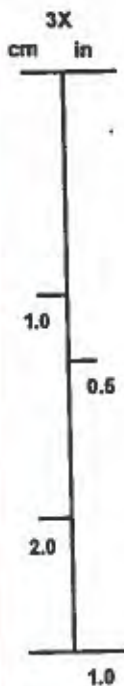
Visible Light



Ultraviolet Light

DEPTH ft	PERM (mD)	POR (%)	OIL% (pure)	WTR% (pore)	GAS% (vol)	PROB PROD	GRAIN DENSITY	LITHOLOGY
9861.0	824.0	22.6					2.62	Sd lt-gy mg ssly

Visible Light



Ultraviolet Light

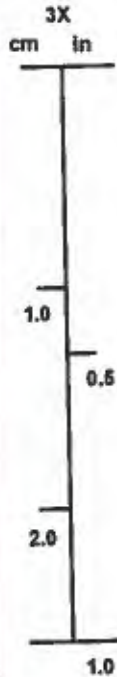
Dupont
 Injection Well # 3, S/T # 1
 Delisle, MS Plant



N-4474
 27-Jan-99
 Harrison Co., MS

DEPTH ft	PERM (mD)	POR (%)	OIL% (pore)	WTR% (pore)	GAS% (vol)	PROB PROD	GRAIN DENSITY	LITHOLOGY
9866.0	0.52	7.7					2.71	Sd lt-gy vf-mg slty w/clay clasts vcalc

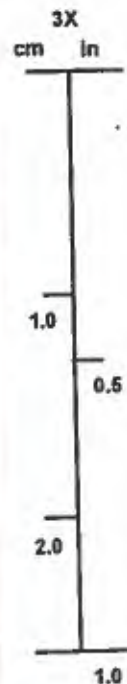
Visible Light



Ultraviolet Light

DEPTH ft	PERM (mD)	POR (%)	OIL% (pore)	WTR% (pore)	GAS% (vol)	PROB PROD	GRAIN DENSITY	LITHOLOGY
9871.0	0.01	5.1					2.69	Sd gy vfg vslty shy calc

Visible Light



Ultraviolet Light

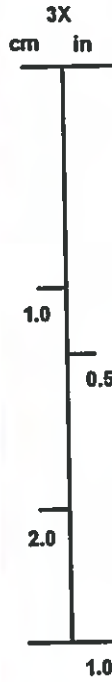
Dupont
 Injection Well # 3, S/T # 1
 Delisle, MS Plant



N-4474
 27-Jan-99
 Harrison Co., MS

DEPTH ft	PERM (mD)	POR (%)	OIL% (pore)	WTR% (pore)	GAS% (vol)	PROB PROD	GRAIN DENSITY	LITHOLOGY
9887.0	90.0	17.0					2.67	Sd lt-gy vf-fg slty scalc

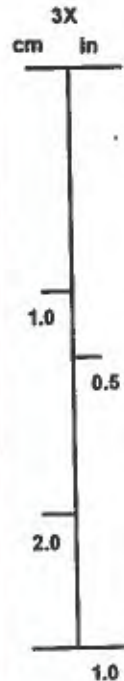
Visible Light



Ultraviolet Light

DEPTH ft	PERM (mD)	POR (%)	OIL% (pore)	WTR% (pore)	GAS% (vol)	PROB PROD	GRAIN DENSITY	LITHOLOGY
9899.0	509.0	19.5					2.63	Sd lt-gy f-vfg slty w/scarb lams

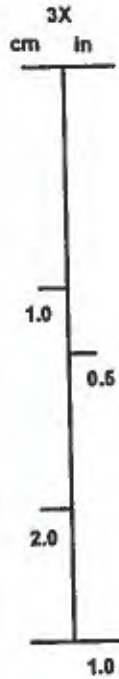
Visible Light



Ultraviolet Light

DEPTH ft	PERM (mD)	POR (%)	OIL% (pore)	WTR% (pore)	GAS% (vol)	PROB PROD	GRAIN DENSITY	LITHOLOGY
9904.0	618.0	20.3					2.63	Sd lt-gy vf-fg slty

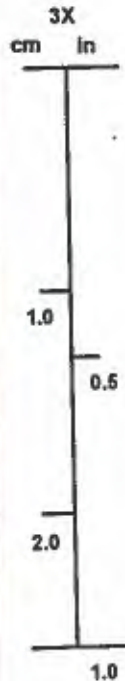
Visible Light



Ultraviolet Light

DEPTH ft	PERM (mD)	POR (%)	OIL% (pore)	WTR% (pore)	GAS% (vol)	PROB PROD	GRAIN DENSITY	LITHOLOGY
9916.0	391.0	20.3					2.64	Sd lt-gy vf-fg slty

Visible Light



Ultraviolet Light

Dupont
 Injection Well # 3, S/T # 1
 Delisle, MS Plant



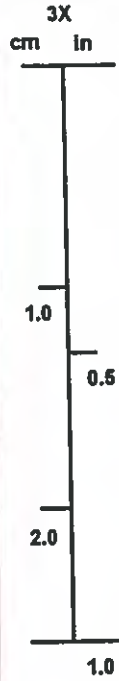
N-4474
 27-Jan-99
 Harrison Co., MS

DEPTH ft	PERM (mD)	POR (%)	OIL% (pore)	WTR% (pore)	GAS% (vol)	PROB PROD	GRAIN DENSITY	LITHOLOGY
9929.0	419.0	19.7					2.63	Sd lt-gy f-vfg slty w/scarb lams

Visible Light



Ultraviolet Light

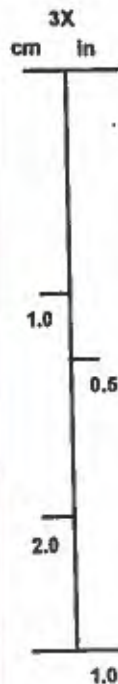


DEPTH ft	PERM (mD)	POR (%)	OIL% (pore)	WTR% (pore)	GAS% (vol)	PROB PROD	GRAIN DENSITY	LITHOLOGY
9938.0	400.0	20.9					2.68	Sd lt-gy f-vfg slty

Visible Light



Ultraviolet Light



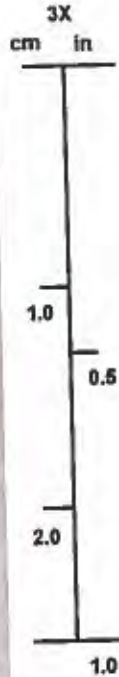
Dupont
 Injection Well # 3, S/T # 1
 Delisle, MS Plant



N-4474
 27-Jan-99
 Harrison Co., MS

DEPTH ft	PERM (mD)	POR (%)	OIL% (pore)	WTR% (pore)	GAS% (vol)	PROB PROD	GRAIN DENSITY	LITHOLOGY
9952.0	0.01	4.3					2.7	Sd lt-gy vf-fg vslty vcalc

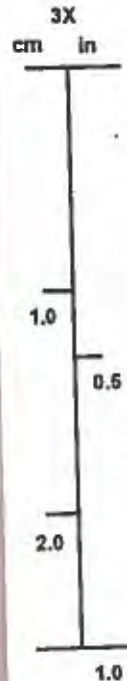
Visible Light



Ultraviolet Light

DEPTH ft	PERM (mD)	POR (%)	OIL% (pore)	WTR% (pore)	GAS% (vol)	PROB PROD	GRAIN DENSITY	LITHOLOGY
9962.0	39.0	17.7					2.72	Sd lt-gy vf-fg slty

Visible Light



Ultraviolet Light

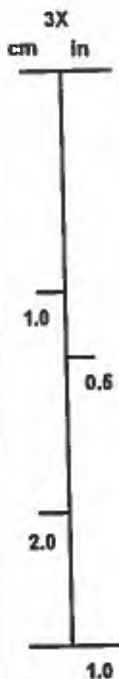
Dupont
 Injection Well # 3, S/T # 1
 Delisle, MS Plant



N-4474
 27-Jan-99
 Harrison Co., MS

DEPTH ft.	PERM (mD)	POR (%)	OIL% (pore)	WTR% (pore)	GAS% (vol)	PROB PROD	GRAIN DENSITY	LITHOLOGY
9970.0	35.0	14.7					2.79	Sd lt-gy vfg slty

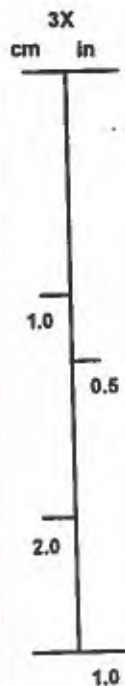
Visible Light



Ultraviolet Light

DEPTH ft.	PERM (mD)	POR (%)	OIL% (pore)	WTR% (pore)	GAS% (vol)	PROB PROD	GRAIN DENSITY	LITHOLOGY
9992.0	18.0	14.1					2.67	Sd lt-gy vfg vslty calc

Visible Light



Ultraviolet Light

Dupont
 Injection Well # 3, S/T # 1
 Delisle, MS Plant



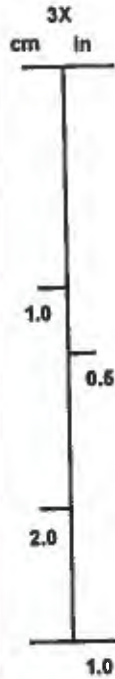
N-4474
 27-Jan-99
 Harrison Co., MS

DEPTH ft	PERM (mD)	POR (%)	OIL% (pore)	WTR% (pore)	GAS% (vol)	PROB PROD	GRAIN DENSITY	LITHOLOGY
9996 -0	47.0	17.8					2.66	Sd lt-gy slty

Visible Light

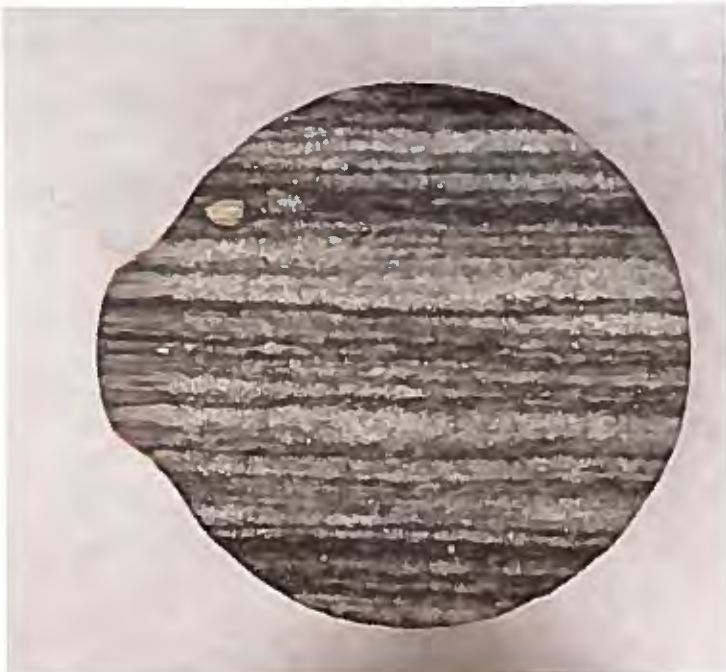


Ultraviolet Light

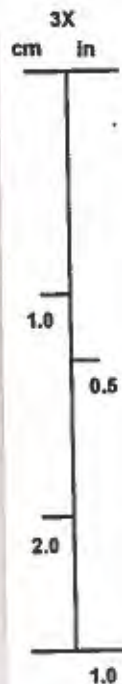


DEPTH ft	PERM (mD)	POR (%)	OIL% (pore)	WTR% (pore)	GAS% (vol)	PROB PROD	GRAIN DENSITY	LITHOLOGY
1000 8.0	0.14	10.4					2.69	Sd gy vfg slty w/carb lams spyr mica

Visible Light



Ultraviolet Light



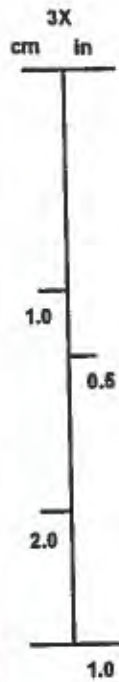
Dupont
 Injection Well # 3, S/T # 1
 Delisle, MS Plant



N-4474
 27-Jan-99
 Harrison Co., MS

DEPTH ft	PERM (mD)	POR (%)	OIL% (pore)	WTR% (pore)	GAS% (vol)	PROB PROD	GRAIN DENSITY	LITHOLOGY
10016.0	259.0	20.2					2.63	Sd lt-gy f-vfg slty

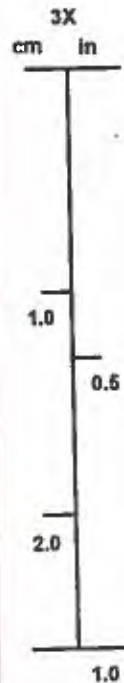
Visible Light



Ultraviolet Light

DEPTH ft	PERM (mD)	POR (%)	OIL% (pore)	WTR% (pore)	GAS% (vol)	PROB PROD	GRAIN DENSITY	LITHOLOGY
10023.0	508.00	20.4					2.63	Sd lt-gy f-vfg slty

Visible Light



Ultraviolet Light

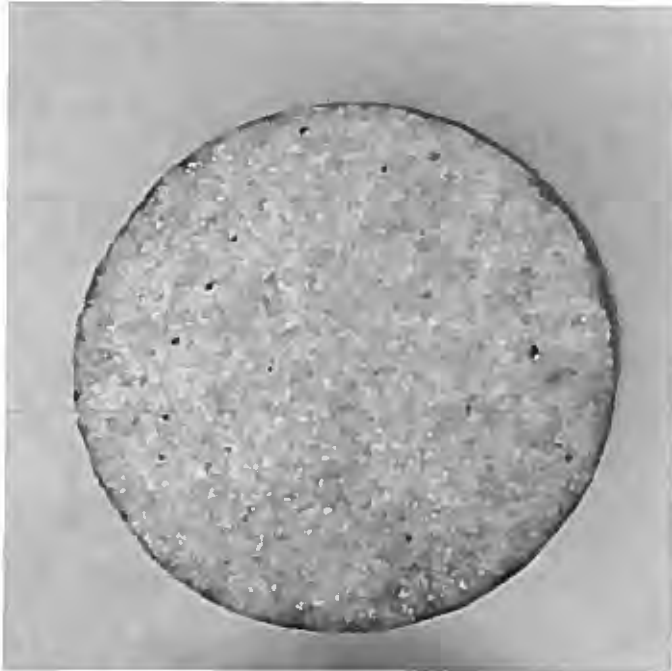
Dupont
 Injection Well # 3, S/T # 1
 Delisle, MS Plant



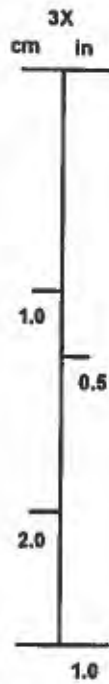
N-4474
 27-Jan-99
 Harrison Co., MS

DEPTH ft	PERM (mD)	POR (%)	OIL% (pore)	WTR% (pore)	GAS% (vol)	PROB PROD	GRAIN DENSITY	LITHOLOGY
10032.0	1121.0	23.4					2.62	Sd lt-gy fg slty

Visible Light



Ultraviolet Light



**-FINAL REPORT-
CAPROCK PERMEABILITY
AND WASTE FLUID COMPATIBILITY STUDY
FOR
SANDIA TECHNOLOGIES, LLC
INJECTION WELL NO. 3 S/T 1
DUPONT DELISLE PLANT
HARRISON COUNTY, MISSISSIPPI
S-99003**

June 7, 1999

June 7, 1999

Mr. Philip Papadeus
Sandia Technologies, LLC
140 Cypress Station Drive, Suite 140
Houston, Texas 77090

Subject: Caprock Permeability and Waste Fluid Compatibility Study
Injection Well No. 3 S/T 1
Dupont Delisle Plant
Harrison County, Mississippi
S-99003

Dear Mr. Papadeus:

An advanced core analysis study to determine caprock permeability and shale compatibility on core material from the subject site has been completed for Sandia Technologies LLC (Sandia). The shale permeability testing was authorized in an electronic mail transmission from Mr. Papadeus of Sandia dated February 8, 1999. The waste fluid compatibility work was authorized in a telephone conversation between Mr. Papadeus of Sandia and Ms. Melanie Dunn of OMNI Laboratories in April 1999. Final results of two caprock permeability tests and three shale compatibility tests are presented herein.

Fluid Preparation

Synthetic formation brine was prepared to match the supplied analysis, adjusted for the expected total salinity for the sample depth, using reagent grade chemicals and deionized water and was evacuated of air and prefiltered through a 0.45 micron Millipore™ filter prior to injection. Four containers of ferric chloride waste fluid were received from the DeLisle plant on April 1999. This fluid was used as received.

Sample Preparation

The 2 shale rotary sidewall samples from the subject site, 8184 and 9212 feet respectively, which had been preserved in Saran Wrap™ and aluminum foil, were saturated with synthetic formation brine prior to permeability testing. Representative pieces of the rotary sidewall samples from the three intervals selected for shale compatibility testing were taken from the preserved samples and tested as received.

Caprock Permeability

Caprock permeability testing was performed on the two selected samples as outlined on Page i. Both samples demonstrated low values of permeability to brine (Sample 1 from 8184 feet $K_b < 1.85E-07$ md, and Sample 3 from 9212 feet $K_b = 1.45E-04$ md). These data are presented in summary form at the end of this discussion.

Waste Fluid Compatibility

Three shale samples were selected from the sidewall samples obtained from the Dupont Delisle Plant Injection Well No. 3 S/T 1 (9663 feet, 9724 feet, and 9804 feet) to evaluate waste fluid compatibility.

A portion of each sample was placed in a beaker and immersed in the supplied waste fluid. The three beakers were then placed in an oven for 14 days at 190°F and periodically observed. After testing the

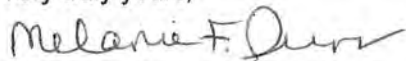
Sandia Technologies LLC
File: S-99003
Page Two

samples were removed from the test fluids and allowed to air dry. A photograph of each sample was taken and is enclosed in this report.

Visual observation of these samples during the course of testing indicated that little to no reaction of the shale to the waste fluid occurred. Shale pieces remained intact during testing with no visible effect indicating that the shale confining zone should not be affected by the waste fluid.

Thank you for this opportunity to be of service to Sandia Technologies LLC. If you have any questions concerning the enclosed information, or if we can be of any additional service, please contact me at 713-462-4800.

Very truly yours,



Melanie F. Dunn
Manager, Special Core Analyses Laboratory

EXPERIMENTAL PROCEDURES

Caprock Permeability to Liquid

1. The preserved samples were saturated with synthetic formation brine.
2. Each sample was loaded in a hydrostatic coreholder and 2300 psi net confining pressure was applied.
3. Synthetic formation brine were injected at a suitable constant pressure while recording produced fluid volumes, elapsed time, and differential pressure until an equilibrium produced flow rate was observed over a 24 hour period (or no flow was observed over a 48 hour period).
4. Permeability to liquid was calculated from the experimental data and measured sample parameters using Darcy's law.

SYNTHETIC FORMATION BRINE
Adjusted to Expected Salinity at 10000 feet

Sandia Technologies LLC
DuPont DeLisle Plant Well No. 5
Formation Fluid

Harrison County, Mississippi
File: S-99003

Constituent		Concentration, gm/l
Sodium Chloride	(NaCl)	157.694
Barium Chloride	(BaCl ₂ · 2H ₂ O)	0.010
Sodium Sulfate	(Na ₂ SO ₄)	0.258
Sodium Carbonate	(Na ₂ CO ₃)	0.469

The brine composition was calculated based on the following analyses:

Constituent	Concentration, mg/l	Constituent	Concentration, mg/l
Sodium	0.0	Chloride	71750
Calcium	0.0	Sulfate	131
Magnesium	0.0	Bicarbonate	0
Barium	4.3	Carbonate	199
Potassium	0.0	Iodide	0
Strontium	4.5		



SUMMARY OF CAPROCK PERMEABILITY TEST RESULTS

Preserved-State Samples
Net Confining Stress: 2300 psi
Ambient Temperature

Sandia Technologies, LLC
Injection Well No. 3 S/T 1
Dupont Delisle Plant

Harrison County, Mississippi
S-99003

Sample Number	Sample Depth, feet	Caprock Permeability to Brine, millidarcys
1	8184	< 1.85E-07
3	9212	1.45E-04

Sandia Technologies, LLC
Dupont Delisle Plant
Injection Well No. 3 S/T 1

Harrison County, Mississippi
S-99003

**Shale Sample 9663 feet
After Immersion Waste Fluid for 2 weeks**



**Shale Sample 9724 feet
After Immersion Waste Fluid for 2 weeks**



Sandia Technologies, LLC
Dupont Delisle Plant
Injection Well No. 3 S/T 1

Harrison County, Mississippi
S-99003

**Shale Sample 9804 feet
After Immersion Waste Fluid for 2 weeks**



Appendix 2-32

O'Malley Laboratories, Inc. Core Analysis

Well No. 4 Original Borehole (1982)

DATE 7-18-82 FILE NO. 782-21

CUMMINS LABORATORIES, INC.
Core Analysis
 NATCHEZ, MISS.

COMPANY E.I. DU PONT DE NEMOURS & CO. WELL MS WASTE WELL # 4 - PROJECT 2613 FIELD

LOCATION COUNTY HARRISON STATE MISSISSIPPI ELEV.

FORMATION CORES GEARHART-OWEN S/W REPORT TO MR. K.L. CORNWELL ANALYSTS JPT-DO-KP

SAMPLE NUMBER	DEPTH FEET	PERMEABILITY MILLIDARLAYS	POROSITY PER CENT	RESIDUAL SATURATION VALUES			FLUORESCENCE	UNITS TOTAL GAS	DESCRIPTION
				% PORE SPACE	OIL %	WATER %			
1.	7930	0.0	4.1	---	---	---	0	SH GY VY CALC	
2.	7936	0.0	3.5	---	---	---	0	AS ABOVE	
3.	7952	0.0	4.6	---	---	---	0	LS GY	
4.	7962	0.0	3.4	---	---	---	0	SH GY VY CALC	
5.	7969	0.0	3.6	---	---	---	0	LS GY DNSE	
6.	7976	0.0	3.5	---	---	---	0	AS ABOVE	
7.	7986	0.0	3.1	---	---	---	0	LS GY SHLY	
8.	8010	0.0	3.3	---	---	---	0	LS GY	
9.	8017	0.0	3.0	---	---	---	0	AS ABOVE-SHLY	
10.	8024	0.0	2.9	---	---	---	0	AS ABOVE	
11.	8034	0.0	2.7	---	---	---	0	AS ABOVE-VY SHLY	
12.	8046	0.0	3.1	---	---	---	0	LS GY SHLY	
13.	8054	0.0	3.0	---	---	---	0	AS ABOVE	
14.	8068	0.0	2.9	---	---	---	0	AS ABOVE	
15.	8076	0.0	3.0	---	---	---	0	AS ABOVE	
16.	8086	0.0	2.8	---	---	---	0	AS ABOVE	
17.	8122	0.0	4.8	---	---	---	0	AS ABOVE	
18.	8126	0.0	4.2	---	---	---	0	AS ABOVE	
19.	8130	0.0	4.9	---	---	---	0	AS ABOVE	
20.	8136	0.0	4.0	---	---	---	0	AS ABOVE	
21.	9218	10.2	20.6	---	---	---	0	VFG GY ASHY SD	
22.	9428	387.	24.7	---	---	---	0	FN/MED GR GY SD	
23.	9462	194.	25.9	---	---	---	0	FN/MED GR GY SL CALC SD	
24.	9464	153.	25.5	---	---	---	0	AS ABOVE	
25.	9540	230.	27.2	---	---	---	0	AS ABOVE	
26.	9592	395.	26.7	---	---	---	0	FN/MED GR GY SD	
27.	9778	61.	23.4	---	---	---	0	FN GR GY CALC SD	
28.	9786	810.	28.7	---	---	---	0	MED GR GY SD	
29.	9790	----	----	---	---	---	0	WALL-CAKE	
30.	9794	672.	27.2	---	---	---	0	MED GR GY SD	

0111003

SAMPLE NUMBER	DEPTH FEET	PERMEABILITY MILLIDARCS		POROSITY PER CENT	RESIDUAL SATURATION VALUES			PROB. PROD.	FLUORESCENCE	UNITS TOTAL GAS	DESCRIPTION
		VERTICAL	HORIZONTAL		OIL %/o	WATER %/o	PORE SPACE				
31.	9798	118.		23.8	---	---	---	---	0	MED GR GY SL CALC SD	
32.	9800	84.		22.9	---	---	---	---	0	FM GR GY SL CALC SD	
33.	9802	312.		24.2	---	---	---	---	0	AS ABOVE	
34.	9804	525.		26.0	---	---	---	---	0	MED GR GY SL CALC SD	
35.	9806	492.		25.8	---	---	---	---	0	AS ABOVE	
36.	9808	364.		23.5	---	---	---	---	0	AS ABOVE	
37.	9810	28.		20.7	---	---	---	---	0	VFG GY SHLY VY CALC SD	
38.	9812	31.		22.3	---	---	---	---	0	FN GR GY VY CALC SD	
39.	9814	236.		24.1	---	---	---	---	0	FN GR GY CALC SD	
40.	9820	0.0		13.7	---	---	---	---	0	VFG GY SHLY SD	
41.	9854	36.		22.6	---	---	---	---	0	VFG GY CALC SD	
42.	9880	18.		20.3	---	---	---	---	0	VFG GY SL CALC SD	
43.	9881	15.		20.1	---	---	---	---	0	AS ABOVE	
44.	9884	34.		22.6	---	---	---	---	0	AS ABOVE	
45.	9892	17.		21.0	---	---	---	---	0	AS ABOVE	
46.	9896	31.		21.7	---	---	---	---	0	AS ABOVE	
47.	9898	194.		23.9	---	---	---	---	0	FN GR GY SL CALC SD	
48.	9900	12.		18.4	---	---	---	---	0	FN GR GY SL LIG SD	
49.	9906	0.0		9.1	---	---	---	---	0	VFG GY DNSE CALC SD	
50.	9930	84.		18.6	---	---	---	---	0	FN GR GY VY CALC SD	
51.	9932	72.		21.6	---	---	---	---	0	FN GR GY SL CALC SD	
52.	9938	558.		22.1	---	---	---	---	0	FN GR GY SL CALC SD	
53.	9940	614.		22.5	---	---	---	---	0	MED GR GY SD	
54.	9942	238.		21.4	---	---	---	---	0	AS ABOVE	
55.	9948	78.		20.8	---	---	---	---	0	FN GR GY SL CALC SD	
56.	9952	0.0		2.7	---	---	---	---	0	AS ABOVE	
57.	9956	32.		18.9	---	---	---	---	0	SH BLK	
58.	9958	46.		19.4	---	---	---	---	0	FN GR GY SL CALC SD	
59.	9962	71.		20.2	---	---	---	---	0	AS ABOVE	
60.	9964	63.		19.7	---	---	---	---	0	AS ABOVE	
61.	9968	578.		23.6	---	---	---	---	0	AS ABOVE	
62.	9970	620.		24.2	---	---	---	---	0	MED GR GY SD	
63.	9982	142.		21.3	---	---	---	---	0	AS ABOVE	
64.	9984	117.		21.0	---	---	---	---	0	AS ABOVE CALC VFG GY SD	

0111003

Appendix 2-33

Omni Laboratories, Inc. Petrographic Study Final Report

Well No. 4 Sidetrack #1 (1995)

**-FINAL REPORT-
PETROGRAPHIC STUDY
FOR
DUPONT ENVIRONMENTAL
DELISLE PLANT NO. 4, S/T NO. 1 WELL
DELISLE PLANT
HARRISON COUNTY, MISSISSIPPI**

August 23, 1995

Mr. Phillip Papadeas
DuPont Environmental Remediation Services
140 Cypress Station, Suite 240
Houston, Texas 77090

SUBJECT: Final Report - Petrographic Study
Delisle Plant No. 4, S/T No. 1 Well
Delisle Plant
Harrison County, Mississippi
File No. GH-2562

Dear Mr. Papadeas,

Ten (10) rotary sidewall core samples from the above referenced well were submitted for complete petrographic analysis, which includes X-ray diffraction (XRD), thin section petrography, and scanning electron microscopy (SEM). Five (5) additional samples were analyzed by XRD only. This final report includes all data, interpretations, and photomicrographs associated with these analyses. Eight (8) copies of this report are provided.

It has been a pleasure to provide this study for DuPont Environmental Remediation Services. Please feel free to contact us if you have any questions concerning this report or if we can be of further service.

Sincerely,
OMNI LABORATORIES



Michael Dixon
Manager, Geologic Services



Monte C. Manske
Senior Geologist

SUMMARY OF RESULTS

Ten rotary (drilled) sidewall core samples from the referenced well were submitted for complete petrographic analysis, which includes X-ray diffraction (XRD), thin section petrography, and scanning electron microscopy (SEM). Based on these results, the samples display a range of porosity development from good (9757', 9782', 9842', 9907', 9917', and 9928'), to moderate (9779'), to poor (9672', 9789', 9876').

The samples with good porosity development (9757', 9782', 9842', 9907', 9917', and 9928') are generally massive, moderately to moderately well sorted, medium- to fine-grained sandstones. These sands are typically very quartzose, providing a chemically stable framework for these sandstones. Primary intergranular porosity (7%-16%) is the dominant porosity type. Porosity is generally open and evenly distributed, but is occasionally blocked by secondary cements. The most common cements are quartz overgrowths, pyrite, and authigenic kaolinite. The authigenic kaolinite occurs as aggregates of booklets which form as a patchy pore-filling. Moderate amounts of secondary dissolution porosity (4%-7%) augments the primary pores and were formed by the partial to complete leaching of relatively unstable framework grains, such as feldspars and lithic fragments. The upper four sandstones with good reservoir quality (9757', 9782', 9842', 9907') also contain significant amounts of a titanium-rich material which partially fills and encrusts the pores in each sample. This material is found coating authigenic kaolinite particles, which is one of the last minerals to form during the diagenesis of this sandstone. The composition of this titanium-rich material was characterized by the X-ray (EDS) detector attached to the SEM. This detector can qualitatively identify elements with an atomic number of 11 (sodium) to 92 (uranium). Titanium is the dominant elemental constituent identified in this material, with variable amounts of silicon, iron, and nickel (possibly an artifact). Halite (NaCl) can also be found overlaying the titanium-rich material. The titanium material could occur as an oxide, a carbonate, or in association with organic material, but it is amorphous, or poorly crystalline. Thin section modal analysis results include this titanium material in the "other opaques" category.

The sample with moderate porosity development at 9779' is very similar, both mineralogically and chemically, to those with good development, except for common ankerite. Ankerite is an iron-rich form of the carbonate mineral dolomite. This ankerite locally occludes available porosity at this depth, and has acted to reduce effective pore volume.

Samples with poor porosity development (9672', 9789', 9876') are very shaly, with the samples from 9789' and 9876' containing abundant ankerite cement as well. This carbonate mineral has acted to almost totally infill effective porosity in portions of each sample which are relatively clean. Calcareous fossil fragments are also a common constituent of the sample at 9876'. Both vertical and horizontal permeabilities should be very low in rocks of this type.

INTRODUCTION

X-ray diffraction (XRD) analysis, thin section petrography, and scanning electron microscopy (SEM) were performed on ten core samples from the referenced well (see Appendices B through D, respectively). XRD only was performed on five additional samples. Table 1 below outlines the sample depths and the analyses performed.

TABLE 1
SAMPLE DEPTHS AND ANALYSES PERFORMED

<u>SAMPLE DEPTH</u> <u>(feet)</u>	<u>THIN SECTION</u> <u>PETROGRAPHY</u>	<u>SEM</u>	<u>XRD</u>
9672	X	X	X
9747	-	-	X
9757	X	X	X
9764	-	-	X
9779	X	X	X
9782	X	X	X
9789	X	X	X
9842	X	X	X
9861	-	-	X
9876	X	X	X
9892	-	-	X
9907	X	X	X
9917	X	X	X
9928	X	X	X
9952	-	-	X

The objectives of these analyses were to: 1) characterize the texture and mineralogy; 2) examine porosity development and determine controls on porosity and permeability; and 3) identify any materials introduced into the formation, if present.

PETROGRAPHIC RESULTS

The following sections briefly characterize the sand intervals with respect to sedimentary texture, composition, porosity development, and the effects of mineralogy on log response. Specific information on individual samples is included in the Appendices.

Sedimentary Texture

The ten samples examined by thin section (see Appendix C) are medium-grained (9757', 9779'), fine-grained (9782', 9842', 9907', 9917', and 9928'), and very fine-grained (9672', 9789', and 9876') sandstones. The average grain size ranges from 0.07 mm (9876') to 0.37 mm (9779'). The samples at 9757', 9779', 9782', 9842', 9907', 9917', and 9928' are generally massive and moderately to moderately well sorted. The samples at 9672', 9789', and 9876' contain common shale laminations. Bioturbation is observed in the sample at 9789'. Bioturbation refers to the reworking of sediment by organisms shortly after deposition. The framework grains in the samples range from angular to subrounded, with subangular grains being most common. Compositionally, the sandstones are classified as subarkoses (9672', 9842', 9876', 9917', and 9928'), quartz arenites (9757', 9779', and 9907'), and sublitharenites (9782' and 9789'), based on the classification scheme of Folk, 1980. The relatively low amounts of feldspars in some of these sands may be a function of both a quartzose sediment source and removal of these less stable grains by secondary dissolution.

Framework Grains

Monocrystalline quartz (27%-55%) is the dominant framework grain in the sandstones analyzed in thin section (Appendix C). Other common framework constituents include polycrystalline quartz (3%-13%), plagioclase feldspar (1%-5%), potassium (K-) feldspar (trace-3%), and various lithic fragments (trace-4% total lithics). The most common lithic types are sedimentary (mostly chert, mudstone, and calcareous types) and volcanic in origin. Lesser amounts of plutonic and metamorphic rock fragments are also present. The feldspars are fresh to strongly altered to sericite and kaolin minerals. Minor constituents present in these samples include organic material, glauconite, calcareous fossil fragments (up to 23% at 9876'), muscovite, biotite, tourmaline, garnet, and zircon. The presence of glauconite indicates marine depositional influence.

Secondary Constituents

The ten samples analyzed by thin section are cemented mainly by secondary quartz overgrowths (1%-9%), and ankerite (1%-25%) in selective samples (9672', 9779', 9789', and 9876'). The quartz overgrowths typically occur as flat to pseudohexagonal crystal faces on host detrital quartz sand grains. The formation of quartz overgrowths appear to be locally inhibited by early

authigenic chlorite grain-coatings in some samples. Ankerite cement was observed in four samples, and occurs as a patchy, pore-filling constituent. Minor cementing agents in these samples include pyrite (trace-4%), authigenic clays (0%-3%), siderite (0%-4%), and iron oxides (0%-trace). Pyrite occurs as scattered framboidal forms, microcrystalline aggregates, and as a grain replacement. The clays are discussed further in the following section on "Clay Mineralogy". Siderite is found as scattered patches of pore-filling microcrystals. Iron oxides are typically found as grain-coatings.

Two components appears to have been introduced into the formation, having precipitated directly within the pore system or on adjacent mineral surfaces. The upper four sandstones with good reservoir quality (9757', 9782', 9842', and 9907') contain significant amounts of a titanium-rich material which partially fills and encrusts the pores in each sample. This material is found coating authigenic kaolinite particles, which is one of the last minerals to form during the diagenesis of this sandstone, as well as other fines associated with the pore system. The composition of this titanium-rich material was characterized by the X-ray (EDS) detector attached to the SEM. This detector can qualitatively identify elements with an atomic number of 11 (sodium) to 92 (uranium). Titanium is the dominant elemental constituent identified in this material, with variable amounts of silicon, iron, and nickel (possibly an artifact). Halite (NaCl) can also be found overlaying (post-dating) the titanium-rich material. The titanium material could occur as an oxide, a carbonate, or in association with organic material, but it is amorphous, or poorly crystalline. Thin section modal analysis results include this titanium material in the "other opaques" category.

Clay Mineralogy

X-ray diffraction (XRD) analyses (Appendix B) of fifteen total samples reveal that the total clay content ranges from 2% (9747') to 41% (9892'), and averages 10%. Mixed-layer illite/smectite (trace-22%), illite (1%-8%), chlorite (trace-8%), and kaolinite (0%-8%) are the clay types present.

Scanning electron microscope (SEM) analyses (Appendix D) of ten samples show that the clays occurs as 1) patchy illitic detrital matrix; 2) illitic shale laminations (9672', 9789', and 9876'); 3) patchy, pore-filling authigenic (secondary) kaolinite; 3) grain-coating authigenic chlorite (9779' and 9842'); and 4) lithic fragments. Mixed-layer illite/smectite and illite are frequently intermixed and occur as a detrital (depositional) matrix, or as discrete shale laminations. Minor illite of possible authigenic origin is rarely observed. Authigenic kaolinite occurs as loose aggregates of minute booklets which have a patchy, pore-filling habit. The individual kaolinite particles are poorly attached to pore walls and represent a fines migration concern. In the more permeable sands with the titanium precipitate, the kaolinite acts as a substrate for the titanium material, probably due to its extremely high surface area. The authigenic chlorite forms as flat platelets with a face-to-edge orientation in the samples at 9779' and 9842'. The grain-coating chlorite developed relatively early during diagenesis. This chlorite appears to locally inhibit the formation of local quartz overgrowth cement, thereby preserving selective intergranular pores. All clay types can also occur as components of various lithic fragments. The authigenic clay

minerals (kaolinite and chlorite) have a very high associated microporosity. Relatively high irreducible water saturations are expected in the intervals analyzed due to abundant water bound between loosely arranged clay particles.

Porosity Development

Primary intergranular porosity (0%-16%), secondary dissolution porosity (trace-7%), and microporosity (trace-4%) are the porosity types present in these samples. Primary intergranular porosity is generally open and evenly distributed, but is occasionally blocked by naturally-occurring secondary cements. The most common cements are quartz overgrowths, pyrite, and authigenic kaolinite. The upper four sandstones with good reservoir quality (9757', 9782', 9842', 9907') also contain significant amounts of a titanium-rich material which partially fills and encrusts the pores in each sample. The lower two samples (9917' and 9928') show only trace amounts of this material. Moderate to minor amounts of secondary dissolution porosity augments the primary pores, and were formed by the partial to complete leaching of relatively unstable framework grains, such as feldspars and lithic fragments. Microporosity is closely associated with authigenic clays in these samples. As previously discussed, this microporosity is ineffective and typically contains irreducible water.

Mineralogic Influences on Log Response

The following section discusses the effects on log response of the mineralogy and associated porosity types found in these samples.

1. Resistivity Logs: The main components which may cause low resistivity in these intervals are dispersed clay and shale laminations. Sands containing the titanium-bearing material, however, may be more resistive than normal because it is believed that this material is organic in nature.

Dispersed clay - Authigenic dispersed clays are present in these samples. Authigenic clay types are predominantly pore-filling kaolinite and, to a lesser extent, grain-coating chlorite. These clays contain a high amount of microporosity which can hold surface bound water and significantly reduce formation resistivity, even in the presence of pore-filling hydrocarbons. The influence of the titanium-bearing material on resistivity log response is not clear, but it is believed to be relatively resistive.

2. Density Logs: The sandstones examined contain generally low amounts of high density minerals including carbonate minerals and pyrite, except in selective samples. Local concentrations of carbonate minerals (e.g. 25% ankerite and 23% calcareous fossil fragments at 9876', by volume from thin section analysis) are present in the interval analyzed, however. Appropriate density values should be used in intervals which contain minerals with anomalously high or low density.

3. Gamma-Ray Log: Gamma-ray logs respond to radioactive isotopes. The clay minerals chlorite (trace-8% by weight from XRD) and kaolinite (0%-8% by weight from XRD) will not be detected by gamma-ray logs due to the absence of potassium in these minerals. Conversely, the mineral K-feldspar (0%-4% by weight from XRD) will be detected as "clay" by gamma-ray logs due to the presence of potassium in this mineral.

APPENDIX A

PETROGRAPHIC ANALYTICAL PROCEDURES

X-ray Diffraction (XRD) Analysis

A representative portion of each sample was dried, extracted if necessary, and then ground in a Brinkman MM-2 Retsch Mill to a fine powder. This ground sample was next loaded into an aluminum sample holder. This "bulk" sample mount was scanned with a Philips X-ray diffractometer using nickel-filtered copper K-alpha radiation at standard scanning parameters. Computer analysis of the diffractograms provide qualitative identification of mineral phases and semiquantitative analysis of the relative abundance (in weight percent) of the various mineral phases. It should also be noted that X-ray diffraction **does not** allow the detection and identification of non-crystalline (amorphous) material, such as organic material.

An oriented clay fraction mount was also prepared for each sample from the ground powder. The samples were further size fractionated by centrifuge to separate the <4 micron fraction. Ultrasonic treatment was used to suspend the material, then a dispersant was used to prevent flocculation when noted. The solution containing the clay fraction was then passed through a Fisher filter membrane apparatus allowing the solids to be collected on a cellulose membrane filter. These solids were then mounted on a glass slide, dried, and scanned with the Philips diffractometer. The oriented clay mount was then glycolated and another diffractogram prepared to identify the expandable, water sensitive minerals. When necessary, the patterns were deconvoluted, or the samples heat treated, to aid in distinguishing kaolinite and chlorite.

Scanning Electron Microscopy (SEM) Analysis

Samples selected for scanning electron microscopy analysis were first broken, or split, to expose fresh surfaces. The samples were then mounted on sample holders with a conductive carbon paste and coated with gold in a "cool" sputter coater to prevent heat damage to sensitive clay minerals or friable samples. The samples were analyzed with a Model SX-40 International Scientific Instruments (ISI) Scanning Electron Microscope and PGT Energy Dispersive Spectrometer (EDS).

Thin Section Petrographic Analysis

Samples selected for thin section analysis were prepared by first vacuum impregnating with blue-dyed epoxy. The samples were then mounted on an optical glass slide and cut and lapped in water to a thickness of 0.03 mm. The prepared sections were then covered with index oil and temporary cover slips, and then analyzed using standard petrographic techniques.

APPENDIX B

X-RAY DIFFRACTION DATA

OMNI LABORATORIES, INC.
X-RAY DIFFRACTION
 (WEIGHT %)

Client: DUPONT ENVIRON. REMEDIATION SERVICES
Well #: DELISLE PLANT WELL NO. 4 S/T NO.1

File No: H-2562
Date: 8/1/95

Sample Depth	CLAYS				CARBONATES				OTHER MINERALS							TOTALS		
	Chlorite	Kaolinite	Illite	Ill/Smec.	Calcite	Ankerite	Siderite	Quartz	Plag.	K-Spar	Halite	Fe Oxide*	Pyrite	Other	Clays	Carb.	Other	
9672'	8	4	3	3	1	TR	TR	65	6	3	0	0	7	0	18	1	81	
9747'	TR	0	1	1	TR	0	0	96	1	TR	1	TR	TR	0	2	TR	98	
9757'	1	0	2	TR	0	0	0	96	TR	TR	1	TR	0	0	3	0	97	
9764'	TR	2	2	1	0	0	0	90	TR	4	1	0	0	0	5	0	95	
9779'	TR	8	2	3	19	TR	0	59	3	0	3	0	3	0	13	19	68	
9782'	TR	0	1	4	0	0	0	94	1	0	TR	TR	0	0	5	0	95	
9789'	3	2	4	7	14	TR	0	61	2	1	0	0	6	0	16	14	70	
9842'	3	2	5	TR	0	0	0	85	4	1	TR	TR	0	0	10	0	90	
9861'	TR	3	2	TR	0	0	0	92	2	1	TR	0	0	0	5	0	95	
9876'	2	5	8	2	41	TR	0	32	9	TR	0	0	1	0	17	41	42	
9892'	6	5	8	22	0	TR	0	51	2	3	0	0	3	0	41	TR	59	
9907'	TR	TR	2	1	0	0	0	96	TR	0	1	TR	0	0	3	0	97	
9917'	1	3	4	TR	0	0	0	82	7	2	1	0	0	0	8	0	92	
9928'	1	1	1	TR	0	0	0	90	5	1	TR	0	0	0	4	0	96	
9952'	2	TR	2	1	24	0	0	59	9	3	0	0	0	0	5	24	71	
AVERAGE	2	2	3	3	7	TR	0	78	3	1	TR	TR	1	0	10	7	83	

* XRD methods cannot quantify amorphous components; limonite (a common Fe oxide) was detected in thin section in greater abundance than indicated here.

APPENDIX C

**THIN SECTION ANALYSES
AND
THIN SECTION PHOTOMICROGRAPHS**

THIN SECTION MODAL ANALYSIS

DuPont Environmental
 Delisle Plant No. 4 S/T No. 1
 Harrison County, Mississippi

DEPTH	9672'	9757'	9779'	9782'
Grain Size Avg. (mm):	0.12	0.31	0.37	0.29
Grain Size Range (mm):	<0.01-0.73	<0.01-0.88	<0.01-> 1.00	<0.01-0.79
Sorting:	Poor	Moderately well	Poor	Moderately
Rock Name (Folk):	Subarkose	Quartz Arenite	Quartz Arenite	Sublitharenite
FRAMEWORK GRAINS				
Quartz	<u>50</u>	<u>65</u>	<u>61</u>	<u>56</u>
Monocrystalline	43	51	55	44
Polycrystalline	7	14	6	12
Feldspar	<u>6</u>	<u>1</u>	<u>2</u>	<u>1</u>
K-Feldspar	3	tr	1	tr
Plagioclase	3	1	1	1
Lithic Fragments	<u>1</u>	<u>tr</u>	<u>1</u>	<u>3</u>
Plutonic	tr	0	tr	tr
Volcanic	tr	tr	tr	0
Metamorphic	0	tr	tr	tr
Chert	1	tr	1	3
Mudstone	tr	0	tr	tr
Calcareous	0	0	tr	0
ACCESSORY GRAINS	<u>tr</u>	<u>tr</u>	<u>tr</u>	<u>tr</u>
Muscovite	tr	tr	0	tr
Biotite	tr	tr	0	0
Heavy Minerals*	tr	0	tr	tr
ENVIRON. INDICATORS	<u>5</u>	<u>0</u>	<u>0</u>	<u>0</u>
Organics	2	**	**	**
Glauconite	tr	0	0	0
Fossil Fragments	3	0	0	0
MATRIX	<u>27</u>	<u>tr</u>	<u>1</u>	<u>1</u>
AUTHIGENIC CEMENT	<u>8</u>	<u>17</u>	<u>23</u>	<u>22</u>
Kaolinite	tr	**	3	**
Quartz Overgrowths	3	6	3	4
Calcite	0	0	0	0
Dolomite	0	0	0	0
Ankerite	1	0	17	0
Siderite	tr	0	tr	0
Pyrite	4	tr	tr	tr
Iron Oxides	tr	**	**	**
Zeolite	0	0	0	0
Barite	0	0	0	0
Gypsum	0	0	0	0
Anhydrite	0	0	0	0
Other Opaques	0	11	tr	18
POROSITY	<u>3</u>	<u>17</u>	<u>12</u>	<u>17</u>
Primary	tr	11	8	9
Secondary	tr	5	tr	7
Microscopic	3	1	4	1
TOTALS:	<u>100</u>	<u>100</u>	<u>100</u>	<u>100</u>

* Tourmaline

** may be included with "other opaques".

THIN SECTION MODAL ANALYSIS

DuPont Environmental
 Delisle Plant No. 4 S/T No. 1
 Harrison County, Mississippi

DEPTH	9789'	9842	9876'	9907'
Grain Size Avg. (mm):	0.12	0.23	0.07	0.24
Grain Size Range (mm):	<0.01-0.58	<0.01-0.56	<0.01-0.34	<0.01-0.66
Sorting:	Poor	Moderately	Poor	Moderately
Rock Name (Folk):	Sublitharenite	Subarkose	Subarkose	Quartz Arenite
FRAMEWORK GRAINS				
<i>Quartz</i>	<u>42</u>	<u>61</u>	<u>30</u>	<u>63</u>
Monocrystalline	35	49	27	50
Polycrystalline	7	12	3	13
<i>Feldspar</i>	<u>2</u>	<u>4</u>	<u>4</u>	<u>1</u>
K-Feldspar	1	1	tr	tr
Plagioclase	1	3	4	1
<i>Lithic Fragments</i>	<u>4</u>	<u>tr</u>	<u>tr</u>	<u>tr</u>
Plutonic	tr	tr	tr	tr
Volcanic	3	tr	tr	tr
Metamorphic	0	tr	0	tr
Chert	1	tr	0	tr
Mudstone	tr	tr	tr	tr
ACCESSORY GRAINS	<u>tr</u>	<u>1</u>	<u>tr</u>	<u>tr</u>
Muscovite	tr	1	tr	tr
Biotite	tr	tr	tr	tr
Heavy Minerals*	tr	0	tr	tr
ENVIRON. INDICATORS	<u>3</u>	<u>0</u>	<u>23</u>	<u>0</u>
Organics	2	**	tr	**
Glauconite	0	0	tr	0
Fossil Fragments	1	0	23	0
MATRIX	<u>33</u>	<u>6</u>	<u>11</u>	<u>3</u>
AUTHIGENIC CEMENT	<u>15</u>	<u>13</u>	<u>32</u>	<u>13</u>
Kaolinite	tr	tr	0	**
Quartz Overgrowths	1	5	2	5
Calcite	0	0	0	0
Dolomite	0	0	0	0
Ankerite	11	0	25	0
Siderite	0	0	4	0
Pyrite	3	tr	1	tr
Iron Oxides	tr	**	0	**
Zeolite	0	0	0	0
Barite	0	0	0	0
Gypsum	0	0	0	0
Anhydrite	0	0	0	0
Other Opaques	0	8	0	8
POROSITY	<u>1</u>	<u>15</u>	<u>tr</u>	<u>20</u>
Primary	tr	7	0	12
Secondary	tr	4	tr	5
Microscopic	1	4	tr	3
TOTALS:	<u>100</u>	<u>100</u>	<u>100</u>	<u>100</u>

* Garnet, tourmaline, zircon

** may be included with "other opaques".

THIN SECTION MODAL ANALYSIS

DuPont Environmental
 Delisle Plant No. 4 S/T No. 1
 Harrison County, Mississippi

DEPTH	9917'	9928'		
Grain Size Avg. (mm):	0.14	0.20		
Grain Size Range (mm):	<0.01-0.41	<0.01-0.53		
Sorting:	Moderately well	Moderately		
Rock Name (Folk):	Subarkose	Subarkose		
FRAMEWORK GRAINS				
<i>Quartz</i>	<u>60</u>	<u>57</u>		
Monocrystalline	51	53		
Polycrystalline	9	4		
<i>Feldspar</i>	<u>6</u>	<u>5</u>		
K-Feldspar	1	1		
Plagioclase	5	4		
<i>Lithic Fragments</i>	<u>1</u>	<u>2</u>		
Plutonic	tr	tr		
Volcanic	tr	tr		
Metamorphic	1	1		
Chert	tr	1		
Mudstone	tr	tr		
ACCESSORY GRAINS	<u>1</u>	<u>1</u>		
Muscovite	1	1		
Biotite	tr	tr		
Heavy Minerals*	tr	tr		
ENVIRON. INDICATORS	<u>tr</u>	<u>tr</u>		
Organics	tr	tr		
Glauconite	0	0		
Fossil Fragments	0	0		
MATRIX	<u>1</u>	<u>2</u>		
AUTHIGENIC CEMENT	<u>7</u>	<u>10</u>		
Kaolinite	tr	tr		
Quartz Overgrowths	7	9		
Calcite	0	0		
Dolomite	0	0		
Ankerite	0	0		
Siderite	0	0		
Pyrite	tr	tr		
Iron Oxides	tr	1		
Zeolite	0	0		
Barite	0	0		
Gypsum	0	0		
Anhydrite	0	0		
Other Opaques	tr	tr		
POROSITY	<u>24</u>	<u>23</u>		
Primary	15	16		
Secondary	7	7		
Microscopic	2	tr		
TOTALS:	<u>100</u>	<u>100</u>		

* Tourmaline, zircon.

DuPont Environmental Remediation Services
Delisle Plant No. 4 S/T No. 1 Well
Harrison County, Mississippi

File No. GH-2562

SAMPLE DEPTH: 9672 FEET

PLATE 1A

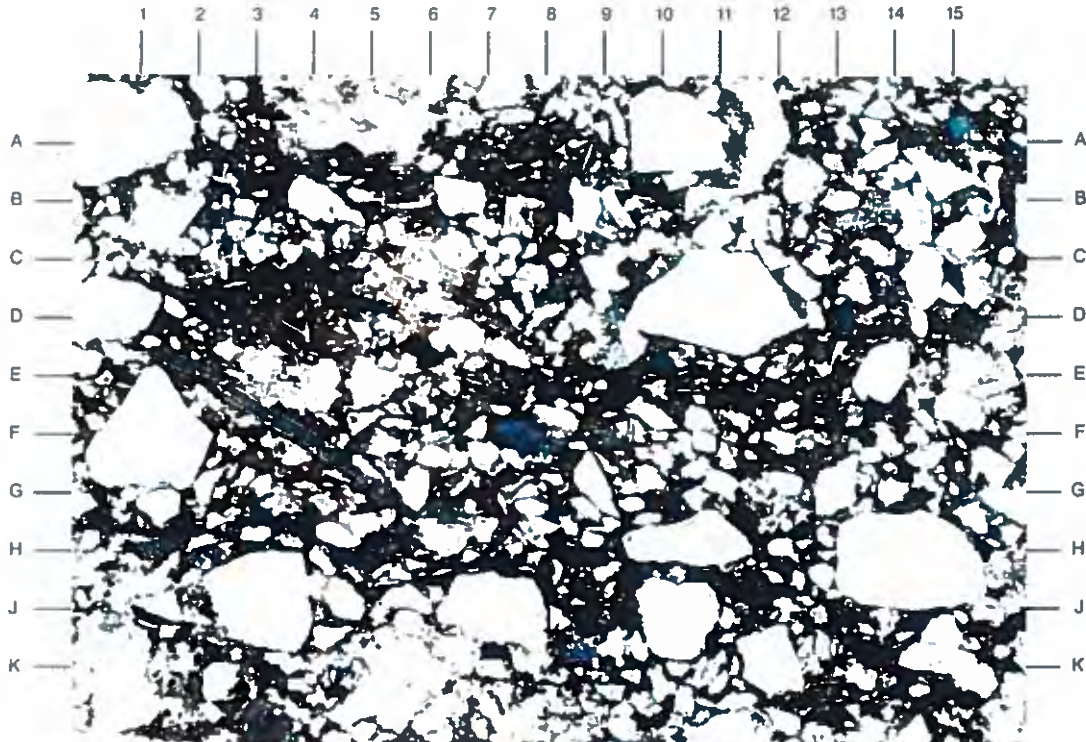
A low magnification view shows the vague laminar fabric of this poorly sorted, very fine-grained sandstone. Laminations are defined by subparallel oriented, organic-rich shale areas (E7-E13,B3-A8). Quartz grains range in size from medium sand (D11,H14) to silt (A13,C7). Scattered calcareous fossil fragments (F4,H1.5) comprise 3% of the sample.

MAGNIFICATION: 40X

PLATE 1B

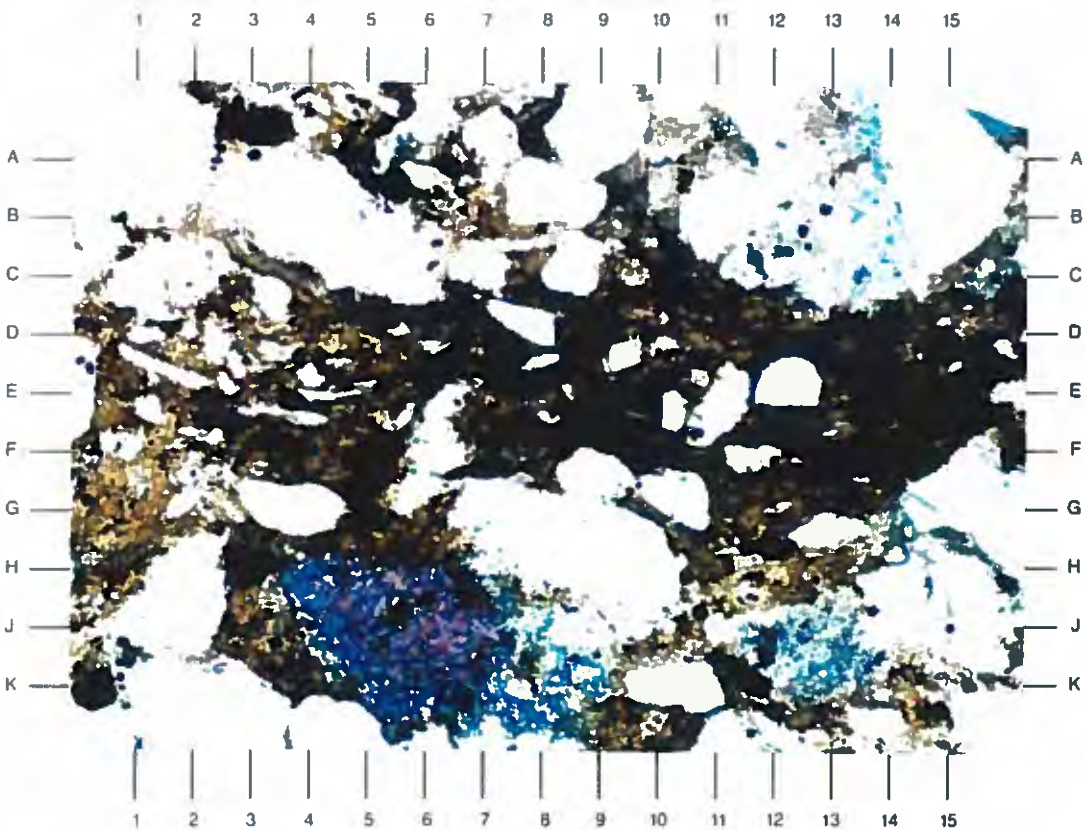
An enlarged view of the area near E8 in Plate 1A is shown in this photomicrograph. An organic-rich shale lamination (E2-E15) is laterally discontinuous. Patches of blue-stained ankerite cement (H4-J7) are widely scattered. The dominant porosity type in this sample is microporosity (A13.5,J8) associated with the matrix.

MAGNIFICATION: 200X



A

0.25 mm



B

0.05 mm

SAMPLE DEPTH: 9757 FEET

PLATE 2A

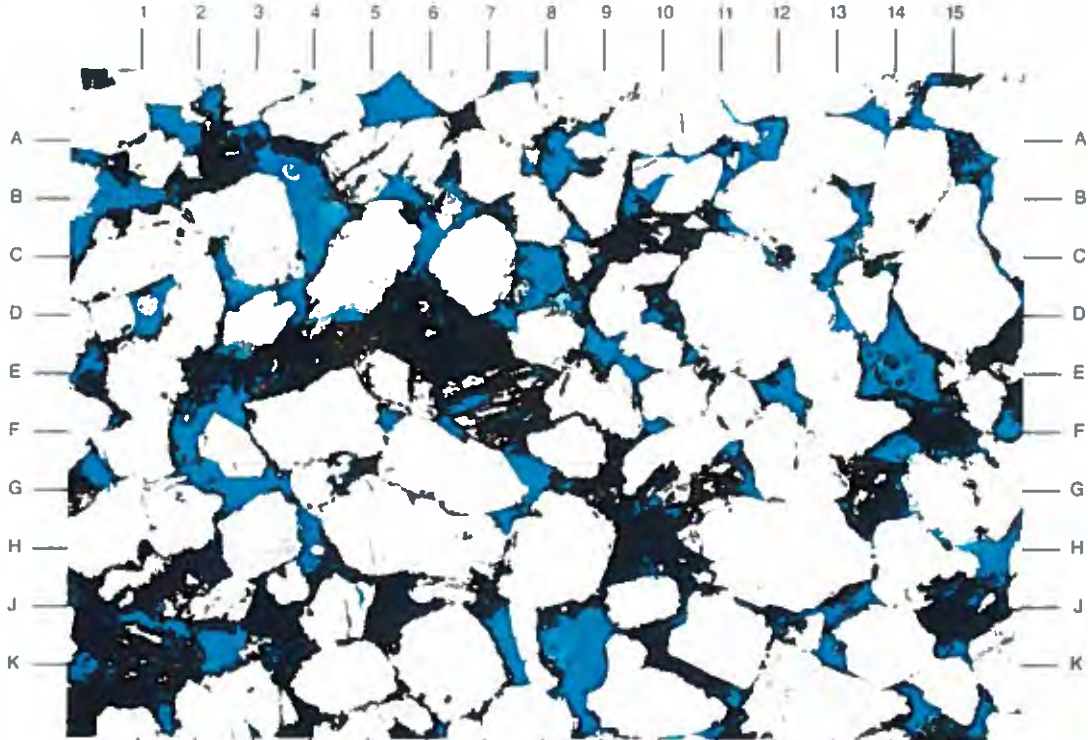
A massive, moderately well sorted, medium-grained sandstone is displayed in this low magnification view. Opaque constituents (black material; E2.5,F15,H10) were determined by SEM analysis to be titanium-rich. This material has an erratic distribution, and tends to be closely associated with clays and partially leached grains (E-F7,G11,K1).

MAGNIFICATION: 40X

PLATE 2B

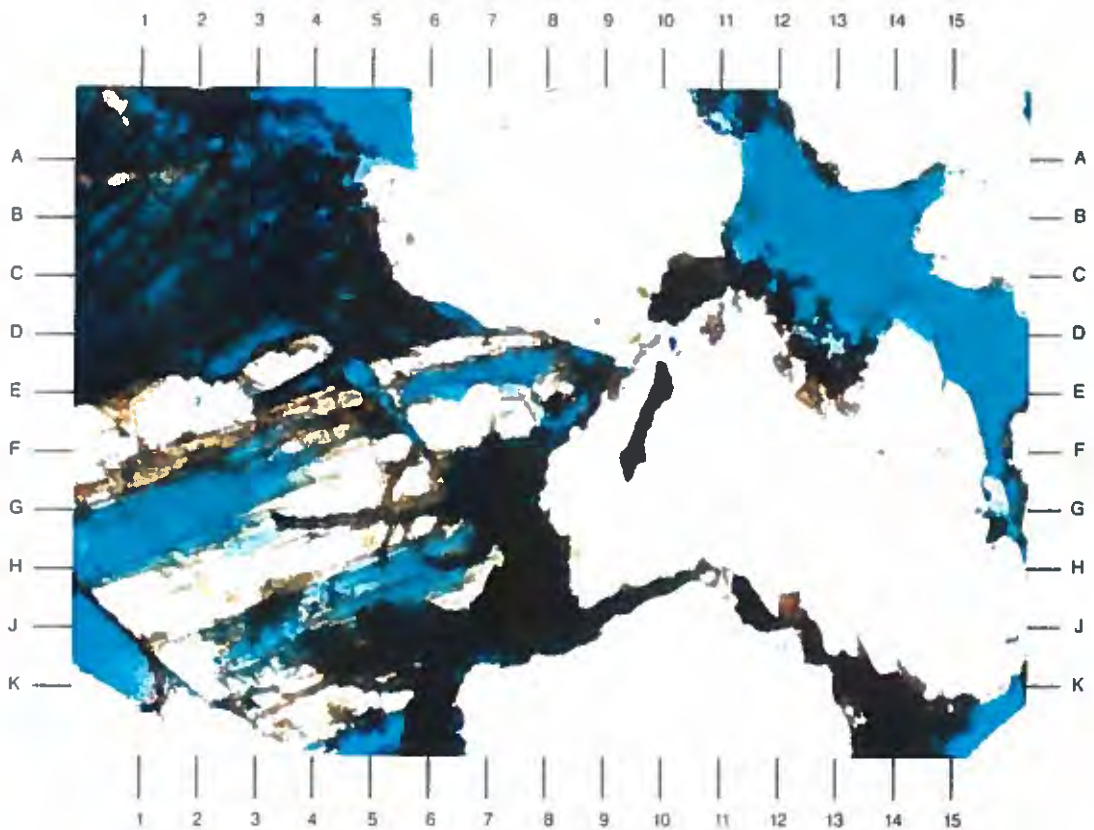
An enlarged view of the area near E8 in Plate 2A is shown in this photomicrograph. Primary intergranular pores (B12,D15,A5) are commonly lined by opaque, titanium-rich material (A4,C11.5, above A11.5). This material has also infiltrated a partly leached plagioclase feldspar grain at E4 to K5.

MAGNIFICATION: 200X



A

0.25 mm



B

0.05 mm

SAMPLE DEPTH: 9779 FEET

PLATE 3A

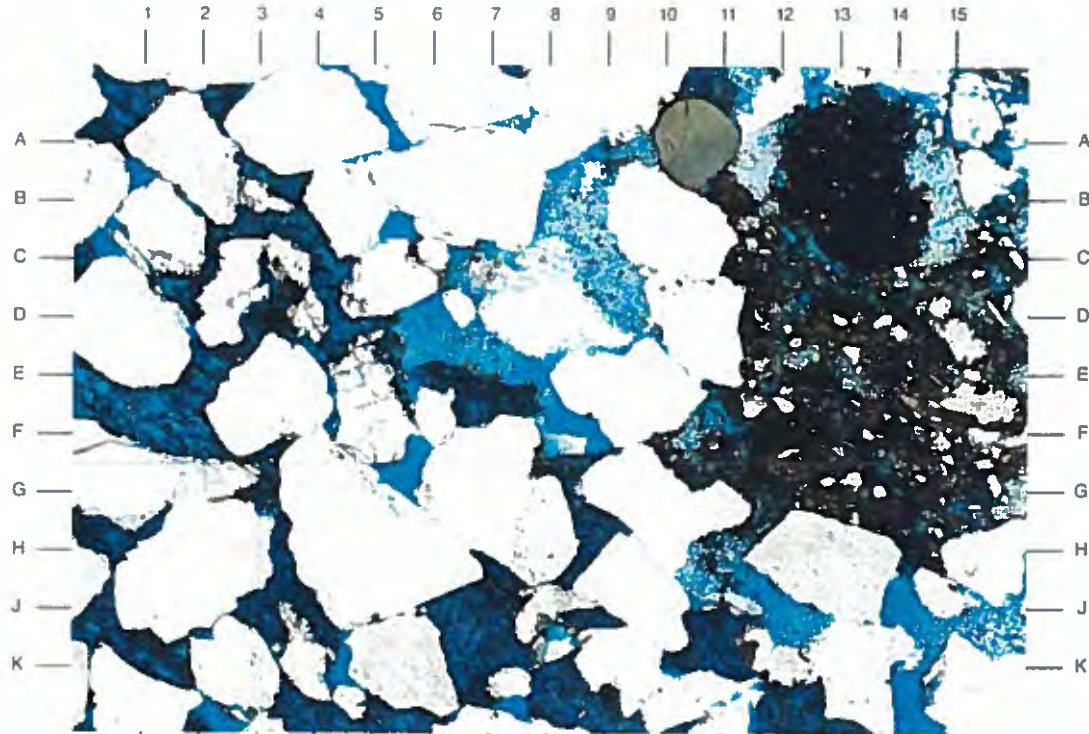
A general overview shows several erratically distributed components in this poorly sorted, medium-grained sandstone. Ankerite cement (stained dark blue; F1.5,J7,J-K11) occluded porosity within limited regions of the sample. Both detrital clays (C12-G15) and authigenic kaolinite (B-C8.5,D9,A-B14.5) have a patchy, pore-filling habit as well. Note the relatively uncommon tourmaline grain at A10.5.

MAGNIFICATION: 40X

PLATE 3B

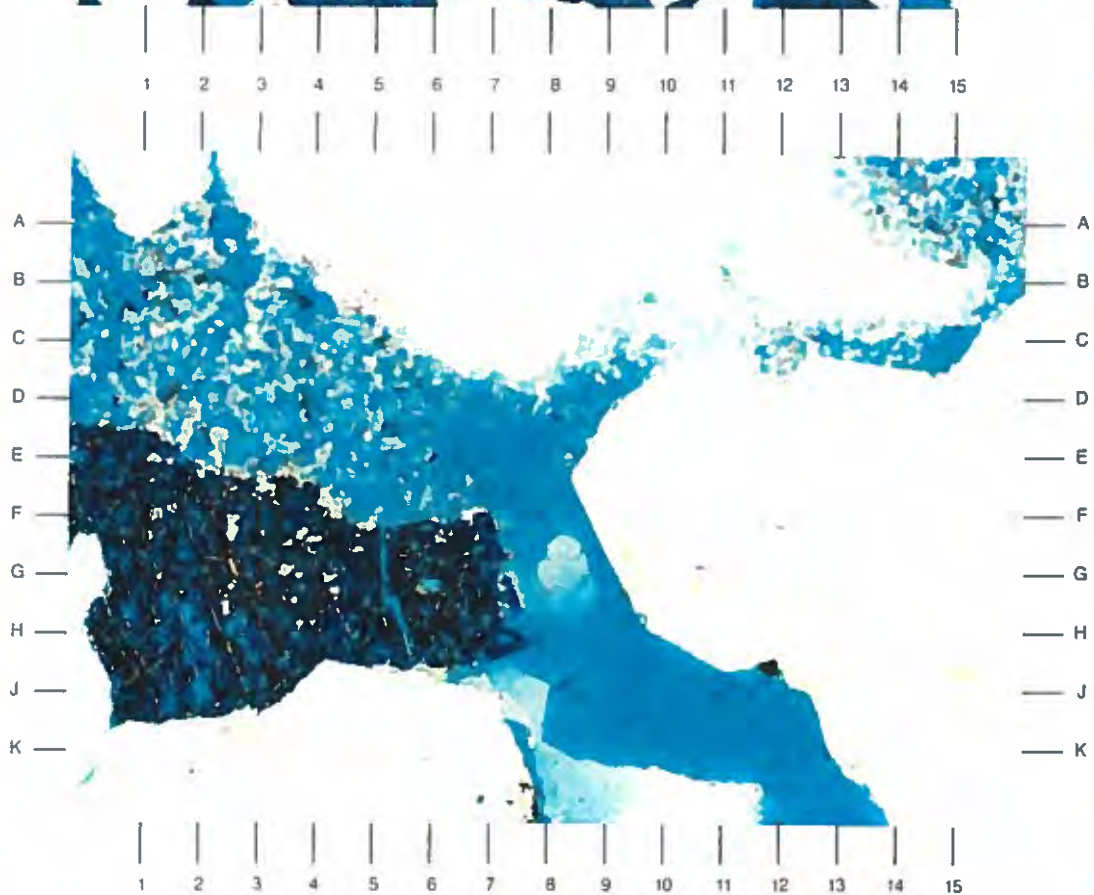
An enlarged view of the area near E8 in Plate 3A is shown in this photomicrograph. Primary intergranular pores range from open (H9-K12) to largely blocked by ankerite (G1-G7) and microporous, authigenic kaolinite (D1-D5,A15). The flat edges of quartz grains (G9.5,D9.5,J6) represent secondary quartz overgrowths.

MAGNIFICATION: 200X



A

0.25 mm



B

0.05 mm

SAMPLE DEPTH: 9782 FEET

PLATE 4A

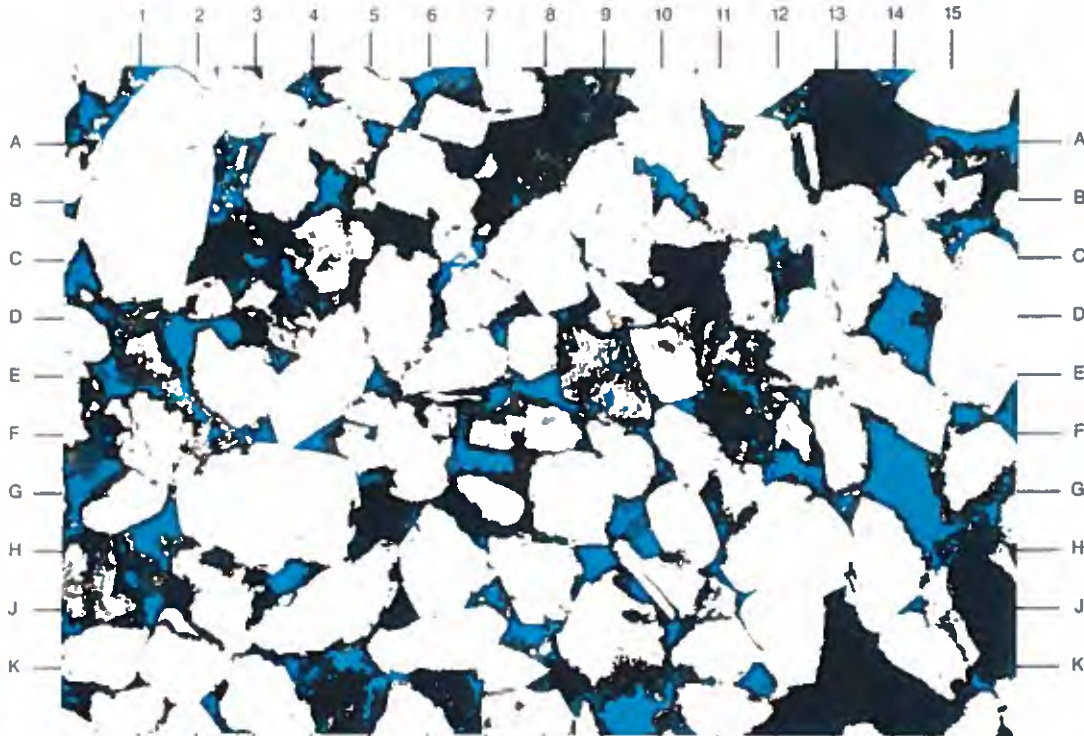
A massive, moderately sorted, fine-grained sandstone is displayed in this low magnification view. Titanium-rich opaque constituents (black material) lines pore walls (D14.5,B4.5), infills open pore space (J-K13,C10.5), and replaces selective grains (A13). Most of the framework grains are monocrystalline and polycrystalline quartz (B1,G3,H12).

MAGNIFICATION: 40X

PLATE 4B

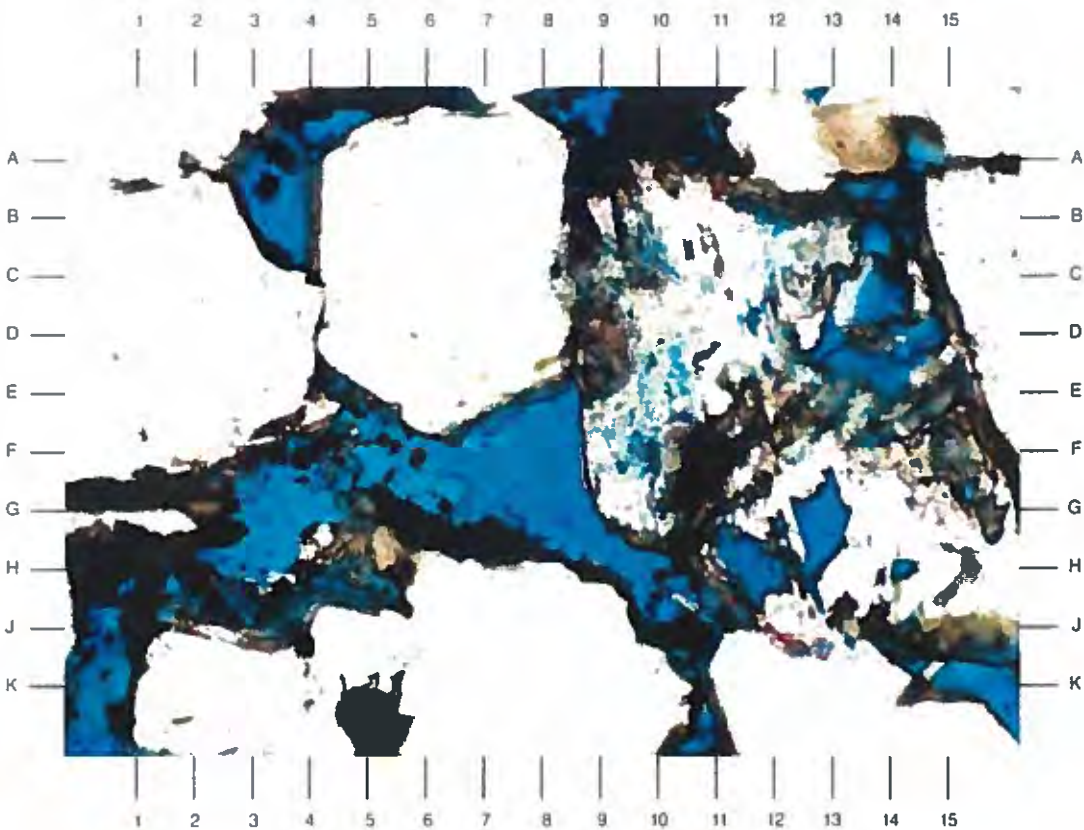
An enlarged view of the area near E8 in Plate 4A is shown in this photomicrograph. Both secondary pores (F11) and primary intergranular pores (A4,G4,A9) are lined or filled by opaque, titanium-rich material. Considerable amounts of secondary (E10,F9.5) and primary (G8) porosity remain open.

MAGNIFICATION: 200X



A

0.25 mm



B

0.05 mm

SAMPLE DEPTH: 9789 FEET

PLATE 5A

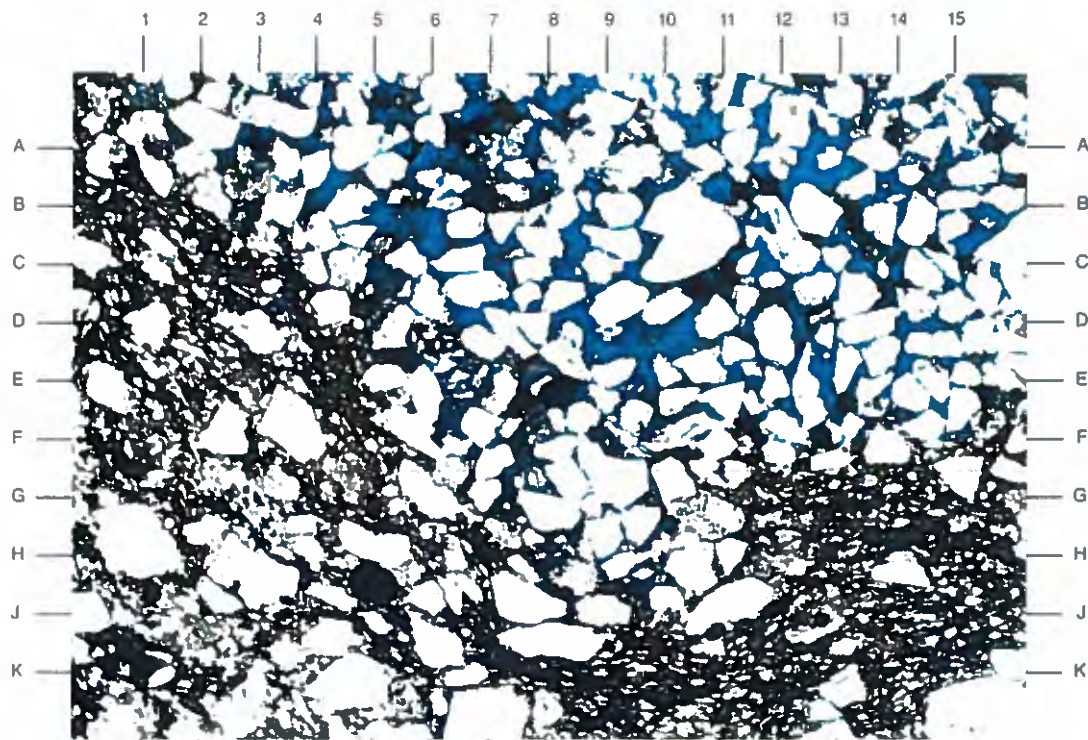
Generally poor reservoir quality is displayed in this poorly sorted, very fine-grained sandstone. Contorted shale laminations (B1-K7-J15) are the result of bioturbation, and lie adjacent to relatively clean sand laminations which are well cemented by ankerite (B4-B15.5). Almost all of the primary intergranular pore space is occluded by detrital clay and ankerite.

MAGNIFICATION: 40X

PLATE 5B

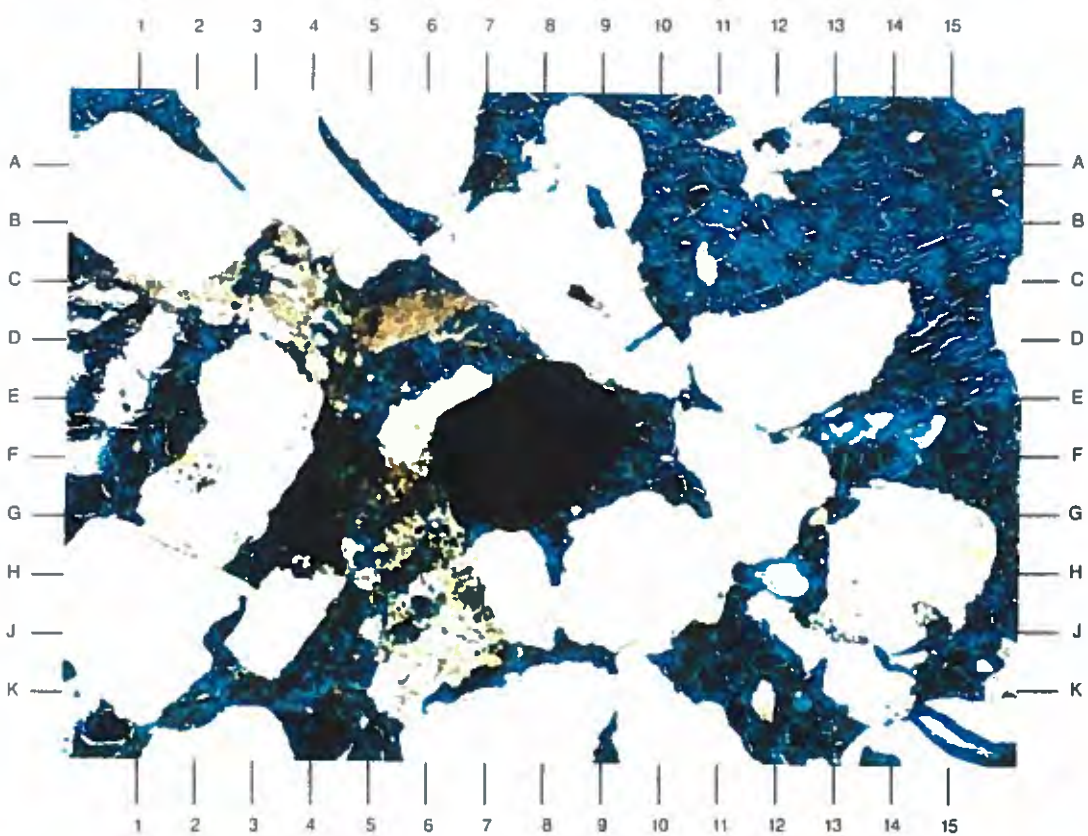
An enlarged view of the area near E8 in Plate 5A is shown in this photomicrograph. Framework grains of quartz (B1,H10,J1) and lithic fragments (J6.5,D5) are cemented initially by quartz overgrowths (B3,G11), and then later cemented by pervasive ankerite (A15-F15,E1.5,A10). Only trace amounts of visible porosity (above F14) remain.

MAGNIFICATION: 200X



A

0.25 mm



B

0.05 mm

DuPont Environmental Remediation Services
Delisle Plant No. 4 S/T No. 1 Well
Harrison County, Mississippi

File No. GH-2562

SAMPLE DEPTH: 9842 FEET

PLATE 6A

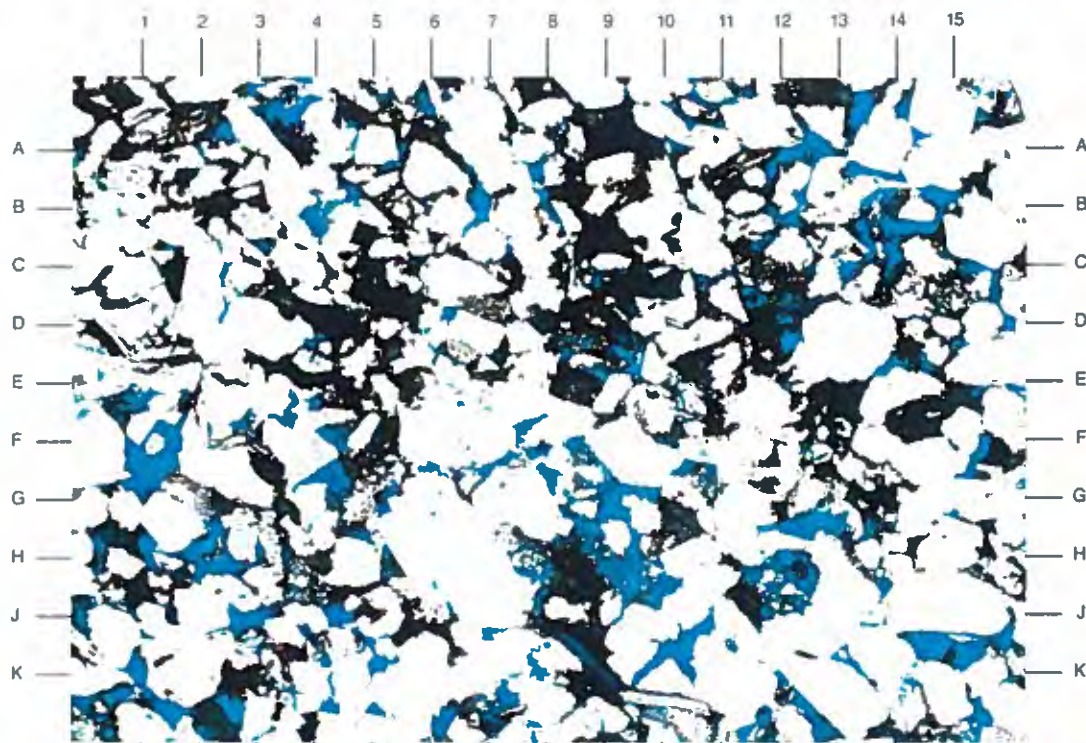
A low magnification view shows the massive nature of this moderately sorted, fine-grained sandstone. Titanium-rich opaque constituents (black material; A9,D4.5) have precipitated within portions of the pore system, whereas other areas retain fairly open pore bodies (F1.5,J-K10.5). While most of the framework grains are quartz (J15,D3), low amounts of feldspar (G2,G5) and muscovite (below K10) are observed.

MAGNIFICATION: 40X

PLATE 6B

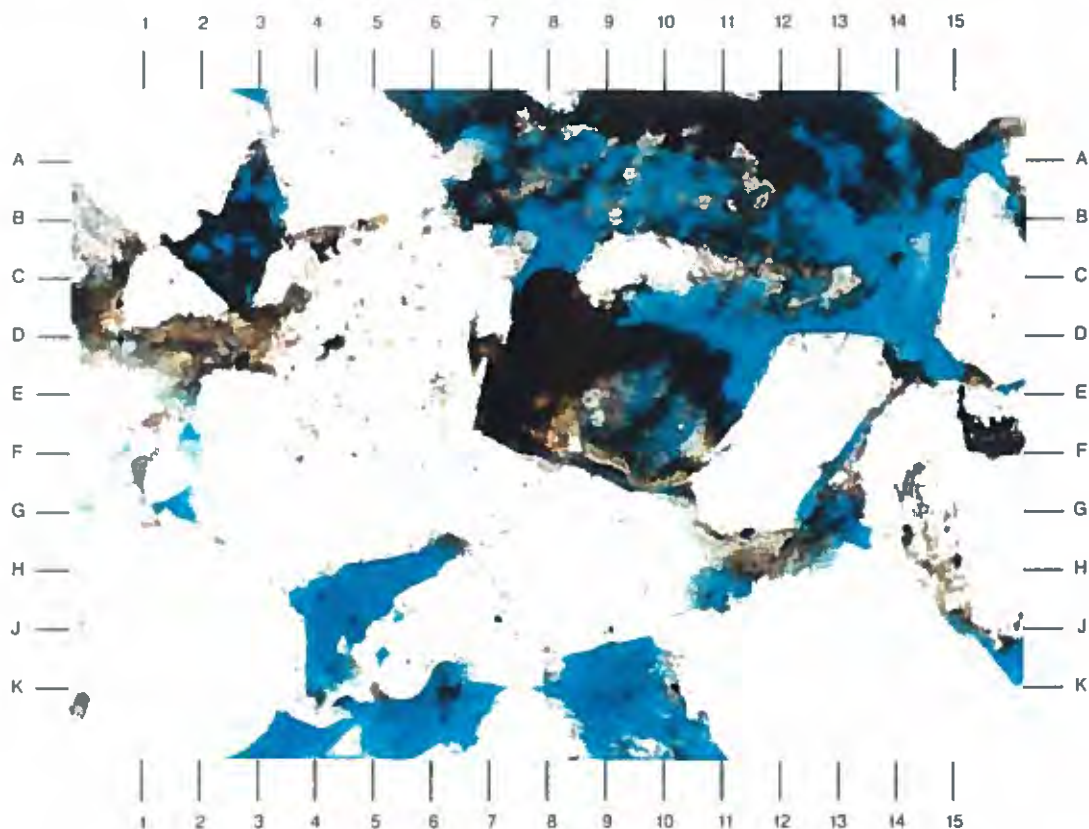
An enlarged view of the area near E8 in Plate 6A is shown in this photomicrograph. The black to dark brown material (A12,D8,B3) was found to be titanium-rich by SEM analysis, and has partially blocked intergranular pores (C-D14) and grain-moldic secondary pores (C8-E11). This material is also observed along thin dust rims (F15) which define quartz overgrowth (E15) contacts.

MAGNIFICATION: 200X



A

0.25 mm



B

0.05 mm

SAMPLE DEPTH: 9876 FEET

PLATE 7A

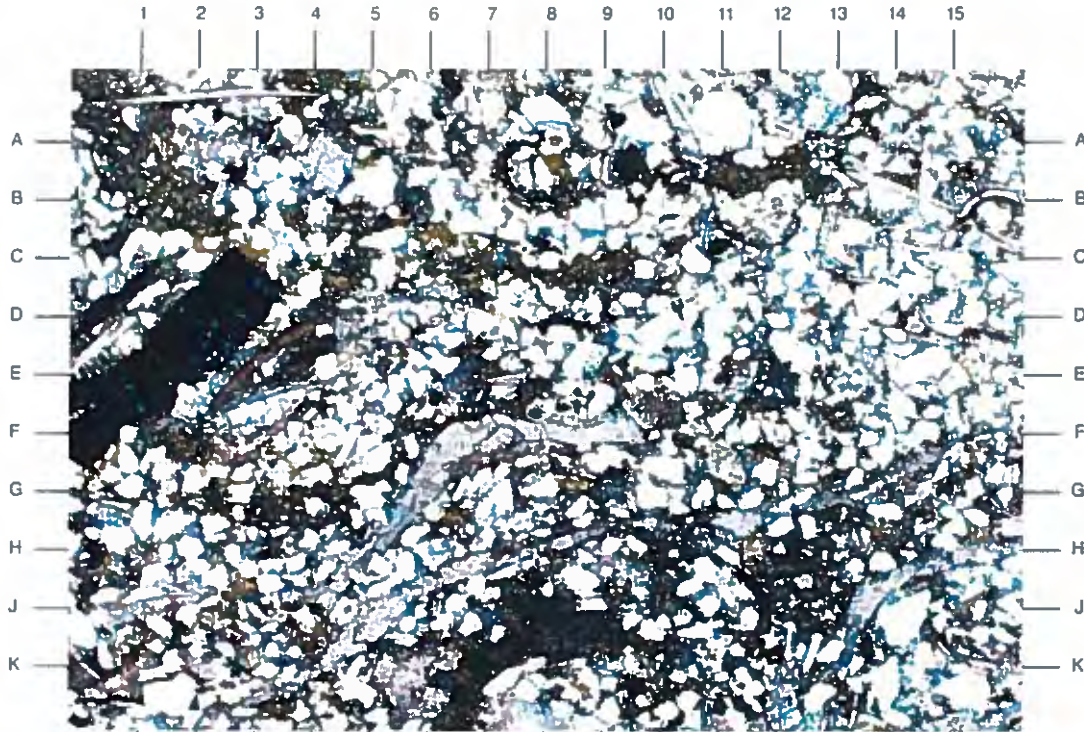
A poorly sorted, very fine-grained sandstone with abundant calcareous fossil fragments is shown in this low magnification view. The elongate fossil fragments (J13.5,J5,F7) show a subparallel orientation with minor shale laminations (C9,G3.5). Plant fragments (D2.5) and secondary siderite (J-K8) have an erratic distribution.

MAGNIFICATION: 40X

PLATE 7B

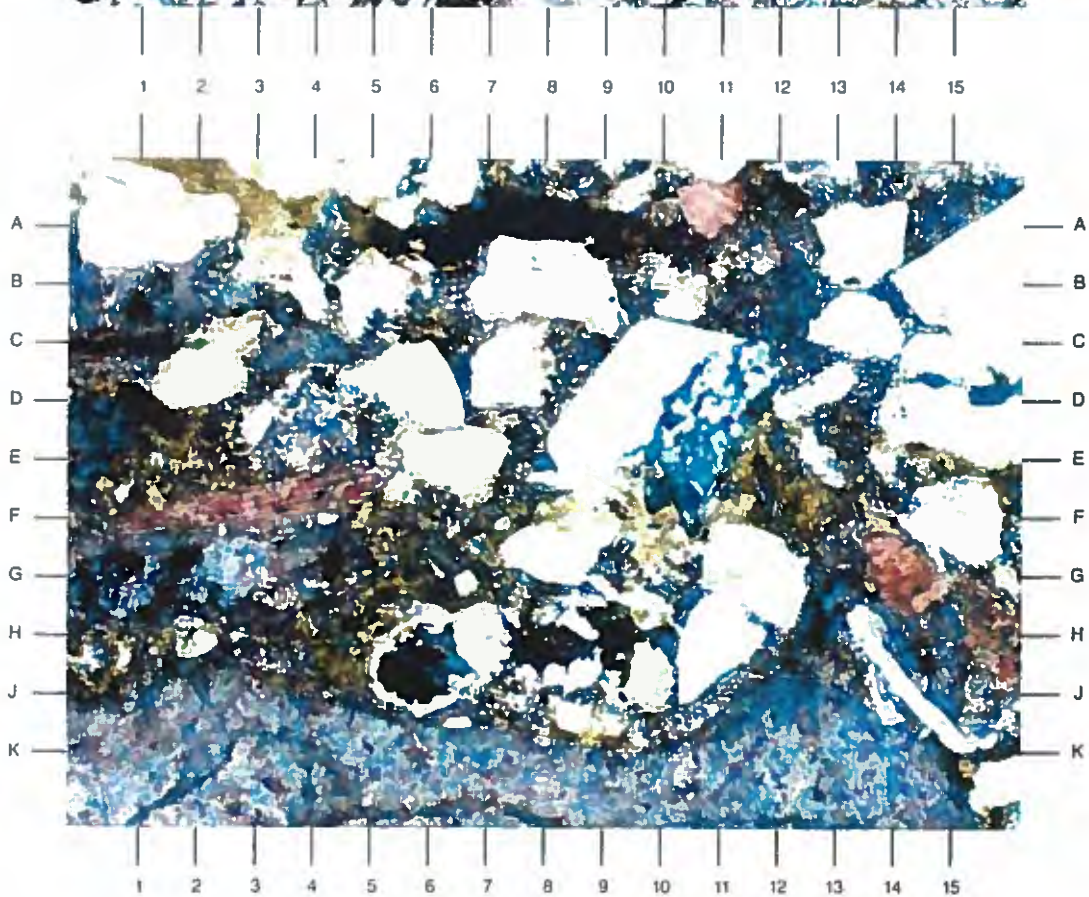
An enlarged view of the area near E8 in Plate 7A is shown in this photomicrograph. Primary intergranular pores have been mostly infilled by detrital matrix clays (E-F12,A3,G5.5) and secondary ankerite (B-C12,G3,B2). Fossil fragments are composed of calcite (red stained; A11,F1.5,G14) and iron-rich ankerite (K1-K14).

MAGNIFICATION: 200X



A

0.25 mm



B

0.05 mm

DuPont Environmental Remediation Services
Delisle Plant No. 4 S/T No. 1 Well
Harrison County, Mississippi

File No. GH-2562

SAMPLE DEPTH: 9907 FEET

PLATE 8A

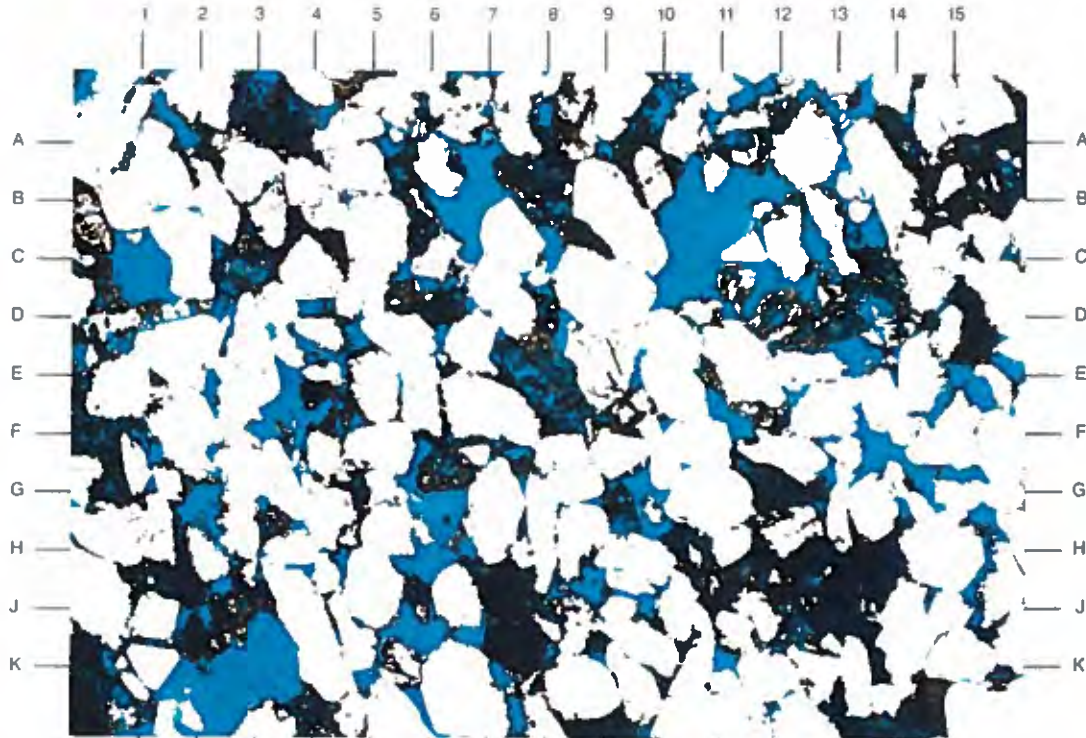
This general overview shows a massive, moderately sorted, fine-grained sandstone. Secondary pores are generally large in size and range from open (C10.5,K3) to largely blocked (A3.5,J13) by titanium-rich opaque constituents. This material is also found erratically distributed within primary intergranular pore system (A14,H-J1.5).

MAGNIFICATION: 40X

PLATE 8B

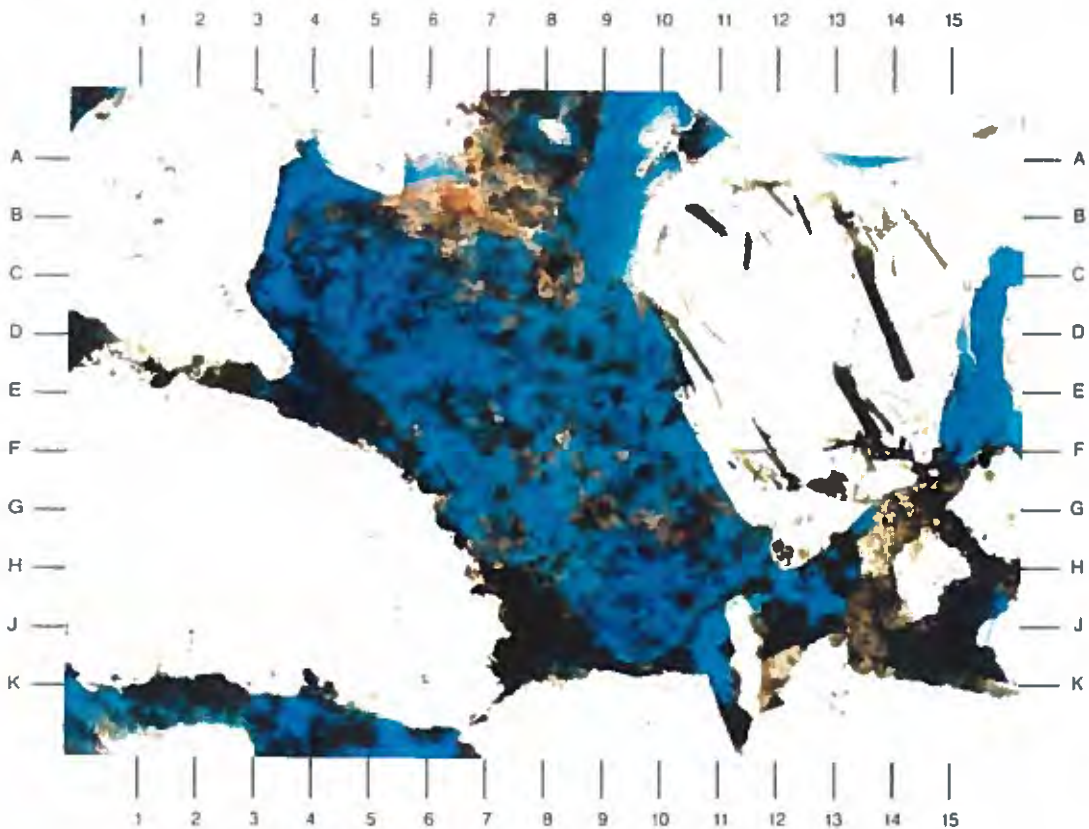
An enlarged view of the area near E8 in Plate 8A is shown in this photomicrograph. A relatively unstable framework grain, probably feldspar, was almost completely removed by secondary dissolution (B4-J10). Titanium-rich material (E4,J15,J8) is commonly observed lining pore walls and partially infilling available pore space.

MAGNIFICATION: 200X



A

0.25 mm



B

0.05 mm

DuPont Environmental Remediation Services
Delisle Plant No. 4 S/T No. 1 Well
Harrison County, Mississippi

File No. GH-2562

SAMPLE DEPTH: 9917 FEET

PLATE 9A

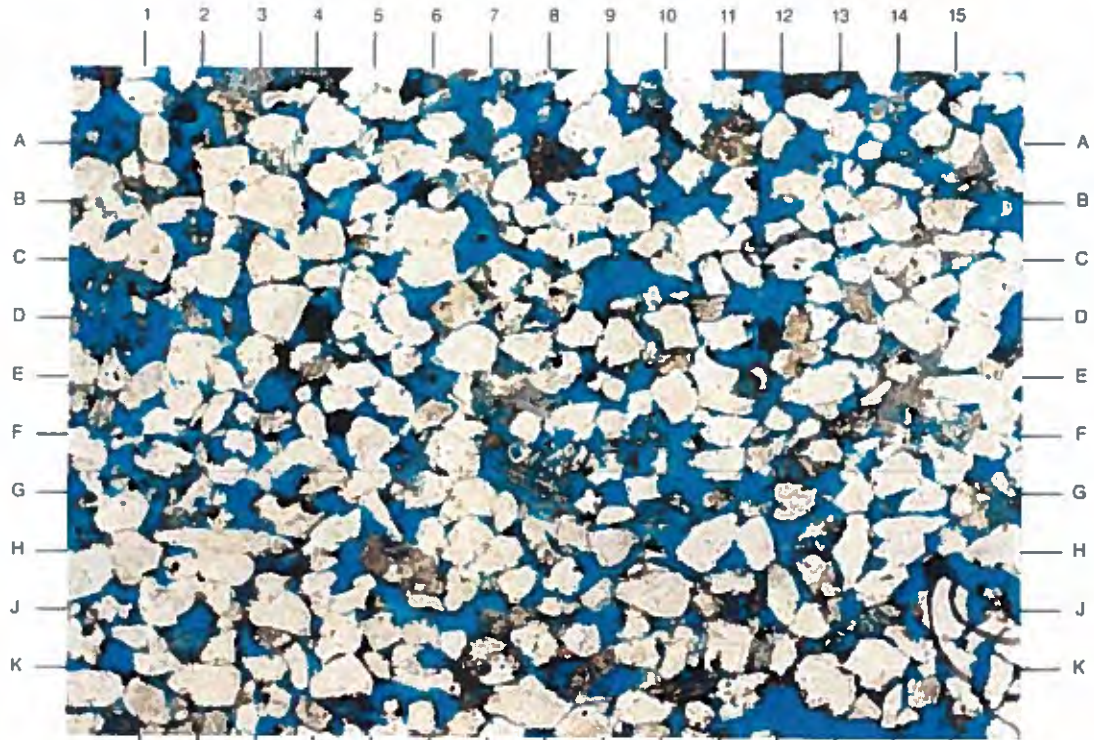
A general overview shows the good porosity development (blue epoxy-filled areas) in this massive, moderately well sorted, fine-grained sandstone. Primary intergranular pores (A14,J14) and secondary pores (below C9,G8) are generally open and evenly distributed. Some areas are moderately well cemented by secondary quartz overgrowths (D15.5,H-J2).

MAGNIFICATION: 40X

PLATE 9B

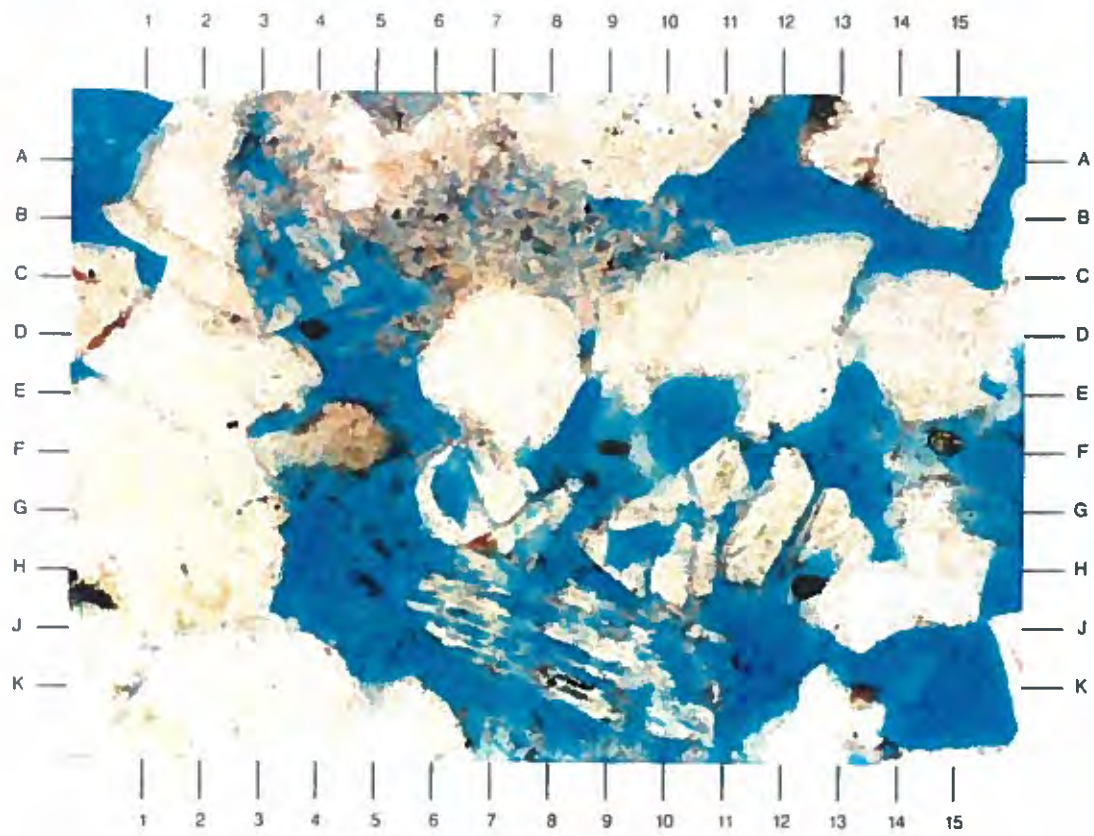
An enlarged view of the area near F8 in Plate 9A is shown in this photomicrograph. Diagenesis has significantly influenced porosity development in this sandstone. Porosity-reducing events include compaction, quartz overgrowth cementation (C2,J1), and precipitation of pore-filling kaolinite (C6-B8). On the other hand, secondary dissolution (C3,G6.5,J7.5) has enhanced porosity.

MAGNIFICATION: 200X



A

0.25 mm



B

0.05 mm

SAMPLE DEPTH: 9928 FEET

PLATE 10A

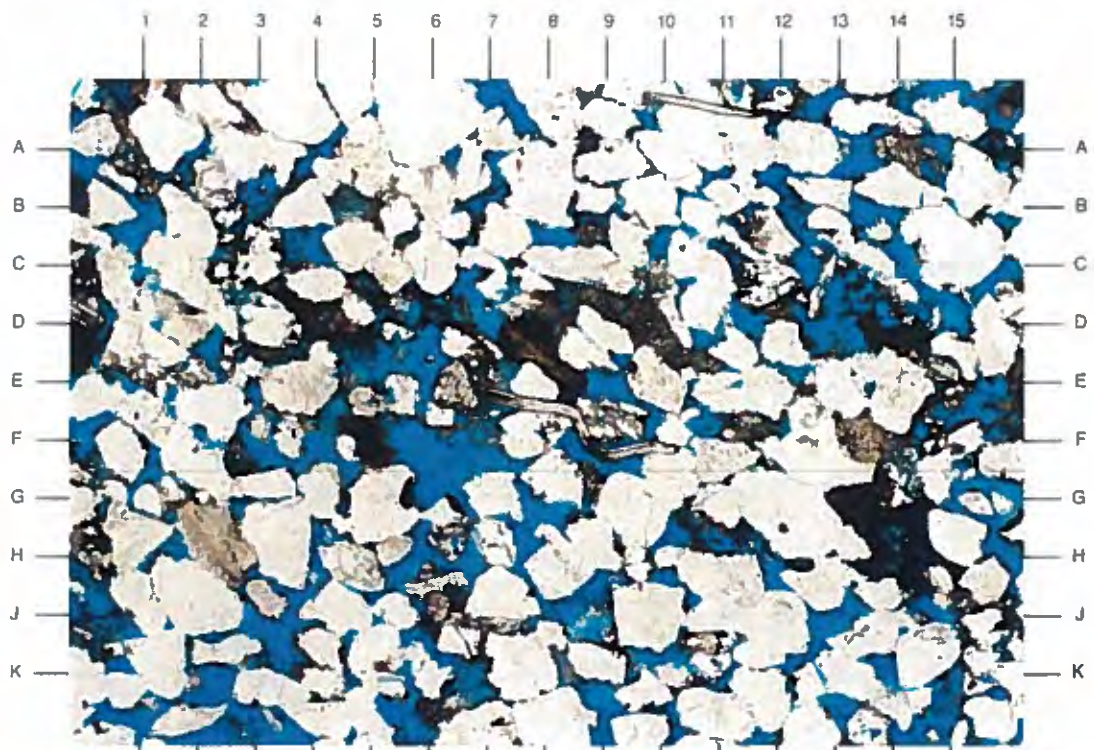
A massive, moderately sorted, fine-grained sandstone is displayed in this low magnification view. The pore system is a combination of primary intergranular porosity (B13.5,J13) and secondary porosity (F-G6,D13), and has a variable distribution. The dominant framework grain is quartz (G12,H3.5,A6), with lesser amounts of lithic fragments (F13.5,D9.5) and plagioclase (H2.5).

MAGNIFICATION: 40X

PLATE 10B

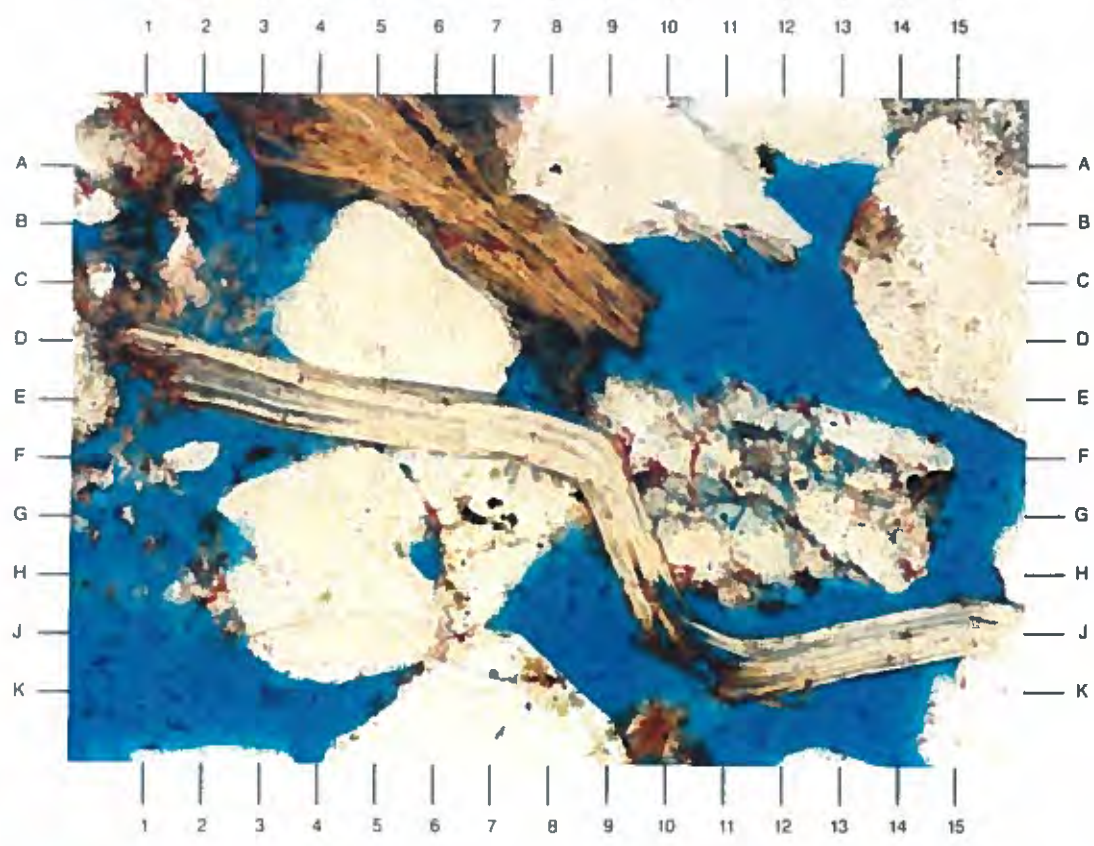
An enlarged view of the area near E8 in Plate 10A is shown in this photomicrograph. The detrital muscovite flakes at E2 to J15 have been strongly contorted against more resistant framework grains, due to compaction. The biotite at A4 to C8 has been pinched between two quartz grains (C5,B9).

MAGNIFICATION: 200X



A

0.25 mm



B

0.05 mm

APPENDIX D

**SCANNING ELECTRON MICROSCOPE
PHOTOMICROGRAPHS AND DESCRIPTIONS**

(Note the micron bar at the lower right portion of each photomicrograph for scale)

DuPont Environmental Remediation Services
Delisle Plant No. 4 S/T No. 1 Well
Harrison County, Mississippi

File No. GH-2562

SAMPLE DEPTH: 9672 FEET

PLATE 11A

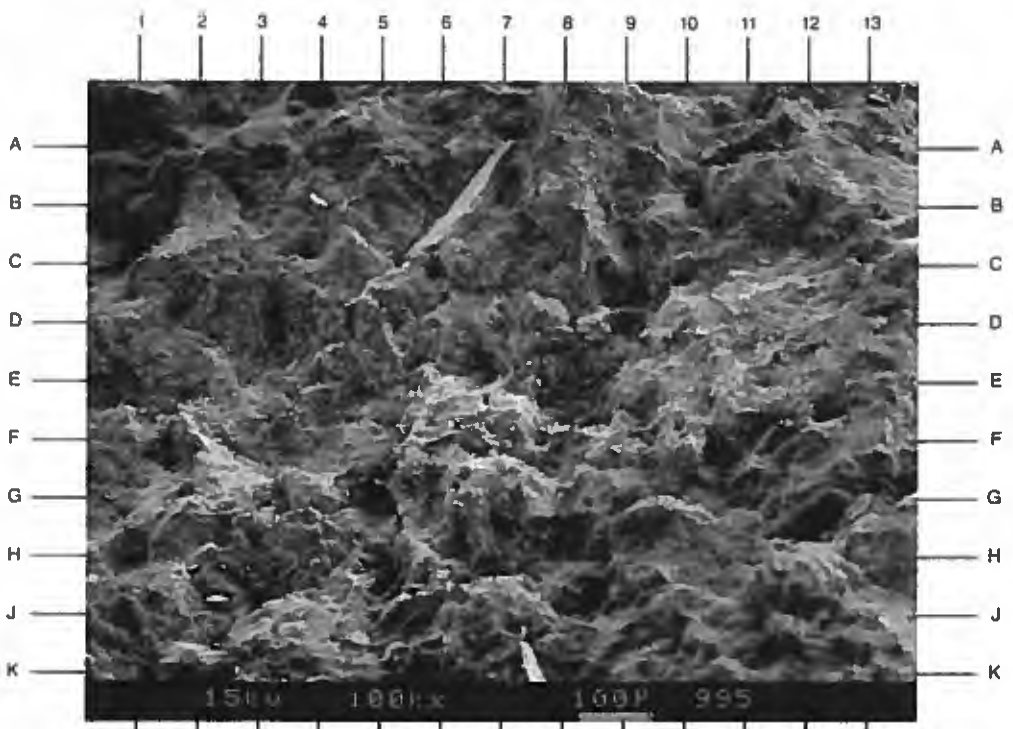
Low porosity development is exhibited at this depth. The shaly, very fine-grained sandstone contains abundant detrital matrix (F8,B-C11) which infills most of the primary intergranular pore space. Relatively large flakes of detrital muscovite (B6.5) show only slight deformation due to compactional effects.

MAGNIFICATION: 100X

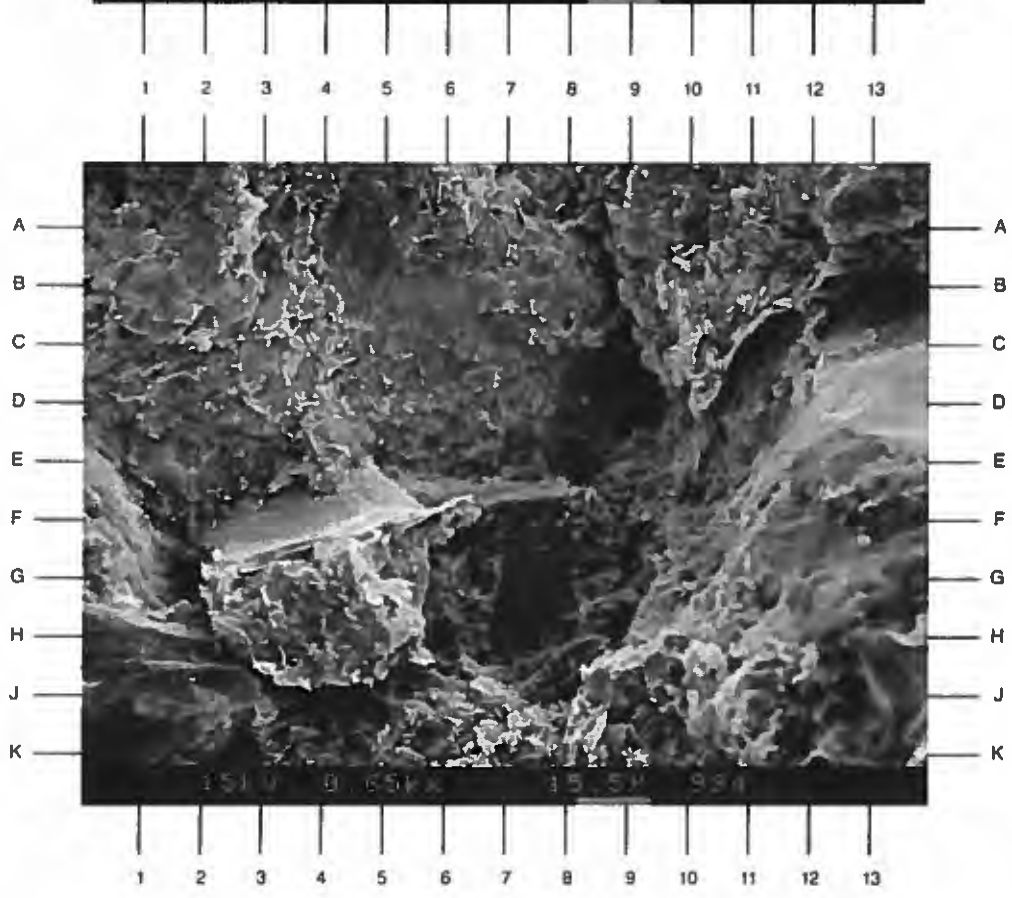
PLATE 11B

An enlarged view of the area near D9 in Plate 11A is shown in this photomicrograph. Chlorite is finely intermixed with illitic clay types to form a pervasive matrix (A11-G9,K4,C-D4) which is detrital in origin. Minor detrital muscovite flakes (F5) are also observed. Note the incipient quartz overgrowths at D13.

MAGNIFICATION: 650X



A



B

SAMPLE DEPTH: 9672 FEET

PLATE 12A

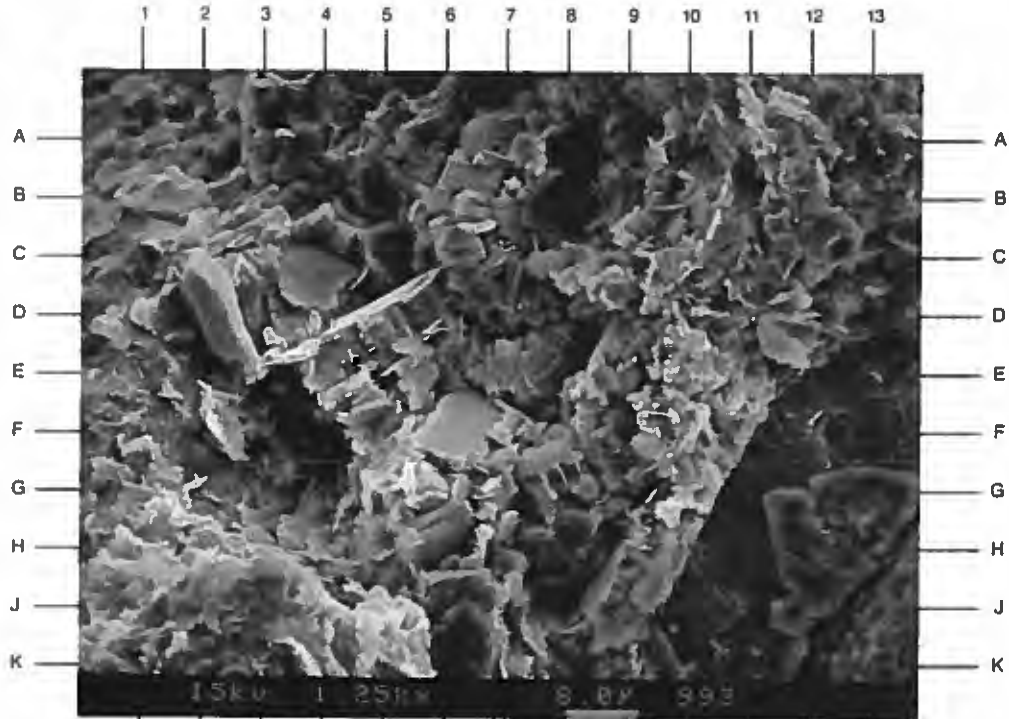
Authigenic kaolinite is highlighted in the photomicrograph on the facing page. A primary intergranular pore has been completely infilled by kaolinite (A7-J7,D3-D9). This secondary kaolinite occurs as aggregates of stacked platelets, or booklets, which have a high associated microporosity (A8.5,E5).

MAGNIFICATION: 1,250X

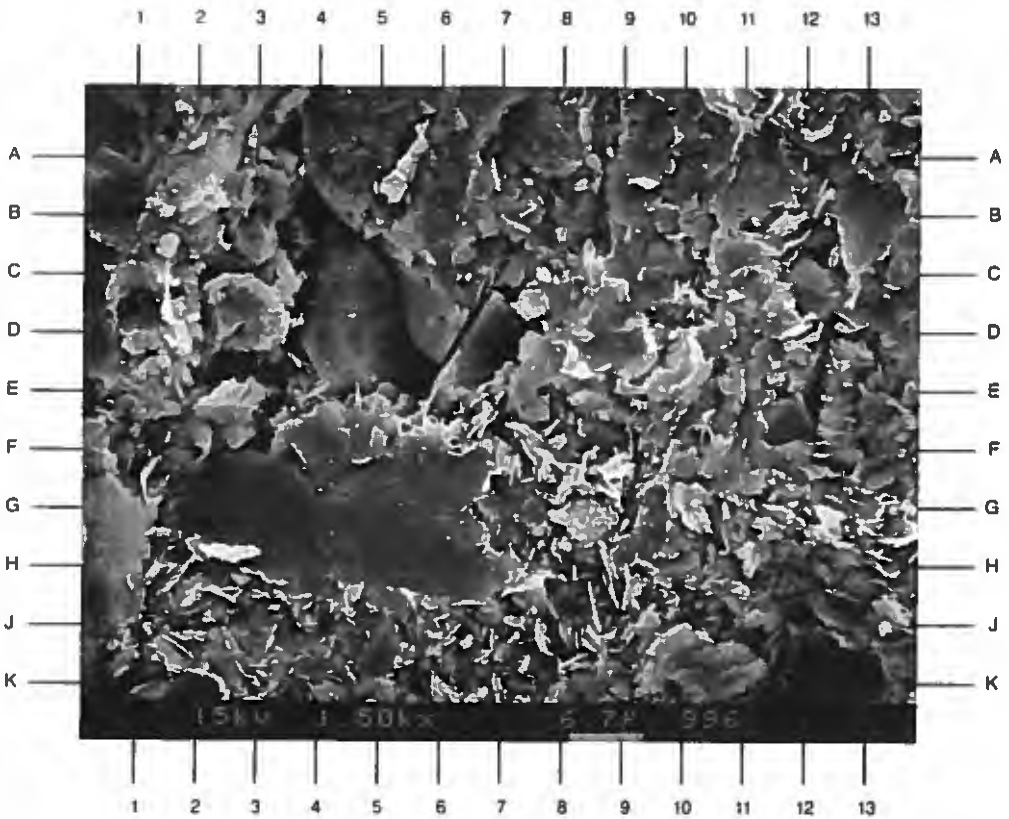
PLATE 12B

A poorly developed porosity system is presented in this field of view. Intergranular pores have been largely occluded by detrital matrix clays, and remaining open pores (B4,E5.5) are widely scattered and poorly interconnected. Microporosity (A12,J8,H2) is the dominant pore type present in this sandstone, and is largely associated with the chloritic and illitic matrix (K6-F13,H-J2,A8.5-A13).

MAGNIFICATION: 1,500X



A



B

DuPont Environmental Remediation Services
Delisle Plant No. 4 S/T No. 1 Well
Harrison County, Mississippi

File No. GH-2562

SAMPLE DEPTH: 9757 FEET

PLATE 13A

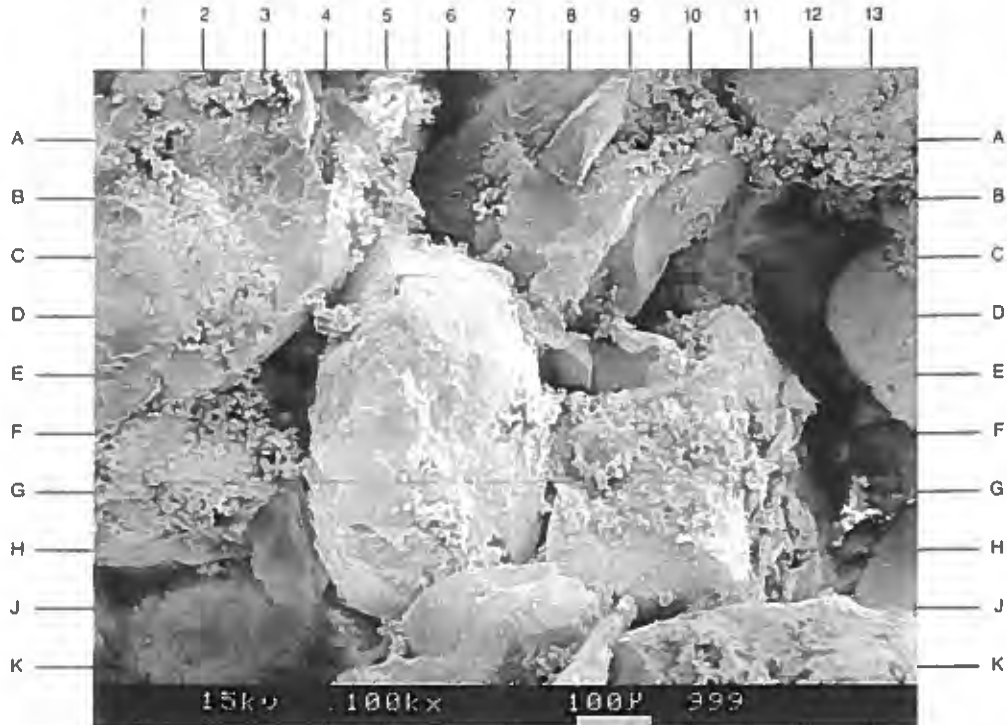
A well developed intergranular pore system (E-F12,E3.5,A6) is displayed in this low magnification view. Quartz sand grains (F5,C1,J7) are typically subangular and medium sand-sized, and are cemented primarily by secondary quartz overgrowths (C-D9,J5). The fine, granular material (F-G3.5,A10,F10) represents titanium-rich material deposited within the pore system.

MAGNIFICATION: 100X

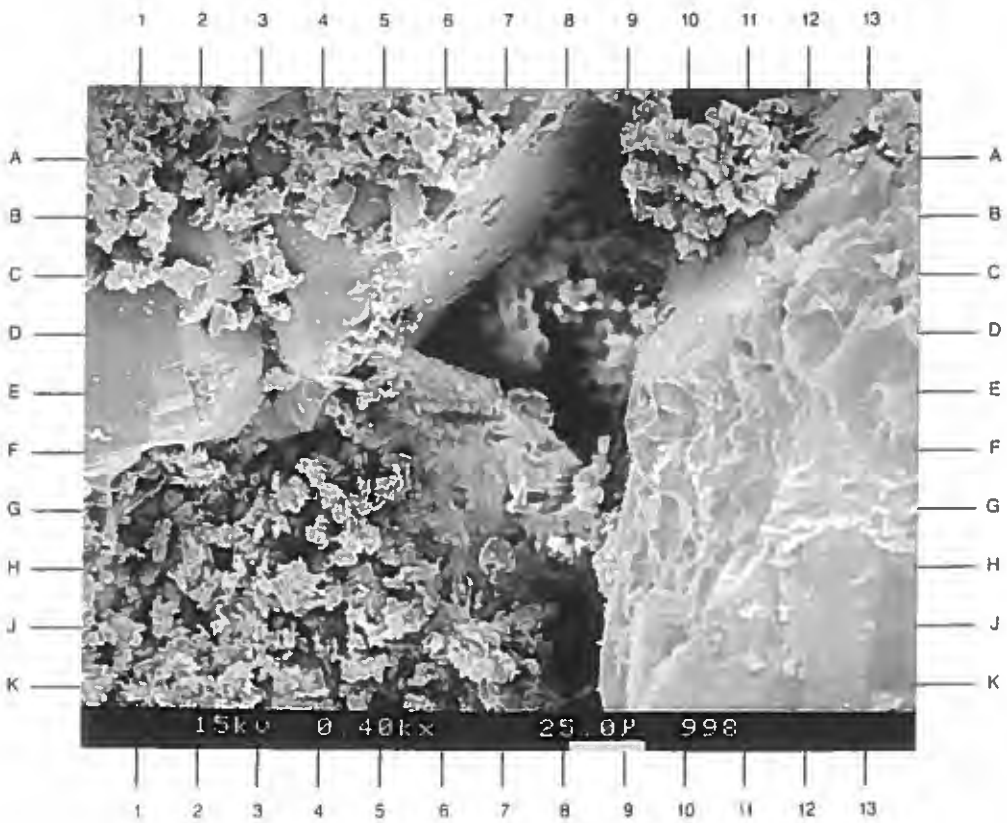
PLATE 13B

An enlarged view of the area near E3 in Plate 13A is shown in this photomicrograph. Secondary quartz overgrowths (E1,D3.5,B12) occur as flat to pseudo-hexagonal crystal surfaces on host quartz sand grains. Aggregates of very fine granular material (A9-A11.5,H1-H6,A1-A6) represent a titanium-rich compound deposited within the pore system.

MAGNIFICATION: 400X



A



B

DuPont Environmental Remediation Services
Delisle Plant No. 4 S/T No. 1 Well
Harrison County, Mississippi

File No. GH-2562

SAMPLE DEPTH: 9757 FEET

PLATE 14A

Secondary quartz overgrowths (D9-B11,A11,D7,D5.5) are well developed in portions of this sandstone. These overgrowths act to fuse adjacent sand grains (F13,A6) and partially occlude associated pores (G6,J4) and pore throats (C9). Precipitates deposited within the pore system include titanium-rich material (G5-K5) and halite (above C9.5,B10).

MAGNIFICATION: 1,250X

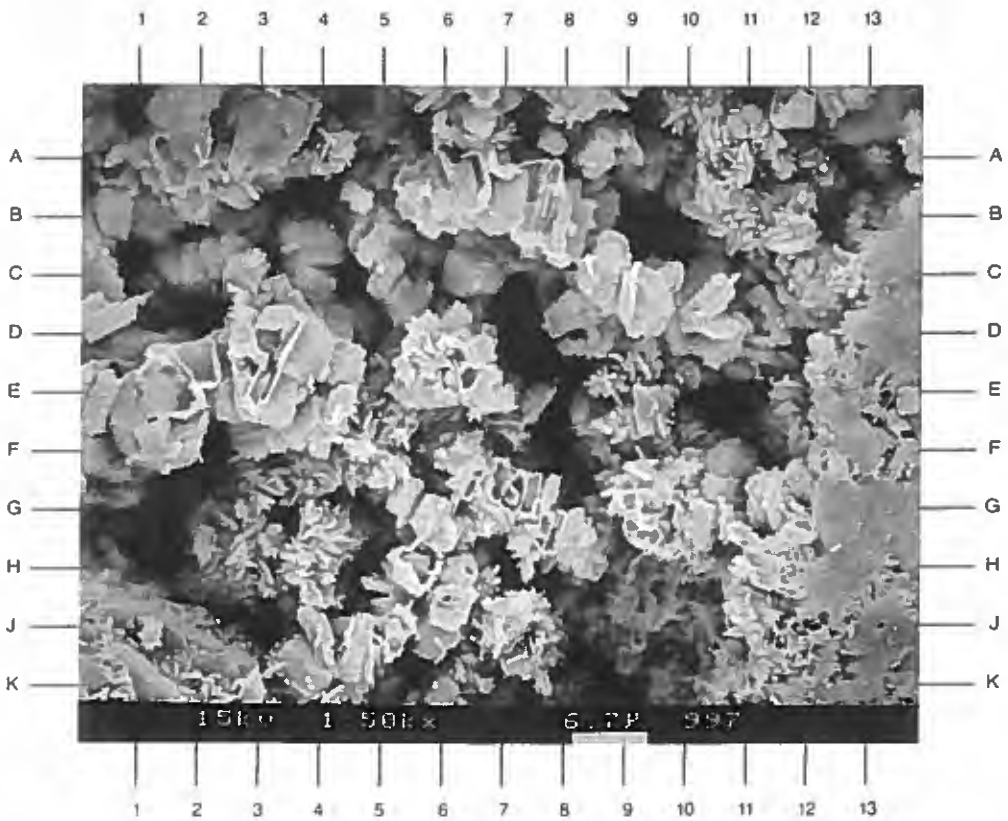
PLATE 14B

Authigenic kaolinite and the titanium-rich material are closely associated in this sandstone. Loose aggregates of kaolinite booklets (B7.5,G7.5) occur as a patchy pore-filling prior to deposition of the titanium material (G-H4,A10.5). The kaolinite acts as a filter upon which the titanium-based material has been deposited. This material displays a microbladed texture in areas.

MAGNIFICATION: 1,500X



A



B

SAMPLE DEPTH: 9779 FEET

PLATE 15A

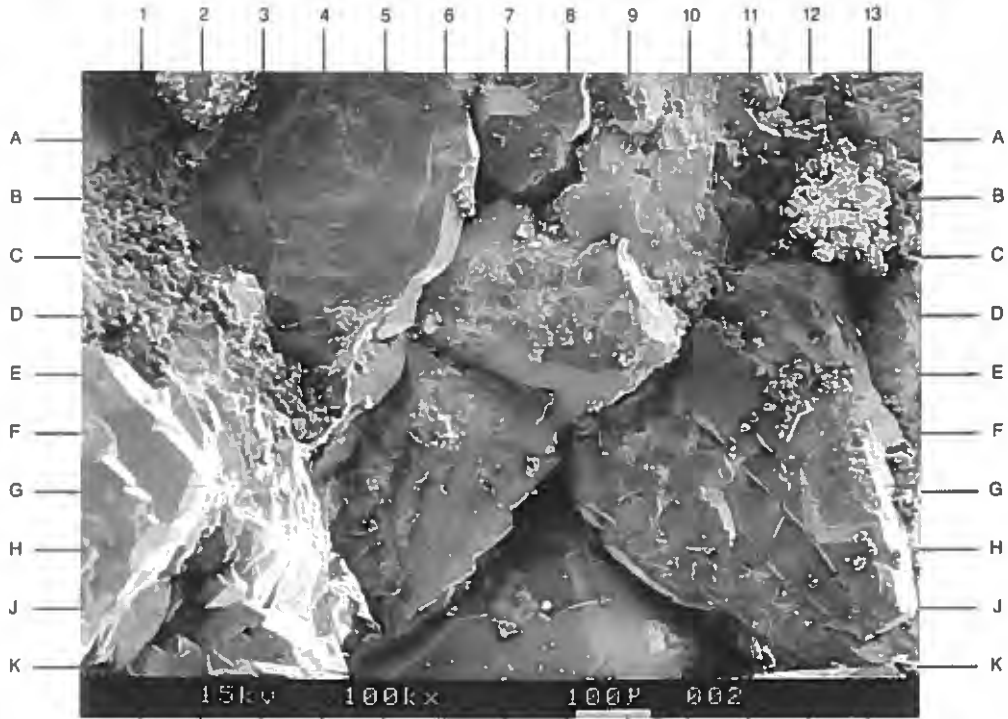
This low magnification view shows a sandstone with the coarsest average grain size (0.37 mm) of those analyzed in this study. The primary intergranular pores range from open (K10.5,G8) to largely occluded by clays (B1,E-F3.5) and a titanium-rich material (D10,B11.5). Secondary quartz overgrowths (H9,E8) are fairly well developed and also act to occlude local porosity.

MAGNIFICATION: 100X

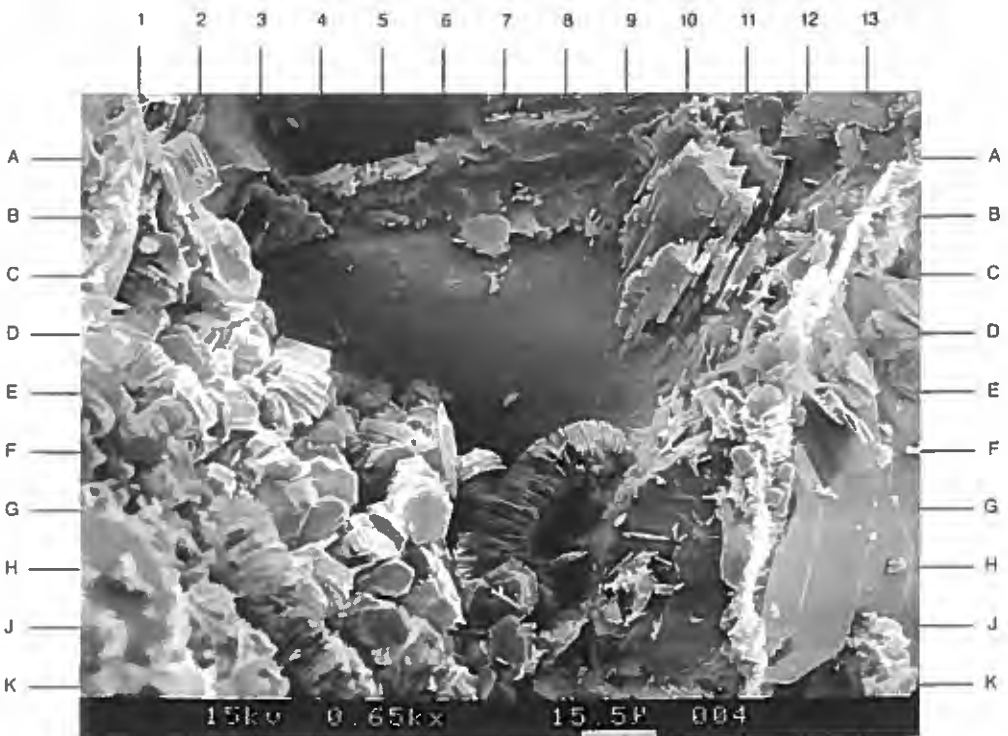
PLATE 15B

An enlarged view of the area near E4 in Plate 15A is shown in this photomicrograph. The void from approximately B3 to B11.5 represents a feldspar grain which was almost completely removed by secondary dissolution. Minor amounts of remnant feldspar (B3.5,B-C10) still exist. Closely associated authigenic kaolinite occurs as aggregates of booklets (A2-J6), which occasionally display a vermicular form (G7-F8.5).

MAGNIFICATION: 650X



A



B

SAMPLE DEPTH: 9779 FEET

PLATE 16A

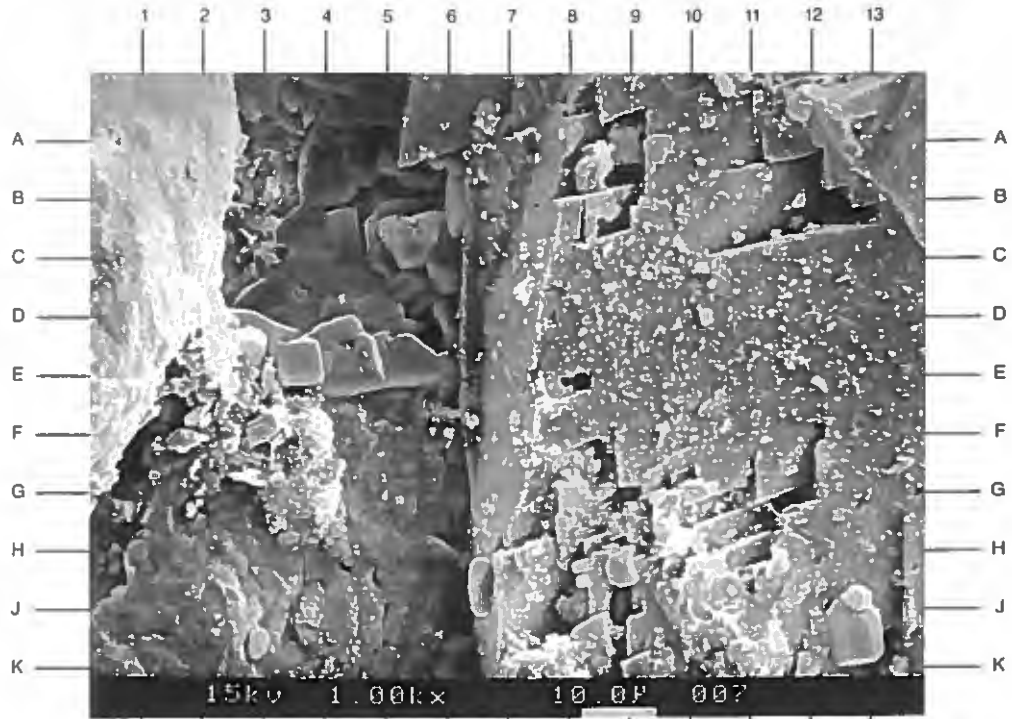
While total feldspar content is relatively low (2% by volume) in this sandstone, the existing feldspars are typically partially leached by secondary dissolution. The plagioclase grain on the right side of this photomicrograph exhibits intragranular porosity (B12,A-B9,G12,J9). Secondary halite (A4-E4) occurs as aggregates of cubic crystals which partially block available pore space. Titanium-rich material (E2-G4) is observed on grain surfaces.

MAGNIFICATION: 1,000X

PLATE 16B

The pore throat at A6 to E13 contains loose pseudohexagonal platelets of authigenic kaolinite (A5,C8,D10). Secondary quartz overgrowths (A3-D6,A8-C13) have reduced pore throat size and are locally inhibited by the earlier formation of grain-coating authigenic chlorite (F4-K3.5,E7). This secondary chlorite occurs as minute platelets with a face-to-edge orientation.

MAGNIFICATION: 1,250X



A



B

SAMPLE DEPTH: 9782 FEET

PLATE 17A

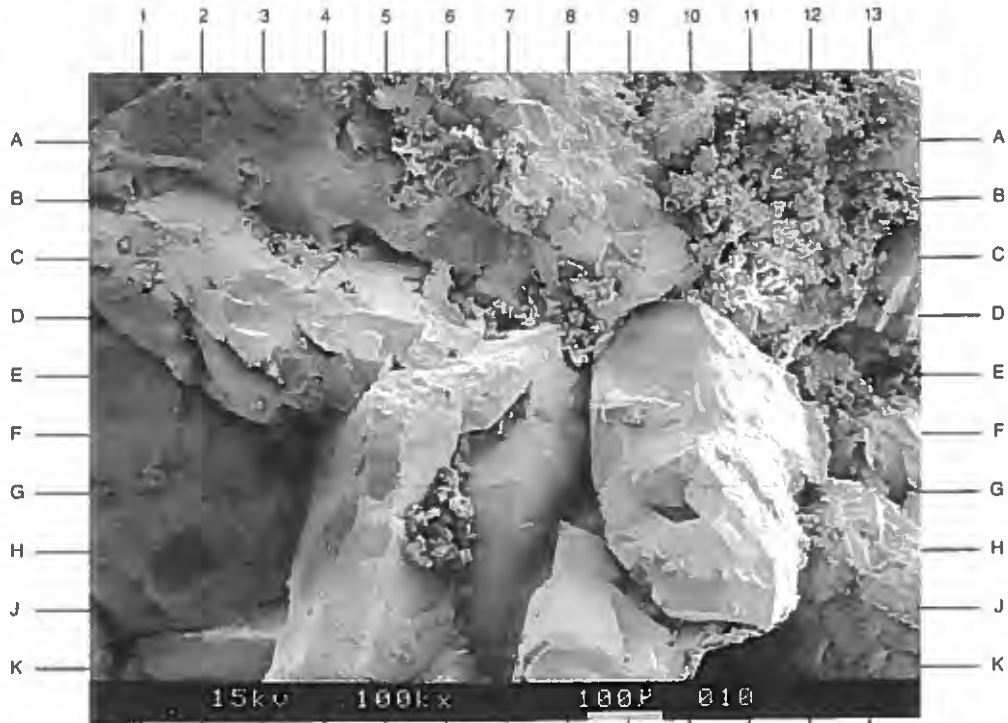
Much of the pore space in this fine-grained sandstone is occupied by a titanium-rich compound (B10-B13,D8,G-H6). A few remaining intergranular pores are partially open (E13,F4,K11). The dominant naturally-occurring secondary cement is quartz overgrowths (J10,J1,B4) which typically occur as flat crystal faces on most quartz sand grains.

MAGNIFICATION: 100X

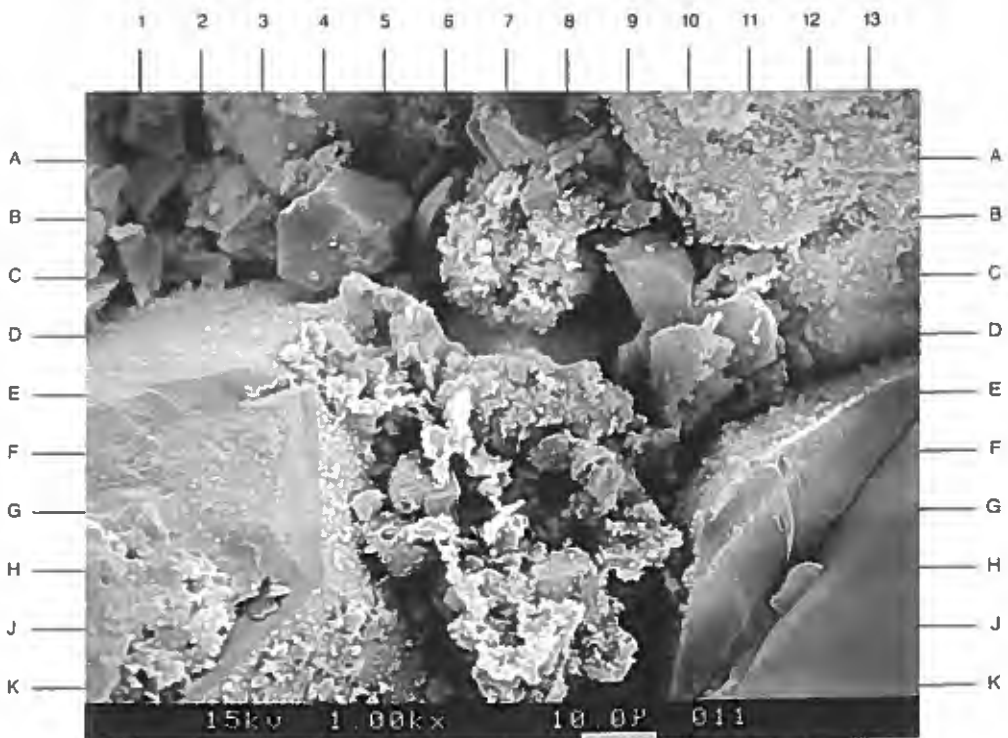
PLATE 17B

An enlarged view of the area near D8 in Plate 17A is shown in this photomicrograph. A titanium-rich material coats the surface of illitic matrix fines (C6-C8,E7,J8.5), as well as the surface of quartz sand grains (A10-A13,K3-K5). The angular fines at B-C4 and C9 appear to have been produced during sample preparation.

MAGNIFICATION: 1,000X



A



B

DuPont Environmental Remediation Services
Delisle Plant No. 4 S/T No. 1 Well
Harrison County, Mississippi

File No. GH-2562

SAMPLE DEPTH: 9782 FEET

PLATE 18A

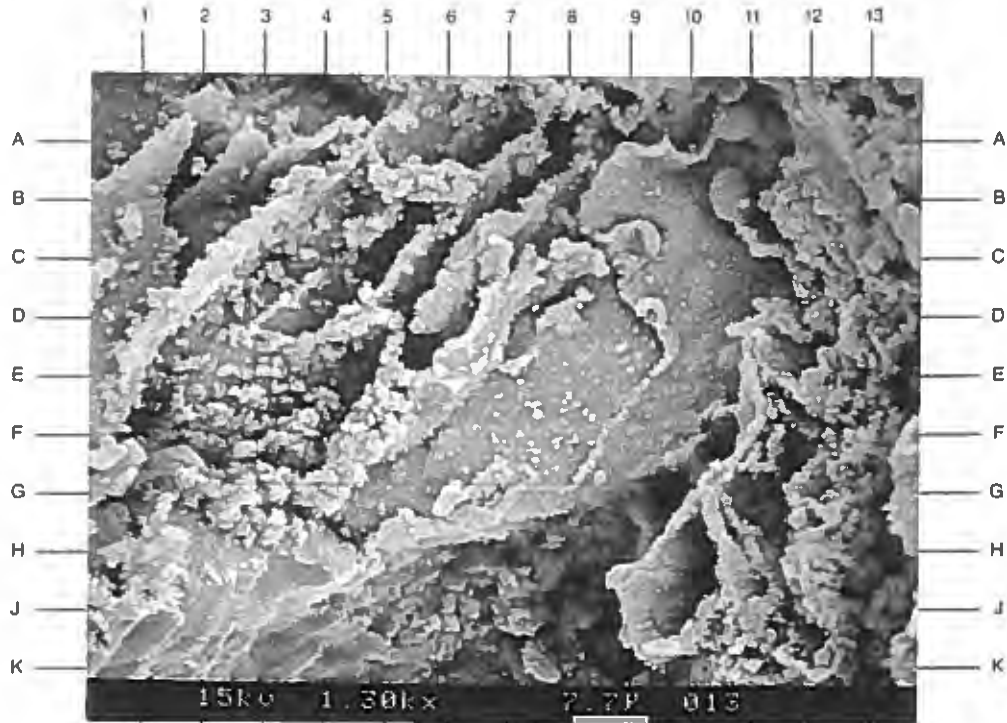
This photomicrograph highlights a feldspar grain which was strongly leached by secondary dissolution. Since dissolution occurred along the cleavage traces of the feldspar grain, remnant grain surfaces have a parallel orientation. Later precipitation of a titanium-rich material (F4-B6,D1,J12-B12) has coated most of the intragranular pore space within this feldspar grain.

MAGNIFICATION: 1,300X

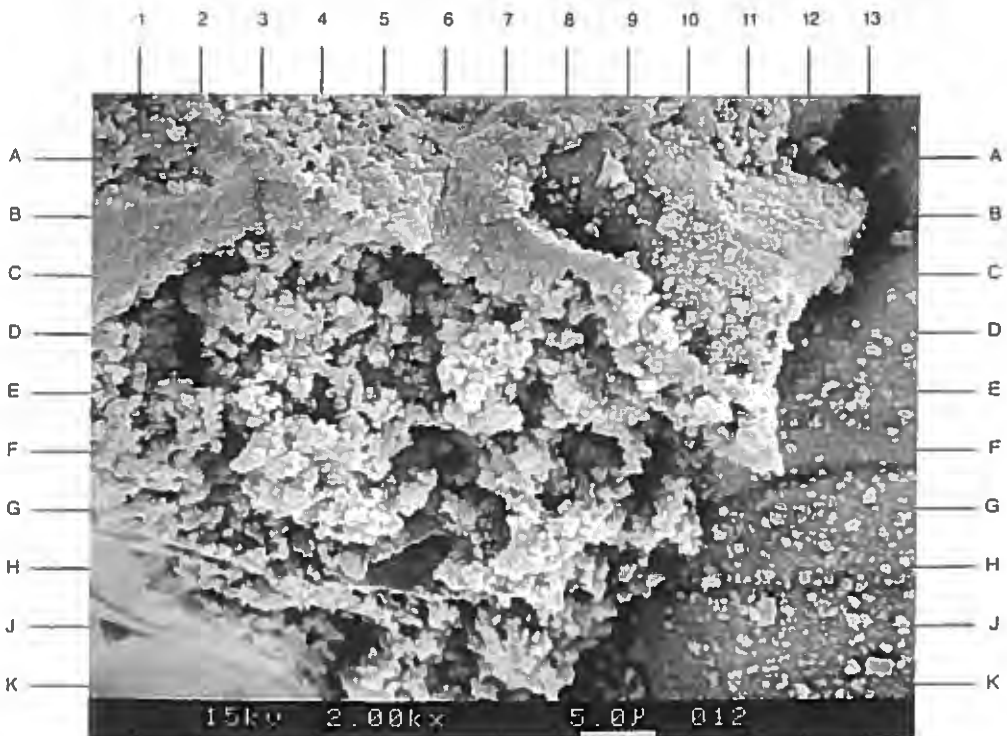
PLATE 18B

A close-up of the titanium-rich compound is highlighted in this photomicrograph. This material fills selective pores (E1-E11) and coats pore walls (D13-K13). The material is apparently amorphous or poorly crystalline, and the granular texture is made up of aggregates of minute particles which are less than 1 micron in diameter.

MAGNIFICATION: 2,000X



A



B

SAMPLE DEPTH: 9789 FEET

PLATE 19A

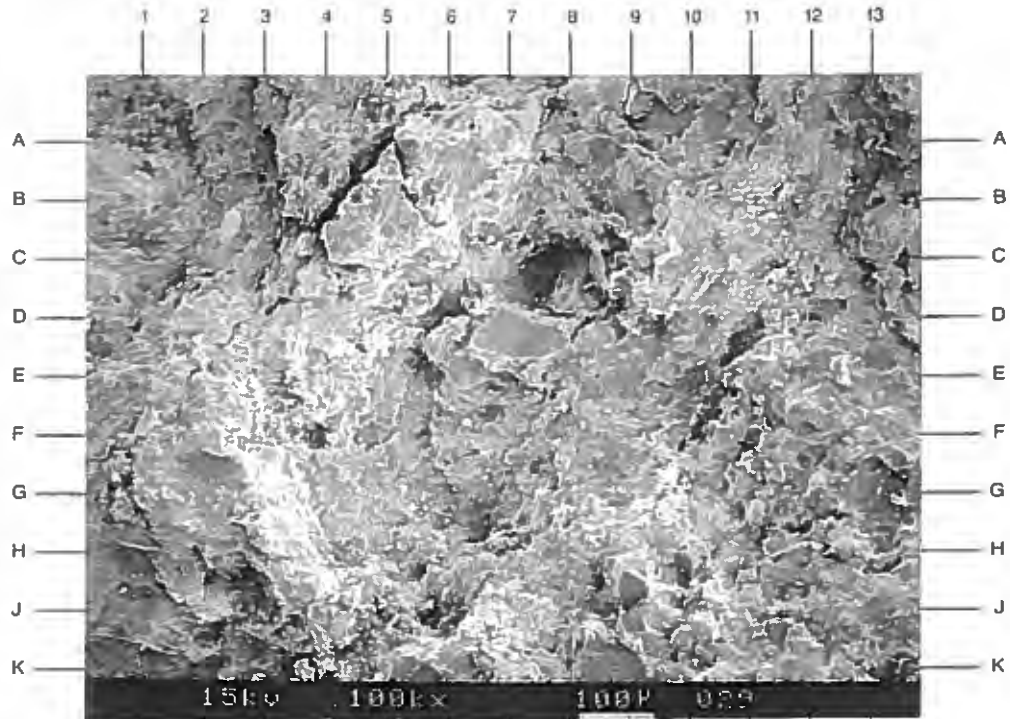
Low porosity development is exhibited in this low magnification view. The only visible porosity consists of microporous portions of the matrix (F10,A1) and widely scattered primary intergranular pores (C8). The majority of the primary pore space in this very fine-grained sandstone is infilled by matrix clays (J5,G11.5) and ankerite (A10, below F3).

MAGNIFICATION: 100X

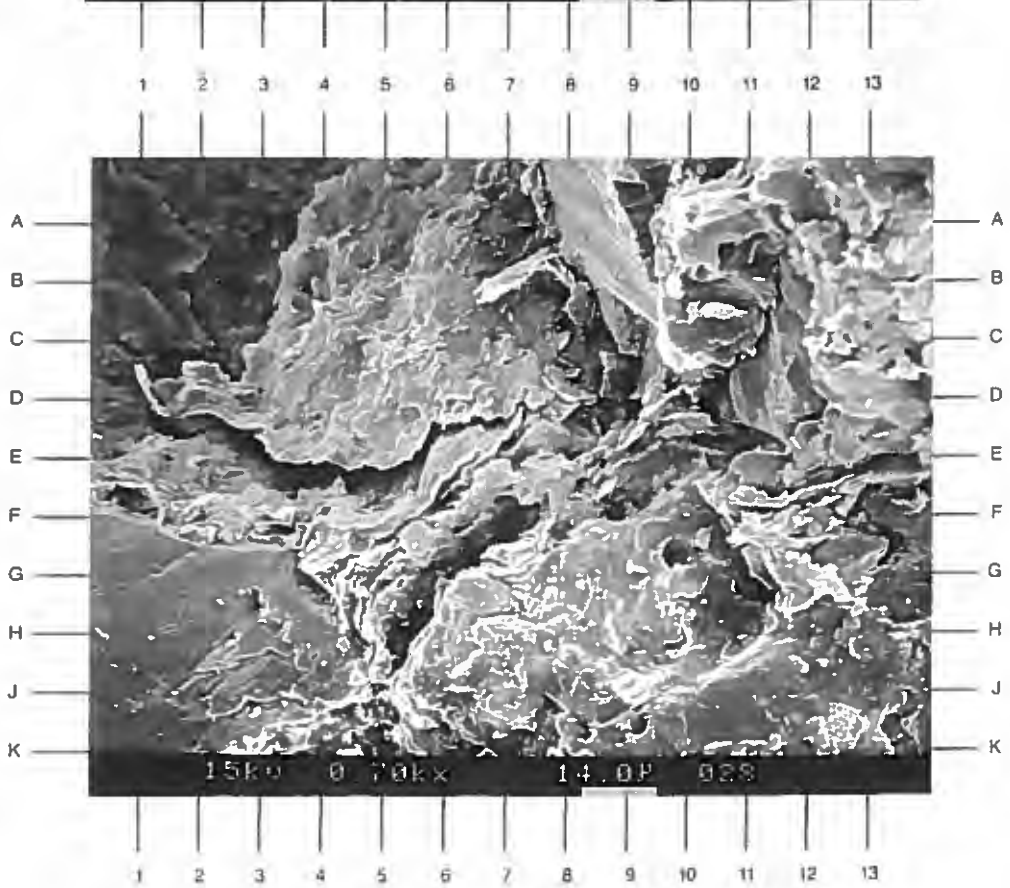
PLATE 19B

An enlarged view of the area near D8 in Plate 19A is shown in this photomicrograph. Mixed-layer illite/smectite and illite are finely intermixed and comprise the majority of the detrital matrix. These clays occur as ragged sheets (G5-E10,F12,D3) which display a subparallel orientation.

MAGNIFICATION: 700X



A



B

DuPont Environmental Remediation Services
Delisle Plant No. 4 S/T No. 1 Well
Harrison County, Mississippi

File No. GH-2562

SAMPLE DEPTH: 9789 FEET

PLATE 20A

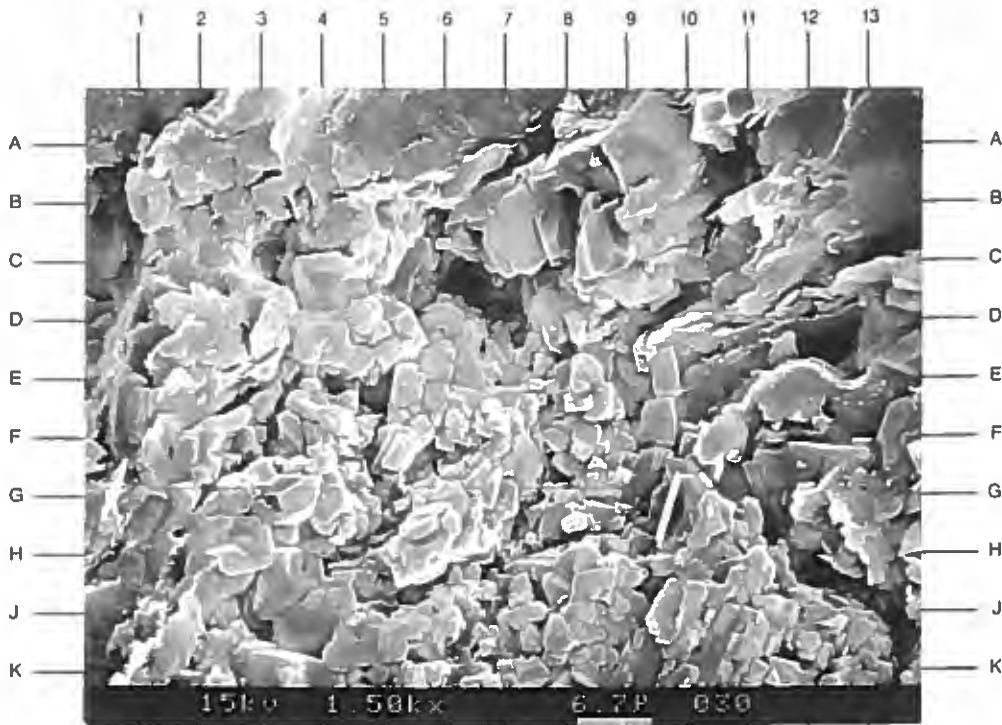
Portions of this sample contain local concentrations of sodium chlorite, or halite. This halite occurs as aggregates of interlocking cubic crystals (F2-F9.5,D6-K8) and is found overlying detrital illitic clay types (E10-D12,B5). Note the microporosity (D-E12,A11,C-D6) associated with these components.

MAGNIFICATION: 1,500X

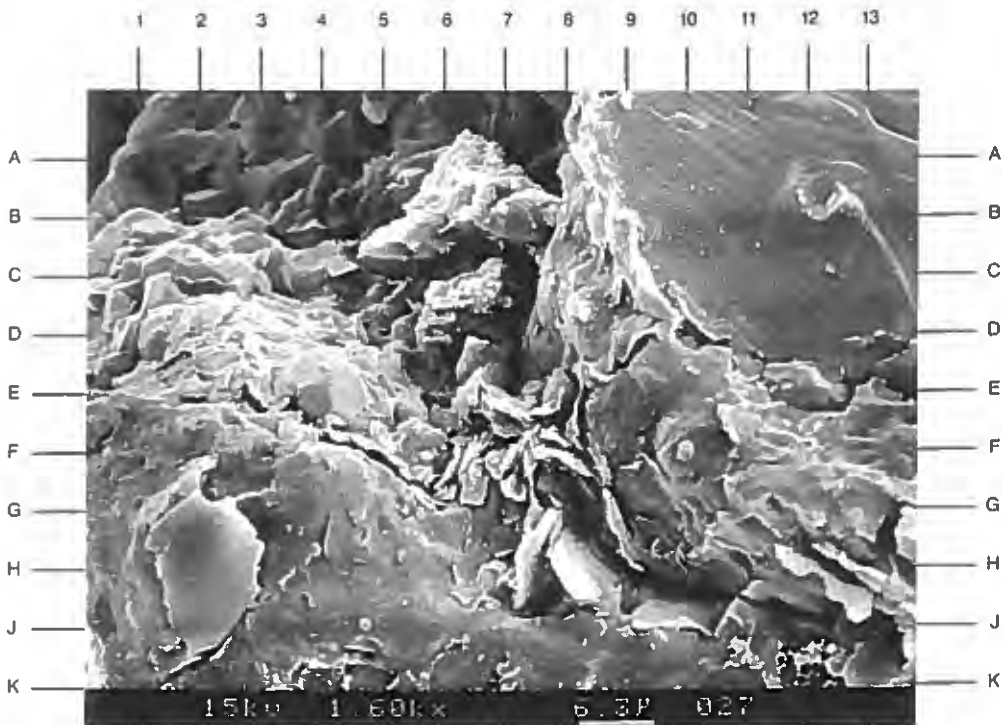
PLATE 20B

Bioturbation has produced areas in the sample with increased microporosity (G8,F6.5,J13) associated with the matrix clays. The clays in this field of view (F6-F8,H7-H9) are mainly composed of illite. Secondary pyrite occurs as aggregates of microcrystals (D6-C7) which fill a small intergranular pore.

MAGNIFICATION: 1,600X



A



B

DuPont Environmental Remediation Services
Delisle Plant No. 4 S/T No. 1 Well
Harrison County, Mississippi

File No. GH-2562

SAMPLE DEPTH: 9842 FEET

PLATE 21A

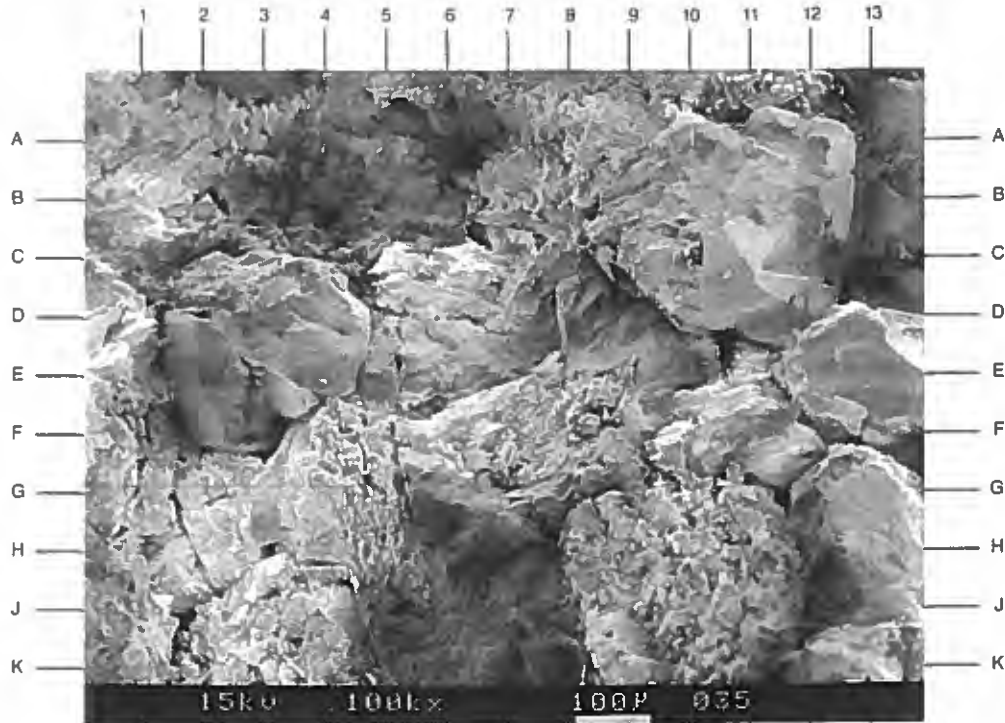
A general overview shows the massive nature of this fine-grained sandstone. Primary intergranular porosity (E10.5,F3, below A6.5) is erratically distributed due to varying amounts of pore-filling titanium-rich material (F8,H5,A4). Secondary quartz overgrowths (C11,B12.5,E2) are a common cement in this sandstone.

MAGNIFICATION: 100X

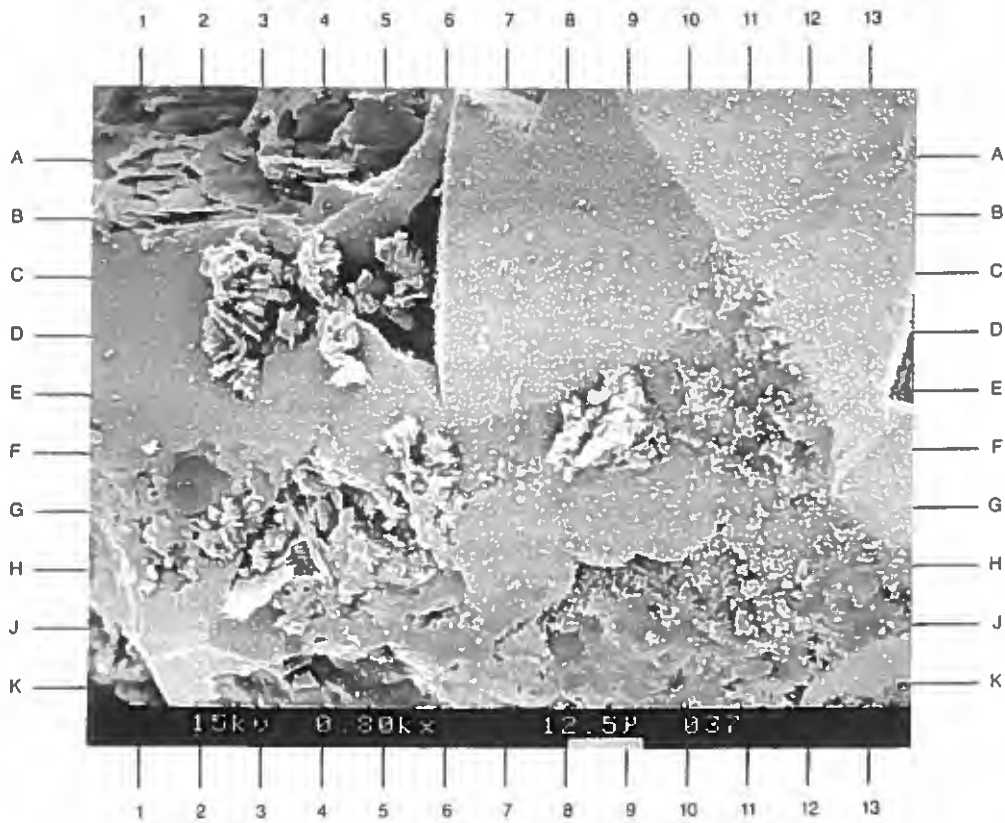
PLATE 21B

An enlarged view of the area near C10 in Plate 21A is shown in this photomicrograph. The flat grain surfaces (D6-D13,E1-E5) represent secondary quartz overgrowths. Note how the titanium-rich material both fills pore space (C5,C3) and coats grain surfaces (G3-E11). Probably authigenic grain-coating chlorite is also coated by titanium-based material at H8.5-H11.

MAGNIFICATION: 800X



A



B

SAMPLE DEPTH: 9842 FEET

PLATE 22A

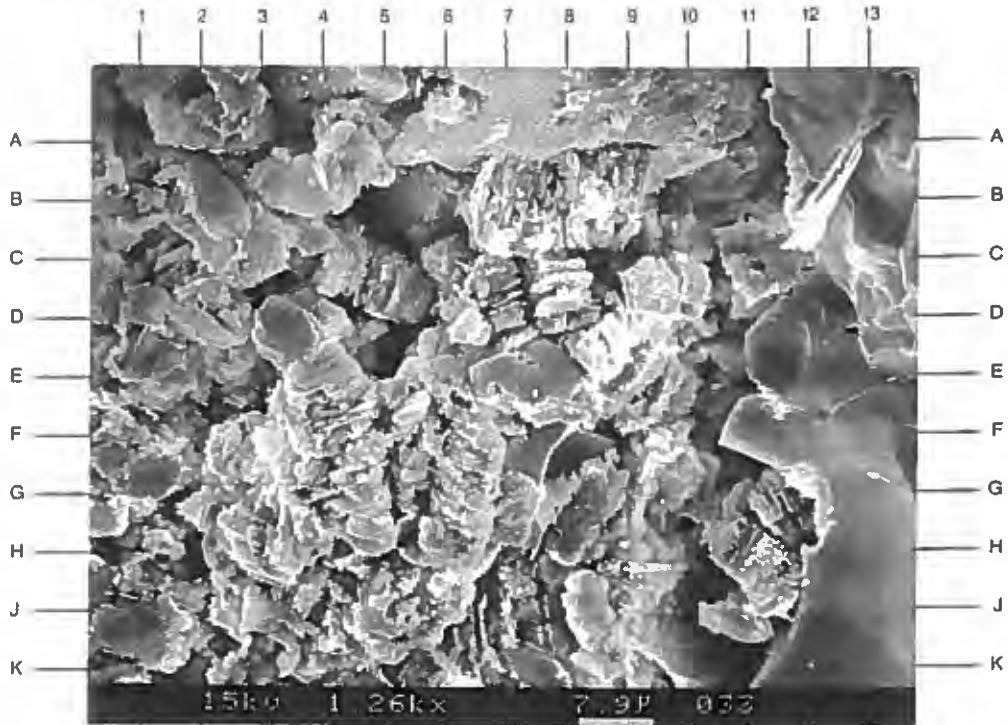
Pore-filling authigenic kaolinite is highlighted in this photomicrograph. As observed in other samples, the kaolinite occurs as loose aggregates of booklets (B7,F4,G6,G-H11.5) with a high associated microporosity. A titanium-rich compound has coated many of these kaolinite booklets (H-J11,F-G6).

MAGNIFICATION: 1,260X

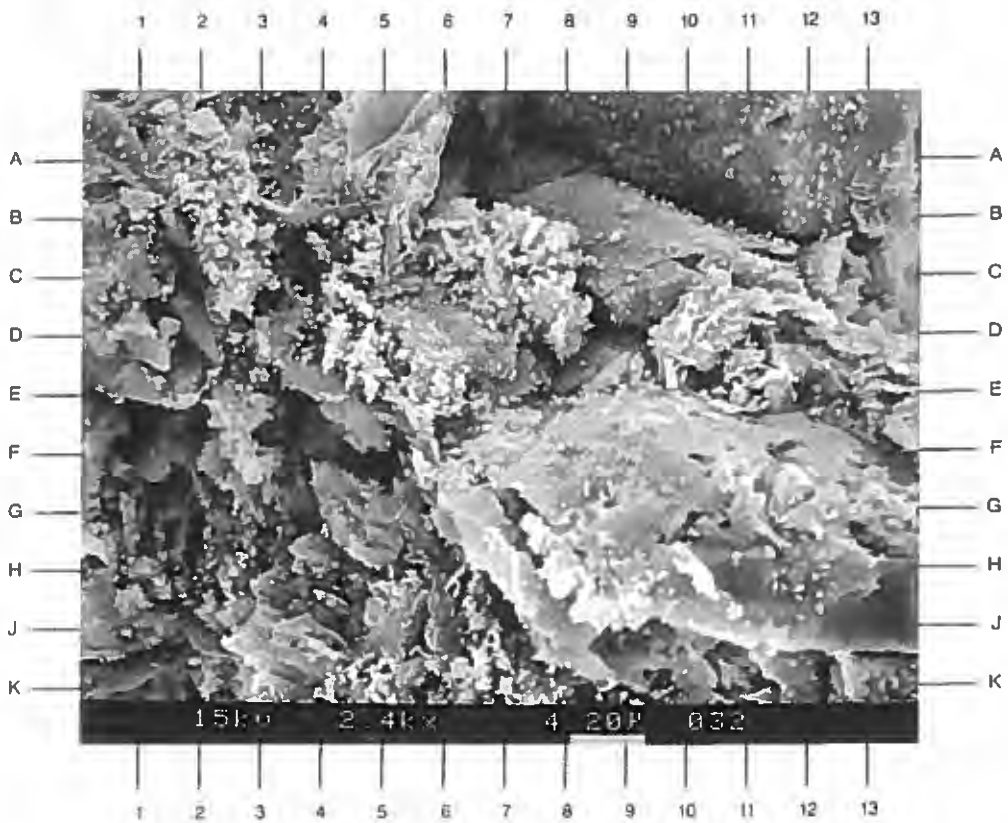
PLATE 22B

A titanium-rich compound has encrusted most of the pore walls in this field of view. This material has a microgranular texture (B2.5,C7,E5.5), or occurs as minute, evenly distributed particles A9-A12.5) along flat pore walls. Aggregates of this material tend to be closely associated with fines in the pore system.

MAGNIFICATION: 2,400X



A



B

DuPont Environmental Remediation Services
Delisle Plant No. 4 S/T No. 1 Well
Harrison County, Mississippi

File No. GH-2562

SAMPLE DEPTH: 9876 FEET

PLATE 23A

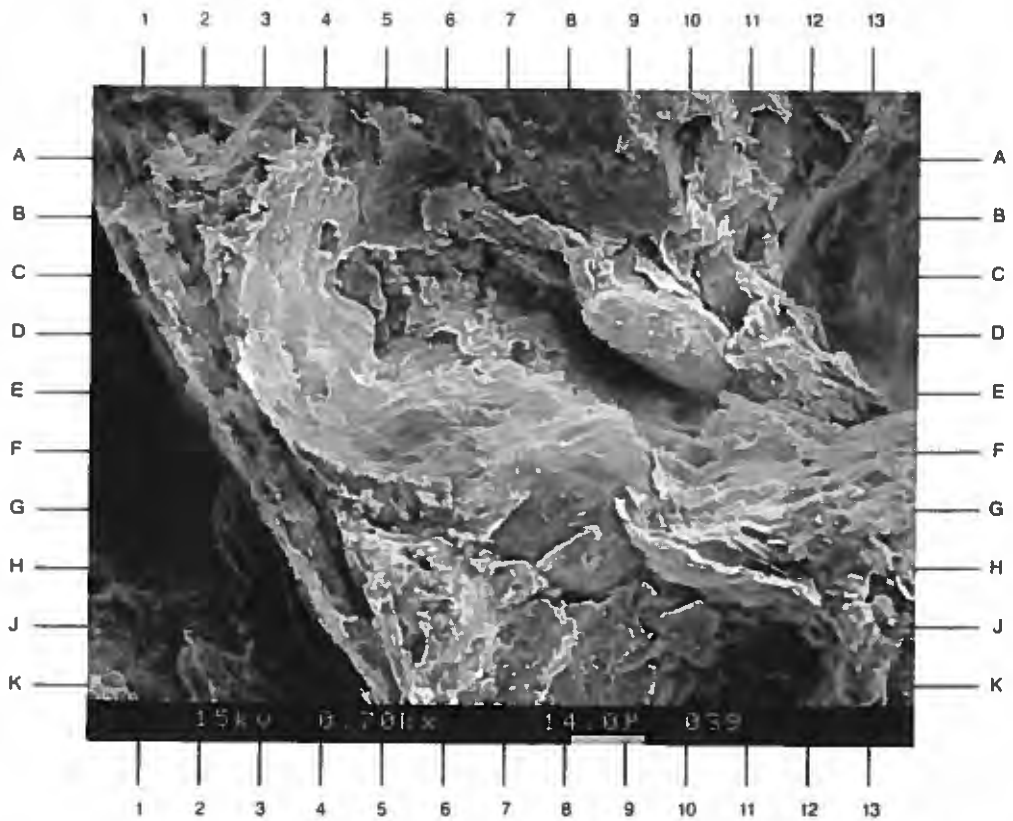
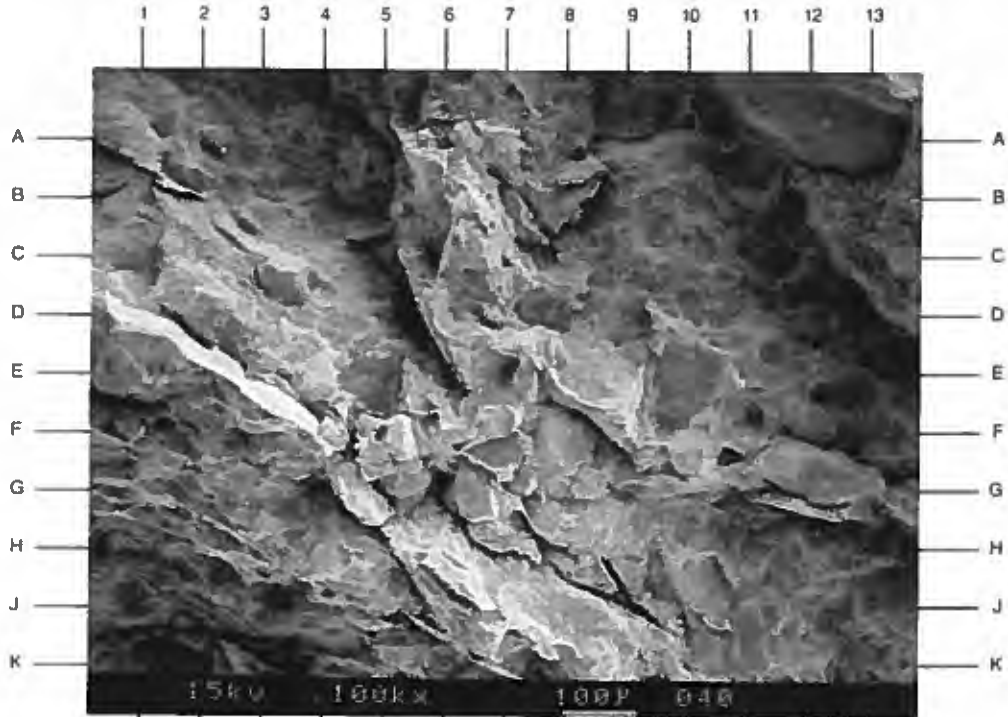
The laminar fabric of this sample (trending upper left to lower right in photo) is defined by abundant, subparallel oriented fossil fragments (F9,E2,B5). These fossil fragments are calcareous in composition. Primary intergranular pores have been infilled largely by detrital matrix clays (A4,B12.5) and ankerite cement (E11.5,H-J11.5).

MAGNIFICATION: 100X

PLATE 23B

An enlarged view of the area near D6.5 in Plate 23A is shown in this photomicrograph. Elongate calcareous fossil fragments (B1-K5,B-C7) are common in this sample, and are frequently set in a matrix of illitic clay (D6,C11,J-K9). Most primary intergranular pores have been infilled by these clays (K11), or by ankerite (not shown in this field of view).

MAGNIFICATION: 700X



SAMPLE DEPTH: 9876 FEET

PLATE 24A

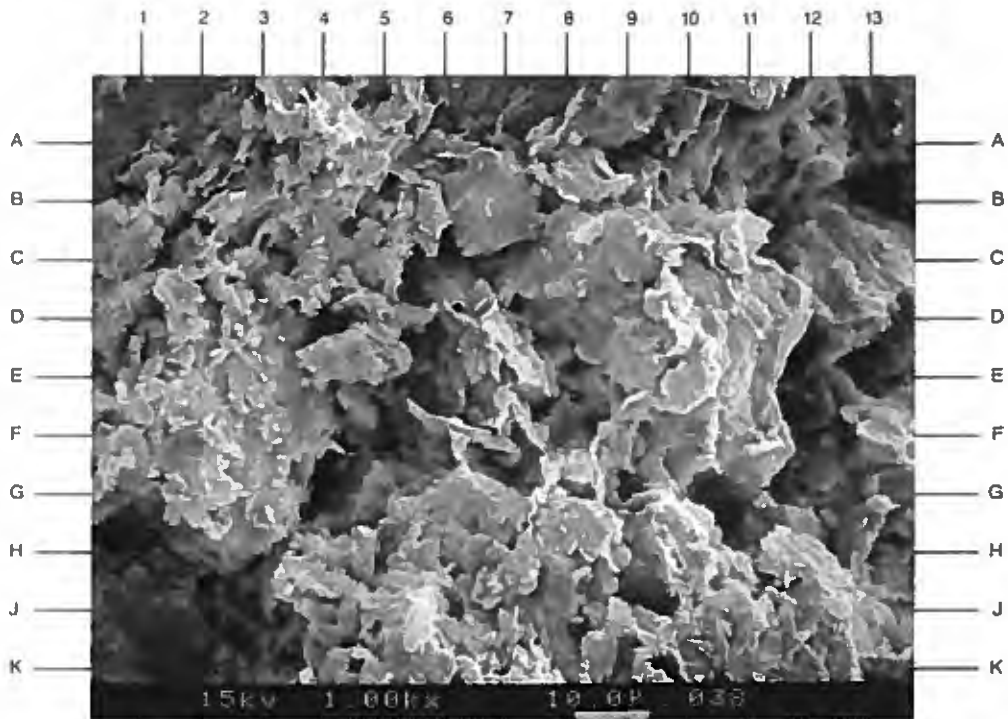
The matrix of this sandstone is composed largely of finely intermixed illite and mixed-layer illite/smectite, which is highlighted in this field of view. These illitic clays (A2-A8,F6,J-K9) occur as aggregates of ragged, curved platelets. Microporosity (B-C2,B5,A9) is commonly associated with this matrix material.

MAGNIFICATION: 1,000X

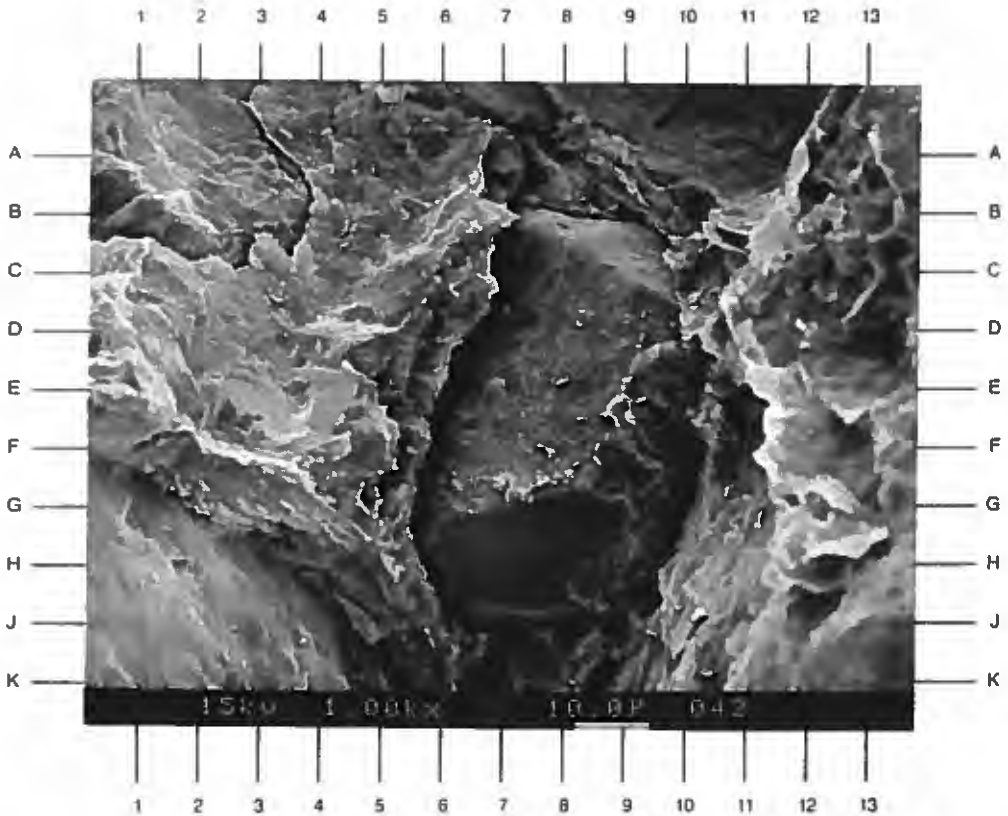
PLATE 24B

A subrounded quartz sand grain (C8-H8) is surrounded by an illite-rich matrix in this high magnification photomicrograph. The original intergranular pore system (A-B7.5,J-K8.5) has been mostly occluded by this relatively dense, depositional matrix (A6.5-H5,A8-C10). Clay platelets show a subparallel orientation.

MAGNIFICATION: 1,000X



A



B

SAMPLE DEPTH: 9907 FEET

PLATE 25A

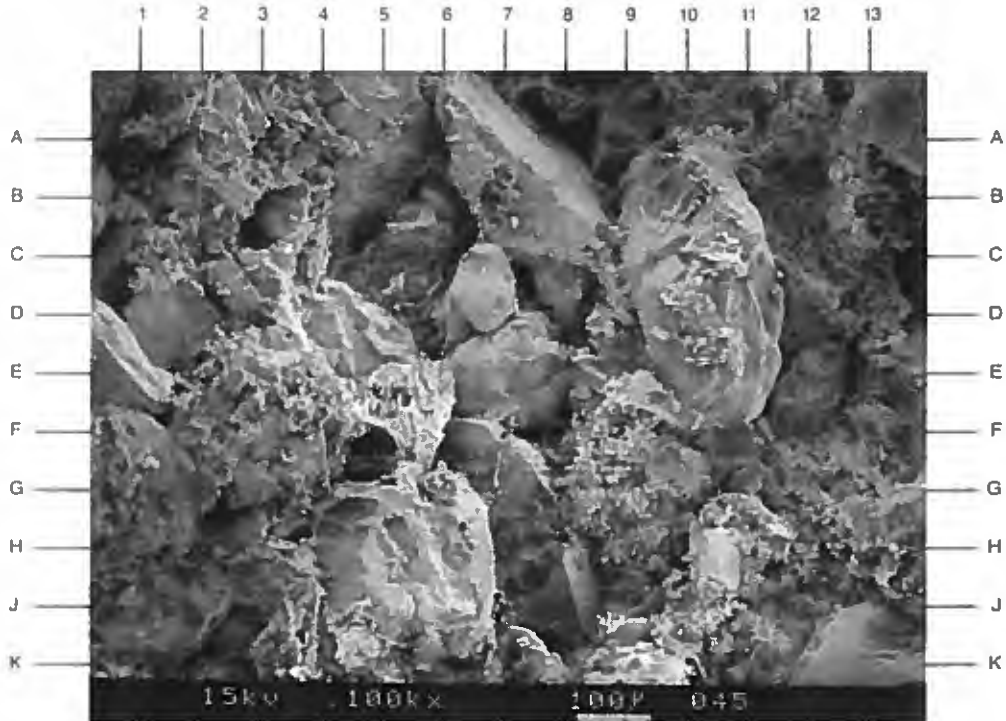
A low magnification view shows the massive nature of this fine-grained sandstone. A titanium-rich material (F9,B13,H12) has precipitated within the pore system of this sandstone, partially blocking local primary intergranular porosity (A8,A1). Secondary quartz overgrowths (J8,F11) formed relatively early during sandstone diagenesis.

MAGNIFICATION: 100X

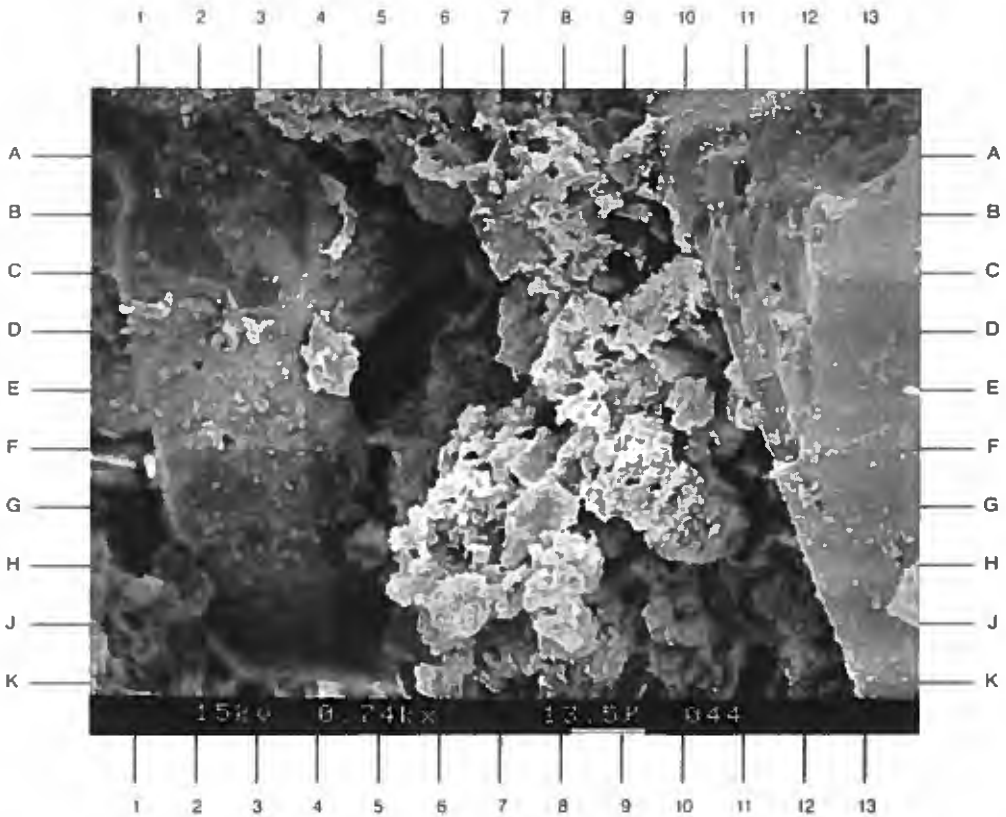
PLATE 25B

An enlarged view of the area near D9 in Plate 25A is shown in this photomicrograph. Most of the intergranular pore from D5 to F11 has been infilled by titanium-rich material (A8-G10,G6.5,J8), but it is not clear if this material locally coats natural matrix fines. The flat grain surfaces (B13-J13) represent secondary quartz overgrowths.

MAGNIFICATION: 740X



A



B

SAMPLE DEPTH: 9907 FEET

PLATE 26A

An intergranular pore (J9) and associated pore throat (D4.5) are highlighted in this photomicrograph. Coatings (A1-D3.5,B7) and linear aggregates (F10-J12.5, above F7) of a titanium-rich material are found within this pore system. Elongate to cubic crystals of halite (A3,C5,E7) overlie, and post-date, the titanium material.

MAGNIFICATION: 800X

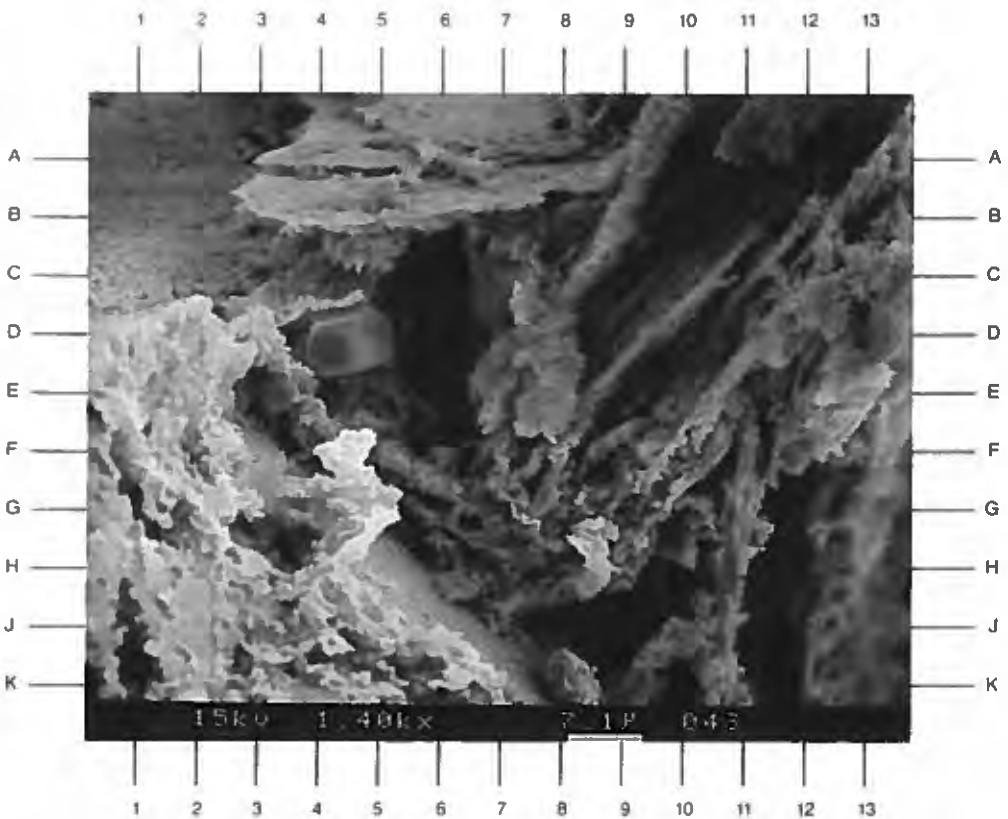
PLATE 26B

A titanium-rich compound has precipitated on remnant debris from feldspar leaching (G6-F10) in this field of view. Secondary dissolution has produced intragranular porosity (A10-E9) within many of the feldspar sand grains. The titanium-based compound tends to deposit on fines and other components with a high surface area.

MAGNIFICATION: 1,400X



A



B

DuPont Environmental Remediation Services
Delisle Plant No. 4 S/T No. 1 Well
Harrison County, Mississippi

File No. GH-2562

SAMPLE DEPTH: 9917 FEET

PLATE 27A

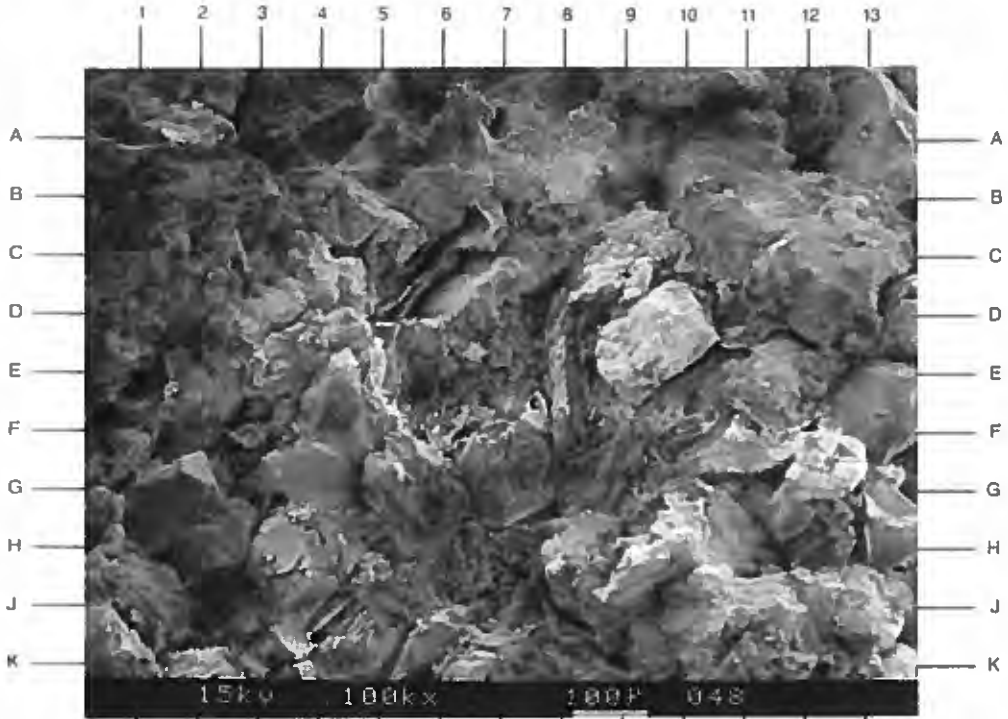
A general overview shows the massive fabric of this fine-grained sandstone. Primary intergranular porosity exists (below A12,F3,K9), but is variably occluded by secondary quartz overgrowths (G2,F4.5), clays (E12,E7), and titanium-rich material (F3). Relatively large flakes of muscovite (D5, J4) are occasionally observed.

MAGNIFICATION: 100X

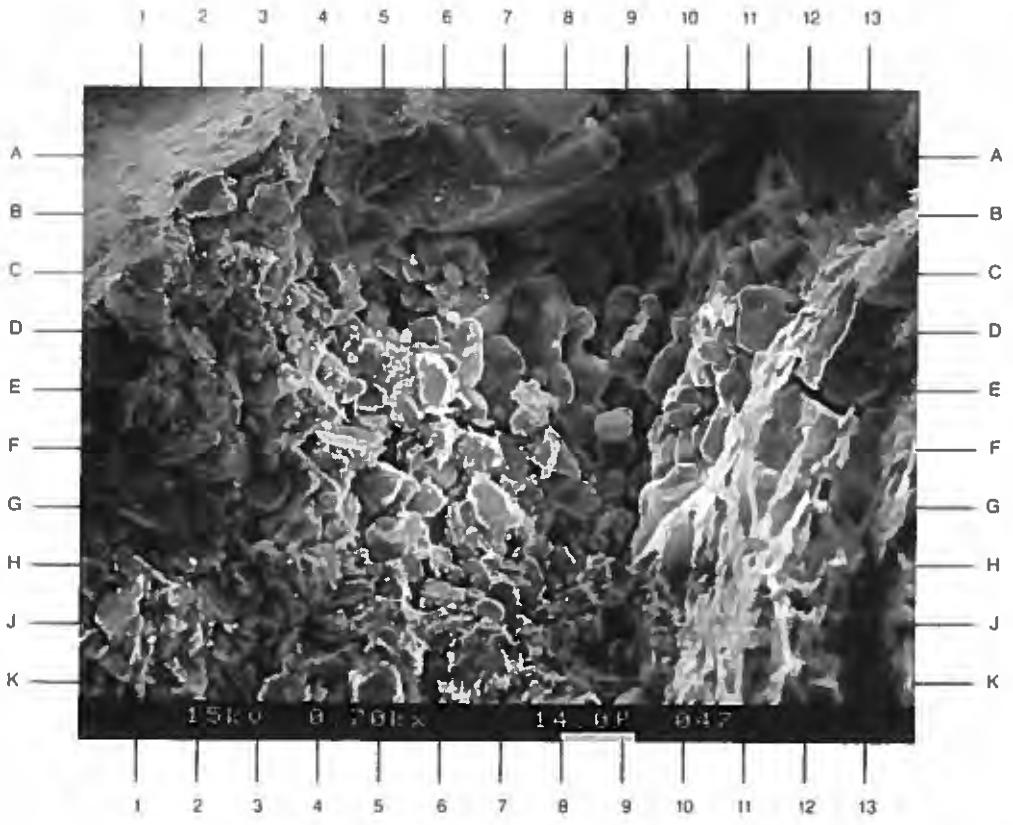
PLATE 27B

An enlarged view of the area near D7.5 in Plate 27A is shown in this photomicrograph. The clay minerals at C2 to J4 are largely kaolinite and display associated microporosity (D5,J4). Sodium chloride, halite (C8-F9,E7-E9.5) occurs as a very late-stage pore-filling, possibly precipitating from brine as the core were brought to the surface.

MAGNIFICATION: 700X



A



B

DuPont Environmental Remediation Services
Delisle Plant No. 4 S/T No. 1 Well
Harrison County, Mississippi

File No. GH-2562

SAMPLE DEPTH: 9917 FEET

PLATE 28A

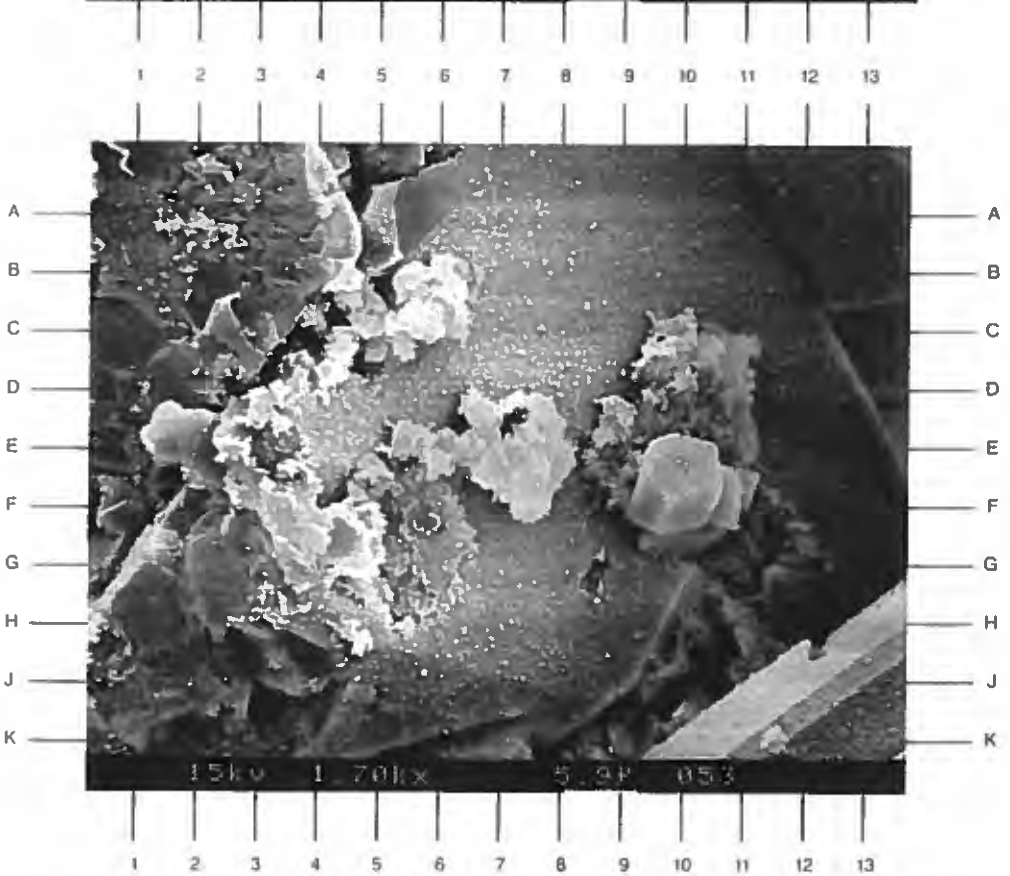
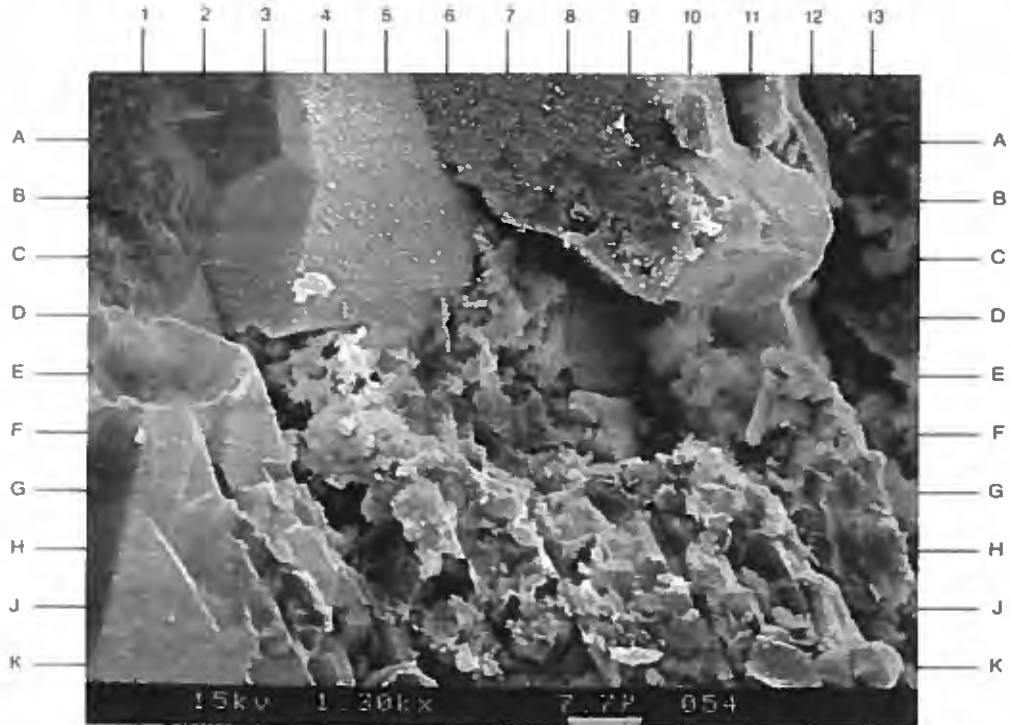
Minor amounts of the titanium-rich material (E4,D-E6,D10) are observed within the pore system of this sandstone. This material significantly coats pore-lining illitic clays (F4-F11), and also occurs as evenly dispersed microgranules (A4-A9) on the surface of smoother quartz overgrowth crystal faces.

MAGNIFICATION: 1,300X

PLATE 28B

Clots of a titanium-rich compound (D10,C5.5,E3) are found on the surface of flat quartz overgrowths. The overgrowths are a natural cementing agent, whereas the titanium material appears to be a contaminant. Note the minor secondary dissolution porosity within a feldspar grain at A2 to B3.5.

MAGNIFICATION: 1,700X



DuPont Environmental Remediation Services
Delisle Plant No. 4 S/T No. 1 Well
Harrison County, Mississippi

File No. GH-2562

SAMPLE DEPTH: 9928 FEET

PLATE 29A

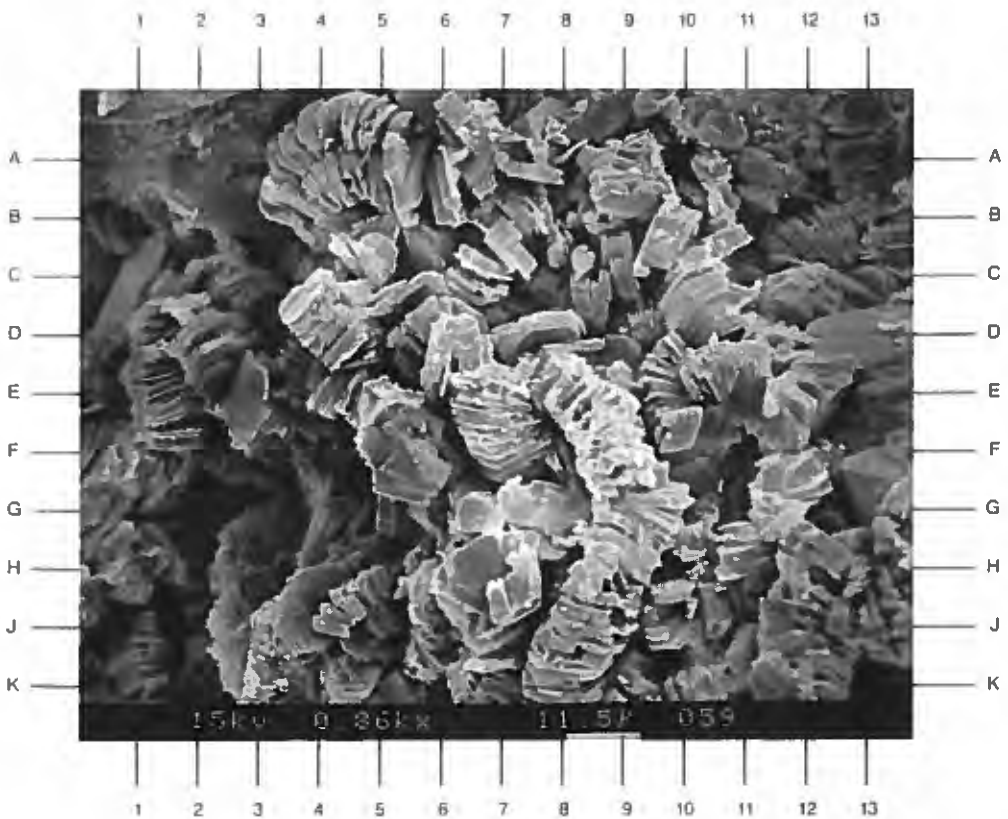
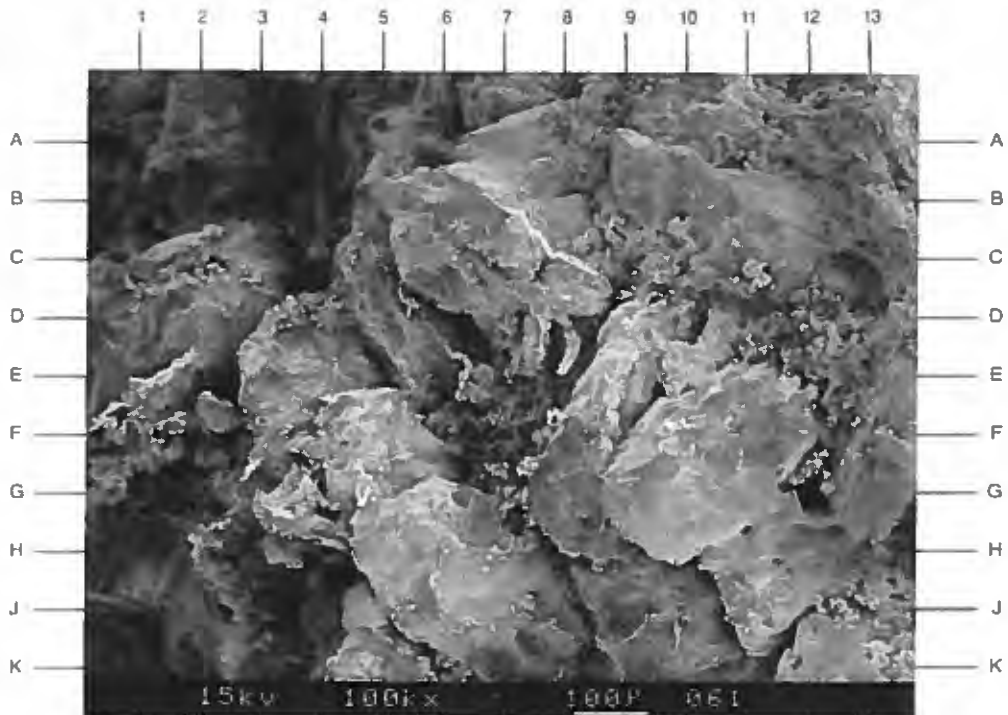
This fine-grained sandstone displays good overall porosity development. Both primary and secondary pore bodies range from open (J3.5,C4) to partially occluded by clays (D-E12) and secondary dissolution remnant debris (D-E8). Secondary quartz overgrowths (F9.5,B10) are the dominant cementing agent.

MAGNIFICATION: 100X

PLATE 29B

An enlarged view of the area near D12 in Plate 29A is shown in this photomicrograph. Booklets of authigenic kaolinite are evident throughout most of the field of view, displaying a characteristic vermicular habit. No evidence of the titanium-rich compound (found in other samples in this study) was observed on the surface of kaolinite particles.

MAGNIFICATION: 860X



DuPont Environmental Remediation Services
Delisle Plant No. 4 S/T No. 1 Well
Harrison County, Mississippi

File No. GH-2562

SAMPLE DEPTH: 9928 FEET

PLATE 30A

Secondary quartz overgrowths (B10-D10,F5-F7,J9) are well developed in portions of this sample. These overgrowths have occluded adjacent pore volume (J10.5,E6) and reduced pore throat size (F2-E5). Strands of illitic clay are found within the pore system at approximately E3 and H10.5.

MAGNIFICATION: 700X

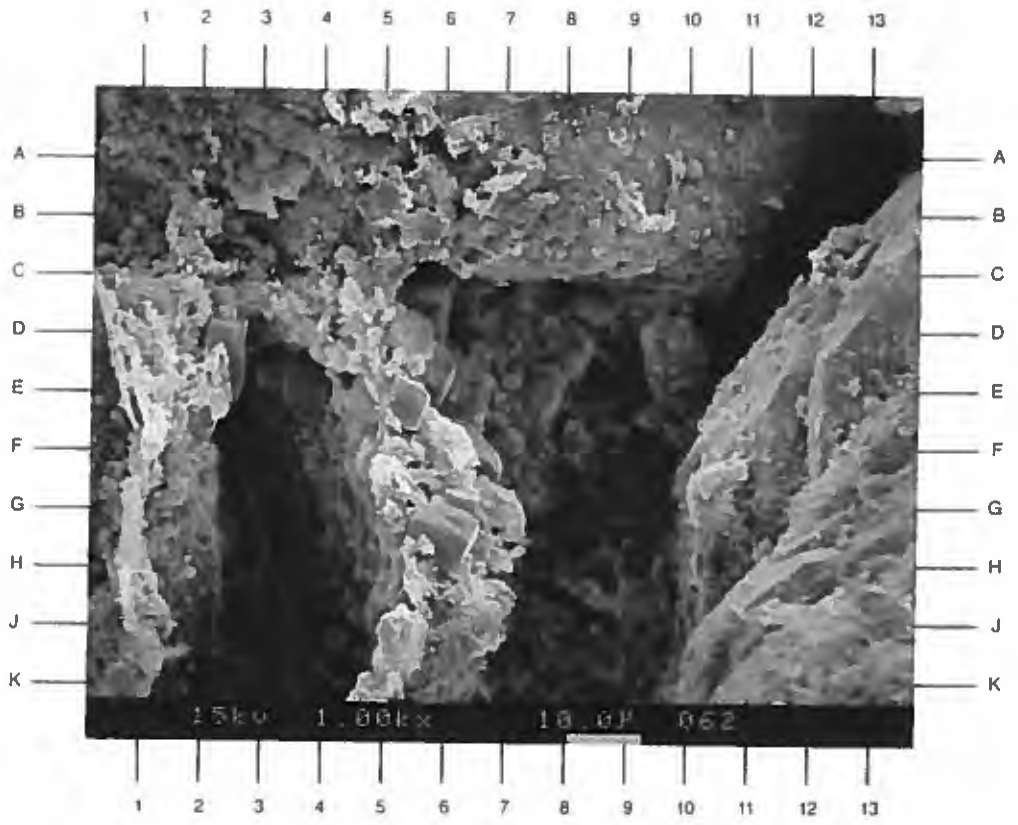
PLATE 30B

The elongate grain surfaces at D1-J1 and D5-K5 represent remnants from dissolution of a feldspar sand grain. These surfaces are now composed largely of illite and kaolinite. The blocky crystals at E5 and G6 are later-forming halite crystals. Grain-coating illite is also observed at G11 and B2-B7.

MAGNIFICATION: 1,000X



A



B

ROTARY SIDEWALL ANALYSIS
FOR

**DUPONT ENVIRONMENTAL
DELISLE PLANT NO. 4, SIDETRACK 1
HARRISON COUNTY, MISSISSIPPI**

DUPONT ENVIRONMENTAL
DELISLE PLANT NO. 4, S/T NO. 1
DELISLE PLANT
HARRISON COUNTY, MISSISSIPPI

FILE NO.: H-2562
ANALYST: MONTI
DATE: 6-26-95
CORES: ROTARY

SAMPLES DRIED ONLY

SMP NO.	DEPTH FEET	PERM mD	POR% He	GRN DEN	LITHOLOGIC DESCRIPTION
1	9672	0.02	9.2	2.71	SS VFG VSHY STKD SCALC NO FLU
2	9747	1156.	23.9	2.63	SS MG CLN NO FLU
3	9757	1691.	20.7	2.64	SS MG CLN NO FLU
4	9764	1200.	19.9	2.64	SS MG CLN NO FLU
5	9779	16.	12.3	2.69	SS M-CG CONG CALC NO FLU
6	9782	41.	20.4	2.68	SS MG CLN NO FLU
7	9789	0.10	5.9	2.71	SS VFG VSHY STKD VCALC NO FLU
8	9842	200.	21.2	2.64	SS F-MG CLN NO FLU
9	9861	480.	22.6	2.64	SS FG CLN NO FLU
10	9876	0.15	3.8	2.73	SS VFG-SILT VSHY STKD VCALC NO FLU
11	9892	0.35	6.6	2.74	SH DK GY SSDY NO FLU
12	9907	510.	25.5	2.60	SS F-MG CLN NO FLU
13	9917	200.	23.3	2.64	SS FG SSHY LAMS NO FLU
14	9928	571.	23.8	2.63	SS F-MG CLN NO FLU
15	9952	0.02	5.1	2.69	SS VFG SSHY LAM NO FLU

DUPONT ENVIRONMENTAL
DELISLE PLANT NO. 4, S/T NO. 1
DELISLE PLANT
HARRISON COUNTY, MISSISSIPPI

FILE NO.: H-2562
ANALYST: MONTI
DATE: 6-29-95
CORES: ROTARY

SAMPLES EXTRACTED & DRIED

SMP NO.	DEPTH FEET	PERM mD	POR% He	GRN DEN	LITHOLOGIC DESCRIPTION
1	9672	0.06	9.9	2.72	SS VFG VSHY STKD SCALC NO FLU
2	9747	1206.	24.2	2.64	SS MG CLN NO FLU
3	9757	1784.	21.3	2.65	SS MG CLN NO FLU
4	9764	1228.	20.2	2.64	SS MG CLN NO FLU
5	9779	17.	12.4	2.69	SS M-CG CONG CALC NO FLU
6	9782	51.	21	2.69	SS MG CLN NO FLU
7	9789	*6.53	7.3	2.72	SS VFG VSHY STKD VCALC NO FLU
8	9842	2.14.	21.8	2.64	SS F-MG CLN NO FLU
9	9861	517.	23.6	2.65	SS FG CLN NO FLU
10	9876	0.3	4.6	2.74	SS VFG-SILT VSHY STKD VCALC NO FLU
11	9892	*2.55	8.0	2.75	SH DK GY SSDY NO FLU
12	9907	547.	26.2	2.60	SS F-MG CLN NO FLU
13	9917	230.	23.6	2.64	SS FG SSHY LAMS NO FLU
14	9928	614.	24.5	2.63	SS F-MG CLN NO FLU
15	9952	0.02	5.3	2.69	SS VFG SSHY LAM NO FLU

*DENOTES FRACTURED PERMEABILITY



9747



9764



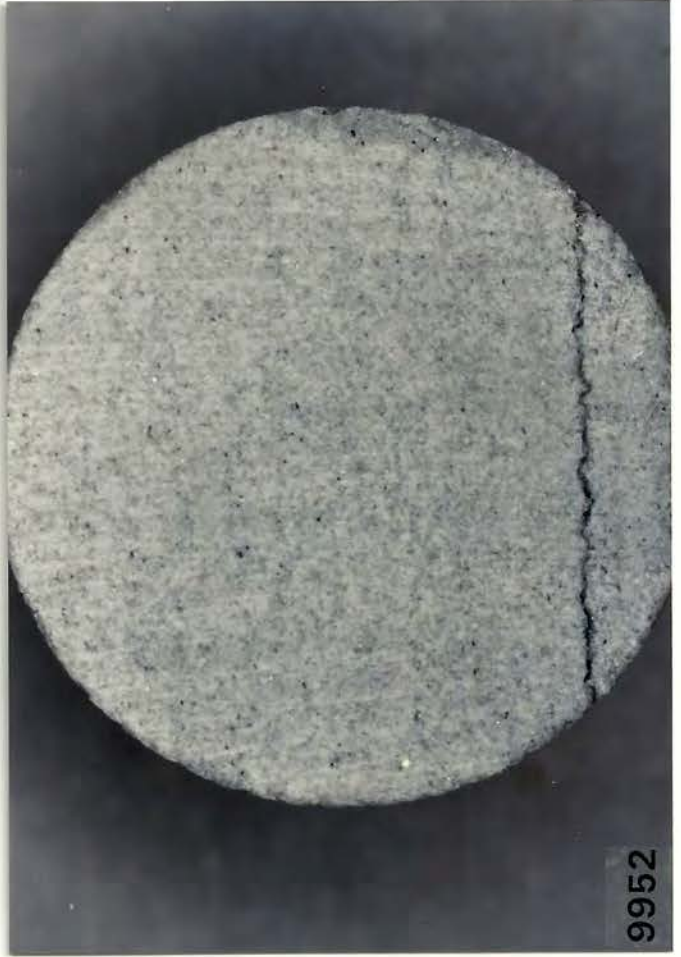
9672



9757







Appendix 2-34

Envirocorp Services and Technology, Inc. Core Analysis Report

Well No. 5 (1993)

PLANT WELL 5



CORE ANALYSIS REPORT

**E. I. DUPONT DE NEMOURS & COMPANY
HARRISON COUNTY, MISSISSIPPI**

ENVIROCORP PROJECT NO. 50Z2485

JUNE 1993

PREPARED BY:

**ENVIROCORP SERVICES & TECHNOLOGY, INC.
HOUSTON, TEXAS**

TABLE OF CONTENTS

EXECUTIVE SUMMARY	iii
1.0 INTRODUCTION	1
2.0 CONCLUSIONS	1
3.0 SAMPLES RECEIVED FOR ANALYSIS	1
4.0 TEST PROCEDURES	2
4.1 POROSITY MEASUREMENTS	2
4.2 PERMEABILITY MEASUREMENTS TO AIR	2
4.3 LOW PERMEABILITY TEST (VERTICAL PLUGS FROM CONFINING INTERVAL)	3
4.4 LITHOLOGIC DESCRIPTIONS	4
5.0 TEST RESULTS AND DISCUSSION	5
5.1 POROSITY MEASUREMENTS	5
5.2 PERMEABILITY MEASUREMENTS TO AIR	6
5.3 LOW PERMEABILITY TESTS (VERTICAL PLUGS FROM CONFINING INTERVAL)	6
5.4 LITHOLOGIC DESCRIPTIONS	7
6.0 X-RAY DIFFRACTION ANALYSIS	7

TABLES

TABLE 5.0-I: PLUG PERMEABILITY AND POROSITY

TABLE 5.2-II: AVERAGE AIR PERMEABILITY AND POROSITY OF EACH ZONE

FIGURE

FIGURE 4.3-1: CORE FLOW APPARATUS

APPENDICES

APPENDIX 5.4-1: LITHOLOGIC DESCRIPTIONS

APPENDIX 6.0-1: X-RAY DIFFRACTION ANALYSES

EXECUTIVE SUMMARY

At the request of E. I. DuPont de Nemours & Company (DuPont), Envirocorp Services & Technology, Inc. (Envirocorp) performed routine core analysis on cores obtained from Dupont's recently drilled Class I Hazardous Waste Disposal Well No. 5 (WDW-5) at its DeLisle, Mississippi facility. Ten (10) conventional sets of cores were collected between 6912 feet and 9907 feet. Core plug samples were dried prior to performing porosity and air permeability measurements. Drying of plug samples can alter the samples which, in turn, will alter the measured permeability. The seven vertical plugs taken from Core Nos. 1 and 4, which were measured for permeability with brine, provide more relevant information as to actual formation permeability. Based on the experimental results obtained during this testing, the following information was gathered:

- Core No. 1 (6912 to 6942 feet) yielded an average porosity of 16% and an average air permeability of 2.45 millidarcies (md). An X-ray diffraction analysis for this zone demonstrated that the samples analyzed consisted mainly of clay and quartz. Four (4) brine permeabilities were measured on vertical plugs taken from this section of core and an average of 3.273×10^5 md was obtained. Brine permeability is more representative of the actual in-situ permeability due to more relevant overburden pressures (~1000 psi versus 200 psi) and the saturated condition of cores versus the dried condition used for air permeability measurements.
- Core No. 2 (7679 to 7711 feet) yielded an average porosity of 8% and an average air permeability of .084 md. An X-ray diffraction analysis for this zone demonstrated that the samples analyzed consisted mainly of calcite.
- Core No. 3 (8311 to 8340 feet) yielded an average porosity of 7% and an average air permeability of .766 md. An X-ray diffraction analysis for this zone demonstrated that the samples analyzed consisted mainly of clay and quartz.
- Due to the condition of the as-received cores, no core plug samples could be obtained from Core No. 4 (8785 to 8815 feet) for porosity and air permeability measurements. However, three vertical plugs were drilled and consolidated in lead sleeves so that brine permeability measurements could be performed. An average of 1.929×10^5 md was measured on three vertical plugs. However, lithologic descriptions provided that

this zone consisted mainly of shale, with some sandstone and shale/claystone between 8805 feet and 8809 feet.

- Core No. 5 (9100 to 9132 feet) yielded an average porosity of 17% and an average air permeability of 65.5 md. An X-ray diffraction analysis for this zone demonstrated that the samples analyzed consisted mainly of quartz.
- Core No. 6 (9386 to 9418 feet) yielded an average porosity of 24% and an average air permeability of 2100 md. An X-ray diffraction analysis for this zone demonstrated that the samples analyzed consisted mainly of quartz.
- Core No. 7 (9606 to 9637 feet) yielded an average porosity of 8% and an average air permeability of .631 md. An X-ray diffraction analysis for this zone demonstrated that the samples analyzed consisted mainly of carbonate and quartz.
- Core No. 8 (9667 to 9697 feet) yielded an average porosity of 6% and an average air permeability of .209 md. An X-ray diffraction analysis for this zone demonstrated that the samples analyzed consisted mainly of carbonate and quartz.
- Core No. 9 (9817 to 9849 feet) yielded an average porosity of 23% and an average air permeability of 1024 md. An X-ray diffraction analysis for this zone demonstrated that the samples analyzed consisted mainly of quartz.
- Core No. 10 (9849 to 9907 feet) yielded an average porosity of 21% and an average air permeability of 799 md. An X-ray diffraction analysis for this zone demonstrated that the samples analyzed consisted mainly of quartz.

The data above show that the confining unit clays exhibit permeabilities of 10^5 md for a 50,000 parts per million (ppm) potassium chloride brine. Thus, it is concluded that current confining material will provide adequate protection against vertical migration. The injection interval sands appear to have sufficient permeability for long-term injection.

1.0 INTRODUCTION

At the request of Dupont, Envirocorp obtained the following data from 10 conventional sets of cores that were collected between 6912 feet and 9907 feet in Dupont's recently drilled Class I Hazardous Waste Disposal Well No. 5 (WDW-5) at its DeLisle, Mississippi facility:

- Two hundred sixteen (216) horizontal core plug porosity measurements.
- Two hundred sixteen (216) horizontal core plug permeability measurements to air.
- Lithologic descriptions were performed on each one-foot section of core received by Envirocorp.

In addition to these measurements, the trimmings from the core plug ends were sent to an outside laboratory for X-ray diffraction analyses (Section 6.0).

The experimental procedures and data interpretation methods are presented in Section 4.0 of this report, specific test results are presented in Section 5.0, and the conclusions are presented in Section 2.0.

2.0 CONCLUSIONS

Testing of the vertical plugs from the confining interval, with respect to 50,000 ppm potassium chloride, yielded an average of 2.7×10^5 md. These data show that the confining unit clays will provide adequate protection against vertical migration. Injection interval testing provided adequate permeability ranges for injection. Core No. 6 (9386 to 9418 feet) demonstrated the highest average permeability (2100 md), with respect to air.

3.0 SAMPLES RECEIVED FOR ANALYSIS

Envirocorp's laboratory received approximately 335 feet of core from WDW-5. Dupont originally requested that one horizontal plug be drilled from each one-foot section of whole core. Due to the condition of some areas of core, mainly shales, plugs could not be drilled in ambient conditions from those areas. Selected samples of whole cores were sent to an outside laboratory so that core plugs could be drilled using liquid nitrogen. Seven (7) vertical plugs were drilled, placed in lead sleeves, and the ends

were screened to consolidate the core plug samples. These seven vertical plugs were used in the low permeability tests using a KCl solution (Section 5.3). Two hundred sixteen (216) horizontal plug samples were drilled in Envirocorp's laboratory. Porosity and air permeability measurements were performed on the horizontal plug samples (Sections 5.1 and 5.2). In addition to these measurements, the trimmings from the core plug ends were sent to an outside laboratory for X-ray diffraction analyses (Section 6.0).

4.0 TEST PROCEDURES

4.1 Porosity Measurements

Porosity measurements were performed using a Coberly-Stevens Boyle's Law porosimeter designed to accommodate 1 inch diameter samples up to 2 inches long. It is operated by admitting gas (helium) at 100 pounds per square inch gauge (psig) into a reference section, shutting in the reference section and reading the pressure, and then opening the reference section to the sealed sample section and reading the resulting lower pressure. The ratio of load pressure to final pressure is used to calculate the sample grain volume. Once the grain volume is obtained, the grain volume is subtracted from the bulk volume of the sample (obtained by mercury emersion), which provides pore volume. Pore volume is then divided by bulk volume to obtain porosity.

4.2 Permeability Measurements to Air

The permeameter, like the porosimeter, is designed to measure 1 inch diameter cylindrical plug samples up to 2 inches long. The instrument operates by providing a means to supply gas (nitrogen) at a regulated and measured pressure to the inlet face of the sample held in a Hassler sleeve cell and to measure the flow rate of the gas issuing from the downstream face of the sample. Permeability is calculated using the upstream and downstream gas pressures, flow rate of gas from the sample, physical dimensions of the sample, and gas viscosity:

$$k = \frac{2000 B Q \mu L/A}{(P_{ug} + B)^2 - (P_{og} + B)^2}$$

where:

- k = permeability, md
- B = barometric pressure, atm
- Q = gas flow rate at B, ml/sec
- μ = gas viscosity, cp
- L = sample length, cm
- A = sample cr. sec. area, cm²
- P_{ug} = gauge pressure, upstream, atmg
- P_{og} = gauge pressure, downstream, atmg

4.3 Low Permeability Tests (Vertical Plugs from Confining Interval)

The basic equation used to evaluate the permeability of low permeability materials is presented below and is derived directly from Darcy's flow equation:

$$\ln \Delta P(t) = \frac{14.08 kAt}{cV_o n l = \ln \Delta P_o}$$

where:

- $\Delta P(t)$ = pressure drop across the test core at time, t (psi)
- k = core permeability darcy
- A = core cross-sectional area (cm²)
- c = compressibility of fluid in core (psi⁻¹)
- V_o = volume upstream of the core (cm³)
- μ = fluid viscosity (centipoise)
- l = core length (cm)
- t = time since pressure drop across core was initiated (min)
- 4.08 = conversion factor

The cores used in these tests are loaded into a core holder as demonstrated in Figure 4.3-1. The experiment is conducted by placing a desired overburden (confining pressure) on the core and then establishing an initial pore pressure in the entire core. The experiment is initiated by slowly opening a downstream valve so that the downstream end of the core is at atmospheric pressure. A transducer is used to measure the pressure drop across the core. The signal from the transducer is fed to a

time-driven recorder. Thus, the raw data are plots of the pressure drop across the core versus time.

The observed decrease in pressure across the core is due to expansion of the fluid in the fixed volume V_0 as fluid is driven through the core.

A plot of $\ln \Delta P$ versus t is then made. This plot is a straight line with:

$$\text{slope } m = \frac{-4.08 k A}{c V_0 \mu l}$$

Since m , A , c , μ , and l are known, the sample permeability can be determined.

Although it is not obvious, system leaks will cause higher permeabilities to be measured and can also cause the plot of $\ln \Delta P$ versus t to be non-linear. Thus, the measuring system is biased in the direction of higher permeability due to fluid movement out of V_0 not related to fluid movement through the core.

4.4 Lithologic Descriptions

Ten (10) conventional cores from WDW-5 were examined and described with respect to rock composition, rock texture, and sedimentary structures.

For each core, core segments were visually examined and general petrologic categories were established based on rock composition, texture, and internal sedimentary structure. Selected samples within the categories were then examined by binocular microscope and subjected to simple chemical and physical tests. Rock composition was described with respect to grain mineralogy, nature of matrix, cement, and authigenic and secondary minerals. Rock texture was recorded as to size range (Wentworth scale), sorting, rounding, and color. The type of bedding, bedding alteration, and miscellaneous bedding characteristics were also noted. Based on this more detailed examination, the previously established categories were further subdivided, as necessary.

Each core was then reexamined and the amount (length) of each specific petrographic type was recorded down to 0.1-foot lengths. Where lithology changed in less than 0.1-foot intervals, an additional narrative was added to the lithology description number. Unusual or unique features or characteristics were also added during this examination.

The results of the descriptions were tabulated by core and are presented in Appendix 5.4-1.

5.0 TEST RESULTS AND DISCUSSION

5.1 Porosity Measurements

The results of the porosity measurements are presented in Table 5.0-I and a summary is provided for each of the 10 core sections in Table 5.0-II. As can be seen by reviewing the data in Table 5.0-II:

- An average of 16% porosity was measured on core plug samples taken from the depths of 6912 to 6942 feet (Core No. 1).
- An average of 8% porosity was measured on core plug samples taken from the depths of 7679 to 7711 feet (Core No. 2).
- An average of 7% porosity was measured on core plug samples taken from the depths of 8311 to 8340 feet (Core No. 3).
- Due to the condition of the as-received cores, no core plug samples could be obtained for testing from the depths of 8785 to 8815 feet (Core No. 4).
- An average of 17% porosity was measured on core plug samples taken from the depths of 9100 to 9132 feet (Core No. 5).
- An average of 24% porosity was measured on core plug samples taken from the depths of 9386 to 9418 feet (Core No. 6).
- An average of 8% porosity was measured on core plug samples taken from the depths of 9606 to 9637 feet (Core No. 7).
- An average of 6% porosity was measured on core plug samples taken from the depths of 9667 to 9697 feet (Core No. 8).
- An average of 23% porosity was measured on core plug samples taken from the depths of 9817 to 9849 feet (Core No. 9).
- An average of 21% porosity was measured on core plug samples taken from the depths of 9849 to 9907 feet (Core No. 10).

5.2 Permeability Measurements to Air

The results of the permeability measurements to air are presented in Table 5.0-I and a summary is provided for each of the 10 core sections in Table 5.0-II. As can be seen by reviewing the data in Table 5.0-II:

- An average permeability of 2.45 md was measured on core plug samples taken from Core No. 1.
- An average permeability of 0.084 md was measured on core plug samples taken from Core No. 2.
- An average permeability of 0.766 md was measured on core plug samples taken from Core No. 3.
- Due to the condition of the as-received cores, no core plug samples could be obtained for testing from Core No. 4.
- An average permeability of 65.5 md was measured on core plug samples taken from Core No. 5.
- An average permeability of 2100 md was measured on core plug samples taken from Core No. 6.
- An average permeability of 0.631 md was measured on core plug samples taken from Core No. 7.
- An average permeability of 0.209 md was measured on core plug samples taken from Core No. 8.
- An average permeability of 1024 md was measured on core plug samples taken from Core No. 9.
- An average permeability of 799 md was measured on core plug samples taken from Core No. 10.

5.3 Low Permeability Tests (Vertical Plugs from Confining Interval)

The results of the pulse test permeability measurements on the seven vertical confining interval cores, using 50,000 ppm potassium chloride (50,000 mg/l KCl) are presented in Table 5.0-I. The depth from which these plugs were taken from the following well depths: 6916.6, 6917.5, 6924.8, 6926.0, 8804.7, 8805.7, and 8807.6. These data show results of 10^5 md and an average of 2.7×10^5 md for the seven vertical plugs measured. Furthermore, these data show that the confining unit clays have low permeability with

respect to the KCl brine. Thus, it is concluded that current confining material will provide adequate protection against vertical migration.

5.4 Lithologic Descriptions

The results of the lithologic descriptions are presented in Appendix 5.4-1 and in Table 5.0-I.

6.0 X-RAY DIFFRACTION ANALYSIS

Trimblings from the core plug ends were sent to an outside laboratory for X-ray diffraction analyses. X-ray diffraction is performed to identify the minerals which compose the sample. The results of the X-ray diffraction analysis appear in Appendix 6.0-1 and in Table 5.0-I.

TABLES

TABLE 5.0-II

AVERAGE AIR PERMEABILITY AND POROSITY OF EACH ZONE

CORE NO.	DEPTH OF ZONE (feet)	NUMBER OF PLUGS MEASURED FROM ZONE	AVERAGE AIR PERMEABILITY OF ZONE (md)	AVERAGE POROSITY OF ZONE (%)
1	6912-6942	18	2.45	16
2	7679-7711	31	.084	8
3	8311-8340	10	.766	7
4	8785-8815	----	----	----
5	9100-9132	14	65.5	17
6	9386-9418	32	2100	24
7	9606-9637	15	.631	8
8	9667-9697	7	.209	6
9	9817-9849	31	1024	23
10	9849-9907	58	799	21

COMPANY: Dupont
WELL: WDW-5

TABLE 5.0-1

STATE: Mississippi
COUNTY: Harrison

DATE: March 1983
ENVIROCORP JOB NO.: 5022485

PLUG PERMEABILITY AND POROSITY

SAMPLE NUMBER	DEPTH (feet)	PERMEABILITY TO AIR		PERMEABILITY TO BRINE		POROSITY %	GRAIN DENSITY (gm/cc)	X-RAY DIFFRACTION (WEIGHT %)				LITHOLOGIC DESCRIPTIONS
		HORIZONTAL (mcd)		VERTICAL (md)				TOTALS				
								CLAYS	CARBONATE	QUARTZ	OTHER MINERALS	
* 6912-13												(1)
1 6913-14	.204					3	2.688	10	38	37	15	(1) (2)
2 6914-15	.154					4	2.681	8	TR	70	22	(2) (3)
* 6915-16												(1) flaser bedding
6916.6V												(1) fine laminae of (2)
6917.5V												(1)
3 6918-19	17.5					26	2.66	9	1	68	22	(1) (3)
4 6919-20	6.93					22	2.651	2	42	38	18	(3) (2)
5 6920-21	5.02					21	2.663	8	1	64	27	(2) (1)
6 6921-22	3.78					21	2.658	16	0	63	21	(1) (2)
7 6922-23	.161					5	2.709	7	48	31	14	(2)
8 6923-24	.158					5	2.692	12	42	33	13	(1) (2)
6924.8V												(2) and (4) finely interbedded
9 6924-25	1.86					21	2.634	19	TR	63	18	(2) and (4) finely interbedded

CORE 1

* Plug sample could not be drilled due to condition of core.
 1 See key at end of table for descriptions.
 2 Failed During Analysis (FDA)

SAMPLE NUMBER	DEPTH (feet)	PERMEABILITY TO AIR		PERMEABILITY TO BRINE		POROSITY %	GRAIN DENSITY (gm/cc)	X-RAY DIFFRACTION (WEIGHT %)				LITHOLOGIC DESCRIPTIONS
		HORIZONTAL (md)	VERTICAL (md)	CLAYS	CARBONATE			QUARTZ	OTHER MINERALS			
										TOTALS		
10	6925-26	1.27				20	2.664	13	1	61	75	(1), (2), and (4) finely interbedded
6926.0V	6926-27		1.819 X 10 ⁻³									(1), (2), and (3) finely interbedded
11	6926-27	.664				17	2.680	16	0	49	35	(1), (2), and (3) finely interbedded
*	6927-28											(1) silty, (3)
12	6928-29	1.65				21	2.657	21	0	55	24	(1) and (3)
*	6929-30											(1) and (3)
*	6930-31											(1), (1) and (2) intercalated
*	6931-32											(1) and (2) intercalated
13	6932-33	.277				10	2.687	11	17	57	15	(3) and (4)
14	6933-34	1.38				17	2.651	26	5	47	22	(4)
15	6934-35	.970				18	2.498	23	0	55	22	(4), (1) and (3) intercalated
16	6935-36	.895				18	2.651	26	5	47	22	(4)
17	6936-37	.661				18	2.855	23	0	55	22	(4), (1) and (3) intercalated
*	6937-38											(1) and (3)
*	6938-39											(1)
*	6939-40											(1)
18	6940-41	.494				16	2.653	29	5	43	23	(4)
19	6941-42	² FDA				² FDA		39	0	41	20	(1)

* Plug sample could not be drilled due to condition of core.

¹ See key at end of table for descriptions.

² Failed During Analysis (FDA)

SAMPLE NUMBER	DEPTH (feet)	PERMEABILITY TO AIR		PERMEABILITY TO BRINE		POROSITY %	GRAIN DENSITY (gm/cc)	X-RAY DIFFRACTION (WEIGHT %)				LITHOLOGIC DESCRIPTIONS
		HORIZONTAL (md)		VERTICAL (md)				CLAYS	TOTALS			
									CARBONATE	QUARTZ	OTHER MINERALS	
20	7679-80	.072				10	2.678	TR	83	7	0	
21	7680-81	.069				11	2.687	1	83	6	0	(5), (6) and 7
22	7681-82	.204				11	2.702	TR	84	6	0	(5) and (6)
23	7682-83	.065				10	2.683	1	82	7	0	(6)
24	7683-84	.59				9	2.674	5	89	6	0	(6)
25	7684-85	.058				6	2.674	1	83	6	0	(5) and (7)
26	7685-86	.062				7	2.679	3	88	7	2	(6)
27	7686-87	.083				8	2.677	1	84	5	0	(6) and (7)
28	7687-88	.053				9	2.680	TR	86	4	0	(5) and (6)
29	7688-89	.070				8	2.666	TR	83	7	0	(6) and (7)
30	7689-90	.054				8	2.661	TR	85	5	0	(6)
31	7690-91	.079				10	2.705	3	89	5	3	(6) and (7)
32	7691-92	.048				9	2.680	3	91	6	0	(6) and (7)
33	7692-93	.070				8	2.673	1	83	6	0	(6) and (7)
34	7693-94	.046				8	2.692	3	89	7	1	(6) and (7)
35	7694-95	.063				9	2.682	3	91	6	0	(6) and (7)
36	7695-96	.051				7	2.679	2	90	5	3	(6)
*	7696-97											(5) and (7)
37	7697-98	.047				9	2.701	3	83	4	0	(5) and (6)

CORE 2

* Plug sample could not be drilled due to condition of core.

¹ See key at end of table for descriptions.

² Failed During Analysis (FDA)

SAMPLE NUMBER	DEPTH (feet)	PERMEABILITY TO AIR		PERMEABILITY TO BRINE		POROSITY %	GRAIN DENSITY (gm/cc)	X-RAY DIFFRACTION (WEIGHT %)				LITHOLOGIC DESCRIPTIONS
		HORIZONTAL (md)		VERTICAL (md)				CLAYS	TOTALS			
									CARBONATE	QUARTZ	OTHER MINERALS	
38	7698-99	.050				9	2.686	4	89	7	0	(6) and (7)
39	7698-700	.062				9	2.696	1	85	4	0	(6) and (7)
40	7700-01	.042				7	2.641	2	90	8	2	(6)
41	7701-02	.102				7	2.660	3	91	6	0	(6)
42	7702-03	.060				7	2.654	3	90	6	1	(6)
43	7703-04	.066				7	2.678	5	89	6	0	(5), (6) and (7)
44	7704-05	.048				7	2.690	TR	83	5	2	(5) and (6)
45	7705-06	.073				8	2.688	4	92	4	0	(5)
46	7706-07	.056				8	2.689	1	94	5	0	(5)
47	7707-08	.087				8	2.680	TR	85	5	0	(5)
48	7708-09	.042				8	2.671	1	83	6	0	(5) and (6)
49	7708-10	.058				7	2.678	1	94	5	0	(6) and (7)
50	7710-11	.046				9	2.683	TR	85	5	0	(6) and (7)
CORE 3												
51	8311-12	.282				7	2.685	15	6	55	24	(8)
52	8312-13	2.891				8	2.688	28	8	49	19	(8)
53	8313-14	.251				8	2.681	22	10	52	17	(8)
54	8314-15	.211				7	2.688	19	15	51	15	(8)
55	8315-16	.136				4	2.706	15	64	28	15	(8)
56	8316-17	.334				9	2.708	20	6	55	19	(8)

* Plug sample could not be drilled due to condition of core.

¹ See key at end of table for descriptions.

² Failed During Analysis (FDA)

SAMPLE NUMBER	DEPTH (feet)	PERMEABILITY TO AIR		PERMEABILITY TO BRINE		POROSITY %	GRAIN DENSITY (gm/cc)	X-RAY DIFFRACTION (WEIGHT %)				LITHOLOGIC DESCRIPTIONS
		HORIZONTAL (md)	VERTICAL (md)	CLAYS	CARBONATE			QUARTZ	OTHER MINERALS			
57	8317-18	.072		.6	2.696	3	39	48	8	(8)		
58	8318-19	.283		8	2.687	18	3	61	17	(8) and (9)		
59	8318-20	.235		8	2.678	28	TR	54	18	(8) and (9)		
60	8320-21	3.04		8	2.700	33	2	52	13	(8) and (9)		
*	8321-22									(8) and (9)		
*	8322-23									(8)		
*	8323-24									(8)		
*	8324-25									(8)		
*	8325-26									(8) and (9)		
*	8326-27									(8)		
*	8327-28									(8)		
*	8328-29									(8)		
*	8329-30									(8)		
*	8330-31									(8)		
*	8331-32									(8)		
*	8332-33									(8)		
*	8333-34									(8)		
*	8334-35									(8)		
*	8335-36									(8)		
*	8336-37									(8)		

* Plug sample could not be drilled due to condition of core.

¹ See key at end of table for descriptions.

² Failed During Analysis (FDA)

SAMPLE NUMBER	DEPTH (feet)	PERMEABILITY TO AIR		PERMEABILITY TO BRINE		POROSITY %	GRAIN DENSITY (gm/cc)	X-RAY DIFFRACTION (WEIGHT %)				LITHOLOGIC DESCRIPTIONS
		HORIZONTAL (md)		VERTICAL (md)				CLAYS	CARBONATE	QUARTZ	OTHER MINERALS	
		TOTALS										
*	8337-38											(9) with occasional concentrations of shells on some shale parting surfaces; occasional siltkenisides
*	8338-39											(9) with occasional concentrations of shells on some shale parting surfaces; occasional siltkenisides
*	8339-40											(8) and (9) with some occasional concentrations of shells on some shale parting surfaces; occasional siltkenisides
CORE 4												
*	8785-86											(10)
*	8786-87											(10)
*	8787-88											(10)
*	8788-89											(10)
*	8789-90											(10)
*	8790-91											(10)
*	8791-92											(10)
*	8792-93											(10)
*	8793-94											(10)
*	8794-95											(10)
*	8795-96											(10)
*	8796-97											(10)
*	8797-98											(10)

* Plug sample could not be drilled due to condition of core.

¹ See key at end of table for descriptions.

² Failed During Analysis (FDA)

SAMPLE NUMBER	DEPTH (feet)	PERMEABILITY TO AIR		PERMEABILITY TO BRINE		POROSITY %	GRAIN DENSITY (gm/cc)	X-RAY DIFFRACTION (WEIGHT %)				LITHOLOGIC DESCRIPTIONS	
		HORIZONTAL (md)		VERTICAL (md)				TOTALS	CLAYS	CARBONATE	QUARTZ		OTHER MINERALS
*	8798-89												
*	8799-8800											(10)	
*	8800-01											(10)	
*	8801-02											(10)	
*	8802-03											(10)	
*	8803-04											(10)	
8804.7V	8804-05			1.071 X 10 ⁻⁵								(10) becoming calcareous and blocky	
8805.7V	8805-06			2.939 X 10 ⁻⁵								(11)	
*	8806-07											(11)	
8807.6V	8807-08			1.777 X 10 ⁻⁵								(11)	
*	8808-09											(10) and (11)	
*	8809-10											(10)	
*	8810-11											(10)	
*	8811-12											(10)	
*	8812-13											(10)	
*	8813-14											(10)	
*	8814-15											(10)	
CORE 5													
*	8100-01											(12) and (13)	
*	8101-02											(13) and (14)	

* Plug sample could not be drilled due to condition of core.

1 See key at end of table for descriptions.

2 Failed During Analysis (FDA)

SAMPLE NUMBER	DEPTH (feet)	PERMEABILITY TO AIR		PERMEABILITY TO BRINE		POROSITY %	GRAIN DENSITY (gm/cc)	X-RAY DIFFRACTION (WEIGHT %)				LITHOLOGIC DESCRIPTIONS
		HORIZONTAL (md)	VERTICAL (md)	CLAYS	CARBONATE			QUARTZ	OTHER MINERALS			
*	8102-03											(14) and (15)
*	8103-04											(14) and (15)
*	8104-05											(12) and (15)
*	8105-06											(15), (16) with clay clasts
61	8106-07	1.44				15	2.669	2	1	77	20	(16) with clay clasts
62	8107-08	.434				13	2.660	2	TR	78	19	(15)
*	8108-09											(12) and (15), (16) very micaceous, dark
*	8109-10											(15) and (16)
*	8110-11											(12) and (15)
*	8111-12											(12) and (15) and (16)
63	8112-13	.763				9	2.687	21	0	66	13	(15) and (16)
64	8113-14	.675				13	2.687	16	1	68	15	(12) and (15)
65	8114-15	.176				8	2.694	21	0	65	14	(14) and (16)
66	8115-16	4.57				18	2.691	13	0	73	14	(14) and (16)
67	8118-17	125				25	2.654	4	0	81	15	(14) and (16)
68	8117-18	148				22	2.651	8	1	87	6	(16)
69	8118-19	211				25	2.640	2	0	83	15	(16)
70	8119-20	113				24	2.710	4	0	85	11	(16)
*	8120-21											
71	8121-22	86.7				20	2.662	2	0	87	11	(15) and (16)

* Plug sample could not be drilled due to condition of core.

¹ See key at end of table for descriptions.

² Failed During Analysis(FDA)

SAMPLE NUMBER	DEPTH (feet)	PERMEABILITY TO AIR		PERMEABILITY TO BRINE		POROSITY %	GRAIN DENSITY (gm/cc)	X-RAY DIFFRACTION (WEIGHT %)				LITHOLOGIC DESCRIPTIONS
		HORIZONTAL (md)		VERTICAL (md)				TOTALS				
								CLAYS	CARBONATE	QUARTZ	OTHER MINERALS	
72	8122-23		227			23	1.783	2	0	85	13	(15) and (16)
*	8123-24											(15)
*	8124-25											(15)
*	8125-26											(15)
*	8126-27											(14) and (15)
73	8127-28	1.2				16	2.654	5	1	80	14	(12) and (14) and (16)
*	8128-29											(12) and (14) and (15)
*	8129-30											(14)
*	8130-31											(14) slickensides noted, (15), (16) but no green mineral, large scale cross-beds
74	8131-32	.128				5	2.711	7	17	66	10	(14) slickensides noted
CORE 6												
75	8386-87	643				25	2.674	4	1	8	5	(17)
76	8387-88	1527				18	2.671	1	11	88	0	(17) with coal clasts
77	8388-89	4849				28	2.648	1	TR	96	3	(17) with very thin coal stringers
78	8389-90	1224				24	2.708	1	3	96	0	(17) with shale, (18) clasts, (17) with thin shale laminae
79	8390-91	6665				28	2.655	1	0	97	2	(17)
80	8391-92	3186				25	2.646	1	2	96	1	(17) with sparse thin laminae of carbonaceous shale, very micaceous; sparse possible low-angle cross beds

* Plug sample could not be drilled due to condition of core.

1 See key at end of table for descriptions.

2 Failed During Analysis (FDA)

SAMPLE NUMBER	DEPTH (feet)	PERMEABILITY TO BRINE		POROSITY %	GRAIN DENSITY (gm/cc)	X-RAY DIFFRACTION (WEIGHT %)				LITHOLOGIC DESCRIPTIONS
		HORIZONTAL (md)	VERTICAL (md)			TOTALS				
						CLAYS	CARBONATE	QUARTZ	OTHER MINERALS	
81	8382-83	2246		27	2.683	2	1	89	8	(17) with sparse, thin laminae of carbonaceous shale, very micaceous; sparse possible low-angle cross beds
82	8383-84	2188		25	2.655	2	1	91	6	(17) with sparse, thin laminae of carbonaceous shale, very micaceous; sparse possible low-angle cross beds
83	8384-85	2486		23	2.647	3	0	83	4	(17) with sparse, thin laminae of carbonaceous shale, very micaceous; sparse possible low-angle cross beds
84	8385-86	2830		25	2.712	3	0	85	2	(17)
85	8386-87	2488		24	2.644	2	0	88	0	(17)
86	8387-88	128		22	2.684	8	6	71	85	(17) increasing frequency of carbonaceous laminae, carbonaceous laminae common, some shale; flaser bedding
87	8388-89	80,807		18	2.668	6	1	85	8	(17) carbonaceous laminae common, some shale; flaser bedding
88	8389-8400	2483		24	2.687	1	3	93	3	(17) interbedded sand and shale (18), beds approximately 0.5 inches, decreasing bedded shale and carbonaceous laminae, cross bedding present
89	8400-01	834		23	2.658	6	0	88	6	(17) increasing shale and carbonaceous laminae, cross bedding, ripple marks, flaser bedding, rip up clasts, some bioturbation
90	8401-02	81.1		16	2.652	11	0	82	7	(17) increasing shale and carbonaceous laminae, cross bedding, ripple marks, flaser bedding, rip up clasts, some bioturbation
81	8402-03	1413		22	2.663	6	0	86	8	(17) with rip up clay clasts, (18) with convolute bedding at base (at sand contact) and internal sand inclusions

* Plug sample could not be drilled due to condition of core.

¹ See key at end of table for descriptions.

² Failed During Analysis (FDA)

SAMPLE NUMBER	DEPTH (feet)	PERMEABILITY TO AIR		PERMEABILITY TO BRINE		POROSITY %	GRAIN DENSITY (gm/cc)	X-RAY DIFFRACTION (WEIGHT %)					LITHOLOGIC DESCRIPTIONS
		HORIZONTAL (md)	VERTICAL (md)	CLAYS	CARBONATE			QUARTZ	OTHER MINERALS	TOTALS -			
82	8403-04	3877			27	2.647	2	0	86	2	(17)		
83	8404-05	3184			26	2.650	2	TR	84	4	(17)		
84	8405-06	4834			28	2.653	4	0	81	5	(17)		
85	8406-07	978			23	2.651	3	0	85	2	(17)		
86	8407-08	1552			25	2.648	1	0	86	3	(17)		
87	8408-09	2234			26	2.653	4	0	83	3	(17)		
88	8409-10	1521			24	2.656	3	0	85	2	(17)		
89	8410-11	1095			23	2.646	2	2	81	5	(17)		
100	8411-12	1269			23	2.655	1	0	86	3	(17)		
101	8412-13	1680			22	2.650	11	0	86	3	(17)		
102	8413-14	1587			24	2.657	5	2	89	4	(17)		
103	8414-15	1721			24	2.656	2	0	87	1	(17)		
104	8415-16	3162			26	2.651	3	0	85	2	(17)		
105	8416-17	1868			25	2.660	3	0	86	1	(17)		
106	8417-18	1373			23	2.657	1	0	87	2	(17)		
CORE 7													
*	8606-07											(22) and (23)	
*	8607-08											(19)	
107	8608-09	.408			8	2.668	2	13	81	4		(20) flaser bedding, and (23)	
108	8608-10	.167			7	2.678	5	3	78	13		(20) and (23)	

* Plug sample could not be drilled due to condition of core.

1 See key at end of table for descriptions.

2 Failed During Analysis (FDA)

SAMPLE NUMBER	DEPTH (feet)	PERMEABILITY TO AIR		PERMEABILITY TO BRINE		POROSITY %	GRAIN DENSITY (gm/cc)	X-RAY DIFFRACTION (WEIGHT %)					LITHOLOGIC DESCRIPTIONS
		HORIZONTAL (md)	VERTICAL (md)	CLAYS	CARBONATE			QUARTZ	OTHER MINERALS	TOTALS			
109	9610-11	.705				13	2.666	2	2	80	6	(20) and (22) and (23), (22) and (23) interbedded	
110	9611-12	.506				15	2.704	6	26	58	10	(19) and (20) interbedded, laser bedding, (23)	
111	9612-13	1.329				6	2.706	21	5	60	14	(19) and (20) interbedded, laser bedding; (20) and (21) interbedded, and (23)	
112	9613-14	.237				8	2.721	8	6	72	16	(20) and (21) interbedded, finely laminated, cross bedded; (20) and (23) interbedded	
113	9614-15	.176				8	2.684	5	2	82	11	(20) and (21) interbedded, finely laminated, cross bedded; (20) and (21) interbedded, delicate cross bedding, laser bedding	
114	9615-16	.261				5	2.670	14	1	72	13	(23) with thin interbeds of (20)	
*	9616-17											(22)	
*	9617-18											(22)	
*	9618-19											(22)	
*	9619-20											(22) and (23)	
*	9620-21											(22) and (23) thinly interbedded	
*	9621-22											(22)	
*	9622-23											(22) interbedded with (20) and (21) interbedded, laser bedding	
115	9623-24	.135				10	2.670	7	9	72	12	(22)	
*	9624-25											(22)	
*	9625-26											(22)	
*	9626-27											(22)	
*	9627-28											(24)	

* Plug sample could not be drilled due to condition of core.

1 See key at end of table for descriptions.

2 Failed During Analysis (FDA)

SAMPLE NUMBER	DEPTH (feet)	PERMEABILITY TO AIR		PERMEABILITY TO BRINE		POROSITY %	GRAIN DENSITY (gm/cc)	X-RAY DIFFRACTION (WEIGHT %)				LITHOLOGIC DESCRIPTIONS
		HORIZONTAL (mcd)	VERTICAL (mcd)	CLAYS	CARBONATE			QUARTZ	OTHER MINERALS			
*	9628-29											(24)
*	9629-30											(24)
116	9630-31	4.16				11	2.874	17	5	65	13	(24)
117	9631-32	.280				7	2.732	16	4	89	11	(24)
118	9632-33	.562				6	2.682	24	4	59	13	(24)
119	9633-34	.178				6	2.687	22	3	64	11	(24)
120	9634-35	.182				6	2.685	18	3	68	11	(24)
*	9635-36											(24)
121	9636-37	.175				6	2.687	13	2	73	12	(24)

* Plug sample could not be drilled due to condition of core.

1 See key at end of table for descriptions.

2 Failed During Analysis (FDA)

SAMPLE NUMBER	DEPTH (feet)	PERMEABILITY TO AIR		PERMEABILITY TO BRINE		POROSITY %	GRAIN DENSITY (gm/cc)	X-RAY DIFFRACTION (WEIGHT %)				LITHOLOGIC DESCRIPTIONS
		HORIZONTAL (md)		VERTICAL (md)				CLAYS	CARBONATE	QUARTZ	OTHER MINERALS	
		TOTALS										
		CORE B										
*	9667-68											(25)
*	9668-69											(25)
*	9669-70											(25)
*	9670-71											(25)
*	9671-72											(25)
*	9672-73											(25)
*	9673-74											(25)
*	9674-75											(25)
*	9675-76											(25)
*	9676-77											(25)
*	9677-78											(25)
*	9678-79											(25)
*	9679-80											(25)
*	9680-81											(25)
*	9681-82											(25)
*	9682-83											(25)
*	9683-84											(25)
*	9684-85											(25)
*	9685-86											(25)

* Plug sample could not be drilled due to condition of core.

¹ See key at end of table for descriptions.

² Failed During Analysis (FDA)

SAMPLE NUMBER	DEPTH (feet)	PERMEABILITY TO AIR		PERMEABILITY TO BRINE		POROSITY %	GRAIN DENSITY (gm/cc)	X-RAY DIFFRACTION (WEIGHT %)				LITHOLOGIC DESCRIPTIONS
		HORIZONTAL (md)	VERTICAL (md)	CLAYS	CARBONATE			QUARTZ	OTHER MINERALS	TOTALS		
*	9686-87											(25)
*	9687-88											(25) and (26)
122	9688-89	.503				2	2.876	13	62	20	5	(25)
*	9689-90											(25)
123	9690-91	.224				8	2.857	7	2	63	28	(25) and (27) gradational, finely interbedded
124	9691-92	.248				10	2.861	4	2	60	34	(27)
125	9692-93	.216				8	2.87	2	12	64	22	(27) and (28)
126	9693-94	.078				1	3.469	TR	28	45	27	(25)
127	9694-95	.089				7	2.828	3	57	38	2	(25) and (27)
128	9695-96	.108				3	2.784	2	36	52	10	(25) and (29)
*	9696-97											(25) and (29)
CORE 9												
129	9817-18	64.9				18	2.873	1	0	88	11	(30) with clay clasts (3), (31)
130	9818-19	7.48				22	2.868	2	0	86	12	(30) and (31)
131	9819-20	7.48				24	2.857	2	0	88	9	(30) and (31)
132	9820-21	1298				21	2.855	2	1	87	10	(30) with clay clasts (31) up to 10 mm
133	9821-22	1522				25	2.860	1	0	90	9	(30) with clay clasts (31) up to 10 mm
134	9822-23	1330				22	2.855	1	0	92	7	(30) and (31)
135	9823-24	1377				24	2.853	1	0	98	3	(30)
136	9824-25	1014				24	2.854	2	1	73	4	(30)

* Plug sample could not be drilled due to condition of core.

1 See key at end of table for descriptions.

2 Failed During Analysis (FDA)

SAMPLE NUMBER	DEPTH (feet)	PERMEABILITY TO AIR		PERMEABILITY TO BRINE		POROSITY %	GRAIN DENSITY (gm/cc)	X-RAY DIFFRACTION (WEIGHT %)				¹ LITHOLOGIC DESCRIPTIONS
		HORIZONTAL (md)	VERTICAL (md)	CLAYS	CARBONATE			QUARTZ	OTHER MINERALS			
137	9825-26	834		23	2.652	1	0	89	10	(30)		
138	9826-27	2070		25	2.653	1	0	97	12	(30)		
139	9827-28	1455		24	2.655	1	0	95	4	(30)		
140	9828-29	1826		24	2.650	1	TR	99	0	(30)		
141	9829-30	276		20	2.664	1	TR	90	9	(30) and (31)		
142	9830-31	1207		23	2.653	1	0	94	5	(30)		
143	9831-32	918		23	2.659	1	0	96	3	(30)		
144	9832-33	521		21	2.661	1	TR	94	5	(30)		
145	9833-34	1254		23	2.659	1	0	87	2	(30)		
146	9834-35	520		21	2.659	1	TR	93	6	(30)		
147	9835-36	1431		23	2.648	1	0	87	2	(30)		
148	9836-37	836		23	2.649	1	0	87	2	(30)		
149	9837-38	1363		26	2.651	2	0	84	4	(30)		
150	9838-39	656		22	2.656	1	0	83	6	(30)		
151	9839-40	543		21	2.659	TR	0	86	4	(30)		
152	9840-41	² FDA		² FDA	² FDA	2	0	83	15	(30) and (31)		
153	9841-42	840		22	2.657	1	TR	97	2	(30)		
154	9842-43	1310		23	2.651	1	TR	83	6	(30)		
155	9843-44	881		22	2.651	2	0	82	6	(30)		
156	9844-45	1476		23	2.647	TR	0	84	6	(30)		

* Plug sample could not be drilled due to condition of core.

¹ See key at end of table for descriptions.

² Failed During Analysis (FDA)

SAMPLE NUMBER	DEPTH (feet)	PERMEABILITY TO AIR		PERMEABILITY TO BRINE		POROSITY %	GRAIN DENSITY (gm/cc)	X-RAY DIFFRACTION (WEIGHT %)				LITHOLOGIC DESCRIPTIONS
		HORIZONTAL (md)		VERTICAL (md)				CLAYS	TOTALS			
									CARBONATE	QUARTZ	OTHER MINERALS	
157	9845-46		733			22	2.654	1	91	7		(30)
158	9846-47		453			21	2.652	1	93	6		(30)
159	9847-48		1219			23	2.652	2	86	2		(30)
160	9848-49		716			21	2.650	1	95	4		(30)
CORE 10												
161	9849-50		449			21	2.652	2	TR	90	8	(32) and (33)
162	9850-51		475			22	2.653	1	1	91	7	(32)
163	9851-52		334			21	2.656	1	0	86	13	(32)
164	9852-53		441			22	2.653	1	0	82	7	(32)
165	9853-54		268			21	2.660	1	0	87	12	(32)
166	9854-55		1797			24	2.658	1	0	94	5	(32)
167	9855-56		816			23	2.648	TR	0	85	5	(32)
168	9856-57		1043			24	2.653	2	TR	94	4	(32)
169	9857-58		956			23	2.653	1	0	85	4	(32)
170	9858-59		1138			24	2.650	1	0	91	8	(32) with occasional thin layers (up to 1/4 inches) of micaceous and carbonaceous (M-C) material
171	9859-60		1043			24	2.651	TR	TR	82	8	(32) with occasional thin layers of M-C material
172	9860-61		662			22	2.648	1	TR	87	12	(32)
173	9861-62		638			23	2.658	1	0	82	7	(32)
174	9862-63		1296			24	2.655	3	0	91	6	(32)
175	9863-64		2048			24	2.647	1	0	95	4	(32)

* Plug sample could not be drilled due to condition of core.

¹ See key at end of table for descriptions.

² Failed During Analysis (FDA)

SAMPLE NUMBER	DEPTH (feet)	PERMEABILITY TO AIR		PERMEABILITY TO BRINE		POROSITY %	GRAIN DENSITY (gm/cc)	X-RAY DIFFRACTION (WEIGHT %)				LITHOLOGIC DESCRIPTIONS
		HORIZONTAL (md)	VERTICAL (md)	CLAYS	CARBONATE			QUARTZ	OTHER MINERALS			
176	9864-65	2781			25	2.657	1	0	83	6	(32)	
177	9865-66	4100			25	2.648	1	0	96	3	(32)	with occasional small lenses of M-C material
178	9866-67	2172			23	2.657	1	2	83	4	(32)	
179	9867-68	219			17	2.672	1	5	91	3	(32)	
180	9868-69	205			18	2.680	1	7	86	6	(32)	
181	9869-70	224			22	2.660	1	2	96	1	(32)	
182	9870-71	2359			23	2.663	1	0	98	1	(32)	
183	9871-72	2037			23	2.681	1	TR	87	2	(32)	
184	9872-73	1828			23	2.655	1	1	85	3	(32)	
185	9873-74	571			21	2.665	1	0	83	6	(32)	
186	9874-75	375			23	2.670	1	TR	95	4	(32)	with small lenses of shale (33) and M-C material
187	9875-76	486			23	2.659	1	0	81	8	(32)	
188	9876-77	414			22	2.681	TR	0	96	4	(32)	
189	9877-78	430			22	2.663	2	1	90	7	(32)	
190	9878-79	131			9	2.680	6	5	60	27	(32)	interbedded with fine layers of M-C material some M-C layers up to 1/2 inches thick, most very thin
191	9878-80	426			22	2.654	1	0	91	8	(32)	
192	9880-81	1036			23	2.654	2	3	88	7	(32)	
193	9881-82	450			22	2.655	1	0	82	7	(32)	
194	9882-83	312			20	2.666	1	0	88	10	(32)	

* Plug sample could not be drilled due to condition of core.

¹ See key at end of table for descriptions.

² Failed During Analysis (FDA)

SAMPLE NUMBER	DEPTH (feet)	PERMEABILITY TO BRINE		POROSITY %	GRAIN DENSITY (gm/cc)	X-RAY DIFFRACTION (WEIGHT %)				LITHOLOGIC DESCRIPTIONS
		HORIZONTAL (md)	VERTICAL (md)			TOTALS				
						CLAYS	CARBONATE	QUARTZ	OTHER MINERALS	
195	9883-84	333		21	2.658	2	3	86	9	(32)
196	9884-85	54.8		17	2.673	2	0	89	9	(32)
197	9885-86	128		19	2.669	2	0	86	12	(32)
198	9886-87	222		21	2.664	2	0	90	8	(32)
199	9887-88	380		22	2.646	1	0	88	11	(32) with occasional M-C laminae
200	9888-89	346		21	2.653	2	0	83	15	(32)
201	9889-90	284		21	2.656	1	0	89	10	(32) with occasional M-C laminae
202	9890-91	583		21	2.660	1	0	91	8	(32) with occasional M-C laminae
203	9891-92	1425		24	2.650	2	0	94	4	(32) with occasional M-C laminae
204	9892-93	235		20	2.655	1	TR	86	13	(32) with occasional M-C laminae
205	9893-94	403		21	2.654	1	1	91	7	(32) with occasional M-C laminae
206	9894-95	707		23	2.657	2	0	93	5	(32) with occasional M-C laminae
207	9895-96	877		24	2.659	1	0	94	5	(32) with occasional M-C laminae, in places slightly calcareous
208	9896-97	232		14	2.675	1	0	82	7	(32) with occasional M-C laminae, in places slightly calcareous
209	9897-98	417		22	2.665	1	0	90	8	(32) with occasional M-C laminae, in places slightly calcareous
210	9898-99	427		22	2.668	1	TR	82	7	(32) in places moderately calcareous
211	9899-9900	1910		25	2.662	1	5	90	4	(32) in places moderately calcareous
212	9900-01	1220		31	2.661	1	0	84	5	(32) in places moderately calcareous
213	9901-02	477		19	2.662	TR	0	87	3	(32) and (33)

* Plug sample could not be drilled due to condition of core.

¹ See key at end of table for descriptions.

² Failed During Analysis (FDA)

SAMPLE NUMBER	DEPTH (feet)	PERMEABILITY TO AIR		PERMEABILITY TO BRINE		POROSITY %	GRAIN DENSITY (gm/cc)	X-RAY DIFFRACTION (WEIGHT %)				LITHOLOGIC DESCRIPTIONS
		HORIZONTAL (md)	VERTICAL (md)	CLAYS	CARBONATE			QUARTZ	OTHER MINERALS			
										TOTALS		
214	8902-03	.336		8	TR	80	12	(32)	with abundant thin shale laminae, cross bedding in lower portion			
215	8903-04	6.31		2	TR	83	15	(32)	with shale and light brown claystone rip-up clasts			
216	8904-05	46.9		2	0	90	8	(32)				
217	8905-06	.167		2	36	54	8	(32)	with shale and light brown claystone rip-up clasts			
218	8906-07	.110		2	35	59	4	(32)				

* Plug sample could not be drilled due to condition of core.

1 See key at end of table for descriptions.

2 Failed During Analysis (FDA)

LITHOLOGIC DESCRIPTION KEY

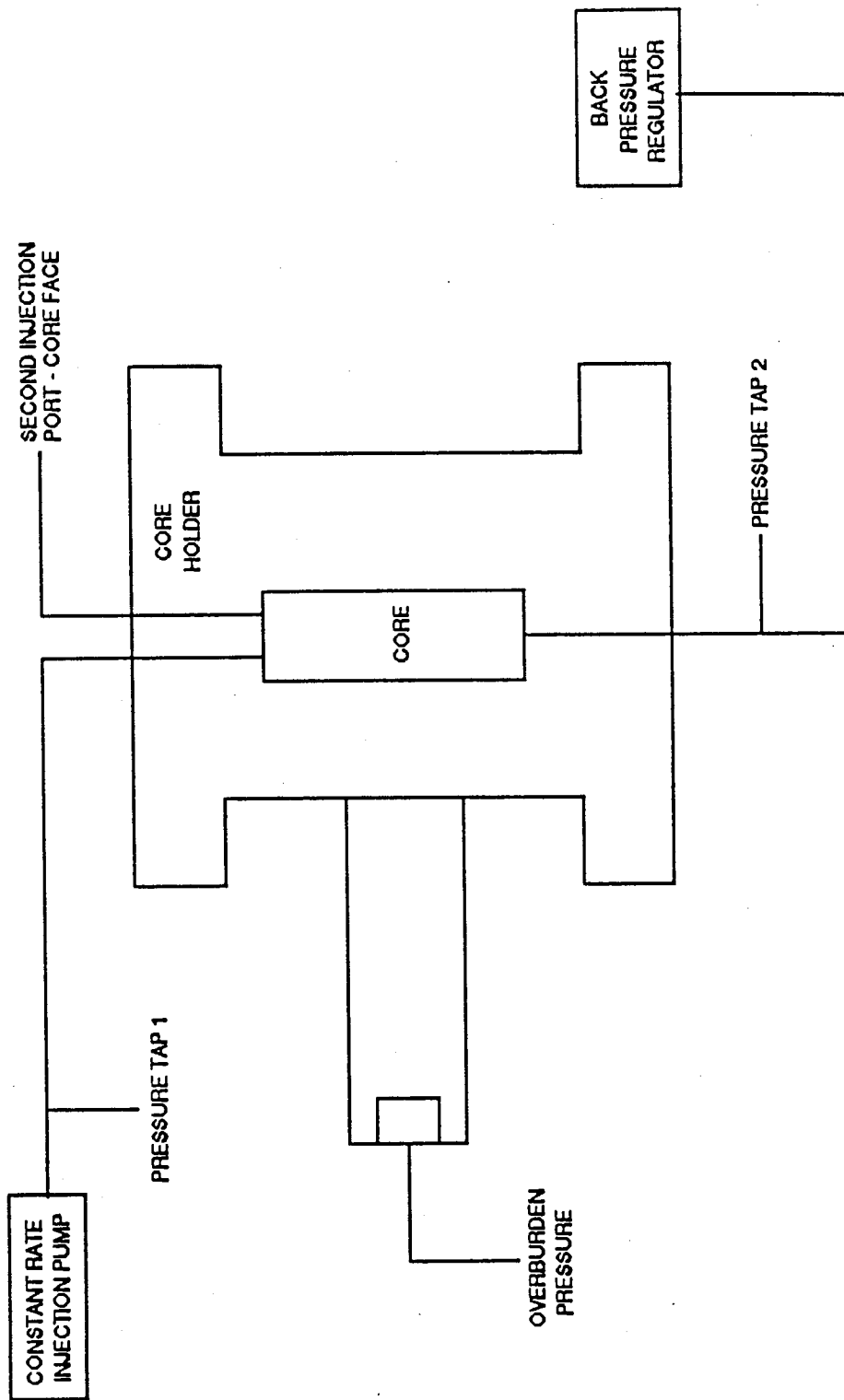
- (1) Shale - dark gray to black, fissile to blocky, carbonaceous, pyritic.
- (2) Sandstone - medium to dark gray, 85% quartz, 15% rock fragments, and dark minerals, fine to very fine grain, moderate sorting, laminated, calcareous, carbonaceous, burrowed, slightly friable, micaceous.
- (3) Sandstone - medium to light gray, 90% quartz, 10% rock fragments and dark minerals, very fine grain, moderately to well sorted, micaceous, carbonaceous, burrowed, slightly friable.
- (4) Sandstone - medium to dark gray, 85% quartz, 15% rock fragments and dark minerals, fine to very fine grain, moderate sorting, micaceous, carbonaceous, burrowed, slightly friable.
- (5) Chalk - light gray (most) and dark gray in lenticular laminations, dark gray probably greater % of shale, bioturbated, burrowed, fossiliferous.
- (6) Chalk - light gray, massive, sparse, fossils, sparse burrows.
- (7) Shale - dark gray to black, fissile, pyritic, carbonaceous.
- (8) Shale - dark gray, slightly fissile, very silty, very sandy (fine to very fine grain quartz sand), micaceous, pyritic, fossiliferous (small pelecypods or brachiopods [lingula (?)]), occasionally laminated (intercalated) with light gray shale which may have a slightly higher silt content.
- (9) Shale - dark gray, fissile, very little sand or silt, micaceous, sparsely fossiliferous (small pelecypods or brachiopods [lingula (?)]), noncalcareous.
- (10) Shale - dark gray, very fissile, micaceous, very few fossils (small pelecypods or brachiopods [lingula (?)]), noncalcareous.
- (11) Sandstone and Shale/Claystone - finely laminated - laminae, generally .5 inch to <.1 inch; sandstone - white, very fine grain, quartz, sub-angular to sub-rounded, slightly calcareous; shale/claystone - dark gray, blocky, hard, micaceous, few fossils, slightly calcareous.
- (12) Shale/Claystone - dark gray, slightly micaceous, slightly pyritic, blocky, hard, sparsely fossiliferous, noncalcareous.
- (13) Shale/Claystone - dark gray, slightly micaceous, blocky, hard, very fossiliferous (large pelecypods), matrix noncalcareous.

- (14) Shale - dark gray, micaceous, fissile to blocky, fossiliferous (pelecypods, brachiopods [lingula (?)]), noncalcareous.
- (15) Shale - dark gray, micaceous, very fissile, fossiliferous, noncalcareous, slickensides.
- (16) Sandstone - greenish white, quartz, fine to very fine grain, well sorted, sub-angular to sub-rounded, micaceous, occasionally very micaceous, 2% - 3% soft, green, waxy mineral (glauconite), very finely laminated to finely bedded, well indurated, slightly calcareous.
- (17) Sandstone - quartz, medium to fine grain, well sorted, angular to sub angular, sparsely micaceous, noncalcareous, well indurated, if not otherwise indicated, structure is massive.
- (18) Shale - dark gray, silty, micaceous, carbonaceous, moderately firm, noncalcareous.
- (19) Sandstone - light gray to medium gray, quartz, fine grain to very fine grain, moderately sorted, angular to sub-rounded, very silty, very shaley, micaceous, well indurated, sparsely carbonaceous, small scale flaser bedding common.
- (20) Sandstone - light gray, quartz, very fine grain, moderately sorted, angular to sub-angular, silty, probably shaley, < 3% dark fragments.
- (21) Sandstone - dark gray, quartz, very fine grain, moderately sorted, angular to sub-angular, carbonaceous, silty, probably shaley.
- (22) Shale - dark gray, micaceous, carbonaceous, sparsely fossiliferous, slickensides, blocky.
- (23) Shale - dark gray, micaceous, carbonaceous, sparsely fossiliferous, fissile.
- (24) Siltstone - dark gray, sandy, shaley, micaceous, carbonaceous, pyritic, blocky to massive.
- (25) Shale - dark gray to black, fissile to massive, very micaceous, slightly calcareous, sparsely pyritic, well indurated.
- (26) Sandstone - quartz, light gray, fine to very fine grain, silty, sub-angular to sub-rounded, moderately sorted micaceous, slightly calcareous, slightly pyritic, finely laminated.
- (27) Sandstone - quartz, light gray to light brown-gray, fine to very fine grain, moderately sorted, shaley, slightly fossiliferous, very micaceous, scarcely pyritic, some clay fragments, delicate flaser bedding with shale (1).
- (28) Sandstone - quartz, light gray, fine to very fine grain, well sorted, slightly micaceous, well indurated, massive.

- (29) Siltstone - medium gray, well indurated, micaceous, massive.
- (30) Sandstone - very light gray to light gray, quartz, medium to very fine grain, generally moderately well sorted, but the degree of sorting may vary on a small scale from moderate to well sorted, angular to sub-rounded, frosted grains abundant, mica generally sparse, but concentrated in bedding planes and veins with carbonaceous material, somewhat friable, slightly calcareous, massive bedding.
- (31) Shale/Claystone - very dark gray to black, micaceous, carboniferous, sparsely fossiliferous, variable fissile to blocky, hard.
- (32) Sandstone - very light gray to light gray quartz, medium to very fine grain, generally moderately well sorted but degree of sorting may vary on a small scale, angular to subrounded, most grains frosted, mica generally sparse but concentrated in bedding planes and vein fillings with carbonaceous material, somewhat friable, very slightly calcareous except where noted, massive bedding except where noted.
- (33) Shale/Claystone - very dark gray to black, micaceous, carboniferous, sparsely fossiliferous, variable fissile to blocky hard.

FIGURE

FIGURE 4.3-1
CORE FLOW APPARATUS



APPENDICES

APPENDIX 5.4-1

LITHOLOGIC DESCRIPTIONS

**E. I. DUPONT DE NEMOURS & COMPANY
WDW-5
HARRISON COUNTY, MISSISSIPPI**

LITHOLOGIC DESCRIPTIONS

COMPANY: DuPont
 WELL: WDW-5
 STATE: Mississippi

FORMATION: Midway
 COUNTY: Harrison

LITHOLOGY

- (1) Shale - dark gray to black, fissile to blocky, carbonaceous, pyritic.
- (2) Sandstone - medium to dark gray, 85% quartz, 15% rock fragments, and dark minerals, fine to very fine grain, moderate sorting, laminated, calcareous, carbonaceous, burrowed, slightly friable, micaceous.
- (3) Sandstone - medium to light gray, 90% quartz, 10% rock fragments and dark minerals, very fine grain, moderately to well sorted, micaceous, carbonaceous, burrowed, slightly friable.
- (4) Sandstone - medium to dark gray, 85% quartz, 15% rock fragments and dark minerals, fine to very fine grain, moderate sorting, micaceous, carbonaceous, burrowed, slightly friable.

CORE NO. 1		
BOX	DEPTH	DESCRIPTION
10	6912.0 - 13.0	(1)
	6913.0 - 13.4	(1)
	6913.4 - 14.0	(2)
	6914.0 - 14.6	(2)
	6914.6 - 15.0	(3)
9	6915.0 - 15.4	(1)
	6815.4 - 15.6	(1) flaser bedding
	6915.6 - 16.4	(1)
	6916.4 - 16.5	(1) fine laminae of (2)
	6916.5 - 18.0	(1)
8	6918.0 - 18.6	(1)
	6918.6 - 19.9	(3)
	6919.9 - 20.7	(2)
	6920.7 - 21.0	(1)
7	6921.0 - 21.3	(1)
	6921.3 - 23.2	(2)
	6923.2 - 24.0	(1)
6	6924.0 - 24.2	(2)
	6924.2 - 24.3	(1)
	6924.3 - 25.0	(2) & (4) finely interbedded
	6925.0 - 25.2	(1)
	6925.2 - 25.4	(2) & (4) finely interbedded
	6925.4 - 25.6	(1)
	6925.6 - 26.8	(2) & (3) finely interbedded
6926.8 - 27.0	(1)	

CORE NO. 1		
BOX	DEPTH	DESCRIPTION
5	6927.0 - 27.6	(1) silty
	6927.6 - 28.5	(3)
	6928.5 - 29.2	(1)
	6929.2 - 29.9	(2)
	6929.9 - 30.0	(1)
4	6930.0 - 30.2	(1)
	6930.2 - 32.0	(1) & (2) intercalated
	6932.0 - 32.4	(3)
	6932.4 - 33.0	(4)
3	6933.0 - 34.5	(4)
	6934.5 - 36.0	(1) & (3) intercalated
2	6936.0 - 36.7	(3)
	6936.7 - 37.0	(1)
	6937.0 - 37.5	(3)
	6937.5 - 39.0	(1)
1	6939.0 - 40.0	(1)
	6940.0 - 41.0	(4)
	6941.0 - 42.0	(1)

LITHOLOGIC DESCRIPTIONS

COMPANY: DuPont
 WELL: WDW-5
 STATE: Mississippi

FORMATION: Selma
 COUNTY: Harrison

LITHOLOGY

- (1) Chalk - light gray (most) and dark gray in lenticular laminations, dark gray probably greater % of shale, bioturbated, burrowed, fossiliferous.
- (2) Chalk - light gray, massive, sparse, fossils, sparse burrows.
- (3) Shale - dark gray to black, fissile, pyritic, carbonaceous.

CORE NO. 2		
BOX	DEPTH	DESCRIPTION
11	7680.0 - 80.5	(1)
	7680.5 - 80.7	(3)
	7680.7 - 81.0	(2)
10	7681.0 - 81.5	(2)
	7681.5 - 82.0	(1)
	7682.0 - 84.0	(2)
9	7684.0 - 84.4	(3)
	7684.4 - 85.0	(1)
	7685.0 - 86.2	(2)
	7686.2 - 86.4	(3)
	7686.4 - 87.0	(2)
8	7687.0 - 87.8	(2)
	7687.8 - 88.0	(1)
	7688.0 - 88.6	(2)
	7688.6 - 88.7	(3)
	7688.7 - 90.0	(2)
7	7690.0 - 90.7	(2)
	7690.7 - 90.8	(3)
	7690.8 - 91.0	(2)
	7691.0 - 91.3	(2)
	7691.3 - 91.4	(3)
	7691.4 - 92.5	(2)
	7692.5 - 93.0	(3)
6	7693.0 - 93.3	(3)
	7693.3 - 94.4	(2)
	7694.4 - 94.5	(3)
	7694.5 - 96.0	(2)

CORE NO. 2		
BOX	DEPTH	DESCRIPTION
5	7696.0 - 96.3	(3)
	7696.3 - 97.1	(1)
	7697.1 - 98.5	(2)
	7698.5 - 98.6	(3)
	7698.6 - 99.0	(2)
4	7699.0 - 99.5	(2)
	7699.5 - 99.6	(3)
	7699.6 - 7702.0	(2)
3	7702.0 - 03.2	(2)
	7703.2 - 03.3	(1)
	7703.3 - 03.7	(3)
	7703.7 - 04.1	(2)
	7704.1 - 04.4	(1)
	7704.4 - 05.0	(2)
2	7705.0 - 08.0	(1)
1	7708.0 - 08.6	(1)
	7708.6 - 09.0	(2)
	7709.0 - 09.6	(3)
	7709.6 - 09.7	(2)
	7709.7 - 11.0	(3)
		(2)

LITHOLOGIC DESCRIPTIONS

COMPANY: DuPont
 WELL: WDW-5
 STATE: Mississippi

FORMATION: Eutaw
 COUNTY: Harrison

LITHOLOGY

- (1) Shale - dark gray, slightly fissile, very silty, very sandy (fine to very fine grain quartz sand), micaceous, pyritic, fossiliferous (small pelecypods or brachiopods [lingula (?)]), occasionally laminated (intercalated) with light gray shale which may have a slightly higher silt content.
- (2) Shale - dark gray, fissile, very little sand or silt, micaceous, sparsely fossiliferous (small pelecypods or brachiopods [lingula (?)]), noncalcareous.

CORE NO. 3		
BOX	DEPTH	DESCRIPTION
10	8310.0 - 13.0	(1)
9	8313.0 - 16.0	(1)
8	8316.0 - 18.5 8318.5 - 18.7 8318.7 - 19.0	(1) (2) (1)
7	8319.0 - 19.6 8319.6 - 19.9 8319.9 - 20.6 8320.6 - 20.8 8320.8 - 21.7 8321.7 - 21.8 8321.8 - 22.0	(2) (1) (2) (1) (2) (1) (2)
6	8322.0 - 25.0	(2)
5	8325.0 - 25.6 8325.6 - 25.7 8325.7 - 28.0	(2) (1) (2)
4	8328.0 - 31.0	(2)
3	8331.0 - 34.0	(2)
2	8334.0 - 37.0	(2)
1	8337.0 - 39.6 8339.6 - 39.7 8339.7 - 40.0	(2) with occasional concentrations of shells on some shale parting surfaces; occasional slickensides (1) (2)

LITHOLOGIC DESCRIPTIONS

COMPANY: DuPont
 WELL: WDW-5
 STATE: Mississippi

FORMATION: Tuscaloosa
 COUNTY: Harrison

LITHOLOGY

- (1) Shale - dark gray, very fissile, micaceous, very few fossils (small pelecypods or brachiopods [lingula (?)]), noncalcareous.
- (2) Sandstone and Shale/Claystone - finely laminated - laminae, generally .5 inch to <.1 inch; sandstone - white, very fine grain, quartz, sub-angular to sub-rounded, slightly calcareous; shale/claystone - dark gray, blocky, hard, micaceous, few fossils, slightly calcareous.

CORE NO. 4		
BOX	DEPTH	DESCRIPTION
10	8785.0 - 88.0	(1)
9	8788.0 - 91.0	(1)
8	8791.0 - 93.0	(1)
7	8793.0 - 97.0	(1)
6	8797.0 - 8800.0	(1)
5	8800.0 - 03.0	(1)
4	8803.0 - 04.3 8804.3 - 04.7 8804.7 - 06.0	(1) (1) becoming calcareous and blocky (2)
3	8806.0 - 08.8 8808.8 - 09.0	(2) (1)
2	8809.0 - 12.0	(1)
1	8812.0 - 15.0	(1)

LITHOLOGIC DESCRIPTIONS

COMPANY: DuPont
 WELL: WDW-5
 STATE: Mississippi

FORMATION: Tuscaloosa
 COUNTY: Harrison

LITHOLOGY

- (1) Shale/Claystone - dark gray, slightly micaceous, slightly pyritic, blocky, hard, sparsely fossiliferous, noncalcareous.
- (2) Shale/Claystone - dark gray, slightly micaceous, blocky, hard, very fossiliferous (large pelecypods), matrix noncalcareous.
- (3) Shale - dark gray, micaceous, fissile to blocky, fossiliferous (pelecypods, brachiopods (lingula (?))), noncalcareous.
- (4) Shale - dark gray, micaceous, very fissile, fossiliferous, noncalcareous, slickensides.
- (5) Sandstone - greenish white, quartz, fine to very fine grain, well sorted, sub-angular to sub-rounded, micaceous, occasionally very micaceous, 2% - 3% soft, green, waxy mineral (glauconite), very finely laminated to finely bedded, well indurated, slightly calcareous.

CORE NO. 5		
BOX	DEPTH	DESCRIPTION
11	9100.5 - 00.7	(1)
	9100.7 - 01.2	(2)
	9101.2 - 02.0	(3)
10	9102.0 - 02.6	(3)
	9102.6 - 03.3	(4)
	9103.3 - 03.8	(3)
	9103.8 - 04.2	(4)
	9104.2 - 04.4	(1)
	9104.4 - 04.6	(4)
9	9104.6 - 05.0	(1)
	9105.0 - 05.6	(4)
	9105.6 - 07.1	(5) with clay clasts
8	9107.1 - 08.0	(4)
	9108.0 - 08.2	(1)
	9108.2 - 08.7	(4)
	9108.7 - 08.9	(5) very micaceous, dark
	9108.9 - 09.4	(4)
	9109.4 - 09.8	(5)
	9109.8 - 10.0	(4)
	9110.0 - 10.2	(1)
	9110.2 - 10.3	(4)
	9110.3 - 10.6	(1)
9110.6 - 11.0	(4)	

CORE NO. 5		
BOX	DEPTH	DESCRIPTION
7	9111.0 - 11.2	(1)
	9111.2 - 11.5	(5)
	9111.5 - 11.7	(4)
	9111.7 - 12.3	(5)
	9112.3 - 13.6	(4)
	9113.6 - 14.0	(1)
6	9114.0 - 15.4	(5)
	9115.4 - 15.7	(3)
	9115.7 - 16.3	(5)
	9116.3 - 16.4	(3)
	9116.4 - 16.8	(5)
	9116.8 - 17.0	(3)
5	9117.0 - 20.0	(5)
4	9120.0 - 21.9	(5)
	9121.9 - 22.6	(4)
	9122.6 - 22.9	(5)
	9122.9 - 23.0	(4)
3	9123.0 - 26.0	(4)
2	9126.0 - 26.4	(4)
	9126.4 - 27.2	(3)
	9127.2 - 27.8	(5)
	9127.8 - 28.2	(1)
	9128.2 - 28.6	(4)
	9128.6 - 29.0	(3)
1	9129.0 - 29.3	(3)
	9129.3 - 30.1	(5) but no green mineral, large scale cross-beds
	9130.1 - 30.5	(4)
	9130.5 - 32.0	(3) slickensides noted

LITHOLOGIC DESCRIPTIONS

COMPANY: DuPont
 WELL: WDW-5
 STATE: Mississippi

FORMATION: Tuscaloosa
 COUNTY: Harrison

LITHOLOGY

- (1) Sandstone - quartz, medium to fine grain, well sorted, angular to sub angular, sparsely micaceous, noncalcareous, well indurated, if not otherwise indicated, structure is massive.
- (2) Shale - dark gray, silty, micaceous, carbonaceous, moderately firm, noncalcareous.

CORE NO. 6		
BOX	DEPTH	DESCRIPTION
11	9386.0 - 87.6 9387.6 - 88.0	(1) (1) with coal clasts
10	9388.0 - 88.3 9388.3 - 88.4 9388.4 - 89.1 9389.1 - 89.3 9389.3 - 89.5 9389.5 - 90.7 9390.7 - 90.9 9390.9 - 91.0	(1) (1) with very thin coal stringers (1) (1) with shale (2) clasts (1) with thin shale laminae (1) (1) with coal stringers (1)
9	9391.0 - 94.0	(1) with sparse thin laminae of carbonaceous shale, very micaceous; sparse possible low-angle cross beds
8	9394.0 - 94.4 9394.4 - 97.0	(1) with sparse thin laminae of carbonaceous shale, very micaceous; sparse possible lowangle cross beds (1)
7	9397.0 - 97.4 9397.4 - 99.4 9399.4 - 99.6 9399.6 - 9400.0	(1) increasing frequency of carbonaceous laminae (1) Carbonaceous laminae common, some shale; flaser bedding (1) interbedded sand and shale (2), beds approximately .5 inches (1) decreasing bedded shale and carbonaceous laminae; cross bedding present
6	9400.0 - 01.9 9401.9 - 02.3 9402.3 - 02.5 9402.5 - 03.0	(1) increasing shale and carbonaceous laminae, cross bedding, ripple marks, flaser bedding, rip up clasts, some bioturbation (2) with convolute bedding at base (at sand contact) and internal sand inclusions (1) with rip up clay clasts (1)
5	9403.0 - 06.0	(1)
4	9406.0 - 09.0	(1)

CORE NO. 6		
BOX	DEPTH	DESCRIPTION
3	9409.0 - 12.0	(1)
2	9412.0 - 15.0	(1)
1	9415.0 - 18.0	(1)

LITHOLOGIC DESCRIPTIONS

COMPANY: DuPont
 WELL: WDW-5
 STATE: Mississippi

FORMATION: Washita-Fredricksburg
 COUNTY: Harrison

LITHOLOGY

- (1) Sandstone - light gray to medium gray, quartz, fine grain to very fine grain, moderately sorted, angular to sub-rounded, very silty, very shaley, micaceous, well indurated, sparsely carbonaceous, small scale flaser bedding common.
- (2) Sandstone - light gray, quartz, very fine grain, moderately sorted, angular to sub-angular, silty, probably shaley, < 3% dark fragments.
- (3) Sandstone - dark gray, quartz, very fine grain, moderately sorted, angular to sub-angular, carbonaceous, silty, probably shaley.
- (4) Shale - dark gray, micaceous, carbonaceous, sparsely fossiliferous, slickensides, blocky.
- (5) Shale - dark gray, micaceous, carbonaceous, sparsely fossiliferous, fissile.
- (6) Siltstone - dark gray, sandy, shaley, micaceous, carbonaceous, pyritic, blocky to massive.

CORE NO. 7		
BOX	DEPTH	DESCRIPTION
11	9606.0 - 06.0	(5)
	9606.6 - 07.0	(4)
10	9607.0 - 08.0	(1)
	9608.0 - 08.5	(2)
	9608.5 - 08.9	(5)
	9608.9 - 09.0	(2) flaser bedding
	9609.0 - 09.7	(5)
	9609.7 - 09.8	(2)
9	9609.8 - 10.0	(5)
	9610.0 - 10.1	(5)
	9610.1 - 10.2	(4)
	9610.2 - 10.6	(2)
	9610.6 - 11.2	(4) & (5) interbedded
	9611.2 - 11.9	(1) & (2) interbedded, flaser bedding
	9611.9 - 12.2	(5)
	9612.2 - 12.5	(1) & (2) interbedded, flaser bedding
9612.5 - 12.7	(5)	
9612.7 - 13.0	(2) & (3) interbedded	

CORE NO. 7		
BOX	DEPTH	DESCRIPTION
8	9613.0 - 13.7	(2) & (3) interbedded, finely laminated, cross-bedded
	9613.7 - 14.3	(2) & (5) interbedded
	9614.3 - 14.5	(2) & (3) interbedded, finely laminated, cross-bedded
	9614.5 - 14.6	(5)
	9614.6 - 14.7	(2) finely laminated
	9614.7 - 14.8	(5)
	9614.8 - 15.0	(2) & (3) interbedded, delicate cross-bedding, flaser bedding
	9615.0 - 15.1	(5)
	9615.1 - 15.4	(2) & (3) interbedded, delicate cross-bedding, flaser bedding
	9615.4 - 16.0	(5) with thin interbeds of (2)
7	9616.0 - 19.0	(4)
6	9619.0 - 19.5	(4)
	9619.5 - 19.6	(5)
	9619.6 - 20.6	(4)
	9620.6 - 20.7	(5)
	9620.7 - 21.0	(4) & (5) thinly interbedded
	9621.0 - 22.0	(4)
5	9622.0 - 22.3	(4)
	9622.3 - 23.6	(4) interbedded with (2) & (3) interbedded, flaser bedding
	9623.6 - 25.0	(4)
4	9625.0 - 26.7	(4)
	9626.7 - 28.0	(6)
3	9628.0 - 31.0	(6)
2	9631.0 - 34.0	(6)
1	9634.0 - 37.0	(6)

LITHOLOGIC DESCRIPTIONS

COMPANY: DuPont
 WELL: WDW-5
 STATE: Mississippi

FORMATION: Washita-Fredricksburg
 COUNTY: Harrison

LITHOLOGY

- (1) Shale - dark gray to black, fissile to massive, very micaceous, slightly calcareous, sparsely pyritic, well indurated.
- (2) Sandstone - quartz, light gray, fine to very fine grain, silty, sub-angular to sub-rounded, moderately sorted micaceous, slightly calcareous, slightly pyritic, finely laminated.
- (3) Sandstone - quartz, light gray to light brown-gray, fine to very fine grain, moderately sorted, shaley, slightly fossiliferous, very micaceous, scarcely pyritic, some clay fragments, delicate flaser bedding with shale (1).
- (4) Sandstone - quartz, light gray, fine to very fine grain, well sorted, slightly micaceous, well indurated, massive.
- (5) Siltstone - medium gray, well indurated, micaceous, massive.

CORE NO. 8		
BOX	DEPTH	DESCRIPTION
10	9667.0 - 70.0	(1)
9	9670.0 - 73.0	(1)
8	9673.0 - 76.0	(1)
7	9676.0 - 79.0	(1)
6	9679.0 - 82.0	(1)
5	9682.0 - 85.0	(1)
4	9685.0 - 87.2 9687.2 - 87.4 9687.4 - 87.6 9687.6 - 87.7 9687.7 - 88.0	(1) (2) (1) (2) (1)
3	9880.0 - 90.4 9890.4 - 90.6 9890.6 - 91.0	(1) (1) & (3) gradational, finely interbedded (3)
2	9891.0 - 92.9 9892.9 - 93.2 9893.2 - 94.0	(3) (4) (1)

CORE NO. 8		
BOX	DEPTH	DESCRIPTION
1	9894.0 - 94.1	(1)
	9894.1 - 95.6	(3)
	9895.6 - 96.6	(1)
	9896.6 - 96.7	(5)
	9896.7 - 97.0	(1)

LITHOLOGIC DESCRIPTIONS

COMPANY: DuPont
 WELL: WDW-5
 STATE: Mississippi

FORMATION: Washita-Fredricksburg
 COUNTY: Harrison

LITHOLOGY

- (1) Sandstone - very light gray to light gray, quartz, medium to very fine grain, generally moderately well sorted, but the degree of sorting may vary on a small scale from moderate to well sorted, angular to sub-rounded, frosted grains abundant, mica generally sparse, but concentrated in bedding planes and veins with carbonaceous material, somewhat friable, slightly calcareous, massive bedding.
- (2) Shale/Claystone - very dark gray to black, micaceous, carboniferous, sparsely fossiliferous, variable fissile to blocky, hard.

CORE NO. 9		
BOX	DEPTH	DESCRIPTION
11	9817.4 - 17.6	(2)
	9817.6 - 17.8	(1) with clay casts (2)
	9817.8 - 17.9	(2)
	9817.9 - 19.0	(1)
10	9819.0 - 19.3	(1)
	9819.3 - 19.7	(2)
	9819.7 - 22.0	(1) with clay clasts (2) up to 10 mm
9	9822.0 - 22.3	(1)
	9822.3 - 22.8	(2)
	9822.8 - 25.0	(1)
8	9825.0 - 28.0	(1)
7	9828.0 - 29.3	(1)
	9829.3 - 29.5	(2)
	9829.5 - 31.0	(1)
6	9831.0 - 34.0	(1)
5	9834.0 - 37.0	(1)
4	9837.0 - 40.0	(1)
3	9840.0 - 40.4	(1)
	9840.4 - 40.5	(2)
	9840.5 - 43.0	(1)
2	9843.0 - 46.0	(1)
1	9846.0 - 49.0	(1)

LITHOLOGIC DESCRIPTIONS

COMPANY: DuPont
 WELL: WDW-5
 STATE: Mississippi

FORMATION: Washita-Fredricksburg
 COUNTY: Harrison

LITHOLOGY

- (1) Sandstone - very light gray to light gray quartz, medium to very fine grain, generally moderately well sorted, but degree of sorting may vary on a small scale, angular to sub-rounded, most grains frosted, mica generally sparse, but concentrated in bedding planes and vein fillings with carbonaceous material, somewhat friable, very slightly calcareous except where noted, massive bedding except where noted.
- (2) Shale/Claystone - very dark gray to black, micaceous, carboniferous, sparsely fossiliferous, variable fissile to blocky hard.

CORE NO. 10		
BOX	DEPTH	DESCRIPTION
20	9849.0 - 49.4	(1)
	9849.4 - 49.7	(2)
	9849.7 - 50.0	(1)
19	9850.0 - 53.0	(1)
18	9853.0 - 56.0	(1)
17	9856.0 - 58.4	(1)
	9858.4 - 59.0	(1) with occasional thin layers (up to 1/4 inches) of micaceous and carbonaceous (M-C) material
16	9859.0 - 59.2	(1) with occasional thin layers of M-C material
	9859.2 - 62.0	(1)
15	9862.0 - 65.0	(1)
14	9865.0 - 65.2	(1)
	9865.2 - 65.8	(1) with occasional small lenses of M-C material
	9865.8 - 68.0	(1)
13	9868.0 - 71.0	(1)
12	9871.0 - 74.0	(1)
11	9874.0 - 74.2	(1) with small lenses of shale (2) and M-C material.
	9874.2 - 77.0	(1)
10	9877.0 - 77.9	(1)
	9877.9 - 78.3	(1) interbedded with fine layers of M-C material, some M-C layers up to 1/2 inches thick, most very thin
	9878.3 - 80.0	(1)
9	9880.0 - 83.0	(1)
8	9883.0 - 86.0	(1)

CORE NO. 10		
BOX	DEPTH	DESCRIPTION
7	9886.0 - 87.3 9887.3 - 87.9 9887.9 - 89.0	(1) (1) with occasional M-C laminae (1)
6	9889.0 - 92.0	(1) with occasional M-C laminae
5	9892.0 - 95.0	(1) with occasional M-C laminae
4	9895.0 - 98.0	(1) with occasional M-C laminae, in places slightly calcareous
3	9898.0 - 9901.0	(1) in places moderately calcareous
2	9901.0 - 01.3 9901.3 - 01.4 9901.4 - 01.9 9901.9 - 02.6 9902.6 - 03.4 9903.4 - 04.0	(1) in places slightly calcareous (1) with abundant shale rip-up clasts (2) with flaser type lenses of fine to very fine grain, cream colored, quartz sand (2) (1) with abundant thin shale laminae, cross-bedding in lower portion (1) with shale and light brown claystone rip-up clasts
1	9904.0 - 04.4 9904.4 - 05.9 9905.9 - 07.0	(1) (1) with shale and light brown claystone rip-up clasts (1)

APPENDIX 6.0-1
X-RAY DIFFRACTION ANALYSIS

APPENDIX 6.0-1

AUTO X-RAY DIFFRACTION STUDY
FOR
ENVIROCORP,
UNKNOWN WELL
DEPTH INTERVAL 6913.5' - 9906.8'

OMNI LABORATORIES, INC.
 AUTO X-RAY DIFFRACTION
 (WEIGHT%)

FILE NO: G-1992
 DATE : 4-29-93

ENVIROCORP
 UNKNOWN WELL

SAMPLE NUMBER	CLAYS					CARBONATES					OTHER MINERALS							TOTALS		
	KAOLINITE	CHLORITE	ILLITE	ILL./MISC.*	SMECTITE	QUARTZ	PLAG.	K-SPAR	MICA	BARITE	PHYRITE	HALITE	CLAYS	CARB.	OTHER	CLAYS	CARB.	OTHER		
001	0	1	2	7	37	1	12	2	TR	0	1	0	10	38	52					
002	TR	1	2	5	TR	0	17	3	TR	0	2	0	8	TR	92					
003	1	1	2	5	1	0	18	6	0	0	TR	0	9	1	90					
004	TR	TR	TR	2	42	0	11	7	0	0	0	0	2	42	56					
005	1	1	2	4	0	1	21	6	0	0	0	0	8	1	91					
006	1	2	2	11	0	0	19	2	0	0	0	TR	16	0	84					
007	TR	1	1	5	48	0	9	4	0	0	TR	1	7	48	45					
008	1	1	2	8	42	0	10	3	TR	0	0	0	12	42	46					
009	TR	2	2	15	TR	0	16	2	TR	0	0	0	19	TR	81					
010	0	2	2	9	1	0	19	6	TR	0	0	0	13	1	86					
011	2	1	4	9	0	0	28	4	TR	0	0	3**	16	0	84					
012	2	1	3	15	0	0	16	8	0	0	0	0	21	0	79					
013	TR	1	1	9	17	0	12	3	0	0	0	0	11	17	72					
014	1	1	3	23	5	0	16	4	TR	0	0	0	28	5	67					
015	TR	1	2	20	0	0	18	TR	0	0	4	0	23	0	77					
016	1	2	3	15	0	0	25	TR	TR	0	2	0	21	0	79					
017	1	2	3	13	0	TR	20	7	0	0	1	0	19	TR	81					
018	2	2	6	19	5	0	14	6	0	0	3	0	29	5	66					
019	10	4	15	10	0	0	11	5	0	0	4	0	39	0	61					
020	0	0	TR	0	83	0	TR	0	0	0	0	0	TR	93	7					
AVERAGE	1	1	3	10	15	TR	16	4	TR	0	1	TR	15	15	70					

* Random mixed-layer Illite/smectite contains approximately 70-80% expandable (smectite) interlayers.

** Sylvite

OMNI LABORATORIES, INC.
 AUTO X-RAY DIFFRACTION
 (WEIGHT%)

ENVIROCORP
 UNKNOWN WELL

FILE NO: G-1992
 DATE : 4-29-93

SAMPLE NUMBER	CLAYS				CARBONATES						OTHER MINERALS						TOTALS			
	KAOLINITE	CHLORITE	ILLITE	ILL./MISC.*	CALCITE	DOLOMITE	SIDERITE	QUARTZ	FLAQ.	K-SPAR	MICA	SARITE	PHYRITE	MALITE	CLAYS	CARB.	OTHER			
021	0	0	TR	0	93	0	0	6	0	0	TR	0	0	0	1	93	6			
022	0	0	TR	TR	94	0	0	6	0	0	0	0	0	0	TR	94	6			
023	TR	0	1	TR	92	0	0	7	TR	0	TR	0	0	0	1	92	7			
024	0	0	2	3	89	0	0	6	0	0	0	0	0	0	5	89	6			
025	TR	0	TR	1	93	0	0	6	0	0	0	0	0	0	1	93	6			
026	0	TR	2	1	86	0	0	7	2	0	0	0	0	0	3	86	9			
027	0	0	TR	1	94	0	0	5	TR	0	0	0	0	0	1	94	5			
028	0	TR	TR	TR	96	0	0	4	TR	0	0	0	0	0	TR	96	4			
029	0	TR	TR	TR	93	0	0	7	0	0	0	0	0	0	TR	93	7			
030	0	0	TR	TR	95	0	0	5	0	0	0	0	0	0	TR	95	5			
031	TR	0	1	2	89	0	0	5	0	0	0	0	3	0	3	89	8			
032	TR	TR	1	2	91	0	0	6	0	0	0	0	0	0	3	91	6			
033	TR	0	TR	1	93	0	0	6	0	0	TR	0	0	0	1	93	6			
034	TR	0	1	2	89	0	0	7	1	0	0	0	0	0	3	89	8			
035	0	0	1	2	91	0	0	6	0	0	0	0	0	0	3	91	6			
036	TR	0	1	1	90	0	0	5	0	0	TR	0	3	0	2	90	8			
037	TR	0	1	2	93	0	0	4	0	0	0	0	0	0	3	93	4			
038	0	0	1	3	89	0	0	7	TR	0	0	0	0	0	4	89	7			
039	TR	0	TR	1	95	0	0	4	0	0	0	0	0	0	1	95	4			
040	0	TR	TR	2	90	0	0	6	2	0	0	0	0	0	2	90	8			
AVERAGE	TR	TR	1	1	92	0	0	6	TR	TR	TR	0	TR	0	2	92	6			

* Random mixed-layer illite/smectite contains approximately 65-65% expandable (smectite) interlayers.

OMNI LABORATORIES, INC.
 AUTO X-RAY DIFFRACTION
 (WEIGHT%)

FILE NO: G-1992
 DATE : 4-29-93

ENVIROCORP
 UNKNOWN WELL

SAMPLE NUMBER	CLAYS					CARBONATES							OTHER MINERALS							TOTALS		
	KAOLINITE	CHLORITE	ILLITE	ILL./SMECT.*	SMECT.	SMECT.	DOLOMITE	SMECT.	QUARTZ	PLAG.	K-SPAR	MCA	BARITE	PIRITE	HALITE	CLAYS	CARB.	OTHER				
041	0	0	1	2	0	0	0	0	6	0	0	0	0	0	0	3	91	6				
042	0	0	1	2	0	0	0	6	1	0	TR	0	0	0	0	3	90	7				
043	0	0	2	3	0	0	0	6	0	0	0	0	0	0	5	89	6					
044	0	0	TR	TR	0	0	0	5	2	0	0	0	0	0	TR	93	7					
046	TR	0	1	3	0	0	0	4	0	0	0	0	0	0	4	92	4					
048	TR	0	TR	1	0	0	0	5	TR	0	0	0	0	TR	1	94	5					
047	0	0	TR	TR	0	0	0	5	0	0	0	0	0	0	TR	95	5					
048	0	TR	TR	1	0	0	0	6	0	0	0	0	0	0	1	93	6					
049	TR	0	TR	1	0	0	0	5	0	0	0	0	0	0	1	94	6					
050	0	0	TR	TR	0	0	0	5	TR	0	0	0	0	0	TR	95	5					
051	4	0	5	6	0	0	0	55	16	6	TR	0	2	0	15	6	79					
052	5	2	7	12	0	0	0	49	13	2	TR	0	4	0	26	6	68					
053	3	2	5	12	0	0	0	52	12	4	TR	0	0	0	22	10	68					
054	5	TR	7	7	0	0	0	61	12	3	0	0	TR	0	19	15	68					
055	3	0	7	5	0	0	0	26	13	2	TR	0	0	0	15	44	41					
056	7	2	9	2	0	0	0	55	14	5	TR	0	0	0	20	6	74					
057	1	TR	1	1	0	0	0	49	7	2	TR	0	0	0	3	39	58					
058	5	1	6	7	0	0	0	61	17	0	TR	0	0	0	19	3	78					
059	6	2	7	13	0	0	0	54	13	3	TR	0	2	0	28	TR	72					
060	5	2	11	15	0	0	0	52	9	TR	TR	0	4	0	33	2	65					
AVERAGE	2	1	4	5	0	0	0	26	6	1	TR	0	1	TR	12	52	38					

* Random mixed-layer illite/smectite contains approximately 40-50% expandable (smectite) interlayers (samples 041-050);
 ordered mixed-layer illite/smectite contains approximately 25-35% expandable (smectite) interlayers (samples 051-060).

OMNI LABORATORIES, INC.
 AUTO X-RAY DIFFRACTION
 (WEIGHT%)

FILE NO: G-1992
 DATE : 4-29-93

ENVIROCORP
 UNKNOWN WELL

SAMPLE NUMBER	CLAYS				CARBONATES				OTHER MINERALS							TOTALS			
	KAOLINITE	CHLORITE	ILLITE	ILL/SMECT*	CALCITE	DOLOMITE	SIDERITE	QUARTZ	PLAG.	K-SPAR	MICA	BARITE	PHYRITE	MALITE	CLAYS	CARB.	OTHER		
061	1	TR	1	TR	1	0	0	77	17	3	TR	0	0	0	2	1	97		
062	TR	1	1	TR	TR	0	0	79	15	4	0	0	0	0	2	TR	98		
063	4	3	6	8	0	0	0	68	11	2	TR	0	0	0	21	0	79		
064	4	2	3	7	1	0	0	68	12	3	TR	0	0	0	16	1	83		
065	1	3	5	12	0	0	0	65	11	3	TR	0	TR	0	21	0	79		
066	1	1	11	0	0	0	0	73	13	1	0	0	0	0	13	0	87		
067	TR	TR	2	2	0	0	0	81	11	4	0	0	0	TR	4	0	96		
068	1	TR	2	2	1	0	0	87	6	1	0	0	0	TR	5	1	94		
069	TR	TR	1	1	0	0	0	83	8	6	0	0	1	TR	2	0	98		
070	TR	TR	2	2	0	0	0	85	6	1	TR	0	0	4	0	0	96		
071	TR	TR	1	1	0	0	0	87	7	1	0	0	3	0	2	0	98		
072	TR	TR	TR	2	0	0	0	85	10	2	0	0	0	1	2	0	98		
073	TR	1	2	2	1	0	0	80	13	1	TR	0	0	0	5	1	94		
074	1	1	2	3	17	0	0	66	8	2	TR	0	0	0	7	17	76		
075	1	1	1	1	0	0	1	90	5	TR	TR	0	0	0	4	1	95		
076	0	TR	1	TR	11	0	0	88	TR	0	0	0	0	0	1	11	88		
077	TR	TR	1	0	TR	0	0	96	3	TR	0	0	TR	0	1	TR	99		
078	1	TR	TR	0	0	0	3	96	0	0	0	0	0	0	1	3	96		
079	TR	TR	1	TR	0	0	0	97	2	TR	0	0	0	0	1	0	99		
080	1	TR	TR	TR	2	0	0	95	2	0	0	0	0	0	1	2	97		
AVERAGE	1	1	2	2	2	0	TR	82	8	2	TR	0	TR	TR	6	2	92		

* Ordered mixed-layer illite/smectite contains approximately 20-25% expandable (smectite) interlayers.

OMNI LABORATORIES, INC.
 AUTO X-RAY DIFFRACTION
 (WEIGHT%)

FILE NO: G-1992
 DATE : 4-29-93

ENVIROCORP
 UNKNOWN WELL

SAMPLE NUMBER	CLAYS					CARBONATES					OTHER MINERALS								TOTALS		
	KAOLINITE	CHLORITE	ILLITE	ILL./SMECT.*	GLAUCOPHANE	MONTEC.	DOLOMITE	SIDERITE	QUARTZ	PLAG.	K-SPAR	MICA	SARTE	PYRITE	HALITE	CLAYS	CARB.	OTHER			
081	1	TR	1	0	1	TR	0	89	4	4	0	0	0	0	2	1	97				
082	1	1	TR	TR	1	0	0	91	5	1	0	0	0	0	2	1	97				
083	1	1	1	0	0	0	0	93	2	2	0	0	TR	0	3	0	97				
084	2	0	1	0	0	0	0	95	1	1	0	0	0	0	3	0	97				
085	1	TR	1	0	0	0	0	98	TR	TR	0	0	0	0	2	0	98				
086	4	1	3	0	0	0	6	71	12	TR	TR	0	3	0	8	6	86				
087	2	1	2	1	0	0	1	85	6	2	0	0	0	0	6	1	93				
088	TR	TR	1	0	0	0	3	93	TR	0	0	0	3	0	1	3	96				
089	4	1	1	TR	0	0	0	88	5	1	TR	0	0	0	6	0	94				
090	3	2	3	3	0	0	0	82	3	1	TR	0	3	TR	11	0	89				
091	2	1	2	1	0	0	0	86	3	5	0	0	TR	0	6	0	94				
092	TR	1	1	TR	0	0	0	96	2	0	0	0	TR	0	2	0	98				
093	1	TR	1	0	TR	TR	0	94	4	0	0	0	0	0	2	TR	98				
094	2	1	1	0	0	0	0	91	2	2	0	0	1	0	4	0	96				
095	1	1	1	0	0	0	0	95	2	0	0	0	0	0	3	0	97				
096	1	TR	TR	0	0	0	0	96	3	TR	0	0	0	0	1	0	99				
097	1	1	2	0	0	0	0	83	2	1	0	0	0	0	4	0	96				
098	1	1	1	0	0	0	0	95	2	TR	TR	0	0	0	3	0	97				
099	1	TR	1	0	0	0	2	91	3	2	TR	0	0	0	2	2	96				
100	TR	TR	1	0	0	0	0	98	2	1	0	0	0	0	1	0	99				
AVERAGE	2	1	1	TR	TR	TR	1	91	3	1	TR	0	TR	0	4	1	95				

* Mixed-layer Illite/smectite contains approximately 20-25% expandable (smectite) interlayers.

OMNI LABORATORIES, INC.
 AUTO X-RAY DIFFRACTION
 (WEIGHT%)

FILE NO: G-1992
 DATE : 4-29-93

ENVIROCORP
 UNKNOWN WELL

SAMPLE NUMBER	CLAYS					CARBONATES					OTHER MINERALS							TOTALS		
	KALONITE	CHLORITE	ILLITE	ILL./MISC.*	CLAYITE	DOLOMITE	SIDERITE	QUARTZ	PLAG.	K-SPAR	MCA	BARITE	PHYRITE	HALITE	CLAYS	CARB.	OTHER			
101	6	2	3	0	0	0	0	86	2	1	0	0	0	0	11	0	89			
102	2	1	2	TR	0	2	0	89	3	0	TR	0	1	0	5	2	93			
103	1	TR	1	0	0	0	0	97	1	0	0	0	0	0	2	0	98			
104	1	1	1	TR	0	0	0	95	2	TR	0	0	TR	0	3	0	97			
105	TR	1	2	TR	0	0	0	96	1	0	0	0	0	0	3	0	97			
106	1	TR	TR	0	0	0	0	97	2	TR	0	0	0	0	1	0	99			
107	1	TR	1	TR	13	0	0	81	2	0	TR	0	2	0	2	13	85			
108	2	TR	2	1	TR	3	0	79	11	TR	TR	0	2	0	5	3	92			
109	1	TR	1	TR	0	0	2	80	6	0	TR	0	0	0	2	2	96			
110	2	1	2	1	0	0	26	58	7	3	TR	0	0	0	6	26	68			
111	4	3	7	7	0	0	5	60	10	4	0	0	0	0	21	5	74			
112	2	1	2	1	0	0	6	72	13	3	0	0	0	0	6	6	88			
113	2	1	1	1	2	0	TR	82	9	TR	0	0	2	0	5	2	93			
114	5	2	4	3	0	0	1	72	12	TR	0	0	1	0	14	1	85			
115	3	1	2	1	6	0	3	72	12	0	0	0	0	7	9	84				
116	4	2	6	5	0	0	5	65	11	2	TR	0	TR	0	17	5	78			
117	2	2	6	6	0	0	4	69	10	1	TR	0	0	0	16	4	80			
118	6	3	7	9	0	0	4	59	11	2	TR	0	0	0	24	4	72			
119	6	2	9	5	0	0	3	84	11	TR	0	0	0	0	22	3	75			
120	6	2	7	4	0	0	3	68	9	1	TR	0	1	0	18	3	79			
AVERAGE	3	1	3	2	1	TR	3	79	7	1	TR	0	TR	0	9	4	87			

* Mixed-layer illite/smectite contains approximately 20-25% expandable (smectite) interlayers.

OMNI LABORATORIES, INC.
 AUTO X-RAY DIFFRACTION
 (WEIGHT%)

ENVIROCORP
 UNKNOWN WELL

FILE NO: G-1992
 DATE : 4-29-93

SAMPLE NUMBER	CLAYS				CARBONATES							OTHER MINERALS							TOTALS		
	SAOLINITE	CHLORITE	MILRE	ILL./MISC.*	CALCITE	DOLOMITE	SIDERITE	QUARTZ	PLAG.	K-SPAR	MICA	BARITE	PTIRITE	HALITE	CLAYS	CARB.	OTHER				
121	4	2	4	3	TR	TR	2	73	11	1	0	0	0	0	13	2	85				
122	2	3	6	2	0	0	62	20	5	0	0	0	0	0	13	62	25				
123	2	1	3	1	2	0	0	63	28	0	TR	0	2	0	7	2	91				
124	1	TR	1	2	2	0	0	60	34	0	0	0	TR	0	4	2	94				
125	1	TR	1	TR	12	0	0	64	22	0	TR	0	TR	0	2	12	86				
126	TR	0	TR	0	28	0	0	45	27	TR	0	0	0	0	TR	28	72				
127	1	TR	1	1	9	0	48	38	2	0	TR	0	0	0	3	57	40				
128	1	TR	1	0	36	0	TR	52	5	1	0	0	4	0	2	36	62				
129	TR	TR	1	TR	0	0	0	88	6	5	0	0	0	0	1	0	99				
130	1	TR	1	0	0	0	0	86	11	1	0	0	0	0	2	0	98				
131	1	TR	1	0	0	0	0	89	9	TR	TR	0	0	0	2	0	98				
132	1	TR	1	TR	0	1	0	87	7	3	0	0	0	0	2	1	97				
133	TR	TR	1	0	0	0	0	90	9	0	0	0	0	0	1	0	99				
134	1	TR	TR	0	0	0	0	92	6	1	0	0	0	0	1	0	99				
135	TR	TR	1	0	0	0	0	96	3	TR	0	0	0	0	1	0	99				
136	1	TR	1	TR	1	0	0	73	17	7	0	0	0	0	2	1	97				
137	1	TR	TR	0	0	0	0	89	10	0	0	0	0	0	1	0	99				
138	TR	TR	1	0	0	0	0	97	2	0	0	0	0	0	1	0	99				
139	1	TR	TR	0	0	0	0	85	4	0	0	0	0	0	1	0	99				
140	1	TR	0	TR	TR	0	0	88	0	TR	0	0	0	0	1	TR	99				
AVERAGE	1	TR	1	1	5	TR	6	74	11	1	TR	0	TR	0	3	11	86				

* Mixed-layer illite/smectite contains approximately 20-25% expandable (smectite) interlayers.

OMNI LABORATORIES, INC.
 AUTO X-RAY DIFFRACTION
 (WEIGHT%)

ENVIROCORP
 UNKNOWN WELL

FILE NO: G-1992
 DATE : 4-29-93

SAMPLE NUMBER	CLAYS					CARBONATES					OTHER MINERALS							TOTALS		
	KAOHLINITE	CHLORITE	ILLITE	ML/SMECT*		CALCITE	DOLOMITE	SIDERITE	QUARTZ	PLAG.	K-SPAR	MCA	BARITE	PHYRITE	MALITE	CLAYS	CARB.	OTHER		
141	1	TR	TR	TR	TR	TR	0	0	80	8	1	0	0	0	0	1	TR	99		
142	TR	TR	1	0	0	0	0	0	94	5	0	0	0	0	0	1	0	99		
143	TR	TR	1	0	0	0	0	0	98	3	0	0	0	0	0	1	0	99		
144	1	TR	TR	TR	TR	TR	0	0	94	4	1	0	0	0	0	1	TR	99		
145	TR	TR	1	0	0	0	0	0	97	2	TR	0	0	0	0	1	0	99		
146	1	TR	TR	TR	TR	0	TR	0	93	5	1	0	0	0	0	1	TR	99		
147	TR	TR	1	TR	TR	0	0	0	97	2	0	0	0	0	0	1	0	99		
148	TR	TR	1	TR	TR	0	0	0	97	2	0	0	0	0	0	1	0	99		
149	1	TR	1	0	0	0	0	0	94	3	1	0	0	0	0	2	0	98		
150	1	TR	TR	0	0	0	0	0	93	5	1	0	0	0	0	1	0	99		
151	TR	TR	TR	0	0	0	0	0	96	4	0	0	0	0	0	TR	0	100		
152	1	TR	1	0	0	0	0	0	83	15	0	TR	0	0	0	2	0	98		
153	TR	TR	1	0	TR	0	0	0	97	2	0	0	0	0	0	1	TR	99		
154	1	TR	TR	0	TR	0	0	0	93	6	TR	TR	0	0	0	1	TR	99		
155	1	TR	1	TR	TR	0	0	0	92	6	TR	0	0	0	2	0	0	98		
156	TR	TR	TR	0	0	0	0	0	94	4	2	0	0	0	TR	0	0	100		
157	1	TR	TR	0	1	0	1	0	91	5	2	0	0	0	0	1	1	98		
158	1	TR	TR	TR	TR	0	0	0	93	5	1	0	0	0	1	0	0	99		
159	TR	1	1	0	0	0	0	0	96	2	TR	0	0	0	2	0	0	98		
160	TR	TR	1	TR	TR	0	0	0	95	4	0	0	0	0	1	0	0	99		
AVERAGE	1	TR	1	TR	TR	TR	TR	0	93	4	1	TR	0	0	2	TR	0	98		

* Mixed-layer illite/smectite contains approximately 20% expandable (smectite) interlayers.

OMNI LABORATORIES, INC.
 AUTO X-RAY DIFFRACTION
 (WEIGHT%)

ENVIROCORP
 UNKNOWN WELL

FILE NO: G-1992
 DATE : 4-29-93

SAMPLE NUMBER	CLAYS					CARBONATES							OTHER MINERALS							TOTALS		
	KALONITE	CHLORITE	ILLITE	ILL/SMC.*	CAOLCITE	DOLOMITE	SIDERITE	QUARTZ	PLAG.	K-SPAR	MICA	BARITE	PIRITE	HAUTE	CLAYS	CARB.	OTHER					
161	1	TR	1	0	TR	TR	0	90	7	1	0	0	0	0	2	TR	98					
162	1	TR	TR	TR	TR	1	0	91	7	TR	0	0	0	0	1	1	98					
163	1	TR	TR	TR	0	0	0	86	13	TR	0	0	0	0	1	0	99					
164	TR	TR	1	0	0	0	0	92	5	2	TR	0	0	0	1	0	99					
165	TR	TR	1	TR	0	0	0	87	10	2	0	0	0	0	1	0	99					
166	1	TR	TR	TR	0	0	0	94	4	1	0	0	0	0	1	0	99					
167	TR	TR	TR	0	0	0	0	95	4	1	0	0	0	0	TR	0	100					
168	1	TR	1	TR	TR	0	0	94	4	TR	0	0	0	0	2	TR	98					
169	TR	TR	1	TR	0	0	0	95	4	TR	0	0	0	0	1	0	99					
170	1	TR	TR	0	0	0	0	91	7	1	TR	0	0	0	1	0	99					
171	TR	TR	TR	0	0	TR	0	92	6	2	TR	0	0	0	TR	TR	100					
172	TR	1	TR	TR	TR	0	0	87	11	1	TR	0	TR	0	1	TR	99					
173	TR	TR	1	TR	0	0	0	92	5	2	0	0	0	0	1	0	99					
174	2	TR	1	TR	0	0	0	91	8	TR	0	0	0	0	3	0	97					
175	TR	1	TR	TR	0	0	0	95	3	1	0	0	0	0	1	0	99					
176	TR	TR	TR	1	0	0	0	93	6	TR	0	0	0	0	1	0	99					
177	0	1	TR	TR	0	0	0	96	2	1	0	0	0	0	1	0	99					
178	1	TR	TR	0	0	2	0	93	4	0	0	0	0	0	1	2	97					
179	1	TR	TR	0	0	5	0	91	3	TR	0	0	0	0	1	5	94					
180	1	TR	TR	TR	0	7	0	86	6	0	TR	0	0	0	1	7	92					
AVERAGE	1	TR	TR	TR	TR	1	0	91	6	1	TR	TR	TR	0	1	1	88					

* Mixed-layer illite/smectite contains approximately 20% expandable (smectite) interlayers.

OMNI LABORATORIES, INC.
 AUTO X-RAY DIFFRACTION
 (WEIGHT%)

ENVIROCORP
 UNKNOWN WELL

FILE NO: G-1992
 DATE : 4-29-93

SAMPLE NUMBER	CLAYS				CARBONATES								OTHER MINERALS								TOTALS			
	KAOHLINITE	CHLORITE	ILLITE	ILL/SMECT.	CALCITE	DOLOMITE	SIDERITE	QUARTZ	FLUC.	K-SPAR	MCA	BARITE	PIRITE	MALITE	CLAYS	CARB.	OTHER	CLAYS	CARB.	OTHER				
181	1	TR	TR	TR	0	2	0	96	1	0	0	0	0	0	1	2	0	1	2	97				
182	TR	TR	1	TR	0	0	0	98	1	0	0	0	0	0	1	0	0	1	0	99				
183	1	TR	TR	TR	TR	TR	0	97	2	0	0	0	0	0	1	TR	0	1	TR	99				
184	1	TR	TR	0	1	0	0	95	3	0	TR	0	0	0	1	1	0	1	1	98				
185	1	TR	TR	0	0	0	0	93	2	2	0	0	2	0	1	0	0	1	0	99				
186	TR	TR	1	0	0	TR	0	95	4	0	0	0	0	0	1	TR	0	1	TR	99				
187	1	TR	TR	TR	0	0	0	91	7	1	0	0	0	0	1	0	0	1	0	99				
188	TR	0	TR	TR	0	0	0	96	4	0	0	0	0	0	TR	0	0	TR	0	100				
189	1	TR	1	0	0	1	0	90	7	0	0	0	0	0	2	1	0	2	1	97				
190	2	1	3	2	0	TR	5	60	27	TR	0	0	0	0	8	5	0	8	5	87				
191	1	TR	TR	0	0	0	0	91	5	3	0	0	0	0	1	0	0	1	0	99				
192	1	TR	1	0	0	3	0	88	5	2	0	0	0	0	2	3	0	2	3	95				
193	TR	TR	1	0	0	0	0	92	7	TR	0	0	0	0	1	0	0	1	0	99				
194	TR	TR	1	0	0	0	0	89	9	1	0	0	0	0	1	0	0	1	0	99				
195	1	TR	1	TR	0	3	0	86	7	2	0	0	0	0	2	3	0	2	3	95				
196	1	TR	1	TR	0	0	0	89	9	0	0	0	0	0	2	0	0	2	0	98				
197	1	TR	1	TR	0	0	0	86	10	2	0	0	0	0	2	0	0	2	0	98				
198	1	TR	1	TR	0	0	0	90	8	TR	0	0	0	0	2	0	0	2	0	98				
199	TR	TR	1	TR	0	0	0	88	8	0	0	0	3	0	1	0	0	1	0	99				
200	1	TR	1	TR	0	0	0	83	12	3	TR	0	0	0	2	0	0	2	0	98				
AVERAGE	1	TR	1	TR	TR	TR	TR	90	7	1	TR	0	TR	0	2	TR	0	2	TR	88				

* Mixed-layer Illite/smectite contains approximately 20% expandable (smectite) interlayers.

